frontiers | Research Topics

The impact of abiotic stresses on agriculture: Mitigation through climate smart strategies

Edited by
Shuvasish Choudhury, Akbar Hossain, Debojyoti Moulick and Marian Brestic

Published in
Frontiers in Plant Science

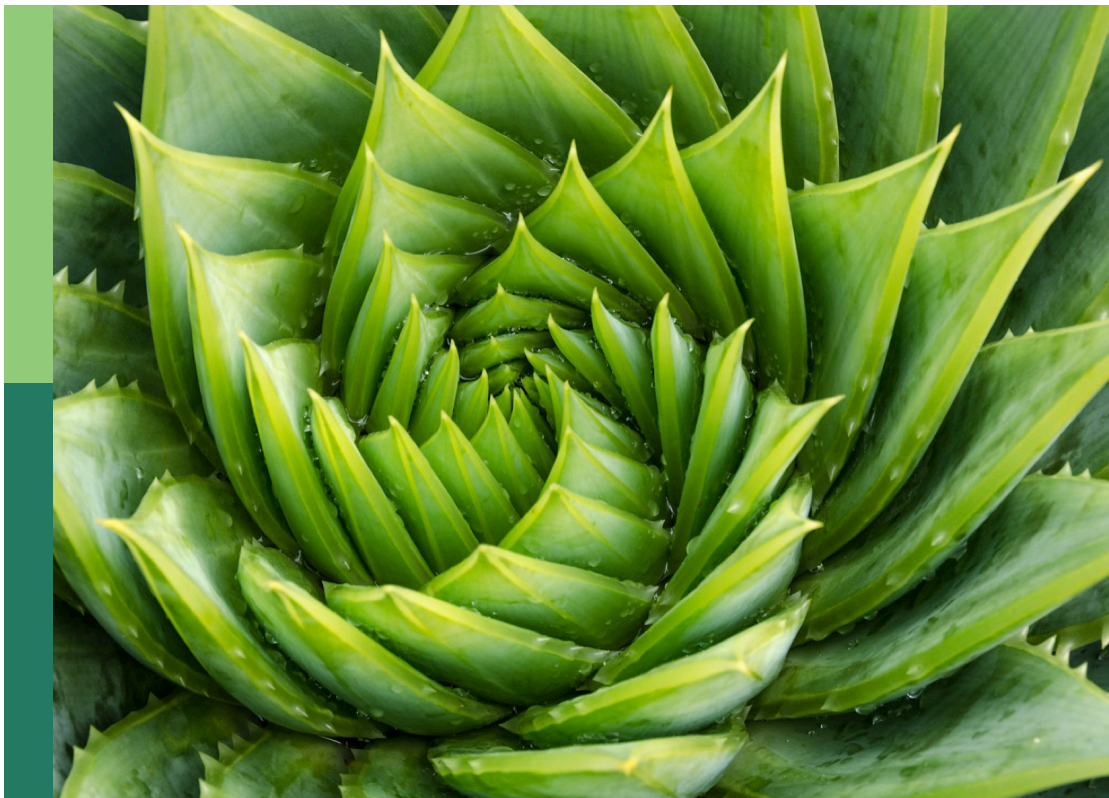

ISSN 1664-8714
ISBN 978-2-8325-4944-5
DOI 10.3389/978-2-8325-4944-5

About Frontiers

Frontiers is more than just an open access publisher of scholarly articles: it is a pioneering approach to the world of academia, radically improving the way scholarly research is managed. The grand vision of Frontiers is a world where all people have an equal opportunity to seek, share and generate knowledge. Frontiers provides immediate and permanent online open access to all its publications, but this alone is not enough to realize our grand goals.

Frontiers journal series

The Frontiers journal series is a multi-tier and interdisciplinary set of open-access, online journals, promising a paradigm shift from the current review, selection and dissemination processes in academic publishing. All Frontiers journals are driven by researchers for researchers; therefore, they constitute a service to the scholarly community. At the same time, the *Frontiers journal series* operates on a revolutionary invention, the tiered publishing system, initially addressing specific communities of scholars, and gradually climbing up to broader public understanding, thus serving the interests of the lay society, too.

Dedication to quality

Each Frontiers article is a landmark of the highest quality, thanks to genuinely collaborative interactions between authors and review editors, who include some of the world's best academicians. Research must be certified by peers before entering a stream of knowledge that may eventually reach the public - and shape society; therefore, Frontiers only applies the most rigorous and unbiased reviews. Frontiers revolutionizes research publishing by freely delivering the most outstanding research, evaluated with no bias from both the academic and social point of view. By applying the most advanced information technologies, Frontiers is catapulting scholarly publishing into a new generation.

What are Frontiers Research Topics?

Frontiers Research Topics are very popular trademarks of the *Frontiers journals series*: they are collections of at least ten articles, all centered on a particular subject. With their unique mix of varied contributions from Original Research to Review Articles, Frontiers Research Topics unify the most influential researchers, the latest key findings and historical advances in a hot research area.

Find out more on how to host your own Frontiers Research Topic or contribute to one as an author by contacting the Frontiers editorial office: frontiersin.org/about/contact

The impact of abiotic stresses on agriculture: Mitigation through climate smart strategies

Topic editors

Shuvasish Choudhury — Assam University, India

Akbar Hossain — Department of Soil Science, Bangladesh Wheat and Maize Research Institute (BWMRI), Bangladesh

Debojyoti Moulick — Independent researcher, Kolkata, India

Marian Brestic — Slovak University of Agriculture, Slovakia

Citation

Choudhury, S., Hossain, A., Moulick, D., Brestic, M., eds. (2024). *The impact of abiotic stresses on agriculture: Mitigation through climate smart strategies*. Lausanne: Frontiers Media SA. doi: 10.3389/978-2-8325-4944-5

Table of contents

frontiers | Frontiers in Plant Science

TYPE Editorial
PUBLISHED 14 May 2024
DOI 10.3389/fpls.2024.1391051

OPEN ACCESS

EDITED AND REVIEWED BY
Saad Sulieman,
University of Khartoum, Sudan

*CORRESPONDENCE
Debojyoti Moulick
drubha31@gmail.com
Akbar Hossain
akbarhossainwrc@gmail.com

RECEIVED 24 February 2024
ACCEPTED 22 April 2024
PUBLISHED 14 May 2024

CITATION
Moulick D, Choudhury S, Brestic M and Hossain A (2024) Editorial: The impact of abiotic stresses on agriculture: mitigation through climate smart strategies.
Front. Plant Sci. 15:1391051.
doi: 10.3389/fpls.2024.1391051

Editorial: The impact of abiotic stresses on agriculture: mitigation through climate smart strategies

Debojyoti Moulick[1]*, Shuvasish Choudhury[2], Marian Brestic[3,4] and Akbar Hossain[5]*

[1]Department of Environmental Science, University of Kalyani, Kalyani, India, [2]Plant Stress Biology and Metabolomics Laboratory, Department of Life Science and Bioinformatics, Assam University, Silchar, India, [3]Institute of Plant and Environmental Sciences, Slovak University of Agriculture, Nitra, Slovakia, [4]Department of Botany and Plant Physiology, Czech University of Life Sciences Prague, Prague, Czechia, [5]Division of Soil Science, Bangladesh Wheat and Maize Research Institute, Dinajpur, Bangladesh

KEYWORDS

abiotic stresses, changing climate, mitigation approaches, climate smart agriculture, food security

Editorial on the Research Topic
The impact of abiotic stresses on agriculture: mitigation through climate smart strategies

Components of agro-ecosystems, whether abiotic or biotic in nature, can be treated as key detrimental factors (for satisfactory growth and yield) or as a *stressor*(s) for crops/cropping systems when they are present below/above the optimum level either alone or in combination (s) (Choudhury and Moulick, 2022). Abiotic stress can be defined as hostile consequences imposed by abiotic component(s) on a crop in a particular agro-environment, resulting in a variety of responses ranging from alterations at the cellular level to gene expression, and metabolomics may have manifested in growth and yield reduction in crops (Choudhury et al., 2021; Zhang et al., 2022; Moulick et al., 2023). The most common abiotic stressors such as Salinity, toxic heavy metals/metalloids, flooding, drought, elevated ozone, carbon dioxide, methane, nitrous oxide, lack of nutrients, extreme temperatures, and nanoparticles pose serious challenges to achieving global food security.

Climate-smart agriculture is a polymathic approach to altering and redesigning the agro-ecosystems to support global food security under the new realities of climate change. Researchers from different parts of the world have contributed their research findings to this topic. Among the published content on this topic, research on both food and forage crops can be found, highlighting that the consequences of salinity, drought, minimizing greenhouse gas emissions, and heat stress are predominant.

In an era of severe global climatic fluctuations, a series of cellular and biochemical manifestations lead to a burst of reactive oxygen species (ROS) upon encountering a stressor, which is subsequently manifested as a reduction in pigments (Shariatipour et al.), the ratio of Fv to Fm, i.e., the chlorophyll fluorescence parameter (Elfanah et al.),

transcriptomic profiles, signaling behavior (Zhao et al.), and alterations in the gene expression of aqua porin and heat shock protein (Hongal et al.). To achieve resilience to abiotic stressors, assessing the intensity of damage caused by stressors on a given crop is vital. Efficacy of hyperspectral reflectance and agro-physiological traits. In addition to its robust and statistically sound experimental design, this approach has been proven to be valuable (Elfanah et al.). Using tolerance indices, Alam et al. identified suitable salt-tolerant onion genotypes.

Melash et al. documented the efficacy of nutrient management on the qualitative aspect of caryopsis and yield attributes of durum wheat under the regime of changing climatic conditions. The article concluded that custom-made (case-by-case) nutrient management strategies, agronomists, breeders, and farmers can play a vital role in durum wheat production, safeguarding food security. N_2O and CH_4 emissions can be effectively reduced in high-yielding transgenic rice with partial aerenchyma by immersing root exudates, which provide substrates for GHGs. Observations made by Iqbal et al. have demonstrated the ability of plant breeders/biotechnologists to serve the goal of sustainable development. In another interesting study, the authors reported that supplementing SiNPs can effectively mitigate salinity stress in lemongrass (*Cymbopogon flexuosus* (Nees ex Steud.) Wats. (Mukarram et al.). Shi et al. provided important insights into the genes and mechanisms underlying the resilience of crop plants to Si-induced low-Fe stress. The authors observed that Si supplementation under Fe-deficient conditions amplified Fe supply to the leaves and roots of tomato plants. With gradual progress in the sowing date, a delayed trend in tiller initiation and a prolongation of later growth phases were observed in the studied wheat varieties cultivated in the Indo-Gangetic Plains. Sattar et al. concluded that the date of sowing and the environment are crucial factors in determining phenology and yield. Qu et al. reported that drought can significantly decrease the carbon (22.7%), nitrogen (21.2%), and phosphorus (21.6%) contents of microbial biomass and the activity levels of enzymes such as β-1,4-glucosidase (26.8%) and acid phosphatase (16.0%) under drought conditions in terrestrial ecosystems.

There is always room for improvement in research, especially in the agro-environmental domain, where multiple factors are operating at different scales. An urgent need to suggest a particular remedial measure is the validation of findings in multiple environments along with multiple crop/cropping systems to deepen our understanding of how a particular variety (existing/newly developed) interacts with the environment and management. Moreover, under constantly fluctuating climates, research on soil conditions should focus on validating the United Nations SDGs. This particular Research Topic provides a platform to highlight some interesting findings; however, there is an urgent need for sustainable and environmentally friendly interventions, such as those related to the molecular response of plants and stressor interactions, the potential for genetic engineering, wild relatives of crops, seed priming, water and nutrient management, and postharvest quality assessment (e.g., eating and cooking attributes), which should be prioritized in the near future (Hossain et al., 2022; Hazra et al., 2023; Moulick et al., 2024). Finally, due emphasis should be given to strategic research to maintain the flow of information/feedback for both basic and applied research.

Author contributions

DM: Conceptualization, Writing – original draft, Writing – review & editing. SC: Conceptualization, Writing – original draft, Writing – review & editing. MB: Conceptualization, Writing – original draft, Writing – review & editing. AH: Conceptualization, Writing – original draft, Writing – review & editing.

Acknowledgments

Editors are thankful to the Frontiers Author Services and the Sustainable Food System Journal Office for the management and publication of this VSI and to the authors who participated in this Research Topic for improving our scientific engagement.

Conflict of interest

The authors declare that the research was conducted in the absence of any commercial or financial relationships that could be construed as potential conflicts of interest.

Publisher's note

References

Choudhury, S., and Moulick, D. (2022). *Response of Field Crops to Abiotic Stress: Current Status and Future Prospects. 1st ed* (CRC Press, 6000 Broken Sound Parkway NW, Suite 300, Boca Raton, FL 33487-2742). doi: 10.1201/9781003258063

Choudhury, S., Sharma, P., Moulick, D., and Mazumder, M. K. (2021). Unrevealing metabolomics for abiotic stress adaptation and tolerance in plants. *J. Crop Sci. Biotechnol.* 24, 479–493. doi: 10.1007/s12892-021-00102-8

Hazra, S., Moulick, D., Mukherjee, A., Sahib, S., Chowardhara, B., Majumdar, A., et al. (2023). Evaluation of efficacy of noncoding RNA in abiotic stress management of field crops: Current status and future prospective. *Plant Physiol. Biochem.* 203, 107940. doi: 10.1016/j.plaphy.2023.107940

Hossain, A., Maitra, S., Pramanick, B., Bhutia, K. L., Ahmad, Z., Moulik, D., et al. (2022). "Wild relatives of plants as sources for the development of abiotic stress

tolerance in plants," in *Plant perspectives to global climate changes* (Academic Press, Elsevier Inc.), 471–518. doi: 10.1016/B978–0-323–85665-2.00011-X

Moulick, D., Bhutia, K. L., Sarkar, S., Roy, A., Mishra, U. N., Pramanick, B., et al. (2023). The intertwining of Zn-finger motifs and abiotic stress tolerance in plants: Current status and future prospects. *Front. Plant Sci.* 13. doi: 10.3389/fpls.2022.1083960

Moulick, D., Mukherjee, A., Das, A., Roy, A., Majumdar, A., Dhar, A., et al. (2024). Selenium–An environmentally friendly micronutrient in agroecosystem in the modern era: An overview of 50-year findings. *Ecotoxicology Environ. Saf.* 270, 115832. doi: 10.1016/j.ecoenv.2023.115832

Zhang, H., Zhu, J., Gong, Z., and Zhu, J.-K. (2022). Abiotic stress responses in plants. Abiotic stress responses in plants. *Nat. Rev. Genet.* 23, 104–119. doi: 10.1038/s41576-021-00413-0

frontiers | Frontiers in Plant Science

TYPE Original Research
PUBLISHED 21 December 2022
DOI 10.3389/fpls.2022.1094451

OPEN ACCESS

EDITED BY
Shuvasish Choudhury,
Assam University, India

REVIEWED BY
Bedabrata Saha,
Agricultural Research Organization (ARO), Israel
Renato De Mello Prado,
São Paulo State University, Brazil
Abbu Zaid,
Govt. Degree College Doda, India

*CORRESPONDENCE
Yi Zhang
harmony1228@163.com
Golam Jalal Ahammed
ahammed@haust.edu.cn

†These authors have contributed equally to this work

SPECIALTY SECTION
This article was submitted to Plant Abiotic Stress, a section of the journal Frontiers in Plant Science

RECEIVED 10 November 2022
ACCEPTED 02 December 2022
PUBLISHED 21 December 2022

CITATION
Shi Y, Guo S, Zhao X, Xu M, Xu J, Xing G, Zhang Y and Ahammed GJ (2022) Comparative physiological and transcriptomics analysis revealed crucial mechanisms of silicon-mediated tolerance to iron deficiency in tomato.
Front. Plant Sci. 13:1094451.
doi: 10.3389/fpls.2022.1094451

Comparative physiological and transcriptomics analysis revealed crucial mechanisms of silicon-mediated tolerance to iron deficiency in tomato

Yu Shi[1†], Shuxun Guo[1†], Xin Zhao[1], Mengzhu Xu[1], Jin Xu[1], Guoming Xing[1], Yi Zhang[1*] and Golam Jalal Ahammed[2,3*]

[1]College of Horticulture, Shanxi Agricultural University, Taigu, Shanxi, China, [2]College of Horticulture and Plant Protection, Henan University of Science and Technology, Luoyang, Henan, China, [3]Henan International Joint Laboratory of Stress Resistance Regulation and Safe Production of Protected Vegetables, Luoyang, Henan, China

Iron (Fe) deficiency is a common abiotic stress in plants grown in alkaline soil that causes leaf chlorosis and affects root development due to low plant-available Fe concentration. Silicon (Si) is a beneficial element for plant growth and can also improve plant tolerance to abiotic stress. However, the effect of Si and regulatory mechanisms on tomato plant growth under Fe deficiency remain largely unclear. Here, we examined the effect of Si application on the photosynthetic capacity, antioxidant defense, sugar metabolism, and organic acid contents under Fe deficiency in tomato plants. The results showed that Si application promoted plant growth by increasing photosynthetic capacity, strengthening antioxidant defense, and reprogramming sugar metabolism. Transcriptomics analysis (RNA-seq) showed that Si application under Fe deficiency up-regulated the expression of genes related to antioxidant defense, carbohydrate metabolism and organic acid synthesis. In addition, Si application under Fe deficiency increased Fe distribution to leaves and roots. Combined with physiological assessment and molecular analysis, these findings suggest that Si application can effectively increase plant tolerance to low Fe stress and thus can be implicated in agronomic management of Fe deficiency for sustainable crop production. Moreover, these findings provide important information for further exploring the genes and underlying regulatory mechanisms of Si-mediated low Fe stress tolerance in crop plants.

KEYWORDS

silicon, low iron, transcriptomics analysis, organic acid, sugar metabolism, oxidative stress

Introduction

Iron (Fe) is not only an essential mineral element for plants but also an activator of many vital enzymes (Chao and Chao, 2022). It is a cofactor for numerous proteases in the redox process including photosynthesis, nitrogen fixation and nucleic acid synthesis (Nikolic et al., 2019). Although Fe is abundantly present in the soil as an element, it commonly occurs in the oxidized form, which is not a suitable form for plant uptake (Ahammed et al., 2020). Notably, Fe solubility is very low in alkaline soils which causes Fe deficiency-induced chlorosis. Fe deficiency inhibits photosynthetic capacity and subsequently sucrose metabolism in plants (Nikolic et al., 2019). Moreover, Fe deficiency-induced disruption in the photosynthetic and respiratory electron transport leads to the massive production of reactive oxygen species (ROS) in chloroplasts and mitochondria (M'Sehli et al., 2014; Zaid et al., 2020).

Silicon (Si) is the second most abundant element in the earth's crust (Khan et al., 2022). Although Si is not a well-established essential element for plant growth and development, recent studies have shown that Si is beneficial to plant growth (Gou et al., 2020; Rastogi et al., 2021). Plant roots mainly absorb silicic acid (H_4SiO_4), which is then transported through the xylem to shoot, eventually forming amorphous Si ($SiO_2{\cdot}nH_2O$) deposited in the cell wall or intercellular space (Zhang et al., 2018; Khan et al., 2021). Dissolved Si (H_4SiO_4), can be readily taken up by plants and it plays an important role as an alleviator of both biotic and abiotic stress (Ahmad et al., 2019; Ahanger et al., 2020; Ahammed and Yang, 2021; Hussain et al., 2021). The absorption of Si by plants consists of active absorption and passive absorption, and both types may exist simultaneously (Ahmed et al., 2014; Zaid et al., 2018). Silicon deposition on the cell wall aids in maintaining the cellular ion balance, osmotic regulation and ROS homeostasis, thus enhancing the resistance of plants to stress (Bakhat et al., 2018).

Recent studies have shown that Si can enhance the re-transfer of Fe from old leaves to new leaves, and promote the transfer of Fe by increasing the content of Fe^{2+} and niacinamide, the chelating agent of Fe^{3+} in the phloem (Pavlovic et al., 2016). Silicon application significantly increased the total Fe content under Fe deficiency, alleviated the symptoms of leaf chlorosis caused by Fe deficiency, and promoted the growth of shoots and roots in cucumber (Bityutskii et al., 2018). Under Fe deficiency, plants treated with Si can absorb Fe faster than those treated without Si, especially Si increases the transport rate of Fe from root to stem, suggesting that the increased expression of transporters affects the absorption and transport of Fe, which is of the great significance of maintaining normal growth of plants under Fe deficiency (Peris-Felipo et al., 2020).

Despite several reports showing that Si can aid plants in Fe uptake, the ameliorative effect of Si on Fe deficiency and its physiological and molecular mechanisms still remain unclear. In this study, the tomato (*Solanum lycopersicum* L.) variety 'Micro-Tom' was used as experimental material in a hydroponic system to study the effects of Si root application on growth characteristics, photosynthetic fluorescence parameters, glucose metabolism, organic acid content and transcriptomics of tomato seedlings under Fe deficiency. Transcriptome analysis and physiological results explained how Si can improve the tolerance of tomato plants to Fe deficiency, which provides a theoretical basis and reference for improving the tolerance of tomato plants to Fe deficiency.

Materials and methods

Plant materials and treatments

Tomato (*S. lycopersicum* L. cultivar "Micro-tom") seeds were purchased from Ball Horticultural Company in the United States. The Si source was $K_2SiO_3{\cdot}nH_2O$ (containing Si 47%-51%), and the Fe source was EDTA-FeNa (containing Fe ≥13%). The nutrient solution used in hydroponics was adopted from the Japanese Yamazaki tomato formula (Qu et al., 2020; Zhang et al., 2019a). The experiment was carried out in the Artificial Climate Room, College of Horticulture, Shanxi Agricultural University, Taigu, China with various environmental parameters as follows: temperature 28/18°C (day/night), light intensity 800 μmol·m^{-2}·s^{-1}, and photoperiod 16/8h. Seedlings at the four-leaf stage were transplanted to hydroponic pots (28cm×19cm×14cm) containing 1/2 strength of the Japanese Yamazaki formula nutrient solution with 100 μM Fe concentration. After a week of recovery of the seedlings, the nutrient solution was replaced with full-strength Japanese Yamazaki formula consistent with different treatments. Treatments were then imposed in different combinations of Fe and Si application which resulted in the following 6 treatments: (i) Control (CK): 100 μmol/L Fe+ 0 mmol/L Si, (ii) Control and Si application (CK+Si): 100 μmol/L Fe + 1.5 mmol/L Si, (iii) Fe deficiency treatment (10 Fe): 10 μmol/L Fe + 0 mmol/L Si, (iv) Fe deficiency and Si application (10 Fe+Si): 10 μmol/L Fe + 1.5 mmol/L Si, (v) Fe deficiency treatment (1 Fe): 1 μmol/L Fe + 0 mmol/L Si, (vi) Fe deficiency and Si application (1 Fe+Si): 1 μmol/L Fe + 1.5 mmol/L Si. The concentration of 1 μM Fe was selected for further experiments based on the results of our preliminary experiments (100 μM Fe was the concentration of the normal nutrient solution, 1 μM and 10 μM Fe were the concentrations of Fe deficient nutrient solution) which eventually results in 4 treatments such as (i) Control (CK): 100 μmol/L Fe+ 0 mmol/L Si, (ii) Control and Si application (CK+Si): 100 μmol/L Fe + 1.5 mmol/L Si, (iii) Fe deficiency treatment (LF): 1 μmol/L Fe + 0 mmol/L Si, (iv) Fe deficiency and Si application (LF+Si): 1 μmol/L Fe + 1.5 mmol/L Si. Since K_2SiO_3 was used as the Si source, K^+ introduced from K_2SiO_3 was subtracted from KNO_3, and the loss of NO_3^- was supplemented with diluted HNO_3. During the experimental period, the nutrient solution was supplied with oxygen in an intermittent manner using an aeration pump, the pH of the nutrient solution was monitored daily and adjusted to 6.0 ± 0.2 using HNO_3, the liquid level was

replenished with distilled water every day and the nutrient solution was changed every 5 days. Biomass, photosynthetic fluorescence parameters, organic acid content, Fe content and transcriptomics were measured at 10 days of treatment, and other indexes such as antioxidant enzyme activity, leaf sucrose content and sucrose-related metabolic enzyme activity, etc. were measured in samples harvested at 5, 10, and 15 days of treatment.

Transcriptomics analysis and quantative real-time PCR assay

At 10 d of treatment, leaf and root samples from the following 4 treatments were harvested and used for RNA-seq: (i) CK, (ii) CK+Si, (iii) LF, and (iv) LF+Si, and the prefixes L and R were used to denote the leaf and root tissues of tomato, respectively for data presentation. Three biological replicates were performed for each treatment, resulting in a total of 24 samples. Total RNA was extracted and purified using TRIzol reagent (Invitrogen, Carlsbad, CA, USA) according to the instruction of the manufacturer. NanoDrop ND-1000 (NanoDrop, Wilmington, DE, USA) was used to quantify the RNA quantity and purity of each sample. Bioanalyzer 2100 (Agilent, CA, USA) with RIN number >7.0, was used to assess the integrity of RNA and confirmed by electrophoresis with denaturing agarose gel. Two rounds of purification were used to purify Poly (A) RNA from 1 μg total RNA using Dynabeads Oligo (dT)25-61005 (Thermo Fisher, CA, USA). Then Magnesium RNA Fragmentation Module (NEB, cat.e6150, USA) was used to fragment the poly(A) RNA into small pieces under 94°C 5-7 min. To generate the cDNA, the cleaved RNA fragments were then reverse-transcribed by SuperScript™ II Reverse Transcriptase (Invitrogen, cat. 1896649, USA). The resulting cDNA were then used to synthesize U-labeled second-stranded DNAs with *E. coli* DNA polymerase I (NEB, cat.m0209, USA), RNase H (NEB, cat.m0297, USA) and dUTP Solution (Thermo Fisher, cat.R0133, USA). Then an A-base was added to the blunt ends of each strand which prepared them for ligation to the indexed adapters.The fragments were ligated to single- or dual-index adapters. After further processing, the ligated products were amplified with PCR under the following conditions: 3 min initial denaturation at 95°C; 8 cycles, 15 sec at 98°C (denaturation), 15 sec at 60°C (annealing), and 30 sec at 72°C (extension); and then 5 min at 72°C (final extension). The final cDNA library was 300 ± 50 bp in terms of the average insert size. At last, the 2×150bp paired-end sequencing (PE150) was performed on an Illumina Novaseq™ 6000 (LC-Bio Technology CO., Ltd., Hangzhou, China) following the recommended protocol. All raw sequencing data from the current study were deposited into the NCBI database under the accession number "PRJNA902026" (https://www.ncbi.nlm.nih.gov/bioproject/PRJNA902026), (Submitted on 15 November 2022). We used fastp software (https://github.com/OpenGene/fastp) to omit the reads that contained adaptor contamination, low quality bases and undetermined bases with default parameters. And fastp was also used to verify the sequence quality. To map reads to the reference genome of *S. lycopersicum L.* SL4.0, HISAT2 (https://ccb.jhu.edu/software/hisat2) was then used. Assembling of the mapped reads of each sample was performed using StringTie (https://ccb.jhu.edu/software/stringtie) with default parameters. Afterward, all transcriptomes from all samples were merged to reconstruct a comprehensive transcriptome using gffcompare (https://github.com/gpertea/gffcompare/). When the final transcriptome was generated, StringTie and was used to estimate the expression levels of all transcripts. StringTie analyzed the expression level for mRNAs by calculating FPKM (FPKM = [total_exon_fragments/mapped_reads(millions) × exon_length(kB)]). The differentially expressed mRNAs were selected with fold change > 2 or fold change < 0.5 and with parametric F-test comparing nested linear models (p-value < 0.05) by R package edgeR (https://bioconductor.org/packages/release/bioc/html/edgeR.html).

The real-time qPCR was performed using the gene-specific primers (Table S1-S2). Samples were added to the 96-well plate and then reacted in the Applied Biosystems Quant Studio 3 real-time fluorescence quantitative PCR instrument with the following conditions: Stage 1: pre-denatured, One cycle at 95°C for 30 s; Stage 2: PCR reaction, 40 cycles, 95°C for 10 s, 60°C for 30 s, and 72°C for 40 s.

Measurements of biochemical and physiological parameters

The roots were cleaned and placed on the Epson Chops V800 Photo tray, scanned the root images and analyzed by the root analysis software WinRHIZO system. The chlorophyll and carotenoid contents were determined according to methods by Lichtenthaler and Wellburn (1983). The net photosynthetic rate (Pn) of functional leaves (the second fully expanded leaf at the growing point) of tomato seedlings on the 10th day of treatment was measured by portable photosynthetic apparatus (Li-6400; LI-COR, Lincoln, NE, USA). The maximum photochemical efficiency (Fv/Fm) of PSII was determined by Li-6400 portable photosynthetic apparatus fluorescence chamber after dark adaptation for 30 min. Then the leaves were activated under light for 1 h, and the effective photochemical quantum efficiency (Fv'/Fm'), actual photochemical quantum efficiency (ΦPSII), photosynthetic electron transfer rate (ETR) was, photochemical quenching coefficient (qP) and non-photochemical quenching coefficient (NPQ) of PSII under 800 $\mu mol \cdot m^{-2} \cdot s^{-1}$ activated light were determined. The Fe^{3+} reductase activity was determined according to 2,2 '-bipyridine-based methods. The Fe content was determined by flame spectrophotometry. The plant samples were digested by the H_2SO_4-H_2O_2 method and iron content was determined by

atomic flame spectrophotometer (AA-3200). Leaf Fe distribution rate = leaf Fe content/(leaf Fe content + stem Fe content + root Fe content), the calculation of stem and root Fe distribution rate is the same as above.

The relative conductivity was measured with a conductivity meter. MDA content was determined by the method of Heath and Packer (1968). H_2O_2 content was determined by the method of Willekens et al. (1997). The superoxide anion content was determined by the method described previously (Zhang et al., 2019a). Antioxidant enzyme activity was determined as described by Sheteiwy et al. (2017).

The sucrose content was determined by the hydrochloric acid-resorcinol method. The activities of sucrose neutral invertase (NI), acid invertase (AI), sucrose synthase (SS) and sucrose phosphate synthase (SPS) were determined using the corresponding enzyme activity assay kits (Beijing Solarbio Science & Technology Co., Ltd., Beijing, China). The content of organic acids was determined by high-performance liquid chromatography as previously described (Shi et al., 2022).

Statistical analysis

All physiological data were checked for statistical significance using ANOVA and presented as the mean ± standard deviation (SD) of 3 biological replicates. Duncan's multiple range test was applied to compare the means at the $P<0.05$ level in SPSS (version-22.0).

Results

Silicon alleviated Fe deficiency-induced growth inhibition

To elucidate the effect of Fe deficiency on tomato plants, the growth of tomato seedlings under Fe deficiency was assessed. As shown in Table 1 and Supplementary Figure 1, Fe deficiency repressed biomass and significantly changed different root features. The superoxide anion However, the application of Si alleviated the growth inhibition caused by Fe deficiency in tomato seedlings. For instance, LF significantly decreased shoot biomass by 56.25% compared with CK; however, LF+Si significantly increased shoot biomass by 69.64% compared with LF (Supplementary Figure 1). Moreover, Si application mitigated the reduction in root length and root surface area caused by Fe deficiency (Table 1). More precisely, LF significantly decreased root length by 54.65% compared with CK; however, LF+Si significantly increased root length by 36.80% compared with LF.

Differentially expressed gene analyses

Compared with the control, 1209 and 909 differentially expressed genes (DEGs) were found in the leaf and root, respectively, under Fe deficiency (Figure 1). Compared with Fe deficiency, 1835 and 1425 DEGs were found in the leaf and root when treated with Si (Figure 1).

KEGG pathway enrichment analysis showed that in leaves, glutathione metabolism was mainly related to Fe deficiency stress and Si application, followed by biosynthesis of amino acids and plant hormone signal transduction (Figures 2A, B). However, in roots, it is mostly correlated with flavonoid biosynthesis, followed by nitrogen metabolism, amino sugar and nucleotide sugar metabolism (Figures 2C, D). In the KEGG pathway, which was significantly enriched in the leaf, we focused on porphyrin and chlorophyll metabolism and photosynthesis-antenna proteins.

GO enrichment analysis showed that response to UV was most related to Fe deficiency and Si application in the leaf, followed by response to salicylic acid and protochlorophyllide reductase activity (Figures 3A, B). However, in roots, it is mostly correlated with L-leucine transaminase activity, followed by the anchored component of plasma membrane, plant−type cell wall organization or biogenesis (Figures 3C, D). In the GO functional enrichment analysis results, we focused on peroxidase activity, ion transport and ferric-chelate reductase activity.

Silicon improved photosynthesis under Fe deficiency

Photosynthetic pigments are one of the most important indicators of the photosynthetic capacity of plants and can be used together with photosynthetic parameters to reflect changes in photosynthetic efficiency and assimilation capacity. After

TABLE 1 Silicon improved different root features in tomato seedlings under Fe deficiency.

Treatments	Total root length (cm)	Total root surface area (cm^2)	Total root volume (cm^3)
CK	377.51 ± 30.85 b	44.15 ± 2.52 bc	1.03 ± 0.09 a
CK+Si	434.68 ± 22.93 a	69.46 ± 3.62 a	0.95 ± 0.03 a
LF	171.19 ± 0.45 d	39.56 ± 0.97 c	0.54 ± 0.01 c
LF+Si	234.18 ± 6.96 c	44.64 ± 3.36 b	0.73 ± 0.02 b

Control (CK): 100 µmol/L Fe+ 0 mmol/L Si, Control and Si application (CK+Si): 100 µmol/L Fe + 1.5 mmol/L Si, Fe deficiency treatment (LF): 1 µmol/L Fe + 0 mmol/L Si, and Fe deficiency and Si application (LF+Si): 1 µmol/L Fe + 1.5 mmol/L Si. Different letters in the same column indicate statistically significant differences (P<0.05).

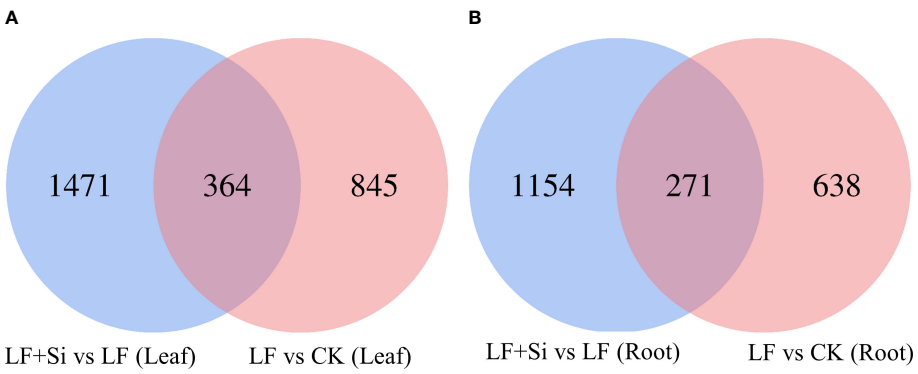

FIGURE 1
Venn diagram of differentially expressed genes in tomato seedlings as influenced by Fe deficiency and Si application. **(A)** The differentially expressed genes in leaves. **(B)** The differentially expressed genes in roots. Control (CK): 100 µmol/L Fe+ 0 mmol/L Si, Fe deficiency treatment (LF): 1 µmol/L Fe + 0 mmol/L Si, and Fe deficiency and Si application (LF+Si): 1 µmol/L Fe + 1.5 mmol/L Si.

enrichment analysis of differentially expressed gene KEGG, DEGs in porphyrin and chlorophyll metabolism and photosynthesis-antenna protein pathways were selected to make heat maps (Figure 4A). We found that the Si application under Fe deficiency mainly upregulated *SEND33*, LOC101263789, LOCLOC101260894, and LOC101266472. *SEND33* encodes Solanum lycopersicum ferredoxin-I, which is also the nuclear gene for chloroplast products. As shown in Figure 4, chlorophyll contents were significantly reduced under Fe deficiency. However, the application of Si increased chlorophyll contents under Fe

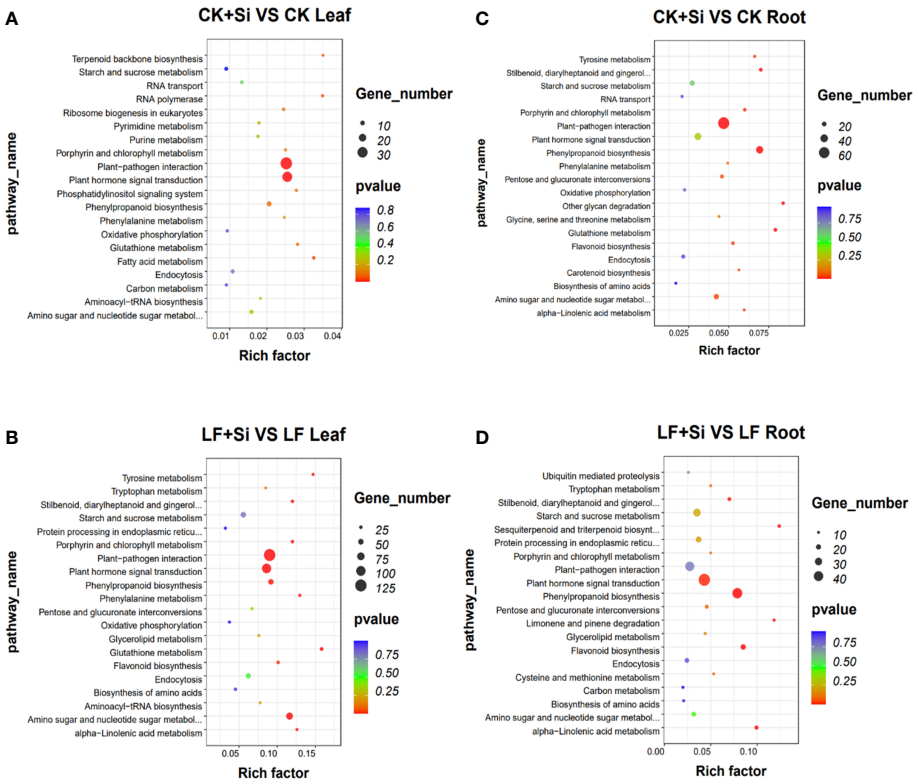

FIGURE 2
The KEGG enrichment analysis of differentially expressed genes. **(A, B)** The KEGG enrichment analysis in leaves. **(C, D)** The KEGG enrichment analysis in roots.

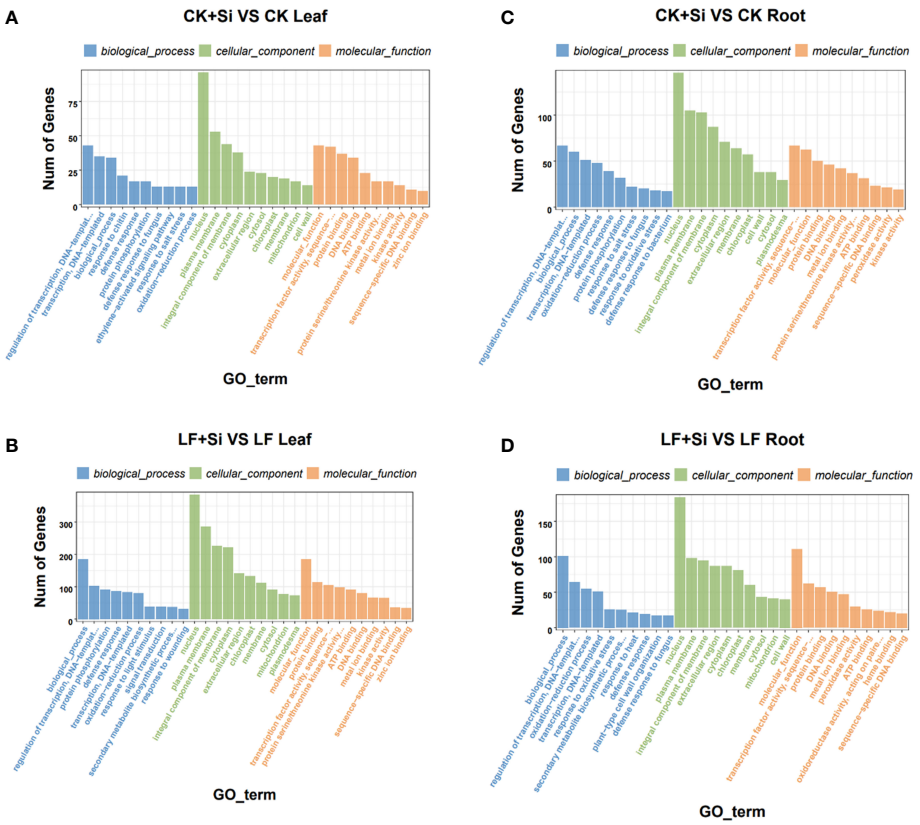

FIGURE 3
The GO enrichment analysis of differentially expressed genes. **(A, B)** The GO enrichment analysis in leaves. **(C, D)** The GO enrichment analysis in roots.

deficiency. LF significantly decreased chlorophyll contents by 65.99% compared with CK; however, LF+Si significantly increased chlorophyll contents by 35.82% compared with LF. As shown in Figures 4B, Fe deficiency reduced Pn, Fv/Fm and ETR. However, the application of Si increased Pn, Fv/Fm and ETR under Fe deficiency (Figures 4C, D, E,. For instance, LF significantly decreased net photosynthetic rate by 57.91% compared with CK; however, LF+Si significantly increased net photosynthetic rate by 70.06% compared with LF. Moreover, the values of ΦPSII, qP and NPQ decreased significantly under Fe deficiency, but the addition of Si increased ΦPSII and NPQ (Table S3). These results indicate that Fe deficiency reduced the photosynthetic capacity of tomato, while Si improved photosynthetic performance.

Silicon alleviated Fe deficiency-induced stress damage

Oxidative stress is intensified under Fe deficiency. Through GO functional gene annotation, we found that part of DEGs was enriched in the response to oxidative stress (GO:0006979), defense response (GO:0006952), peroxidase activity (GO:0004601) and peroxisome (GO:0005777) function (Figure 5A). Moreover, we found that Si application under Fe deficiency mainly upregulated *EREB* and *Eix1* in leaves (Figure 5A), and upregulated *TGAS118* in roots. *EREB* encodes Solanum lycopersicum ethylene responsive element binding protein. As shown in Figures 5C, D, Fe deficiency resulted in increased electrolyte permeability and MDA content in tomato seedlings. However, Si application reduced electrolyte permeability and MDA content. Compared with CK, MDA content in leaves and roots of LF increased 1.08 and 0.96 times, respectively. The MDA content of LF+Si significantly decreased by 26.44% and 45.14% compared with LF in leaves and roots, respectively. Likewise, compared with CK, H_2O_2 content in leaves and roots of LF increased by 42.37% and 69.18%, respectively. However, compared with LF, the H_2O_2 content in LF+Si significantly decreased by 11.97% and 31.11% in leaves and roots, respectively. The excessive accumulation of ROS disrupted the cellular enzymatic antioxidant defense system (Figures 5E, F). However, Si application alleviated the accumulation of ROS and MDA under Fe deficiency stress, by

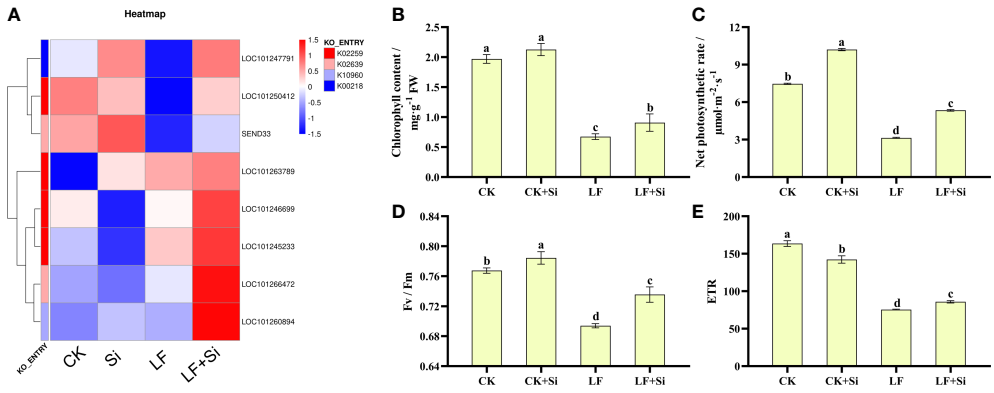

FIGURE 4
Response of photosynthetic capacity of tomato to silicon application under Fe deficiency. **(A)** Heat map of photosynthesis-related differentially expressed genes. **(B)** Total chlorophyll content. **(C)** Net photosynthetic rate. **(D)** Maximum photochemical efficiency of PS II (Fv/Fm). **(E)** Photosynthetic electron transport rate (ETR). Each data point represents the mean of three independent biological replicates (mean ± SD). Different letters above the bars indicate statistically significant differences ($P < 0.05$).

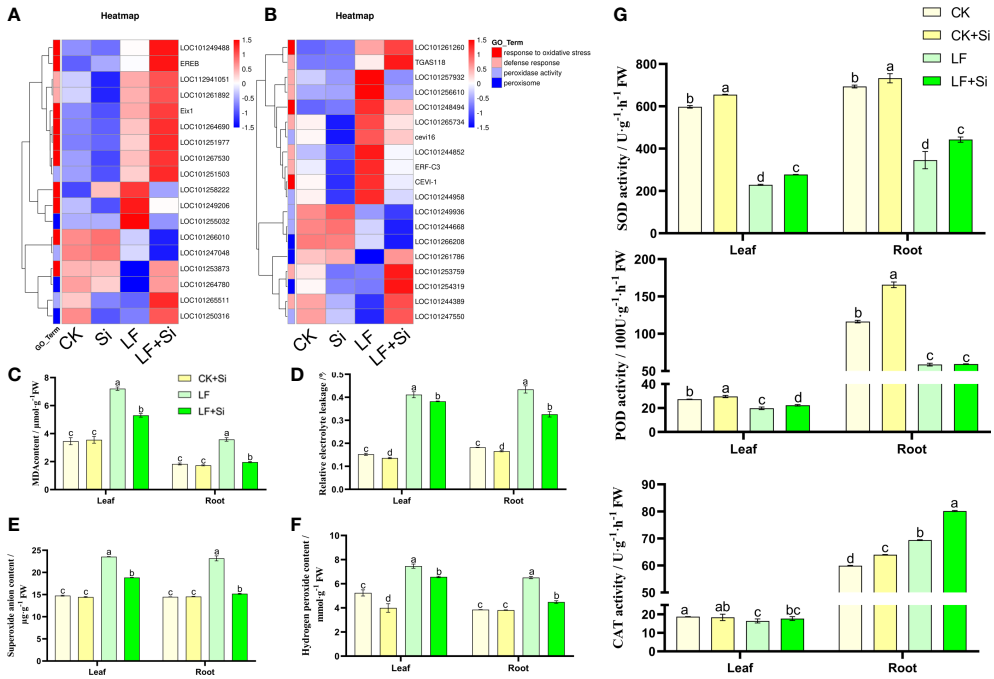

FIGURE 5
Effects of silicon application on antioxidant defense in tomato under Fe deficiency. **(A)** Heat map of antioxidant-related differentially expressed genes in the leaf. **(B)** Heat map of antioxidant-related differentially expressed genes in the root. **(C)** malondialhyde (MDA) content. **(D)** Relative electrolyte leakage. **(E)** Hydrogen peroxide content. **(F)** Superoxide anion content. **(G)** Antioxidant enzyme activity. Each data point represents the mean of three independent biological replicates (mean ± SD). Different letters above the bars indicate statistically significant differences ($P<0.05$).

enhancing the efficiency of the enzymatic antioxidant system such as the activity of SOD in leaves and roots (Figure 5).

Silicon enhanced organic acid metabolism under Fe deficiency

Organic acid metabolism is not only regarded as one of the necessary metabolic processes for plant growth, but also one of the intermediate links for plant iron absorption. Therefore, the content of organic acids in roots, an important organ for absorbing nutrients, was determined. By focusing on the Citrate cycle (ko00020), we found that differentially expressed genes are closely related to citric acid metabolism. We found that the Si application under Fe deficiency upregulated LOC101247353 and LOC101258079, and downregulated *ICDH1* (Figure 6). *ICDH1* encodes Solanum lycopersicum isocitrate dehydrogenase [NAD] regulatory subunit 1. As shown in Figure 6, the content of oxalic acid, malic acid, acetic acid and citric acid contents in tomato roots increased under Fe deficiency. However, increased application of Si further increased the organic acid content (Figure 6). Compared with CK, malic acid, acetic acid and citric acid contents of LF increased by 105.21%, 145.54% and 38.39%, respectively. Interestingly, compared with LF, the malic acid, acetic acid and citric acid contents of LF+Si significantly increased by 53.34%, 166.75% and 150.88%, respectively.

Silicon enhanced sugar metabolism under Fe deficiency

To further investigate the effects of nutrient metabolism under Fe deficiency, we measured the relevant indicators of sucrose metabolism in tomato leaves. By focusing on Starch and sucrose metabolism (ko00500), we found that Si application under Fe deficiency upregulated *ctu1* and *SlArf/Xyl1*, downregulated LOC101257526 and LOC101260501 (Figure 7). *ctu1* encodes solanum lycopersicum glutation-S-transferase. As shown in Figure 7, the sucrose content of the leaves showed an increase at 5 and 10 d and a decrease at 15 d under Fe deficiency. LF significantly decreased sucrose content by 35.29% compared with CK at 15 d. However, LF+Si significantly increased sucrose content by 27.00% compared with LF at 15 d (Figure 7). Subsequently, the activities of key enzymes for synthesis and conversion in sucrose metabolism were measured. As shown in Figures 7C, D, SS and SPS activities followed the same trend as sucrose content, showing an increase at 5 and 10 d and a decrease at 15 d. NI activity decreased under low iron stress, increased in the Si addition, and increased progressively over time in all treatments (Figure 7). AI activity decreased progressively over time and, Si addition also reduced AI activity (Figure 7).

Silicon enhanced iron absorption capacity under Fe deficiency

The root system is main organ for absorbing iron. Through GO functional gene annotation, we found that part of DEGs was enriched in the cellular response to iron ion (GO:0071281), iron ion homeostasis (GO:0055072), and iron ion binding (GO:0005506) function that we were interested in (Figure 8A). Moreover, we found that Si application under Fe deficiency mainly upregulated *GLR2.2* in leaves, and upregulated LOC101268463 in roots. *GLR2.2* encodes solanum lycopersicum glutamate receptor 2.2. The reduction process involving Fe^{3+} reductase is the rate-limiting process by which plants acquire Fe from the soil and can reflect the rate of Fe uptake by plants. As shown in Figure 8, the Fe^{3+} reductase activity was increased by 79.93% under Fe deficiency

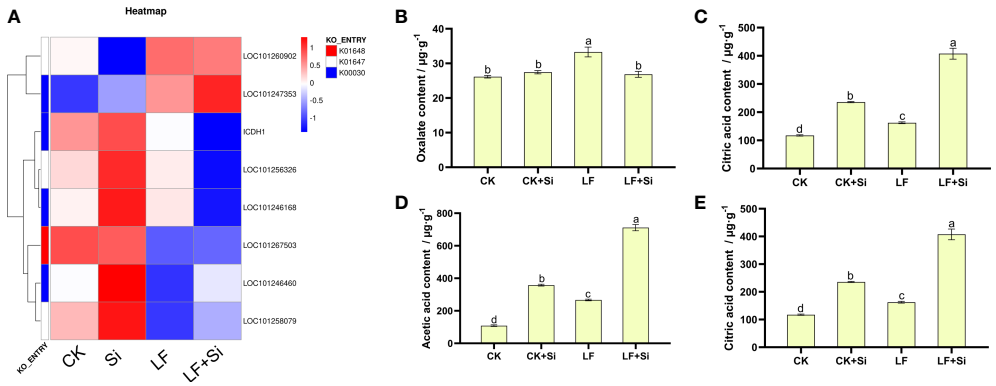

FIGURE 6
Effects of silicon application on organic acid metabolism in tomato roots under Fe deficiency. **(A)** Heat map of related differentially expressed genes. **(B)** Oxalate content. **(C)** Malic acid content. **(D)** Acetic acid content. **(E)** Citric acid content. Each data point represents the mean of three independent biological replicates (mean ± SD). Different letters above the bars indicate statistically significant differences ($P<0.05$).

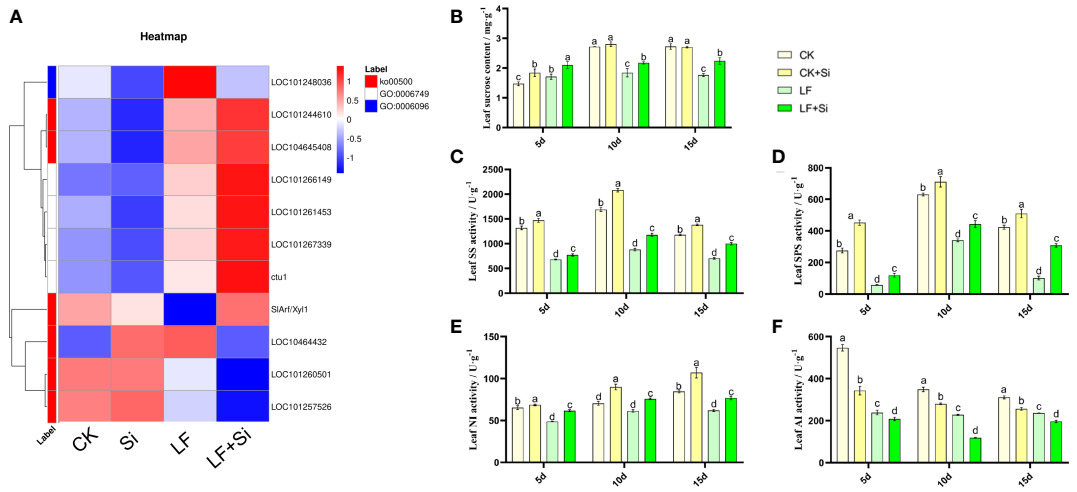

FIGURE 7
Response of sucrose metabolism of tomato leaves to silicon application under Fe deficiency. **(A)** Heat map of related differentially expressed genes. **(B)** Leaf sucrose content. **(C)** Leaf SS activity. **(D)** Leaf SPS activity. **(E)** Leaf NI activity. **(F)** Leaf AI activity. Each data point represents the mean of three independent biological replicates (mean ± SD). Different letters above the bars indicate statistically significant differences ($P<0.05$).

compared with CK, and Si application further enhanced root Fe^{3+} reductase activity. The accumulation of Fe in tomato plants changed under Fe deficiency. For instance, compared with CK, LF reduced the Fe content in leaves by 54.97%; however, LF+Si increased the Fe content in leaves by 31.86% compared with LF (Supplementary Figure 2). Moreover, we found that the application of Si under Fe deficiency significantly promoted the distribution of Fe to leaves and roots in tomato seedlings, suggesting a role for Si in modulating the transport of Fe from root and stem to leaf under Fe deficiency (Figure 8). Consistent with this, the transcript levels of iron transporters such as *FRD3, IRT2* and *FRO6* were significantly uprgulated by LF+Si compared with LF only treatment (Figure S3).

Taken together, we found that Si application under Fe deficiency affected the photosynthetic capacity, sucrose metabolism, antioxidant capacity, Fe absorption capacity and root growth of tomato (Figure 9). Fe deficiency firstly mediated a strong oxidative stress response in tomato, while Si application effectively maintained the stability of the metabolic environment by improving the activity of antioxidant enzymes to remove excess ROS. Si application significantly increased chlorophyll biosynthesis and brought more photosynthetic products, thus promoting the transformation of sugar metabolism in leaves. In roots, Si application increased the root surface area and maintained the dynamic balance of ROS, which together improved the Fe absorption capacity of tomato.

Discussion

Iron deficiency is a major handicap for crop production in many soils worldwide. In the current study, we provided physiological, biochemical and molecular evidence that Si supply could alleviate Fe deficiency and revealed critical mechanisms through which Si improved tolerance to Fe deficiency in tomato. Transcriptomic data combined with physiological analyses provide a novel characterization of the key traits and stress tolerance associated with the adaptation of tomato plants to Fe deficiency. Traits associated with changes in gene expression towards enhanced tolerance to Fe deficiency can be used to improve protected tomato cultivation.

Biomass usually directly reflects the difference in horticultural plant growth and response to the environment, and Fe deficiency significantly decreased plant biomass accumulation as reflected by the decline in the fresh weight of tomato seedlings as well as the changes in root morphology that directly affects the ability of roots to absorb and transport water and nutrients (Zhan et al., 2015). In order to adapt to the Fe deficiency, roots undergo two changes: one is to inhibit the growth of taproots to reduce the consumption of photosynthates; the other is to increase the number of lateral roots to enhance nutrient absorption capacity (Debona et al., 2017; Zhang et al., 2019b; Chao and Chao, 2022). Si application improved the tolerance of tomato to Fe deficiency by improving root architecture (Table 1). Si application promoted lateral root initiation, and such root architecture change was potentially beneficial to increase tomato root nutrient absorption area (Wang et al., 2013).

Photosynthesis is very sensitive to environmental stress, nonetheless, Si has been found to improve photosynthetic gas exchange in a variety of plants, including tomato, sorghum, pumpkin and tobacco (Haghighi and Pessarakli, 2013; Hajiboland and Cheraghvareh, 2014; Li et al., 2015; Siddiqui et al., 2015). The KEGG pathway analysis of differentially expressed genes in leaves revealed 8 DEGs in porphyrin and

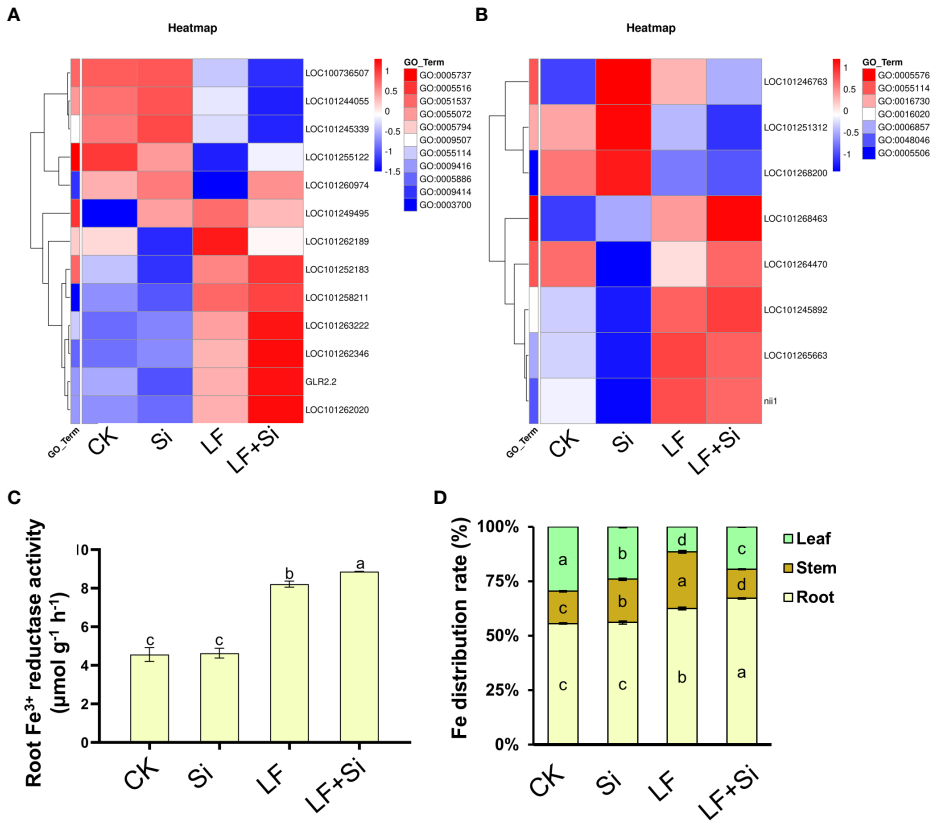

FIGURE 8
Effects of silicon application on absorption capacity of Fe under Fe deficiency in tomato. **(A)** Heat map of related leaf differentially expressed genes. **(B)** Heat map of related root differential genes. **(C)** Root Fe^{3+} reductase activity. **(D)** Fe distribution rate (%) in tomato plants. Each data point represents the mean of three independent biological replicates (mean ± SD). Different letters above the bars indicate statistically significant differences ($P<0.05$).

chlorophyll metabolism in LF+Si treatment compared to LF treatment in leaves (Figure 4). Notably, Si application protected the integrity of the chloroplast structure and also increased the chlorophyll content, leading to improved absorption and transfer of light energy (Zhu and Gong, 2013).

Transcriptome analysis showed that Si application under Fe deficiency increased the activity of Fe chelate reductase and the expression level of ferridoxin in tomato roots. Ferridoxin is a small molecule protein with an electron transport function, and its content can reflect the efficiency of electron transfer, thus affecting photosynthesis (Mazor et al., 2015). In addition, the formation of silicified cells due to Si application can increase the net photosynthetic rate of the plant (Liang et al., 2003). The high photosynthetic rate increases the accumulation of photosynthetic products of the plant and accelerates the process of carbon and nitrogen metabolism, thus increasing biomass accumulation (Noshi et al., 2016; Ahmad et al., 2021).

Chlorophyll fluorescence parameters are used to reflect the various reactive processes in plant photosynthesis under abiotic stress (Zai et al., 2012; Guo and Tan, 2015). Under Fe deficiency, the values of ΦPSII, ETR and qP decreased significantly, but increased after the addition of Si (Supplementary Table 3), indicating that the Si application effectively increased the development and activity of PSII reaction center, which was conducive to using more energy for PSII electron transfer and improving the efficiency of photosynthetic pigments in converting light energy into chemical energy. NPQ decreased under Fe deficiency and Si application increased NPQ, indicating that Fe deficiency damaged the photoprotective system, limiting the dissipation of excess light energy and increasing the risk of damage to the photosystem, while Si application effectively protected the photoprotective system and reduced the damage to the photosystem from the accumulation of excess light energy (Debona et al., 2017; Hussain et al., 2021).

The generation and clearance of ROS in plants are in a state of dynamic balance to maintain normal growth and metabolism (Mittler et al., 2022). Under Fe deficiency, ROS such as H_2O_2, and superoxide anion accumulate in large quantities, causing oxidative damage to proteins, nucleic acids and lipids and thus destroying the normal growth and metabolism of plants (Puyang et al., 2015;

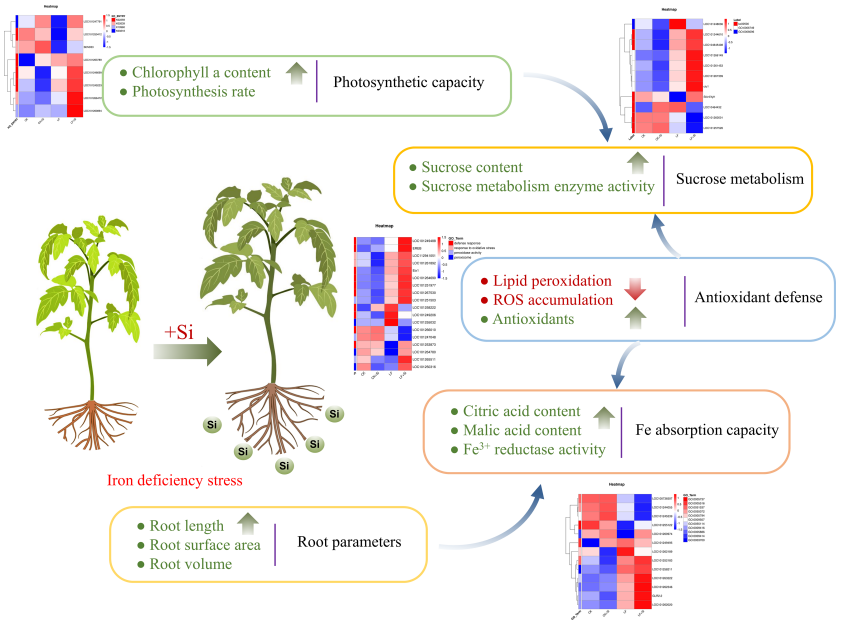

FIGURE 9
A working model of the effect of Si application on tomato under Fe deficiency.

Zhu et al., 2015). Plants deploy their antioxidant defense by increasing the activity of antioxidant enzymes such as SOD, POD and CAT and by accumulating antioxidant substances such as ascorbic acid and glutathione (Ahmad et al., 2019; Zhang et al., 2019a; Ahanger et al., 2020). Transcriptomic analysis showed that Si treatment significantly increased the expression peroxidase *cevi16* under Fe deficiency (Figure 5). Transcriptome data and physiological indicators suggest that Si alleviates the membrane lipid peroxidation induced by Fe deficiency by enhancing the activity of antioxidant enzymes in plants, reduces the accumulation of ROS in plants, and protects the integrity of cell membranes, thus improving the tolerance of plants to Fe deficiency (Zhu et al., 2015).

Transcriptome analysis showed that citrate synthase and malase genes were up-regulated in leaves under Fe deficiency, and the up-regulated genes mainly encoded citrate synthase and malase in roots under Fe deficiency combined with Si application (Figure 6). It is possible that Si promoted the secretion of organic acids and alleviated the Fe deficiency by up-regulating the expression of genes encoding enzymes related to organic acid synthesis. In dicotyledon plants, only divalent Fe can be transported, generally in the chelated form with citric acid or malic acid. Both malic acid and citric acid are involved in the chelation of Fe in the xylem. The Fe-citric acid complex is involved in long-distance Fe transport in plant xylem (Bityutskii et al., 2018). Pavlovic et al. (2013) found that the Si-mediated alleviatory effects on Fe deficiency included Fe activation and Fe absorption in root exoplasms (Pavlovic et al., 2013). The increase in Fe binding transport compounds (such as citric acid) is the main mechanism of Si-induced alleviation of Fe deficiency in cucumber plants (Bityutskii et al., 2014). Moreover, the accumulation of organic compounds associated with Fe absorption and transport in roots and exudation of root exudates largely increase Fe availability due to Fe^{3+} chelation and reduction (Martínez-Cuenca et al., 2013). Bityutskii et al. (2017) showed that the content of citric acid was very low under Fe deficiency at pH 4, indicating that organic acids did not respond to Fe deficiency under acidic conditions (Bityutskii et al., 2017). At pH 6, the concentrations of several organic acids, including citric acid, succinic acid, fumaric acid and gluconic acid increased under Fe deficiency (Bityutskii et al., 2017). Although citric acid is not necessarily accumulated in strawberry roots under Fe deficiency, it is released with root exudates (Valentinuzzi et al., 2015). Therefore, the increase in root organic acid content induced by Si application is important in promoting the long-distance transport of Fe (Bityutskii et al., 2017).

The metabolism of starch and sucrose is one of the important mechanisms of plant response to Fe deficiency. During Fe deficiency, the expression of genes related to glycolytic pathway was significantly up-regulated, and Fe deficiency significantly affected the sugar metabolism in Malus chinensis (Hu et al., 2018). In this study, GO functional enrichment analysis of up-regulated differentially expressed genes showed that Si application under Fe deficiency up-regulated the expression of genes related to starch and sucrose metabolism. The results showed that the synthesis, utilization and distribution of starch and sucrose in tomato leaves and roots were affected by Fe deficiency, and the

regulation of sugar metabolism was a way of tomato plant response to Fe deficiency. Under abiotic stress, a large amount of soluble sugar is accumulated, which further inhibits photosynthesis and slows down plant growth (Erban et al., 2015; Wei et al., 2015) and sucrose is decomposed into hexose for use by leaves to maintain the normal growth of plants (Hütsch et al., 2014). The results showed that in the early stage of Fe deficiency, sucrose accumulation increased in response to Fe deficiency, which could play a role in osmotic regulation. In order to further explore the mechanism of alterations in sucrose content, we further detected the activity of sucrose metabolism enzymes. The results showed that the decrease in sucrose content in leaves under Fe deficiency was due to the decrease in SS, SPS, NI and AI activities (Figure 7). However, with the increase of stress duration, the utilization rate of sugar in plant tissues decreased, which would change the source-sink relationship and lead to the failure of timely transportation of photosynthates, resulting in feedback inhibition (Luo et al., 2021).

The reduction of Fe^{3+} by Fe^{3+} reductase in roots of the Strategy I plant, is the rate-limiting step of Fe absorption (Connolly et al., 2003). The Strategy I plants increase root H^+-ATPase and root Fe^{3+} reductase activities under Fe deficiency, release a large amount of H^+, reduce the rhizosphere pH, and then promote the activation and absorption of Fe (Song et al., 2018). Our results showed that Si application under Fe deficiency promoted the expression of *IRT2* and *FRO6* in roots (Supplementary Figure S2) and increased the activity of Fe^{3+} reductase (Figure 8). Si application promoted Fe absorption and improved Fe transport efficiency from roots to leaves by Fe^{3+} reductase activity (Bityutskii et al., 2017). In addition, Si affects the gene expression in the synthesis of Fe transport-related compounds, resulting in an increased accumulation of organic acids and phenols, thus increasing the availability of Fe in roots (Carrasco-Gil et al., 2018).

Conclusions

In summary, Fe deficiency inhibits tomato plant growth by inducing oxidative stress, and inhibiting photosynthesis and glucose metabolism in tomato seedlings. Transcriptomics analysis coupled with biochemical assays indicated that Si modulated the response of plants to Fe deficiency by regulating antioxidant response, and the expression of related genes involved in carbohydrate metabolism. Moreover, Si application protected photosynthesis possibly by improving the antioxidant defense, and maintained Fe-related physiological metabolism by promoting Fe distribution in tomato leaves and roots under Fe deficiency. The study provides an important reference for the underlying mechanism of Si-induced tolerance to low Fe stress and the potential utilization of Si fertilizer to improve the growth traits of tomato plants under Fe deficiency.

Data availability statement

The data presented in the study are deposited in the NCBI repository (https://www.ncbi.nlm.nih.gov/bioproject/PRJNA902026), accession number: PRJNA902026.

Author contributions

YS: Conceptualization, Methodology, Formal analysis, Investigation, Writing—original draft. SG: Formal analysis, Investigation, Writing—original draft. XZ: Formal analysis, Investigation. MX: Methodology, Investigation. JX: Formal analysis, Investigation. GX: Funding acquisition, Project administration. YZ: Conceptualization, Supervision, Resources, Writing—original draft, Project administration. GA: Conceptualization, Writing—review and editing, Project administration. All authors contributed to the article and approved the submitted version.

Funding

This work was supported by the Basic Research Program in Shanxi Province (202303021211263, 20210302123366), the Shanxi Province Key R&D Plan (201903D211011), the Graduate Student Education Innovation Project in Shanxi Province (2021Y324), and the Ministry of Science and Technology of the People's Republic of China (DL2022026004L).

Conflict of interest

The authors declare that the research was conducted in the absence of any commercial or financial relationships that could be construed as a potential conflict of interest.

Publisher's note

Supplementary material

The Supplementary Material for this article can be found online at: https://www.frontiersin.org/articles/10.3389/fpls.2022.1094451/full#supplementary-material

References

Ahammed, G. J., Wu, M., Wang, Y., Yan, Y., Mao, Q., Ren, J., et al. (2020). Melatonin alleviates iron stress by improving iron homeostasis, antioxidant defense and secondary metabolism in cucumber. *Sci. Hortic.* 265, 109205. doi: 10.1016/j.scienta.2020.109205

Ahammed, G. J., and Yang, Y. X. (2021). Mechanisms of silicon-induced fungal disease resistance in plants. *Plant Physiol. Bioch.* 165, 200–206. doi: 10.1016/j.plaphy.2021.05.031

Ahanger, M. A., Bhat, J. A., Siddiqui, M. H., Rinklebe, J., and Ahmad, P. (2020). Silicon and secondary metabolites integration in plants: A significant association in stress tolerance. *J. Exp. Bot.* 71 (21), 6758–6774. doi: 10.1093/jxb/eraa291

Ahmad, P., Ahanger, M. A., Alam, P., Alyemeni, M. N., Wijaya, L., Ali, S., et al. (2019). Silicon (Si) supplementation alleviates NaCl toxicity in mung bean [Vigna radiata (L.) wilczek] through the modifications of physio-biochemical attributes and key antioxidant enzymes. *J. Plant Growth Regul.* 38, 70–82. doi: 10.1007/s00344-018-9810-2

Ahmad, A., Khan, W. U., Ali Shah, A., Yasin, N. A., Naz, S., Ali, A., et al. (2021). Synergistic effects of nitric oxide and silicon on promoting plant growth, oxidative stress tolerance and reduction of arsenic uptake in brassica juncea. *Chemosphere* 262, 128384. doi: 10.1016/j.chemosphere.2020.128384

Ahmed, M., Asif, M., and Hassan, F. U. (2014). Augmenting drought tolerance in sorghum by silicon nutrition. *Acta Physiol. Plant.* 36 (2), 473–483. doi: 10.1002/etc.2697

Bakhat, H. F., Bibi, N., Zia, Z., Abbas, S., Hammad, H. M., Fahad, S., et al. (2018). Crop protection silicon mitigates biotic stresses in crop plants: A review. *Crop Prot.* 104, 21–34. doi: 10.1016/j.cropro.2017.10.008

Bityutskii, N., Pavlovic, J., Yakkonen, K., Maksimović, V., and Nikolic, M. (2014). Contrasting effect of silicon on iron, zinc and manganese status and accumulation of metal-mobilizing compounds in micronutrient-deficient cucumber. *Plant Physiol. Biochem.* 74, 205–211. doi: 10.1016/j.plaphy.2013.11.015

Bityutskii, N. P., Yakkonen, K. L., Petrova, A. I., Lukina, K. A., and Shavarda, A. L. (2018). Silicon ameliorates iron deficiency of cucumber in a pH-dependent manner. *J. Plant Physiol.* 231, 364–373. doi: 10.1016/j.jplph.2018.10.017

Bityutskii, N. P., Yakkonen, K. L., Petrova, A. I., and Shavarda, A. L. (2017). Interactions between aluminium, iron and silicon in cucumber sativus l. grown under acidic conditions. *J. Plant Physiol.* 218, 100–108. doi: 10.1016/j.jplph.2017.08.003

Carrasco-Gil, S., Rodríguez-Menéndez, S., Fernández, B., Pereiro, R., Vicenta, D., and Hernandez-Apaolaza, L. (2018). Silicon induced fe deficiency affects fe, Mn, Cu and zn distribution in rice (Oryza sativa l.) growth in calcareous conditions. *Plant Physiol. Biochem.* 125, 153–163. doi: 10.1016/j.plaphy.2018.01.033

Chao, Z.-F., and Chao, D.-Y. (2022). Similarities and differences in iron homeostasis strategies between graminaceous and nongraminaceous plants. *New Phytol.* 236, 1655–1660. doi: 10.1111/nph.18482

Connolly, E. L., Campbell, N. H., Grotz, N., Prichard, C. L., and Guerinot, M. L. (2003). Overexpression of the FRO2 ferric chelate reductase confers tolerance to growth on low iron and uncovers posttranscriptional control. *Plant Physiol.* 133 (3), 1102–1110. doi: 10.1104/pp.103.025122

Debona, D., Rodrigues, F. A., and Datnoff, L. E. (2017). Silicon's role in abiotic and biotic plant stresses. *Annu. Rev. Phytopathol.* 55, 85–107. doi: 10.1146/annurev-phyto-080516-035312

Erban, A., Zorb, C., Kopka, J., and Annika, J. (2015). Metabolic contribution to salt stress in two maize hybrids with contrasting resistance. *Plant Sci.: Int. J. Exp. Plant Biol* 233, 107–115. doi: 10.1016/j.plantsci.2015.01.006

Gou, T., Yang, L., Hu, W., Chen, X., Zhu, Y., Guo, J., et al. (2020). Silicon improves the growth of cucumber under excess nitrate stress by enhancing nitrogen assimilation and chlorophyll synthesis. *Plant Physiol. Biochem.* 152, 53–61. doi: 10.1016/j.plaphy.2020.04.031

Guo, Y., and Tan, J. (2015). Recent advances in the application of chlorophyll a fluorescence from photosystem II. *Photochem. Photobiol.* 91, 1–14. doi: 10.1111/php.12362

Haghighi, M., and Pessarakli, M. (2013). Influence of silicon and nano-silicon on salinity tolerance of cherry tomatoes (Solanum lycopersicum l.) at early growth stage. *Sci. Hortic.* 161, 111–117. doi: 10.1016/j.scienta.2013.06.034

Hajiboland, R., and Cheraghvareh, L. (2014). Influence of Si supplementation on growth and some physiological and biochemical parameters in salt-stressed tobacco (*Nicotiana rustica* l.) plants. *J. Sci. Islam. Repub. Iran.* 25, 205–217.

Heath, R. L., and Packer, L. (1968). Photoperoxidation in isolated chloroplasts. i. kinetics and stoichiometry of fatty acid peroxidation. *Arch. Biochem. Biophys.* 125 (1), 189–198. doi: 10.1016/0003-9861(68)90654-1

Hussain, S., Li, S. X., Mumtaz, M., Shafiq, I., Iqbal, N., Brestic, M., et al. (2021). Foliar application of silicon improves stem strength under low light stress by regulating lignin biosynthesis genes in soybean (Glycine max (L.) merr.). *J. Hazard. Mater.* 401, 11. doi: 10.1016/j.jhazmat.2020.123256

Hütsch, B., Jung, S., and Schubert, S. (2014). Comparison of salt and drought-stress effects on maize growth and yield formation with regard to acid invertase activity in the kernels. *J. Agron. Crop Sci.* 201 (5), 353–367. doi: 10.1111/jac.12111

Hu, Y., Zhu, Y. F., Guo, A. X., Jia, X. M., Li, C., Tong, Z., et al. (2018). Transcriptome analysis in malus halliana roots in response to iron deficiency reveals insight into sugar regulation. *Mol. Genet. Genomics* 293, 1–12. doi: 10.1007/s00438-018-1479-5

Khan, I., Awan, S. A., Rizwan, M., Ali, S., Hassan, M. J., Brestic, M., et al. (2021). Effects of silicon on heavy metal uptake at the soil-plant interphase: A review. *Ecotoxicol. Environ. Saf.* 222, 112510. doi: 10.1016/j.ecoenv.2021.112510

Khan, I., Awan, S. A., Rizwan, M., Brestic, M., and Xie, W. (2022). Silicon: an essential element for plant nutrition and phytohormones signaling mechanism under stressful conditions. *Plant Growth Regul.* doi: 10.1007/s10725-022-00872-3

Liang, Y., Chen, Q., Liu, Q., Zhang, W., and Ding, R. (2003). Exogenous silicon (Si) increases antioxidant enzyme activity and reduces lipid peroxidation in roots of salt-stressed barley (Hordeum vulgare l.). *J. Plant Physiol.* 160 (10), 1157–1164. doi: 10.1078/0176-1617-01065

Lichtenthaler, H. K., and Wellburn, A. R. (1983). Determinations of total carotenoids and chlorophylls a and b of leaf extracts in different solvents. *Analysis* 11 (5), 591–592. doi: 10.1042/bst0110591

Li, H., Zhu, Y., Hu, Y., Han, W., and Gong, H. (2015). Beneficial effects of silicon in alleviating salinity stress of tomato seedlings grown under sand culture. *Acta Physiol. Plant.* 37 (4), 1–9. doi: 10.1007/s11738-015-1818-7

Luo, A. R., Zhou, C. N., and Chen, J. L. (2021). The associated with carbon conversion rate and source-sink enzyme activity in tomato fruit subjected to water stress and potassium application. *Front. Plant Sci.* 12. doi: 10.3389/fpls.2021.681145

M'Sehli, W., Houmani, H., Donnini, S., Zocchi, G., Abdelly, C., and Gharsalli, M. (2014). Iron deficiency tolerance at leaf level in medicago ciliaris plants. *Am. J. Plant Sci.* 5 (16), 2541–2553. doi: 10.4236/ajps.2014.516268

Martínez-Cuenca, M. R., Iglesias, D. J., Talón, M., Abadía, J., López-Millán, A. F., Primo-Millo, E., et al. (2013). Metabolic responses to iron deficiency in roots of carrizo citrange [Citrus sinensis (L.) osbeck. x poncirus trifoliata (L.) raf]. *Tree Physiol.* 33 (3), 320–329. doi: 10.1093/treephys/tpt011

Mazor, Y., Borovikova, A., and Nelson, N. (2015). The structure of plant photosystem I super-complex at 2.8 angstrom resolution. *Elife* 4, 18. doi: 10.7554/eLife.07433

Mittler, R., Zandalinas, S. I., Fichman, Y., and Van Breusegem, F. (2022). Reactive oxygen species signalling in plant stress responses. *Nat. Rev. Mol. Cell Biol* 23, 663–679. doi: 10.1038/s41580-022-00499-2

Nikolic, D. B., Nesic, S., Bosnic, D., Kostic, L., Nikolic, M., and Samardzic, J. T. (2019). Silicon alleviates iron deficiency in barley by enhancing expression of strategy II genes and metal redistribution. *Front. Plant Sci.* 10. doi: 10.3389/fpls.2019.00416

Noshi, M., Hatanaka, R., Tanabe, N., Terai, Y., and Shigeoka, S. (2016). Redox regulation of ascorbate and glutathione by a chloroplastic dehydroascorbate reductase is required for high-light stress tolerance in arabidopsis. *J. Agric. Chem. Soc. Japan* 80 (5), 870–877. doi: 10.1080/09168451.2015.1135042

Pavlovic, J., Samardzic, J., Kostic, L., Laursen, K. H., Natic, M., Timotijevic, G., et al. (2016). Silicon enhances leaf remobilization of iron in cucumber under limited iron conditions. *Ann. Bot.* 118 (2), 271–280. doi: 10.1093/aob/mcw105

Pavlovic, J., Samardzic, J., Maksimović, V., Timotijevic, G., Stevic, N., Laursen, K. H., et al. (2013). Silicon alleviates iron deficiency in cucumber by promoting mobilization of iron in the root apoplast. *N. Phytol.* 198 (4), 1096–1107. doi: 10.1111/nph.12213

Peris-Felipo, F. J., Benavent-Gil, Y., and Hernandez-Apaolaza, L. (2020). Silicon beneficial effects on yield, fruit quality and shelf-life of strawberries grown in different culture substrates under different iron status. *Plant Physiol. Biochem.* 152, 23–31. doi: 10.1016/j.plaphy.2020.04.026

Puyang, X., An, M., Han, L., and Zhang, X. (2015). Protective effect of spermidine on salt stress induced oxidative damage in two Kentucky bluegrass (Poa pratensis l.) cultivars. *Ecotoxicol. Environ. Saf.* 117 (jul.), 96–106. doi: 10.1016/j.ecoenv.2015.03.023

Qu, F., Zhang, J., Ma, X., Wang, J., Gao, Z., and Hu, X. (2020). Effects of different n, p, K and Ca levels on tomato yield, quality and fertiliser use efficiency. *Plant. Soil Environ.* 66, 569–575. doi: 10.17221/498/2020-pse

Rastogi, A., Yadav, S., Hussain, S., Kataria, S., Hajihashemi, S., Kumari, P., et al. (2021). Does silicon really matter for the photosynthetic machinery in plants? *Plant Physiol. Biochem.* 169, 40–48. doi: 10.1016/j.plaphy.2021.11.004

Sheteiwy, M., Shen, H., Xu, J., Guan, Y., Song, W., and Hu, J. (2017). Seed polyamines metabolism induced by seed priming with spermidine and 5-aminolevulinic acid for chilling tolerance improvement in rice (Oryza sativa l.) seedlings. *Environ. Exp. Bot.* 137, 58–72. doi: 10.1016/j.envexpbot.2017.02.007

Shi, Y., Zhao, Y., Yao, Q., Liu, F., Li, X., Jin, X., et al. (2022). Comparative physiological and transcriptomic analyses reveal mechanisms of exogenous spermidine-induced tolerance to low-iron stress in solanum lycopersicum l. *Antioxidants* 11, 1260. doi: 10.3390/antiox11071260

Siddiqui, M. H., Al-Whaibi, M. H., Faisal, M., and Sahli, A. A. A. (2015). Nano-silicon dioxide mitigates the adverse effects of salt stress on cucurbita pepo l. *Environ. Toxicol. Chem.* 33 (11), 2429–2437. doi: 10.1002/etc.2697

Song, Y., Dong, Y., Tian, X., Wang, W., and Zhenli, H. (2018). Mechanisms of exogenous nitric oxide and 24-epibrassinolide alleviating chlorosis of peanut plants under iron deficiency. *Pedosphere* 28, 926–942. doi: 10.1016/S1002-0160(17)60446-6

Valentinuzzi, F., Pii, Y., Vigani, G., Lehmann, M., Cesco, S., and Mimmo, T. (2015). Phosphorus and iron deficiencies induce a metabolic reprogramming and affect the exudation traits of the woody plant fragaria×ananassa. *J. Exp. Bot.* 66 (20), 6483–6495. doi: 10.1093/jxb/erv364

Wang, H., Xiao, W. D., Niu, Y. F., Jin, C. W., Chai, R. S., Tang, C. X., et al. (2013). Nitric oxide enhances development of lateral roots in tomato (Solanum lycopersicum l.) under elevated carbon dioxide. *Planta* 237 (1), 137–144. doi: 10.1007/s00425-012-1763-2

Wei, W., Qing-Tian, L., Ya-Nan, C., Reiter, R. J., Xiao-Min, Y., Dan-Hua, Z., et al. (2015). Melatonin enhances plant growth and abiotic stress tolerance in soybean plants. *J. Exp. Bot.* 3), 695–707. doi: 10.1093/jxb/eru392

Willekens, H., Chamnongpol, S., Davey, M., Schraudner, M., Langebartels, C., Van Montagu, M., et al. (1997). Catalase is a sink for H2O2 and is indispensable for stress defence in C3 plants. *EMBO J.* 16 (16), 4806–4816. doi: 10.1093/emboj/16.16.4806

Zaid, A., Ahmad, B., Jaleel, H., Wani, S. H., and Hasanuzzaman, M. (2020). "A critical review on iron toxicity and tolerance in plants: Role of exogenous phytoprotectants," in *Plant micronutrients: Deficiency and toxicity management*. Eds. T. Aftab and K. R. Hakeem (Cham: Springer International Publishing), 83–99. doi: 10.1007/978-3-030-49856-6_4

Zaid, A., Gul, F., Ahanger, M. A., and Ahmad, P. (2018). "Silicon-mediated alleviation of stresses in plants," in *Plant metabolites and regulation under environmental stress* (London EC2Y 5AS, United Kingdom: Academic Press), 377–387. doi: 10.1016/b978-0-12-812689-9.00020-0

Zai, X. M., Zhu, S. N., Qin, P., Wang, X. Y., Che, L., and Luo, F. X. (2012). Effect of glomus mosseae on chlorophyll content, chlorophyll fluorescence parameters, and chloroplast ultrastructure of beach plum (Prunus maritima) under NaCl stress. *Photosynthetica* 50 (3), 323–328. doi: 10.1007/s11099-012-0035-5

Zhang, Y., Liang, Y., Zhao, X., Jin, X., and Ahammed, G. J. (2019a). Silicon compensates phosphorus deficit-induced growth inhibition by improving photosynthetic capacity, antioxidant potential, and nutrient homeostasis in tomato. *Agronomy* 9 (11), 733. doi: 10.3390/agronomy9110733

Zhang, Y., Shi, Y., Gong, H. J., Zhao, H. L., Huan-Li, L. I., Yan-Hong, H. U., et al. (2018). Beneficial effects of silicon on photosynthesis of tomato seedlings under water stress. *J. Integr. Agric* 17, 2151–2159. doi: 10.1016/S2095-3119(18)62038-6

Zhang, Y., Zhou, Y., Chen, S., Liu, J., Fan, K., Li, Z., et al. (2019b). Gibberellins play dual roles in response to phosphate starvation of tomato seedlings, negatively in shoots but positively in roots. *J. Plant Physiol.* 234-235, 145–153. doi: 10.1016/j.jplph.2019.02.007

Zhan, A., Schneider, H., and Lynch, J. P. (2015). Reduced lateral root branching density improves drought tolerance in maize. *Plant Physiol.* 168 (4), 1603–1615. doi: 10.1104/pp.15.00187

Zhu, Y., and Gong, H. (2013). Beneficial effects of silicon on salt and drought tolerance in plants. *Agron. Sustain. Dev.* 34 (2), 455–472. doi: 10.1007/s13593-013-0194-1

Zhu, Y. X., Xu, X. B., Hu, Y. H., Han, W. H., Yin, J. L., Li, H. L., et al. (2015). Silicon improves salt tolerance by increasing root water uptake in cucumis sativus l. *Plant Cell Rep.* 34 (9), 1629–1646. doi: 10.1007/s00299-015-1814-9

frontiers | Frontiers in Plant Science

TYPE Original Research
PUBLISHED 17 February 2023
DOI 10.3389/fpls.2023.1116769

OPEN ACCESS

EDITED BY
Shuvasish Choudhury,
Assam University, India

REVIEWED BY
Owais Ali Wani,
Sher-e-Kashmir University of Agricultural Sciences and Technology of Kashmir, India
Zahoor Ahmad,
University of Central Punjab, Pakistan

*CORRESPONDENCE
Mohammad Mukarram
mdmukarram007@gmail.com

SPECIALTY SECTION
This article was submitted to Plant Abiotic Stress, a section of the journal Frontiers in Plant Science

RECEIVED 05 December 2022
ACCEPTED 30 January 2023
PUBLISHED 17 February 2023

CITATION
Mukarram M, Khan MMA, Kurjak D, Lux A and Corpas FJ (2023) Silicon nanoparticles (SiNPs) restore photosynthesis and essential oil content by upgrading enzymatic antioxidant metabolism in lemongrass (*Cymbopogon flexuosus*) under salt stress.
Front. Plant Sci. 14:1116769.
doi: 10.3389/fpls.2023.1116769

Silicon nanoparticles (SiNPs) restore photosynthesis and essential oil content by upgrading enzymatic antioxidant metabolism in lemongrass (*Cymbopogon flexuosus*) under salt stress

Mohammad Mukarram [1,2*], M. Masroor A. Khan [1], Daniel Kurjak [3], Alexander Lux [4,5] and Francisco J. Corpas [6]

[1]Advance Plant Physiology Section, Department of Botany, Aligarh Muslim University, Aligarh, India, [2]Department of Phytology, Faculty of Forestry, Technical University in Zvolen, Zvolen, Slovakia, [3]Department of Integrated Forest and Landscape Protection, Faculty of Forestry, Technical University in Zvolen, Zvolen, Slovakia, [4]Department of Plant Physiology, Faculty of Natural Sciences, Comenius University in Bratislava, Ilkovicova 6, Bratislava, Slovakia, [5]Institute of Chemistry, Slovak Academy of Sciences, Bratislava, Slovakia, [6]Department of Stress, Development and Signaling in Plants, Antioxidant, Free Radical and Nitric Oxide in Biotechnology, Food and Agriculture Group, Estación Experimental del Zaidín, Consejo Superior de Investigaciones Científicas (CSIC), Granada, Spain

Lemongrass (*Cymbopogon flexuosus*) has great relevance considering the substantial commercial potential of its essential oil. Nevertheless, the increasing soil salinity poses an imminent threat to lemongrass cultivation given its moderate salt-sensitivity. For this, we used silicon nanoparticles (SiNPs) to stimulate salt tolerance in lemongrass considering SiNPs special relevance to stress settings. Five foliar sprays of SiNPs 150 mg L^{-1} were applied weekly to NaCl 160 and 240 mM-stressed plants. The data indicated that SiNPs minimised oxidative stress markers (lipid peroxidation, H_2O_2 content) while triggering a general activation of growth, photosynthetic performance, enzymatic antioxidant system including superoxide dismutase (SOD), catalase (CAT), and peroxidase (POD), and osmolyte proline (PRO). SiNPs amplified stomatal conductance and photosynthetic CO_2 assimilation rate by about 24% and 21% in NaCl 160 mM-stressed plants. Associated benefits contributed to pronounced plant phenotype over their stressed counterparts, as we found. Foliar SiNPs sprays assuaged plant height by 30% and 64%, dry weight by 31% and 59%, and leaf area by 31% and 50% under NaCl 160 and 240 mM concentrations, respectively. SiNPs relieved enzymatic antioxidants (SOD, CAT, POD) and osmolyte (PRO) in lemongrass plants stressed with NaCl 160 mM (9%, 11%, 9%, and 12%, respectively) and NaCl 240 mM (13%, 18%, 15%, and 23%, respectively). The same treatment supported the oil biosynthesis improving essential oil content by 22% and 44% during 160 and 240 mM salt stress, respectively. We found SiNPs can completely overcome NaCl 160 mM stress while significantly palliating NaCl 240 mM stress. Thus, we propose that SiNPs can

be a useful biotechnological tool to palliate salinity stress in lemongrass and related crops.

KEYWORDS

nanoparticles, antioxidants, oxidative stress, photosynthesis, reactive oxygen species, salinity, silica, medicinal plant

1 Introduction

Salt-induced damage to growth and productivity depends on the plant tolerance to salt which varies significantly among species, and since most plants are glycophytes, increasing salinity poses an imminent threat to global agriculture and food security (Munns and Tester, 2008; Butcher et al., 2016). Higher salt concentrations impede plant water uptake creating osmotic stress in a drought-like manner (Munns, 2002). The osmotic stress instigates ion excess and disrupts ion homeostasis staging ionic stress (Van Zelm et al., 2020). The physiological setbacks are further exacerbated by oxidative stress. At this point, the plant has the excessive presence of hydrogen peroxide (H_2O_2), superoxide anion ($O_2^{\cdot-}$), singlet oxygen ($^1O_2$), and hydrogen radical ($^{\bullet}OH$) in the chloroplast, mitochondria, peroxisomes, endoplasmic reticulum, vacuole, cytoplasm, and apoplast (Foyer, 2018; Corpas et al., 2020; Mittler et al., 2022). These oxidative species are collectively known as reactive oxygen species (ROS). ROS degenerate cellular integrity through oxidising lipid bilayer and destabilising the structure and function of the proteins, lipids, and nucleic acids (Miller et al., 2010; Hossain et al., 2017). Most of the cellular organelles comprise a set of specialised compounds capable of scavenging ROS. These compounds, antioxidants, lay the first line of defence against mounting oxidative stress. Therefore, a robust antioxidative system can be indispensable in determining plant stress tolerance (Foyer and Noctor, 2005; Foyer and Shigeoka, 2011; Hasanuzzaman et al., 2020). Further, several attempts to advance crop performance under salt stress manifest a strong correlation with the upregulated antioxidant system (Hernandez et al., 2000; Zhu et al., 2004; Ashraf, 2009; Houmani et al., 2016; Ashraf and Munns, 2022).

Agricultural intensifications to boost crop productivity coupled with climate change and poor agricultural practices such as the excessive use of traditional fertilisers have further worsened the soil biochemical texture and exaggerated the saline influence in the soil (Foucher et al., 2014; Kopittke et al., 2019; Eswar et al., 2021; Hopmans et al., 2021). Thus, recent interventions engage sustainable, non-toxic, economic, and environment-friendly alternatives for yield enhancement during optimal and stressful conditions (Lehmann, 2007; Dodd and Pérez-Alfocea, 2012; Machado and Serralheiro, 2017; Mukarram et al., 2022a). The use of silicon nanoparticles (SiNPs) is one such recent intervention. On many occasions, the growth-promoting potential of SiNPs during both optimal and stressful environments was reported (Tripathi et al., 2015; Nazaralian et al., 2017; Fatemi et al., 2021; González-Moscoso et al., 2022). SiNPs, smaller than bulk silicon, might be absorbed faster and provide a higher surface area to interact with plant signalling molecules (Mukarram et al., 2022b). It renders a better plant performance with SiNPs over bulk silicon during stress. SiNPs can be understood as 'sponges' that can chelate mineral nutrients and hold moisture for plant roots (Mukarram et al., 2022b). SiNPs can further induce secondary and lateral root growth which might also reinforce plant water and nutrient uptake (El-Dengawy et al., 2021). This enables SiNPs to have special relevance in salinity studies worldwide. Additionally, silica deposition in the apoplast may provide structural strength and better leaf posture for maximised photon flux (Tamai and Ma, 2008). This can improve canopy photosynthesis.

Another moiety of SiNPs action is its active participation in ROS and antioxidant metabolism during salt stress. Several studies suggest upregulated activities of superoxide dismutase (SOD), catalase (CAT), and peroxidase (POD) enzymes with SiNPs (Tripathi et al., 2015; Elsheery et al., 2020; Fatemi et al., 2020; El-Saadony et al., 2021; Mukarram et al., 2021a). This can correspond to silicon's potential to upregulate the expression level of several genes encoding these antioxidants (Khandekar and Leisner, 2011; Ma et al., 2016; Farouk et al., 2020; Lesharadevi et al., 2021). SiNPs can also have a significant role in osmotic adjustment by regulating the expression of genes connected to proline (PRO) biosynthesis. On many occasions, SiNPs appeased PRO content and supported total antioxidant capacity in salt-stressed plants (Abdel-Haliem et al., 2017; Kalteh et al., 2018; Larkunthod et al., 2022; Mahmoud et al., 2022). Thus, SiNPs-induced structural and physiological modifications, in concert, can ascribe to higher plant growth, development, and productivity under saline scenarios.

A significant part of agricultural land in India is affected by soil salinity curbing gross national crop productivity (Kumar and Sharma, 2020). While the salt implications were extensively studied in many leading crops of the nation, lemongrass received little attention even when India is one of the largest producers and exporters of lemongrass and its essential oil (Skaria et al., 2006). The primary incentive for lemongrass production is its immense commercial potential in the pharmaceutical, food packaging, and cosmetic industries (Haque et al., 2018). Lemongrass export in India has swollen by >1250% in the past two decades, and the future market could be expected to grow (Mukarram et al., 2021b). However, we recently found that lemongrass is moderately salt-sensitive and higher saline concentrations (>NaCl 80 mM) significantly reduce its essential oil productivity (Mukarram et al., 2022c). Therefore, corrective measures are required to shield the lemongrass oil market from growing salinity. In our previous study, SiNPs did not bring enormous defence elicitation in unstressed lemongrass (Mukarram et al., 2021a). However, considering the special relevance of SiNPs under stress, it would be interesting to quantify the responses of the ROS and antioxidative

system in salt-stressed (NaCl 160 and 240 mM) lemongrass. Thus, the working hypothesis for this study was that SiNPs cushion lemongrass against salt stress and furnish increased growth and yield (H1). Further, the cornerstone of this tolerance is SiNPs-upgraded ROS and antioxidative system that corresponds to cellular homeostasis in lemongrass during salt excess (H2).

2 Material and methods

2.1 Plant material and growth condition

Lemongrass (*Cymbopogon flexuosus* (Steud.) Wats) var. Nima developed by the Central Institute of Medicinal and Aromatic Plants, Lucknow, India, was used as plant material for this study. After surface sterilisation with 0.2% $HgCl_2$ for 5 min, slips were washed repetitively with deionised water. Plant slips were transferred to soil-filled earthen pots (25 × 25 cm) in a net house at the Department of Botany, Aligarh Muslim University (AMU), Aligarh (27°52' N, 78°51' E, and 187 m a.s.l.). The ranges for temperature (27–36 ± 4°C) and relative humidity ranges (68–74 ± 7%) were recorded for the experimental timeline. Soil samples were randomly collected from different pots for soil analyses at the Soil-Testing Laboratory, Indian Agricultural Research Institute, New Delhi. The soil texture was identified as sandy loam while other variables were as follows: pH (1:2): 7.6, E.C. (1:2): 0.52 m mhos cm^{-1}, available N, P and K: 94.8, 8.9, and 136.5 mg kg^{-1} of soil, respectively.

2.2 Salinity treatment

Lemongrass plants were maintained under two NaCl concentrations (160 and 240 mM). These concentrations were selected as per our earlier finding on the salt sensitivity of lemongrass plants (Mukarram et al., 2022c). Salt treatments began 21 days after transplantation. NaCl concentrations were supplied as 300 mL of 40 mM NaCl solutions every alternate day to attain the final concentration and to avoid osmotic shock. The control group was supplied only with 300 mL of double distilled water.

2.3 Acquisition, structural analysis, and application of silicon nanoparticles

SiNPs were obtained as fumed silica from Evonic Industries AG, Germany, in the form of Aerosil R812. The structural analysis of SiNPs was performed by scanning electron microscopy (JOEL, JSM-6510 LV, Japan) at the Ultra Sophisticated Instrumentation Facility, AMU, Aligarh. SiNPs R812 samples were mounted on the holder with carbon tape and gold was used as a coating material for the scanning. An accelerating current of 10 kilovolts was passed and SEM was set at 1,000× magnification with a spot size of 40 to reveal the nanoparticles structural characteristics. Photos were taken at 10 µm using a secondary electron imaging detector. SiNPs were dissolved using 30% ethyl alcohol and de-ionised water to make a concentration of 150 mg L^{-1}. In total, five foliar sprays of SiNPs (50 mL each) were applied every week, starting 5 days after the attainment of the final salt concentration for each group. The schedule in Figure 1 illustrates the experimental timeline and the protocol employed for NaCl and SiNPs treatments.

2.4 Determination of photosynthesis and gas-exchange modules

A saturation-pulse fluorometer PAM-2000 (Walz, Effeltrich, Germany) was used to evaluate chlorophyll fluorescence (Fv/Fm). The plants were dark-adapted for 30 minbefore measuring

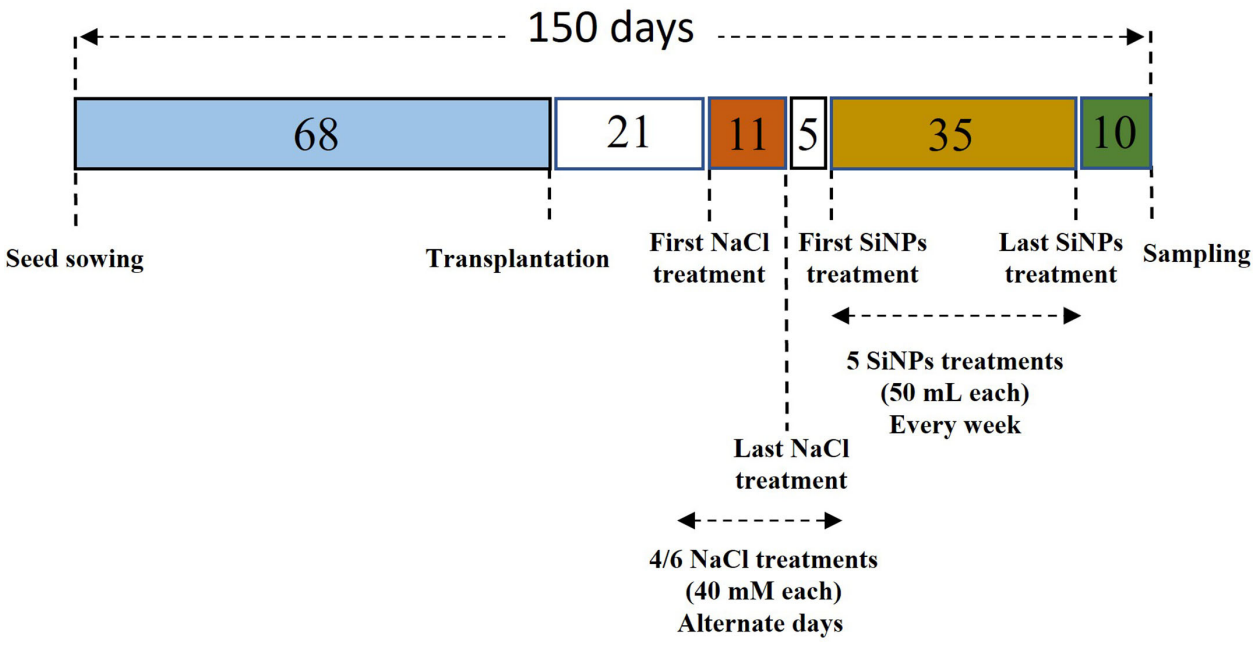

FIGURE 1
The experimental timeline of the significant events during the present study.

fluorescence. We recorded Fv/Fm during daytime in the upper surface of the first stretched-out leaf. Chlorophyll content was quantified in the intact expanded leaves of lemongrass through a Minolta chlorophyll meter (SPAD-502; Konica Minolta Sensing Inc. Japan).

Photosynthetic CO_2 assimilation rate (*A*), stomatal conductance (g_s), and transpiration rate (E) of the first fully expanded leaf of lemongrass were determined with an infra-red gas analyzer (LiCOR 6200, Portable Photosynthesis System, NA, USA). All the modules were determined on a leaf area of 6 cm^2 with air temperature, relative humidity, and atmospheric CO_2 concentration maintained at 25°C, 85%, and 400 ± 5 µmol mol^{-1}, respectively. All the measurements were made between 09:00 and 12:00 h at a photosynthetic photon flux density of 780–800 µmol m^{-2} s^{-1}.

2.5 H_2O2 content and lipid peroxidation assays

Hydrogen peroxide (H_2O_2) content was determined by a peroxidase-dependent assay adopting the method of Okuda et al. (1991). The reaction solution was prepared with crude extract (1 mL), 3- (dimethylamino) benzoic acid (12.5 mM, 0.4 mL), phosphate buffer (37.5 mM, pH 6.5), 3- methyl-2-benzothiazoline hydrazone (0.08 mL). Subsequently, peroxidase (0.02 mL, 0.25 unit) was added as a reaction initiator to the final volume of 1.5 mL at 25°C. The degree of light absorbance was observed for 3 min through a spectrophotometer adjusted at 590 nm.

The thiobarbituric acid reactive substances (TBARS) content was used to signify lipid peroxidation in lemongrass leaves as per Cakmak and Horst (1991). The TBARS concentration was captured as malondialdehyde (MDA) equivalents. For this, leaf tissue (0.5 g) was ground with trichloroacetic acid (0.1% (w/v), 5 ml) with subsequent centrifugation (12,000× g, 5 min). Tetrabutylammonium (0.5% (w/v), 4 mL) in trichloroacetic acid was added to the supernatant followed by incubation and centrifugation. The absorbance was noted at 532 nm and corrected for non-specific turbidity by subtracting the optical density at 600 nm.

2.6 Plant crude extracts

For the enzymatic assays, 0.5 g of fresh and mature lemongrass leaves were ground in liquid N_2 using a mortar and pestle. The resulting coarse powder was transferred to 5 ml (w/v) of chilled extraction medium containing potassium phosphate buffer (100 mM, pH 7.8), 1% (w/v) polyvinylpyrrolidone and 0.5% (v/v) Triton-X-100. Homogenates were centrifuged at 15,000× g for 5 min at 4°C. The supernatant acquired after centrifugation was used to determine enzymatic antioxidant activities (Kuo et al., 1982).

2.7 Enzymatic activity assays

The superoxide dismutase (SOD, E.C. 1.15.1.1) activity was assayed according to Beyer and Fridovich (1987). Riboflavin (1 mM), methionine (9.9 mM), nitrobluetetrazolium (55 mM), EDTA (2 mM), and Triton-X-100 (0.02%) were added to the 0.1 mL of freshly prepared enzyme extract and illuminated and maintained for one hour at 30°C. The reaction mixture was analysed by a spectrophotometer (Shimadzu UV-1700, Tokyo, Japan), and absorbance was recorded at 560 nm. One SOD unit is the amount of the enzyme needed for half inhibition of nitrobluetetrazolium reaction at the set wavelength.

The activity of the catalase (CAT, E.C. 1.11.1.6) was determined with the methods of Beers and Sizer (1952) with slight modification. In the 0.04 mL of the leaf extract, 2.6 mL of potassium phosphate buffer (50 mM with pH 7) was added. The solution was centrifuged afterwards at 12,500× g for 20 min at 4°C. The supernatant was removed and 0.4 mL of H_2O_2 (15 mM) was added as the reaction substrate. The enzyme activity was measured by determining the disappearance of H_2O_2 at 240 nm for 2 minutes with 5 seconds intervals.

The peroxidase (POD, EC 1.11.1.7) activity was estimated by pyrogallol oxidation according to Kumar and Khan (1982). The reaction mixture contained phosphate buffer (0.1 M, pH 6.8, 2 mL), pyrogallol (0.01 M, 1 mL), crude extract (0.5 mL), and H_2O_2 (0.005 M, 1 mL). After the incubation (5 min, 25°C), the reaction was stopped with H_2SO_4 (2.5 N, 1 mL). The purpurogallin formed by pyrogallol oxidation was measured at 420 nm against a reagent blank.

For geraniol dehydrogenase (GeDH, EC 1.1.1.183) activity, the fresh young leaves (0.5 g) were homogenised into Tricine-NaOH (50 mM, pH 7.5), β-mercaptoethanol (2.5 mM), thiourea (5 mM), phenylmethylsulfonylfluoride (1 mM), and glycerol (15% v/v) in the presence of polyvinylpolypyrrolidone (Polyclar AT) and amberlite XAD-4 as described in the earlier study (Sangwan et al., 1993). Enzyme activity was calculated by determining geraniol-dependent-$NADP^+$ reduction and recording absorbance increment at 340 nm.

2.8 Proline (PRO) content

The proline was detected in lemongrass leaves according to Bates et al. (1973). The absorbance of the toluene-aspired layer was noted at 520 nm by a spectrophotometer (Shimadzu UV-1700, Tokyo, Japan).

2.9 Estimation of growth modules

Growth parameters were evaluated in terms of plant height, dry weight, and leaf area. The lemongrass plants were left to dry for 24 h at 80°C in a hot-air oven to acquire dry weights measurement. Further, the leaf area was determined by following the procedure of Pandey and Singh (2011).

2.10 Extraction of lemongrass essential oil

The lemongrass essential oil was acquired by the hydro-distillation method (Guenther, 1972).

2.11 Statistical analyses

The experiment was set up in a simple randomised design. At least five independent biological replicas were used for each treatment and evaluation of various parameters. The normal distribution of the data was first tested for each treatment by the Shapiro–Wilk test. The homogeneity of variance among treatments was tested with Bartlett's test. One-way analysis of variance (ANOVA) was used to test the SiNPs effect on lemongrass growth, development, and productivity under salinity stress. Duncan's mean range *post-hoc* test was used to determine the significance of differences among the treatments. All statistical analyses were conducted at the replicate level and $\alpha = 0.05$ in RStudio (RStudio PBC, Boston, MA, USA). Principal component analysis (PCA) was applied to measured parameters using FactoMineR and factoextra packages to explore the positioning of each treatment with the remaining treatment groups. Further, the relationship among studied parameters was drawn using the PerformanceAnalytics package and presented in the correlation matrix. Correlation analysis was used to analyse relationships among all parameters observed for control and treated plants.

3 Results

3.1 SiNPs characterisation

The average particle diameter of R812 was 7 nm with a specific surface area of 200 $m^2 g^{-1}$ (Figure 2). R812 is a hydrophobic derivative of Aerosil 300 which is composed of untreated fumed silica powder with a BET surface area of 300 $m^2 g^{-1}$. Aerosil 300 are reacted with hexamethyldisilazane to form methylated and hydrophobic R812 nanoparticles.

3.2 SiNPs appease salinity-induced growth constraints in lemongrass

The visible effect of salt stress comprised redundant growth, shorter plants, and fewer green leaves (Figure 3). The saline regime reduced plant height and dry weight under both concentrations (NaCl 160 & 240 mM) (Figures 4A, B). Leaf expansion faced a similar deleterious impact with the highest reduction in leaf area being at NaCl 240 mM (Figure 4C). Nonetheless, when salt-stressed plants were treated with SiNPs, they acquired improved growth. Under NaCl 160 mM treatments, SiNPs sprays improved plant height, dry weight, and leaf area each by about 30% while during NaCl 240 mM stress, it was 64%, 59%, and 50%, respectively. Although SiNPs could restore plant performance significantly under NaCl 240 mM, the complete salinity reversal was observed under NaCl 160 mM.

3.3 SiNPs upgrade photosynthesis and stomatal activity under salinity

Lemongrass plants grown under salt concentrations (160 & 240 mM) displayed minimised photosynthesis. However, the foliar sprays with SiNPs 150 mg L^{-1} improved photosynthetic traits under the physiological and saline domains. The experimental results suggest that the extreme salinity (NaCl 240 mM) minimised chlorophyll biosynthesis. However, SiNPs brought the highest salt amelioration in such plants with improved chlorophyll content (55%) and fluorescence (Fv/Fm) (16%) (Figures 5A, B).

Salinity also negatively influenced stomatal dynamics including *A*, g_s, and E. The maximum reduction in *A*, g_s, and E was observed with NaCl 240 mM followed by NaCl 160 mM. Foliar sprays of SiNPs on lemongrass plants growing under salt conditions improved stomatal opening, transpiration, and CO_2 assimilation. SiNPs treatment to 160 mM NaCl-stressed plants increased E by 16%, g_s by 31%, and *A* by 26% over SiNPs-untreated plants (Figure 6).

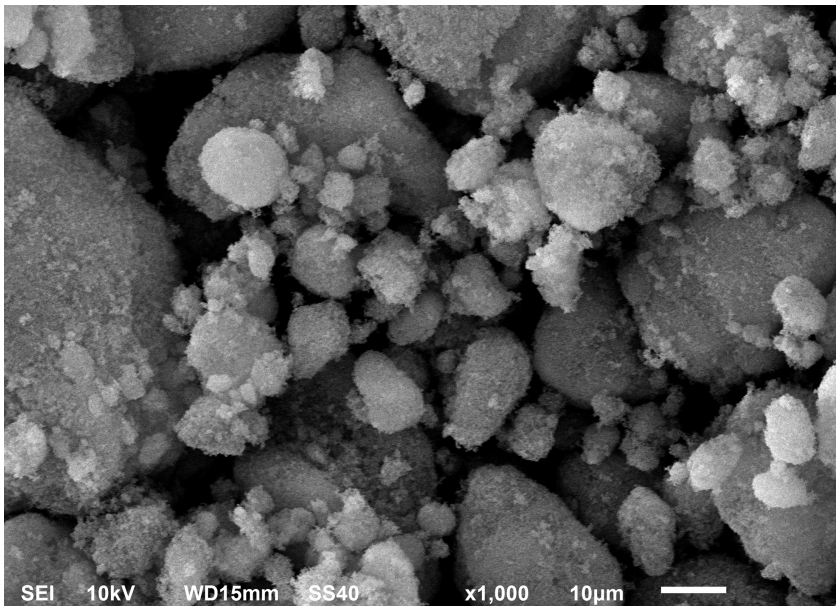

FIGURE 2
Scanning electron microscopy (SEM) representative picture of silicon nanoparticles (SiNPs) used in this study. The average size for R812 SiNPs was calculated as 7 nm with a specific surface area of 200 $m^2 g^{-1}$.

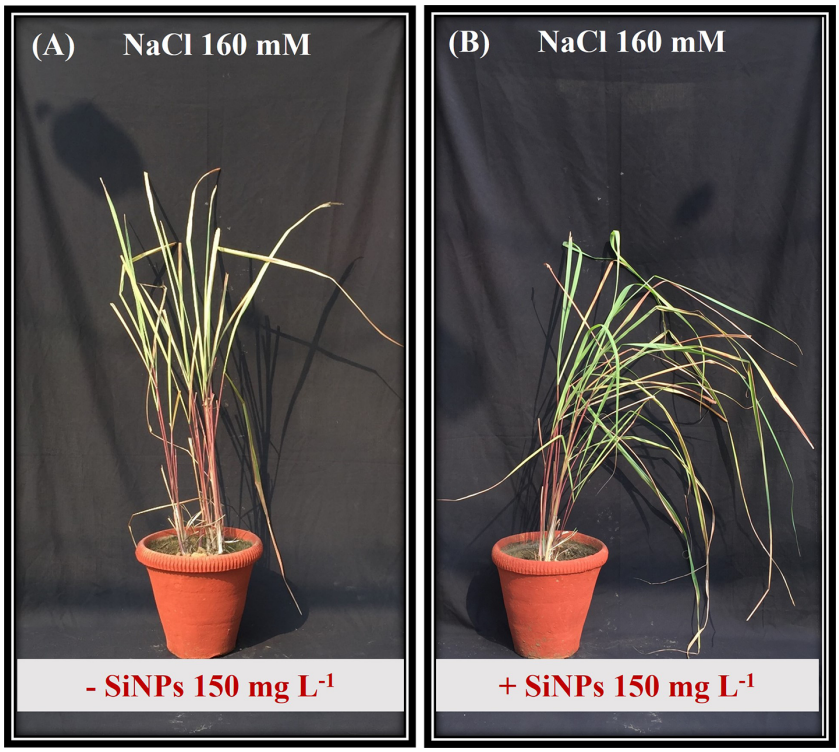

FIGURE 3
Phenotype of lemongrass plant under NaCl 160 mM salinity regime without **(A)** and with **(B)** SiNPs application (150 mg L^{-1}).

3.4 SiNPs bolster ROS metabolism for enhanced salt tolerance

The ROS metabolism was upregulated to combat rising oxidative stress in lemongrass caused by salinity. Both salt concentrations (160 and 240 mM) increased oxidative stress as depicted by enhanced H_2O_2 (28% and 37%) and TBARS (27% and 48%) contents over the control (Figures 7A, B). The lemongrass defence system was strengthened by overproduced antioxidative enzymes SOD, CAT, and POD and osmolyte PRO to minimise cellular damage. SiNPs supported antioxidant and osmolyte production in the absence of salinity which implies a positive SiNPs influence on redox homeostasis. The same SiNPs treatment (150 mg L^{-1}) appeased H_2O_2 contents by 19% and 14% and TBARS contents by 17% and 21% in 160 and 240 mM salt-stressed plants, respectively. Furthermore, SiNPs relieved SOD (9% and 13%), CAT (11% and 18%), and POD (9% and 15%) activities in 160 and 240 mM NaCl-treated plants to achieve a healthier cellular environment (Figures 7C–E). SiNPs also assuaged PRO intensification in 160 (12%) and 240 mM (23%) salt-stressed lemongrass plants suggesting a positive role in restricting salinity-induced osmotic stress (Figure 7F).

3.5 SiNPs appease lemongrass productivity during the saline regime

Salinity adversely affected lemongrass oil productivity and the enzyme responsible for its production. The maximised reduction in GeDH activity (48%) and essential oil content (50%) was noted with the NaCl 240 mg L^{-1}. Nevertheless, SiNPs 150 mg L^{-1} sprays brought significant ($\alpha = 0.05$) improvement in GeDH activity (43% and 76%) and essential oil content (27% and 78%) during both saline regimes (NaCl 160 and 240 mM) (Figure 8).

Principal component analysis (PCA) was done for all plant development and yield variables. We opted for only PC1 and PC2 since they covered about 93% explanation for the total variance during the scree plot analysis (Supplementary Figure 1). The scatter plot analysis demonstrated that each treatment group exhibited significantly different responses in lemongrass (Figure 9). Plants treated with SiNPs sprays held the highest explained variance with both PC1 and PC2. The same treatment also rendered maximum growth and productivity elicitations in the present study. Contrary to this, the variability of control plants and plants treated with 240 mM NaCl were least explained on PC2 and PC1, respectively. Moreover, all the studied modules exhibited significant interconnection during the PCA variable analysis (Figure 10). The variables were further colour-sorted based on their contribution to the principal component. The expected average contribution for each variable to PC1 and PC2 was 6.2% (Supplementary Figure 2). Higher values represent a more significant contribution of the variable to PC1 and PC2. The contribution of each variable to the PC1 can be found in Supplementary Figure 3. At the same time, variable contribution to the PC2 is depicted in Supplementary Figure 4. We also analysed how closely different parameters were related to each other among all treatments. Furthermore, a strong correlation was traced with the correlation matrix chart among all the studied variables (Figure 11).

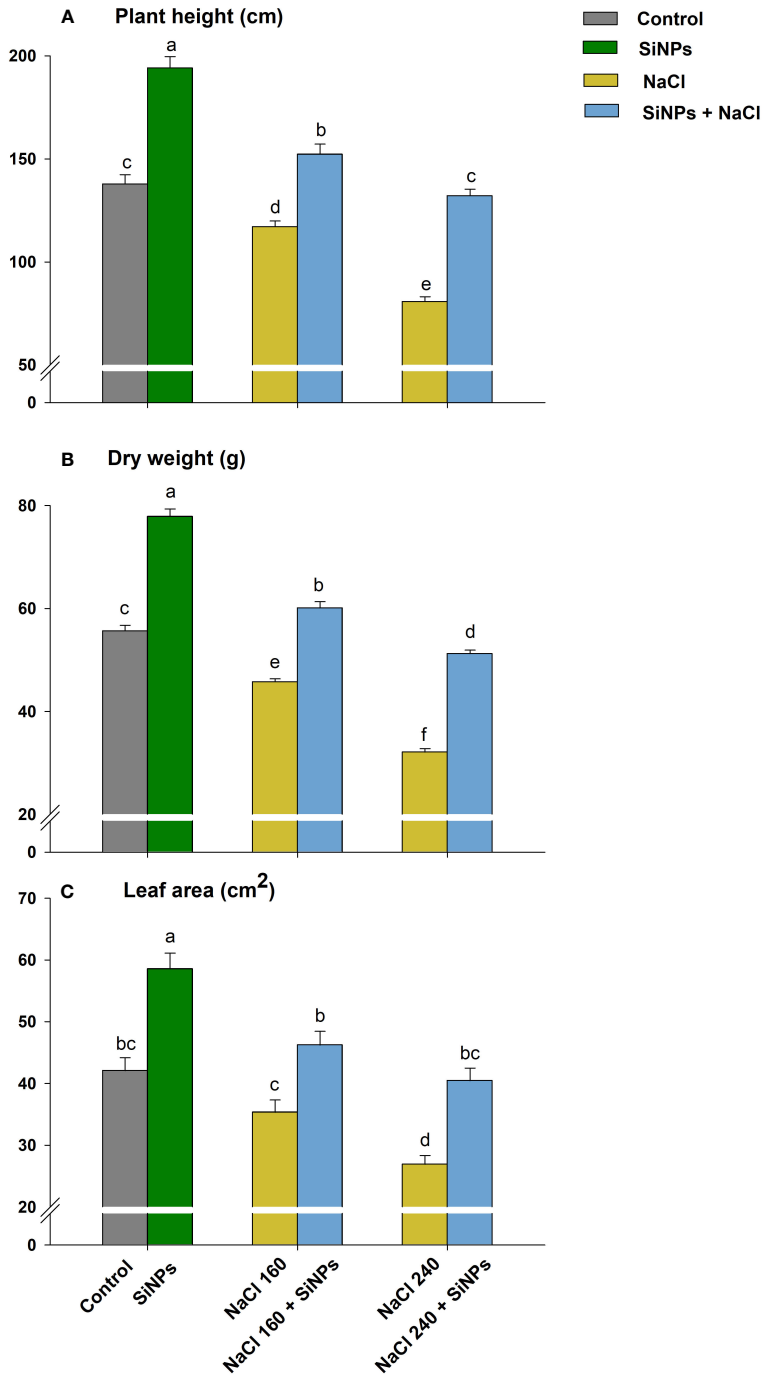

FIGURE 4
Effect of SiNPs on lemongrass plant height **(A)**, dry weight **(B)**, and leaf area **(C)** under salt stress. Replicate mean ± standard deviation is represented for each value. The difference between the mean values having the same letter(s) within a column is insignificant ($\alpha \leq 0.05$) according to Tukey's HSD test. The concentrations are expressed in mM (NaCl) and mg L^{-1} (SiNPs).

4 Discussion

4.1 SiNPs positively affect the lemongrass growth and development

Salt extremities (NaCl 160 and 240 mM) restricted plant growth and development in the lemongrass which could be accredited to its moderate salt sensitiveness (Mukarram et al., 2022c). Salinity initiates ionic and oxidative emergency in most plants and restricts the uptake of water and mineral nutrients (Munns, 1993; Hasegawa et al., 2000; Munns, 2002; Ahmad et al., 2022). This induces physiological drought and carbon starvation (Cheeseman, 1988; Kramer and Boyer, 1995; McDowell, 2011; Mukarram et al., 2021c). Nonetheless, SiNPs can act antagonistically to salinity and palliate salt-induced abnormal functionalities in morphological and biochemical modules (Zulfiqar and Ashraf, 2021). It can be ascribed to silicon's ability to hold various nutrients and water (Savant et al., 1996; Romero-Aranda et al., 2006; Sommer et al., 2006). Further, silicon might promote Na^+ flow out of the cell through

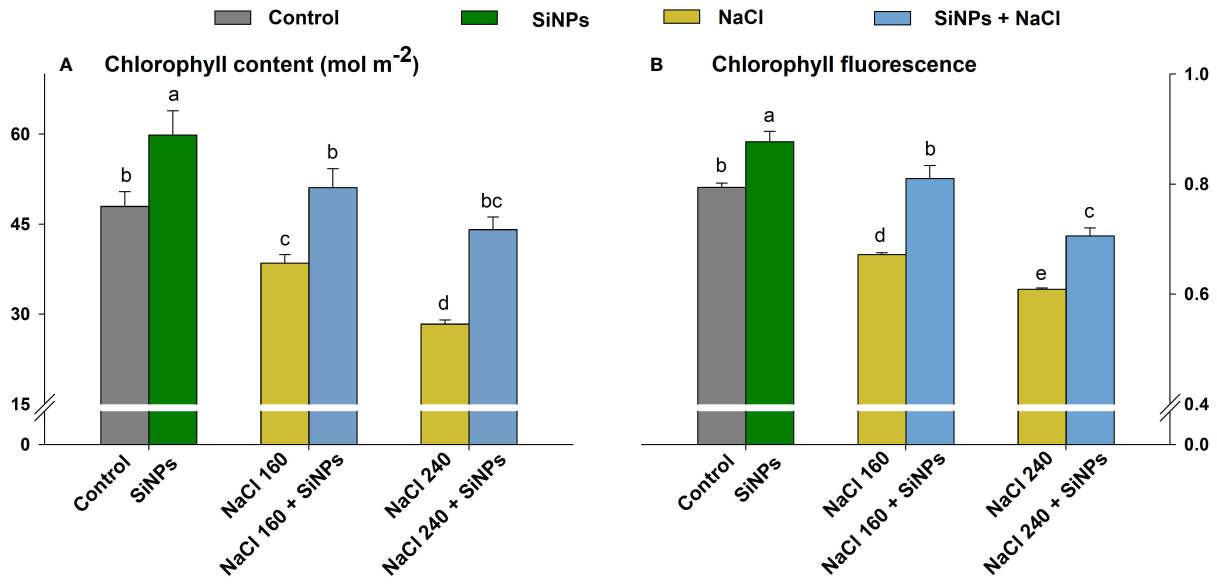

FIGURE 5
SiNPs effect on chlorophyll content **(A)** and chlorophyll fluorescence (Fv/Fm) **(B)** of lemongrass under salinity. Replicate mean ± standard deviation is represented for each value. The difference between the mean values having the same letter(s) within a column is insignificant ($\alpha \leq 0.05$) according to Tukey's HSD test. The concentrations are expressed in mM (NaCl) and mg L^{-1} (SiNPs).

improved H^+-ATPase activity aiding vacuolar accumulation of Na^+ and cell compartmentation to increase plant salt tolerance (Yamaguchi et al., 2013). The foliar sprays of 150 mg L^{-1} SiNPs improved plant height, dry weight, and leaf area in the present study as well during both salt regimes. Similar observations were made in *Phaseolus vulgaris* (Alsaeedi et al., 2017), *Ocimum basilicum* (Kalteh et al., 2018), and *Cucumis sativus* (Yassen et al., 2017) with SiNPs application, where it influenced plant metabolism and improved vegetative growth under salinity stress. SiNPs upgraded lemongrass physiology and biochemical status in our case as well. It could be realised by the fact that silicon can escalate the absorption and incarceration of mineral nutrients including nitrogen, phosphorous, potassium, calcium, magnesium, and silicon, and the content of free amino acids, total soluble carbohydrates, and proteins in various plant species (Li et al., 2012; Schaller et al., 2012; Brackhage et al., 2013; Reboredo et al., 2013; Xu et al., 2015; Neu et al., 2017; Xu et al., 2020; Karimian et al., 2021). Further, SiNPs can induce secondary and lateral root growth during salt severity which must have reinforced plant water and nutrient uptake in *Mangifera indica* (El-Dengawy et al., 2021). The positive influence of SiNPs is not limited to dicot plants and taproot systems. Silicon nanoforms seem to support the growth of lateral roots in gymnosperm *Larix olgensis* (Bao-Shan et al., 2004), and both primary and lateral roots in monocot *Brassica juncea* (Pandey et al., 2016), lateral roots in monocot *Musa acuminata* (El-Kady et al., 2017), and lateral root in the fibrous root system of more closely related member of grass family *Oryza sativa* (Isa et al., 2010). Thus, it seems feasible that SiNPs supported fibrous root growth and development in lemongrass plants, promoting water and mineral uptake during saline regimes. Additionally, the magnitude of SiNPs effects seems to vary depending on the application methods such as seed priming (Janmohammadi and Sabaghnia, 2015), root application (Attia and Elhawat, 2021), or foliar application (Mukarram et al., 2021a). Nonetheless, several studies, in concert, suggest SiNPs can enhance growth variables irrespective of applying methods under different environmental conditions in several crops including *Solanum tuberosum* (Mahmoud et al., 2019), *Hordeum vulgare* (Ghorbanpour et al., 2020), *Oryza sativa* (Banerjee et al., 2021), *Saccharum officinarum* (Elsheery et al., 2020), *Coriandrum sativum* (Fatemi et al., 2021), *Triticum aestivum* (Tripathi et al., 2017), and *Polianthes tuberosa* (Karimian et al., 2021).

4.2 SiNPs treatment palliate the negative impact of salinity on photosynthesis and stomatal behaviour

Foliar deposition of SiNPs and subsequent non-toxic lignification reduce wilting and retain leaves extended to acquire higher photosynthetic photon flux optimising photosynthesis (Mattson and Leatherwood, 2010; Asgari et al., 2018; Kah et al., 2018). In our case, this could have corresponded to improved chlorophyll fluorescence and net photosynthetic CO_2 assimilation rate in control and stressed plants with SiNPs application. Etienne et al. (2021) reported that silicon application in *Brassica napus* could regulate the expression level of 296 differentially expressed genes related to photosynthesis, antenna proteins, ribosomes, pentose phosphate pathway, amino acid biosynthesis, and plant hormone signal transduction pathway. This suggests that SiNPs functionality is much more genomic integrated and complex than mere structural support. Many studies indicate that SiNPs can induce several photosynthetic genes belonging to photosystems (*PsaA*, *PsbA*, *PsbW*, *PsbQ*, *PsbP*, and *Psb28*) and electron transport chain (*PetE* and *PetF*) and proteins (Q332S1, Q7F8E8, and P19312) to support photosystem assembly, light-harvesting complex, and thylakoid membrane (Zhang et al., 2018, 2019; Abdelaal et al., 2020; Lesharadevi et al., 2021). The higher chlorophyll content with SiNPs sprays in lemongrass plants suggests that SiNPs favoured the gene expressions of photosynthetic machinery and associated

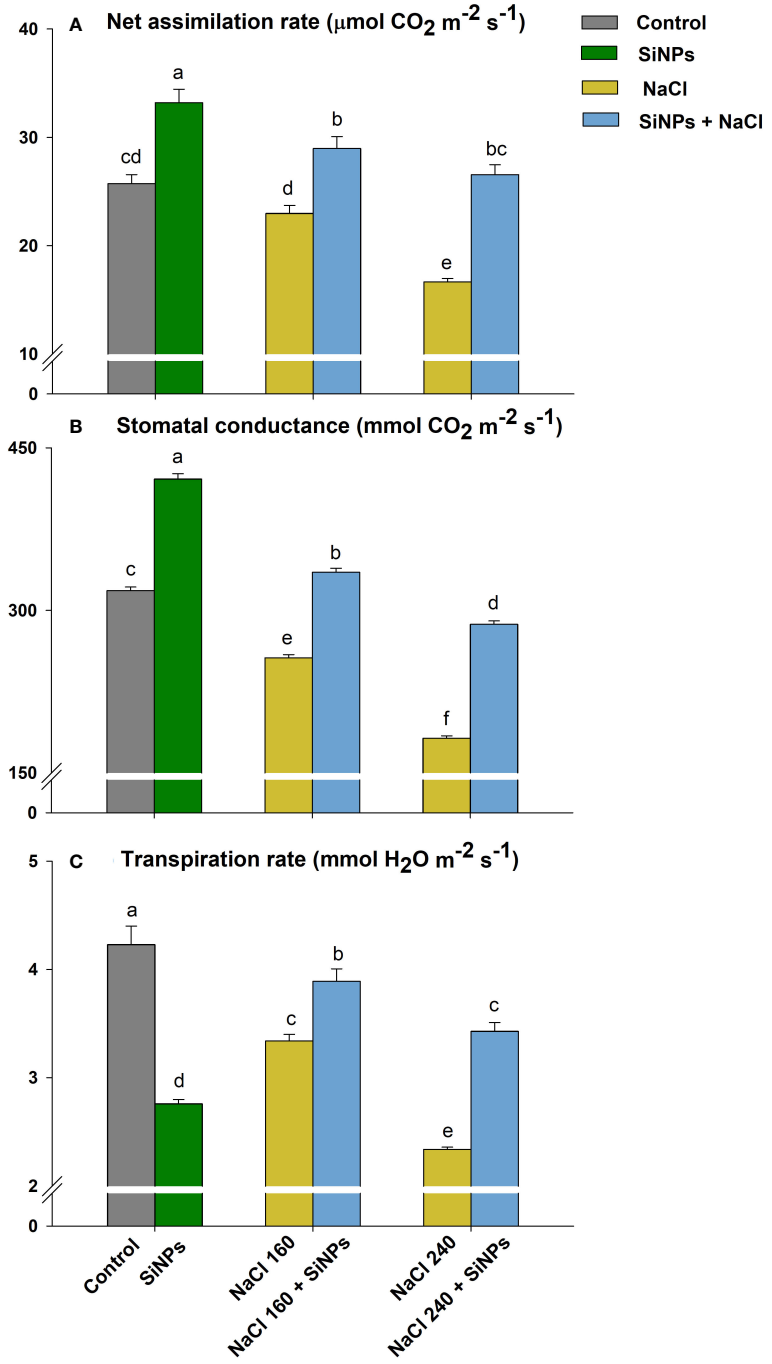

FIGURE 6
SiNPs effect on stomatal dynamics such as net CO_2 assimilation rate **(A)**, stomatal conductance **(B)**, and transpiration rate **(C)** of lemongrass under salinity. Replicate mean ± standard deviation is represented for each value. The difference between the mean values having the same letter(s) within a column is insignificant ($\alpha \leq 0.05$) according to Tukey's HSD test. The concentrations are expressed in mM (NaCl) and mg L^{-1} (SiNPs).

signalling pathways that supported chlorophyll biosynthesis in lemongrass. The higher chlorophyll content along with improved chlorophyll fluorescence could have further supported photosystem biochemistry and palliated salt-induced photosynthetic restrictions in the present study. Similar understandings were developed by Avestan et al. (2019) where SiNPs improved photosynthetic machinery in *Fragaria* × *anansa* plants during salt stress. Siddiqui et al. (2014) argued that SiNPs can reduce the salinity-induced toxic effects in *Cucurbita pepo* by enhancing *A*, g_s, E, and water use efficiency. SiNPs offered similar effects in our study where salt-stressed lemongrass plants exhibited better g_s and E over their non-SiNPs counterparts. Salinity negatively affects stomatal regulation, reducing CO_2 diffusion and carbohydrate assimilation (Singh and Sharma, 2018). Nonetheless, SiNPs might have intensified carbon accumulation and carboxylation efficiency in lemongrass plants by improving their stomatal activity as was reported in another C_4 perennial grass *Saccharum officinarum* with silicon (Frazão et al., 2020). We observed an improved photosynthetic assimilation rate with SiNPs in stressed

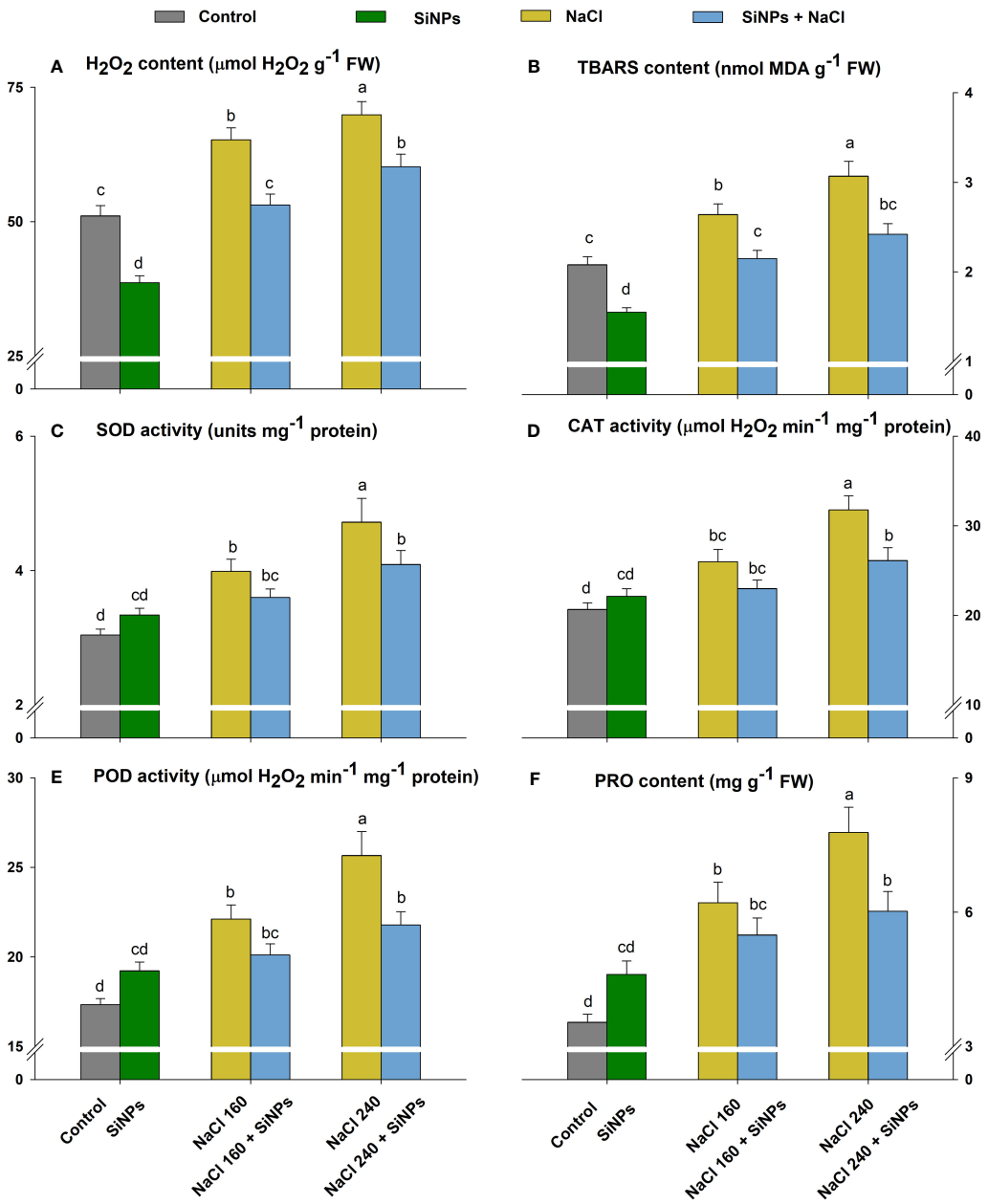

FIGURE 7
Lemongrass ROS metabolism under salinity as influenced by SiNPs. The antioxidant and ROS metabolism was represented in terms of hydrogen peroxide (H_2O_2) content **(A)**, thiobarbituric acid reactive substances (TBARS) content **(B)** , superoxide dismutase (SOD) activity **(C)**, catalase (CAT) activity **(D)**, peroxidase (POD) activity **(E)**, and proline (PRO) content **(F)**. Replicate mean ± standard deviation is represented for each value. The difference between the mean values having the same letter(s) within a column is insignificant ($a \leq 0.05$) according to Tukey's HSD test. The concentrations are expressed in mM (NaCl) and mg L^{-1} (SiNPs).

and non-stressed lemongrass plants that can further support this reasoning. Another understanding of silicon-induced stomatal activity comes from hydraulic conductance and aquaporins activity. Dhiman et al. (2021) suggested that silicon increases water uptake and the expression of plasma membrane intrinsic proteins and thus, aquaporins activity under salinity stress. This downplays the repression in root hydraulic conductance and supports stomatal conductivity and water retention during salt stress. SiNPs could perform similar actions in our study with *Cymbopogon flexuosus*. However, further analyses are needed for the elaborative understanding and evidence to support this narrative in lemongrass.

4.3 SiNPs stimulate antioxidant metabolism

Higher salt concentrations can disrupt redox homeostasis by overproducing reactive species that compromise the structure and functionality of several biomolecules (Miller et al., 2010; Hossain

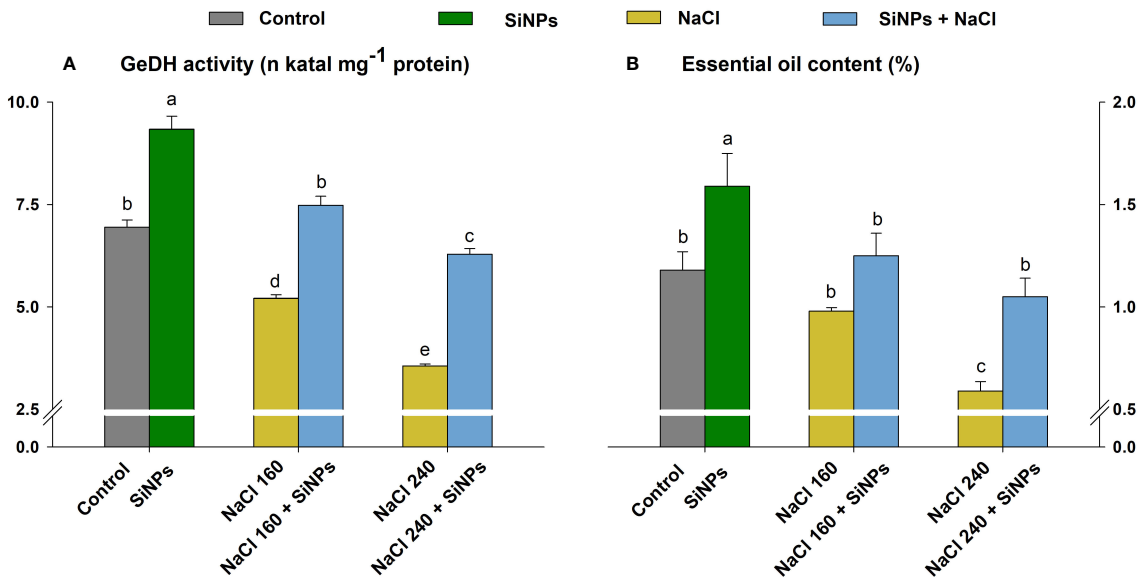

FIGURE 8
Effect of SiNPs sprays on geraniol dehydrogenase (GeDH) activity **(A)** and essential oil content as a percentage to plant dry weight **(B)** in lemongrass leaves during salinity stress. Replicate mean ± standard deviation is represented for each value. The difference between the mean values having the same letter(s) within a column is insignificant ($\alpha \leq 0.05$) according to Tukey's HSD test. The concentrations are expressed in mM (NaCl) and mg L^{-1} (SiNPs).

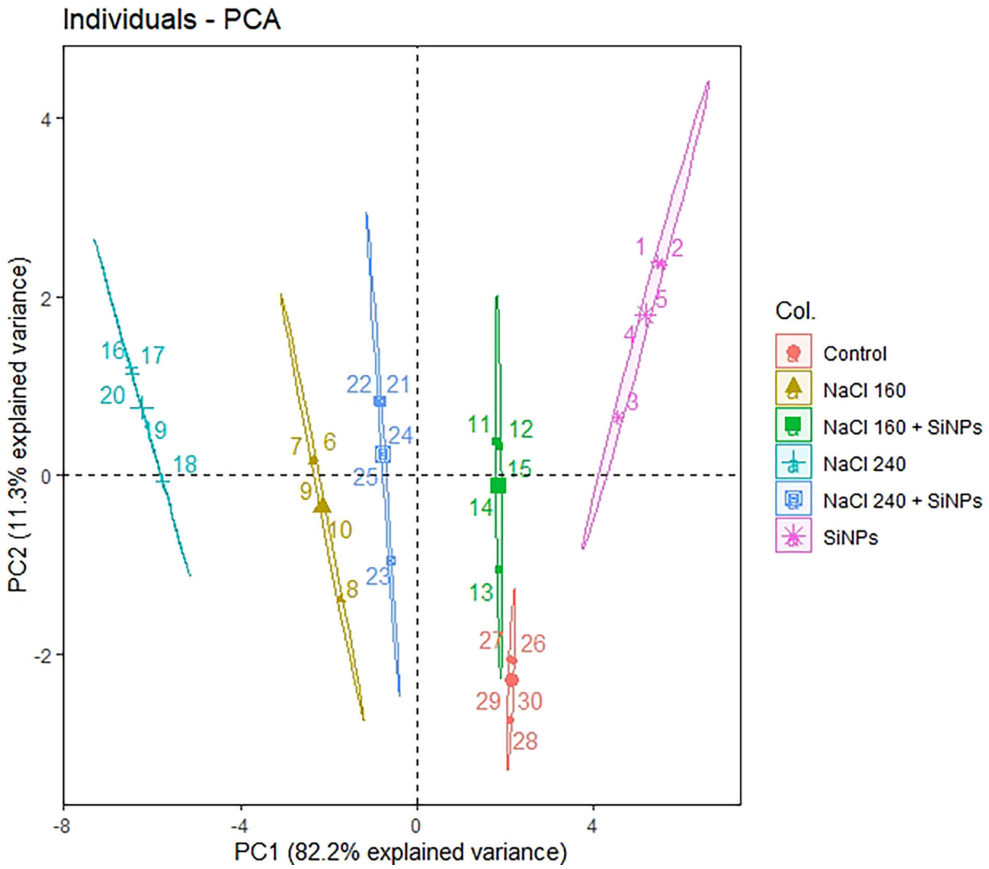

FIGURE 9
The interconnection among the treatment groups as drawn by PCA scatter plot. Non-overlapping groups are significantly different ($\alpha \leq 0.05$) where ellipses hold a 95% confidence level. SiNPs, silicon nanoparticles 150 mg L^{-1}; NaCl concentrations are represented in mM.

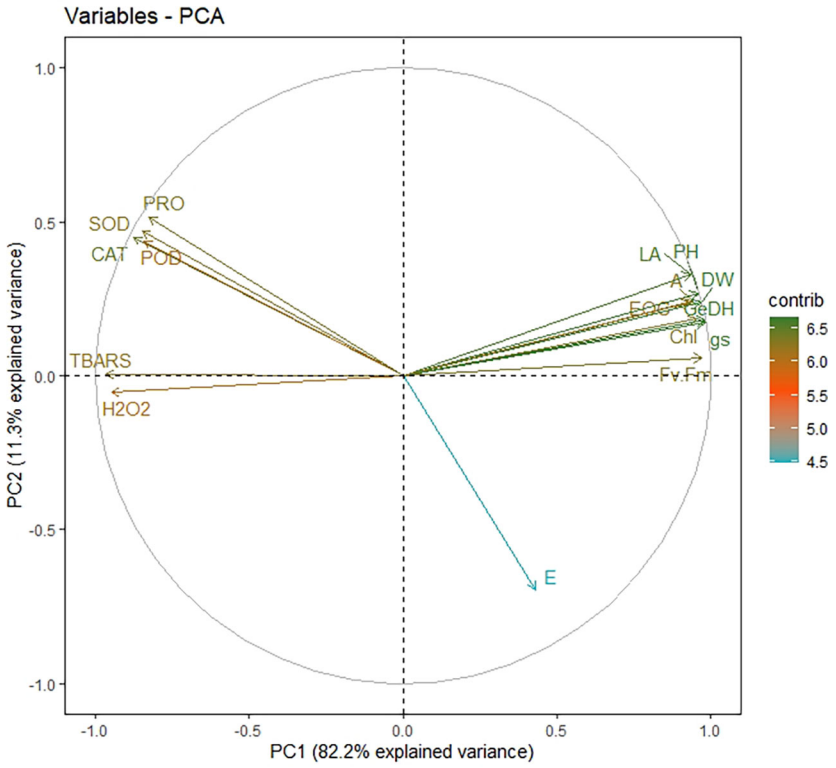

FIGURE 10
Variable correlation plot depicting the relationship among each variable from different treatment groups. The distance between any two parameters represents their relation intensity. The parameters in the same quadrant are positively related, while the ones from the opposite quadrant are negatively correlated. On the other hand, the distance between the variable and its origin point is directly proportional to the variables' quality on the factor map. Colour gradients signify each variable's contribution percentage (contrib) to the principal component. LA, leaf area; GeDH, geraniol dehydrogenase activity; gs, stomatal conductance; Fv/Fm, chlorophyll fluorescence; E, transpiration rate; H_2O_2, hydrogen peroxide content; TBARS, thiobarbituric acid reactive substances content; CAT, catalase activity; POD, peroxidase activity; SOD, superoxide dismutase activity; PRO, proline content (overlapped variables: dry weight, plant height, chlorophyll content, photosynthetic CO_2 assimilation rate, and essential oil content).

et al., 2017; Steinhorst and Kudla, 2019). The intricate cross-talk between oxidative species and antioxidants can minimise stress-inflicted damage, thus, perform a cardinal role in stress tolerance (Foyer, 2018; Considine and Foyer, 2021; Mittler et al., 2022). We observed upregulated H_2O_2 and TBARS contents during NaCl 160 and 240 mM treatments signifying salinity-induced oxidative bursts in lemongrass plants. This compromised overall plant growth, development, and productivity. Nevertheless, SiNPs were able to diminish both H_2O_2 and TBARS contents suggesting an antagonistic mechanism to salinity. It is argued that SiNPs upregulate antioxidant activities for ROS scavenging in stressed cells. Farhangi-Abriz and Torabian (2018); Naguib and Abdalla (2019), and Sharma et al. (2022) concluded that SiNPs can activate the antioxidant system enhancing SOD, CAT, and POD activities to restrict ROS accumulation and associated damage. Data from the present study also suggest a similar feedback mechanism in lemongrass. Several other studies follow this understanding where SiNPs upregulated antioxidative and osmotic defence systems and protected plants against stressful environments (Ashour, 2018; Elsheery et al., 2020; Ghorbanpour et al., 2020; El-Saadony et al., 2021; Alam et al., 2022; Alsamadany et al., 2022). It is suggested that Si-activated isozymes could induce the encoding genes of antioxidant activity under stress (Farouk et al., 2020). Furthermore, SiNPs seem to indulge in gene regulation for PRO biosynthesis thus, having significant osmotic importance during stressful conditions (Siddiqui et al., 2020). Silicon's interaction with PRO further strengthened the antioxidative system in *Phaseolus vulgaris* during stress (Rady et al., 2019). Mahmoud et al. (2022) reported that SiNPs boosted the PRO and antioxidant contents in *Citrus sinensis* under salt severity. Naguib and Abdalla (2019) primed seeds with SiNPs and observed reduced lipid peroxidation *in Zea mays*. Similarly, SiNPs supplementation brought physiological adjustments to *Cucumis sativus* and palliated salt severity (Yassen et al., 2017).

4.4 SiNPs trigger the biosynthesis of lemongrass essential oil

Essential oil productivity has a dual relationship with stressful environments. While milder stress induces essential oil content, severe stress conditions can cause a considerable reduction in overall oil yield (Mirzaei et al., 2020; Mukarram et al., 2022c). The plummet in LEO

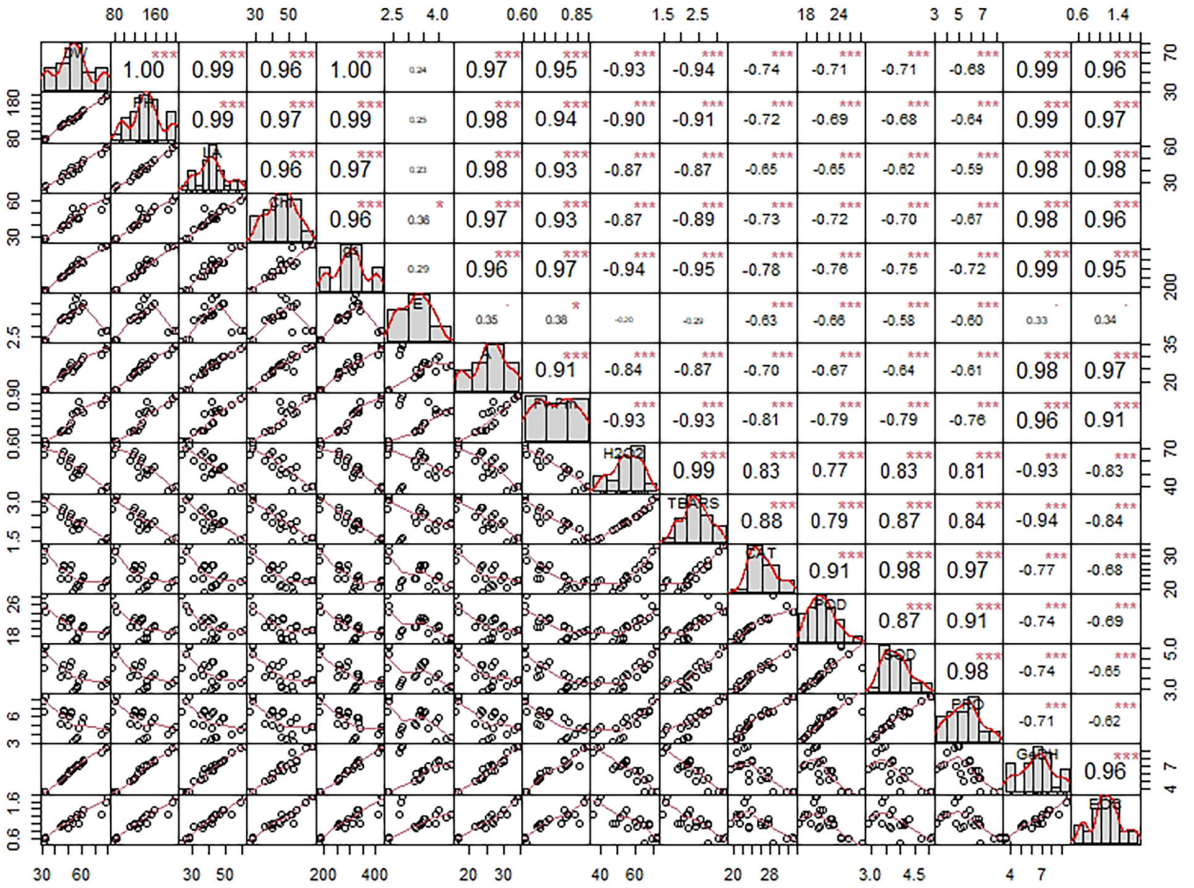

FIGURE 11
Chart of correlation matrix exploring the intricate relation among variables using Pearson's method. Each variable is distributed on the chart diagonal. The bottom of the diagonal corresponds to the bivariate scatter plot with a fitted line between any two variables. Further, each box in the diagonal top consists of the correlation values between any two variables and significance levels. Symbols denote significance levels following p-values: . (a = 0.01), * (a = 0.05), *** (a = 0.001). DW, dry weight; PH, plant height; LA, leaf area; CHL, chlorophyll content; gs, stomatal conductance; E, transpiration rate; A, photosynthetic carbon assimilation; Fv/Fm, chlorophyll fluorescence; H2O2, hydrogen peroxide content; TBARS, thiobarbituric acid reactive substances content; CAT, catalase activity; POD, peroxidase activity; SOD, superoxide dismutase activity; PRO, proline content; GeDH, geraniol dehydrogenase activity; EOC, essential oil content.

content under 160 and 240 mM NaCl could result from poor plant growth and development owing to ionic, osmotic, and oxidative imbalance and retarded plant-water relation, nutrient uptake, photosynthates production, and source-sink potential (Idrees et al., 2012; Dagar et al., 2013; Shahid et al., 2020). However, SiNPs sprays improved essential oil productivity in lemongrass plants during both salt intensities. This can be ascribed to silicon's positive effect on water and nutrient uptake and source-sink potential in grass and legume plant functional types (Xu et al., 2020) or the SiNPs constructive role in photosynthesis, stomatal conductance, and ROS and antioxidant metabolism as we observed in our previous study with *Cymbopogon flexuosus* plants (Mukarram et al., 2021a). Furthermore, SiNPs upregulate GeDH activity which is believed to play a cardinal role in oil enrichment in lemongrass (Mukarram et al., 2021a). Kalteh et al. (2018) and Alsaeedi et al. (2019) observed similar results where SiNPs improved yield components in *Ocimum basilicum* and *Cucumis sativus*, respectively. Our finding agrees with a previous study with *Oryza sativa* where SiNPs application delivered higher crop production during salinity stress (Badawy et al., 2021). The obtained results of higher lemongrass yield with SiNPs find further support from several other studies where SiNPs exhibited similar effects in *Solanum lycopersicum* (Haghighi and Pessarakli, 2013), *Solanum tuberosum* (Kafi et al., 2021), *Triticum aestivum* (Mushtaq et al., 2017), and *Musa acuminata* (Mahmoud et al., 2020) under salt stress.

5 Conclusion

The obtained results support the effectiveness of SiNPs-induced protection in lemongrass against salt stress (NaCl 160 and 240 mM). We found that SiNPs redress photosynthetic performance and stomatal conductance in salt-stressed lemongrass. At the same time, foliar sprays of SiNPs instigated antioxidant production to defend lemongrass plants against salt-induced oxidative stress. Upregulated SOD, CAT, POD, and PRO facilitated cellular homeostasis in the lemongrass. Thus, we noticed reduced H_2O_2 and TBARS content in NaCl 160 and 240 mM treated plants. Further, SiNPs boosted GeDH enzyme activity and essential oil content in both saline regimes. SiNPs could downright redress NaCl 160 mM-induced damages. However,

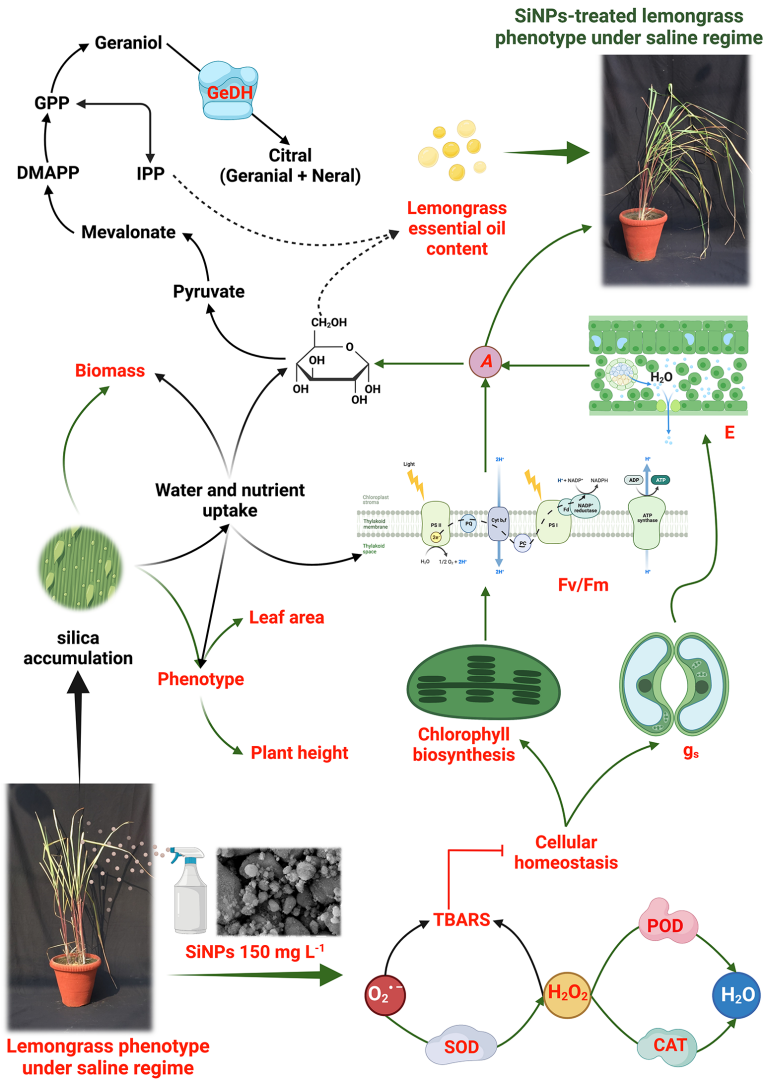

FIGURE 12
Proposed *modus operandi* of silicon nanoparticles (SiNPs) in lemongrass as was developed during the present study. Our results suggest that SiNPs palliate salt-induced oxidative stress by boosting antioxidant metabolism (such as SOD, CAT, and POD). Improved cellular homeostasis could support chlorophyll biosynthesis and PSII efficiency (Fv/Fm). Subsequent upgradation in stomatal dynamics (such as g_s and E) would assist lemongrass with a higher photosynthetic CO_2 assimilation rate (*A*). Further, a higher *A* is expected to generate more glucose which can undergo a mevalonate or mevalonate-independent pathway to confer improved essential oil productivity in salt-stressed lemongrass. The overall upgradation of plant physiology coupled with improved water and nutrient uptake during salt stress can render morphological improvements in lemongrass such as dry weight, leaf area, and plant height. The studied phenomena are coloured in red while the green arrows show SiNPs-induced elicitation of the process.

NaCl 240 mM conferred irreversible damage to the lemongrass growth, development, and productivity modules. A working model for these coordinated biochemical effects is proposed in Figure 12 which is based on our understanding developed during the present study and the insights from our previous studies with lemongrass (see reference list for details). In summary, our results indicate that SiNPs application upgrades plant physiology and triggers cellular defence of lemongrass plants against high salt stress (≤240 mM). These, in concert, brought improved crop productivity in the present study. Therefore, it is proposed that SiNPs could be a useful biotechnological tool to palliate salinity stress in lemongrass crops and that its use could be extrapolated to other agricultural species. On this note, future trends could include the followings:

1. It would be remarkable to know how lemongrass would respond to a mixture of several stresses such as drought, salinity, and high temperature with external SiNPs application.
2. It is high time to know if SiNPs can induce heat-shock proteins or vacuolar H^+-ATPase channels in plants under global climate change scenarios.
3. What individual genes can SiNPs directly target to induce photosynthesis and antioxidant metabolism?
4. Do SiNPs induce Na^+ exclusion at soil-root interphase in saline soil settings?
5. Could the increase in essential oil in stressful situations be considered a reliable marker of stress?

Data availability statement

The original contributions presented in the study are included in the article/Supplementary Material. Further inquiries can be directed to the corresponding author.

Author contributions

MM: Data curation, Formal analysis, Funding acquisition, Investigation, Writing – Original draft preparation. MK: Conceptualization, Funding acquisition, Methodology, Project administration, Resources, Supervision, Validation, Visualization, Writing – Review & Editing. DK: Validation, Visualization, Writing – Review & Editing. AL: Validation, Visualization, Writing – Review & Editing. FC: Validation, Visualization, Writing – Review & Editing. All authors contributed to the article and approved the submitted version.

Funding

MM and MK are funded by the Council of Science and Technology, UP, Lucknow, India through the project grant (Role of radiation-processed chitosan and silicon nanoparticles in regulation of geraniol dehydrogenase for citral production of Lemongrass). MM is also supported by the Slovak Research and Development Agency (APVV-19-0035). DK was supported from the Slovak Grant Agency for Science, No. VEGA 1/0535/20. FJC research is supported by a European Regional Development Fund- co-financed grant from the Ministry of Economy and Competitiveness (PID2019-103924GB-I00), the Plan Andaluz de Investigación, Desarrollo e Innovación (PAIDI 2020) (P18-FR-1359) and Junta de Andalucía (group BIO192), Spain. AL was supported by the Operation Program of Integrated Infrastructure – co-financed by the European Regional Development Fund (ITMS2014+) (313021BUZ3).

Acknowledgments

MM thanks Peter Fleischer Jr (TU, Zvolen) for the useful discussion on the statistical analysis. The graphical abstract and Figure 12 were created with BioRender.com.

Conflict of interest

The authors declare that the research was conducted in the absence of any commercial or financial relationships that could be construed as a potential conflict of interest.

Publisher's note

Supplementary material

The Supplementary Material for this article can be found online at: https://www.frontiersin.org/articles/10.3389/fpls.2023.1116769/full#supplementary-material

References

Abdelaal, K. A., Mazrou, Y. S., and Hafez, Y. M. (2020). Silicon foliar application mitigates salt stress in sweet pepper plants by enhancing water status, photosynthesis, antioxidant enzyme activity and fruit yield. *Plants* 9, 733. doi: 10.3390/plants9060733

Abdel-Haliem, M. E., Hegazy, H. S., Hassan, N. S., and Naguib, D. M. (2017). Effect of silica ions and nano silica on rice plants under salinity stress. *Ecol. Eng.* 99, 282–289. doi: 10.1016/j.ecoleng.2016.11.060

Ahmad, P., Venema, K., and Corpas, F. J. (2022). Unravelling salt tolerance mechanisms in plants: From lab to field. *Plant Physiol. Biochem.* 176, 31–33. doi: 10.1016/j.plaphy.2022.02.006

Alam, P., Arshad, M., Al-Kheraif, A. A., Azzam, M. A., and Al Balawi, T. (2022). Silicon nanoparticle-induced regulation of carbohydrate metabolism, photosynthesis, and ROS homeostasis in *Solanum lycopersicum* subjected to salinity stress. *ACS Omega.* 7 (36), 31834–31844. doi: 10.1021/acsomega.2c02586

Alsaeedi, A. H., El-Ramady, H., Alshaal, T., El-Garawani, M., Elhawat, N., and Almohsen, M. (2017). Engineered silica nanoparticles alleviate the detrimental effects of na^+ stress on germination and growth of common bean (*Phaseolus vulgaris*). *Environ. Sci. pollut. Res.* 24, 21917–21928. doi: 10.1007/s11356-017-9847-y

Alsaeedi, A., El-Ramady, H., Alshaal, T., El-Garawany, M., Elhawat, N., and Al-Otaibi, A. (2019). Silica nanoparticles boost growth and productivity of cucumber under water deficit and salinity stresses by balancing nutrients uptake. *Plant Physiol. Biochem.* 139, 1–10. doi: 10.1016/j.plaphy.2019.03.008

Alsamadany, H., Alharby, H. F., Al-Zahrani, H. S., Alzahrani, Y. M., Almaghamsi, A. A., Abbas, G., et al. (2022). Silicon-nanoparticles doped biochar is more effective than biochar for mitigation of arsenic and salinity stress in quinoa: Insight to human health risk assessment. *Front. Plant Sci.* 13, 989504. doi: 10.3389/fpls.2022.989504

Asgari, F., Majd, A., Jonoubi, P., and Najafi, F. (2018). Effects of silicon nanoparticles on molecular, chemical, structural and ultrastructural characteristics of oat (*Avena sativa* l.). *Plant Physiol. Biochem.* 127, 152–160. doi: 10.1016/j.plaphy.2018.03.021

Ashour, H. A. (2018). Influence of gibberellic acid and silicon different sources on growth and chemical constituents of Monterey cypress (*Cupressus macrocarpa* 'Goldcrest wilma') plants. *Middle East J.* 7, 210–226.

Ashraf, M. (2009). Biotechnological approach of improving plant salt tolerance using antioxidants as markers. *Biotechnol. Adv.* 27, 84–93. doi: 10.1016/j.biotechadv.2008.09.003

Ashraf, M., and Munns, R. (2022). Evolution of approaches to increase the salt tolerance of crops. *Crit. Rev. Plant Sci.* 41(2), 128–160. doi: 10.1080/07352689.2022.2065136

Attia, E. A., and Elhawat, N. (2021). Combined foliar and soil application of silica nanoparticles enhances the growth, flowering period and flower characteristics of marigold (*Tagetes erecta* l.). *Sci. Hortic.* 282, 110015. doi: 10.1016/j.scienta.2021.110015

Avestan, S., Ghasemnezhad, M., Esfahani, M., and Byrt, C. S. (2019). Application of nano-silicon dioxide improves salt stress tolerance in strawberry plants. *Agronomy* 9, 246. doi: 10.3390/agronomy9050246

Badawy, S. A., Zayed, B. A., Bassiouni, S. M., Mahdi, A. H., Majrashi, A., Ali, E. F., et al. (2021). Influence of nano silicon and nano selenium on root characters, growth, ion selectivity, yield, and yield components of rice (*Oryza sativa* l.) under salinity conditions. *Plants* 10, 1657. doi: 10.3390/plants10081657

Banerjee, A., Singh, A., Sudarshan, M., and Roychoudhury, A. (2021). Silicon nanoparticle-pulsing mitigates fluoride stress in rice by fine-tuning the ionomic and metabolomic balance and refining agronomic traits. *Chemosphere* 262, 127826. doi: 10.1016/j.chemosphere.2020.127826

Bao-Shan, L., Chun-hui, L., Li-jun, F., Shu-chun, Q., and Min, Y. (2004). Effect of TMS (nanostructured silicon dioxide) on growth of changbai larch seedlings. *J. For. Res.* 15, 138–140. doi: 10.1007/BF02856749

Bates, L. S., Waldren, R. P., and Teare, I. D. (1973). Rapid determination of free proline for water-stress studies. *Plant Soil* 39, 205–207. doi: 10.1007/BF00018060

Beers, R. F., and Sizer, I. W. (1952). A spectrophotometric method for measuring the breakdown of hydrogen peroxide by catalase. *J. Biol. Chem.* 195, 133–140. doi: 10.1016/S0021-9258(19)50881-X

Beyer, W. F., and Fridovich, I. (1987). Assaying for superoxide dismutase activity: Some large consequences of minor changes in conditions. *Anal. Biochem.* 161, 559–566. doi: 10.1016/0003-2697(87)90489-1

Brackhage, C., Schaller, J., Bäuckner, E., and Dudel, G. D. (2013). Silicon availability affects the stoichiometry and content of calcium and micro nutrients in the leaves of common reed. *Silicon* 5, 199–204. doi: 10.1007/s12633-013-9145-3

Butcher, K., Wick, A. F., DeSutter, T., Chatterjee, A., and Harmon, J. (2016). Soil salinity: A threat to global food security. *J. Agron.* 108, 2189–2200. doi: 10.2134/agronj2016.06.0368

Cakmak, I., and Horst, W. J. (1991). Effect of aluminium on lipid peroxidation, superoxide dismutase, catalase, and peroxidase activities in root tips of soybean (*Glycine max*). *Physiol. Plant* 83, 463–468. doi: 10.1111/j.1399-3054.1991.tb00121.x

Cheeseman, J. M. (1988). Mechanisms of salinity tolerance in plants. *Plant Physiol.* 87, 547–550. doi: 10.1104/pp.87.3.547

Considine, M. J., and Foyer, C. H. (2021). Stress effects on the reactive oxygen species-dependent regulation of plant growth and development. *J. Exp. Bot.* 72, 5795–5806. doi: 10.1093/jxb/erab265

Corpas, F. J., González-Gordo, S., and Palma, J. M. (2020). Plant peroxisomes: A factory of reactive species. *Front. Plant Sci.* 11, 853. doi: 10.3389/fpls.2020.00853

Dagar, J. C., Tomar, O. S., Minhas, P. S., and Kumar, M. (2013). Lemongrass (*Cymbopogon flexuosus*) productivity as affected by salinity of irrigation water, planting method and fertilizer doses on degraded calcareous soil in a semi-arid region of northwest India. *Indian J. Agric. Sci.* 83, 734–738.https://epubs.icar.org.in/index.php/IJAgS/article/view/31168

Dhiman, P., Rajora, N., Bhardwaj, S., Sudhakaran, S. S., Kumar, A., Raturi, G., et al. (2021). Fascinating role of silicon to combat salinity stress in plants: An updated overview. *Plant Physiol. Biochem.* 162, 110–123. doi: 10.1016/j.plaphy.2021.02.023

Dodd, I. C., and Pérez-Alfocea, F. (2012). Microbial amelioration of crop salinity stress. *J. Exp. Bot.* 63, 3415–3428. doi: 10.1093/jxb/ers033

El-Dengawy, E. F. A., EL-Abbasy, U. K., and El-Gobba, M. H. (2021). Influence of nano-silicon treatment on growth behavior of 'Sukkary' and 'Gahrawy' mango root-stocks under salinity stress. *J. Plant Prod.* 12, 49–61. doi: 10.21608/JPP.2021.152020

El-Kady, M. E., El-Boray, M. S., Shalan, A. M., and Mohamed, L. M. (2017). Effect of silicon dioxide nanoparticles on growth improvement of banana shoots *in vitro* within rooting stage. *J. Plant Prod.* 8, 913–916. doi: 10.21608/jpp.2017.40900

El-Saadony, M. T., Desoky, E. S. M., Saad, A. M., Eid, R. S., Selem, E., and Elrys, A. S. (2021). Biological silicon nanoparticles improve *Phaseolus vulgaris* l. yield and minimize its contaminant contents on a heavy metals-contaminated saline soil. *J. Environ. Sci.* 106, 1–14. doi: 10.1016/j.jes.2021.01.012

Elsheery, N. I., Helaly, M. N., El-Hoseiny, H. M., and Alam-Eldein, S. M. (2020). Zinc oxide and silicone nanoparticles to improve the resistance mechanism and annual productivity of salt-stressed mango trees. *Agronomy* 10, 558. doi: 10.3390/agronomy10040558

Eswar, D., Karuppusamy, R., and Chellamuthu, S. (2021). Drivers of soil salinity and their correlation with climate change. *Curr. Opin. Environ. Sustain* 50, 310–318. doi: 10.1016/j.cosust.2020.10.015

Etienne, P., Trouverie, J., Haddad, C., Arkoun, M., Yvin, J. C., Caïus, J., et al. (2021). Root silicon treatment modulates the shoot transcriptome in *Brassica napus* l. and in particular upregulates genes related to ribosomes and photosynthesis. *Silicon* 13, 4047–4055. doi: 10.1007/s12633-020-00710-z

Farhangi-Abriz, S., and Torabian, S. (2018). Nano-silicon alters antioxidant activities of soybean seedlings under salt toxicity. *Protoplasma* 255, 953–962. doi: 10.1007/s00709-017-1202-0

Farouk, S., Elhindi, K. M., and Alotaibi, M. A. (2020). Silicon supplementation mitigates salinity stress on *Ocimum basilicum* l. *via* improving water balance, ion homeostasis, and antioxidant defense system. *Ecotoxicol. Environ. Saf.* 206, 111396. doi: 10.1016/j.ecoenv.2020.111396

Fatemi, H., Esmaiel Pour, B., and Rizwan, M. (2021). Foliar application of silicon nanoparticles affected the growth, vitamin c, flavonoid, and antioxidant enzyme activities of coriander (*Coriandrum sativum* l.) plants grown in lead (Pb)-spiked soil. *Environ. Sci. pollut. Res.* 28, 1417–1425. doi: 10.1007/s11356-020-10549-x

Fatemi, H., Pour, B. E., and Rizwan, M. (2020). Isolation and characterization of lead (Pb) resistant microbes and their combined use with silicon nanoparticles improved the growth, photosynthesis and antioxidant capacity of coriander (*Coriandrum sativum* l.) under Pb stress. *Environ. pollut.* 266, 114982. doi: 10.1016/j.envpol.2020.114982

Foucher, A., Salvador-Blanes, S., Evrard, O., Simonneau, A., Chapron, E., Courp, T., et al. (2014). Increase in soil erosion after agricultural intensification: Evidence from a lowland basin in France. *Anthropocene* 7, 30–41. doi: 10.1016/j.ancene.2015.02.001

Foyer, C. H. (2018). Reactive oxygen species, oxidative signaling and the regulation of photosynthesis. *Environ. Exp. Bot.* 154, 134–142. doi: 10.1016/j.envexpbot.2018.05.003

Foyer, C. H., and Noctor, G. (2005). Redox homeostasis and antioxidant signaling: a metabolic interface between stress perception and physiological responses. *Plant Cell* 17, 1866–1875. doi: 10.1105/tpc.105.033589

Foyer, C. H., and Shigeoka, S. (2011). Understanding oxidative stress and antioxidant functions to enhance photosynthesis. *Plant Physiol.* 155, 93–100. doi: 10.1104/pp.110.166181

Frazão, J. J., de Mello Prado, R., de Souza Júnior, J. P., and Rossatto, D. R. (2020). Silicon changes c: N: P stoichiometry of sugarcane and its consequences for photosynthesis, biomass partitioning and plant growth. *Sci. Rep.* 10, 1–10. doi: 10.1038/s41598-020-69310-6

Ghorbanpour, M., Mohammadi, H., and Kariman, K. (2020). Nanosilicon-based recovery of barley (*Hordeum vulgare*) plants subjected to drought stress. *Environ. Sci. Nano.* 7, 443–461. doi: 10.1039/C9EN00973F

González-Moscoso, M., Juárez-Maldonado, A., Cadenas-Pliego, G., Meza-Figueroa, D., SenGupta, B., and Martínez-Villegas, N. (2022). Silicon nanoparticles decrease arsenic translocation and mitigate phytotoxicity in tomato plants. *Environ. Sci. pollut. Res.* 29, 34147–34163. doi: 10.1007/s11356-021-17665-2

Guenther, E. (1972). The essential oils: History, origin in plants, production. *Analysis* 1, 147–151.

Haghighi, M., and Pessarakli, M. (2013). Influence of silicon and nano-silicon on salinity tolerance of cherry tomatoes (*Solanum lycopersicum* l.) at early growth stage. *Sci. Hortic.* 161, 111–117. doi: 10.1016/j.scienta.2013.06.034

Haque, A. N. M. A., Remadevi, R., and Naebe, M. (2018). Lemongrass (Cymbopogon): A review on its structure, properties, applications and recent developments. *Cellulose* 25, 5455–5477. doi: 10.1007/s10570-018-1965-2

Hasanuzzaman, M., Bhuyan, M. H. M., Zulfiqar, F., Raza, A., Mohsin, S. M., Mahmud, J. A., et al. (2020). Reactive oxygen species and antioxidant defense in plants under abiotic stress: Revisiting the crucial role of a universal defense regulator. *Antioxidants* 9, 681. doi: 10.3390/antiox9080681

Hasegawa, P. M., Bressan, R. A., Zhu, J. K., and Bohnert, H. J. (2000). Plant cellular and molecular responses to high salinity. *Annu. Rev. Plant Biol.* 51, 463–499. doi: 10.1146/annurev.arplant.51.1.463

Hernandez, J. A., Jiménez, A., Mullineaux, P., and Sevilia, F. (2000). Tolerance of pea (*Pisum sativum* l.) to long-term salt stress is associated with induction of antioxidant defences. *Plant Cell Environ.* 23, 853–862. doi: 10.1046/j.1365-3040.2000.00602.x

Hopmans, J. W., Qureshi, A. S., Kisekka, I., Munns, R., Grattan, S. R., Rengasamy, P., et al. (2021). Critical knowledge gaps and research priorities in global soil salinity. *Adv. Agron.* 169, 1–191. doi: 10.1016/bs.agron.2021.03.001

Hossain, M. S., ElSayed, A. I., Moore, M., and Dietz, K. J. (2017). Redox and reactive oxygen species network in acclimation for salinity tolerance in sugar beet. *J. Exp. Bot.* 68, 1283–1298. doi: 10.1093/jxb/erx019

Houmani, H., Rodríguez-Ruiz, M., Palma, J. M., Abdelly, C., and Corpas, F. J. (2016). Modulation of superoxide dismutase (SOD) isozymes by organ development and high long-term salinity in the halophyte *Cakile maritima*. *Protoplasma* 253, 885–894. doi: 10.1007/s00709-015-0850-1

Idrees, M., Naeem, M., Khan, M. N., Aftab, T., and Khan, M. (2012). Alleviation of salt stress in lemongrass by salicylic acid. *Protoplasma* 249, 709–720. doi: 10.1007/s00709-011-0314-1

Isa, M., Bai, S., Yokoyama, T., Ma, J. F., Ishibashi, Y., Yuasa, T., et al. (2010). Silicon enhances growth independent of silica deposition in a low-silica rice mutant, lsi1. *Plant Soil* 331 (1), pp.361–pp.375. doi: 10.1007/s11104-009-0258-9

Janmohammadi, M., and Sabaghnia, N. (2015). Effect of pre-sowing seed treatments with silicon nanoparticles on germinability of sunflower (*Helianthus annuus*). *Bot. Lith.* 21, 13–21. doi: 10.1515/botlit-2015-0002

Kafi, M., Nabati, J., Ahmadi-Lahijani, M. J., and Oskoueian, A. (2021). Silicon compounds and potassium sulfate improve salinity tolerance of potato plants through instigating the defense mechanisms, cell membrane stability, and accumulation of osmolytes. *Commun. Soil Sci. Plant Anal.* 52, 843–858. doi: 10.1080/00103624.2020.1869768

Kah, M., Kookana, R. S., Gogos, A., and Bucheli, T. D. (2018). A critical evaluation of nanopesticides and nanofertilizers against their conventional analogues. *Nat. Nanotechnol.* 13, 677. doi: 10.1038/s41565-018-0131-1

Kalteh, M., Alipour, Z. T., Ashraf, S., Marashi Aliabadi, M., and Falah Nosratabadi, A. (2018). Effect of silica nanoparticles on basil (*Ocimum basilicum*) under salinity stress. *J. Chem. Health Risks* 4, 49–55. doi: 10.22034/jchr.2018.544075

Karimian, N., Nazari, F., and Samadi, S. (2021). Morphological and biochemical properties, leaf nutrient content, and vase life of tuberose (*Polianthes tuberosa* l.) affected by root or foliar applications of silicon (Si) and silicon nanoparticles (SiNPs). *J. Plant Growth Regul.* 40, 2221–2235. doi: 10.1007/s00344-020-10272-4

Khandekar, S., and Leisner, S. (2011). Soluble silicon modulates expression of *Arabidopsis thaliana* genes involved in copper stress. *J. Plant Physiol.* 168, 699–705. doi: 10.1016/j.jplph.2010.09.009

Kopittke, P. M., Menzies, N. W., Wang, P., McKenna, B. A., and Lombi, E. (2019). Soil and the intensification of agriculture for global food security. *Environ. Int.* 132, 105078. doi: 10.1016/j.envint.2019.105078

Kramer, P. J., and Boyer, J. S. (1995). *Water relations of plants and soils* (Academic press, California 92101-4495, USA).

Kumar, K. B., and Khan, P. A. (1982). Peroxidase & polyphenol oxidase in excised ragi (*Eleusine coracana* cv pr 202) leaves during senescence. *Indian J. Exp. Biol.* 20, 412–416.

Kumar, P., and Sharma, P. K. (2020). Soil salinity and food security in India. *Front. Sustain. Food Syst.* 4, 533781. doi: 10.3389/fsufs.2020.533781

Kuo, T. M., Warner, R. L., and Kleinhofs, A. (1982). *In vitro* stability of nitrate reductase from barley leaves. *Phytochemistry* 21, 531–533. doi: 10.1016/0031-9422(82)83134-8

Larkunthod, P., Boonlakhorn, J., Pansarakham, P., Pongdontri, P., Thongbai, P., and Theerakulpisut, P. (2022). Synthesis and characterization of silica nanoparticles from rice husk and their effects on physiology of rice under salt stress. *Chil. J. Agric. Res.* 82, 412–425. doi: 10.4067/S0718-58392022000300412

Lehmann, J. (2007). A handful of carbon. *Nature* 447, 143–144. doi: 10.1038/447143a

Lesharadevi, K., Parthasarathi, T., and Muneer, S. (2021). Silicon biology in crops under abiotic stress: A paradigm shift and cross-talk between genomics and proteomics. *J. Biotechnol.* 333, 21–38. doi: 10.1016/j.jbiotec.2021.04.008

Li, B., Tao, G., Xie, Y., and Cai, X. (2012). Physiological effects under the condition of spraying nano-SiO_2 onto the *Indocalamus barbatus* McClure leaves. *J. Nanjing Univ. Nat. Sci.* 36, 161–164.

Ma, D., Sun, D., Wang, C., Qin, H., Ding, H., Li, Y., et al. (2016). Silicon application alleviates drought stress in wheat through transcriptional regulation of multiple antioxidant defense pathways. *J. Plant Growth Regul.* 35, 1–10. doi: 10.1007/s00344-015-9500-2

Machado, R. M. A., and Serralheiro, R. P. (2017). Soil salinity: effect on vegetable crop growth. management practices to prevent and mitigate soil salinization. *Horticulturae* 3, 30. doi: 10.3390/horticulturae3020030

Mahmoud, L. M., Dutt, M., Shalan, A. M., El-Kady, M. E., El-Boray, M. S., Shabana, Y. M., et al. (2020). Silicon nanoparticles mitigate oxidative stress of *in vitro*-derived banana (*Musa acuminata* 'Grand nain') under simulated water deficit or salinity stress. *S. Afr. J. Bot.* 132, 155–163. doi: 10.1016/j.sajb.2020.04.027

Mahmoud, L. M., El-Kady, M. E., Elboray, M. S., Shalan, A. N., Shabana, Y. M., and Grosser, J. W. (2019). "Silicon nanoparticles mitigate the adverse effect of drought induced by polyethylene glycol of in vitro banana shoots," in *In vitro cellular and developmental biology – animal*, vol. 233. (Spring ST, New York, NY 10013 USA: Springer), S54–S54.

Mahmoud, L. M., Shalan, A. M., El-Boray, M. S., Vincent, C. I., El-Kady, M. E., Grosser, J. W., et al. (2022). Application of silicon nanoparticles enhances oxidative stress tolerance in salt stressed 'Valencia' sweet orange plants. *Sci. Hortic.* 295, 110856. doi: 10.1016/j.scienta.2021.110856

Mattson, N. S., and Leatherwood, W. R. (2010). Potassium silicate drenches increase leaf silicon content and affect morphological traits of several floriculture crops grown in a peat-based substrate. *Hortic. Sci.* 45, 43–47. doi: 10.21273/HORTSCI.45.1.43

McDowell, N. G. (2011). Mechanisms linking drought, hydraulics, carbon metabolism, and vegetation mortality. *Plant Physiol.* 155, 1051–1059. doi: 10.1104/pp.110.170704

Miller, G., Suzuki, N., Ciftci-Yilmaz, S., and Mittler, R. (2010). Reactive oxygen species homeostasis and signalling during drought and salinity stresses. *Plant Cell Environ.* 33 (4), 453–467. doi: 10.1111/j.1365-3040.2009.02041.x

Mirzaei, M., Ladan Moghadam, A., Hakimi, L., and Danaee, E. (2020). Plant growth promoting rhizobacteria (PGPR) improve plant growth, antioxidant capacity, and essential oil properties of lemongrass (*Cymbopogon citratus*) under water stress. *Iran. J. Plant Physiol.* 10, 3155–3166. doi: 10.30495/IJPP.2020.672574

Mittler, R., Zandalinas, S. I., Fichman, Y., and Van Breusegem, F. (2022). Reactive oxygen species signalling in plant stress responses. *Nat. Rev. Mol.* 23(10), 663–679. doi: 10.1038/s41580-022-00499-2

Mukarram, M., Choudhary, S., Khan, M. A., Poltronieri, P., Khan, M. M. A., Ali, J., et al. (2021b). Lemongrass essential oil components with antimicrobial and anticancer activities. *Antioxidants* 11, 20. doi: 10.3390/antiox11010020

Mukarram, M., Choudhary, S., Kurjak, D., Petek, A., and Khan, M. M. A. (2021c). Drought: Sensing, signalling, effects and tolerance in higher plants. *Physiol. Plant* 172, 1291–1300. doi: 10.1111/ppl.13423

Mukarram, M., Khan, M. M. A., and Corpas, F. J. (2021a). Silicon nanoparticles elicit an increase in lemongrass (*Cymbopogon flexuosus* (Steud.) wats) agronomic parameters with a higher essential oil yield. *J. Hazard. Mater.* 412, 125254. doi: 10.1016/j.jhazmat.2021.125254

Mukarram, M., Khan, M., Uddin, M., and Corpas, F. J. (2022a). Irradiated chitosan (ICH): An alternative tool to increase essential oil content in lemongrass (*Cymbopogon flexuosus*). *Acta Physiol. Plant* 44, 1–15. doi: 10.1007/s11738-021-03335-w

Mukarram, M., Khan, M. M. A., Zehra, A., Petrik, P., and Kurjak, D. (2022c). Suffer or survive: Decoding salt-sensitivity of lemongrass and its implication on essential oil productivity. *Front. Plant Sci.* 13, 903954. doi: 10.3389/fpls.2022.903954

Mukarram, M., Petrik, P., Mushtaq, Z., Khan, M. M. A., Gulfishan, M., and Lux, A. (2022b). Silicon nanoparticles in higher plants: Uptake, action, stress tolerance, and crosstalk with phytohormones, antioxidants, and other signalling molecules. *Environ. pollut.* 310, 119855. doi: 10.1016/j.envpol.2022.119855

Munns, R. (1993). Physiological processes limiting plant growth in saline soils: some dogmas and hypotheses. *Plant Cell Environ.* 16, 15–24. doi: 10.1111/j.1365-3040.1993.tb00840.x

Munns, R. (2002). Comparative physiology of salt and water stress. *Plant Cell Environ.* 25, 239–250. doi: 10.1046/j.0016-8025.2001.00808.x

Munns, R., and Tester, M. (2008). Mechanisms of salinity tolerance. *Annu. Rev. Plant Biol.* 59, 651. doi: 10.1146/annurev.arplant.59.032607.092911

Mushtaq, A., Jamil, N., Riaz, M., Hornyak, G. L., Ahmed, N., Ahmed, S. S., et al. (2017). Synthesis of silica nanoparticles and their effect on priming of wheat (*Triticum aestivum* l.) under salinity stress. *In Biol. Forum.* 9, 150–157.

Naguib, D. M., and Abdalla, H. (2019). Metabolic status during germination of nano silica primed *Zea mays* seeds under salinity stress. *J. Crop Sci. Biotechnol.* 22, 415–423. doi: 10.1007/s12892-019-0168-0

Nazaralian, S., Majd, A., Irian, S., Najafi, F., Ghahremaninejad, F., Landberg, T., et al. (2017). Comparison of silicon nanoparticles and silicate treatments in fenugreek. *Plant Physiol. Biochem.* 115, 25–33. doi: 10.1016/j.plaphy.2017.03.009

Neu, S., Schaller, J., and Dudel, G. D. (2017). Silicon availability modifies nutrient use efficiency and content, C:N:P stoichiometry, and productivity of winter wheat (*Triticum aestivum* l.). *Sci. Rep.* 7, 1–8. doi: 10.1038/srep40829

Okuda, T., Matsuda, Y., Yamanaka, A., and Sagisaka, S. (1991). Abrupt increase in the level of hydrogen peroxide in leaves of winter wheat is caused by cold treatment. *Plant Physiol.* 97, 1265–1267. doi: 10.1104/pp.97.3.1265

Pandey, C., Khan, E., Panthri, M., Tripathi, R. D., and Gupta, M. (2016). Impact of silicon on Indian mustard (*Brassica juncea* l.) root traits by regulating growth parameters, cellular antioxidants and stress modulators under arsenic stress. *Plant Physiol. Biochem.* 104, 216–225. doi: 10.1016/j.plaphy.2016.03.032

Pandey, S. K., and Singh, H. (2011). A simple, cost-effective method for leaf area estimation. *J. Bot.* 2011, 1–6. doi: 10.1155/2011/658240

Rady, M. M., Elrys, A. S., Abo El-Maati, M. F., and Desoky, E. S. M. (2019). Interplaying roles of silicon and proline effectively improve salt and cadmium stress tolerance in *Phaseolus vulgaris* plant. *Plant Physiol. Biochem.* 139, 558–568. doi: 10.1016/j.plaphy.2019.04.025

Reboredo, F., Lidon, F. C., Pessoa, F., Duarte, M. P., and Silva, M. J. (2013). The uptake of macronutrients by an active silicon accumulator plant growing in two different substrata. *Emir. J. Food Agric.* 25, 986–993. doi: 10.9755/ejfa.v25i12.16735

Romero-Aranda, M. R., Jurado, O., and Cuartero, J. (2006). Silicon alleviates the deleterious salt effect on tomato plant growth by improving plant water status. *J. Plant Physiol.* 163, 847–855. doi: 10.1016/j.jplph.2005.05.010

Sangwan, R. S., Singh-Sangwan, N., and Luthra, R. (1993). Metabolism of acyclic monoterpenes: Partial purification and properties of geraniol dehydrogenase from lemongrass (*Cymbopogon flexuosus* stapf.) leaves. *J. Plant Physiol.* 142, 129–134. doi: 10.1016/S0176-1617(11)80952-1

Savant, N. K., Snyder, G. H., and Datnoff, L. E. (1996). Silicon management and sustainable rice production. *Adv. Agron.* 58, 151–199. doi: 10.1016/S0065-2113(08)60255-2

Schaller, J., Brackhage, C., Gessner, M. O., Bäker, E., and Dudel, E. G. (2012). Silicon supply modifies C:N:P stoichiometry and growth of *Phragmites australis*. *Plant Biol.* 14, 392–396. doi: 10.1111/j.1438-8677.2011.00537.x

Shahid, M. A., Sarkhosh, A., Khan, N., Balal, R. M., Ali, S., Rossi, L., et al. (2020). Insights into the physiological and biochemical impacts of salt stress on plant growth and development. *Agronomy* 10, 938. doi: 10.3390/agronomy10070938

Sharma, A., Vishwakarma, K., Singh, N. K., Prakash, V., Ramawat, N., Prasad, R., et al. (2022). Synergistic action of silicon nanoparticles and indole acetic acid in alleviation of chromium (CrVI) toxicity in *Oryza sativa* seedlings. *J. Biotechnol.* 343, 71–82. doi: 10.1016/j.jbiotec.2021.09.005

Siddiqui, H., Ahmed, K. B. M., Sami, F., and Hayat, S. (2020). "Silicon nanoparticles and plants: current knowledge and future perspectives," in *Sustainable agriculture reviews 41*. Eds. S. Hayat, J. Pichtel, M. Faizan and Q. Fariduddin (Cham: Springer), 129–142.

Siddiqui, M. H., Al-whaibi, M. H., Faisal, M., and Sahli, A. A. A. (2014). Nano-silicon dioxide mitigates the adverse effects of salt stress on *Cucurbita pepo* l. *Environ. Toxicol. Chem.* 33, 2429–2437. doi: 10.1002/etc.2697

Singh, A., and Sharma, P. C. (2018). Recent insights into physiological and molecular regulation of salt stress in fruit crops. *Adv. Plants Agric. Res.* 8, 171–183. doi: 10.15406/apar.2018.08.00309

Skaria, B. P., Joy, P. P., Mathew, S., and Mathew, G. (2006). "Lemongrass," in *Handbook of herbs and spices* (Woodhead Publishing, Cambridge, UK), 400–419.

Sommer, M., Kaczorek, D., Kuzyakov, Y., and Breuer, J. (2006). Silicon pools and fluxes in soils and landscapes – a review. *J. Plant Nutr. Soil Sci.* 169, 310–329. doi: 10.1002/jpln.200521981

Steinhorst, L., and Kudla, J. (2019). How plants perceive salt. *Nature* 572, 318–320. doi: 10.1038/d41586-019-02289-x

Tamai, K., and Ma, J. F. (2008). Reexamination of silicon effects on rice growth and production under field conditions using a low silicon mutant. *Plant Soil* 307, 21–27. doi: 10.1007/s11104-008-9571-y

Tripathi, D. K., Singh, V. P., Prasad, S. M., Chauhan, D. K., and Dubey, N. K. (2015). Silicon nanoparticles (SiNp) alleviate chromium (VI) phytotoxicity in *Pisum sativum* (L.) seedlings. *Plant Physiol. Biochem.* 96, 189–198. doi: 10.1016/j.plaphy.2015.07.026

Tripathi, D. K., Singh, S., Singh, V. P., Prasad, S. M., Dubey, N. K., and Chauhan, D. K. (2017). Silicon nanoparticles more effectively alleviated UV-b stress than silicon in wheat (*Triticum aestivum*) seedlings. *Plant Physiol. Biochem.* 110, 70–81. doi: 10.1016/j.plaphy.2016.06.026

Van Zelm, E., Zhang, Y., and Testerink, C. (2020). Salt tolerance mechanisms of plants. *Annu. Rev. Plant Biol.* 71, 403–433. doi: 10.1146/annurev-arplant-050718-100005

Xu, D., Fang, X., Zhang, R., Gao, T., Bu, H., and Du, G. (2015). Influences of nitrogen, phosphorus and silicon addition on plant productivity and species richness in an alpine meadow. *AoB Plants* 7, plv125. doi: 10.1093/aobpla/plv125

Xu, D., Gao, T., Fang, X., Bu, H., Li, Q., Wang, X., et al. (2020). Silicon addition improves plant productivity and soil nutrient availability without changing the grass: Legume ratio response to n fertilization. *Sci. Rep.* 10, 10295. doi: 10.1038/s41598-020-67333-7

Yamaguchi, T., Hamamoto, S., and Uozumi, N. (2013). Sodium transport system in plant cells. *Front. Plant Sci.* 4, 410. doi: 10.3389/fpls.2013.00410

Yassen, A., Abdallah, E., Gaballah, M., and Zaghloul, S. (2017). Role of silicon dioxide nano fertilizer in mitigating salt stress on growth, yield and chemical composition of cucumber (*Cucumis sativus* l.). *Int. J. Agric. Res.* 22, 130–135. doi: 10.3923/ijar.2017.130.135

Zhang, Y., Liang, Y., Zhao, X., Jin, X., Hou, L., Shi, Y., et al. (2019). Silicon compensates phosphorus deficit-induced growth inhibition by improving photosynthetic capacity, antioxidant potential, and nutrient homeostasis in tomato. *Agronomy* 9, 733. doi: 10.3390/agronomy9110733

Zhang, Y., Shi, Y., Gong, H., Zhao, H., Li, H., Hu, Y., et al. (2018). Beneficial effects of silicon on photosynthesis of tomato seedlings under water stress. *J. Integr. Agric.* 17, 2151–2159. doi: 10.1016/S2095-3119(18)62038-6

Zhu, Z., Wei, G., Li, J., Qian, Q., and Yu, J. (2004). Silicon alleviates salt stress and increases antioxidant enzymes activity in leaves of salt-stressed cucumber (*Cucumis sativus* l.). *Plant Sci.* 167, 527–533. doi: 10.1016/j.plantsci.2004.04.020

Zulfiqar, F., and Ashraf, M. (2021). Nanoparticles potentially mediate salt stress tolerance in plants. *Plant Physiol. Biochem.* 160, 257–268. doi: 10.1016/j.plaphy.2021.01.028

frontiers | Frontiers in Plant Science

TYPE Original Research
PUBLISHED 20 February 2023
DOI 10.3389/fpls.2023.1128928

OPEN ACCESS

EDITED BY
Debojyoti Moulick,
Independent Researcher, Kolkata, India

REVIEWED BY
Krishan K. Verma,
Guangxi Academy of Agricultural Sciences, China
Sukamal Sarkar,
Ramakrishna Mission Vivekananda Educational and Research Institute, India
Bhaben Chowardhara,
Assam University, India

*CORRESPONDENCE
Shyam Sundar Dey
shyam.iari@gmail.com;
shyam.dey@icar.gov.in
Tusar Kanti Behera
tusar@rediffmail.com

SPECIALTY SECTION
This article was submitted to Plant Abiotic Stress, a section of the journal Frontiers in Plant Science

RECEIVED 21 December 2022
ACCEPTED 06 February 2023
PUBLISHED 20 February 2023

CITATION
Hongal DA, Raju D, Kumar S, Talukdar A, Das A, Kumari K, Dash PK, Chinnusamy V, Munshi AD, Behera TK and Dey SS (2023) Elucidating the role of key physio-biochemical traits and molecular network conferring heat stress tolerance in cucumber. *Front. Plant Sci.* 14:1128928. doi: 10.3389/fpls.2023.1128928

Elucidating the role of key physio-biochemical traits and molecular network conferring heat stress tolerance in cucumber

Dhananjay A. Hongal[1], Dhandapani Raju[2], Sudhir Kumar[2], Akshay Talukdar[3], Anjan Das[1], Khushboo Kumari[1], Prasanta K. Dash[4], Viswanathan Chinnusamy[2], Anilabha Das Munshi[1], Tusar Kanti Behera[1,5*] and Shyam Sundar Dey[1*]

[1]Division of Vegetable Science, ICAR-Indian Agricultural Research Institute, New Delhi, India, [2]Division of Plant Physiology, ICAR-Indian Agricultural Research Institute, New Delhi, India, [3]Division of Genetics, ICAR-Indian Agricultural Research Institute, New Delhi, India, [4]ICAR-National Institute for Plant Biotechnology, New Delhi, India, [5]ICAR-Indian Institute of Vegetable Research, Varanasi, India

Cucumber is an important vegetable crop grown worldwide and highly sensitive to prevailing temperature condition. The physiological, biochemical and molecular basis of high temperature stress tolerance is poorly understood in this model vegetable crop. In the present study, a set of genotypes with contrasting response under two different temperature stress (35/30°C and 40/35°C) were evaluated for important physiological and biochemical traits. Besides, expression of the important heat shock proteins (HSPs), aquaporins (AQPs), photosynthesis related genes was conducted in two selected contrasting genotypes at different stress conditions. It was established that tolerant genotypes were able to maintain high chlorophyll retention, stable membrane stability index, higher retention of water content, stability in net photosynthesis, high stomatal conductance and transpiration in combination with less canopy temperatures under high temperature stress conditions compared to susceptible genotypes and were considered as the key physiological traits associated with heat tolerance in cucumber. Accumulation of biochemicals like proline, protein and antioxidants like SOD, catalase and peroxidase was the underlying biochemical mechanisms for high temperature tolerance. Upregulation of photosynthesis related genes, signal transduction genes and heat responsive genes (HSPs) in tolerant genotypes indicate the molecular network associated with heat tolerance in cucumber. Among the HSPs, higher accumulation of HSP70 and HSP90 were recorded in the tolerant genotype, WBC-13 under heat stress condition indicating their critical role. Besides, *Rubisco S, Rubisco L* and *CsTIP1b* were upregulated in the tolerant genotypes under heat stress condition. Therefore, the HSPs in combination with photosynthetic and aquaporin genes were the underlying important molecular network associated with heat stress tolerance in cucumber. The findings of the present study also indicated negative feedback of *G-protein alpha unit* and oxygen evolving complex in relation to heat stress tolerance in cucumber. These results indicate that the thermotolerant cucumber genotypes enhanced physio-

biochemical and molecular adaptation under high-temperature stress condition. This study provides foundation to design climate smart genotypes in cucumber through integration of favorable physio-biochemical traits and understanding the detailed molecular network associated with heat stress tolerance in cucumber.

KEYWORDS

cucumber, heat stress, physiological and biochemical traits, antioxidant enzymes, RT-PCR, HSPs

Introduction

Agriculture and food safety are threatened by extreme climate change. High temperature (HT) stress restricts plant development and productivity and, in severe cases, even results in plant death (Bita and Gerats, 2013; Gong et al., 2020). Due to global warming, vegetable crops in tropical and subtropical areas, including tomato, pepper, and cucumber experienced decreased fruit number, weight, and shape throughout spring and autumn (Battisti and Naylor, 2009; Zhao et al., 2017). Abiotic stresses, such as drought stress on plants, will also be exacerbated by the high-temperature environment, which will also lead to the outbreak of several diseases (Cohen and Leach, 2020; Cohen et al., 2021). In particular, heat greatly affects plant growth and development, immunity and circadian rhythm, and poses a serious threat to the global food supply chain (Liu et al., 2015).

Cucumber is an annual vine crop is native to the Himalayan foothills (Wóycicki et al., 2011). India is the center of diversity for cultivated cucumber. Secondary centers of diversity for cucumber exist in China and the Near East (Meglic et al., 1996; Staub et al., 1999). Natural and artificial selection has contributed to the genetic differences observed between the cultivated and wild cucumber varieties (Wang et al., 2018). Cucumber is sensitive to high temperatures instead of its origin in tropical regions. The optimal temperature for its growth and development is 25-28°C during the day and 15-20°C at night (Tian et al., 2002). Cucumber plants in the early stage are susceptible to heat stress (HS) with the increasing global temperature, especially during the late spring and early autumn cultivation, where the temperature often exceeds 35°C (Tian et al., 2002). Besides, during the summer season, the temperature of cultivation in open fields often exceeds 35°C even during the seedling stage which leads to sunburn of leaves, growth retardation of stems and roots, and even plant death, which severely affects further growth of cucumber. In general, cucumber prefers a moderately warm environment, and the suitable temperature for growth is 20–30°C and at a temperature above 35°C abnormal growth is very common. Long-term high temperature above 40°C often results in metabolic malfunction, water loss and wilting of cucumber, and short-term extreme high temperature above 50°C leads to macro-molecule degradation, cell structure damage, dehydration and death, which has a great impact on the yield and quality of cucumber (Yu et al., 2018). Heat-related damage to cucumbers causes the blooms to fall easily, the leaves to droop and turn yellow, and the fruit to become malformed. In more extreme situations, the heat can cause the vine to completely wither, the top to die, the blooms to wither, and the leaves to get burnt and wilted. Thus, heat stress poses a significant threat for cucumber development, affecting production and quality during the summer. In the earlier studies, heat tolerance in the seedling stage was conducted using a limited number of genotypes, and studies were limited to the selected physiological traits like electrical conductivity, antioxidant enzymes, and chlorophyll estimation. Till date, no detailed studies regarding the physiological and biochemical basis of heat tolerance and the correlation of the heat stress response with the adult growth stage are reported.

Reactive oxygen species (ROS) are produced when high temperature (HT) is present, and these ROS cause membrane and pigment peroxidation, which reduces membrane permeability (Niu and Xiang, 2018). Additionally, HT changes the chloroplast and metabolite composition of leaves, which lowers the photosynthetic rate and causes plants to have a shorter lifespan and produce less (Djanaguiraman et al., 2018). The direct and indirect impacts of heat on sensor molecules located in many cellular components allow plants to detect heat stress. In response to heat stress, plants have evolved different avoidance and tolerance-based mechanisms. Heat avoidance includes all those strategies that plants adapt to avoid heat stress exposure while to survive under stressful conditions plants have evolved multiple of intrinsic tolerance mechanisms to adapt to high-temperature stress (Wang et al., 2016). To maintain life under high temperatures, plants have developed a variety of tolerance mechanisms. Physio-biochemical and molecular changes are important underlying mechanisms among the standard stress management techniques. Chlorophyll retention under stress is an effective way to sustain biomass production and crop yield (Wang et al., 2008). The ability to tolerate heat is demonstrated by a high membrane stability index and a high relative water content. To counteract the consequences of stress, it is crucial to have stress proteins, osmoprotectants, free-radical scavengers, ion transporters, and components involved in signaling cascades and transcriptional regulation (Wang et al., 2004). The understanding of various physiological, molecular, and biochemical pathways can facilitate the development of superior heat-tolerant genotypes in cucumber. Therefore, this study was conducted to address the aforementioned questions with objectives 1. To investigate the physio-biochemical basis for heat tolerance in cucumber. 2. Understanding the molecular networks for heat tolerance in cucumber for the key genes associated with heat stress tolerance.

Material and methods

Plant materials

The present experiment was carried out during 2021-22 at National phytotron facility, ICAR-Indian Agricultural Research Institute, New Delhi. The materials for present investigation comprised of 10 germplasms of cucumber collected from various parts of India. On the basis of their performance in two rounds of screening and performance under open field conditions, these genotypes are grouped into thermotolerant and thermosensitive. Five thermotolerant 'TT' and five thermosensitive 'TS' cucumber lines were grown in the pots with standard NPH potting mixture of soil, sand and coco peat in ratio 2:1:1 (v/v) (Table 1; Figure 1). Three seeds were sown in each pot and 5 replications were maintained for each genotype in both control and treatment conditions. A completely randomized design (CRD) with three replications per genotype per treatment was used. Data were taken from 3 randomly selected replications from each genotype. Seedlings were irrigated by sprayer cans with water and Hoagland nutrient solution every day morning and kept in such a condition that there was no water deficit. More frequent watering of plants was done under treatment to avoid any moisture stress. To avoid infections with fungal diseases, seedlings were occasionally sprayed with captan 2g/liter.

High-temperature stress treatments

In control conditions plants were maintained at normal temperature (30°C/25°C day/night) in same glass house compartment throughout the experiments, while for treatment, plants were initially grown under normal conditions for twenty days, later seedlings were transferred to growing chamber for high temperature treatment. Therefore, the first HT treatment was set as 35°C for 12 h in the daytime and 30°C for 12 h in the night for 5 days, later growing chamber temperature raised to 40°C for 12 h in the daytime and 35°C for 12 h in the night for 5 days. Under the growth chamber, the plants were grown in growth media and were maintained without any moisture stress. Application of water and Hogland solution was practiced multiple times in a day to avoid water stress for the plants kept under temperature stress condition. Measurements were done on first or second true leaf of seedlings from three replications of each genotype in both control and treatment conditions. The physio-biochemical measurements were carried out at three different time intervals. First reading was recorded before transferring of the plants to growing chamber for treatment (day 0 control and day 0 stress). Remaining two readings were recorded after transferring of the plants to growing chamber for treatment. Second reading was noted on the last day of moderate stress (35°C/30°C) treatment (day 5 stress) and on same day readings were recorded under control conditions (day 5 control). Third reading was observed on the last day of high temperatures stress (40°C/35°C) treatment (day 10 stress) and on the same day data were recorded in control conditions (day 10 control).

Chlorophyll measurement

The relative chlorophyll content of the leaves was measured by a SPAD chlorophyll meter (Apogee chlorophyll content meter). The measurements were done on the adaxial surface of the first and second true leaves in a single plant in five points uniformly distributed throughout the leaves and the average values were taken for analysis. The average value of two leaves was used to estimate the chlorophyll content. Chlorophyll was measured in CCI units. The CCI values of the instrument ranges from 1 to 100.

Membrane stability index

Membrane stability index (MSI) of fresh leaves was determined as per the method suggested by Bailly et al. (1996). For this purpose, two plants of each genotype were randomly chosen per replicate and two leaf samples per plant were taken as follows. One sample from first true leaf and the second sample from second true leaf to represent mature and developing leaves, respectively. The conductivity of solutions was measured using a conductivity bridge meter and MSI calculated using following formulae:

TABLE 1 List of the diverse set of genotypes expressed variable response to heat stress along with their key features.

	Genotype	Heat stress response	Salient feature	Yield under control conditions
1	DARL 106	Tolerant	Monoecious, non-parthenocarpic	2.4 Kg/Plant
2	DGC-103	Tolerant	Gynoecious non-parthenocarpic	2.8 Kg/Plant
3	WBC 13	Very Tolerant	Monoecious, non-parthenocarpic	2.0 Kg/Plant
4	WBC 39-1	Tolerant	Monoecious, non-parthenocarpic	2.0 Kg/Plant
5	DC83	Very Tolerant	Monoecious, non-parthenocarpic	3.0 kg/Plant
6	BAROPATTA	Sensitive	Monoecious, non-parthenocarpic	2.0 kg/Plant
7	EC-753493	Sensitive	Monoecious, non-parthenocarpic	2.0 kg/Plant
8	WBC 22	Sensitive	Monoecious, non-parthenocarpic	2.2 kg/Plant
9	DC-206	Sensitive	Monoecious, non-parthenocarpic	2.8 kg/Plant
10	DGPC-59	Very Sensitive	Predominantly gynoecious, parthenocarpic	2.6 kg/Plant

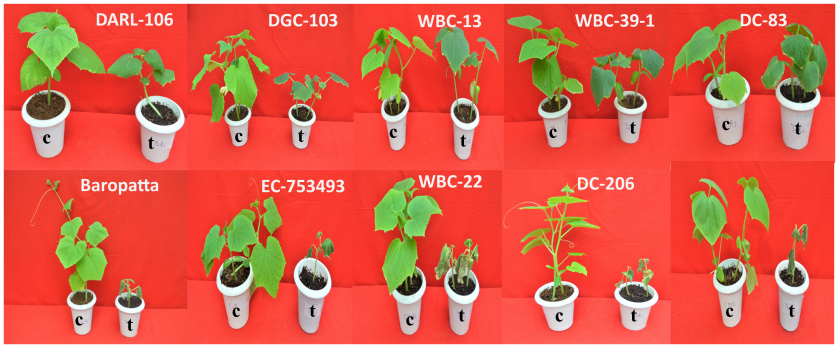

FIGURE 1
Heat stress response of the ten diverse cucumber genotypes under growth chamber with temperature stress treatment (40°C/35°C) along with controls (30°C/25°C); c-Control conditions, t-Treatment conditions (40°C/35°C).

$$\text{Membrane stability index MSI} = 1 - \frac{C1}{C2}$$

Where C1 conductivity at 40°C; C2 conductivity at 100°C

Relative water content (RWC)

Leaf samples were used for Relative water content (RWC) assay according to the method described by Barrs and Weatherley, 1962. RWC in leaves of the plants was measured from two randomly chosen fully developed leaves. A 10 cm long segment was excised from the middle portion of the leaf and cut into two equal halves; FW was recorded and the leaf segments were immediately immersed into distilled water in a Petri plate for 4 h at room temperature. The leaf segments were blotted properly and turgid weight (TW) was recorded. Then, the samples were placed in a paper bag and dried in a hot air oven at 70°C for 24 h and the dry weight (DW) was recorded. The fresh weight (W1), turgid weight (W2), and dry weight (W3) of leaves were measured, and the RWC was calculated as follows:

$$\text{RWC}(\%) = \frac{(W1 - W3)}{(W2 - W3)} \times 100$$

Photosynthesis and canopy temperature

Gas exchange measurements were performed using a portable photosynthesis system (Li-6400; LI-COR, Inc., Lincoln, NE, USA) in the morning between 9:00-10: 30am, on the first fully expanded leaf between 1 and 6 h of the light period on the third day of control (day 3 control), and moderate stress (day 3 stress) and high temperature treated (day 8 stress) plants. Air temperature was between 25°C - 30°C as per the temperature of the growth chamber. The light response curves were measured at ambient CO_2 concentrations (350-400 µmol) during photosynthetic observations. Leaves were illuminated with photon flux densities 1500 µmol photons $m^{-2}s^{-1}$. Net photosynthetic rate (P_N), stomatal conductance (g_s), transpiration rate (E), and intracellular CO_2 concentration (Ci) was measured. Canopy temperature of cucumber leaves was performed using an imaging FLUKE thermal imager.

Morphological parameters

Morphological parameters like shoot length, fresh weight and dry weight, measurements were taken only once in both control and treatment conditions (10-day control and 10-day stress). Three plants from each genotype were for recording observations. Fresh weight and shoot length were measured immediately after harvesting of genotypes, whereas dry weight was measured by drying the samples in an oven at 85°C for two days.

Biochemical parameters

Proline content

Proline (Pro) content was determined according to the protocol described previously by Bates et al. (1973). The second true leaf (0.5 g) were used to extract the proline, homogenized in 3% sulfosalicylic acid, and the supernatant was mixed with an equal volume of glacial acetic acid and acidic ninhydrin for the reaction. Following heating under 100°C for 30 min, a volume of 5 ml toluene was added to the mixture. The absorbance of the supernatant was measured at 520 nm using a UV–vis spectrometer and the standard curves which were made using l-proline in the same way. Proline activity is expressed as $\mu molg^{-1}FW$.

Super oxide dismutase

Super oxide dismutase content was determined according to the protocol described previously by Hwang et al. (1999). The activity of superoxide dismutase was measured by the ability of the enzyme to inhibit the light-dependent reduction of nitro blue tetrazolium chloride (NBT). The mixture was read at 560 nm and the amount of enzyme required to produce a 50% inhibition in the photoreduction rate of NBT was defined as one unit of SOD activity calculated as enzyme units (EU) per g of sample per minute ($Ug^{-1}FW\ min^{-1}$).

Catalase and guaiacol peroxidise

The catalase and guaiacol peroxidise activities were assayed as per the protocol of Pereira et al. (2002) and guaiacol peroxidase as per the protocol of Ramiro et al. (2006). CAT activity was measured by following the decomposition of H_2O_2 at 240 nm in a reaction mixture containing 50 mM phosphate buffer (pH 7.0) and 15 Mm H_2O_2. Enzyme activity was expressed as $Ug^{-1}FW$ For GPX, the oxidation of guaiacol was measured by following the increase in absorbance at 470 nm for 1 min. The assay mixture contained 50 mM phosphate buffer (pH 7.0), 0.1 mM EDTA, 10 mM guaiacol and 10 mM H_2O_2. GPOX activity was expressed as $\mu molg^{-1}min^{-1}$

MDA analysis

Determination of malonaldehyde (MDA) content was described by Dhindsa et al. (1981) and modified by Wang et al. (2018). A total of 0.5 g leaves were ground into powder using 0.5% trichloroacetic acid (TCA), then centrifuged at 3000g for 20 min. The supernatant (2 mL) was added the same volume of 0.5% thibabituric acid (TBA). After that the mixture was boiled at 100°C for 30 min to obtain the supernatants. Finally, we recorded the absorption wavelengths of supernatants on 450 532 and 600 nm. MDA activity was expressed as $nmolg^{-1}FW$.

Protein content

Protein quantification

Total soluble proteins were determined according to the method of Bradford (1976) with bovine serum albumin as a calibration standard. The homogenised leaf samples were used for preparation of the aliquot and estimation of protein. Protein content is expressed in terms of mgg^{-1}.

Ascorbate peroxidase content

Ascorbate peroxidase activity was determined according to Wang et al. (1991) by estimating the decreasing rate of ascorbate oxidation at 290 nm. APOD extraction was performed in 50 mM Tris–HCl (pH 7.2), 2% PVP, 1 mM EDTA, and 2 mM ascorbate. The reaction mixture consisted of 50 mM KH_2PO_4 buffer (pH 6.6), 2.5 mM ascorbate, 10 mM H_2O_2, and enzyme, containing 100 µg proteins in a final volume of 1 mL. The enzyme activity was calculated from the initial rate of the reaction using the extinction coefficient of ascorbate (E = 2.8 mM cm−1 at 290 nm). APOX activity expressed in terms of $\mu mol\ min^{-1}g^{-1}$.

Hydrogen peroxidase content

Hydrogen peroxidase contents were determined by the method Ohkawa et al. (1979). For determination of hydrogen peroxide, 0.5 mL of 0.1 M Tris–HCl (pH 7.6) and 1 mL of 1 M KI were added to 0.5 mL of supernatant. After 90 min, the absorbance was measured at 390 nm. A standard curve for hydrogen peroxide was prepared to calculate hydrogen peroxide concentration in each sample. Hydrogen peroxidase is expressed in terms of $\mu mol\ g^{-1}FW$.

RT-PCR analysis

Two contrasting genotypes, WBC-13 and DGPC-59 (Supplementary Figure 1) were used for gene expression analysis under two different stress conditions (35°C/30°C and 40°C/35°C) along with control without any stress (30°C/25°C). Total RNA from cucumber leaves under different stress conditions was extracted using Trizol reagent. RNA was quantified by spectrophotometric analysis and the quality was evaluated through agarose gel electrophoresis. First-strand complementary DNA (cDNA) synthesis was carried out using the user instruction (Promega, USA). Relative expression of 18 important genes associated with heat tolerance were conducted using two contrasting genotypes under two different stress conditions (Table S1). Quantitative real-time PCR was carried out using Light Cycler (Roche) with Light Cycler Fast Start DNA Master SYBR Green kit (Roche). Amplification of stress-related genes was carried out according to the manufacturer's protocol. Reaction mixture of 20 µl contains 1.5 µl cDNA, 0.3 µl of primer (forward and reverse), 12.5 µl SYBR Premix, and 5.4 µl dH_2O. Expression analysis of all genes were tested in triplicate with appropriate primers along with *Actin* used as an internal control. The gene expression data were calculated comparative to *Actin*, and Ct values of the used target genes were normalized using the Ct values of *Actin*. The levels of mRNA were also normalized with *Actin* and its value was expressed relative to that of the control, which was given an arbitrary value 1 (Liu et al., 2012). The relative differential gene expression was measured according to the equation $2-\Delta\Delta Ct$ (Livak and Schmittgen, 2001). The final data of RT-PCR were calculated from three experimental replicates.

Statistical analysis

The data collected were analyzed in R software using one- or two-way ANOVA after verifying data for homogeneity and normality. The correlation among the variables was analyzed using Spearman correlation and a correlogram was constructed for each temperature treatment in the controlled heat-stress experiment and total plant responses from two stages for the field experiment. The multiple comparisons of means were made using Tukey's HSD (Honestly Significant Difference) under $\alpha \leq 0.05$. For only the significant main effects of stage, mean separation for the two stages were done within each level of varieties using Tukey's HSD (Honestly Significant Difference) at $\alpha \leq 0.05$.

Results

Based on screening of genotypes under controlled environmental conditions and their validation under natural field conditions one set of 5 genotypes each in the tolerant and susceptible were selected for their detailed studies on important physiological and biochemical traits.

Physiological basis of high temperature tolerance

Chlorophyll content

Chlorophyll content significantly decreased in all genotypes under heat stress treatments over the control (Table 2). However, TT genotypes were able to maintain chlorophyll content, shown decrease of 5.5% and 19.1% whereas susceptible genotypes shown higher chlorophyll degradation, shown decrease of 14.9% and 30.4% in moderate temperature treatment (35°C/30°C) and high temperature treatment (40°C/35°C), respectively. Among the genotypes, DC-83 (20.8 CCI units) and DGC-103 (17.7 CCI units) had highest chlorophyll at moderate stress condition. In peak stress condition, higher chlorophyll concentration was retained by DC-83 (18.1 CCI units) and DARL-106 (15. 3 CCI units) whereas DC-206 (11.0 CCI units, 7.6 CCI units) and EC-753493 (11.7 CCI units, 7.7 CCI units) shown lowest chlorophyll content at moderate as well as high temperature conditions (Table 3). This differential rate of decrease in chlorophyll content across cucumber genotypes showed the presence of genetic variability for chlorophyll retention under high temperature conditions. For chlorophyll concentration, genotype and genotype × temperature interaction effects were highly significant ($p<0.05$) (Table S2).

Membrane stability index (MSI)

Significant genetic variability in high temperature induced electrolyte leakage was also observed in cucumber genotypes taken for study. Tolerant genotypes showed slight decrease in MSI under heat stress condition, whereas drastic reduction in MSI was recorded in case of sensitive genotypes under temperature stress condition (Table 2). MSI decreased by 7.0% and 13.8% in tolerant group in contrast to 24.3% and 32.5% in susceptible group under moderate and high treatment conditions, respectively. In Table 3, it was depicted that at 35°C/30°C treatment and 40°C/35°C treatment, highest membrane stability was observed WBC-13 (78.5%,73.7%) and DC-83 (76.2%, 71.8%) whereas minimum in DGPC-59 (58.6%) followed by Baropatta (60.2%) at moderate stress conditions and DGPC-59 (49.2%) followed by EC-753493 (53.1%) at high stress conditions. Genotype, temperature and genotype × temperature interaction had an impact on membrane stability and significant effects were observed (Table S2).

Relative water content

In cucumber seedlings, RWC was measured under different heat stress conditions. Under stress combination, RWC levels showed a significant decrease as compared to control (Table 2). Heat stress resulted drastic reduction in RWC in all susceptible genotypes compared to tolerant genotypes. RWC levels decreased by 9.4% and 12.7% in tolerant group whereas RWC decreased by 20.2% and 26.2% in susceptible group under heat treatment over the control. It was depicted that under 35°C/30°C and 40°C/35°C treatments, highest tension of relative water content was observed WBC-13 (79.4%,76.3%) and DGC-103 (78.5%, 75.9%) whereas minimum water content was seen in WBC-22 (60.8%, 56.7%) followed by DGPC-59 (63.1%, 59.5%) at moderate and high temperature stress conditions, respectively (Table 3). The effects of genotype, temperature, and genotype × temperature interaction on RWC were presented in Table S1 and were significant ($p<0.05$).

Canopy temperature

It was evident that the tolerant genotypes were maintaining comparatively less canopy temperature by transpirational cooling than the susceptible genotypes in high temperature treatment conditions (Figure 2; Supplementary Figure 2). Lowest canopy temperature was recorded in the tolerant genotypes WBC-13, DGC-103 and DC-83 at moderate temperature stress and the same of set of genotypes also maintained a comparatively lowerer canopy temperature under high temperature stress condition (Table 3). The effects of genotypes, temperature, and genotype × temperature interaction effects on canopy temperature were significant (Table S2).

Photosynthetic rate and leaf gas exchange related parameters

Leaf Pn, Gs, Ci, and Tr were significantly decreased on exposure to heat stress conditions in susceptible genotypes compared to tolerant genotypes. The net photosynthesis of susceptible genotypes was significantly lower than the tolerant genotypes under temperature stress conditions (Supplementary Figure 3A). Percentage decrease of Pn was 29.4% and 67.7% in susceptible groups in contrast to 7.9% and 24.1% in tolerant group under heat stress conditions (Table 4).

TABLE 2 Effect of high temperature treatment on important physiological parameters in cucumber.

Parameter	Tolerant group					Susceptible group				
	Control (mean)	35°C/30°C (mean)	Loss (%) at 35°C/30°C	40°C/35 (mean)	Loss (%) at 40°C/35°C	Control (mean)	35°C/30°C (mean)	Loss (%) at 35°C/30°C	40°C/35°C(mean)	Loss (%) at 40°C/35°C
Chlorophyll (CCI)	17.2	16.2***	5.8	13.9**	19.1	17.1	14.5**	14.9	11.9**	30.4
MSI (%)	81.7	76.0**	7.0	70.4**	13.8	82.7	62.6***	24.3	55.9***	32.5
RWC (%)	84.0	76.2**	9.4	73.3***	12.7	83.1	66.3***	20.2	61.3***	26.2
CFC	0.819	0.811***	0.9	0.806**	1.5	0.813	0.799*	1.8	0.774*	4.9

Significant at *p = 0.05, **p = 0.01 and ***p = 0.001.

TABLE 3 Evaluation of diverse genotypes for chlorophyll content, membrane stability Index, relative water content and canopy temperature at control, moderate and high temperature conditions.

		Chlorophyll content					Membrane stability index				
Sl.no	Genotype	Control (m ± SE)	35°C/ 30°C(m ± SE)	Loss (%) at 35°C/ 30°C	40°C/ 35°C(m ± SE)	Loss (%) at 40°C/ 35°C	Control (m ± SE)	35°C/ 30°C(m ± SE)	Loss (%) at 35°C/ 30°C	40°C/ 35°C(m ± SE)	Loss (%) at 40°C/ 35°C
1	DARL-106	17.7 ± 0.24^{bc}	16.8 ± 1.57^{abc}	4.9	15.3 ± 1.58^{ab}	13.7	82.7 ± 0.36^{a}	74.6 ± 0.82^{a}	9.9	69.0 ± 0.35^{bc}	16.6
2	DGC-103	18.7 ± 0.35^{b}	17.7 ± 0.50^{ab}	5.5	14.9 ± 0.74^{abc}	20.3	79.6 ± 1.59^{a}	74.5 ± 1.58^{a}	6.4	70.8 ± 0.84^{abc}	11.0
3	WBC-13	14.3 ± 0.17^{fg}	13.4 ± 1.23^{bcd}	5.8	12.0 ± 1.46^{bcd}	16.1	83.0 ± 1.48^{a}	78.5 ± 0.87^{a}	5.4	73.7 ± 1.51^{a}	11.2
4	WBC-39-1	13.6 ± 0.12^{g}	12.3 ± 0.49^{cd}	9.6	9.4 ± 0.29^{cd}	30.9	82.6 ± 1.69^{a}	75.8 ± 0.68^{a}	8.2	66.4 ± 0.31^{cd}	19.6
5	DC-83	21.8 ± 0.08^{a}	20.8 ± 0.12^{a}	4.6	18.1 ± 0.64^{a}	17.1	80.4 ± 0.55^{a}	76.2 ± 0.16^{a}	5.1	71.8 ± 0.55^{ab}	10.6
6	BAROPATTA	15.8 ± 0.25^{de}	12.3 ± 0.27^{cd}	21.9	9.8 ± 0.70^{bcd}	38.2	82.5 ± 1.05^{a}	60.2 ± 0.28^{c}	27.1	59.9 ± 0.48^{e}	27.4
7	EC-753493	17.0 ± 0.30^{cd}	11.7 ± 0.53^{cd}	31.4	7.7 ± 0.46^{d}	54.9	82.4 ± 0.91^{a}	67.9 ± 0.09^{b}	17.6	53.1 ± 0.77^{fg}	35.6
8	WBC-22	17.6 ± 0.20^{bc}	14.3 ± 0.43^{bcd}	18.6	11.7 ± 0.67^{bcd}	33.7	84.4 ± 1.36^{a}	65.8 ± 0.95^{b}	22.0	54.1 ± 0.74^{f}	35.9
9	DC-206	18.6 ± 0.17^{b}	11.0 ± 1.44^{d}	40.7	7.6 ± 1.31^{d}	59.1	81.5 ± 0.01^{a}	60.4 ± 1.26^{c}	25.9	62.9 ± 0.37^{de}	22.8
10	DGPC-59	15.6 ± 0.26^{ef}	13.3 ± 0.19^{bcd}	14.6	10.4 ± 0.78^{bcd}	33.0	82.5 ± 1.12^{a}	58.6 ± 0.60^{c}	29.0	49.2 ± 0.38^{g}	40.4
		Relative water content					Canopy temperature				
Sl.no	Genotype	Control	35°C/ 30°C	Loss (%) at 35°C/ 30°C	40°C/ 35°C	Loss (%) at 40°C/ 35°C	Control	35°C/ 30°C	CTD	40°C/ 35°C	CTD
1	DARL-106	85.9 ± 0.79^{ab}	72.6 ± 0.89^{bc}	15.5	71.5 ± 1.04^{bcd}	16.7	28.1 ± 0.58^{ab}	32.6 ± 0.15^{cd}	2.3 ± 0.12	34.0 ± 0.37^{b}	6.0 ± 0.30
2	DGC-103	85.9 ± 0.11^{ab}	78.5 ± 0.57^{a}	8.6	75.9 ± 0.19^{ab}	11.7	27.9 ± 0.49^{ab}	32.4 ± 0.22^{d}	2.5 ± 0.18	35.8 ± 0.49^{b}	4.2 ± 0.40
3	WBC-13	83.5 ± 0.89^{ab}	79.4 ± 1.42^{a}	4.9	76.3 ± 0.75^{a}	8.7	26.8 ± 0.54^{ab}	32.1 ± 0.03^{d}	2.8 ± 0.03	34.2 ± 0.19^{b}	5.8 ± 0.15
4	WBC-39-1	81.8 ± 0.24^{bc}	72.3 ± 0.31^{bc}	11.6	69.3 ± 0.59^{cd}	15.2	29.1 ± 0.58^{a}	32.9 ± 0.12^{bcd}	2.1 ± 0.09	34.2 ± 0.47^{b}	5.8 ± 0.38
5	DC-83	82.8 ± 0.95^{bc}	77.7 ± 1.62^{ab}	6.1	73.4 ± 0.19^{abc}	11.3	27.6 ± 0.25^{ab}	32.3 ± 0.31^{d}	2.7 ± 0.25	34.3 ± 0.47^{b}	5.7 ± 0.39
6	BAROPATTA	87.7 ± 0.07^{a}	72.1 ± 1.09^{ab}	17.7	67.2 ± 0.49^{d}	23.3	26.7 ± 0.35^{b}	34.4 ± 0.06^{abc}	0.6 ± 0.05	38.3 ± 0.49^{a}	1.7 ± 0.40
7	EC-753493	78.6 ± 0.20^{c}	64.9 ± 0.91^{de}	17.4	60.5 ± 0.44^{ef}	23.0	27.2 ± 0.52^{ab}	34.7 ± 0.09^{ab}	0.3 ± 0.07	38.8 ± 0.84^{a}	1.2 ± 0.68
8	WBC-22	82.9 ± 0.28^{bc}	60.8 ± 0.21^{e}	26.7	56.7 ± 0.80^{f}	31.6	27.0 ± 0.71^{ab}	34.6 ± 0.19^{ab}	0.4 ± 0.15	39.7 ± 0.43^{a}	0.3 ± 0.35
9	DC-206	83.4 ± 0.85^{ab}	67.1 ± 0.66^{cd}	19.5	62.6 ± 0.96^{e}	25.0	27.1 ± 0.43^{ab}	34.7 ± 0.09^{ab}	0.3 ± 0.07	39.2 ± 0.59^{a}	0.8 ± 0.48
10	DGPC-59	82.5 ± 0.84^{bc}	63.1 ± 0.72^{de}	23.5	59.5 ± 1.16^{ef}	27.9	27.4 ± 0.40^{ab}	34.9 ± 0.09^{a}	0.1 ± 0.07	39.6 ± 0.36^{a}	0.4 ± 0.29

Values within a group in a column bearing different letters are significantly different as determined by Tukey's test.

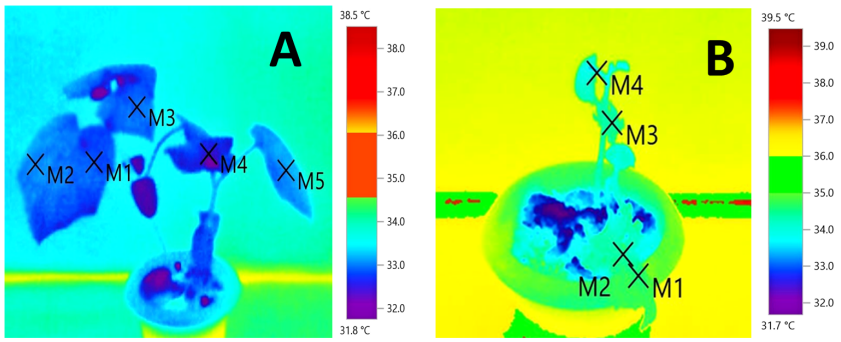

FIGURE 2
Infrared thermography of the thermotolerant cucumber genotype, WBC-13 **(A)** along with susceptible genotype, DGPC-59 **(B)** at high stress conditions 40°C/35°C.

Similarly, stomatal conductance (Gs) of all genotypes decreased to varied extent at high temperature treatments compared to the controls. Tolerant genotypes expressed higher stomatal conductance compared to susceptible genotypes under heat stress conditions (Supplementary Figure 3B). Reduction in stomatal conductance was 23.6% and 37.7% in tolerant group and 55.8% and 80.2% among the susceptible genotypes (Table 4). Tolerant genotypes recorded higher internal CO_2 concentration (Ci) at high temperature treatments compared to the susceptible genotypes (Supplementary Figure 4A). Tolerant plants shown less reduction in Ci percentage (29.5% and 46.1%) as compared to drastic reduction in susceptible genotypes (37.7% and 58.9%) under stress conditions (Table 4). Transpiration rate (Tr) was significantly reduced at high temperature treatment in susceptible genotypes compared to tolerant genotypes (Supplementary Figure 4B). High temperature adversely affected transpiration rate of susceptible genotypes (55.5% and 66.3% reduction) compared to tolerant varieties (15.36% and 14.87%) as shown in Table 4.

The tolerant genotype, DC-83 (19.2 µmol $CO_2m^{-2}s^{-1}$, 16.1 µmol $CO_2m^{-2}s^{-1}$) and WBC-13(18.3 µmol $CO_2m^{-2}s^{-1}$, 16 µmol $CO_2m^{-2}s^{-1}$) had stable net photosynthesis in moderate and high temperature stress conditions, respectively. Drastic reduction in photosynthesis was recorded in Baropatta (12.7 µmol $CO_2m^{-2}s^{-1}$), WBC-22 (13.2 µmol $CO_2m^{-2}s^{-1}$) at moderate heat stress conditions and DGPC-59 (4.5 µmol $CO_2m^{-2}s^{-1}$) and EC-753493 (5.1 µmol $CO_2m^{-2}s^{-1}$) in peak stress conditions. Maximum stomatal conductance was observed in DC-83 (0.57 mol $H_2Om^{-2}s^{-1}$) followed by WBC-13(0.57 mol $H_2Om^{-2}s^{-1}$) and minimum was seen in DGPC-59 (0.24 mol $H_2Om^{-2}s^{-1}$), followed by DC-206 (0.25 mol $H_2Om^{-2}s^{-1}$) in moderate stress. Similarly, WBC-13 (0.53 mol $H_2Om^{-2}s^{-1}$) and DC-83 (0.49 mol $H_2Om^{-2}s^{-1}$) had high stomatal conductance where as drastic drop in stomatal conductance was recorded in DGPC-59 (0.08 mol $H_2Om^{-2}s^{-1}$) and Baropatta (0.11 mol $H_2Om^{-2}s^{-1}$) at peak stress conditions (Table 5).

Maximum internal CO_2 concentration was observed in DC-83 (558.9 µmolCO_2mol^{-1}) followed by DARL 106 (548.9 µmolCO_2mol^{-1}) and minimum was recorded in DGPC-59 (407.9 µmolCO_2mol^{-1}), followed by WBC-22 (457.4 µmolCO_2mol^{-1}) in moderate stress. WBC-13 (490.9 µmolCO_2mol^{-1}) and DGC-103 (413.0 µmolCO_2mol^{-1}) had high internal CO_2 concentration where as drastic drop in stomatal conductance was recorded in DGPC-59 (272.3 µmolCO_2mol^{-1}) and WBC-22 (260.4 µmolCO_2mol^{-1}) at peak stress conditions. Similarly, highest transpiration rate was recorded in DC-83 (4.8 m mol $H_2Om^{-2}s^{-1}$) followed by WBC-13 (4.5 m mol $H_2Om^{-2}s^{-1}$) and minimum was recorded in WBC-22 (2.3 m mol $H_2Om^{-2}s^{-1}$) followed by DGPC-59 (2.4 m mol $H_2Om^{-2}s^{-1}$) in moderate stress and WBC-13 (4.7 m mol $H_2Om^{-2}s^{-1}$), DC 83 (4.7 m mol $H_2Om^{-2}s^{-1}$) shown highest transpiration rate whereas WBC-22 (1.8 m mol $H_2Om^{-2}s^{-1}$) followed by DGPC-59 (1.9 m mol $H_2Om^{-2}s^{-1}$) had lowest transpiration rate at peak stress conditions (Table 5).

Genotype, temperature and genotype × temperature interaction had an impact on photosynthetic pigment and leaf gas exchange–related parameters and significant effects were observed (Table S3).

TABLE 4 Effect of high temperature treatment on photosynthetic and gaseous parameters in cucumber genotypes.

Parameter	Tolerant group					Susceptible group				
	Control (mean)	35°C/30° C (mean)	Loss (%) at 35°C/30°C	40°C/35 (mean)	Loss (%) at 40°C/35°C	Control (mean)	35°C/ 30°C (mean)	Loss (%) at 35°C/30°C	40°C/35° C(mean)	Loss (%) at 40°C/35°C
Pn	18.7	17.2*	7.9	14.2*	24.1	19.5	13.7**	29.4	6.3**	67.7
Gs	0.691	0.528*	23.6	0.431*	37.7	0.685	0.303*	55.8	0.136*	80.2
Ci	763.9	538.4***	29.5	412.0***	46.1	739.6	460.8***	37.7	304.3***	58.9
Tr	5.0	4.2**	15.3	4.2**	14.8	6.8	3.0*	55.5	2.3*	66.3

Significant at *p = 0.05, **p = 0.01 and ***p = 0.001.

TABLE 5 Evaluation of ten diverse genotypes for Net Photosynthesis, Stomatal Conductance, Internal CO_2 concentration and Transpiration rate under control, moderate and high temperature conditions.

		Net Photosynthesis					Stomatal Conductance				
Sl.no	Genotype	Control (m ± SE)	35°C/ 30°C(m ± SE)	Loss (%) at 35°C/ 30°C	40°C/ 35°C(m ± SE)	Loss (%) at 40°C/ 35°C	Control (m ± SE)	35°C/ 30°C(m ± SE)	Loss (%) at 35°C/ 30°C	40°C/ 35°C(m ± SE)	Loss (%) at 40°C/ 35°C
1	DARL-106	16.9 ± 0.23^{cd}	15.5 ± 0.12^{de}	3.5	13.5 ± 0.02^{b}	16.2	0.83 ± 0.07^{b}	0.51 ± 0.03^{a}	38.4	0.40 ± 0.001^{b}	51.3
2	DGC-103	17.1 ± 0.36^{cd}	15.8 ± 0.03^{cd}	7.3	12.5 ± 0.03^{b}	26.4	0.66 ± 0.02^{bcd}	0.47 ± 0.02^{a}	28.1	0.42 ± 0.007^{ab}	34.4
3	WBC-13	18.6 ± 0.01^{b}	18.3 ± 0.46^{a}	1.6	15.9 ± 0.40^{a}	14.2	0.67 ± 0.105^{bcd}	0.56 ± 0.01^{a}	15.8	0.53 ± 0.008^{a}	20.1
4	WBC-39-1	21.0 ± 0.05^{a}	16.9 ± 0.12^{bc}	19.6	12.6 ± 0.43^{b}	39.8	0.61 ± 0.04^{bcd}	0.50 ± 0.004^{a}	25.2	0.27 ± 0.007^{c}	60.2
5	DC-83	19.2 ± 0.19^{b}	17.3 ± 0.58^{ab}	5.6	16.0 ± 0.58^{a}	21.1	0.60 ± 0.01^{cd}	0.57 ± 0.005^{a}	5.0	0.49 ± 0.004^{ab}	16.8
6	BAROPATTA	17.6 ± 0.23^{c}	12.6 ± 0.04^{g}	28.2	7.9 ± 0.45^{c}	55.2	1.36 ± 0.04^{a}	0.36 ± 0.002^{a}	73.2	0.11 ± 0.004^{de}	92.3
7	EC-753493	21.9 ± 0.02^{a}	13.3 ± 0.06^{fg}	39.0	5.0 ± 0.05^{ef}	76.8	0.79 ± 0.02^{bc}	0.26 ± 0.001^{a}	67.1	0.20 ± 0.003^{cd}	75.3
8	WBC-22	16.4 ± 0.17^{d}	13.2 ± 0.07^{fg}	19.6	7.7 ± 0.07^{cd}	53.2	0.49 ± 0.001^{de}	0.38 ± 0.005^{a}	22.4	0.18 ± 0.001^{cde}	66.0
9	DC-206	19.3 ± 0.06^{b}	14.4 ± 0.17^{ef}	25.3	6.2 ± 0.08^{de}	67.9	0.35 ± 0.009^{e}	0.25 ± 0.005^{a}	27.8	0.22 ± 0.001^{c}	64.1
10	DGPC-59	21.9 ± 0.02^{a}	14.9 ± 0.04^{de}	31.8	4.4 ± 0.004^{f}	79.5	0.61 ± 0.001^{bcd}	0.24 ± 0.002^{a}	41.1	0.08 ± 0.004^{e}	80.7
		Internal CO_2 Concentration					Transpiration Rate				
Sl.no	Genotype	Control (m ± SE)	35°C/ 30°C(m ± SE)	Loss (%) at 35°C/ 30°C	40°C/ 35°C(m ± SE)	Loss (%) at 40°C/35° C	Control (m ± SE)	35°C/ 30°C(m ± SE)	Loss (%) at 35°C/ 30°C	40°C/ 35°C(m ± SE)	Loss (%) at 40°C/ 35°C
1	DARL-106	767.2 ± 4.38^{ab}	548.3 ± 11.88^{ab}	28.5	372.9 ± 0.02^{f}	51.4	4.7 ± 0.002^{cd}	4.1 ± 0.03^{abc}	13.6	4.1 ± 0.01^{b}	12.3
2	DGC-103	772.1 ± 1.26^{a}	533.1 ± 7.68^{bc}	31.0	413.6 ± 0.30^{b}	46.4	4.1 ± 0.04^{d}	3.8 ± 0.13^{bcd}	7.5	3.5 ± 0.01^{c}	13.9
3	WBC-13	760.4 ± 6.08^{bc}	526.2 ± 5.38^{bc}	30.8	490.6 ± 5.07^{a}	35.5	5.4 ± 0.01^{bcd}	4.5 ± 0.15^{ab}	15.9	4.7 ± 0.01^{a}	13.5
4	WBC-39-1	753.6 ± 0.14^{cd}	525.0 ± 1.31^{c}	30.3	401.7 ± 0.60^{c}	46.7	4.8 ± 0.38^{cd}	3.8 ± 0.38^{bcd}	20.6	4.2 ± 0.01^{b}	13.4
5	DC-83	766.2 ± 0.48^{ab}	558.9 ± 0.36^{a}	27.1	381.1 ± 0.18^{e}	50.3	5.9 ± 0.01^{abcd}	4.8 ± 0.03^{a}	17.6	4.7 ± 0.01^{a}	20.0
6	BAROPATTA	774.9 ± 2.37^{a}	488.0 ± 4.47^{d}	37.0	391.4 ± 0.37^{d}	49.5	7.7 ± 0.83^{ab}	3.7 ± 0.17^{bcd}	51.7	2.2 ± 0.01^{e}	70.3
7	EC-753493	769.0 ± 3.51^{ab}	477.3 ± 1.06^{de}	37.9	303.6 ± 1.25^{g}	60.5	6.6 ± 0.57^{abc}	3.1 ± 0.07^{de}	53.0	3.1 ± 0.03^{d}	53.1
8	WBC-22	747.4 ± 0.69^{d}	457.4 ± 2.93^{e}	38.8	260.4 ± 0.55^{j}	65.2	7.8 ± 0.48^{a}	2.3 ± 0.02^{e}	70.1	1.8 ± 0.01^{f}	77.0
9	DC-206	688.4 ± 0.45^{f}	471.6 ± 7.16^{de}	31.5	293.5 ± 0.34^{h}	57.4	7.5 ± 1.42^{ab}	3.5 ± 0.42^{cd}	53.0	2.3 ± 0.01^{e}	69.3
10	DGPC-59	718.0 ± 0.84^{e}	409.7 ± 0.91^{f}	42.9	272.3 ± 0.53^{i}	62.1	4.4 ± 0.01^{cd}	2.4 ± 0.01^{e}	44.7	1.9 ± 0.01^{ef}	55.4

Values within a group in a column bearing different letters are significantly different as determined by Tukey's test.

10.3389/fpls.2023.1128928

TABLE 6 Effect of high temperature on important morphological characteristics in cucumber genotypes.

Shoot length				Fresh weight			Dry weight		
Tolerant Genotype	Control (m ± SE)	Treatment (m ± SE)	%Reduction	Control (m ± SE)	Treatment (m ± SE)	%Reduction	Control (m ± SE)	Treatment (m ± SE)	%Reduction
DARL 106	21.6 ± 0.45	15.3 ± 0.56	29.3	40.0 ± 0.26	12.9 ± 0.09	67.7	2.3 ± 0.05	1.3 ± 0.01	42.7
DGC-103	23.2 ± 4.56	14.1 ± 0.73	39.4	50.5 ± 0.17	15.4 ± 0.22	69.4	2.7 ± 0.01	1.6 ± 0.02	38.8
WBC 13	28.0 ± 0.16	20.0 ± 0.94	28.5	45.4 ± 0.83	21.1 ± 0.20	53.3	4.1 ± 0.01	2.5 ± 0.27	37.5
WBC 39-1	23.3 ± 1.19	14.6 ± 0.54	37.1	42.9 ± 0.42	14.6 ± 0.18	65.8	2.6 ± 0.05	1.8 ± 0.13	30.5
DC83	12.6 ± 0.76	9.3 ± 0.49	26.3	21.9 ± 0.12	10.5 ± 0.05	51.7	1.6 ± 0.02	1.1 ± 0.04	29.1
Average	21.7	14.6**	32.1	40.1	14.9**	62.7	2.6	1.7**	36.3
Susceptible Genotype	Control (m ± SE)	Treatment (m ± SE)	%Reduction	Control (m ± SE)	Treatment (m ± SE)	%Reduction	Control (m ± SE)	Treatment (m ± SE)	%Reduction
BAROPATTA	52.7 ± 0.29	11.2 ± 0.39	78.7	62.5 ± 0.40	7.6 ± 0.10	87.7	1.2 ± 0.02	0.5 ± 0.01	54.3
EC-753493	26.3 ± 1.91	10.1 ± 0.72	61.3	32.1 ± 0.11	6.5 ± 0.10	79.7	1.3 ± 0.02	0.4 ± 0.01	64.3
WBC 22	17.5 ± 1.50	10.0 ± 0.19	42.5	35.5 ± 0.54	7.8 ± 0.06	78.0	2.3 ± 0.01	0.2 ± 0.01	88.3
DC-206	48.6 ± 8.31	8.7 ± 0.53	81.9	57.5 ± 0.49	3.2 ± 0.07	94.3	2.2 ± 0.03	0.7 ± 0.01	67.4
DGPC-59	20.3 ± 1.44	6.6 ± 0.45	67.3	30.9 ± 0.45	3.1 ± 0.03	89.7	1.6 ± 0.02	0.8 ± 0.04	50.1
Average	33.1	9.3*	71.7	43.7	5.6**	87.0	1.7	0.5*	67.4

Significant at *p = 0.05, **p = 0.01 and ***p = 0.001.

TABLE 7 Evaluation of ten diverse genotypes for shoot length, fresh weight and dry weight under control, moderate and high temperature conditions.

		Control (m ± SE)	Treatment (m ± SE) (40°C/35°C)	Control (m ± SE)	Treatment (m ± SE) 40°C/35°C)	Control(m ± SE)	Treatment (m ± SE) 40°C/35°C)
Sl.no	Genotype	Shoot length		Fresh weight		Dry weight	
1	DARL106	21.6 ± 0.45^{b}	15.3 ± 0.56^{b}	40.0 ± 0.26^{e}	12.9 ± 0.09^{c}	2.3 ± 0.05^{c}	1.3 ± 0.01^{bcd}
2	DGC-103	23.2 ± 4.56^{b}	14.1 ± 0.73^{bc}	50.5 ± 0.17^{c}	15.4 ± 0.22^{b}	2.7 ± 0.01^{b}	1.6 ± 0.02^{bc}
3	WBC-13	28.0 ± 0.16^{b}	20.0 ± 0.94^{a}	45.4 ± 0.83^{d}	21.1 ± 0.20^{a}	4.1 ± 0.01^{a}	2.6 ± 0.27^{a}
4	WBC-39-1	23.3 ± 1.19^{b}	14.6 ± 0.54^{bc}	42.9 ± 0.42^{d}	14.6 ± 0.18^{b}	2.6 ± 0.05^{b}	1.8 ± 0.13^{b}
5	DC83	12.6 ± 0.76^{b}	9.3 ± 0.49^{de}	21.9 ± 0.12^{h}	10.5 ± 0.05^{d}	1.6 ± 0.02^{d}	1.1 ± 0.04^{cde}
6	BAROPATTA	52.7 ± 0.29^{a}	11.2 ± 0.39^{cd}	62.5 ± 0.40^{a}	7.6 ± 0.10^{e}	1.2 ± 0.02^{e}	0.5 ± 0.01^{ef}
7	EC-753493	26.3 ± 1.91^{b}	10.1 ± 0.72^{de}	32.1 ± 0.11^{g}	6.5 ± 0.10^{f}	1.3 ± 0.02^{e}	0.4 ± 0.01^{f}
8	WBC-22	17.5 ± 1.50^{b}	10.0 ± 0.19^{de}	35.5 ± 0.54^{f}	7.8 ± 0.06^{e}	2.3 ± 0.01^{c}	0.2 ± 0.01^{f}
9	DC-206	48.6 ± 8.31^{a}	8.7 ± 0.53^{de}	57.5 ± 0.49^{b}	3.2 ± 0.07^{g}	2.2 ± 0.03^{c}	0.7 ± 0.01^{def}
10	DGPC-59	20.3 ± 1.44^{b}	6.6 ± 0.45^{e}	30.9 ± 0.45^{g}	3.1 ± 0.03^{g}	1.6 ± 0.02^{d}	0.8 ± 0.04^{def}

Values within a group in a column bearing different letters are significantly different as determined by Tukey's test.

Morphological characteristics

Shoot length, fresh weight and dry weight of all genotypes as well as percentage change are presented in Table 6. Fresh weight, shoot length and dry weight were significantly reduced in seedlings grown under high temperature stress condition in all the genotypes. However, tolerant group showed less reduction (32.1%) in shoot length whereas higher reduction was recorded in susceptible group (71.7%) under high temperature stress condition. Significant reduction was also observed in fresh weight in both tolerant and susceptible genotypes. But tolerant genotypes were able to maintain the fresh weight in treatment conditions in contrast to susceptible genotypes. Reduction in fresh weight was higher in susceptible group of genotypes (87.0%) whereas in tolerant group shown much lower (62.7%) reduction in treatment conditions. Significant reduction in dry weight was recorded in all genotypes, however, percent of reduction was high in susceptible genotypes (67.4%) compared tolerant group (36.3%) under heat stress conditions.

It was found that highest shoot length was observed in WBC-13 (20 cm), DARL-106 (15.3 cm) and lowest in DGPC-59 (6.6 cm), DC-206 (8.7cm) under stress conditions. Fresh weight was higher in WBC-13 (21.1 g), DGC-103 (15.5 g) and much lower low in DGPC-59 (3.1 g), DC-206 (3.2 g) under high temperature conditions. Highest dry weight was recorded in WBC-13 (2.6g) and WBC 39-1 (1.8 g) and lowest in WBC-22 (0.2 g) and EC-753493 (0.4g) under stress conditions. Significant effects were seen ($p< 0.05$) for the effects of genotype, temperature, and genotype × temperature interaction on shoot length, fresh weight, and dry weight (Table 7; Table S4).

Biochemical traits

Proline content

Higher amount of proline accumulation was recorded in tolerant group of genotypes under heat stress conditions (Supplementary Figure 5A). Tolerant group accumulated 44.9% and 50.8% more proline in moderate temperature treatment (35°C/30°C) and high temperature treatment (40°C/35°C), respectively over control condition. There was no significant increase in proline level in susceptible group of genotypes under stress conditions (Table 8). The tolerant genotypes WBC-13 (15.93 $\mu molg^{-1}FW$) and DC-83 (14.50 $\mu molg^{-1}FW$) had accumulated maximum proline content whereas DC-206 (6.39 $\mu molg^{-1}FW$) and EC-753493 (6.63 $\mu molg^{-1}FW$) had minimum proline accumulation at 35°C/30°C treatment. Maximum proline was recorded in WBC-13 (17.9 $\mu molg^{-1}FW$) and DARL-106 (15.0 $\mu molg^{-1}FW$) and minimum accumulation was recorded in DC-206 (6.3 $\mu molg^{-1}FW$) and EC-753493 (7.0 $\mu molg^{-1}FW$) at 40°C/35°C treatment (Table 9). The effects of genotype, temperature, and genotype × temperature interaction for proline content were all significant (Table S5).

Super oxide dismutase content

In our study, the activity of superoxide dismutase enhanced with variable magnitude under heat stress conditions. Supplementary Figure 5B shown that amount of SOD accumulated in three conditions and significance difference among genotypes were recorded both in control and high temperature treatments. Table 8 indicated that SOD level increased by 23.2% and 50.7% under moderate and high heat stress conditions in tolerant group compared to control conditions, respectively. Among tolerant genotypes, maximum percent of SOD accumulated in DC-83 (45.2 $Ug^{-1}FW\ min^{-1}$) and WBC-13 (34.3 $Ug^{-1}FW\ min^{-1}$) whereas low SOD was observed in WBC-22 (10.7 $Ug^{-1}FW\ min^{-1}$) and DGPC-59 (15.4 $Ug^{-1}FW\ min^{-1}$) at 35°C/30°C treatment. In high temperature stress (40°C/35°C treatment), WBC-13 (72.8 $Ug^{-1}FW\ min^{-1}$) accumulated highest SOD followed by DC-83 (59.0 $Ug^{-1}FW\ min^{-1}$). Among the susceptible genotypes DC-206 (16.2 $Ug^{-1}FW\ min^{-1}$) and EC-753493 (26.3 $Ug^{-1}FW\ min^{-1}$) had accumulated lowest SOD content (Table 9). There was significant effects of genotype,

TABLE 8 Effect of high temperature treatment on biochemical parameters in cucumber genotypes under control, moderate and high temperature conditions.

Parameter	Tolerant group					Susceptible group				
	Control (mean)	35°C/30° C (mean)	Gain (%) at 35°C/ 30 °C	40°C/35 (mean)	Gain (%) at 40°C/35°C	Control (mean)	35°C/ 30°C (mean)	Gain (%) at 35°C/30°C	40°C/35° C (mean)	Gain (%) at 40°C/35°C
Proline	6.9	12.5**	44.9	14.0**	50.8	7.4	7.1ns	-4.1	7.2 ns	-2.6
Super oxide dismutase	26.5	34.5*	23.2	53.8*	50.7	31.7	16.7*	-56.5	33.8 ns	-6.5
Catalase	6.2	11.1**	44.4	12.8**	51.6	5.2	6.4*	19.8	6.8 ns	24.4
Guaiacol peroxidase	8.5	21.7**	60.7	22.8**	62.6	7.6	9.7*	21.8	10.4*	27.0
Malondialdehyde	11.5	16.6*	30.9	19.0**	39.6	12.1	24.5***	50.7	29.9***	129.3
Protein	1.8	3.4*	46.6	2.5*	29.2	1.8	1.1**	-65.9	0.8***	-112.0
Ascorbate peroxidase	5.1	5.4*	4.4	6.0*	13.7	4.4	3.6*	-26.7	2.7**	-62.4
Hydrogen peroxidase	25.6	20.2*	-29.2	14.5**	-84.1	22.0	25.9*	14.9	30.7**	27.8

Significant at *p = 0.05, **p = 0.01 and ***p = 0.001.

TABLE 9 Evaluation of ten diverse genotypes for proline, super oxide dismutase, catalase, guaiacol peroxidase, malondialdehyde, protein, ascorbate peroxidase and hydrogen peroxide under different temperature conditions.

		Control (m ± SE)	35°C/30°C (m ± SE)	Gain (%) at 35°C/30°C	40°C/35°C (m ± SE)	Gain (%) at 40°C/35°C	Control (m ± SE)	35°C/30°C (m ± SE)	Gain (%) at 35°C/30°C	40°C/35°C (m ± SE)	Gain (%) at 35°C/30°C
Sl.no	Genotype	Proline					Super oxide dismutase				
1	DARL106	6.4 ± 0.06^{de}	12.1 ± 0.04^{c}	46.5	15.0 ± 0.16^{b}	56.9	17.6 ± 0.13^{e}	26.2 ± 0.61^{c}	32.7	43.9 ± 1.10^{de}	59.9
2	DGC-103	7.0 ± 0.11^{c}	10.3 ± 0.03^{d}	31.8	12.9 ± 0.06^{c}	45.2	29.0 ± 0.09^{d}	33.7 ± 0.68^{b}	13.9	39.2 ± 0.04^{e}	26.1
3	WBC-13	6.3 ± 0.14^{e}	15.9 ± 0.12^{a}	60.2	17.9 ± 0.39^{a}	64.7	18.5 ± 0.37^{e}	34.4 ± 0.30^{b}	46.0	72.8 ± 1.77^{a}	74.5
4	WBC-39-1	6.6 ± 0.14^{cde}	9.6 ± 0.13^{e}	31.3	11.5 ± 0.19^{c}	42.9	31.2 ± 0.13^{c}	33.1 ± 0.43^{b}	5.7	53.9 ± 1.32^{c}	42.1
5	DC83	7.9 ± 0.15^{b}	14.5 ± 0.12^{b}	45.2	12.6 ± 0.30^{c}	37.2	36.1 ± 0.36^{b}	45.2 ± 0.12^{a}	20.0	5 9.0 ± 0.89^{b}	38.7
6	BAROPATTA	7.0 ± 0.09^{cd}	7.7 ± 0.12^{f}	9.6	7.0 ± 0.12^{de}	2.1	11.2 ± 0.08^{f}	21.6 ± 0.52^{d}	48.0	41.2 ± 0.94^{de}	72.7
7	EC-753493	7.8 ± 0.11^{b}	6.6 ± 0.06^{h}	-18.7	7.0 ± 0.36^{de}	-11.6	35.1 ± 0.16^{b}	16.8 ± 0.26^{ef}	-109.4	26.3 ± 0.27^{f}	-33.5
8	WBC-22	8.8 ± .03^{a}	7.3 ± 0.06^{fg}	-19.4	8.0 ± 0.18^{d}	-9.2	17.0 ± 0.21^{e}	10.7 ± 0.23^{g}	-58.4	39.6 ± 0.14^{e}	57.0
9	DC-206	6.3 ± 0.08^{e}	6.3 ± 0.04^{h}	0.8	6.3 ± 0.47^{e}	0.0	31.2 ± 0.02^{c}	18.7 ± 0.15^{e}	-66.4	16.2 ± 0.37^{g}	-91.6
10	DGPC-59	6.8 ± 0.11^{cde}	7.2 ± 0.07^{g}	5.8	7.2 ± 0.16^{de}	6.5	63.7 ± 0.90^{a}	15.4 ± 0.06^{f}	-312.0	45.2 ± 1.13^{d}	-40.9
Sl.no	Genotype	Catalase					Guaiacol Peroxidase				
1	DARL106	4.4 ± 0.03^{e}	9.0 ± 0.21^{c}	51.1	12.4 ± 0.29^{b}	64.5	11.4 ± 0.17^{a}	19.5 ± 0.41^{c}	41.6	23.3 ± 0.07^{b}	51.2
2	DGC-103	10.0 ± 0.07^{a}	12.4 ± 0.14^{b}	19.4	13.2 ± 0.34^{b}	24.2	6.7 ± 0.08^{cde}	22.4 ± 0.30^{b}	69.8	23.2 ± 0.42^{b}	70.9
3	WBC-13	5.2 ± 0.12^{c}	13.4 ± 0.23^{a}	61.2	15.0 ± 0.17^{a}	65.3	11.8 ± 0.07^{a}	22.0 ± 0.48^{b}	46.2	17.1 ± 0.31^{d}	30.8
4	WBC-39-1	6.8 ± 0.14^{b}	9.2 ± 0.14^{c}	26.1	10.8 ± 0.06^{c}	37.0	6.0 ± 0.11^{de}	18.8 ± 0.03^{c}	68.1	19.8 ± 0.03^{c}	69.8
5	DC83	4.6 ± 0.11^{de}	11.8 ± 0.15^{b}	61.0	12.6 ± 0.18^{b}	63.5	6.5 ± 0.04^{cde}	25.5 ± 0.21^{a}	74.2	30.3 ± 0.38^{a}	78.3
6	BAROPATTA	5.0 ± 0.06^{cd}	7.0 ± 0.03^{de}	28.6	8.6 ± 0.12^{d}	41.9	5.3 ± 0.13^{e}	7.7 ± 0.01^{g}	30.8	9.3 ± 0.19^{g}	42.0
7	EC-753493	4.4 ± 0.05^{e}	6.8 ± 0.16^{e}	35.3	6.8 ± 0.06^{e}	35.3	8.9 ± 0.16^{bc}	10.2 ± 0.16^{e}	13.3	11.8 ± 0.15^{ef}	24.4
8	WBC-22	6.8 ± 0.13^{b}	7.6 ± 0.08^{d}	10.5	7.2 ± 0.08^{e}	5.6	6.0 ± 0.15^{de}	8.7 ± 0.06^{fg}	31.4	10.9 ± 0.27^{f}	44.8

(Continued)

TABLE 9 Continued

Sl.no	Genotype	Catalase					Guaiacol Peroxidase				
9	DC-206	5.0 ± 0.01^{cd}	5.6 ± 0.07^{f}	10.7	7.0 ± 0.07^{e}	28.6	7.8 ± 0.02^{bcd}	12.3 ± 0.21^{d}	36.5	12.8 ± 0.03^{e}	39.0
10	DGPC-59	4.8 ± 0.01^{cde}	5.4 ± 0.21^{f}	11.1	4.8 ± 0.03^{f}	0.0	9.7 ± 0.05^{ab}	9.3 ± 0.07^{ef}	-4.7	7.1 ± 0.10^{h}	-36.9
Sl.no	Genotype	Malondialdehyde					Protein				
1	DARL106	11.3 ± 0.11^{de}	14.1 ± 0.29^{fg}	20.0	17.2 ± 0.42^{f}	34.3	2.1 ± 0.02^{b}	3.1 ± 0.03^{c}	31.8	1.9 ± 0.02^{d}	-9.1
2	DGC-103	13.0 ± 0.30^{b}	15.0 ± 0.27^{f}	13.7	15.6 ± 0.01^{g}	16.5	1.2 ± 0.02^{e}	3.1 ± 0.01^{c}	59.8	2.4 ± 0.05^{c}	49.1
3	WBC-13	12.6 ± 0.26^{bc}	17.6 ± 0.23^{e}	28.5	20.3 ± 0.14^{e}	38.0	2.4 ± 0.06^{a}	3.8 ± 0.03^{b}	36.8	3.0 ± 0.08^{b}	20.0
4	WBC-39-1	7.3 ± 0.08^{f}	13.6 ± 0.13^{g}	46.2	16.5 ± 0.08^{fg}	55.5	2.1 ± 0.01^{b}	2.7 ± 0.02^{d}	22.0	1.7 ± 0.01^{e}	-18.5
5	DC83	13.1 ± 0.27^{ab}	22.5 ± 0.24^{cd}	41.7	25.4 ± 0.34^{d}	48.2	1.0 ± 0.01^{f}	4.0 ± 0.04^{a}	73.6	3.4 ± 0.01^{a}	69.0
6	BAROPATTA	10.3 ± 0.10^{e}	21.4 ± 0.42^{d}	51.8	30.4 ± 0.21^{c}	66.1	1.6 ± 0.01^{d}	0.6 ± 0.01^{h}	-169.0	0.4 ± 0.01^{h}	-270.7
7	EC-753493	14.1 ± 0.10^{a}	25.0 ± 0.25^{b}	43.3	32.9 ± 0.48^{b}	56.9	1.9 ± 0.05^{c}	1.6 ± 0.03^{e}	-18.4	1.1 ± 0.02^{f}	-77.7
8	WBC-22	13.1 ± 0.32^{ab}	23.2 ± 0.07^{c}	43.3	25.0 ± 0.33^{d}	47.4	1.7 ± 0.02^{d}	1.3 ± 0.02^{f}	-33.8	0.8 ± 0.01^{g}	-102.4
9	DC-206	11.0 ± 0.07^{de}	24.6 ± 0.36^{b}	55.0	26.1 ± 0.38^{d}	57.6	1.6 ± 0.04^{d}	0.9 ± 0.01^{g}	-81.2	0.9 ± 0.01^{g}	-80.1
10	DGPC-59	11.6 ± 0.24^{cd}	28.2 ± 0.34^{a}	58.9	34.9 ± 0.29^{a}	66.8	1.9 ± 0.04^{bc}	0.9 ± 0.02^{g}	-113.7	0.9 ± 0.01^{g}	-118.7
Sl.no	Genotype	Ascorbate Peroxidase					Hydrogen Peroxidase				
1	DARL106	5.4 ± 0.03^{b}	5.9 ± 0.06^{a}	8.7	6.5 ± 0.06 ^{a}	17.0	29.8 ± 0.19 ^{b}	27.4 ± 0.03 ^{b}	-8.8	18.3 ± 0.11^{e}	-63.1
2	DGC-103	4.8 ± 0.02^{c}	5.0 ± 0.04^{b}	3.1	5.6 ± 0.10 ^{b}	14.7	19.2 ± 0.34^{g}	12.4 ± 0.10 ^{h}	-54.6	9.5 ± 0.02^{h}	-102.1
3	WBC-13	5.8 ± 0.10^{a}	6.0 ± 0.02^{a}	3.9	6.5 ± 0.09 ^{a}	10.5	23.9 ± 0.18^{d}	21.5 ± 0.25 ^{f}	-11.2	16.4 ± 0.18^{f}	-45.5
4	WBC-39-1	4.9 ± 0.01^{c}	5.0 ± 0.07^{b}	0.2	5.0 ± 0.02 ^{c}	1.6	21.4 ± 0.04^{ef}	17.5 ± 0.22 ^{g}	-22.2	16.3 ± 0.10^{f}	-31.4
5	DC83	4.8 ± 0.0^{c}	5.1 ± 0.08^{b}	5.9	6.4 ± 0.11^{a}	24.7	33.6 ± 0.07^{a}	22.5 ± 0.38 ^{ef}	-49.3	12.1 ± 0.13^{g}	-178.4
6	BAROPATTA	4.9 ± 0.10 ^{c}	4.5 ± 0.05^{c}	-8.1	3.4 ± 0.01^{d}	-42.3	26.1 ± 0.40 ^{c}	30.4 ± 0.21^{a}	14.1	35.6 ± 0.24^{a}	26.7
7	EC-753493	4.4 ± 0.02 ^{d}	4.2 ± 0.04^{d}	-3.9	2.7 ± 0.05^{e}	-61.3	22.4 ± 0.04 ^{e}	25.1 ± 0.36 ^{cd}	10.6	27.6 ± 0.54^{d}	18.8
8	WBC-22	3.8 ± 0.07 ^{e}	3.1 ± 0.04^{e}	-21.9	2.2 ± 0.01^{f}	-73.9	21.6 ± 0.05^{ef}	23.7 ± 0.33 ^{de}	9.0	27.0 ± 0.36^{d}	20.0

(Continued)

TABLE 9 Continued

Sl.no	Genotype	Ascorbate Peroxidase					Hydrogen Peroxidase				
9	DC-206	4.9 ± 0.03 ^{c}	2.9 ± 0.01^{e}	-67.2	2.7 ± 0.02^{e}	-84.9	20.7 ± 0.01^{f}	25.8 ± 0.23 ^{c}	19.6	30.3 ± 0.09^{c}	31.6
10	DGPC-59	4.0 ± 0.07 ^{e}	3.0 ± 0.01^{e}	-32.5	2.7 ± 0.02^{e}	-49.5	19.3 ± 0.25^{g}	24.5 ± 0.19 ^{de}	21.3	33.1 ± 0.62^{d}	41.8

Values within a group in a column bearing different letters are significantly different as determined by Tukey's test.

temperature, and genotype × temperature interaction for SOD (Table S5).

Catalase content

Catalase content in all genotypes under control and heat treatments conditions are depicted in Supplementary Figure 5C. Catalase content has increased in all genotypes irrespective of tolerance and susceptibility, but tolerant genotypes accumulated higher amount of catalase compared to susceptible genotypes. Percent increase in catalase was 44.4% and 51.6% in tolerant genotypes where as in susceptible genotypes, percentage increase was by 19.8% and 24.4% in moderate and high temperature stress conditions, respectively (Table 8).

Highest catalase activity was recorded in WBC-13 (13.4 Ug^{-1}FW min^{-1}) and DGC-103 (12.4 Ug^{-1}FW min^{-1}) and lowest in DGPC-59 (5.4 Ug^{-1}FW min^{-1}) and DC-206 (5.6 Ug^{-1}FW min^{-1}) at 35°C/30°C treatment. The genotypes WBC-13(13.2 Ug^{-1}FW min^{-1}) and DGC-103 (13.2 Ug^{-1}FW min^{-1}) had recorded highest catalase activity and DGPC-59 (4.8 Ug^{-1}FW min^{-1}), EC-753493 (6.8 Ug^{-1}FW min^{-1}) had lowest catalase activity at 40°C/35°C treatment (Table 9). Temperature, genotype, and genotype × temperature interaction was significant for catalase (Table S5).

Guaiacol peroxidase content

Peroxidase content of leaves increased significantly with increase in temperature than that from control conditions in all genotypes (Supplementary Figure 5D). Significant differences were noted among genotypes under different conditions. In tolerant genotypes GPX increased by 60.7% and 62.6%, where as in susceptible genotypes amount increased by 21.8% and 27% in moderate and high temperature stress conditions, respectively over control conditions (Table 8). Maximum peroxidase activity was recorded in DC-83 (25.55 μmol$g^{-1}$$min^{-1}$) and DGC-103 (22.43 μmol$g^{-1}$$min^{-1}$) and minimum in Baropatta (7.78 μmol$g^{-1}$$min^{-1}$) and WBC-22 (8.78 μmol$g^{-1}$$min^{-1}$) at 35°C/30°C treatment. At 40°C/35°C treatment, lowest peroxidase activity was recorded in DGPC-59 (7.13 μmol$g^{-1}$$min^{-1}$), Baropatta (9.30 μmol$g^{-1}$$min^{-1}$) and highest was in DC-83 (30.36 μmol$g^{-1}$$min^{-1}$), DARL-106 (23.28 μmol$g^{-1}$$min^{-1}$) at high temperature stress conditions (Table 9). There were significant ($p<0.05$) effects of genotype, temperature, and genotype × temperature interaction on GPX content (Table 5S).

Malondialdehyde content

In response of high temperature stress, high endogenous malondialdehyde content levels were observed in cucumber plants (Supplementary Figure 5E). In susceptible genotypes, malondialdehyde content significantly increased with increase in temperature as compared to control conditions. Malondialdehyde content increased by 50.7% and 129.3% in susceptible group in contrast to tolerant group with an increase by 30.9% and 39.6% in moderate and high temperature stress conditions, respectively. (Table 8). The genotype DGPC-59 (28.25 nmolg^{-1}FW, 34.9 nmolg^{-1}FW) had shown highest malonaldehyde content under both high temperature treatments whereas WBC 39-1 (13.6 nmolg^{-1}FW) and DGC-103(15.6 nmolg^{-1}FW) had shown lowest malonaldehyde content in 35°C/30°C treatment and 40°C/35°C treatment, respectively (Table 9). Temperature, genotype, and genotype × temperature interaction all had significant effects on Malondialdehyde accumulation in the plants (Table S5).

Protein content

Greater increase in protein content was noticed in 35°C/30°C treatment compared to 40°C/35°C treatment (Supplementary Figure 5F). Tolerant group accumulated 46.6% and 29.2% of protein in moderate and high temperature conditions over the control, whereas protein level was significantly reduced in susceptible genotypes (Table 8). Highest protein was recorded in DC-83 (4.05 mg g^{-1}, 3.45 mg g^{-1}) followed by WBC-13 (3.8 mg g^{-1}, 3.03 mg g^{-1}) and lowest was recorded in Baropatta (0.6 mg g^{-1}, 0.4 mg g^{-1}) and DC-206 (0.9 mg g^{-1}, 0.9 mg g^{-1}) under both treatment conditions (Table 9). Significant difference has been observed among genotypes under all three conditions. The effects of genotype, temperature, and genotype × temperature interaction on protein content were significant (Table S4).

Ascorbate peroxidase content

Greater increase in ascorbate peroxidase was noticed 40°C/35°C treatment in treatment compared to 35°C/30°C (Supplementary Figure 5G). Tolerant group accumulated 4.4% and 37.6% of APX content in moderate and high temperature conditions over the control, whereas APX level was significantly reduced in susceptible genotypes (Table 8). Highest APX was recorded in WBC-13 (6.0 μmol$min^{-1}$$g^{-1}$1 6.5 μmol$min^{-1}$$g^{-1}$) in moderate and high stress conditions. Lowest was recorded in DC-206 (2.9 μmol$min^{-1}$$g^{-1}$) under moderate stress and WBC 22 (2.2 μmol$min^{-1}$$g^{-1}$) under high stress conditions (Table 9). The effects of genotype, temperature, and genotype × temperature interaction on protein content were significant (Table S4).

Hydrogen peroxidase content

In response of high temperature stress, high levels of hydrogen peroxide was content levels were observed in cucumber plants (Supplementary Figure 5H). In susceptible genotypes, hydrogen

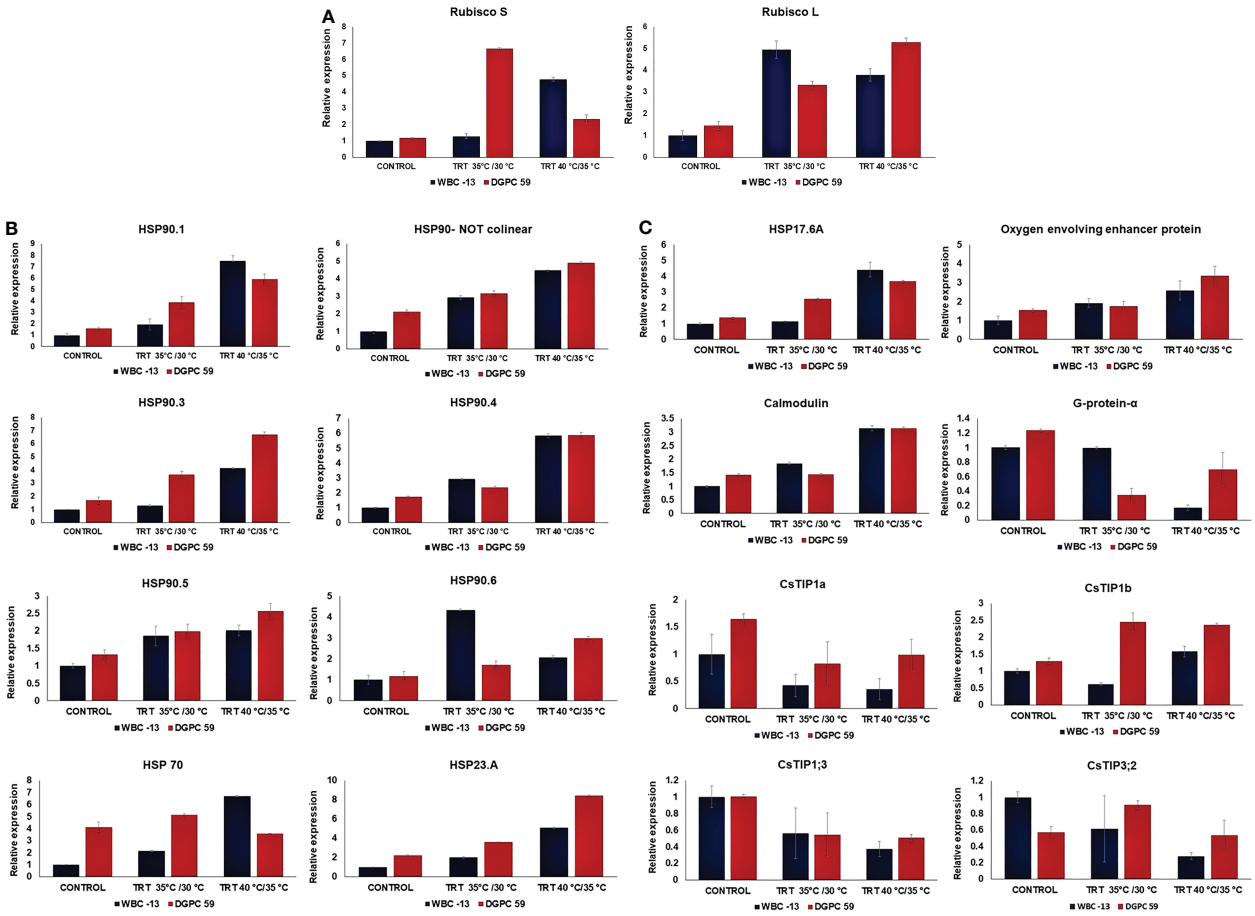

FIGURE 3
(A) Relative expression (means± SE) of Photosynthesis related genes (Rubisco S and Rubisco L) in cucumber leaves under in control, moderate temperature treatment (35°C/30°C) and high temperature treatment (40°C/35°C). **(B)** Relative expression (means± SE) of Heat shock proteins (HSPs) in cucumber leaves under in control, moderate temperature treatment (35°C/30°C) and high temperature treatment (40°C/35°C). **(C)** Relative expression (means± SE) of HSP 17.6 A and signal transduction genes in cucumber leaves under in control, moderate temperature treatment (35°C/30°C) and high temperature treatment (40°C/35°C).

peroxide content significantly increased with increase in temperature as compared to control conditions. Hydrogen peroxidase content increased by 14.9% and 27.8% in susceptible group in contrast to significant decrease in tolerant at stress conditions (Table 8). The genotype Baropatta(30.4 μmolg^{-1}FW, 35.6 μmolg^{-1}FW) had shown highest hydrogen peroxidase content under both high temperature treatments whereas DGC-103(12.4 μmolg^{-1}FW, 9.5 μmolg^{-1}FW) had shown lowest hydrogen peroxidase content in moderate and high stress conditions (Table 9). The effects of genotype, temperature, and genotype × temperature interaction on hydrogen peroxidase content were significant (Table S4).

RT-PCR of selected genes associated with heat stress

Based on the performance and analysis of physio-biochemical characters in 10 different genotypes, two genotypes namely, WBC-13 (heat tolerant) and DGPC-59 (heat susceptible) were selected for gene expression studies of selected heat responsive genes. Expression profiling of 18 selected heat responsive genes was conducted in two contrasting genotypes under three different temperature conditions (Control: 30°C/25°C, Moderate stress: 35°C/30°C and High stress: 40°C/35°C). Genes used in study are mentioned in Table S5. Rubisco S gene showed highest expression of 6-7 folds at moderate heat stress in DGPC-59 whereas WBC-13 showed highest expression of 4-5 folds at high stress condition. Analysis of result showed that Rubisco L gene was 5-6 folds upregulated in DGPC-59 at high heat stress whereas WBC-13 showed increase in 5-6 folds expression at moderate heat stress (Figure 3A).

A remarkable up-regulation in relative accumulation of some HSPs under high stress conditions were recorded in tolerant genotypes. At the same time, few HSPs were shown down regulation under high heat stress conditions in the tolerant genotype, WBC-13 (Figure 3B). In control conditions, no significant differences were observed between the genotypes except for the HSP70 which showed higher expression in susceptible genotypes. It was observed that at moderate heat stress condition, only HSP 90.6 shown higher expression in WBC-13 as compared with other stress condition. At high heat stress condition, HSP 90.1, HSP 70 and HSP 17.6A shown higher expression in tolerant genotype, WBC-13. Some HSPs like HSP90.3, HSP90.6, HSP 23.A, HSP 90.5 shown upregulation in DGPC-59 whereas HSP90.4 shown no

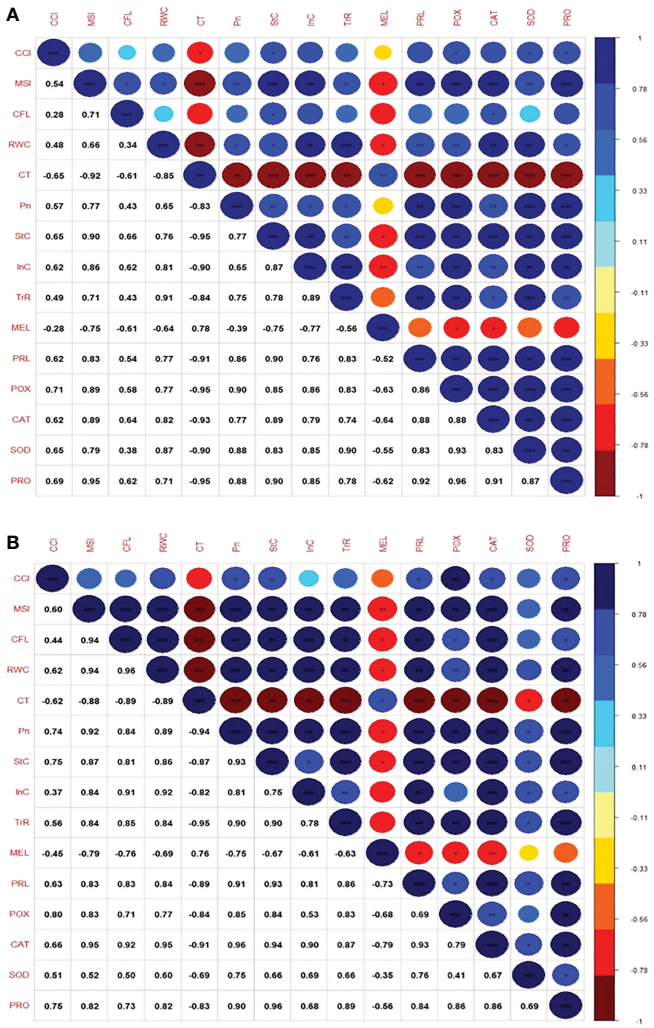

FIGURE 4
(A) Correlogram showing the relationship between average values of the variables at moderate high temperature stress conditions 35°C/30°C. **(B)** Correlogram showing the relationship between average values of the variables at moderate high temperature stress conditions 40°C/35°C; The intensity of color and size of the circle increases with an increase in the significance of correlation. Dark red denotes a high negative correlation, whereas dark blue denotes a high positive correlation.

significant difference between the genotypes at high heat stress condition. Additionally, the genes corresponding to signal transduction were also studied under control and heat stress conditions. In control and treatment conditions, significant differences were seen among the genotypes (Figure 3C). Under high heat stress conditions tolerant genotype, WBC-13 expressed downregulation for CsTIP1;3, CsTIP3;2, CsTIP1a whereas WBC-13 shown upregulation for CsTIP1b gene (Figure 5). In case of Calmodulin gene expression, both contrasting genotypes had same level of expression with no significant difference. G-protein-α and oxygen evolving enhancer genes were upregulated in DGPC-59 at high heat stress condition and downregulated in WBC-13.

Correlation analysis

Moderate temperature stress (35°C/30°C)

A correlogram (Figure 4A) depicts the correlation between the all parameters measured between all parameters in all genotypes at moderate heat stress conditions 35°C/30°C. Chlorophyll content (CCI) was significantly and positively correlated with membrane stability index (r=0.54), relative water content (r=0.48), net photosynthesis (r=0.57) and transpiration rate(r= 0.49), proline (r=0.62), catalase (r=0.62), stomatal conductance (r=0.65), internal CO_2 concentration (r=0.62), peroxidase (r=0.71), super oxide dismutase (r=0.65), protein (r=0.69) and with chlorophyll florescence (r=0.33). However, there was a significant negative correlation of the parameters chlorophyll and canopy temperature (r=-0.78) and malonaldehyde (r=-0.33). The MSI was positively and significantly correlated to stomatal conductance (r=0.90), internal CO_2 concentration (r=0.86), proline(r=0.83), peroxidase(r=0.89), catalase (r=0.89), protein (r=0.95), chlorophyll florescence(r=0.71), relative water content(r=0.66), net photosynthesis(r=0.77), transpiration rate (r=0.71) and super oxide dismutase (0.79) and there was a significant negative correlation of the parameters MSI and CT (r=-0.1) and malonaldehyde (r=-0.78). Chlorophyll fluorescence is positively correlated with stomatal conductance, catalase, internal CO_2 concentration, protein with r value 0.78 and net photosynthesis,

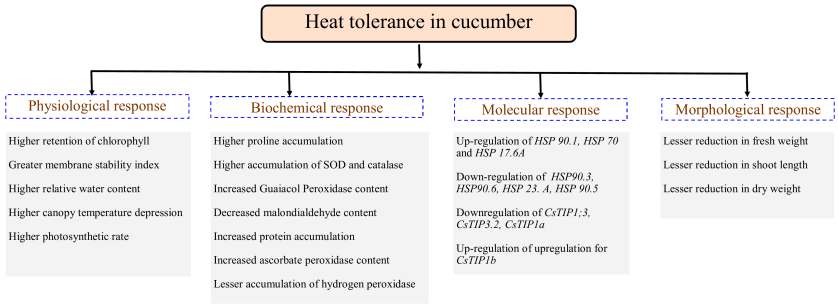

FIGURE 5
Important physiological, biochemical, molecular and morphological factors associated with heat stress tolerance in cucumber.

transpiration rate, proline, peroxidase with r=0.56 and relative water content and super oxide dismutase with r=0.33, negative correlation exists between CFC and malonaldehyde and canopy temperature with r=-0.78. Similarly, canopy temperature was positively correlated with malonaldehyde (r=0.78). Additionally, net photosynthesis is positively correlated with proline, peroxidase, SOD, and protein with r value near to 1 and with stomatal conductance, internal CO_2 concentration, transpiration rate and catalase with r=0.78. Besides, internal CO_2 concentration was positively correlated with transpiration rate, peroxidase, SOD and proline content. In edition biochemical parameters proline, peroxidase, SOD and protein are positively and significantly correlated to each other.

High temperature stress (40°C/35°C)

A correlogram (Figure 4B) depicts the correlation between the all parameters measured between all parameters in all genotypes at moderate heat stress conditions 40°C/35°C. Chlorophyll content (CCI) is significantly and positively correlated with peroxidase (r=0.8), relative water content(r=0.62), membrane stability index (r=0.60), net photosynthesis (r=0.74), stomatal conductance (r=0.75), proline (r=0.74), catalase (r=0.66) and protein (r=0.75), chlorophyll florescence (0.44), transpiration rate (r=0.56), super oxide dismutase (r=0.51), internal CO_2 concentration (r=0.33) and CCI is negatively correlated with canopy temperature (r = -0.78), malonaldehyde (r=-0.56). Membrane stability index was highly correlated with chlorophyll florescence, relative water content, net photosynthesis, stomatal conductance, internal CO_2 concentration, transpiration rate, proline, peroxidase, catalase and protein with r value near to 1. SOD (r=0.56) and MSI were negatively correlated with malonaldehyde (r=-0.78) and canopy temperature (r=-1). Chlorophyll fluorescence had significant positive correlation with relative water content, net photosynthesis, stomatal conductance, internal CO_2 concentration, transpiration rate, proline, catalase with r value near to 1 and peroxidase and protein with r value near to 0.78, SOD (r=0.56) and negative correlation with malonaldehyde (r=-0.78) and canopy temperature (r=-1). Relative water content had significant positive correlation (r=1) with parameters net photosynthesis, stomatal conductance, internal CO_2 concentration, transpiration rate, proline and catalase and protein and peroxidase (r=0.78), SOD (r=0.56) and negatively correlated with Malondialdehyde (-0.78) and canopy temperature (r=-1). Canopy temperature shown positive significance with malondialdehyde (r=0.78). Net photosynthesis was significantly and positively correlated with stomatal conductance, internal CO_2 concentration, transpiration rate, proline, peroxidase, catalase and protein with r value near to 1, SOD with r=0.78 and negatively correlated with malondialdehyde content (-0.78). Stomatal conductance and transpiration rate were showing significant and positive correlation with proline, peroxidase, catalase, SOD, protein except with malondialdehyde. Biochemical parameters had positive correlation among themselves except malondialdehyde content.

Discussion

Plants being sessile are constantly exposed to several abiotic stresses comprising drought, heat or different stress combinations that results in several metabolic disparities leading to oxidative damage due to ROS production and accumulation. ROS build-up in plants triggers organelle integrity, oxidation of cellular components, and even can lead to cell death (Suzuki et al., 2014; Nath et al., 2016; Raja et al., 2017). Thus, plants may have evolved different physiological, biochemical and molecular mechanisms to adopt for heat stress conditions. We are reporting the comprehensive physio-biochemical response of a contrasting set of cucumber genotypes under varied level of high-temperature stress conditions (Figure 5). Expression analysis of selected important genes were performed to examine the molecular responses of the cucumber genotypes to heat stress.

Physiological basis of heat stress tolerance

In our present experiment, analysis of variance for different physiological and biochemical parameters was significant indicating the existence of significant genetic variability among the genotypes and differential response of genotypes to heat stress conditions. In chloroplast, the chlorophyll is harbored by thylakoid which are

considered as the most heat labile cell structures (Vacha et al., 2007). Any damage to thylakoid caused by heat is expected to result in chlorophyll loss. This showed that chlorophyll is linked with dry matter accumulation and can be utilized in screening the genotypes for high-temperature tolerance at seedling stage of cucumber. We found variations in the percent degradation of chlorophyll in the present investigation suggesting that some of the cucumber genotypes were able to maintain more chlorophyll under stress conditions. Chlorophyll content in leaves decreased as HT days increased, and the decrease was faster in a heat-susceptible cultivar compared to tolerant cultivar as was observed in other crops like hot pepper (Arnaoudova et al., 2020) and tomato genotypes (Bhattarai et al., 2021). The higher chlorophyll content in heat-tolerant cultivar gives better photosynthetic stability than heat-susceptible tomato cultivars (Zhou et al., 2017). By elevating unsaturated fatty acids and making the plasma membrane more fluid, HS causes the plasma membrane to become disorganized (Hofmann, 2009). It also affects cellular processes by starting a signal cascade (Firmansyah and Argosubekti, 2020; Hassan et al., 2021). The ability to adapt to high temperatures appears to be governed by a stable cell membrane system that keeps working under heat stress. High temperature stress can directly affect membrane integrity through photochemical modifications during photosynthesis or ROS (Bita and Gerats, 2013). It is also suggested that the membrane disruption may alter water, ion and organic solutes movement across the plant membrane which interferes with photosynthesis and transpiration. In this study we evaluated the membrane stability index and it was found that tolerant genotypes maintained high stability index. Recently, it was demonstrated that tolerant genotype of cucumber shown less relative conductivity and less damage of membrane lipid (Wang et al., 2020). The thermosensitive cucumber genotypes had high relative conductivity after high-temperature stress compared to tolerant genotypes (Yu et al., 2022). Similarly, cucumber genotypes with less electrolyte leakage ability tend to be more heat tolerant than genotypes with more electrolyte leakage at a high temperature of 40°C (Ali et al., 2019). Heat-tolerant cultivars of cauliflower expressed more cell membrane thermostability than susceptible ones (Aleem et al., 2021). Under different stress conditions, plants maintain their physiological balance through higher RWC values particularly under higher rates of transpiration. In the present study, plants subjected to heat stress conditions displayed decreased RWC values suggesting the sensitivity of cucumber plants towards heat stress. The difference in RWC under stress conditions did not differ significantly among the tolerant and susceptible genotypes suggesting its limited role in heat tolerance in cucumber. Raja et al. (2020) reported decreased RWC in tomato plants under high-temperature stress.

Chlorophyll fluorescence is a rapid, reliable, and inexpensive procedure for predicting photosynthetic performance under HS. Reduced *Fv/Fm* values indicate damage to the light-harvesting complex (Moradpour et al., 2021). Chlorophyll fluorescence has been used as screening tool in common bean (Stefanov et al., 2011) and okra (Hayamanesh, 2018). Several recent studies also supported our finding that tolerant genotypes shown higher *Fv/Fm* ratio with stable photosynthetic system under heat stress conditions. High temperature seriously impaired the photosynthetic system of susceptible plants as compared to the tolerant genotypes (Yu et al., 2022).

In our study, HT significantly decreased the photosynthetic rate in thermos-sensitive genotypes but stable rate of photosynthesis was maintained in the tolerant cultivar. The stable photosynthetic rate of heat-tolerant cultivar in HT might be due to the increased stomatal conductivity and transpiration rate. Under the condition of 40°C/35°C heat treatment, rate of photosynthesis and stomatal conductance were drastically reduced in the susceptible genotypes in contrast to the tolerant genotypes suggesting the ability of the tolerant genotypes to sustain the photosynthetic activities even under high-temperature stress conditions. Yu et al. (2022) demonstrated thermo-tolerant plants showed stable photosynthesis under high-temperature stress whereas sensitive plants had extremely unstable photosynthesis in cucumber. Photosynthetic rate was significantly reduced in susceptible cultivar but not in tolerant seedlings even with the exposure to 42°C in hot pepper. Similarly, stomatal conductivity and transpiration rate was significantly higher in tolerant genotypes compared to susceptible genotypes (Rajametov et al., 2021). In tomato, high stomatal conductivity and transpiration rate under heat stress facilitate reduced canopy temperature in heat-tolerant genotypes, providing better protection for chlorophyll and maintaining a relatively high photosynthetic rate (Zhou et al., 2017). Therefore, it was concluded that the ability of the tolerant genotypes to maintain a stable photosynthetic rate was one of the important factors for thermotolerance.

Growth parameters in response to heat stress

In the present study, plants were subjected to high temperature stress conditions exhibited reduction in shoot length, fresh weight and dry weight values suggesting the effect of heat stress on biomass of the plants. However, the tolerant genotypes were able to maintain the higher biomass compared to susceptible genotypes. Reduction in plant growth under high temperatures varied among the genotypes and tolerant genotypes exhibited significantly better morphological traits when compared with the sensitive genotypes in tomato (Shaheen et al., 2016). Lower height reduction under heat-stress in tolerant genotypes signified that their ability to maintain their growth properly when exposed to heat stress conditions. The changes in plant diameter under heat stress may be related to changes in stem tissue hydration. Reduction in growth because of reduced water content in cell and cell size is common when plants are exposed to high temperature stress conditions (Ashraf and Hafeez, 2004; Rodríguez et al., 2005). Besides, retarded relative growth in the susceptible genotypes because of reduction in net assimilation rate (NAR) was reported in maize, millet (Wahid et al., 2007) and sugarcane (Srivastava et al., 2012).

Biochemical basis of heat stress tolerance

Variability in increasing the activities of these antioxidants across cucumber genotypes indicates their differential ability to acquire thermo-tolerance. Even the heat tolerance was found directly linked with the percent increase in catalase, superoxide dismutase, guaiacol peroxidase accumulation in most genotypes. Thus, our results show

that tolerance mechanism for heat stress exists in cucumber genotypes for a variable extent. Proline serves as a membrane protectant, and due to its zwitter ion character, accumulates in high-concentration in cell cytoplasm under stress conditions without interfering with cellular structure or metabolism. Proline in plants functions as an osmoprotectant and allows them to tolerate stress (Akram et al., 2018; Alzahrani et al., 2018). Higher levels of proline accumulation in plants occur under stress conditions. In this study, we evaluated the contents of proline and found that tolerant genotypes accumulated significantly higher proline content under heat stress in comparison to susceptible genotypes. Tomato genotypes accumulated high amount of proline under heat stress conditions (Raja et al., 2020). Proline content was also significantly higher in tolerant genotypes compared to susceptible genotypes after heat treatment in hot pepper (Rajametov et al., 2021). Several recent studies reported that proline accumulation occurs in plants with exposure to stress conditions (Kaur and Asthir, 2015; Moreno-Galván et al., 2020) because of its property to stabilize subcellular structures, scavenging free radicals and buffer cellular redox potential (Hazman et al., 2015; Dar et al., 2016; Nurdiani et al., 2018). Heat stress is known to accompany with the formation of reactive oxygen species such as H_2O_2 and OH^-, which damage membranes and macromolecules. SOD is usually considered as the first line of defense against oxidative stress. In plants, we found significant difference between genotypes with respect to SOD accumulation and SOD activity was increased under heat stress conditions in tolerant genotype. No significant difference in superoxide dismutase enzyme (SOD) activity was detected between contrasting genotypes under normal conditions, whereas tolerant genotypes exhibited significant increase in SOD activity during heat stress compared with susceptible genotype (Wang et al., 2020). Tolerant genotypes of brinjal were reported to have higher amount of superoxide dismutase, peroxidase and catalase (Faiz et al., 2020). Superoxide dismutase (SOD) and peroxidase (POD) are two necessary antioxidant enzymes that protect plants from heat-induced oxidative stress. Catalase and peroxidises are the most important enzymes involved in regulation of intracellular level of H_2O_2. They convert H_2O_2 into OH^- along with the regeneration of NADP, thus helping the plants under stress conditions (Sairam et al., 1997; Xu et al., 2008). We found higher accumulation of catalase and peroxidises in tolerant genotypes under heat stress conditions compared to susceptible genotypes. The heat tolerance was found directly linked with the percent increase in catalase/superoxide dismutase/guaiacol peroxidase accumulation in wheat genotypes. During present study, MDA content was increased in susceptible genotypes as compared to tolerant genotypes under heat stress conditions. Potential resistance mechanisms of plants exposed to heat stress may involve higher osmotic regulation capacity related to an increase in leaf protein content (Ding et al., 2016). We also observed increased protein levels in tolerant genotypes under heat stress conditions was instrumental in conferring heat tolerance in cucumber genotypes.

Gene expression in response to high temperature stress treatment

The acquisition of plant heat tolerance is closely associated with the synthesis of chaperone proteins and the levels of non-enzymatic antioxidants in response to HT (Kotak et al., 2007; Wahid et al., 2007). Heat shock proteins play an essential role in the regulation of HSFs and subsequently, the expression of heat responsive genes associated with heat tolerance. The plants generally activate and accumulate a large amount of the HSPs to response to heat shock exposure to maintain the stability of cells under stress conditions (Richter et al., 2010; Li et al., 2018). In our study, HSP 90.1 and HSP 70 shown seven-fold and six-fold increased expression, respectively in tolerant genotype in response to heat stress conditions. Earlier, Yu et al. (2018) also reported the role of heat shock proteins in thermotolerance in cucumber. Besides, lower expression of HSP70 has been recorded in susceptible genotypes of chilies in response to heat stress while the tolerant ones showed overexpression of HSP70 which enhanced the thermostability of cell membranes (Usman et al., 2015). Similarly, significant increase in BoHSP70 in cabbage, HSP60/CPN60, HSP70, HSP90, HSP100/ClpB, and HSP90 activator and HSP70/HSP90 organizing protein in spinach and ClHSP11.1A, ClHSP50.3, and ClHSP17.4 in watermelon are reported to play key role in response to high temperature stress (Park et al., 2013; He et al., 2018; Zhao et al., 2018). Recent studies revealed that chilli specific many HSPs including CaHSP70, CaHSP60, CaHSP20, and CaHSP16.4 are upregulated in pepper under HS and significant difference between the genotypes (Guo et al., 2015; Usman et al., 2015).

The AQPs channel proteins to facilitate the transport of water primarily through the plasma and tonoplast membranes in the plant cells (Chaumont and Tyerman, 2014). They are often designated as plasma membrane intrinsic proteins (PIPs) or tonoplast intrinsic proteins (TIPs) (Danielson and Johanson, 2008). Participation of AQPs in different abiotic stress responses is reported earlier (Matsumoto et al., 2009; Sreedharan et al., 2013; Wang et al., 2017). Besides, the differential expression of aquaporin isoforms is reported under different stress conditions (Alexandersson et al., 2010). Regulation of TIP controlled water transport across vacuolar membranes by different environmental signals is determined both at the transcriptional and the post-transcriptional levels (Li et al., 2014). Salinity, drought, gibberellic acid, and abscisic acid level are associated with regulation of TIPs (Hachez et al., 2006, Maurel et al., 2008; Moshelion et al., 2009; Hachez et al., 2012; Zarrouk et al., 2016). Transgenic approaches demonstrate that the overexpression of aquaporins in plants confers enhanced tolerance against abiotic stress, including drought (An et al., 2018; Lu et al., 2018; Wang et al., 2018; Patankar et al., 2019; Rosales et al., 2019; Wang et al., 2019). In the present study, varied expression of cucumber specific *CsAQPs* was recorded in the genotypes with contrasting response to heat stress. In control conditions, significant difference was found for genes *CsTIP3.2, CsTIP1a* in contrast to high temperature stress

conditions. Therefore, *CsTIP3.2, CsTIP1a* were instrumental in providing heat stress response in the cucumber genotypes. No significant difference in calmodulin genes in the contrasting genotypes under the heat stress conditions indicated its limited role in conferring heat tolerance in cucumber. Upregulation of the G-protein-α and oxygen evolving enhancer genes in the susceptible genotype, DGPC-59 at high heat stress condition indicated their role as negative feedback in heat tolerance in cucumber. In pea and Chinese pear, induced level of the in response to the heat stress has been reported (Misra et al., 2007; Bhardwaj et al., 2020). Negative role of the GPA1 was also reported in *Arabidopsis* mutants in response to the heat stress (Chakraborty et al., 2015). Inhibition of electron transport from the oxygen evolving complex (OEC) of PSII is because of its dissociation by heat stress (Havaux and Tardy, 1996; Allakhverdiev et al., 1997; Wahid et al., 2007; Allakhverdiev et al., 2008). Therefore, negative feedback of the G-protein and OEC is established in cucumber in relation to the heat stress tolerance.

Conclusion

Efforts to sustain crop production under steadily increasing global temperature remain imperative for food security. Exploring tolerance mechanisms to determine genotypes that can perform best under temperature extremes is of high priority to avoid significant shortage in food production in the following years. Thus, this study was conducted to explore the potential of different cucumber genotypes to sustain under high-temperature conditions and understanding the physio-biochemical and molecular mechanisms of high temperature tolerance in cucumber.

In our experiment, we categorized selected genotypes into various classes on the basis of important parameters analyzed in this study. Cucumber genotypes WBC-13 and DC-83 have been identified as high heat tolerant, and DGPC-59 and WBC-22 as highly heat susceptible whereas DARL-106, DGC-103, WBC-39-1 as tolerant and Baropatta, EC-753493, DC-206 as susceptible genotypes. We understood high chlorophyll retention, stable membrane stability index, higher retention of water content in plants, stability in net photosynthesis, good stomatal conductance and transpiration rate and maintaining less canopy temperatures in tolerant genotypes are the key physiological mechanisms in cucumber associated with heat tolerance. Accumulation of biochemicals like proline, protein and antioxidants like SOD, catalase and peroxidase formed the biochemical basis of high temperature tolerance. Upregulation of photosynthesis related genes, signal transduction genes and heat responsive genes (HSPs) in tolerant genotypes indicated their key role in determining molecular basis of heat stress tolerance in cucumber. These results indicate that the thermotolerant cucumber genotypes enhanced physio-biochemical and molecular adaptation under high-temperature stress conditions. It is suggested that these heat tolerant genotypes can be used in breeding programme, and information generated can be utilized in functional genomics in identifying the genomic regions and candidate genes associated with heat tolerance in cucumber.

Data availability statement

The original contributions presented in the study are included in the article/Supplementary Material. Further inquiries can be directed to the corresponding authors.

Author contributions

Conceived theme of the study and designed experiment: SD; Data curation: DH, DR, and SK; Investigation: DH, AD, SD, and KK; Resources: SD, TB, and AM, and VC; Supervision: SD, AM, TB; VC, AT, and PD; Visualization: SD, TB, and AM; Writing original draft: DH and SD; Review and editing: SD, TB, and AM. All authors contributed to the article and approved the submitted version.

Acknowledgments

Authors are thankful to the ICAR-Indian Agricultural Research Institute, New Delhi for providing financial support and conduct of the research program of the PhD student, DH. Besides, authors are also thankful to the NAHEP-CAAST programme of Indian Council of Agricultural Research (ICAR) for partially funding the research work.

Conflict of interest

The authors declare that the research was conducted in the absence of any commercial or financial relationships that could be construed as a potential conflict of interest.

Publisher's note

All claims expressed in this article are solely those of the authors and do not necessarily represent those of their affiliated organizations, or those of the publisher, the editors and the reviewers. Any product that may be evaluated in this article, or claim that may be made by its manufacturer, is not guaranteed or endorsed by the publisher.

Supplementary material

The Supplementary Material for this article can be found online at: https://www.frontiersin.org/articles/10.3389/fpls.2023.1128928/full#supplementary-material

References

Akram, N. A., Iqbal, M., Muhammad, A., Ashraf, M., Al-Qurainy, F., and Shafiq., S. (2018). Aminolevulinic acid and nitric oxide regulate oxidative defense and secondary metabolisms in canola (*Brassica napus* l.) under drought stress. *Protoplasma* 255 (1), 163–174. doi: 10.1007/s00709-017-1140-x

Aleem, S., Sharif, I., Tahir, M., Najeebullah, M., Nawaz, A., and Khan, M. I. (2021). Impact of heat stress on cauliflower (*Brassica oleracea* var. *Botrytis*): A physiological assessment. *Pak J. Agric. Sci.* 34 (3), 479–486. doi: 10.17582/journal.pjar/2021/34.3.479.486

Alexandersson, E., Danielson, J. A., Råde, J., Moparthi, V. K., Fontes, M., and Kjellbom, P. (2010). Transcriptional regulation of aquaporins in accessions of arabidopsis in response to drought stress. *Plant J.* 61 (4), 650–660. doi: 10.1111/j.1365-313X.2009.04087.x

Ali, M., Ayyub, C. M., Amjad, M., and Ahmad, R. (2019). Evaluation of thermo-tolerance potential in cucumber genotypes under heat stress. *Pak J. Agric. Sci.* 56 (1), 53–61.

Allakhverdiev, S. I., Kreslavski, V. D., Klimov, V. V., Los, D. A., Carpentier, R., and Mohanty, P. (2008). Heat stress: An overview of molecular responses in photosynthesis. *Photosynth Res.* 98 (1-3), 541–550. doi: 10.1007/s11120-008-9331-0

Allakhverdiev, S. I., Yruela, I., Picorel, R., and Klimov, V. (1997). Bicarbonate is an essential constituent of the water-oxidizing complex of photosystem II. *Proc. Natl. Acad. Sci. U S A.* 94 (10), 5050–5054. doi: 10.1073/pnas.94.10.5050

Alzahrani, Y., Kuşvuran, A., Alharby, H. F., Kuşvuran, S., and Rady, M. (2018). The defensive role of silicon in wheat against stress conditions induced by drought, salinity or cadmium. *Ecotoxicol Environ. Saf.* 154, 187–196. doi: 10.1016/j.ecoenv.2018.02.057

An, J., Cheng, C., Hu, Z., Chen, H., Cai, W., and Yu, B. (2018). The panax ginseng PgTIP1 gene confers enhanced salt and drought tolerance to transgenic soybean plants by maintaining homeostasis of water, salt ions and ROS. *Environ. Exp. Bot.* 155, 45–55. doi: 10.1016/j.envexpbot.2018.06.025

Arnaoudova, Y., Topalova, E., and Todorova, V. (2020). High temperature effect on the male gametophyte and the photosynthetic activity of two *Capsicum annuum* L. cultivars. *Bulgar. J. Agric. Sci.* 26 (2), 409–415.

Ashraf, M., and Hafeez, M. (2004). Thermotolerance of pearl millet and maize at early growth stages: growth and nutrient relations. *Biol. Plant* 48 (1), 81–86. doi: 10.1023/B:BIOP.0000024279.44013.61

Bailly, C., Benamar, A., Corbineau, F., and Cone, D. (1996). Changes in malondialdehyde content and in superoxide dismutase, catalase and glutathione reductase activities in sunflower seeds as related to deterioration during accelerated aging. *Physiol. Plant* 97, 104–110. doi: 10.1111/j.1399-3054.1996.tbOO485

Barrs, H. D., and Weatherley, E. (1962). A re-examination of the relative turgidity technique for estimating water deficits in leaves. *Aust. Jnl Bio Sci.* 15 (3), 413–428. doi: 10.1071/BI9620413

Bates, L. S., Waldren, R. P., and Teare, I. (1973). Rapid determination of free proline for water-stress studies. *Plant Soil.* 39 (1), 205–207. doi: 10.1007/BF00018060

Battisti, D. S., and Naylor, R. (2009). Historical warnings of future food insecurity with unprecedented seasonal heat. *Science* 323 (5911), 240–244. doi: 10.1126/science.1164363

Bhardwaj, D., Sahoo, R. K., Naqvi, A. R., Lakhanpaul, S., and Tuteja, N. (2020). Pea gβ subunit of G proteins has a role in nitric oxide-induced stomatal closure in response to heat and drought stress. *Protoplasma* 257 (6), 1639–1654. doi: 10.1007/s00709-020-01529-6

Bhattarai, S., Harvey, J. T., Djidonou, D., and Leskovar, D. (2021). Exploring morpho-physiological variation for heat stress tolerance in tomato. *Plants (Basel).* 10 (2), 347. doi: 10.3390/plants10020347

Bita, C. E., and Gerats, T. (2013). Plant tolerance to high temperature in a changing environment: scientific fundamentals and production of heat stress-tolerant crops. *Front. Plant Sci.* 4. doi: 10.3389/fpls.2013.00273

Bradford, M. M. (1976). A rapid and sensitive method for the quantitation of microgram quantities of protein utilizing the principle of protein–dye binding. *Anal. Biochem.* 72, 248–254. doi: 10.1006/abio.1976.9999

Chakraborty, N., Singh, N., Kaur, K., and Raghuram, N. (2015). G-Protein signaling components GCR1 and GPA1 mediate responses to multiple abiotic stresses in arabidopsis. *Front. Plant Sci.* 6. doi: 10.3389/fpls.2015.01000

Chaumont, F., and Tyerman, S. D. (2014). Aquaporins: Highly regulated channels controlling plant water relations. *Plant Physiol.* 164 (4), 1600–1618. doi: 10.1104/pp.113.233791

Cohen, S. P., and Leach, E. (2020). High temperature-induced plant disease susceptibility: more than the sum of its parts. *Curr. Opin. Plant Biol.* 56, 235–241. doi: 10.1016/j.pbi.2020.02.008

Cohen, I., Zandalinas, S. I., Huck, C., Fritschi, F. B., and Mittler, R. (2021). Meta-analysis of drought and heat stress combination impact on crop yield and yield components. *Physiol. Plant* 171 (1), 66–76. doi: 10.1111/ppl.13203

Danielson, J. A., and Johanson, U. (2008). Unexpected complexity of the aquaporin gene family in the moss physcomitrella patens. *BMC Plant Biol.* 8, 45. doi: 10.1186/1471-2229-8-45

Dar, M. I., Naikoo, M. I., Rehman, F., Naushin, F., and Khan, A. (2016). *Proline accumulation in plants: Roles in stress tolerance and plant development* (India: Springer).

Dhindsa, R. S., Plumb-Dhindsa, P., and Thorpe, T. (1981). Leaf senescence: Correlated with increased levels of membrane permeability and lipid peroxidation and decreased levels of superoxide dismutase and catalase. *J. Exp. Bot.* 32 (1), 93–101. doi: 10.1093/jxb/32.1.93

Ding, X., Jiang, Y., Hao, T., Jin, H., Zhang, H., and He, L. (2016). Effects of heat shock on photosynthetic properties, antioxidant enzyme activity, and downy mildew of cucumber (*Cucumis sativus* l.). *PloS One* 11 (4), e0152429. doi: 10.1371/journal.pone.0152429

Djanaguiraman, M., Boyle, D. L., Welti, R., Jagadish, S. K., and Prasad, V. (2018). Decreased photosynthetic rate under high temperature in wheat is due to lipid desaturation, oxidation, acylation, and damage of organelles. *BMC Plant Biol.* 18 (1), 55. doi: 10.1186/s12870-018-1263-z

Faiz, H., Ayyub, C. M., Khan, R. W., and Ahmad, R. (2020). Morphological, physiological and biochemical responses of eggplant (*Solanum melongena* L.) seedling to heat stress. *J. Agric. Sci.* 57, 371–380.

Firmansyah, A.N., and Argosubekti, N. (2020). A review of heat stress signaling in plants. *In IOP Conference Series: Earth and Environmental Science*; Bristol, UK: IOP Publishing, Volume 484.

Gong, Z., Xiong, L., Shi, H., Yang, S., Herrera-Estrella, L. R., and Xu, G. (2020). Plant abiotic stress response and nutrient use efficiency. *Sci. China Life Sci.* 63 (5), 635–674. doi: 10.1007/s11427-020-1683-x

Guo, M., Lu, J. P., Zhai, Y. F., Chai, W. G., Gong, Z. H., and Lu, H. (2015). Genome-wide analysis, expression profile of heat shock factor gene family (CaHsfs) and characterisation of CaHsfA2 in pepper (*Capsicum annuum* l.). *BMC Plant Biol.* 15, 151. doi: 10.1186/s12870-015-0512-7

Hachez, C., Moshelion, M., Zelazny, E., Cavez, D., and Chaumont, F (2006). Localization and quantifcation of plasma membrane aquaporin expression in maize primary root: a clue to understanding their role as cellular plumbers. *Plant Mol Biol.* 62 (1-2), 305–23. doi: 10.1007/s11103-006-9022-1

Hachez, C., Veselov, D., Ye, Q., Reinhardt, H., Knipfer, T., and Fricke, W. (2012). Short-term control of maize cell and root water permeability through plasma membrane aquaporin isoforms. *Plant Cell Environ.* 35 (1), 185–198. doi: 10.1111/j.1365-3040.2011.02429.x

Hayamanesh, S. (2018). *The effect of high temperature on physiological and metabolic parameters and reproductive tissues of okra (Abelmoschus esculentus (L.) Moench)* [doctoral dissertation]

Hassan, M. U., Chattha, M. U., Khan, I., Chattha, M. B., Barbanti, L., and Aamer, M. (2021). Heat stress in cultivated plants: nature, impact, mechanisms, and mitigation strategies-a review. *Plant Biosyst.* 155 (2), 211–234. doi: 10.1080/11263504.2020.1727987

Havaux, M., and Tardy, F. (1996). Temperature-dependent adjustment of the thermal stability of photosystem II *in vivo*: Possible involvement of xanthophyll-cycle pigments. *Planta* 198 (3), 324–333. doi: 10.1007/BF00620047

Hazman, M., Hause, B., Eiche, E., Nick, P., and Riemann, M. (2015). Increased tolerance to salt stress in OPDA-deficient rice allene oxide cyclase mutants is linked to an increased ROS scavenging activity. *J. Exp. Bot.* 66 (11), 3339–3352. doi: 10.1093/jxb/erv142

He, Y., Fan, M., Sun, Y., and Li, L. (2018). Genome-wide analysis of watermelon HSP20s and their expression profiles and subcellular locations under stresses. *Int. J. Mol. Sci.* 20 (1), 12. doi: 10.3390/ijms20010012

Hofmann, R. (2009). The plasma membrane as first responder to heat stress. *Plant Cell.* 21 (9), 2544. doi: 10.1105/tpc.109.210912

Hwang, S. Y., Lin, H. W., Chern, R. H., Lo, H. F., and Li, L. (1999). Reduced susceptibility to waterlogging together with highlight stress is related to increases in superoxide dismutase and catalase activities in sweet potato. *Plant Growth Regul.* 27 (3), 167–172. doi: 10.1023/A:1006100508910

Kaur, G., and Asthir, B. (2015). Proline: A key player in plant abiotic stress tolerance. *Biol. Plant* 59 (4), 609–619. doi: 10.1007/s10535-015-0549-3

Kotak, S., Larkindale, J., Lee, U., Vierling, E., and Scharf, D. (2007). Complexity of the heat stress response in plants. *Curr. Opin. Plant Biol.* 10 (3), 310–316. doi: 10.1016/j.pbi.2007.04.011

Li, B. J., Gao, K., Ren, H. M., and Tang, Q. (2018). Molecular mechanisms governing plant responses to high temperatures. *J. Integr. Plant Biol.* 60 (9), 757–779. doi: 10.1111/jipb.12701

Li, G., Santoni, V., and Maurel, C. (2014). Plant aquaporins: roles in plant physiology. *Biochim Biophys Acta* 1840 (5), 1574–82. doi: 10.1016/j.bbagen.2013.11.004

Liu, S., Chen, C., Chen, G., Cao, B., Chen, Q., and Lei, J. (2012). RNA-Sequencing tag profiling of the placenta and pericarp of pungent pepper provides robust candidates contributing to capsaicinoid biosynthesis. *Plant Cell Tiss Organ Cult (PCTOC)* 110 (1), 111–121. doi: 10.1007/s11240-012-0135-8

Liu, J. Z., Feng, L. L., Li, J. M., and He, Z. H. (2015). Genetic and epigenetic control of plant heat responses. *Front. Plant Sci.* 6. doi: 10.3389/fpls.2015.00267

Livak, K. J., and Schmittgen, T. D. (2001). Analysis of relative gene expression data using real-time quantitative PCR and the 2-ΔΔCT method. *Methods* 25 (4), 402–408. doi: 10.1006/meth.2001.1262

Lu, L., Dong, C., Liu, R., Zhou, B., Wang, C., and Shou, H. (2018). Roles of soybean plasma membrane intrinsic protein GmPIP2; 9 in drought tolerance and seed development. *Front. Plant Sci.* 9. doi: 10.3389/fpls.2018.00530

Matsumoto, T., Lian, H. L., Su, W. A., Tanaka, D., Liu, C., and Iwasaki, I. (2009). Role of the aquaporin PIP1 subfamily in the chilling tolerance of rice. *Plant Cell Physiol.* 50 (2), 216–229. doi: 10.1093/pcp/pcn190

Maurel, C., Verdoucq, L., Luu, D. T., and Santoni, V. (2008). Plant aquaporins: membrane channels with multiple integrated functions. *Annu. Rev. Plant Biol.* 59, 595–624. doi: 10.1146/annurev.arplant.59.032607.092734

Meglic, V., Serquen, F., and Staub, J. E. (1996). Genetic diversity in cucumber (*Cucumis sativus* l.): I. a reevaluation of the US germplasm collection. *Genet. Resour Crop Evol.* 43 (6), 533–546. doi: 10.1007/BF00138830

Misra, S., Wu, Y., Venkataraman, G., Sopory, S. K., and Tuteja, N. (2007). Heterotrimeric G-protein complex and G-protein-coupled receptor from a legume (Pisum sativum): Role in salinity and heat stress and cross-talk with phospholipase. *C. Plant J.* 51 (4), 656–669. doi: 10.1111/j.1365-313X.2007.03169.x

Moradpour, M., Abdullah, A., and Namasivayam, P. (2021). The impact of heat stress on morpho-physiological response and expression of specific genes in the heat stress-responsive transcriptional regulatory network in *Brassica oleracea*. *Plants (Basel).* 10 (6), 1–19. doi: 10.3390/plants10061064

Moreno-Galván, A. E., Cortés-Patiño, S., Romero-Perdomo, F., Uribe-Vélez, D., Bashan, Y., and Bonilla, R. R. (2020). Proline accumulation and glutathione reductase activity induced by drought-tolerant rhizobacteria as potential mechanisms to alleviate drought stress in Guinea grass. *Appl. Soil Ecol.* 147, 103367. doi: 10.1016/j.apsoil.2019.103367

Moshelion, M., Hachez, C., Ye, Q., Cavez, D., Bajji, M., and Jung, R. (2009). Membrane water permeability and aquaporin expression increase during growth of maize suspension cultured cells. *Plant Cell Environ.* 32 (10), 1334–1345. doi: 10.1111/j.1365-3040.2009.02001.x

Nath, M., Bhatt, D., Prasad, R., Gill, S. S., Anjum, N. A., and Tuteja, N. (2016). Reactive oxygen species generation-scavenging and signaling during plant-arbuscular mycorrhizal and piriformospora indica interaction under stress condition. *Front. Plant Sci.* 7. doi: 10.3389/fpls.2016.01574

Niu, Y., and Xiang, Y. (2018). An overview of biomembrane functions in plant responses to high-temperature stress. *Front. Plant Sci.* 9. doi: 10.3389/fpls.2018.00915

Nurdiani, D., Widyajayantie, D., and Nugroho, S. (2018). OsSCE1 encoding SUMO E2-conjugating enzyme involves in drought stress response of *Oryza sativa*. *Rice Sci.* 25 (2), 73–81. doi: 10.1016/j.rsci.2017.11.002

Ohkawa, H., Ohishi, N., and Yagi, N. Y. (1979). Assay of lipid peroxides in animal tissue by thiobarbituric acid reaction. *Anal. Biochem.* 95, 351–358. doi: 10.1016/0003-2697(79)90738-3

Park, H. J., Jung, W. Y., Lee, S. S., Song, J. H., Kwon, S. Y., and Kim, H. (2013). Use of heat stress responsive gene expression levels for early selection of heat tolerant cabbage (*Brassica oleracea* l.). *Int. J. Mol. Sci.* 14 (6), 11871–11894. doi: 10.3390/ijms140611871

Patankar, H. V., Al-Harrasi, I., Al-Yahyai, R., and Yaish, M. W. (2019). Functional characterization of date palm aquaporin gene PdPIP1; 2 confers drought and salinity tolerance to yeast and arabidopsis. *Genes* 10 (5), 390. doi: 10.3390/genes10050390

Pereira, G. G., Molina, S. G., Lea, P. J., and Azevedo, R. A. (2002). Activity of antioxidant enzymes in response to cadmium in *Crotalaria juncea*. *Plant Soil.* 239 (1), 123–132. doi: 10.1023/A:1014951524286

Raja, V., Majeed, U., Kang, H., Andrabi, K. I., and John, R. (2017). Abiotic stress: interplay between ROS, hormones and MAPKs. *Environ. Exp. Bot.* 137, 142–157. doi: 10.1016/j.envexpbot.2017.02.010

Raja, V., Qadir, S. U., Alyemeni, M. N., and Ahmad, P. (2020). Impact of drought and heat stress individually and in combination on physio-biochemical parameters, antioxidant responses, and gene expression in *Solanum lycopersicum*. *3 Biotech.* 10 (5), 208. doi: 10.1007/s13205-020-02206-4

Rajametov, S. N., Yang, E. Y., Cho, M. C., Chae, S. Y., Jeong, H. B., and Chae, W. B. (2021). Heat-tolerant hot pepper exhibits constant photosynthesis *via* increased transpiration rate, high proline content and fast recovery in heat stress condition. *Sci. Rep.* 11 (1), 14328. doi: 10.1038/s41598-021-93697-5

Ramiro, D. A., Guerreiro-Filho, O., and Mazzafera, P. (2006). Phenol contents, oxidase activities, and the resistance of coffee to the leaf miner *Leucoptera coffeella*. *J. Chem. Ecol.* 32 (9), 1977–1988. doi: 10.1007/s10886-006-9122-z

Richter, K., Haslbeck, M., and Buchner, J. (2010). The heat shock response: life on the verge of death. *Mol. Cell.* 40 (2), 253–266. doi: 10.1016/j.molcel.2010.10.006

Rodríguez, M., Canales, E., and Borrás- Hidalgo, O. (2005). Molecular aspects of abiotic stress in plants. *Biotechnol. Appl.* 22, 1–10.

Rosales, M. A., Maurel, C., and Nacry, P. (2019). Abscisic acid coordinates dose-dependent developmental and hydraulic responses of roots to water deficit. *Plant Physiol.* 180 (4), 2198–2211. doi: 10.1104/pp.18.01546

Sairam, R. K., Deshmukh, P. S., and Shukla, D. S. (1997). Tolerance of drought and temperature stress in relation to increased antioxidant enzyme activity in wheat. *J. Agron. Crop Sci.* 178 (3), 171–178. doi: 10.1111/j.1439-037X.1997.tb00486.x

Shaheen, M. R., Ayyub, C. M., Amjad, M., and Waraich, E. A. (2016). Morpho-physiological evaluation of tomato genotypes under high temperature stress conditions. *J. Sci. Food Agric.* 96 (8), 2698–2704. doi: 10.1002/jsfa.7388

Sreedharan, S., Shekhawat, U. K., and Ganapathi, T. R. d. (2013). Transgenic banana plants overexpressing a native plasma membrane aquaporin m usa PIP 1; 2 display high tolerance levels to different abiotic stresses. *Plant Biotechnol. J.* 11 (8), 942–952. doi: 10.1111/pbi.12086

Srivastava, S., Pathak, A. D., Gupta, P. S., and Srivastava, A. K. (2012). Hydrogen peroxide-scavenging enzymes impart tolerance to high temperature induced oxidative stress in sugarcane. *J. Environ. Biol.* 33 (3), 657–661.

Staub, J. E., Serquen, F. C., Horejsi, T., and Chen, J. F. (1999). Genetic diversity in cucumber (*Cucumis sativus* l.): IV. an evaluation of Chinese germplasm1. *Genet. Resour Crop Evol.* 46 (3), 297–310. doi: 10.1023/A:1008663225896

Stefanov, D., Petkova, V., and Denev, I. D. (2011). Screening for heat tolerance in common bean (*Phaseolus vulgaris* l.) lines and cultivars using JIP-test. *Sci. Hortic.* 128 (1), 1–6. doi: 10.1016/j.scienta.2010.12.003

Suzuki, N., Rivero, R. M., Shulaev, V., Blumwald, E., and Mittler, R. (2014). Abiotic and biotic stress combinations. *New Phytol.* 203 (1), 32–43. doi: 10.1111/nph.12797

Tian, J., Trader, B.W., Reddy, K.R., Harkess, R.L., Harkess, R.L., and Harkess, R.L. (2002). Research progress on high-temperature stress injury and heat tolerance of cucumber. *China Veget* 46 (6), 878–84. doi: 10.21273/HORTSCI.46.6.878

Usman, M. G., Rafii, M. Y., Ismail, M. R., Malek, M. A., and Latif, M. A. (2015). Expression of target gene Hsp70 and membrane stability determine heat tolerance in chili pepper. *J. Am. Soc. Hortic. Sci.* 140 (2), 144–150. doi: 10.21273/JASHS.140.2.144

Vacha, F., Adamec, F., Valenta, J., and Vacha, M. (2007). Spatial location of photosystem pigment-protein complexes in thylakoid membranes of chloroplast of *Pisum sativum* studied by chlorophyll fluroscence. *J. Luminesc.* 122-123, 301–303. doi: 10.1016/j.jlumin.2006.01.148

Wahid, A. (2007). Physiological implications of metabolite biosynthesis for net assimilation and heat-stress tolerance of sugarcane (*Saccharum officinarum*) sprouts. *J. Plant Res.* 120 (2), 219–228. doi: 10.1007/s10265-006-0040-5

Wahid, A., Gelani, S., Ashraf, M., and Foolad, M. R. (2007). Heat tolerance in plants: An overview. *Environ. Exp. Bot.* 61 (3), 199–223. doi: 10.1016/j.envexpbot.2007.05.011

Wang, X., Bao, K., Reddy, U. K., Bai, Y., Hammar, S. A., and Jiao, C. (2018). The USDA cucumber (Cucumis sativus l.) collection: genetic diversity, population structure, genome-wide association studies, and core collection development. *Hortic. Res.* 5, 64. doi: 10.1038/s41438-018-0080-8

Wang, X., Gao, F., Bing, J., Sun, W., Feng, X., and Ma, X. (2019). Overexpression of the jojoba aquaporin gene, ScPIP1, enhances drought and salt tolerance in transgenic arabidopsis. *Int. J. Mol. Sci.* 20 (1), 153. doi: 10.3390/ijms20010153

Wang, M., He, X., Peng, Q., Liang, Z., Peng, Q., and Liu, W. (2020). Understanding the heat resistance of cucumber through leaf transcriptomics. *Funct. Plant Biol.* 47 (8), 704–715. doi: 10.1071/FP19209

Wang, M., Jiang, B., Peng, Q. W., Liu, W. R., He, X. M., and Liang, Z. J. (2018). Transcriptome analyses in different cucumber cultivars provide novel insights into drought stress responses. *Int. J. Mol. Sci.* 19 (7), 2067. doi: 10.3390/ijms19072067

Wang, S. Y., Jiao, H., and Faust, M. (1991). Changes in ascorbate, glutathione and related enzyme activity during thidiazuron-induced bud break of apple. *Plant Physiol.* 82, 231–236. doi: 10.1111/j.1399-3054.1991.tb00086.x

Wang, D., Qin, B. X., Li, X., Tang, D., Zhang, Y. E., and Cheng, Z. K. (2016). Nucleolar DEAD-box RNA helicase TOGR1 regulates thermotolerant growth as a pre-rRNA chaperone in rice. *PloS Genet.* 12 (2), e1005844. doi: 10.1371/journal.pgen.1005844

Wang, W., Vinocur, B., Shoseyov, O., and Altman, A. (2004). Role of plant heat-shock proteins and molecular chaperones in the abiotic stress response. *Trends Plant Sci.* 9 (5), 244–252. doi: 10.1016/j.tplants.2004.03.006

Wang, F., Wang, G. X., Li, X. Y., Huang, J. L., and Zheng, J. K. (2008). Heredity, physiology and mapping of a chlorophyll content gene of rice (*Oryza sativa* l.). *J. Plant Physiol.* 165 (3), 324–330. doi: 10.1016/j.jplph.2006.11.006

Wang, X., Zhang, J. L., Feng, X. X., Li, H. J., and Zhang, G. F. (2017). The molecular mechanisms of plant plasma membrane intrinsic proteins trafficking and stress response. *Yi Chuan.* 39 (4), 293–301. doi: 10.16288/j.yczz.16-290

Wang, L., Zhang, C., Wang, Y., Wang, Y., Yang, C., and Lu, M. (2018). Tamarix hispida aquaporin ThPIP2; 5 confers salt and osmotic stress tolerance to transgenic tamarix and arabidopsis. *Environ. Exp. Bot.* 152, 158–166. doi: 10.1016/j.envexpbot.2017.05.018

Wóycicki, R., Witkowicz, J., Gawroński, P., Dąbrowska, J., Lomsadze, A., and Pawełkowicz, M. (2011). The genome sequence of the north-European cucumber (*Cucumis sativus* l.) unravels evolutionary adaptation mechanisms in plants. *PloS One* 6 (7), e22728. doi: 10.1371/journal.pone.0022728

Xu, P. L., Guo, Y. K., Bai, J. G., Shang, L., and Wang, X. J. (2008). Effects of long-term chilling on ultrastructure and antioxidant activity in leaves of two cucumber cultivars under low light. *Physiol. Plant* 132 (4), 467–478. doi: 10.1111/j.1399-3054.2007.01036.x

Yu, B., Ming, F., Liang, Y., Wang, Y., Gan, Y., and Qiu, Z. (2022). Heat stress resistance mechanisms of two cucumber varieties from different regions. *Int. J. Mol. Sci.* 23 (3), 1817. doi: 10.3390/ijms23031817

Yu, B., Yan, S., Zhou, H., Dong, R., Lei, J., and Chen, C. (2018). Overexpression of CsCaM3 improves high temperature tolerance in cucumber. *Front. Plant Sci.* 9. doi: 10.3389/fpls.2018.00797

Zarrouk, O., Garcia-Tejero, I., Pinto, C., Genebra, T., Sabir, F., and Prista, C. (2016). Aquaporins isoforms in cv. touriga nacional grapevine under water stress and recovery-regulation of expression in leaves and roots. *Agric. Water Manage.* 164, 167–175. doi: 10.1016/j.agwat.2015.08.013

Zhao, Q., Chen, W., Bian, J., Xie, H., Li, Y., and Xu, C. (2018). Proteomics and phosphoproteomics of heat stress-responsive mechanisms in spinach. *Front. Plant Sci.* 9. doi: 10.3389/fpls.2018.00800

Zhao, C., Liu, B., Piao, S., Wang, X., Lobell, D. B., and Huang, Y. (2017). Temperature increase reduces global yields of major crops in four independent estimates. *Proc. Natl. Acad. Sci. U S A.* 114 (35), 9326–9331. doi: 10.1073/pnas.1701762114

Zhou, R., Kjaer, K. H., Rosenqvist, E., Yu, X., Wu, Z., and Ottosen, C. O. (2017). Physiological response to heat stress during seedling and anthesis stage in tomato genotypes differing in heat tolerance. *J. Agron. Crop Sci.* 203 (1), 68–80. doi: 10.1111/jac.12166

frontiers | Frontiers in Plant Science

TYPE Original Research
PUBLISHED 22 February 2023
DOI 10.3389/fpls.2023.1133643

OPEN ACCESS

EDITED BY
Shuvasish Choudhury,
Assam University, India

REVIEWED BY
Dr. Owais Ali Wani,
Sher-e-Kashmir University of Agricultural Sciences and Technology of Kashmir, India
Arun Jyoti Nath,
Assam University, India

*CORRESPONDENCE
Xiaorong Fan
xiaorongfan@njau.edu.cn
Xin Xiao
xiaoxin8088@126.com

†These authors have contributed equally to this work

SPECIALTY SECTION
This article was submitted to Plant Abiotic Stress, a section of the journal Frontiers in Plant Science

RECEIVED 29 December 2022
ACCEPTED 31 January 2023
PUBLISHED 22 February 2023

CITATION
Iqbal MF, Zhang Y, Kong P, Wang Y, Cao K, Zhao L, Xiao X and Fan X (2023) High-yielding nitrate transporter cultivars also mitigate methane and nitrous oxide emissions in paddy.
Front. Plant Sci. 14:1133643.
doi: 10.3389/fpls.2023.1133643

High-yielding nitrate transporter cultivars also mitigate methane and nitrous oxide emissions in paddy

Muhammad Faseeh Iqbal[1,2†], Yong Zhang[3†], Pulin Kong[1,2], Yulong Wang[1,2], Kaixun Cao[4], Limei Zhao[1,2], Xin Xiao[4,5*] and Xiaorong Fan[1,2,6*]

[1]National Key Laboratory of Crop Genetics, Germplasm Enhancement and Utilization, College of Resources and Environmental Sciences, Nanjing Agricultural University, Nanjing, China, [2]Key Laboratory of Plant Nutrition and Fertilization in Lower-Middle Reaches of the Yangtze River, Ministry of Agriculture, College of Resources and Environmental Sciences, Nanjing Agricultural University, Nanjing, China, [3]Institute of Food Crops, Jiangsu Academy of Agricultural Sciences, Jiangsu High Quality Rice Research and Development Center, Nanjing Branch of China National Center for Rice improvement, Nanjing, China, [4]College of Resource and Environment, Anhui Science and Technology University, Chuzhou, China, [5]College of Resource and Environment, Anqing Normal University, Anqing, China, [6]Zhongshan Biological Breeding Laboratory, Nanjing, China

Development of high yield rice varieties is critical to ensuring global food security. However, the emission of greenhouse gases (GHG) such as Methane (CH_4) and Nitrous oxide (N_2O) from paddy fields threatens environmental sustainability. In this study, we selected overexpressed high-affinity nitrate transporters (NRT2.3 along with their partner protein NAR2.1) cultivars, which are effective nitrogen use efficient transgenic lines *pOsNAR2.1: OsNAR2.1* (Ox2) and *p35S:OsNRT2.3b* (O8). We used high (270 kg N/ha) and low (90 kg N/ha) nitrogen (N) fertilizers in paddy fields to evaluate morphophysiological traits, including GHG emission. We found that Ox2 and O8 reduced CH_4 emissions by 40% and 60%, respectively, compared to their wild type (WT). During growth stages, there was no consistent N_2O discharge pattern between WT and transgenics (Ox2, O8) in low and high N application. However, total cumulative N_2O in a cropping season reduced in O8 and increased in Ox2 cultivars, compared to WT. Root aerenchyma formation reduced by 30-60% in transgenic lines. Methanogens like *mcrA* in low and high N were also reduced by up to 50% from rhizosphere of Ox2 and O8. However, the nitrifying bacterial population such as *nosZ* reduced in both transgenics significantly, but *nirK* and *nirS* did not show a consistent variation. The high yield of transgenic rice with limited aerenchyma mitigates the discharge of CH_4 and N_2O by reducing root exudates that provide substrates for GHG. Our results improve understanding for breeders to serve the purpose of sustainable development.

KEYWORDS

sustainable agriculture, food security, greenhouse gases mitigation, climate-smart strategies, methanogens, nitrate transporters

Introduction

Greenhouse gases (GHG) pose a significant threat to the environment with nitrous oxide (N_2O) and methane (CH_4) are among the chief contributors to global warming. The global warming potential of CH_4 and N_2O is 28 and 265 times that of carbon dioxide (CO_2) over a 100-year period (Liu S. et al., 2016; IPCC, 2014). Rice cultivation is a major contributor to GHG emission, with paddy fields responsible for 48% of CH_4 and 50% of N_2O emission among total agricultural emissions (Oo et al., 2018; Iqbal et al., 2021). Rice used as a staple food for almost half of the global population. It projected 60% increase in rice production in next few decades to meet rapidly growing demand (Dong et al., 2011; Chen et al., 2016; Frona et al., 2019). Excessive production could lead to a 60% increase in anthropogenic GHG emission (Hofstra and Vermeulen, 2016; Frona et al., 2019). To address this, research on balancing GHG mitigation and high yield is inevitable for the development of modern agriculture techniques (Oo et al., 2018).

The agriculture environment such as periodic wet/dry conditions, intensive organic material and fertilizers application like nitrogen creates suitable conditions for CH_4 and N_2O discharge in paddy conditions (Akiyama et al., 2005; Hu et al., 2012; Kritee et al., 2018). Nitrogen (N) is vital for plant growth and development, as it is an essential element in the amino acids that make up cell structures and proteins. It is also a key component of many chemical and biological process in plants, including the production of chlorophyll, the compound that allows plants to use sunlight to produce sugars from carbon dioxide and water (Xu et al., 2012; Leghari et al., 2016; Xuan et al., 2017). Rice is traditionally grown in flooded conditions (anaerobic soil), where ammonium is the primary source of N. In such conditions, aerenchyma cells in the shoots transfer O_2 from shoot to root and into rhizosphere, where process of nitrification (ammonium to nitrate) occurs (Shimamura et al., 2002; Li et al., 2008). Nitrification in paddy fields can provide 25-40% of the total N taken up in the form of nitrate, primarily through a high-affinity transport system (HATS). Additionally, NUE lines facilitate uptake of phosphorus, potassium and other micro nutrients (Fan et al., 2016). These lines not only contribute to plant and root development but also produce green cultivars with less greenhouse effects. Therefore, the benefits of using nitrogen efficient cultivars extend beyond facilitating O_2 transport and N uptake (Hirel et al., 2007; Leghari et al., 2016; Naz et al., 2019; Zhang et al., 2021).

Elevated CO_2, N and microbial biomass in rhizosphere are vital for soil GHG emission. Therefore, addressing these areas to mitigate GHG emission is a useful approach (Yang et al., 2022). Several effective methods have been reported to reduce GHG emission, such as management practices, effective drainage, controlling soil microbial and chemical properties, roots aerenchyma, introducing genetically modified crops to reduce usage of fertilizers (Thomson et al., 2012; Carlson et al., 2016; Lévesque et al., 2020; Iqbal et al., 2021). Aerenchyma in plants not only removes gases (such as N_2O, CH_4, ethylene, CO_2, and H_2O_2) into the rhizosphere, but also provides a channel for gaseous exchange between the aerial and flooded parts in submerged plants, like rice. Furthermore, it facilitates oxygen diffusion to the root tip (Armstrong, 1980; Justin and Armstrong, 1991). Microbes play an essential role in fixing GHG in soil during paddy conditions. In waterlogged conditions, N_2O discharge is possible after microbial transformation of N in the soil and nutrients. It is often increased where N availability surpasses plant requirements like in paddy conditions (Smith et al., 2008). In case of CH_4, organic materials decomposed during anaerobic conditions and CH_4 gas is produced after oxidation (Smith et al., 2008). The N_2O emission from agriculture is primarily owed to ammonia oxidation and bacterial fixation, the initiation to nitrification (Thomson et al., 2012). Methanotrophs are also known as methane-oxidizing bacteria (MOB) use CH_4 as an energy source and ingest 30% methane before reaching into the atmosphere (Liu et al., 2011; Shrestha et al., 2010; Yang et al., 2014).

A critical soil procedure that is directly affected by changes in plant biotic and abiotic stress is CH_4 oxidation. A plant stress response is an essential factor for the oxidation of CH_4 (Zhou et al., 2013). The practice of using high-yielding cultivars (less stress) of rice in agriculture accounts for almost 50% of the recent yield growth in developing countries. These new cultivars mainly focused on increasing the harvest index, but this strategy may also be beneficial for reducing GHG emissions. As harvest index increases with higher plant biomass, it can alternatively decrease the production of root exudates that fuel CH_4 production (Denier et al., 2002; Su et al., 2015; Jiang et al., 2017). The Key source for N_2O in the soil is N and the balanced use of N is imperative for mitigating N_2O emission in agriculture (Thomson et al., 2012). Therefore, in this study, we have used *pOsNAR2.1: OsNAR2.1* (Ox2) (Chen et al., 2017) and *p35S: OsNRT2.3b* (O8) overexpression materials (Fan et al., 2016) previously reported as high-yield nitrate transporter cultivars and very efficient for NUE.

The Hypothesis of this study is that the use of high-yielding N efficient rice cultivars will result in reduced GHG emissions under low and high N regimes through limited aerenchyma formation, methanotrophs population, and efficient utilization of available N in soil. The objectives of this study are:

- To measure the CH_4, N_2O, and CO_2 emission from high-yielding nitrate transporter rice cultivars under low and high N regimes.
- To investigate the effect of high-yielding nitrate transporter rice cultivars on aerenchyma formation in roots and methanotrophs population in rhizosphere.
- To suggest high-yielding cultivars which can also mitigate GHG emission under low and high N regimes, thus contributing to a sustainable environment.

Materials and methods

Experimental site and transgenic materials

We selected two different types of transgenic cultivars. The first one was the *OsNAR2.1* overexpression line (Ox2) with a background of *Oryza sativa* L. ssp. *Japonica* cv. Wuyunjing7 as described in (Chen et al., 2017). The second was the *OsNRT2.3b* overexpression plant (O8) with a background of *Oryza sativa* L. ssp. *Japonica* cv.

Nipponbare as described in (Fan et al., 2016). Both cultivars (Ox2, O8) have different phenotypic backgrounds; therefore, we used and compared them with their own wildtypes. This experiment was performed in the experimental site of Anhui Science and Technology University in 2017 and 2018. The site is located in Fengyang County, Anhui Province, on south bank of the middle reaches of the Huaihe River, north latitude (32°37′-33°03′N, 117°19′-117°57′E). We also calculated soil chemical properties, the soil was yellow-brown in color, and initial soil profile was as follows: pH 7.54, available phosphorus 393.98mg/kg, available potassium 114.81mg/kg, total nitrogen 0.37g/kg, and organic matter content 8.02g/kg. Soil and plants samples were collected for further experiments in lab and examination of chemical properties before and after rice harvest. The data collection on plant phenotype and agronomic traits in field conditions were recorded following standard protocol (Chen et al., 2016).

Field experiment

The Plants were planted in a field plots that was fertilized at a rate of 270 kg N/ha for high nitrogen (HN) field and 90kg N/ha for low nitrogen (LN) field. Three plots were used to set the replicates for the test and forty-five seedlings were grown in each plot. the plot area was 3.75 square meters. Before transplantation, nylon bags with a diameter of 30um, a width of 7.5cm, and a height of 12cm were buried around the plot in advance. Each bag contained 475 grams of soil for collecting soil samples during the experiment for GHG emission, aerenchyma formation, and microbial population abundance (Nie et al., 2015; Iqbal et al., 2021). The seedlings were raised in the nursery on May 10-12, transplanted on June 7-9 and harvested on October 20-22 during planting year of 2017 and 2018. A total of 60kg/ha of urea was applied in each plot, 50% was used as a base fertilizer on June 13-14, 20% as a tiller fertilizer on July 1-2, and 30% as a spike fertilizer on August 28-29. During the basal fertilizer period, 75 kg/ha of superphosphate (containing 12% P_2O_5) and 150kg/ha of potassium chloride (containing 60% K_2O) were applied at one time. Field management and farming practices were followed according to local agricultural practices.

Methane, carbon dioxide and nitrous oxide flux measurements

The simultaneous determination of methane, carbon dioxide and nitrous oxide fluxes was calculated by using static black chamber method. We used closed box-gas chromatography (Zhang et al., 2015). Before transplanting rice to the plot, a PVC flux loop was permanently embedded in each plot to continuously monitor GHG emissions during the experiment period. A 5cm deep groove on the edge of each base was used to inject water and seal the gas chamber during gas production, in order to prevent gas exchange. The cross-sectional area of the gas tank was 0.25m^2 (50cm*50cm) and the height was 50cm. Once the rice grew taller, the height was increased to 1m.

Sponge and aluminum foil were wrapped around the exterior of the gas box to prevent drastic changes in temperature inside the chamber. The gas chamber was also equipped with a small fan to ensure that the gas in the box was fully mixed. Sampling was conducted 9:00 a.m. and 11:00 a.m. every time, using a 60ml medical syringe to collect gas from the top of the chamber, once every 5 minutes, for a total of four times (Hao et al., 2001).

Before gas chromatography analysis, the gas was transferred to a vacuum airbag for less than a day to ensure that the gas was not mixed with the outside environment. A gas chromatograph was equipped with an electron capture detector (ECD) and a flame ionization detector (Agilent 7890A network gas chromatograph, Gow Mac instruments, Bethlehem, PA, USA). It was used for the simultaneous analysis of methane, carbon dioxide, and nitrous oxide gas concentrations (Liu S. et al., 2016). The linear regression slope for the greenhouse gas concentration of the continuous samples was calculated, and the data with the linear regression value r^2<0.9 was removed from the dataset for gas flux calculation (Liu et al., 2013). The gas flux calculation formula is as follows:

$$F = H \times \rho \times (273.2 + 273.2 + T) \times (dC/dt)$$

Where F is the gas emission flux (mg m^{-2} h^{-1}), H is the height of the sampling chamber, ρ is the gas density in the standard state, and dC/dt is the slope of the concentration growth of the gas concentration fitted by a linear equation (mg m^{-3} h^{-1}). T is the temperature in the sampling chamber at the time of sampling(°C). During the test, cumulative methane, carbon dioxide, and nitrous oxide emissions were sequentially accumulated from the flux of each two adjacent intervals. For N_2O cumulative emission, the final value was multiplied by atomic mass of N_2 divided by atomic mass of N_2O (Liu et al., 2013; Liu S. et al., 2016; Iqbal et al., 2021). The gas flux calculation formula and the total cumulative GHG emission during one growing season was also calculated according to protocol given in (Iqbal et al., 2021).

Determination and quantification of root aerenchyma

Roots of WT and overexpress lines (5-6cm in length) at the tillering stage (July 9) at the experimental site of Anhui Science and Technology University were collected for the determination of aerenchyma. On the sampling day we selected five to six random plants, WT and overexpress plants' complete root tips of about 5-6cm in length and the same size were gently removed with a sharp blade and quickly placed into FAA fixative. Before embedding the root slices in resin, the root was divided into six short segments with a length of 0.5cm from the root tip, and the root samples were vacuumed in a vacuum chamber. Then, the root samples were embedded in EPON812 embedding resin (SPI, USA) (Zhu et al., 2015). The resin-embedded root tissues were sectioned using a Leica automated microtome (RM 2265, Leica, Germany), mounted on a microscope slide and dried at 42°C. The cross-sections of root tissues were observed with a fluorescence microscope (OLYMPUS BX51), and the images were recorded from the microscope using the cellSens standard software. Ventilation tissues formation was calculated from section images using Image J® software (Zhu et al., 2015).

Collection of soil and extraction of its DNA and qPCR analysis

We used WT and transgenic lines to understand microbial population dynamics under field conditions in root zones. We collected soil from the rhizosphere after transplanting seedlings from nursery (day1), at the vegetative stage (day 14 and 28) and at the reproductive stage (day 43). A quantitative analysis of soil microorganism was conducted. We quantified the relative abundance of particulate methane monooxygenase (*pmoA*), methyl coenzyme M reductase (*mcrA*) used as functional marker genes to determine methanotrophs in soil. Nitrite reductase genes (*nirK, nirS*) were used as functional marker genes to determine denitrifying bacteria in soil samples, and for active and total N_2O consuming bacteria in soil, nitrous oxide reductase genes (*nosZ*) were used as a biomarker. Soil samples were also taken before and after plantation for chemical analysis to determine the nutrient content. Nylon bags were used to collect rhizosphere soil in the field. Fresh soil with a weight of about 0.5g attached to the roots was scratched, and the total DNA was extracted from the soil using FastDNA Spin Kit for soil (MP Biomedicals LLC USA). A QuantStudio 6Flex instrument was used to conduct a soil DNA quantitative experiment, which was repeated twice for each sample. The 20ul qRT-PCR system is as follows: 10.0ul SYBR PremixExTaq (TaKaRa Norrie Biotech Auckland New Zealand), 0.4ul each of the forward and reverse primers, 2.0ul template DNA, 0.4ul DyII, 6.8ul ddH_2O (Iqbal et al., 2021).

Statistical analysis

Data were analyzed by using a *t*-test for comparing two groups and one-way analysis of variance (ANOVA) for comparing more than two groups were used followed by Tukey's test ($P<0.05$). Significant difference between two groups was shown by small alphabet letters (a, b) like 'a' shows higher value and 'b' shows smaller value. The data from Ox2 always compared with WT (Wuyunjing7 background) and O8 always compared with WT-N (Nipponbare background). Statistical analyses and Pearson correlation were conducted using the SPSS software (version 25.0) (SPSS Inc., Chicago, USA).

Results

Nitrate transporter cultivars (Ox2, O8) reduced greenhouse gases emission in paddy

We grew plants *pOsNAR2.1:OsNAR2.1* (Ox2) and *p35:OsNRT2.3b* (O8) along with their respective WT to quantify the discharge of GHG emission after planting in paddy field conditions. The details of research plot area and plant material is given in material method section. The first measurement of greenhouse gases was set to day-one after the transplanting seedlings from the nursery to the field. We separately used two kinds of Nitrogen (N) applications low nitrogen (LN) and high nitrogen (HN) in the paddy fields. Whether under high or low N conditions, methane (CH_4) emission fluxes were lower in overexpression (OE) lines as compared to their WT (Figure 1). The CH_4 discharge in Ox2 was lower than WT at the initial stages of growth, especially during the vegetative stage. However, with the passage of growth, the difference of discharge between Ox2 and its WT was minimal in high and low N conditions (Figures 1A, B). Likewise, in the O8 line, CH_4 emission fluxes show a similar pattern during the vegetative growth. However, in high N conditions, the difference between WT and N increases to more than two folds (Figures 1C, D). Total CH_4 emission significantly increased to two folds in high N conditions in WT compared to OE lines. However, the significant difference of cumulative methane emission in low N application in both Ox2 and O8 compared to their WT was less than 1.5 folds (Figure 1E).

We further calculated nitrous oxide (N_2O) emission rates among OE lines in high and low N applications. In Ox2 the emission fluxes in N_2O were significantly lower in HN regime, but it was not consistent during all plant growth stages as compared to WT (Figures 2A, B). The N_2O emission was increased significantly at LN application in Ox2 after 29 days (Figure 2A). In contrast, the O8 line shows a significant difference in N_2O emission rate during different growth stages of paddy (Figures 2C, D). The cumulative N_2O emission rate shows a similar pattern in low and high N applications. The Ox2 line slightly up-regulated the N_2O emission rate compared to its WT at LN, but the O8 reduced the N_2O emission significantly in LN and HN emission in its rhizosphere (Figure 2E). We also calculated CO_2 emission fluxes (Figure 3). The CO_2 emission was higher in both transgenic lines (Ox2, O8) as compared to their WT (Figure 3). In Ox2 line produced higher amount of CO_2 as compared to WT both in high and low N regimes (Figures 3A, B). Therefore, the cumulative emission from Ox2 was significantly higher as compared to WT in both low and high nitrogen (Figure 3E). Similarly, for line O8 significant emission was noticed for CO_2 emission compared to its WT in low N application but there was not any consistent pattern at high nitrogen application (Figures 3C, D). However, the O8 line compared to its WT for cumulative emission was significantly higher in O8 in LN and no difference was recorded for HN (Figure 3E).

Limited aerenchyma formation in Ox2 and O8 cultivars

Root aerenchyma is the passage for the discharge of gases between aerial and flooded parts in a paddy field. Therefore, we observed the development of aerenchyma among Ox2 and O8 lines. The rice root system develops during the tillering stage; we collected rice root samples to observe the aerenchyma. Through root sections, we can see that aerenchyma of WT developed earlier than Ox2 (Figure 4). At the distance of 0.5-1.0cm from the root tip, aerenchyma of WT began to form while Ox2 was not formed yet. Root aerenchyma formation was increased with continuous root development. The aerenchyma formation percentage was significantly higher in WT than Ox2, even at different distances from the root apex (Figures 4A, B). The aerenchyma formation in WT at the distance of 1.5-2.5 cm from the root apex was twofold increased as compared to Ox2 (Figures 4A,B). During the aerenchyma study in O8 line, we observed a similar pattern (Figure 5). At the distance of 0.5-2.0 cm from the apex, the

10.3389/fpls.2023.1133643

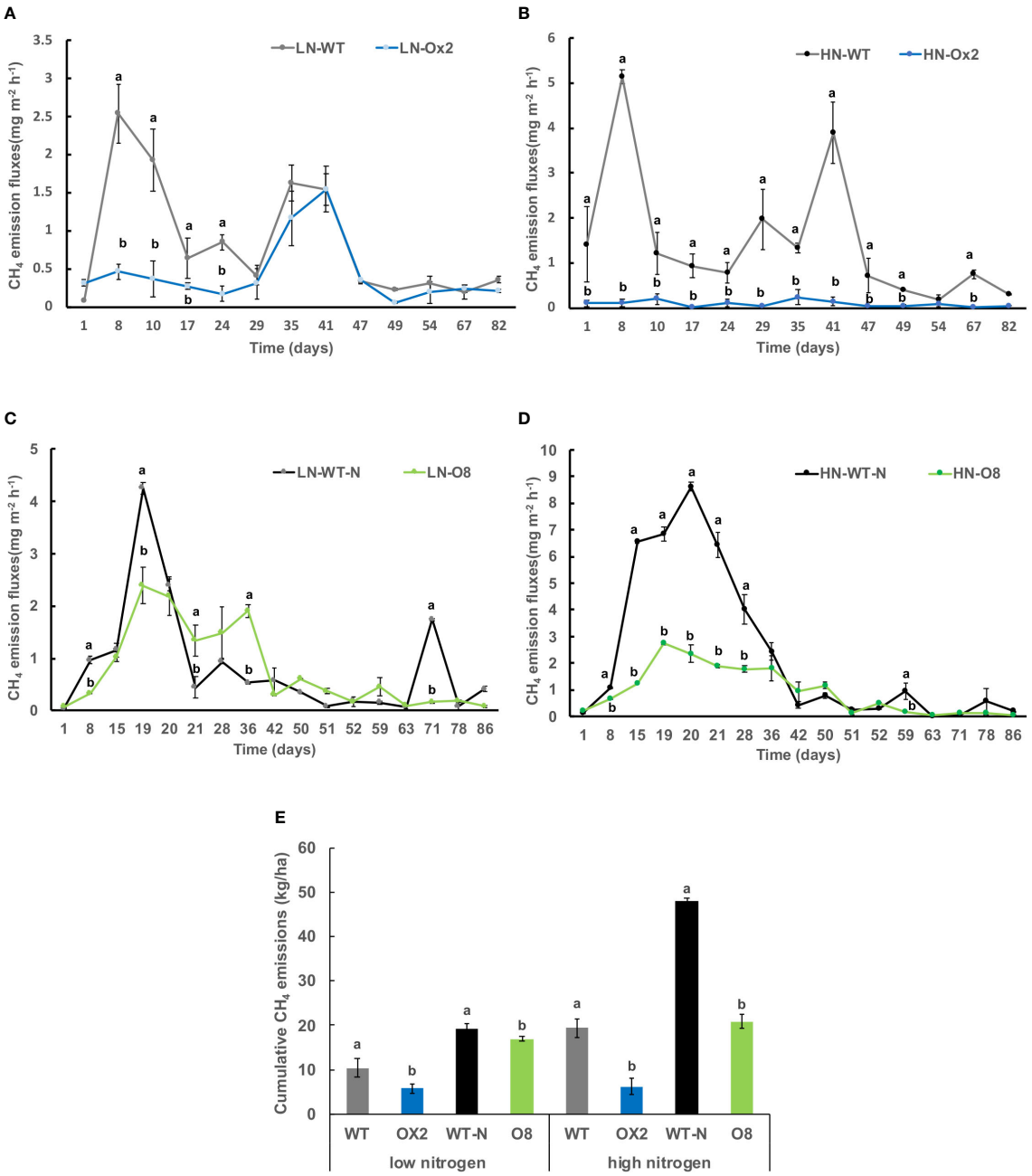

FIGURE 1
Detailed CH_4 gas emission fluxes ($mgm^{-2}h^{-1}$) from rhizosphere of WT, Ox2, WT-N and O8. The (LN) low nitrogen soil application shows in figure **(A, C)** and (HN) high nitrogen soil application shows in figure **(B, D)**. X-axis shows CH_4 gas emission recording time (days), from the first measurement after transplanting seedlings from nursery to field is day1 to onwards **(A-D)**. CH_4 emission flux ($mgm^{-2}h^{-1}$) from the rhizosphere was compared between Ox2 in figures a-b and O8 in figure **(C, D)** with their respective wildtypes (WT) separately. Figure **(E)** shows cumulative CH_4 emission during full growing season in kilogram per hectare (kg/ha). Cumulative emission data consist of 13 individual values taken during various growth stages (n=13). Error bars: SE (n = 3). Significant difference between two cultivars (transgenic and respective WT) are indicated by different letters: a= high value, b= lower value (*t*-test, $p< 0.05$).

aerenchyma formation was significantly lower in O8 lines than WT (Figures 5A,B). At the distance of 2.0 to 3.0 cm from the root tip, the aerenchyma formation showed a similar downward percentage in the O8 line than WT (Figures 5A,B). Therefore, it can speculate that transgenic rice with overexpression of *OsNAR2.1* and *OsNRT2.3b* regulates the formation of aerenchyma structure somehow. This may be regulated directly or through interaction with related genes. As for the specific molecular mechanism, it requires further investigation.

Nitrate transporter cultivars (Ox2, O8) regulated methanotrophs and nitrifying bacterial population in soil

Greenhouse gas emissions from rice fields are also associated with multiple microorganisms; methanogenic bacteria *mcrA* and *pmoA* are important methanotrophs. In addition, nitrification and denitrification bacteria; *nirK*, *nirS* and *nosZ* are involved in the

10.3389/fpls.2023.1133643

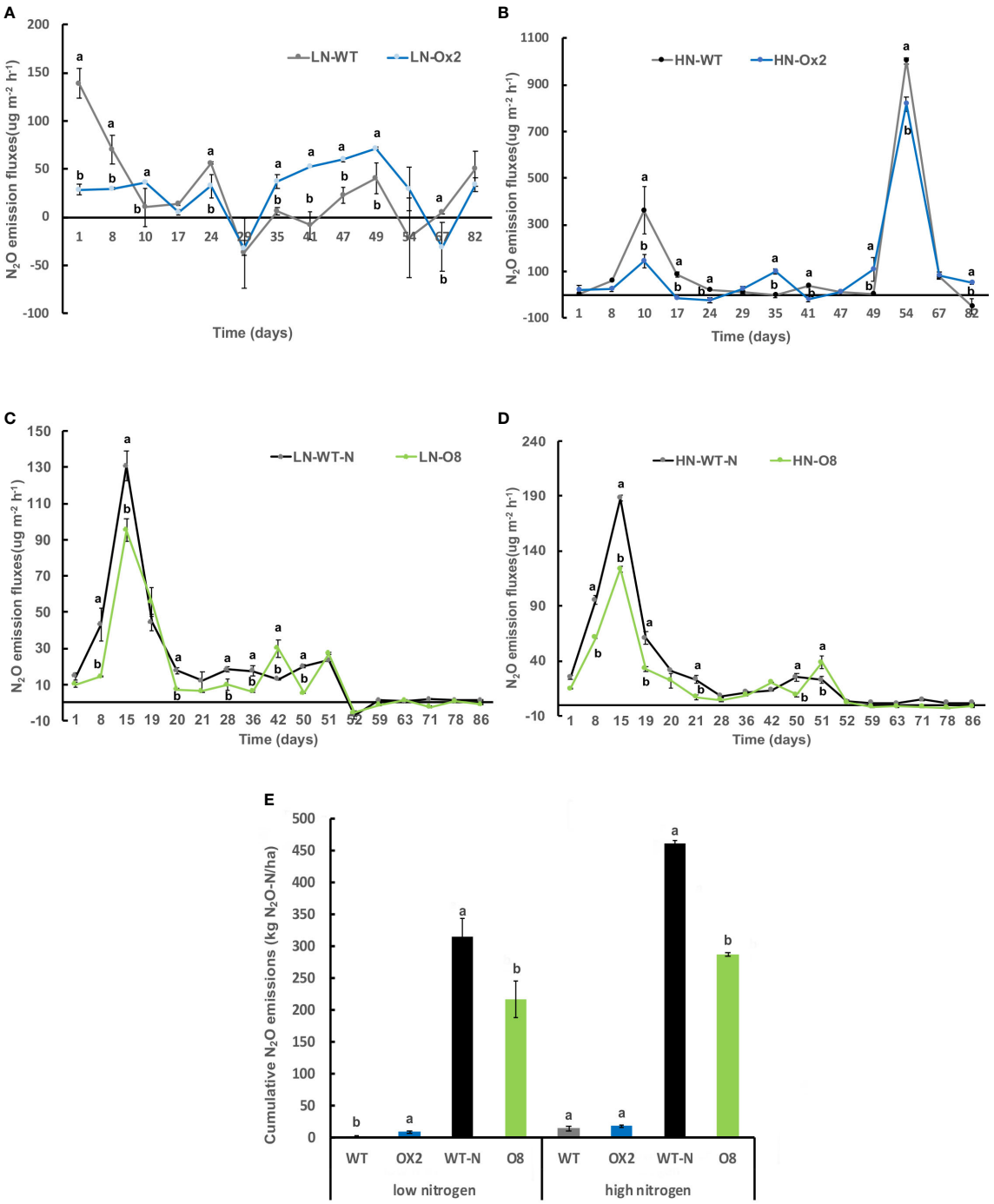

FIGURE 2
Detailed N_2O gas emission fluxes ($ugm^{-2}h^{-1}$) from rhizosphere of WT, Ox2, WT-N and O8. The (LN) low nitrogen soil application shows in figure **(A, C)** and (HN) high nitrogen soil application shows in figure **(B, D)**. X-axis shows N_2O gas emission recording time (days), from the first measurement after transplanting seedlings from nursery to field is day1 to onwards **(A-D)**. N_2O emission flux ($ugm^{-2}h^{-1}$) from the rhizosphere was compared between Ox2 in figures **(A, B)** and O8 in figure **(C, D)** with their respective wildtypes (WT) separately. Figure **(E)** shows cumulative N_2O emission during full growing season (kg N_2O-N/ha). Cumulative emission data consist of 13 individual values taken during various growth stages (n=13). Error bars: SE (n = 3 Significant difference between two cultivars (transgenic and respective WT) are indicated by different letters: a= high value, b= lower value (*t*-test, $p< 0.05$).

generation and oxidation of greenhouse gases such as N_2O. The significant difference was calculated in transgenic lines after transplanting from nursery to field called day 1 (Figures 6–9). The abundance of *mcrA* copy number was significantly decreased in Ox2 both in low and high N regimes (Figures 6A, C). The difference was maximum during the vegetative growth stage. However, in the O8 line, the *mcrA* copy number was not consistent even in high or low N applications (Figures 7A,C). The abundance of the *pmoA* microbial

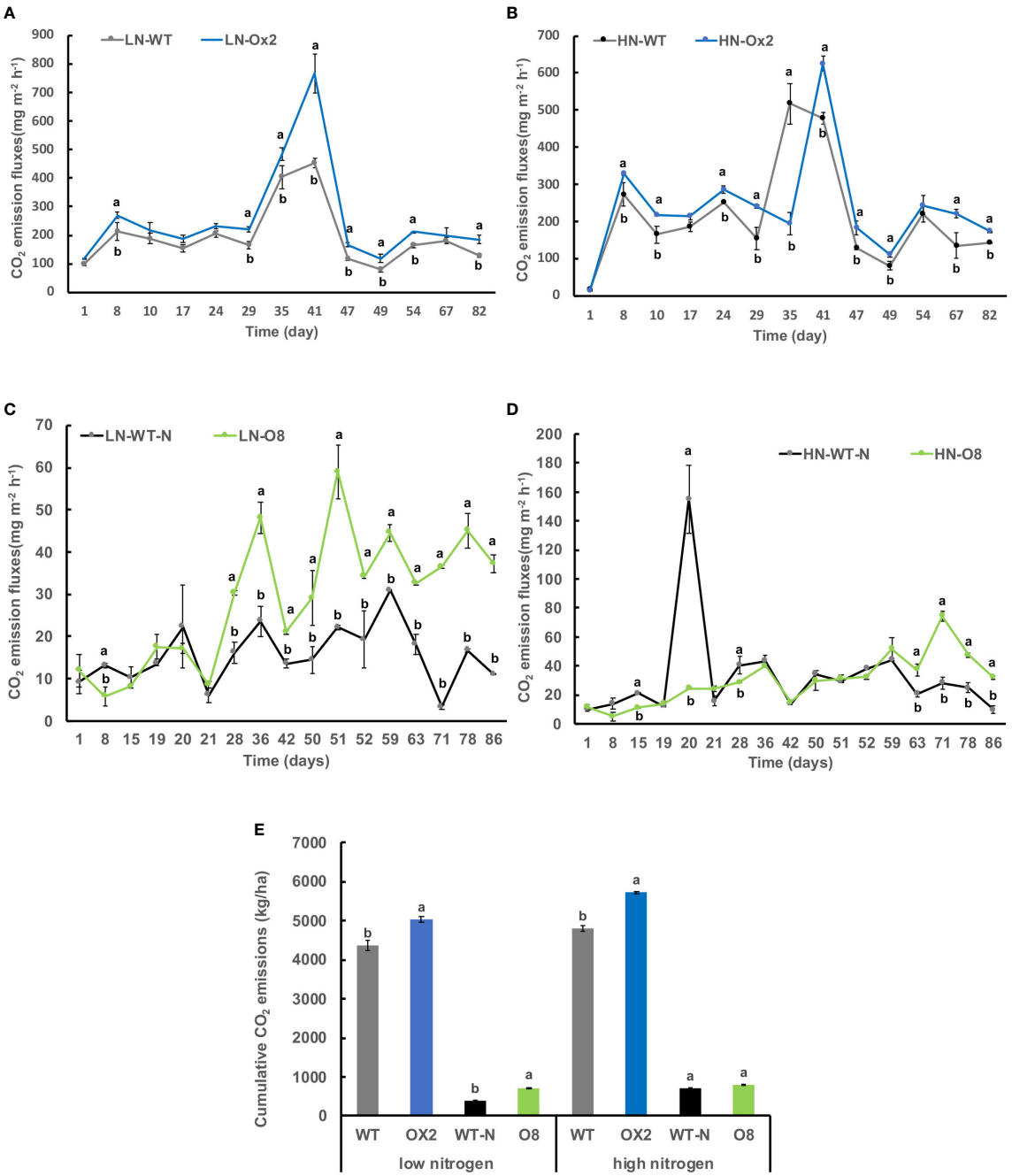

FIGURE 3
Detailed CO_2 gas emission fluxes ($mgm^{-2}h^{-1}$) from rhizosphere of WT, Ox2, WT-N and O8. The (LN) low nitrogen soil application shows in figure **(A, C)** and (HN) high nitrogen soil application shows in figure **(B, D)**. X-axis shows CO_2 gas emission recording time (days), from the first measurement after transplanting seedlings from nursery to field is day1 to onwards **(A-D)**. CO_2 emission flux ($mgm^{-2}h^{-1}$) from the rhizosphere was compared between Ox2 in figures **(A, B)** and O8 in figure **(C, D)** with their respective wildtypes (WT) separately. Figure **(E)** shows cumulative CO_2 emission during full growing season in kilogram per hectare (kg/ha). Cumulative emission data consist of 13 individual values taken during various growth stages (n=13). Error bars: SE (n = 3). Significant difference between two cultivars (transgenic and respective WT) are indicated by different letters: a= high value, b= lower value (*t*-test, $p< 0.05$).

population regulated significantly even in high and low N applications both in Ox2 and O8 lines (Figures 6, 7). However, the Ox2 was significantly higher than WT in early stage and late stage (28 days) in high nitrogen application, but there was no difference after 14 days of transplanting (Figures 6B, D). In case of O8 the *pmoA* microbial population was increased as compared to WT after 28 days in both low and high N application (Figures 7B–D).

The *nirK* abundance of WT at the mid-tiller stage was significantly higher in Ox2 and O8 lines than WT in both low and high N regimes (Figures 8, 9A, D). The trend of *nirS* microbial

10.3389/fpls.2023.1133643

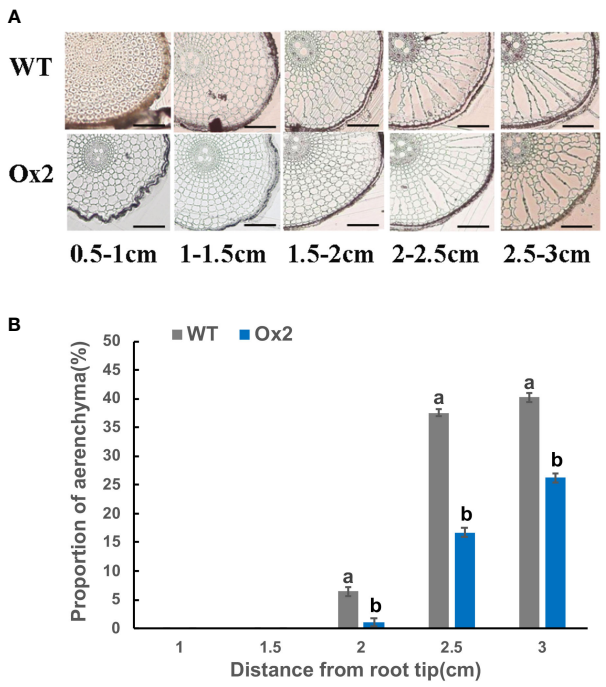

FIGURE 4
Describe aerenchyma formation in rice roots of WT and Ox2. Figure a-b show resin sections results of roots and aerenchyma formation (%) 0-0.5 cm, 0.5-1.0 cm, 1.0–1.5 cm, 1.5–2.0 cm and 2.0-2.5 cm from root apex in WT and Ox2 and significant difference between WT and Ox2 in each group are indicated by different letters: a= high value, b= lower value. Aerenchyma pics scale bar: 200um, Error bars: SE (n = 3) (*t*-test, $p< 0.05$).

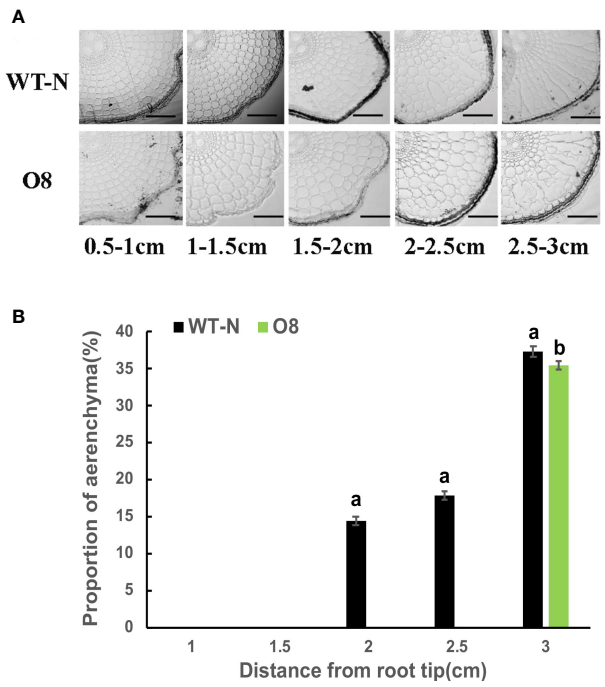

FIGURE 5
Describe aerenchyma formation in rice roots of WT and O8. Figures **(A, B)** show resin sections results of roots and aerenchyma formation (%) 0-0.5 cm, 0.5-1.0 cm, 1.0–1.5 cm, 1.5–2.0 cm and 2.0-2.5 cm from root apex in WT and O8 and significant difference between WT and O8 in each group are indicated by different letters: a= high value, b= lower value. Aerenchyma pics scale bar: 200um, Error bars: SE (n = 3) (*t*-test, $p< 0.05$).

abundance changing with time was not consistent in Ox2 and O8 even at different N regimes (Figures 8, 9B, E). The *nosZ* abundance in the Ox2 line was significantly higher than that of WT in the early stage of rice after transplanting, showed an opposite trend in the middle stage, and no significant difference in the later stage in both low and high N application (Figures 8C, F). A similar trend in line O8 compared to its WT was observed (Figures 9C, F).

Paddy soil from cultivars regulated by nutrient use efficiency

Paddy soil is a complex ecological environment. Many factors influence physical and chemical properties in paddy soil. The Ox2 and O8 lines didn't show any impact on soil pH compared to their WT (Table 1). The available P (AP) was significantly lower in O8 than its WT during low N application. But no significant difference was recorded for AP in both overexpress lines in low or high N (Table 1). The available K (AK) was significantly higher in both overexpress lines (Ox2, O8) even in low and high N regimes except the O8 line in high N application was not significant than WT (Table 1).

The total nitrogen content (TN) in rhizosphere soil in WT was significantly higher than Ox2 (Table 1). In terms of Ammonium ($NH_4^+ - N$) and nitrate (NO_3^-N) in rhizosphere soil, WT and Ox2 showed no significant difference. We recorded similar results in O8 lines in both low and high N regimes. We calculated the above-ground N concentration of Ox2 and O8 under low and high N applications. Under low and high N treatment, the nitrogen concentration of the culm and leaf of WT was significantly higher than Ox2 (Figure S1A, B). It was higher in leaf in O8 lines as compared to WT (Figure S1C). But when high N was applied, the concentration of N in culm and leaf was lower in O8 than WT-N (Figure S1D). However, the nitrogen concentration in the panicle was significantly higher in Ox2 and O8 than in their respective WT, irrespective of high or low N regimes (Figure S1). It demonstrates that these transgenic lines used N for high yield production. Therefore total N concentration of Ox2 (Figures S2A, C) and O8 (Figures S2B, D) in both low and high application of N fertilizer was higher in panicles than their leaf and culm. In addition, grain yield (Figures S2A-S3A), grain number per panicle (Figures S2B, S3B), grain weight (Figures S2C, S3C), effective tiller (Figures S2D, S3D), seed setting rate (Figures S2E, S3E), plant height (Figures S2F, S3F) and dry biomass (Figures S4A, B) were significantly higher in both Ox2 and O8 lines as compared to their WT in both low and high N regimes.

Discussion

The co-relation of N use efficient transgenic lines and GHG's emission

It has been reported that nitrogen-efficient materials can efficiently absorb and transport available N in soil (Chen et al.,

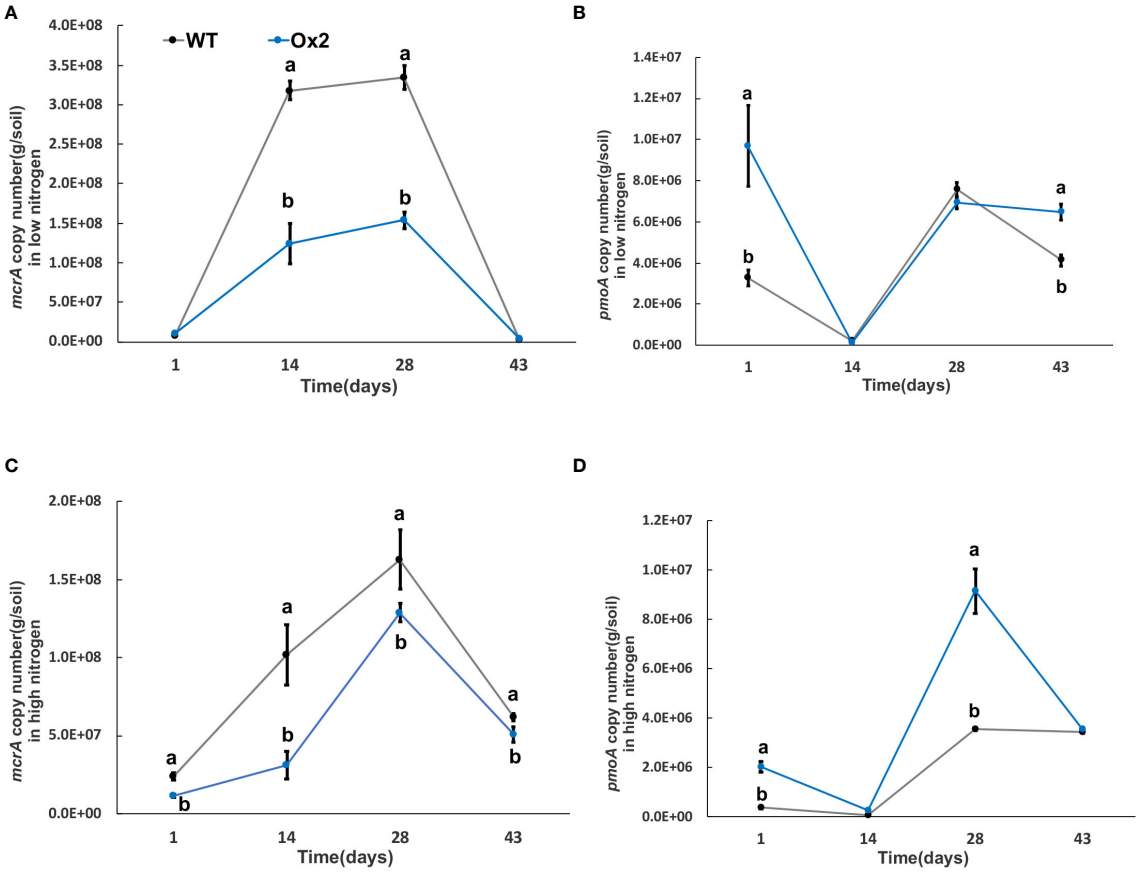

FIGURE 6
The abundance of *mcrA and pmoA* genes in low and high Nitrogen soil of WT and Ox2. X-axis shows the soil sampling time (days), from the first measurement after transplanting seedlings from nursery to field. Figures **(A, C)** show the *mcrA* copy number/g of soil. Figures **(B, D)** show the *pmoA* copy number/g of soil. Error bars: SE (n = 3). Significant difference between WT and Ox2 are indicated by different letters: a= high value, b= lower value (*t*-test, $p < 0.05$).

2017). Applications of non-sulfate, NH_4 based (e.g., urea, $(NH_4)_2HPO_4$) fertilizers have been linked to higher CH_4 emissions in paddy fields (Kumaraswamy et al., 2000). This is due to the increased plant growth and carbon supply that results from high N applications, which in turn provides more methanogenic substrate and improves the efficiency of CH_4 transport to the atmosphere (Bodelier et al., 2000; Schimel, 2000; Dong et al., 2011; Abalos et al., 2014). N_2O originates from both nitrification and denitrification (produced more N_2O) in paddy. The addition of N fertilizers to the soil directly increases the potential for N_2O emission (Dobbie and Smith, 2003; Yan et al., 2008). However, N efficient transgenic lines discharge less N_2O (Figure 2) as they utilized accessible N in the rhizosphere, leaving less available N which is vital for N_2O discharge. Moreover, the long-term N application also regulates the N_2O discharge in soil. The combined application of organic N and mineral N (inorganic fertilizer) could also mitigate N_2O emission (Liu et al., 2017; Liu et al., 2020; Yuan et al., 2022).

Our transgenic lines (Ox2, O8) previously reported as high-affinity nitrate transporters cultivars utilize available N in their panicles and grains (Figures S1–S4). It seems they provide less substrate for CH_4 emission in paddy soil. The plant growth, grain yield and biomass were significantly increased in Ox2 and O8 lines compared to WT in both high and low N applications (Figures S2–S4). The high agronomic yield, plant biomass and nitrogen utilization for seeds formation in our results (Figures S2–S4) are compatible with previous results (Fan et al., 2016; Chen et al., 2017). Here, our cultivars utilized available N and mitigated CH_4 and N_2O in soil alternatively (Figures 1, 2). Nitrification and denitrification are linked to N_2O production in soil. It is an intermediate product of these processes which are influenced by the amount of ammonium and nitrate in the soil and other factors including soil water-filled pore spaces. (Dobbie and Smith, 2003). Soil type and land-use might have direct relationship with nitrification and denitrification to N_2O production from agricultural soil (Liu R. et al., 2016). Also, after microbial decomposition of N in soil and fertilizers, and N_2O is often increased where N availability surpasses plant requirements like in paddy conditions. However, in case of our transgenic lines, they didn't have much available N for nitrification and denitrification than WT in the respective rhizosphere (Table 1).

Relationship of excessive CO_2 with reduced $CH_4$and N_2O emissions

Most of CH_4 emissions occur right after transplanting seedlings from nursery into field until first growing stage (Wu et al., 2019). Our

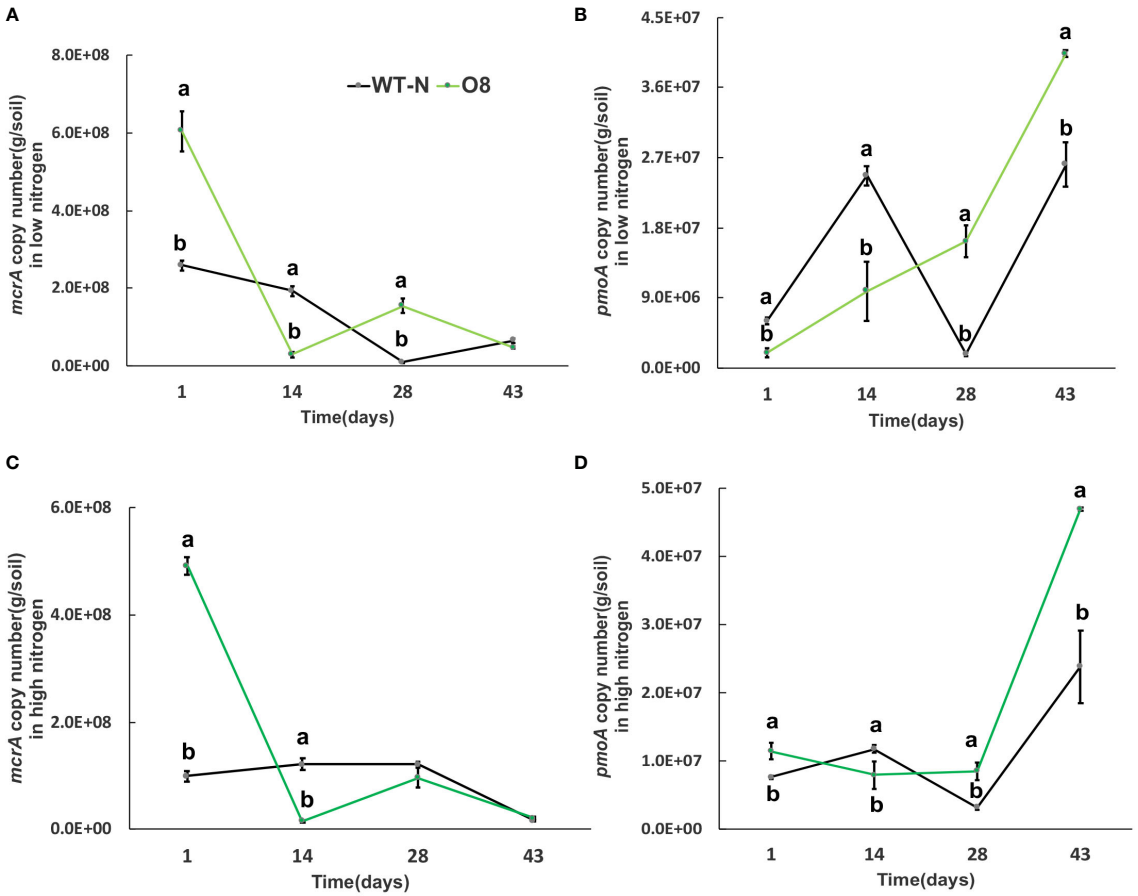

FIGURE 7
The abundance of *mcrA and pmoA* genes in low and high Nitrogen soil of WT-N and O8. X-axis shows the soil sampling time (days), from the first measurement after transplanting seedlings from nursery to field. Figures **(A, C)** show the *mcrA* copy number/g of soil. Figures **(B, D)** show the *pmoA* copy number/g of soil. Error bars: SE (n = 3). Significant difference between WT and O8 are indicated by different letters: a= high value, b= lower value (*t*-test, $p < 0.05$).

results were compatible with previous findings of high discharge in CH_4 in WT (Iqbal et al., 2021) during an early growth stage except for transgenic lines which show a decline in CH_4 emission (Figure 1). Our results also verified a decrease in N_2O emission rate (Figure 2). Reduced aerenchyma also reduced other gases which affect oxidation of CH_4 and nitrification of N_2O (Dobbie and Smith, 2003; Gutierrez et al., 2014).

However, our results revealed higher CO_2 emission from transgenic (Ox2, O8) lines (Figure 3). The relationship of CO_2 and CH_4 emission is co-related. Elevated CO_2 in paddy conditions reduced N_2O and CH_4 emission during field conditions (Yu et al., 2022). The reduction in CH_4 and N_2O induced by excessive CO_2 emission in our transgenics is might be attributed to higher soil Eh, higher O_2 transport into soil. As, CO_2 and N are potentially involved in production of more tillers and rice biomass (Fan et al., 2016; Yu et al., 2022). However, in some previous findings the elevated CO_2 also stimulate CH_4 and N_2O emission along with high yield in some breeding cultivars (Liu et al., 2018; Hu et al., 2020).

Another potential reason behind high values of CO_2 and N_2O from transgenics are different phenotypes as Ox2 is Wuyunjing7 and O8 is Nipponbare background. Different genotype and phenotypic backgrounds possibly produce different amount of yield, plant growth, O_2 and water usage (Fan et al., 2016; Chen et al., 2017). Therefore, GHG discharge is also associated with said factors (Figures 2, 3).

Restricted aerenchyma formation regulates GHG emission

Aerenchyma is a specific structure formed by plants to adapt anoxic or anaerobic environment. Here, a primary purpose is to transport oxygen and also a meaningful way to excrete CH_4 from paddy fields (Sorrell et al., 2013). Limited aerenchyma was one of the additional factors in reducing N_2O and CH_4 emissions. It is reported that about 90% of CH_4 from paddy was released into atmosphere was through aerenchyma, that signifies their role in discharge of CH_4 and other GHG (Kim et al., 2018; Iqbal et al., 2021). Aerenchyma formation has a regulatory correlation with gaseous exchange in rice. During submerged conditions,

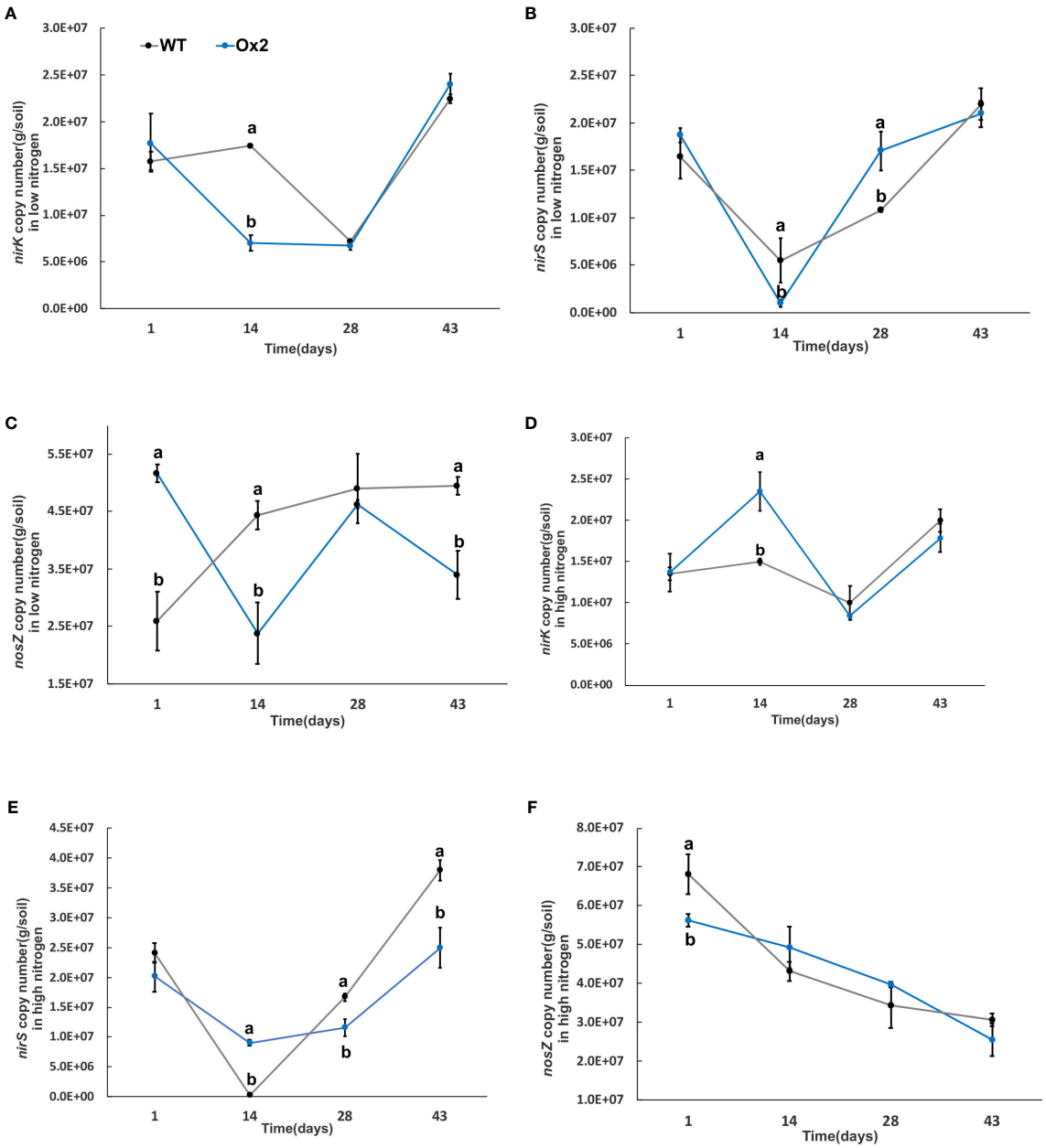

FIGURE 8
The abundance of *nirK, nirS and nosZ* genes in low and high Nitrogen soil of WT and Ox2. X-axis shows the soil sampling time (days), from the first measurement after transplanting seedlings from nursery to field, Figures **(A, D)** show the *nirK* copy number/g of soil in low and high nitrogen application. Figures **(B, E)** show the *nirS* copy number/g of soil in low and high nitrogen application. Figures **(C, F)** show the *nosZ* copy number/g of soil in low and high nitrogen application Error bars: SE (n = 3). Significant difference between WT and Ox2 are indicated by different letters: a= high value, b= lower value (*t*-test, $p < 0.05$).

aerenchyma provides passage for O_2 to a tip of the root, then into rhizosphere and removes gases (ethylene, N_2O, CH_4 and CO_2) into soil (Butterbach-Bahl et al., 1997; Colmer, 2003; Colmer and Voesenek, 2009). The continuous formation of aerenchyma in wet plants is inevitable because it provides the passage for gaseous exchange between aerial and anaerobic (flooded) soil (Vartapetian and Jackson, 1997).

Limited aerenchyma in our transgenic lines (Figures 4, 5) also played a significant role in reducing GHG emissions (Figures 1, 2). Limited aerenchyma formation was a crucial factor for less CH_4 emission in our cultivars. CH_4 oxidation in plants depends on the transport pathways like aerenchyma formation (Van den Berg et al., 2016). The formation of gaseous spaces during flooded conditions is common in plants. Such plants can directly regulate CH_4 oxidation. (Wagatsuma et al., 1990). In waterlogged plants (rice, reeds) the GHG emission is controlled by constant existence of aerenchyma in the roots (Wagatsuma et al., 1990; Vartapetian and Jackson, 1997; Van den Berg et al., 2016).

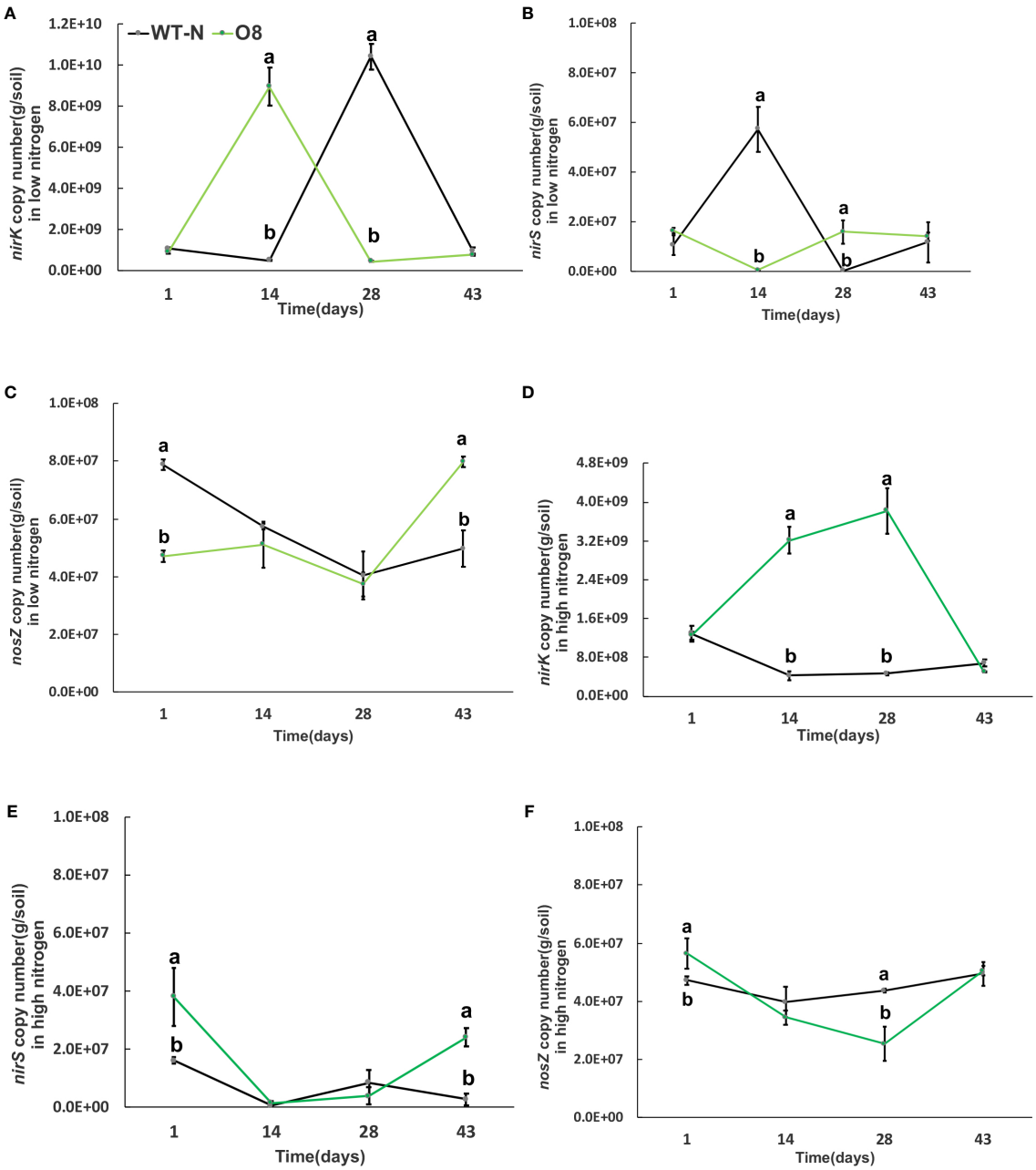

FIGURE 9
The abundance of *nirK, nirS and nosZ* genes in low and high Nitrogen soil of WT-N and O8. X-axis shows the soil sampling time (days), from the first measurement after transplanting seedlings from nursery to field. Figures **(A, D)** show the *nirK* copy number/g of soil in low and high nitrogen application. Figures **(B, E)** show the *nirS* copy number/g of soil in low and high nitrogen application. Figures **(C, F)** show the *nosZ* copy number/g of soil in low and high nitrogen application Error bars: SE (n = 3). Significant difference between WT and O8 are indicated by different letters: a= high value, b= lower value (*t*-test, $p < 0.05$).

Methanotrophs impact on GHG emission

Methane production requires the participation of *mcrA* and an anaerobic environment, so there are higher levels of methanogenic bacteria in paddy environment. The methane-oxidizing bacteria will oxidize a portion of methane during methane emission. Therefore, the distribution of methane-oxidizing bacteria increases in soil with high permeability (Judd, 2011). Methanotrophs play a significant role in mitigating GHG. It is reported that some methanotrophs consume 10-30% CH_4 before it reaches the atmosphere. These bacteria utilize CH_4 as their sole carbon and energy source (Bodelier et al., 2000; Shrestha et al., 2010). According to an estimation, about 62% of global N_2O emissions are through natural and agricultural soils, mainly due to bacterial nitrification and denitrification (ammonia oxidation) (Okereke, 1993; Zumft, 1997; Thomson et al., 2012). The information of bacterial

TABLE 1 The chemical characteristics i.e., pH, available phosphorus (AP) mg/kg, available potassium (AK) mg/kg, Total Nitrogen (TN) g/kg, Total organic carbon (TOC) g/kg, ammonium NH4+-N mg/kg and nitrate $N0_3N$ in mg/kg in low and high nitrogen application from the rhizosphere soil of the WT, Ox2, WT-N and O8 in the field experiment.

Genotype	pH	AP(mg/kg)	AK(mg/kg)	TN(g/kg)	TOC(g/kg)	NH_4^+-N (mg/kg)	NO_3^- (mg/kg)
WT (low nitrogen)	6.52±0.10a	48.82±6.02ab	111.00±29.88b	0.57±0.24a	17.49±1.13a	4.53±0.24a	1.08±0.06a
Ox2(low nitrogen)	6.56±0.06a	43.35±5.10b	157.00±20.26a	0.68±0.12a	16.74±0.17ab	4.15±0.09a	1.09±0.06a
WT-N (low nitrogen)	7.21±0.02a	37.50±2.45a	104.23±9.91b	0.59±0.23b	21.26±1.12b	4.25±0.25b	0.87±0.0ca
O8 (low nitrogen)	7.24±0.02a	32.15±1.26ab	123.58±16.59a	0.62±0.25a	22.24±1.29ab	4.46±0.26a	1.10±0.10b
WT (high nitrogen)	6.60±0.03a	39.86±3.39a	99.50±13.18b	0.63±0.06a	16.85±0.28b	4.94±0.70b	1.14±0.11a
Ox2 (high nitrogen)	6.62±0.05a	41.99±5.60a	125.50±2.08a	0.55±0.06b	17.73±0.26ab	5.12±0.27b	1.03±0.03b
WT-N (high nitrogen)	7.08±0.08a	34.83±1.88a	88.32±5.32b	0.59±0.24a	24.78±1.77a	4.16±0.25b	1.11±0.09b
O8 (high nitrogen)	7.06±0.10a	31.57±2.69b	87.12±1.96	0.52±0.18b	21.80±1.37b	5.64±0.28a	2.91±0.71a

Significant difference between two lines (transgenic and respective WT) are indicated by different letters: a= high value, b= lower value, *p* values shown with every value where n = 3 (*t*-test).

populations (methanotrophs, nitrification and denitrification) in soil is directly associated with N_2O and CH_4 fluxes from paddies. The CH_4 flux was positively correlated with *mcrA* and *nosZ* genes and negatively correlated with *pmoA*. Nitrous oxide flux was positively correlated with *pmoA* and *nirK* and negatively correlated with *nosZ* gene abundance (Figures 6-9). By observing quantitative results of *pmoA*, *nirK* and *nosZ*, it was found that abundance of *pmoA* in Ox2 was higher than WT at some points (Figures 6–9). The CH_4 oxidation to ammonia, methanol and hydroxylamine is regulated by mono-oxygenase enzymes, which have homologous copper membrane (Klotz and Stein, 2008). The stimulation or inhibition of methane oxidizing bacteria in rhizosphere depends on N from NO_3 and NH_4, carbon from CH_4 and genetic potential of methane oxidizing bacteria (Stein and Klotz, 2011).

In this study two N efficient transgenic lines were utilized (Ox2, O8) in order to increase N uptake and utilization efficiency, which in turn aimed to increase rice yield and growth. The transgenic cultivars were found to have an impact on the microbes related to CH_4 and N_2O emissions (Figures 6–9). As seen in the abundance of *nosZ* and the cumulative emissions of CH_4 and N_2O (Figures 1E, 2E). Additionally, the abundance of certain microbial enzymes such as *pmoA, mcrA* and *nirK* were observed to be affected by the N regimes and growth stages. We found that under paddy conditions, the *nirK* abundance of WT was significantly higher than Ox2 (Figure 8). Besides methane and oxygen, N can also have an essential function in CH_4 oxidation and N_2O emission and may become an inhibiting or stimulating factor for growth of methanotrophs and nitrifying bacteria (Dobbie and Smith, 2003; Bodelier and Laanbroek, 2004; Smith et al., 2008; Shrestha et al., 2010; Thomson et al., 2012).

The abundance of the microbial enzymes *pmoA* and *mcrA* were observed too be significantly higher at certain growth stages, specifically at 14 days. This was found to correspond with a higher cumulative nitrous oxide emission in WT compared to Ox2 (Figure 2E). A similar trend was also observed in the microbial abundance of WT and Ox2 under various other treatments. However, the cultivar O8 did not display a consistent pattern. Additionally, our study found that both high and low N applications played a significant role in the microbial growth, as seen in Figures 6–9. Microorganisms that use ammonia as an energy source (nitrifiers) and microorganisms that use methane as an energy source (methanotrophs) have many similarities in terms of their energy requirements and enzymes they use, such as methane monooxygenase enzyme, ammonia monooxygenase/particulate enzyme family (Stein et al., 2012). This suggests that the populations of both nitrifying and methanotrophs microorganisms maybe regulated by transgenic cultivars Ox2 and O8 (Figures 6–9).

Conclusion

In conclusion, our study demonstrated that the use of Overexpressed transgenic cultivars (Ox2, O8) in paddy fields can effectively regulate yield, nitrogen consumption, oxygen transport and greenhouse gases (CH_4, N_2O, CO_2) emission. These transgenic lines accomplish this through the utilization of excessive nitrogen and carbon dioxide in the rhizosphere, regulation of associated functional microorganisms in the soil, and development of aerenchyma in rice roots.

Our findings provide valuable suggestions and future recommendations:

1. Our findings provide useful insight into the potential for developing sustainable agriculture cultivars that can enhance crop production for food security while also reducing greenhouse gas emissions and addressing the challenge of global warming.
2. Our data highlights the crucial role that nitrogen plays in the emissions of CH_4 and N_2O, and suggest that transgenic cultivars (Ox2, O8) that increase N uptake may provide reduced substrate for these emissions.
3. Our study revealed a significant negative correlation between N remobilization into grains and the emission of N_2O

Data availability statement

The original contributions presented in the study are included in the article/Supplementary Material. Further inquiries can be directed to the corresponding authors.

Author contributions

MI and YZ considered the experiments and wrote the manuscript. YW, PK, KC and LZ performed the experiments. XF and XX designed, supervised the project, performed the statistical data analysis and wrote the manuscript. All authors contributed to the article and approved the submitted version.

Acknowledgments

We would like to thanks all funding sources includes, The National Key Research and Development Program of China (2021YFF1000404), The National Natural Science Foundation of China (32172665) and The Introduction Project of High-level Talents in Xinjiang Uygur Autonomous Region.

Conflict of interest

The authors declare that the research was conducted in the absence of any commercial or financial relationships that could be construed as a potential conflict of interest.

Publisher's note

Supplementary material

The Supplementary Material for this article can be found online at: https://www.frontiersin.org/articles/10.3389/fpls.2023.1133643/full#supplementary-material

References

Abalos, D., Sanchez-martin, L., Garcia-torres, L., Willem, J., Groenigen, V., and Vallejo, A. (2014). Management of irrigation frequency and nitrogen fertilization to mitigate GHG and NO emissions from drip-fertigated crops. *Sci. Total. Environ.* 490, 880–888. doi: 10.1016/j.scitotenv.2014.05.065

Akiyama, H., Yagi, K., and Yan, X. (2005). Direct N_2O emissions from rice paddy fields: Summary of available data. *Global Biogeochem. Cycles*. 19, 1–10. doi: 10.1029/2004GB002378

Armstrong, W. (1980). Aeration in higher plants. *Adv. Bot. Res.* 7, 225–332. doi: 10.1016/S0065-2296(08)60089-0

Bodelier, P. L. E., and Laanbroek, H. J. (2004). Nitrogen as a regulatory factor of methane oxidation in soils and sediments. *FEMS Microbiol. Ecol.* 47, 265–277. doi: 10.1016/S0168-6496(03)00304-0

Bodelier, P. L. E., Roslev, P., Henckel, T., and Frenzel, P. (2000). Stimulation by ammonium-based fertilizers of methane oxidation in soil around rice roots. *Nature* 403, 421–424. doi: 10.1038/35000193

Butterbach-Bahl, K., Papen, H., and Rennenberg, H. (1997). Impact of gas transport through rice cultivars on methane emission from rice paddy fields. *Plant. Cell Environ.* 20, 1175–1183. doi: 10.1046/j.1365-3040.1997.d01-142.x

Carlson, K. M., Gerber, J. S., Mueller, N. D., Herrero, M., MacDonald, G. K., Brauman, K. A., et al. (2016). Greenhouse gas emissions intensity of global croplands. *Nat. Clim. Change* 7, 63–68. doi: 10.1038/nclimate3158

Chen, J., Fan, X., Qian, K., Zhang, Y., Song, M., Liu, Y., et al. (2017). pOsNAR2.1: OsNAR2.1 expression enhances nitrogen uptake efficiency and grain yield in transgenic rice plants. *Plant Biotechnol. J.* 15, 1273–1283. doi: 10.1111/pbi.12714

Chen, J., Zhang, Y., Tan, Y., Zhang, M., Zhu, L., Xu, G., et al. (2016). Agronomic nitrogen-use efficiency of rice can be increased by driving OsNRT2.1 expression with the OsNAR2.1 promoter. *Plant Biotechnol. J.* 14, 1705–1715. doi: 10.1111/pbi.12531

Colmer, T. D. (2003). Aerenchyma and an inducible barrier to radial oxygen loss facilitate root aeration in upland, paddy and deep-water rice (Oryza sativa l.). *Ann. Bot.* 91, 301–309. doi: 10.1093/aob/mcf114

Colmer, T. D., and Voesenek, L. A. C. J. (2009). Flooding tolerance: Suites of plant traits in variable environments. *Funct. Plant Biol.* 36, 665–681. doi: 10.1071/FP09144

Denier, H. A. C., DerGon, V., Kropff, M. J., Van Breemen, N., Wassmann, R., Lantin, R. S., et al. (2002). Optimizing grain yields reduces CH_4 emissions from rice paddy fields. *Proc. Natl. Acad. Sci. U. S. A.* 99, 12021–12024. doi: 10.1073/pnas.192276599

Dobbie, K. E., and Smith, K. A. (2003). Impact of different forms of n fertilizer on N_2O emissions from intensive grassland. *Nutr. Cycl. Agroecosyst.* 67, 37–46. doi: 10.1023/A:1025119512447

Dong, H., Yao, Z., Zheng, X., Mei, B., Xie, B., Wang, R., et al. (2011). Effect of ammonium-based, non-sulfate fertilizers on CH_4 emissions from a paddy field with a typical Chinese water management regime. *Atmos. Environ.* 45, 1095–1101. doi: 10.1016/j.atmosenv.2010.11.039

Fan, X., Tang, Z., Tan, Y., Zhang, Y., Luo, B., Yang, M., et al. (2016). Overexpression of a pH-sensitive nitrate transporter in rice increases crop yields. *Proc. Natl. Acad. Sci.* 113, 7118–7123. doi: 10.1073/pnas.1525184113

Frona, D., Szenderak, J., and Harangi-Rakos, M. (2019). The challenge of feeding the poor. *sustainablity* 11 (20), 5816. doi: 10.3390/su11205816

Gutierrez, J., Atulba, S. L., Kim, G., and Kim, P. J. (2014). Importance of rice root oxidation potential as a regulator of CH_4 production under waterlogged conditions. *Biol. Fertil. Soils.* 50, 861–868. doi: 10.1007/s00374-014-0904-0

Hao, X., Chang, C., Larney, F. J., and Travis, G. R. (2001). Greenhouse gas emissions during cattle feedlot manure composting. *J. Environ. Qual.* 30, 376–386. doi: 10.2134/jeq2001.302376x

Hirel, B., Le Gouis, J., Ney, B., and Gallais, A. (2007). The challenge of improving nitrogen use efficiency in crop plants: Towards a more central role for genetic variability and quantitative genetics within integrated approaches. *J. Exp. Bot.* 58, 2369–2387. doi: 10.1093/jxb/erm097

Hofstra, N., and Vermeulen, L. C. (2016). Impacts of population growth, urbanisation and sanitation changes on global human cryptosporidium emissions to surface water. *Int. J. Hyg. Environ. Health* 219, 599–605. doi: 10.1016/j.ijheh.2016.06.005

Hu, Z., Chen, X., Yao, J., Zhu, C., Zhu, J., and Liu, M. (2020). Plant-mediated effects of elevated CO_2 and rice cultivars on soil carbon dynamics in a paddy soil. *New Phytol.* 225, 2368–2379. doi: 10.1111/nph.16298

Hu, Z., Lee, J. W., Adhikari, R., Wagle, A., and You, K. (2012). Nitrous oxide (N_2O) emission from aquaculture: A review. *Environ. Sci. Technol.* 46, 6470–6480. doi: 10.1021/es300110x

IPCC (2014). *Climate change, (2014): Synthesis report. contribution of working groups I, II and III to the fifth assessment report of the intergovernmental panel on climate change.* Eds. Core Writing Team,, R. K. Pachauri and L. A. Meyer (Geneva, Switzerland: IPCC), 151. doi: ipcc.ch/report/ar5/syr/

Iqbal, M. F., Liu, S., Zhu, J., Zhao, L., Qi, T., Liang, J., et al. (2021). Limited aerenchyma reduces oxygen diffusion and methane emission in paddy. *J. Environ. Manage.* 279, 111583. doi: 10.1016/j.jenvman.2020.111583

Jiang, Y., Van Groenigen, K. J., Huang, S., and Hungate, B. A. (2017). Higher yields and lower methane emissions with new rice cultivars. *Glob. Chang. Biol.* 23, 4728–4738. doi: 10.1111/gcb.13737

Judd, C. R. (2011). *IMPACT OF METHANOTROPH ECOLOGY ON UPLAND METHANE BIOGEOCHEMISTRY IN GRASSLAND SOILS* [master's thesis]. Fort Collins (CO):(Colorado State University).

Justin, S. H. F. W., and Armstrong, W. (1991). Evidence for the involvement of ethene in aerenchyma formation in adventitious roots of rice (Oryza sativa l.). *New Phytol.* 118, 49–62. doi: 10.1111/j.1469-8137.1991.tb00564.x

Kim, W. J., Bui, L. T., Chun, J. B., McClung, A. M., and Barnaby, J. Y. (2018). Correlation between methane (CH_4) emissions and root aerenchyma of rice varieties. *Plant Breed. Biotechnol.* 6, 381–390. doi: 10.9787/PBB.2018.6.4.381

Klotz, M. G., and Stein, L. Y. (2008). Nitrifier genomics and evolution of the nitrogen cycle. *FEMS Microbiol. Lett.* 278, 146–156. doi: 10.1111/j.1574-6968.2007.00970.x

Kritee, K., Nair, D., Zavala-Araiza, D., Proville, J., Rudek, J., K. Aadhya, K., et al. (2018). High nitrous oxide fluxes from rice indicate the need to manage water for both long- and short-term climate impacts. *Proc. Natl. Acad. Sci.* 115, 9720–9725. doi: 10.1073/pnas.1809276115

Kumaraswamy, S., Kumar Rath, A., Ramakrishnan, B., and Sethunathan, N. (2000). Wetland rice soils as sources and sinks of methane: A review and prospects for research. *Biol. Fertil. Soils.* 31, 449–461. doi: 10.1007/s003740000214

Leghari, S. J., Wahocho, N. A., Laghari, G. M., HafeezLaghari, A., MustafaBhabhan, G., HussainTalpur, K., et al. (2016). Role of nitrogen for plant growth and development: A review. *Adv. Environ. Biol.* 10 (9), 209–218.

Lévesque, V., Rochette, P., Hogue, R., Jeanne, T., Ziadi, N., Chantigny, M. H., et al. (2020). Greenhouse gas emissions and soil bacterial community as affected by biochar amendments after periodic mineral fertilizer applications. *Biol. Fertil. Soils.* 56, 907–925. doi: 10.1007/s00374-020-01470-z

Li, Y. L., Fan, X. R., and Shen, Q. I. R. (2008). The relationship between rhizosphere nitrification and nitrogen-use efficiency in rice plants. *Plant Cell Environ.* 31, 73–85. doi: 10.1111/j.1365-3040.2007.01737.x

Liu, D. Y., Ding, W. X., Jia, Z. J., and Cai, Z. C. (2011). Relation between methanogenic archaea and methane production potential in selected natural wetland ecosystems across China. *Biogeosciences* 8, 329–338. doi: 10.5194/bg-8-329-2011

Liu, R., Hu, H., Suter, H., Hayden, H. ,. L., He, J., Mele, P., et al. (2016). Nitrification is a primary driver of nitrous oxide production in laboratory microcosms from different land-use soils. *Front. Microbiol.* 7. doi: 10.3389/fmicb.2016.01373

Liu, S., Hu, Z., Wu, S., Li, S., Li, Z., and Zou, J. (2016). Methane and nitrous oxide emissions reduced following conversion of rice paddies to inland crab-fish aquaculture in southeast China. *Environ. Sci. Technol.* 50, 633–642. doi: 10.1021/acs.est.5b04343

Liu, S., Ji, C., Wang, C., Chen, J., Jin, Y., Zou, Z., et al. (2018). Climatic role of terrestrial ecosystem under elevated CO_2: A bottom-up greenhouse gases budget. *Ecol. Lett.* 21, 1108–1118. doi: 10.1111/ele.13078

Liu, S., Lin, F., Wu, S., Ji, C., Sun, Y., Jin, Y., et al. (2017). A meta-analysis of fertilizer-induced soil NO and combined NO + N_2O emissions. *Glob. Chang. Biol.* 23, 2520–2532. doi: 10.1111/gcb.13485

Liu, Q., Qin, Y., Zou, J., Guo, Y., and Gao, Z. (2013). Annual nitrous oxide emissions from open-air and greenhouse vegetable cropping systems in China. *Plant Soil.* 370, 223–233. doi: 10.1007/s11104-013-1622-3

Liu, D., Sun, H., Liao, X., Luo, J., Lindsey, S., Yuan, J., et al. (2020). N_2O and NO emissions as affected by the continuous combined application of organic and mineral n fertilizer to a soil on the north China plain. *Agronomy* 10, 1965. doi: 10.3390/agronomy10121965

Naz, M., Luo, B., Guo, X., Li, B., Chen, J., and Fan, X. (2019). Overexpression of nitrate transporter osnrt2.1 enhances nitrate-dependent root elongation. *Genes (Basel).* 10, 1–18. doi: 10.3390/genes10040290

Nie, S., Li, H., Yang, X., Zhang, Z., Weng, B., Huang, F., et al. (2015). Nitrogen loss by anaerobic oxidation of ammonium in rice rhizosphere. *ISME. J.* 9, 2059–2067. doi: 10.1038/ismej.2015.25

Okereke, G. U. (1993). Growth yield of denitrifiers using nitrous oxide as a terminal electron acceptor. *World J. Microbiol. Biotechnol.* 9, 59–62. doi: 10.1007/BF00656518

Oo, A. Z., Sudo, S., Inubushi, K., Mano, M., Yamamoto, A., Ono, K., et al. (2018). Methane and nitrous oxide emissions from conventional and modified rice cultivation systems in south India. *Agric. Ecosyst. Environ.* 252, 148–158. doi: 10.1016/j.agee.2017.10.014

Schimel, J. (2000). Rice, microbes and methane. *Nature* 403, 375–377. doi: 10.1038/35000325

Shimamura, S., Mochizuki, T., Nada, Y., and Fukuyama, M. (2002). Secondary aerenchyma formation and its relation to nitrogen fixation in root nodules of soybean plants (Glycine max) grown under flooded conditions. *Plant Prod. Sci.* 5, 294–300. doi: 10.1626/pps.5.294

Shrestha, M., Shrestha, P. M., Frenzel, P., and Conrad, R. (2010). Effect of nitrogen fertilization on methane oxidation, abundance, community structure, and gene expression of methanotrophs in the rice rhizosphere. *ISME. J.* 4, 1545–1556. doi: 10.1038/ismej.2010.89

Smith, P., Martino, D., Cai, Z., Gwary, D., Janzen, H., Kumar, P., et al. (2008). Greenhouse gas mitigation in agriculture. *Philos. Trans. R. Soc. B. Biol. Sci.* 363, 789–813. doi: 10.1098/rstb.2007.2184

Sorrell, B. K., and Brix, H. (2013). *Gas Transport and Exchange through Wetland Plant Aerenchyma. In Methods in Biogeochemistry of Wetlands* (eds R. D. DeLaune, K. R. Reddy, C. J. Richardson and J. P. Megonigal). pp. 177–196. doi: 10.2136/sssabookser10.c11

Stein, L. Y., and Klotz, M. G. (2011). Nitrifying and denitrifying pathways of methanotrophic bacteria. *Biochem.soc.Trans* 39, 1826–1831. doi: 10.1042/BST20110712

Stein, L. Y., Roy, R., and Dunfield, P. F. (2012). *Aerobic methanotrophy and Nitrification: Processes and connections aerobic methanotrophy and Nitrification: Processes and connections* (Chichester: eLS. John Wiley & Sons, Ltd). doi: 10.1002/8780470015902.a0022213

Su, J., Hu, C., Yan, X., Jin, Y., Chen, Z., Guan, Q., et al. (2015). Expression of barley SUSIBA2 transcription factor yields high-starch low-methane rice. *Nature* 523, 602–606. doi: 10.1038/nature14673

Thomson, A. J., Giannopoulos, G., Pretty, J., Baggs, E. M., and Richardson, D. J. (2012). Biological sources and sinks of nitrous oxide and strategies to mitigate emissions. *Philos. Trans. R. Soc. B. Biol. Sci.* 367, 1157–1168. doi: 10.1098/rstb.2011.0415

Van den Berg, M., Ingwersen, J., van den Elzen, E., Lamers, L. P. ~. M., and Streck, T. (2016). "Role of plant-mediated gas transport in CH4 emissions from phragmites-dominated peatlands," in *EGU general assembly conference abstracts* (EGU General Assembly Conference Abstracts), EPSC2016–12193. https://ui.adsabs.harvard.edu/abs/2016EGUGA..1812193V/abstract

Vartapetian, B. B., and Jackson, M. B. (1997). Plant adaptations to anaerobic stress 79, 2–20. doi: 10.1093/oxfordjournals.aob.a010303

Wagatsuma, T., Nakashima, T., Tawaraya, K., Watanabe, S., Kamio, A., and Ueki, A. (1990). "Role of plant aerenchyma in wet tolerance of and methane emission from plants," in *Plant nutrition — physiology and applications: Proceedings of the eleventh international plant nutrition colloquium, 30 July–4 august 1989, wageningen, the Netherlands*. Ed. M. L. van Beusichem (Dordrecht: Springer Netherlands), 455–461.

Wu, X., Wang, W., Xie, K., Yin, C., Hou, H., and Xie, X. (2019). Combined effects of straw and water management on CH_4 emissions from rice fields. *J. Environ. Manage.* 231, 1257–1262. doi: 10.1016/j.jenvman.2018.11.011

Xu, G., Fan, X., and Miller, A. J. (2012). Plant nitrogen assimilation and use efficiency. *Annu. Rev. Plant Biol.* 63, 153–182. doi: 10.1146/annurev-arplant-042811-105532

Xuan, W., Beeckman, T., and Xu, G. (2017). Plant nitrogen nutrition: sensing and signaling. *Curr. Opin. Plant Biol.* 39, 57–65. doi: 10.1016/j.pbi.2017.05.010

Yan, Y., Sha, L., Cao, M., Zheng, Z., Tang, J., Wang, Y., et al. (2008). Fluxes of CH_4 and N_2O from soil under a tropical seasonal rain forest in xishuangbanna, southwest China. *J. Environ. Sci.* 20, 207–215. doi: 10.1016/S1001-0742(08)60033-9

Yang, X., Liu, D., Fu, Q., Li, T., Hou, R., Li, Q., et al. (2022). Characteristics of greenhouse gas emissions from farmland soils based on a structural equation model: Regulation mechanism of biochar. *Environ. Res.* 206, 112303. doi: 10.1016/j.envres.2021.112303

Yang, Y., Shan, J., Zhang, J., Zhang, X., Xie, X., and Liu, Y. (2014). Ammonia- and methane-oxidizing microorganisms in high-altitude wetland sediments and adjacent agricultural soils. *Environ. Biotch.* 98, 10197–10209. doi: 10.1007/s00253-014-5942-x

Yu, H., Zhang, G., Ma, J., Wang, T., Song, K., Huang, Q., et al. (2022). Elevated atmospheric CO_2 reduces CH_4 and N_2O emissions under two contrasting rice cultivars from a subtropical paddy field in China. *Pedosphere.* 32 (5), 707–717. doi: 10.1016/j.pedsph.2022.05.003

Yuan, H., He, X., Luo, J., Hu, C., Li, X., and Lindsey, S. (2022). Differential immediate and long-term effects of nitrogen input on denitrification $N_2O/(N_2O+N_2)$ ratio along a 0-5.2 m soil profile. *PloS One* 17 (10), e0276891. doi: 10.1371/journal.pone.0276891

Zhang, Y., Jiang, Y., Li, Z., Zhu, X., Wang, X., Chen, J., et al. (2015). Aboveground morphological traits do not predict rice variety effects on CH_4 emissions. *Agric. Ecosyst. Environ.* 208, 86–93. doi: 10.1016/j.agee.2015.04.030

Zhang, S., Zhang, Y., Li, K., Yan, M., Zhang, J., Yu, M., et al. (2021). Nitrogen mediates flowering time and nitrogen use efficiency *via* floral regulators in rice. *Curr. Biol.* 31 (4), 671–683.e5. doi: 10.1016/j.cub.2020.10.095.

Zhou, X., Smaill, S. J., and Clinton, P. W. (2013). Methane oxidation needs less stressed plants. *Trends Plant Sci.* 18, 657–659. doi: 10.1016/j.tplants.2013.09.011

Zhu, J., Liang, J., Xu, Z., Fan, X., Zhou, Q., Shen, Q., et al. (2015). Root aeration improves growth and nitrogen accumulation in rice seedlings under low nitrogen. *AoB. Plants.* 7, plv131. doi: 10.1093/aobpla/plv131

Zumft, W. G. (1997). Cell biology and molecular basis of denitrification. *Microbiol. Mol. Biol. Rev.* 61, 533–616. doi: 10.1128/mmbr.61.4.533-616.1997

frontiers | Frontiers in Plant Science

TYPE Original Research
PUBLISHED 31 March 2023
DOI 10.3389/fpls.2023.1154051

OPEN ACCESS

EDITED BY
Bhumi Nath Tripathi,
Indira Gandhi National Tribal University, India

REVIEWED BY
Owais Ali Wani,
Sher-e-Kashmir University of Agricultural Sciences and Technology of Kashmir, India
Zahoor Ahmad,
University of Central Punjab, Pakistan

*CORRESPONDENCE
Md. Ashraful Alam
a.alam_83@yahoo.com
Akbar Hossain
akbarhossainwrc@gmail.com

SPECIALTY SECTION
This article was submitted to Plant Abiotic Stress, a section of the journal Frontiers in Plant Science

RECEIVED 30 January 2023
ACCEPTED 13 March 2023
PUBLISHED 31 March 2023

CITATION
Alam MA, Rahman MA, Rahman MM, Hasan MM, Naher S, Fahim AHF, Mottalib MA, Roy S, Islam MR, Mozumder SN, Alsuhaibani AM, Gaber A and Hossain A (2023) Performance valuation of onion (*Allium cepa* L.) genotypes under different levels of salinity for the development of cultivars suitable for saline regions.
Front. Plant Sci. 14:1154051.
doi: 10.3389/fpls.2023.1154051

Performance valuation of onion (*Allium cepa* L.) genotypes under different levels of salinity for the development of cultivars suitable for saline regions

Md. Ashraful Alam[1]*, Md. Atikur Rahman[2], Md. Marufur Rahman[3], Md. Mahmudul Hasan[4], Shamsun Naher[2], Abu Hena Faisal Fahim[5], Md. Abdul Mottalib[6], Srabanti Roy[7], Md. Rafiqul Islam[8], Shailendra Nath Mozumder[4], Amnah Mohammed Alsuhaibani[9], Ahmed Gaber[10] and Akbar Hossain[11]*

[1]Plant Breeding Division, Spices Research Centre, Bangladesh Agricultural Research Institute, Bogura, Bangladesh, [2]Division of Soil Science, Spices Research Centre, Bangladesh Agricultural Research Institute, Bogura, Bangladesh, [3]Regional Station, Bangladesh Institute of Research and Training on Applied Nutrition, Rangpur, Bangladesh, [4]Division of Horticulture, Spices Research Centre, Bangladesh Agricultural Research Institute, Bogura, Bangladesh, [5]Division of Agronomy, Spices Research Centre, Bangladesh Agricultural Research Institute, Bogura, Bangladesh, [6]Division of Agricultural Engineering, Spices Research Centre, Bangladesh Agricultural Research Institute, Bogura, Bangladesh, [7]Department of Agricultural Chemistry, Bangladesh Agricultural University, Mymensingh, Bangladesh, [8]Division of Agronomy, Regional Agricultural Research Station, Bangladesh Agricultural Research Institute (BARI), Ishwardi, Pabna, Bangladesh, [9]Department of Physical Sport Science, College of Education, Princess Nourah bint Abdulrahman University, Riyadh, Saudi Arabia, [10]Department of Biology, College of Science, Taif University, Taif, Saudi Arabia, [11]Division of Soil Science, Bangladesh Wheat and Maize Research Institute, Dinajpur, Bangladesh

Abiotic stress, especially salt stress, is one of the major barriers to crop production worldwide. Crops like onion that belong to the glycophytic group are more sensitive to salinity stress. A huge study regarding the influence of salinity stress on the growth and development of crops has already been done and is still ongoing. One of the major targets of the research is to develop genotypes that have enhanced performance under stress environments. The world needs more of these types of genotypes to combat the ever-growing salt-stressed soils. Therefore, a number of germplasm were studied during the 2019–2020 and 2020–2021 seasons under different salt concentrations to identify tolerant genotypes as well as to study the plants' responses at different growth stages against elevated salinity levels. A 2-year study was conducted where germination potential was evaluated in the first year and carried out in petri dish culture of seeds, followed by plastic pot culture for plant establishment and bulb development evaluation during the second year. Four different saline water solutions having different salt concentrations (0, 8, 10, and 12 dS m^{-1}) were applied to the petri dishes and pots as the source of water for plants in both seasons. Results indicated that a significant reduction in plants' performance occurs under higher salinity levels. Salt concentration had an adverse impact on germination, leaf development and growth, the height of plants, bulb size and shape, and the bulb weight of onion. All the growth phases of onion are sensitive

to elevated concentrations. Variable performances were observed in the genotypes under stress conditions, and a few genotypes (Ac Bog 409, Ac Bog 414, Ac Bog 424, Ac Bog 430, Ac Bog 417, Ac Bog 419, Ac Bog 420, Ac Bog 422, and Ac Bog 425) having some sort of tolerance to salt stress were identified, which might be recommended for mass production. Tolerance indices could successfully be applied in selecting the salt-tolerant genotypes. Thus, the present findings and the identified genotypes could be further utilized in salt stress improvement research on onion.

KEYWORDS

salinity, onion, STI, stress, bulb growth, germination

1 Introduction

Onion (*Allium cepa* L.) is one of the most important vegetables and spice crops. It is one of the most popular vegetables around the globe, carrying a pungent flavor and often used as a condiment to prepare multiple delicious cuisines in every corner of the world. It has important medicinal properties to combat several diseases especially blood pressure and heart disease. Two-thirds of the total onion production come from Asia, among which India and China hold the major share (FAOSTAT, [[NoYear]]). Bangladesh ranks third in the list in terms of production (Star Business Report, 2022). Bangladesh produced 19.54 lakh M tons of onion bulbs from 1.85 lakh ha of land in 2020, with an average yield of 10.55 t/ha (FAOSTAT, [[NoYear]]), which is very low compared to other countries. Onion ranks the highest among the spice crops in Bangladesh based on production and generally grows all over the country mostly in the winter season. It is an important ingredient in many food preparations and is mostly used as a spice rather than as a vegetable in different daily dishes. Although the country is producing a lot of onion, it is still has a huge shortage and, thus, has to import a large amount from abroad to meet the domestic demand (BBS, 2019).

To feed the ever-increasing population, food production by irrigation is common in arid and semiarid regions, resulting in 20% to 50% of the land being affected by salinity called secondary salinization, bringing unprecedented agricultural losses over time (Pitman and Läuchli, 2006). A similar statement was also concluded in a prediction that highlights that approximately 50% of today's arable land worldwide would be lost from agricultural use due to the worse effect of salinity by 2050 (Wang et al., 2003). It is estimated that there is a loss of more than US$12 billion per year worldwide due to salinity-induced agricultural input losses (Shabala, 2013).

Soil salinity is one of the harsh outputs of global climate change and has an immense impact on arable land, especially coastal agricultural land (Qadir et al., 2014; Rahman et al., 2018). Soil degradation by salinization is one of the consequences of climate change caused by natural and anthropogenic activities (Yeo, 1998). An elevated salinity level adversely affects the morphology, physiology, and yield of a crop and is similar to the case of onion production as well (Shoaib et al., 2018; Regessa et al., 2022; Sanwal et al., 2022; Venâncio et al., 2022). Germination and emergence become difficult (Khan, 2003; Regessa et al., 2010; Hanci and Cebeci, 2015; Ullah and Bano, 2019) and subsequent yield reduction occurs (Chinnusamy et al., 2005) for glycophytes under saline-affected soils (Hanci et al., 2016), although they have a different threshold level of salinity, such as the onion, which is very sensitive to salinity beyond 1.2 dS m^{-1} (Maas and Hoffman, 1977).

In Bangladesh, onion is being grown all over the country, but production is hampered in saline-prone areas around the coastal belt as it is a glycophytic crop. A total of 1.06 million ha of land area (32% of the total coastal and offshore land) in the country is affected by different degrees of salinity (Ahsan and Bhuiyan, 2010; SRDI, 2010; Parvin et al., 2017). Soil salinity was classified by Soil Research Development Institute (SRDI) (2010) as non-saline (2.0–4.0 dS m^{-1}), very slightly saline (4.1–8.0 dS m^{-1}), moderately saline (8.1–12.0 dS m^{-1}), strongly saline (12.1–16.0 dS m^{-1}), and very strongly saline (>16 dS m^{-1}), which occupied approximately 0.328 (31%), 0.274 (26%), 0.190 (18%), 0.162 (15%), and 0.102 (10%) m ha of land, respectively (Ahsan and Bhuiyan, 2010; SRDI, 2010). During the growing season, salinity level varies between 6 and 12 dS m^{-1}, which reaches up to 20 dS m^{-1} in extreme cases (SRDI, 2010). Thus, the cropping intensity is low in the coastal areas compared to the national average. A substantial amount of land has always remained fallow in coastal areas during the winter season after Aman rice (wet season rice) cultivation due to salinity problems. Onion has the potential as a cash crop to fit in this area to increase cropping intensity and save foreign currency by reducing the import of the crop, if cultivated after harvesting T. Aman rice. Moreover, onion cultivation in the mainland has almost plateaued, thus requiring a higher production to meet the shortage. Public research institutes in the country developed several varieties of onion suitable for both winter and rainy seasons, mainly on the mainland. However, those also suffer from salinity stress when cultivated in coastal areas. Therefore, the yield of onion in this area is very low compared to other parts of the country. Hence, genotypes suitable for cultivation under low to moderate levels of salinity level are a crying need for this zone. The potential genotype tolerant to salt stress will increase

the total onion production in the country and improve the socio-economic condition of farmers. It will also play a role in increasing the onion cultivation area in the coastal belt. By keeping the above view, the present study was hypothesized as an attempt to evaluate and identify suitable genotypes that have a tolerance to moderate salinity (8–12 dS m^{-1}) levels to increase onion production in saline-prone regions.

2 Materials and methods

2.1 Location of the current study

The present study was carried out at the Spices Research Centre, BARI, Bogura during two consecutive winter seasons (*Rabi*): 2019 and 2020. The details of prevailing weather conditions during the pot experiment are given in Table S1.

2.2 Properties of soil used in the study

Physicochemical analysis of initial soil under field conditions was carried out at the central soil science laboratory of BARI. The soil employed in the study had a sandy loam texture and was slightly neutral in nature in response, with a field capacity of 29.6% and a pH of 6.0, and organic matter percentage was low (1.33), having an average EC of 2.06 dS m^{-1}. Total nitrogen (0.07%) was very low, available phosphorus (40.77 µg/g soil) was very high, exchangeable potassium was low (0.15 meq/100 g soil), and available sulfur was low (10.57 µg/g soil). Available iron (85.91 µg/g soil) was very high, available zinc (1.63 µg/g soil) was optimum, available boron (0.2 µg/g soil) was low, available manganese (18.21 µg/g soil) was very high, available copper was very high (2.31 µg/g soil), exchangeable calcium (4.70 meq/100 g soil) was optimum, and exchangeable magnesium (1.59 meq/100 g soil) was high.

2.3 Genotypes used in the study

A set of 25 onion genotypes was included in the current study; details of the studied genotypes are presented in Table S1 (Khan et al., 2022). A local cultivar BARI Piaz-4 released from a public research institute (BARI) was incorporated as a check cultivar.

2.4 Treatments and design

Four different salinity levels were applied in the present experiment (0, 8, 10, and 12 dS m^{-1}) for both petri dish and pot experiments. The saline solutions were prepared using normal NaCl salt following the method recommended by Yaron and Mokady (1962). In the first year, the observation was done in petri dishes by arranging all treatments in a completely randomized design (CRD) and repeated three times. In the second-year experiment, all genotypes were accommodated in small-sized pots placed in the field and also laid out in a CRD by repeating all treatments two times.

2.5 Experimental plan

In the first season, all the genotypes were tested for their ability to germinate and subsequent plumule development under different salinity treatments. Autoclaved petri dishes were used, where blotting papers (Whatman no. 1) were placed. Then, seeds of the studied genotypes were placed in different petri dishes. Four levels of saline water were applied for each genotype to indulge the germination process. Spraying of saline water as per treatments was applied every other day. The percentage of germination and growth repression was observed after 7 days.

During the second season, the genotypes under study were accommodated in small-sized pots placed in the field. At first, seeds of the different genotypes were sown on a well-prepared seed bed to grow seedlings. The seedlings were then transplanted into the pot and kept in the field at 35 days after sowing. Uniform sandy loam soil was collected from AEZ-4 and then recommended doses of compost and chemical fertilizers were incorporated for this experiment. The experimental pot was fabricated by biodegradable plastic materials having an internal volume of 500 ml. Each pot was filled with 400 g of soil mixture. A 15 cm × 10 cm spacing was maintained from row to row and hill to hill while arranging pots in the field. Starting from transplanting, irrigations were applied with particular saline solutions to reach the field capacity of soil as per aforesaid treatments. Other intercultural practices were followed as and when required, in which timely irrigation was provided to ensure moisture availability and plant protection measures were taken to repel pest and disease infestation.

2.6 Observations recorded

Various morpho-physiological trait observations were recorded using a standard protocol for onion phenotyping. The germination percentage was recorded after 7 days of seed placement on petri dishes. Subsequent growth repression (further growth and development arrested despite seed germination) was observed after 14 days of seed placement on each petri dish. The number of plants with dried leaves, number of green plants, maximum leaf length (MLL), and number of total leaves were counted on each pot basis. Individual bulb weight (IBW), bulb length (BL), and bulb diameter (BD) were recorded at harvest. Data on soil salinity level were observed eight times during the entire crop cycle from the seedling to the harvesting stage with an EC meter (model: HI 993310) after 15 days of each irrigation as indicated by Slavich and Petterson (1993) (Slavich and Petterson, 1993).

2.7 Statistical analysis

All the observed data were subjected to statistical analysis following the standard formulas. The Data Analysis tool of the

Microsoft Excel program was used to estimate the statistical parameters. CV% was estimated based on output from the analyzed results. Shoot tolerance index (ShTI), stress tolerance index (STI), and percent yield reduction (PYR) were calculated on the MS Excel program following the formula given below (Fischer and Maurer, 1978; Choukan et al., 2006; Takahashi et al., 2015; Zafar et al., 2015; Guellim et al., 2019).

The ShTI was estimated according to the following equation:

$$\text{ShTI} = \frac{\text{MLL at different dS/m}}{\text{MLL at 0 dS/m}} \times 100 \quad \ldots\ldots\ldots\ldots\ldots\ldots \text{[i]}$$

The STI was estimated according to the following equation:

$$\text{STI} = \frac{\text{IBW at 0 dS/m x IBW at different dS/m}}{(\text{Grand mean of IBW})2} \quad \ldots\ldots\ldots\ldots\ldots\ldots \text{[ii]}$$

The PYR was estimated according to the following equation:

$$\text{PYR} = \frac{\text{IBW at 0 dS/m} - \text{IBW at different dS/m}}{\text{IBW at 0 dS/m}} \times 100 \quad \ldots\ldots\ldots\ldots\ldots\ldots \text{[iii]}$$

Regression analysis was performed to determine the extent of the relationship between IBW and salinity levels at different phases. Stepwise regression was also performed to find out the critical phase for salinity stress to IBW. Regression analysis and visualization were performed by using the "ggplot2" package (Wickham, 2009) in the "R" platform (R Core Team R, 2021).

3 Results

3.1 First-year observation

3.1.1 Germination and subsequent growth repression percentage

Soil salinity markedly influenced the germination percentage of onion (Table 1). Germination percentage was recorded the highest in Ac Gaz 379 (98%) followed by Ac Bog 418 (90%), Ac Bog 432 (84%), and Ac Bog 422 (78%) compared to the rest of the germplasm, whereas the lowest germination (36%) was recorded in BARI Piaz-4 (check cultivar) under 8 dS m^{-1}. Under normal water treatment, germination percentage was found to be higher in Ac Gaz 379 (100%), Ac Bog 428 (92%), Ac Bog 423 (92%), Ac Bog 422 (90%), Ac Bog 421 (94%), Ac Bog 420 (90%), Ac Bog 422 (96%), and Ac Bog 409 (90%) than the rest of the germplasm, and the lowest germination (60%) was recorded in Ac Bog 417. Under 10 dS m^{-1}, germination percentage ranged from 36% (Ac Bog 418) to 92% (Ac Gaz 379). On the other hand, the highest germination percentage was recorded in Ac Gaz 379 (100%), which was followed by Ac Bog 418 (76%), Ac Bog 423 (72%), and Ac Bog 424 (72%), and the lowest germination was recorded in BARI Piaz-4, which was only 14% under the 12 dS m^{-1} salinity level. Finally, after subjecting all levels of salinity (0, 8, 10, and 12 dS m^{-1}), germination percentage was found to range from 38% to 97.50%.

Under all levels of salinity (8, 10, and 12 dS m^{-1}), the growth of germinated onion bulb was repressed in a significant way (Table 1) compared to untreated control as it ranged from 1% to 6% and 1% to 22% in control and 12 dS m^{-1} treatment, respectively. After imposing 8 dS m^{-1} salinity, the lowest growth repression % was recorded in Ac Gaz 379 (0) and the highest was recorded in Ac Bog 422 (9). After exerting 10 dS m^{-1} salinity, the lowermost growth repression % was noted in Ac Gaz 418 (3), Ac Gaz 420 (3), and Ac Gaz 421 (3), and the highest was noted in Ac Bog 429 (20) and BARI Piaz-4 (20). When 12 dS m^{-1} salinity was applied, the lowest growth repression % was found in Ac Gaz 379 (1) and the highest was found in Ac Bog 416 (22). Considering the mean values of all treatments (0, 8, 10, and 12 dS m^{-1}), the lowest growth repression % was observed in Ac Gaz 379 (1.5) and the highest was observed in BARI Piaz-4 (11.25).

From Figure 1, it was revealed that the germination percentage gradually decreased with the increase of irrigation water salinity concentration. In contrast, the subsequent growth repression among the genotypes was minimum in the control treatment (0 dS m^{-1}), and it was increased along the salinity level. Ultimately, the highest percentage of seized growth or death of germinated seed was observed at the 12 dS m^{-1} treatment.

3.2 Second-year observation

3.2.1 Analysis of variance

Variance analysis was carried out among the studied traits of the second-year study and substantial variations ($p< 0.01$) were observed (Table S2). Variance due to genotypes (σ^2g) and salinity levels (σ^2s) were significant for all the studied traits, while variance due to genotypes:salinity level (σ^2g×s) was significant for all the traits except MLL.

3.2.2 Progression of soil salinity

The studied soil was non-saline during the entire growing period of onion as the salinity range of soil under untreated control ranged from 1.67 to 2.58 dS m^{-1} (Table S4). In contrast, soil salinity was gradually built up with the advancement of different phases of onion plants depending on the concentration of salt in the solution (0, 8, 10, and 12 dS m^{-1}) after eight spells of application (Tables S5-S7). After the application of irrigation water having 8, 10, and 12 dS m^{-1} of salinity, it was found that minimum levels of ECs (electrical conductivity in pot soil) were recorded in the first phase and maximum levels were recorded in the eighth phase. For example, 3.14, 2.57, and 3.33 dS m^{-1} were recorded from the first phase of 8, 10, and 12 dS m^{-1} treatments, respectively, whereas 6.92, 9.18, and 11.26 dS m^{-1} were obtained from 8, 10, and 12 dS m^{-1} treatments at the eighth phase, respectively. In the last phase of crops, soil salinity was increased by 168.22%, 255.81%, and 336.43% in 8, 10, and 12 dS m^{-1} treatments compared to the control treatment (0 dS m^{-1}), respectively. The salinity profile in pot soil

TABLE 1 Scanning the germination ability of onion genotypes at different salinity stress levels in the first year.

Genotype	Germination percentage (%)					Growth repressed (%)				
	C (0 dS m^{-1})	8 dS m^{-1}	10 dS m^{-1}	12 dS m^{-1}	Mean	C (0 dS m^{-1})	8 dS m^{-1}	10 dS m^{-1}	12 dS m^{-1}	Mean
Ac Bog 409	90	66	62	44	65.5	6	14	24	42	21.5
Ac Bog 410	74	64	64	56	64.5	8	8	20	18	13.5
Ac Bog 411	78	62	44	50	58.5	8	6	26	24	16
Ac Bog 412	86	50	66	26	57	8	12	24	22	16.5
Ac Bog 414	86	66	48	56	64	4	16	16	24	15
Ac Bog 415	64	68	48	48	57	6	16	22	18	15.5
Ac Bog 416	84	74	76	36	67.5	6	6	26	44	20.5
Ac Bog 417	60	68	80	66	68.5	8	14	26	36	21
Ac Bog 418	96	90	36	76	74.5	4	4	6	4	4.5
Ac Bog 419	86	58	70	52	66.5	8	16	14	20	14.5
Ac Bog 420	90	74	52	56	68	4	8	6	12	7.5
Ac Bog 421	94	72	68	50	71	4	8	6	24	10.5
Ac Bog 422	90	78	48	54	67.5	4	18	10	22	13.5
Ac Bog 423	92	72	72	72	77	2	8	22	12	11
Ac Bog 424	84	42	52	72	62.5	6	12	28	12	14.5
Ac Bog 425	82	74	64	74	73.5	4	6	10	16	9
Ac Bog 426	82	66	54	52	63.5	12	8	12	26	14.5
Ac Bog 427	74	60	60	46	60	8	18	12	22	15
Ac Bog 428	92	74	46	46	64.5	8	12	30	12	15.5
Ac Bog 429	82	58	72	44	64	6	12	40	14	18
Ac Bog 430	86	72	74	54	71.5	4	16	16	16	13
Ac Bog 431	80	70	44	70	66	6	4	14	16	10
Ac Bog 432	84	82	50	56	68	2	4	10	18	8.5
Ac Gaz 379	100	98	92	100	97.5	2	0	8	2	3
BARI Piaz-4	66	36	36	14	38	8	16	40	26	22.5
Mean	83.28	67.76	59.12	54.8	66.24	5.84	10.48	18.72	20.08	13.78
SD	9.8	13.28	14.34	17.28		2.44	5.1	9.86	9.96	
Min	60	36	36	14		2	0	6	2	
Max	100	98	92	100		12	18	40	44	

SD, standard deviation; Min, minimum; Max, maximum; C, control treatment, 0 dS m^{-1}.

was in ascending order from the start to the end of the crop cycle, i.e., first to eighth phase (Figure 2). The soil salinity levels (EC_s) reached at the eighth phase in all treatments (8, 10, and 12 dS m^{-1}) were lower than those of the respective irrigation water salinity (Figure 3). However, it was expected to be the same at the irrigation treatments in an equilibrium state.

3.2.3 Impact of different levels of salinity on leaf-associated traits

Drying out of onion plant leaves was markedly influenced by the different levels (0, 8, 10, and 12 dS m^{-1}) of salinity (Table 2 and Table S3). Almost 100% of the seedlings of onion plants were green under non-saline treatment, but at 8 dS m^{-1}, no plants with dried

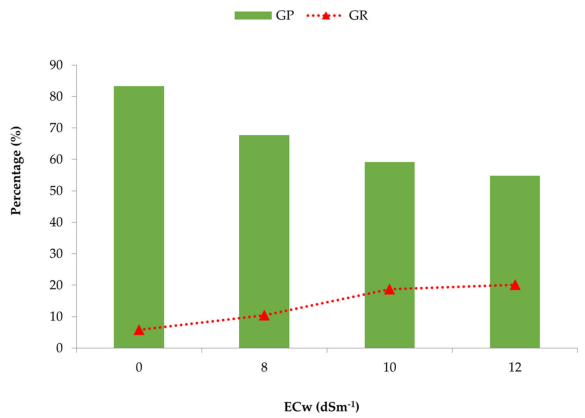

FIGURE 1
Comparison of the mean germination percentage (GP) and growth repression (GR) of 25 onion genotypes at different concentrations or salinity levels of irrigation water.

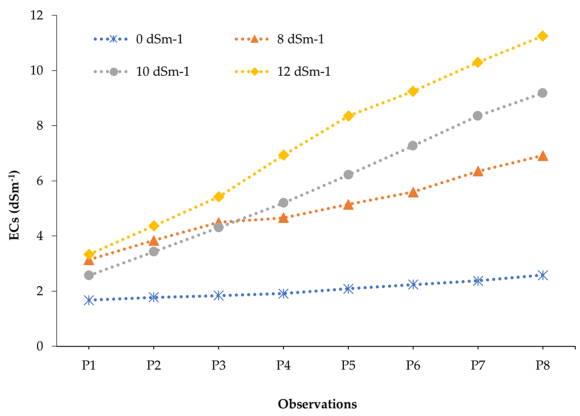

FIGURE 2
Development of soil salinity (EC_s) over the periods of the onion life cycle at different salinity concentrations. All the data points are the mean values of EC_s recorded in replicated experimental pots representing 25 different onion genotypes (150 pots).

leaves were found in Ac Bog 414, Ac Bog 415, Ac Bog 416, Ac Bog 417, Ac Bog 418, Ac Bog 419, Ac Bog 420, Ac Bog 422, Ac Bog 424, and Ac Bog 425 where the highest percentage of plants with dried leaves (PPDL) was recorded in Ac Bog 410 (100%), Ac Bog 432 (100%), and Ac Bog 428 (83.33%). After applying 10 dS m^{-1} salinity, no plants with dried leaves were found in Ac Bog 418, Ac Bog 420, and Ac Bog 424, but the highest PPDL was found in Ac Bog 432 (100%) and Ac Gaz 379 (83.33%).

At 12 dS m^{-1} salinity, no plants with dried leaves were found in Ac Bog 412, Ac Bog 422, and BARI Piaz-4, but the highest PPDL was found in Ac Bog 411 (100%), Ac Bog 412 (100%), Ac Bog 420 (100%), and Ac Bog 432 (100%). Mean PPDL ranged from 4.17% (Ac Bog 422) to 75% (Ac Bog 432) after subjecting all levels (0, 8, 10, and 12 dS m^{-1}) of salinity.

The percentage of green plants (PGP) was noticeably influenced by imposing salinity (Table 2 and Table S3). Almost all studied plants remain green under control treatments, but under 8 dS m^{-1}, 100% of plants were dead in Ac Bog 410 and Ac Bog 432 genotypes where, under the same treatment, the highest PPG (100%) was observed in Ac Bog 414, Ac Bog 415, Ac Bog 416, Ac Bog 420, and Ac Bog 424. Under 10 dS m^{-1} of salinity, the highest percentage (100%) of green plants was found in Ac Bog 418, Ac Bog 420, and Ac Bog 424 where the lowest number of green plants was recorded in Ac Bog 432 (0%). Under 12 dS m^{-1} of salinity, in the Ac Bog 422 genotype, the highest percentage (100%) of green plants was noted and the lowest (0%) was obtained from Ac Bog 410, Ac Bog 411, Ac Bog 430, and Ac Bog 432. After subjecting all levels (0, 8, 10, and 12 dS m^{-1}) of salinity, PGP was found to range from 1.5 to 5.25.

MLL was prominently affected by imposing salinity (Table 3 and Table S3). The MLL (cm) of onion seedlings ranged from 13.67 to 26.00 under untreated control treatment. The highest MLL (cm) under 8 dS m^{-1} was recorded in Ac Bog 409 (25.67), which was followed by Ac Bog 415 (24.33), Ac Bog 414 (23.80), and Ac Bog 416 (23.60), and the lowest MLL was found in Ac Bog 432 (0.0001). Under 10 dS m^{-1}, MLL (cm) was noted to be the highest in Ac Bog 422 (21.17), which was followed by Ac Bog 416 (20.67) and Ac Bog 423 (20.30), and the lowest was obtained in Ac Bog 410 (7.50). The highest MLL (cm) under 12 dS m^{-1} salinity was recorded in Ac Bog 414 (23.40) and the lowest was recorded in Ac Bog 432 (0.0001). After subjecting all levels of treatments (0, 8, 10, and 12 dS m^{-1}), the average MLL of onion seedlings was between 9.44 and 22.76 cm.

The number of leaves (NL) was markedly influenced by the application of salinity (0, 8, 10, and 12 dS m^{-1}) treatments (Tables 3 and S3). The number of leaves of onion seedlings ranged from 1.67 to 7.17 under untreated control treatment. Under the 8 dS m^{-1} salinity level, the highest NL was recorded in Ac Bog 420 (5.83) and Ac Bog 425 (5.83), and the lowest NL was recorded in Ac Bog 428 (2.50). The highest NL was found in Ac Bog 416 (6.67) under 10 dS m^{-1} salinity, whereas the lowest NL was found in Ac Bog 410 (1.33). Under 12 dS m^{-1} salinity treatment, the lowest NL was observed in Ac Bog 411 (1.83), whereas the highest NL was found in Ac Bog 424 (5.50). Considering the mean values of NL over the different salinity levels, the leaf number varied between 2.63 and 5.71.

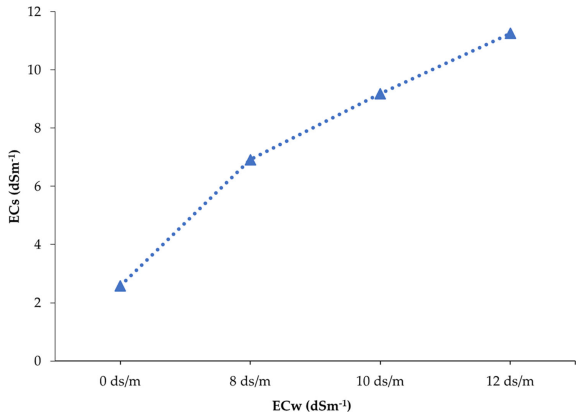

FIGURE 3
Soil salinity development after the application of different treatments at the end of the cropping season. Each point represents the mean of EC_s values recorded in replicated experimental pots of 25 genotypes (150 pots).

TABLE 2 Performance of onion genotypes for greenness-related traits under different salinity stress levels in pot culture in the second year.

Genotype	Plants with dried leaves (%)					Green plants (%)				
	C (0 dS m^{-1})	8 dS m^{-1}	10 dS m^{-1}	12 dS m^{-1}	Mean	C (0 dS m^{-1})	8 dS m^{-1}	10 dS m^{-1}	12 dS m^{-1}	Mean
Ac Bog 409	0 (1.65)*	33.33 (35.26)	33.33 (35.26)	33.33 (35.26)	25 (26.86)	100 (88.35)	66.67 (54.74)	83.33 (71.54)	66.67 (54.74)	79.17 (67.34)
Ac Bog 410	0 (1.65)	100 (88.35)	66.67 (54.74)	100 (88.35)	66.67 (58.27)	100 (88.35)	0 (1.65)	50 (45)	0 (1.65)	37.5 (34.16)
Ac Bog 411	0 (1.65)	50 (45)	66.67 (54.74)	100 (88.35)	54.17 (47.43)	100 (88.35)	33.33 (35.26)	33.33 (35.26)	0 (1.65)	41.67 (40.13)
Ac Bog 412	0 (1.65)	33.33 (35.26)	16.67 (18.46)	0 (1.65)	12.5 (14.26)	100 (88.35)	50 (45)	83.33 (71.54)	66.67 (54.74)	75 (64.91)
Ac Bog 414	0 (1.65)	0 (1.65)	16.67 (18.46)	33.33 (35.26)	12.5 (14.26)	100 (88.35)	100 (88.35)	83.33 (71.54)	66.67 (54.74)	87.5 (75.74)
Ac Bog 415	0 (1.65)	0 (1.65)	16.67 (18.46)	50 (45)	16.67 (16.69)	100 (88.35)	100 (88.35)	83.33 (71.54)	33.33 (35.26)	79.17 (70.87)
Ac Bog 416	0 (1.65)	0 (1.65)	16.67 (18.46)	83.33 (71.54)	25 (23.33)	100 (88.35)	100 (88.35)	66.67 (54.74)	16.67 (18.46)	70.83 (62.47)
Ac Bog 417	0 (1.65)	0 (1.65)	16.67 (18.46)	66.67 (54.74)	20.83 (19.13)	100 (88.35)	100 (88.35)	83.33 (71.54)	33.33 (35.26)	79.17 (70.87)
Ac Bog 418	0 (1.65)	0 (1.65)	0 (1.65)	33.33 (35.26)	8.33 (10.06)	100 (88.35)	50 (45)	100 (88.35)	66.67 (54.74)	79.17 (69.11)
Ac Bog 419	0 (1.65)	0 (1.65)	16.67 (18.46)	16.67 (18.46)	8.33 (10.06)	100 (88.35)	83.33 (71.54)	83.33 (71.54)	83.33 (71.54)	87.5 (75.74)
Ac Bog 420	0 (1.65)	0 (1.65)	0 (1.65)	100 (88.35)	25 (23.33)	100 (88.35)	100 (88.35)	100 (88.35)	16.67 (18.46)	79.17 (70.87)
Ac Bog 421	0 (1.65)	33.33 (35.26)	16.67 (18.46)	16.67 (18.46)	16.67 (18.46)	100 (88.35)	66.67 (54.74)	83.33 (71.54)	66.67 (54.74)	79.17 (67.34)
Ac Bog 422	0 (1.65)	0 (1.65)	16.67 (18.46)	0 (1.65)	4.17 (5.86)	100 (88.35)	83.33 (71.54)	66.67 (54.74)	100 (88.35)	87.5 (75.74)
Ac Bog 423	0 (1.65)	16.67 (18.46)	33.33 (35.26)	50 (45)	25 (25.09)	100 (88.35)	83.33 (71.54)	66.67 (54.74)	50 (45)	75 (64.91)
Ac Bog 424	0 (1.65)	0 (1.65)	0 (1.65)	33.33 (35.26)	8.33 (10.06)	100 (88.35)	100 (88.35)	100 (88.35)	66.67 (54.74)	91.67 (79.94)
Ac Bog 425	0 (1.65)	0 (1.65)	16.67 (18.46)	16.67 (18.46)	8.33 (10.06)	100 (88.35)	83.33 (71.54)	66.67 (54.74)	83.33 (71.54)	83.33 (71.54)
Ac Bog 426	0 (1.65)	16.67 (18.46)	33.33 (35.26)	33.33 (35.26)	20.83 (22.66)	100 (88.35)	66.67 (54.74)	66.67 (54.74)	33.33 (35.26)	66.67 (58.27)
Ac Bog 427	16.67 (18.46)	50 (45)	66.67 (61.8)	83.33 (71.54)	54.17 (49.2)	83.33 (71.54)	33.33 (28.19)	33.33 (35.26)	16.67 (18.46)	41.67 (38.36)
Ac Bog 428	16.67 (18.46)	83.33 (71.54)	66.67 (54.74)	33.33 (35.26)	50 (45)	83.33 (71.54)	16.67 (18.46)	33.33 (35.26)	66.67 (54.74)	50 (45)
Ac Bog 429	0 (1.65)	16.67 (18.46)	16.67 (18.46)	16.67 (18.46)	12.5 (14.26)	100 (88.35)	66.67 (54.74)	66.67 (54.74)	66.67 (54.74)	75 (63.14)
Ac Bog 430	0 (1.65)	16.67 (18.46)	33.33 (35.26)	50 (45)	25 (25.09)	100 (88.35)	66.67 (61.81)	50 (45)	0 (1.65)	54.17 (49.2)
Ac Bog 431	0 (1.65)	66.67 (54.74)	50 (45)	16.67 (18.46)	33.33 (29.96)	100 (88.35)	16.67 (18.46)	33.33 (35.26)	66.67 (54.74)	54.17 (49.2)
Ac Bog 432	0 (1.65)	100 (88.35)	100 (88.35)	100 (88.35)	75 (66.67)	100 (88.35)	0 (1.65)	0 (1.65)	0 (1.65)	25 (23.33)

(Continued)

TABLE 2 Continued

Genotype	Plants with dried leaves (%)					Green plants (%)				
	C (0 dS m^{-1})	8 dS m^{-1}	10 dS m^{-1}	12 dS m^{-1}	Mean	C (0 dS m^{-1})	8 dS m^{-1}	10 dS m^{-1}	12 dS m^{-1}	Mean
Ac Gaz 379	0 (1.65)	50 (45)	83.33 (71.54)	66.67 (54.74)	50 (43.23)	100 (88.35)	50 (45)	16.67 (18.46)	33.33 (35.26)	50 (46.77)
BARI Piaz-4	0 (1.65)	66.67 (54.74)	16.67 (18.46)	0 (1.65)	20.83 (19.13)	100 (88.35)	33.33 (35.26)	83.33 (71.54)	16.67 (18.46)	58.33 (53.4)
Mean	1.33 (3)	29.33 (27.55)	32.67 (31.2)	45.33 (41.99)	27.17 (25.94)	98.67 (87)	62 (54.84)	64.67 (56.68)	44.67 (39.62)	67.5 (59.53)
CV %	50.83				–	21.88				–
LSD (0.05)	5.23				–	12.93				–

CV, coefficient of variation; LSD (0.05), least significant difference; C, control treatment, 0 dS m^{-1}; *data in parentheses represent the transformed value of the corresponding data.

3.2.4 Impact of different levels of salinity on bulb-associated traits

The BL (cm) of onion seedlings was decisively influenced by the salinity treatments (Table 4 and S3).

BL (cm) ranged from 12.76 to 38.74 in the control treatment. The highest BL (cm) was found in Ac Bog 417 (50.2), which was followed by Ac Bog 424 (49.58), and the lowest was recorded in Ac Bog 432 (6.84) under 8 dS m^{-1} salinity. Moreover, under 10 dS m^{-1} salinity, the highest BL (cm) was found in Ac Bog 417 (47.38), which was followed by Ac Bog 424 (47.2), Ac Bog 420 (44.62), and Ac Bog 414 (44.02), and the lowest was recorded in Ac Bog 432 (8.52).

On the other hand, the highest BL (cm) was obtained from Ac Bog 426 (54.46), and the lowest was recorded in Ac Bog 432 (17) under 12 dS m^{-1} salinity. After assessing the mean of BL (cm) of all treatments, BL ranged from 12.64 to 43.32 cm.

The BD (cm) of onion seedlings was remarkably influenced by the salinity treatments (Tables 4 and S3). BD (cm) ranged from 11.2 to 39.56 in the untreated control. The highest BD (cm) under 8 dS m^{-1} salinity was observed in Ac Bog 426 (38.36) and the lowest was recorded in BARI Piaz-4 (10.4). Furthermore, under 10 dS m^{-1} salinity, the highest BD (cm) was found in Ac Bog 429 (31.68), which was followed by Ac Bog 420 (31.46), and the lowest was recorded in Ac Bog 432 (7.02). In contrast, the highest BD (cm) under 12 dS m^{-1} salinity was found in Ac Bog 420 (29.4) and the lowest was recorded in Ac Bog 432 (7.52). After evaluating the mean of BD (cm) of all treatments, the average BD ranged from 12.1 to 26.28 cm.

The IBW (g) of onion seedlings was markedly influenced by the salinity treatments (Tables 4 and S3). IBW (g) oscillated from 7.65 to 38.15 in the untreated control. The highest IBW (g) under 8 dS m^{-1} salinity was observed in Ac Bog 409 (22.2) and the lowest was recorded in Ac Bog 424 (2.1). Moreover, under 10 dS m^{-1} salinity, the highest IBW (g) was found in Ac Bog 420 (16.2), which was followed by Ac Bog 424 (15.6), and the lowest was noted in Ac Bog 428 (1.5). In comparison, the highest IBW (g) under 12 dS m^{-1} salinity was found in Ac Bog 420 (17) and the lowest was documented in Ac Bog 428 (1.4). The mean IBW (g) of all salinity treatments varied between 3.9 and 16.5 g for all the studied genotypes.

3.2.5 Associated indices of soil salinity stress

ShTI, STI, and PYR were distinctly influenced by the application of different levels of salinity in comparison with the untreated control (Tables 5 and 6). The ShTI under 8 dS m^{-1} ranged from 0.00 to 99.31 with a mean of 88.62 (Table 5). The highest ShTI was recorded in Ac Bog 415, which was followed by Ac Bog 414 (99.17) and Ac Bog 409 (98.36), and the lowest ShTI was recorded in Ac Bog 432 under 8 dS m^{-1} salinity treatment. Under 10 dS m^{-1}, the ShTI ranged from 31.91 to 96.03 with a mean of 75.56. The highest ShTI was documented in Ac Bog 425, and the lowest ShTI was documented in Ac Bog 410. The mean ShTI under 12 dS m^{-1} was 63.56 with a range from 0.00 to 97.50, where the highest ShTI was recognized in Ac Bog 414 but the lowest was recognized in Ac Bog 411 and Ac Bog 432.

Under 8 dS m^{-1}, the STI ranged from 0.22 to 4.19 with a mean of 1.79 (Table 5). Maximum STI was noted in Ac Bog 430, and the lowest was noted in Ac Bog 432 under 8 dS m^{-1} salinity treatment. The mean STI under 10 dS m^{-1} was 1.19 with a range of 0.13 to 3.43. The highest STI was documented in Ac Bog 424, which was followed by Ac Bog 420 (3.25), and the lowest was noted in Ac Bog 432. The STI under 12 dS m^{-1} ranged from 0.12 to 3.41 with a mean of 1.16. The highest STI under 12 dS m^{-1} salinity treatment was found in Ac Bog 420, which was followed by Ac Bog 424 (3.22), but the lowest was found in the Ac Bog 432 genotype. The mean PYR under 8 dS m^{-1} was 56.00 with a range of 0.89 to 92.59. The highest PYR under 8 dS m^{-1} salinity treatment was recorded in Ac Bog 424, which was followed by Ac Bog 426 (89.91) and Ac Bog 379 (86.92), and the lowest was noted in Ac Bog 409. The PYR under 10 dS m^{-1} ranged from 37.33 to 94.13 with a mean of 73.62. Under 10 dS m^{-1}, the highest PYR was obtained in Ac Bog 428, which was followed by Ac Bog 413 (93.64) and Ac Bog 423 (89.52), and the lowest was obtained in Ac Bog 420. Under 12 dS m^{-1}, the PYR ranged from

TABLE 3 Performance of onion genotypes for leaf-related traits under different salinity stress levels in pot culture in the second year.

Genotypes	Maximum leaf length					Number of leaves				
	C (0 dS m^{-1})	8 dS m^{-1}	10 dS m^{-1}	12 dS m^{-1}	Mean	C (0 dS m^{-1})	8 dS m^{-1}	10 dS m^{-1}	12 dS m^{-1}	Mean
Ac Bog 409	25.67	25.25	16.17	17.6	21.17	6.17	4.00	5.17	4.17	4.88
Ac Bog 410	23.5	11.33	7.5	10	13.08	2.83	4.17	1.33	2.83	2.79
Ac Bog 411	22	19.5	11.5	0.0001	13.25	2.83	4.00	2.83	1.83	2.87
Ac Bog 412	25	17	15.8	17.2	18.75	5.33	5.33	4.00	4.50	4.79
Ac Bog 413	21.5	18.83	15.67	8.4	16.10	6.00	4.17	4.83	4.50	4.29
Ac Bog 414	24	23.8	19.83	23.4	22.76	5.17	5.67	5.83	4.67	5.54
Ac Bog 415	24.5	24.33	19	19.4	21.81	4.67	5.00	6.00	4.67	5.21
Ac Bog 416	25.67	23.6	20.67	12	20.49	6.00	4.50	6.67	3.50	4.83
Ac Bog 417	23.33	22.33	17.5	21.8	21.24	3.67	5.50	5.50	4.83	5.46
Ac Bog 419	24.33	14.5	20	18.17	19.25	6.33	4.83	3.17	5.00	4.83
Ac Bog 420	25.83	17.5	18.17	17.5	19.75	6.17	5.83	3.83	4.67	5.13
Ac Bog 421	18.8	18.2	14.83	14.33	16.54	4.50	5.17	5.50	4.00	4.79
Ac Bog 422	24.33	22	21.17	15.33	20.71	5.83	5.17	4.83	4.50	5.08
Ac Bog 423	22.17	20.6	20.3	20.25	20.83	7.17	5.00	5.83	4.83	5.71
Ac Bog 424	25.83	21.67	18.5	20.75	21.69	6.17	5.67	3.17	5.50	5.13
Ac Bog 425	20.17	19.67	19.37	18.5	19.43	6.33	5.83	3.33	4.33	4.96
Ac Bog 426	24.2	22.8	17.83	12.67	19.38	6.00	5.00	5.00	4.00	5.00
Ac Bog 427	19.67	19	12.33	12	15.75	5.33	3.17	5.67	3.17	4.33
Ac Bog 428	13.67	12.5	10.67	8.25	11.27	1.67	2.50	3.00	3.33	2.63
Ac Bog 429	26	23.33	13.83	16.4	19.89	4.83	5.50	4.67	4.83	4.96
Ac Bog 430	21.17	17	19.8	17.4	18.84	5.67	4.83	2.67	4.83	4.50
Ac Bog 431	21.75	20	18.5	15	18.81	2.50	3.00	4.67	3.83	3.50
Ac Bog 432	22.75	0.0001	15	0.0001	9.44	3.17	2.83	2.00	2.67	2.67
Ac Gaz 379	20.33	19	15.67	10	16.25	3.00	2.83	5.33	2.83	3.50
BARI Piaz-4	21.5	18	10	15.25	16.19	2.50	5.00	2.67	4.83	3.75
Mean	22.69	17.17	20.72	15.51	19.11	4.8	4.3	4.58	4.11	4.45
CV%	20.76				–	20.97				–
LSD (0.05)	–				–	0.92				

CV, coefficient of variation; LSD (0.05), least significant different; C, control treatment; 0 dS m^{-1}.

34.24 to 94.52 with a mean of 73.87. The highest PYR was found in Ac Bog 428, which was followed by Ac Bog 413 (93.64) and Ac Bog 423 (92.40), and the lowest was found in the Ac Bog 420 genotype.

3.2.6 Ranking of the genotypes

Genotypes were ranked against salinity stress tolerance to select potential ones (Table 5). Based on different tolerance indices (ShTI and STI), genotypes were ranked, where dissimilarities in ranking positions were observed within a particular index for some of the potential genotypes. Thus, mean ranking (MR) was estimated for all the indices. Many of the genotypes are observed in the upper order among the MR of different indices, though differential results are also in place. Ranking and mean ranking were also estimated for yield reduction (%) (PYR), and a reflection of a similar ranking pattern from the previous result was observed (Table 6). Finally, to select better genotypes having good yield, better tolerance, and minimum yield loss under stress, ranking based on IBW and re-ranking of MR (of ShTI, STI, and PYR) was carried out (Table 7).

Genotypes' position in those ranks was marked and their position within the top 10 was counted. The genotypes that present a maximum of four times in the top 10 were regarded as tolerant genotypes and those that present three times were denoted as

TABLE 4 Performance of onion genotypes for bulb-related traits under different salinity stress levels in pot culture in the second year.

Genotype	Bulb length (mm)					Bulb diameter (mm)					Individual bulb weight (g)				
	C (0 dS m^{-1})	8 dS m^{-1}	10 dS m^{-1}	12 dS m^{-1}	Mean	C (0 dS m^{-1})	8 dS m^{-1}	10 dS m^{-1}	12 dS m^{-1}	Mean	C (0 dS m^{-1})	8 dS m^{-1}	10 dS m^{-1}	12 dS m^{-1}	Mean
Ac Bog 409	18.8	35.92	34.56	48.78	34.52	39.56	15.7	24.26	22.2	25.44	22.4	22.2	8.75	8.85	15.55
Ac Bog 410	19.46	15.54	17.64	30.92	20.88	21	19.02	19.48	18.42	19.48	14.2	5.25	4.75	5.25	7.35
Ac Bog 411	15.2	15.98	26.34	37.18	23.68	21.14	12.14	20.74	13.98	17	14.25	7.45	2.8	2.6	6.8
Ac Bog 412	15.38	29.76	31.48	30.3	26.72	16	11.9	16.56	13.96	14.6	12.75	4.9	5.8	6.35	7.45
Ac Bog 413	20.8	18.16	26.04	44.28	27.32	24.72	18.84	9.56	9.34	15.62	25.95	9.4	1.65	1.65	9.65
Ac Bog 414	27.76	26.92	44.02	43.02	35.44	27.8	23.36	22.82	22.64	24.16	30.5	12	11.4	11.85	16.4
Ac Bog 415	28.36	37.08	37.72	40.74	35.98	23.74	26.1	24.3	19.02	23.28	25.55	11.4	6.7	4.1	11.95
Ac Bog 416	25.66	23.84	37.96	44.76	33.06	24.56	20.52	26.5	14.22	21.44	27.2	16.65	3.4	3.65	12.7
Ac Bog 417	28.04	50.2	47.38	47.66	43.32	30.3	22.3	27.54	24.96	26.28	22.85	19.7	5.8	3.6	13
Ac Bog 419	36.08	36.44	36.76	30.18	34.86	14.38	35.72	17.4	16.86	21.1	39.05	5.35	7.45	7.25	14.75
Ac Bog 420	25.32	45.26	44.62	31.66	36.72	20.12	23.62	31.46	29.4	26.14	25.85	6.9	16.2	17	16.5
Ac Bog 421	17.5	27	29.24	35.32	27.26	17.54	15.4	19.68	20.92	18.38	18.45	5.1	5.75	5.4	8.65
Ac Bog 422	27.14	34.46	37.12	33.02	32.94	24.3	27.84	23.56	24.3	25	30.85	10.7	8	8.55	14.5
Ac Bog 423	38.74	34.08	35.66	33.72	35.56	17.06	34	15.34	14.16	20.14	38.15	5.5	4	2.9	12.65
Ac Bog 424	27.9	49.58	47.2	46.46	42.78	20.64	21.62	27.2	25.7	23.78	28.35	2.1	15.6	14.65	15.15
Ac Bog 425	29.72	38.86	40.22	36.28	36.26	27.7	30.08	23.1	23.98	26.22	33.35	12	7.25	7.05	14.9
Ac Bog 426	36.7	33.16	34.76	54.46	39.78	33.26	38.36	14.46	13.26	24.84	35.2	3.55	3.85	3.85	11.6
Ac Bog 427	22.94	30.62	24	27.66	26.3	26.56	16.9	18.28	11.44	18.3	18.2	17.7	2.75	3.15	10.45
Ac Bog 428	16.14	23.2	22.64	23.64	21.4	11.2	15.02	20.84	8.32	13.84	25.55	9	1.5	1.4	9.35
Ac Bog 429	17.64	27	30.82	43.72	29.8	26.62	14.52	31.68	15.38	22.04	20.3	11.75	4.15	4.7	10.25
Ac Bog 430	24.88	39.74	37.76	34.64	34.26	25.9	24.84	24.84	25.02	25.14	30.5	17.7	8.05	8.7	16.25
Ac Bog 431	19.54	24.56	33.04	39.18	29.08	20.78	17.18	16.02	17.48	17.86	17.65	9.25	3.9	3.35	8.55
Ac Bog 432	18.18	6.84	8.52	17	12.64	18.26	15.62	7.02	7.52	12.1	7.65	3.7	2.2	2.1	3.9
Ac Gaz 379	17.22	27.04	30.26	26.36	25.22	16.34	15.9	29.26	18.44	19.98	23.7	3.1	4.55	4.45	8.95
BARI Piaz-4	12.76	36.04	29.82	28.46	26.78	16.44	10.4	14.28	14.36	13.88	9.05	3.5	3.55	4.15	5.05
Mean	23.51	30.69	33.02	36.38	30.90	22.64	21.08	21.05	17.81	20.64	23.90	9.43	5.99	5.86	11.29
CV%	20.52					35.11					48.23				
LSD (0.05)	3.11					3.55					1.07				

CV, coefficient of variation; LSD (0.05), least significant different; C, control treatment; 0 dS m^{-1}.

moderate genotypes. The genotypes present four times in the top 10 were Ac Bog 409, Ac Bog 414, Ac Bog 424, and Ac Bog 430, whereas the genotypes that occurred three times within the top 10 were Ac Bog 417, Ac Bog 419, Ac Bog 420, Ac Bog 422, and Ac Bog 425. Those genotypes could be selected as salinity-tolerant candidates.

3.3 Regression study

A simple linear regression analysis was carried out involving salinity concentration (EC_w) in irrigation water and IBW of onion corresponding to the salinity levels where IBW was considered as the dependent variable. The result showed that 61% of the IBW variation was accounted for by the irrigation water salinity levels (Figure 4).

The soil salinity levels (EC_s) had significant effects on bulb formation and its subsequent development. The soil salinity levels at different phases were regressed on IBWs of the studied genotypes. The regression analysis helps to examine the strength of the relationship between dependent and independent variables. It helped to identify the relative importance of predictor variables in terms of contributing to the variation in dependent variables. The

10.3389/fpls.2023.1154051

TABLE 5 Stress indices and their ranks for the different studied onion genotypes under different salinity treatments in pot culture in the second year.

Genotype	ShTI_8 dS m^{-1}	R	ShTI_10 dS m^{-1}	R	ShTI_12 dS m^{-1}	R	MR	STI_8 dS m^{-1}	R	STI_10 dS m^{-1}	R	STI_12 dS m^{-1}	R	MR
Ac Bog 409	98.36	3	62.99	20	68.56	13	12	3.86	2	1.52	8	1.54	8	4.5
Ac Bog 410	48.21	24	31.91	25	42.55	22	23.67	0.58	20	0.52	19	0.58	18	14.25
Ac Bog 411	88.64	16	52.27	23	0	24	21	0.82	18	0.31	22	0.29	22	15.5
Ac Bog 412	68	21	63.2	19	68.8	12	17.33	0.48	22	0.57	17	0.63	17	14
Ac Bog 413	87.58	17	72.88	15	39.07	23	18.33	1.89	10	0.33	21	0.33	21	13
Ac Bog 414	99.17	2	82.63	6	97.5	1	3	2.84	6	2.7	3	2.81	3	3
Ac Bog 415	99.31	1	77.55	11	79.18	7	6.33	2.26	9	1.33	9	0.81	12	7.5
Ac Bog 416	91.94	12	80.52	8	46.75	21	13.67	3.52	3	0.72	15	0.77	14	8
Ac Bog 417	95.71	7	75.01	13	93.44	2	7.33	3.49	4	1.03	12	0.64	16	8
Ac Bog 419	59.6	23	82.2	7	74.68	9	13	1.62	14	2.26	4	2.2	4	5.5
Ac Bog 420	67.75	22	70.34	17	67.75	14	17.67	1.38	15	3.25	2	3.41	1	4.5
Ac Bog 421	96.81	5	78.88	9	76.22	8	7.33	0.73	19	0.82	14	0.77	13	11.5
Ac Bog 422	90.42	14	87.01	4	63.01	16	11.33	2.56	7	1.92	5	2.05	6	4.5
Ac Bog 423	92.92	10	91.57	3	91.34	4	5.67	1.63	13	1.18	10	0.86	10	8.25
Ac Bog 424	83.89	18	71.62	16	80.33	6	13.33	0.46	23	3.43	1	3.22	2	6.5
Ac Bog 425	97.52	4	96.03	1	91.72	3	2.67	3.11	5	1.88	7	1.83	7	4.75
Ac Bog 426	94.21	8	73.68	14	52.36	19	13.67	0.97	17	1.05	11	1.05	9	9.25
Ac Bog 427	96.59	6	62.68	21	61.01	17	14.67	2.5	8	0.39	20	0.45	20	12
Ac Bog 428	91.44	13	78.05	10	60.35	18	13.67	1.79	12	0.3	23	0.28	24	14.75
Ac Bog 429	89.73	15	53.19	22	63.08	15	17.33	1.85	11	0.65	16	0.74	15	10.5
Ac Bog 430	80.3	20	93.53	2	82.19	5	9	4.19	1	1.91	6	2.06	5	3
Ac Bog 431	91.95	11	85.06	5	68.97	11	9	1.27	16	0.53	18	0.46	19	13.25
Ac Bog 432	0	25	65.93	18	0	24	22.33	0.22	25	0.13	25	0.12	25	18.75
Ac Gaz 379	93.46	9	77.08	12	49.19	20	13.67	0.57	21	0.84	13	0.82	11	11.25
BARI Piaz-4	83.72	19	46.51	24	70.93	10	17.67	0.25	24	0.25	24	0.29	23	17.75
Mean	88.62		75.56		63.56			1.83		1.19		1.16		
SD	26.48		19.64		24.73			1.25		0.94		0.96		
Min	0.00		31.91		0.00			0.22		0.13		0.12		
Max	99.31		96.03		97.50			4.19		3.43		3.41		

ShTI, shoot tolerance index; STI, stress tolerance index; R, rank; MR, mean rank; SD, standard deviation; Min, minimum; Max, maximum.

regression analysis showed that salinity levels at different phases negatively contributed to the IBW (Table 8).

Coefficient of determination (R^2) values for linear regression varied between 0.39 and 0.58. Multiple regression results revealed that combining all the phases accounted for 61% of the contribution towards the total IBW variation (Table 8). Figure 5 shows the contribution of different phases to the IBW variation. It was clear from the graph that, after phase 4, the attainment of soil salinity level is very distinct.

A further analysis (stepwise regression) was done to find the most critical phases for crop when undergoing salinity stress. Results showed that phases 3, 5, and 7 were responsible for 63% variability and are the most important phases under salinity stress (Tables 8 and 9).

4 Discussion

Salinity is a major environmental stressor that reduces agricultural production and sustainability in arid and semiarid settings by delaying the commencement of germination and subsequent seedling establishment (Uçarlı, 2021). Worldwide, salt has a negative impact on agricultural yield. Approximately 30

TABLE 6 The yield reduction (%) and their ranks for the different studied onion genotypes under different saline water treatments.

Genotype	PYR_8 dS m^{-1}	R	PYR_10 dS m^{-1}	R	PYR_12 dS m^{-1}	R	MR
Ac Bog 409	0.89	1	60.94	5	60.49	5	3.67
Ac Bog 410	63.03	14	66.55	7	63.03	7	9.33
Ac Bog 411	47.72	8	80.35	17	81.75	17	14.00
Ac Bog 412	61.57	13	54.51	3	50.2	3	6.33
Ac Bog 413	63.78	15	93.64	24	93.64	24	21.00
Ac Bog 414	60.66	11	62.62	6	61.15	6	7.67
Ac Bog 415	55.38	10	73.78	11	83.95	19	13.33
Ac Bog 416	38.79	4	87.5	21	86.58	21	15.33
Ac Bog 417	13.79	3	74.62	13	84.25	20	12.00
Ac Bog 419	86.3	22	80.92	19	81.43	16	19.00
Ac Bog 420	73.31	20	37.33	1	34.24	1	7.33
Ac Bog 421	72.36	19	68.83	8	70.73	8	11.67
Ac Bog 422	65.32	18	74.07	12	72.29	10	13.33
Ac Bog 423	85.58	21	89.52	23	92.4	23	22.33
Ac Bog 424	92.59	25	44.97	2	48.32	2	9.67
Ac Bog 425	64.02	16	78.26	15	78.86	13	14.67
Ac Bog 426	89.91	24	89.06	22	89.06	22	22.67
Ac Bog 427	2.75	2	84.89	20	82.69	18	13.33
Ac Bog 428	64.77	17	94.13	25	94.52	25	22.33
Ac Bog 429	42.12	6	79.56	16	76.85	12	11.33
Ac Bog 430	41.97	5	73.61	10	71.48	9	8.00
Ac Bog 431	47.59	7	77.9	14	81.02	14	11.67
Ac Bog 432	51.63	9	71.24	9	72.55	11	9.67
Ac Gaz 379	86.92	23	80.8	18	81.22	15	18.67
BARI Piaz-4	61.33	12	60.77	4	54.14	4	6.67
Mean	56.00		73.62		73.87		
SD	28.28		14.27		15.48		
Min	0.89		37.33		34.24		
Max	92.59		94.13		94.52		

PYR, percent yield reduction (over 0 dS m^{-1} treatment); R, rank; MR, mean rank; SD, standard deviation; Min, minimum; Max, maximum.

agricultural plants currently provide 90% of plant-based human food, and the bulk of these crops, known as glycophytes, are neither salt-tolerant nor salt-sensitive. Because of salt sensitivity, glycophytes make up the majority of cultivated plants. Osmotic stress, ion toxicity, and oxidative stress all have an impact on seed germination and seedling establishment. The negative influence of abiotic stresses, such as salt, heat, and drought, has an undesirable impact on seed germination (Wahid et al., 2007). Inhibition of seed germination, fall in germination percentage, and germination delay are the initial outcomes of salinity (Uçarlı, 2021) and are caused by altering the levels of seed germination stimulants (i.e., Gibberellic Acids (GAs), Abscisic Acid (ABA), membrane permeability, and water behavior) in the seed (Uçarlı, 2021).

Results of the year I study stated that germination percentage was hampered by the different salinity treatments. Germination percentage decreased with the increase in salt concentration. Seed germination primarily increases at low concentrations of salt (NaCl), but at rising concentrations, it was significantly reduced (Abdel-Fattah et al., 1972; Sudha and Riazunnisa, 2015). A similar scenario was also observed in different types of salt solutions (NaCl,

10.3389/fpls.2023.1154051

TABLE 7 Ranking of onion genotypes based on bulb weight, stress indices, and yield reduction (%) under different salinity treatments in pot culture in the second year.

Genotype	Rank based on				Occurrence* (in the top 10)
	IBW	MR (ShTI)	MR (STI)	MR (PYR)	
Ac Bog 409	4	8	2	1	4
Ac Bog 410	22	18	17	7	1
Ac Bog 411	23	16	19	13	0
Ac Bog 412	21	13	16	2	1
Ac Bog 413	16	15	14	18	0
Ac Bog 414	2	2	1	5	4
Ac Bog 415	12	4	6	12	2
Ac Bog 416	10	11	7	15	2
Ac Bog 417	9	5	7	11	3
Ac Bog 419	7	9	4	17	3
Ac Bog 420	1	14	2	4	3
Ac Bog 421	19	5	12	10	2
Ac Bog 422	8	7	2	12	3
Ac Bog 423	11	3	8	19	2
Ac Bog 424	5	10	5	8	4
Ac Bog 425	6	1	3	14	3
Ac Bog 426	13	11	9	20	1
Ac Bog 427	14	12	13	12	0
Ac Bog 428	17	11	18	19	0
Ac Bog 429	15	13	10	9	2
Ac Bog 430	3	6	1	6	4
Ac Bog 431	20	6	15	10	2
Ac Bog 432	25	17	21	8	1
Ac Gaz 379	18	11	11	16	0
BARI Piaz-4	24	14	20	3	1

IBW, individual bulb weight; MR, mean rank; ShTI, shoot tolerance index; STI, stress tolerance index; and PYR, percent yield reduction. *Total number of times a genotype is present within the top 10 at different rankings.

$CaCl_2$, and $MgCl_2$) (Malik and Singh, 1977). Therefore, the selection of genotypes based on salinity stress performance would produce better results (Regessa et al., 2010; Regessa et al., 2022). Though the germination percentage was negatively affected by salt treatment, the impact was not so detrimental for this particular trait as quite a few genotypes showed better performance in terms of germinability. In contrast, many of the genotypes were greatly influenced, showing subsequent growth repression and ultimately dying under different salt treatments. Very high growth repression was observed at elevated salinity treatments for different genotypes that previously showed better germination percentage under an ideal environment. As a whole, the germination process (emergence to first leaf development) is vulnerable to salt stress. This harmful effect may be prompted by Na and Cl ions' direct influence on embryo viability (Jahromi et al., 2008; Daszkowska-Golec, 2011) or

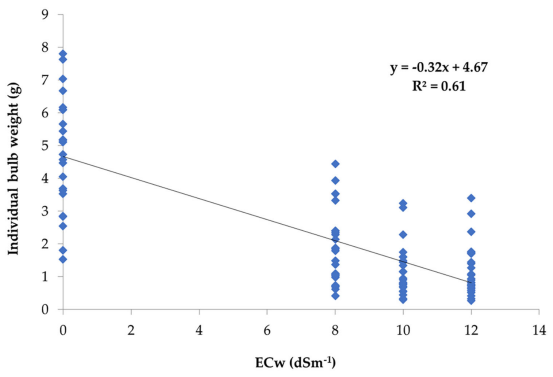

FIGURE 4
Regression of salinity concentration EC_w (dS m^{-1}) of irrigation water on individual bulb weight (g).

TABLE 8 Regression analysis for IBW based on soil salinity developed at different phases.

Item / Phase	SLR								MLR	SWR
	1	2	3	4	5	6	7	8		
b	−1.68	−1.36	−1.07	−0.76	−0.61	−0.54	−0.48	−0.44	–	–
R^2	0.39	0.53	0.58	0.55	0.54	0.55	0.57	0.56	0.61	0.63
p-value	<0.001	<0.001	<0.001	<0.001	<0.001	<0.001	<0.001	<0.001	<0.001	<0.001

SLR = simple linear regression; MLR = multiple linear regression; SWR = stepwise regression; b = regression coefficient; R^2 = coefficient of determination. Numbers 1 to 8 represent the different dates/phases when observation on EC_s was recorded.

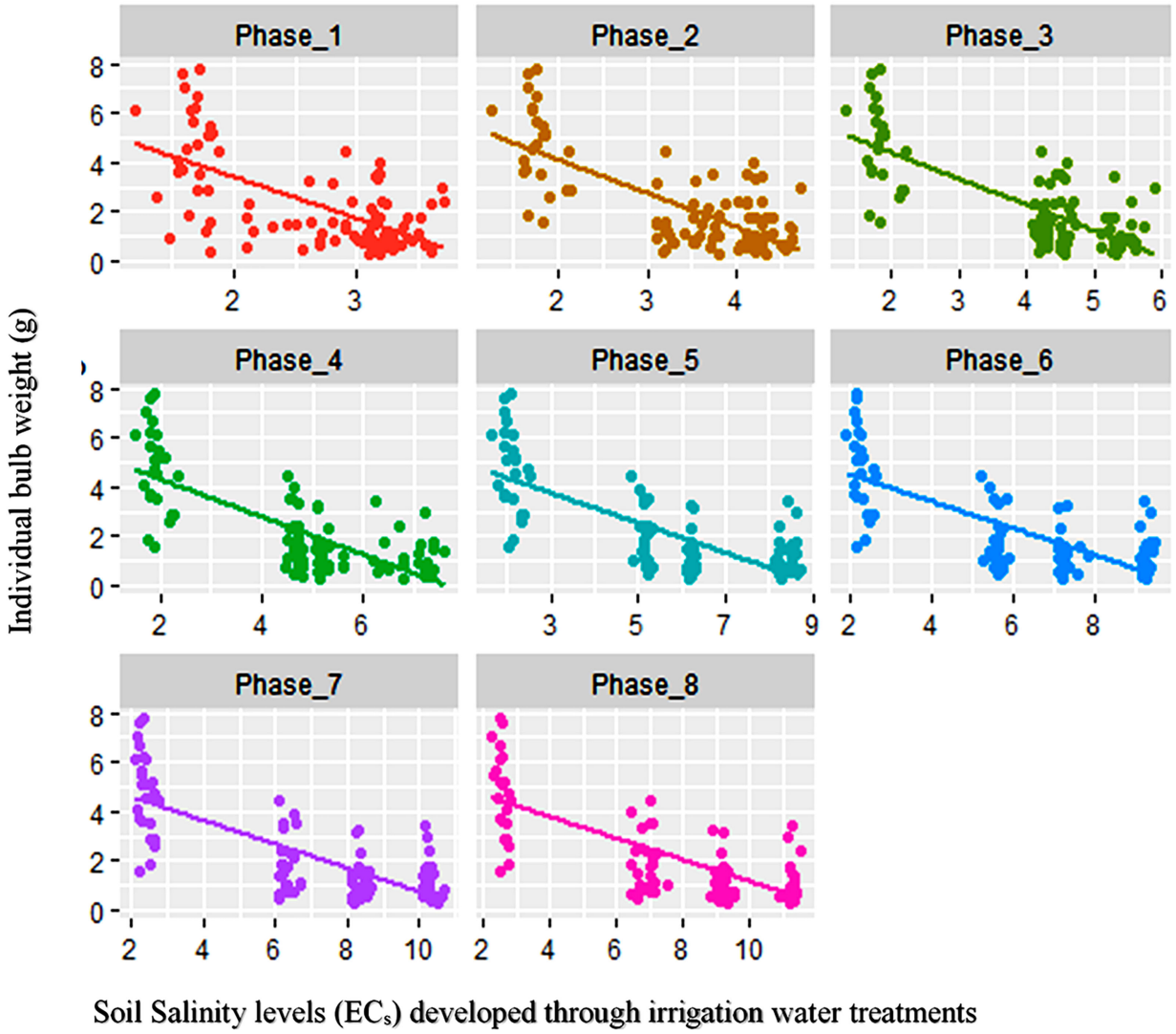

FIGURE 5
Regression of EC_s at different phases on the individual bulb weight of 25 different onion genotypes.

TABLE 9 Initial and final model after stepwise regression of different phases of soil salinity levels (EC_s) on individual bulb weight.

Type	Model
Initial model	IBW ~ Phase_1 + Phase_2 + Phase_3 + Phase_4 + Phase_5 + Phase_6 + Phase_7 + Phase_8
Final model	IBW ~ Phase_3 + Phase_5 + Phase_7

IBW, individual bulb weight; different phases representing the EC_s values of all the experimental pots at different phases of the crop cycle.

indirectly by decreasing the water availability around seeds (Koyro et al., 2008).

After each irrigation treatment, plants turn brown and ultimately older leaves tend to dry. Sometimes, all the leaves in plants of a few genotypes become completely dry within a week of saline water application. Thus, onion plants' growth in terms of the number of dried plants, number of green plants, number of total leaves, and MLL was severely affected by salinity stress. The interplay between saline treatments and plant age would result in significant changes in onion leaves, especially in terms of weight (Sta-Baba et al., 2005; Sta-Baba et al., 2010), which might be due to the changes in cells' osmotic potential following water intake reduction (El-Hendawy et al., 2019). Although many of the dried plants started to produce new leaves after the older leaves became dry, in this process, plant growth was hampered and could not contribute to accumulating the assimilates towards the bulb formation and subsequent development. However, practically robust foliage during the vegetative stage is a must for maximum production (Bosch Serra and Casanova, 2000; Sta-Baba et al., 2005). Similar to this (Bernstein and Ayers, 1953), 50% reduced growth in onion in field plots in Riverside, CA, at an EC value of 4.1 dS m^{-1}, was also observed. In the present study, the number of dried plants increased with the increase in salinity levels. Drying out or death of seedlings due to exposure to the shallow root system of onion at high salt concentration (Sta-Baba et al., 2005) was also reported under salt water irrigation in a previous study conducted by De Malach et al. (1989). In contrast, the number of green plants was reduced with the elevated salinity level. Similar to this, the number of total leaves also decreased with the increasing salinity treatments. A reduction in leaf numbers by up to 50% was reported after 45 days in onion in an earlier study (Sta-Baba et al., 2010). Apart from this, it was also revealed that MLL was reduced with the increase in salinity levels. This indicates that salt stress has a negative impact on MLL, i.e., the height of onion plants, and approximately 21% reduction in height was recorded due to this abiotic stress (Sta-Baba et al., 2010). Some of the genotypes showed better leaf length despite the elevated salinity level, which indicates that there was some sort of tolerance mechanism. Those plants had the capability to grow under higher salt stress conditions. The height of onion plants was also studied by different research groups in previous studies, and they reported that plant height reduced as salt levels rose (Janki et al., 2020). Interestingly, many research findings (Bernstein and Hayward, 1958; Bernstein, 1962; Allison, 1964) reported that on saline soils, plant height can be limited or completely inhibited by the following factors: (a) the osmotic effect on plant roots, (b) the toxic effect of accumulated ions in plant tissues, (c) the specific effect of constituent ions, or (d) a combination of all three. Reduction in onion's vegetative growth and development in terms of plant height, number of green leaves, leaf length, etc. was also reported in earlier findings (Hanci and Cebeci, 2018; Shoaib et al., 2018; Regessa et al., 2022; Sanwal et al., 2022).

Both varietal potential and salt concentration had an extensive effect on different growth and yield attributes of onion (Janki et al., 2020). Onion is very much vulnerable to salt stress (Mangal et al., 1989) with a low EC threshold (Maas and Hoffman, 1977). In the present study, traits related to bulb size and weight were observed under different salinity levels. Differences in the performances of the studied genotypes were recorded at different salt stresses. An increase in BL along with a decrease in BD as well as bulb weight was observed with the increase in salt concentration of irrigation water. A similar finding of hampered onion bulb firmness and size was reported in an earlier study (Venâncio et al., 2022). It denotes that bulb development or growth is adversely influenced by the salt stress accompanied by soil water unavailability triggered by salt concentration. Bulb growth is the most vulnerable (Kadayifci et al., 2005) and tends to escape the stress by reducing the duration of different stages, leading to a faster bulb growth stage under salinized soil (Kamran et al., 2019; Paudel et al., 2020), and ultimately ends with small-sized bulbs, which was common in previous studies. In a previous study (Ayers and Westcot, 1985), it was concluded that onion yield potential is 100% for EC_w = 0.8 dS m^{-1}, 90% for 1.2 dS m^{-1}, 75% for 1.8 dS m^{-1}, 50% for 2.9 dS m^{-1}, and 0% for 5.0 dS m^{-1}. The reduction in yield might be due to fewer bulbs per unit area, as well as reduced bulb size (Sta-Baba et al., 2005). A considerable decrease in fresh bulb weight and bulb volume was associated with the increasing salt concentration (Janki et al., 2020; Regessa et al., 2022; Sanwal et al., 2022; Venâncio et al., 2022). Fifty percent and 80% bulb loss were reported at 3.7 and 9.51 dS m^{-1} solution plots, respectively, compared to the control plot in an earlier study (Sta-Baba et al., 2010).

By delaying the start of germination and subsequent seedling establishment, salinity becomes a significant environmental constraint that lowers agricultural production and stability in arid and semiarid situations. When salt (NaCl) content is low, seed germination is predominantly increased, but as the concentration rises, it is greatly decreased. Onion leaves grow and develop differently depending on plant age and saline treatments. In this investigation, the number of dried plants increased as salinity levels rose. When the salt concentration was higher, the growth rate was significantly slower. MLL, or the height of onion plants, is negatively impacted by salinity exertion. Onion growth and yield characteristics varied greatly depending on both varietal potential and salt content (Hanci and Cebeci, 2018; Shoaib et al., 2018; Regessa et al., 2022; Sanwal et al., 2022). Onion has a low EC threshold, making it extremely susceptible to salt stress. Bulb growth is most susceptible to salinity stress and tends to avoid it by shortening the time between stages.

Soil salinity levels gradually increase with the saline water application as irrigation (Venâncio et al., 2022). The progression increased after consecutive applications up to the fourth irrigation for all the levels and reached the highest point at the end of the crop season. At this point, soil salinity (EC_s) was almost nearer to the corresponding levels of irrigation water solutions (EC_w). Similar to this, the gradual evolution pattern and the highest levels of EC_s nearer to EC_w at the end of the onion crop cycle were also concluded in a study (Sta-Baba et al., 2010).

Stress-associated indices help to select superior genotypes having tolerance to particular stresses. Ranking depending on the stress index values makes it easier to identify the best-performing genotypes. Three different indices were estimated in the current study consisting of indicators based on shoot growth (ShTI), bulb

weight (STI), and bulb weight loss under stress (PYR). ShTI recognizes the genotypes that show better shoot growth under salinity stress, while STI could differentiate the better genotypes that have the potential of producing sizable onion bulbs under a salinity stress environment. On the other hand, PYR identifies the genotypes that show minimum bulb yield loss under stress conditions. Results of the present study revealed that the ranking of ShTI, STI, and PYR at different salinity levels showed a dissimilar genotype at the upper positions. For example, Ac Bog 415, Ac Bog 425, and Ac Bog 414 were at the top of the position (rank 1) under salinity levels 8, 10, and 12 dS m^{-1}, respectively, for the stress index ShTI. A similar pattern was also observed for the other two indices (STI and PYR). Thus, a combined rank position, including the stress indices and the rank of IBW, was intended to be estimated. In doing so, mean rank (MR) was calculated for all the indices, and subsequently, a fresh ranking was employed based on the mean ranking of indices. To identify the best genotypes, presence in the top 10 ranking in multiple categories (i.e., the rank of IBW and MRs of indices) was counted. The maximum occurring genotypes were believed to have better vegetative growth, yielding ability, and minimum yield loss and ultimately had some sort of tolerance mechanism under salt stress conditions. In the present study, nine genotypes that had those characteristic features were recorded. Genotype performance under stress and sustainable selection would result depending on this (Venâncio et al., 2022).

The result from the regression analysis indicated the significant effects of saline water irrigation towards the bulb weight variation. Corresponding to water salinity (EC_w), soil salinity had a similar contribution to the variation in IBW. Elevated salinity levels are directly associated with impaired soil nutrient availability, which hampers not only nutrient absorption but also water uptake. Plants under salt stress were forced to undergo physiological changes to combat unfavorable conditions. All these lead to the reduction in onion bulb yield under such stress conditions. Simple as well as multiple linear regressions yielded similar results of soil salinity impact on the IBW. Soil salinity levels of all the phases individually and also combined significantly contributed to the yield variation. A report from a regression analysis on onion bulb yield was found to be affected by stress during the growth stage (Lee et al., 2019). The result of stepwise regression indicated that the middle phases of the growth cycle are the vulnerable stage under salinity stress (phases 3 to 7). This may be due to the fact that at the early vegetative stage, crop plants can recover quickly, while at the last stage, salinity level had very minimal effects, if any, on the crop as, at this point, bulb formation had already been completed. Stepwise regression was employed to account for the variability contributed by predictor variables on onion bulb yield in the previous study and identified the most responsible traits related to the early growth stage (Sanwal et al., 2022). From the regression graph, it was also evident that salinity development in soil due to the saline water was more distinct after consecutive applications of few irrigations (fourth in the case of the present study).

6 Conclusions

Onion is one of the most sensitive crops to salt stress as compared to other spice crops. Starting from germination to bulb maturity, all the stages are vulnerable to salinity stress. Reduction in germination percentage along with repression in subsequent growth indicated the adverse influence of higher salt concentration towards early plant formation. Interruption in leaf growth due to stress ensured limited or no food production as well as successive translocation to the bulb, which ultimately ends with reduced production. A higher salt concentration during the bulb formation stage interferes with the bulb development process, resulting in a reduced and irregular bulb shape, volume, and weight of onion bulbs. All these ultimately lead to a reduction in bulb fresh yield. The significant reduction in bulb weight compared to the control treatment clearly defines the detrimental effect of salt stress on onion yield. The variable performance of the studied genotypes under stress conditions specifies the availability of variability among the germplasm for salinity tolerance. The better sustainability and the subsequent bulb formation of several salinity-tolerant genotypes can be used in further research and for cultivation in saline-prone areas. The present findings will improve the current understanding of the salinity tolerance of onion. The present output allows the scope of the developing gene pool to have certain characteristics associated with tolerance to salt stress. Further advanced research related to genomic-level studies can dissect the underlying molecular mechanism behind the salinity tolerance of onion.

Data availability statement

The original contributions presented in the study are included in the article/Supplementary Material, further inquiries can be directed to the corresponding author/s.

Author contributions

Conceptualization: MA, MAR, MMR, MH, MN, AF, MM, SR, MI, and SM; methodology: MA, MAR, MMR, MH, MN, AF, MM, SR, MI, and SM; validation: MA, MAR, MMR, MH, MN, AF, MM, SR, MI, and SM; formal analysis: MA, AG, AA, and AH; investigation: MA and MAR; resources: MA and AH; data curation: MA, AG, AA, and AH; writing—original draft preparation: MA, MAR, MMR, MH, MN, AF, MM, SR, MI, and SM; editing: AG, AH, and AA; visualization: MA, MAR, MMR,

MH, MN, AF, MM, SR, MI, and SM; supervision: AH and MA; funding: AA, AG, SM, and AH. All authors contributed to the article and approved the submitted version.

Funding

This research was partially funded by the "Strengthening spices crops research in Bangladesh" project and Princess Nourah bint Abdulrahman University Researchers Supporting Project number (PNURSP2023R65), Princess Nourah bint Abdulrahman University, Riyadh, Saudi Arabia.

Acknowledgments

The authors would also like to extend their sincere appreciation to Bangladesh Agricultural Research Institute and Princess Nourah bint Abdulrahman University Researchers Supporting Project number (PNURSP2023R65), Princess Nourah bint Abdulrahman University, Riyadh, Saudi Arabia, for supporting the current research.

Conflict of interest

The authors declare that the research was conducted in the absence of any commercial or financial relationships that could be construed as a potential conflict of interest.

Publisher's note

Supplementary material

The Supplementary Material for this article can be found online at: https://www.frontiersin.org/articles/10.3389/fpls.2023.1154051/full#supplementary-material

References

Abdel-Fattah, M. A., Abdel-Salam, A. S., Elmofty, I. A., and Abdel-Gawwad, M. M. (1972). Salt tolerance of onion during germination and early seedling growth. *Desert Inst. Bull. A.R.E* 22, 157–165.

Ahsan, M., and Bhuiyan, M. R. (2010). Soil and water salinity, their management in relation to the climate changes in coastal areas of Bangladesh. *Khulna Univ. Stud.* 2010, 31–42. doi: 10.53808/KUS.SI.SESB.2010.31-42-ls

Allison, L. E. (1964). Salinity in relation to irrigation. *Adv. Agron.* 16, 139–180. doi: 10.1016/S0065-2113(08)60023-1

Ayers, R. S., and Westcot, D. W. (1985). *Water quality for agriculture* Vol. 29 (Rome, italy: FAO UNITED NATIONS), 97.

BBS (2019). *Household income and expenditure survey* (Bangladesh: Bangladesh Bureau of Statistics (BBS), Statistics and Informatics Division (SID), Ministry of Planning).

Bernstein, L. (1962). "Salt-affected soils and plants," in *Proceedings of the proceedings of the Paris symposium*, vol. 18. (Paris: UNESCO), 139–174.

Bernstein, L., and Ayers, A. D. (1953). Salt tolerance of five varieties of carrots. *J. Am. Soc Hortic. Sci.* 61, 360–366.

Bernstein, L., and Hayward, H. E. (1958). Physiology of salt tolerance. *Annu. Rev. Plant Physiol.* 9, 25–46. doi: 10.1146/annurev.pp.09.060158.000325

Bosch Serra, A. D., and Casanova, D. (2000). Estimation of onion (Allium cepa, l.) biomass and light interception from reflectance measurements at field level. *Acta Hortic.* 519, 53–63. doi: 10.17660/actahortic.2000.519.4

Chinnusamy, V., Jagendorf, A., and Zhu, J. K. (2005). Understanding and improving salt tolerance in plants. *Crop Sci.* 45, 437–448. doi: 10.2135/cropsci2005.0437

Choukan, R., Taherkhani, T., Ghannadha, M. R., and Khodarahmi, M. (2006). Evaluation of drought tolerance in grain maize inbred lines using drought tolerance indices. *Iran. J. Agric. Sci.* 8, 79–89.

Daszkowska-Golec, A. (2011). Arabidopsis seed germination under abiotic stress as a concert of action of phytohormones. *Omi. A J. Integr. Biol.* 15, 763–774. doi: 10.1089/omi.2011.0082

De Malach, Y., Pasternak, D., Mendlinger, S., and Borovic, I. (1989). Irrigation with brackish water under desert conditions. *VIII* 16, 201–215. doi: 10.1016/0378-3774(89)90003-6

El-Hendawy, S., Elshafei, A., Al-Suhaibani, N., Alotabi, M., Hassan, W., Dewir, Y. H., et al. (2019). Assessment of the salt tolerance of wheat genotypes during the germination stage based on germination ability parameters and associated SSR markers. *J. Plant Interact.* 14, 151–163. doi: 10.1080/17429145.2019.1603406

FAOSTAT *Statistical database* (Rome, Italy: Food and Agriculture Organization of the United Nations). Available at: http://fenix.fao.org/faostat/internal/en/#data (Accessed 13 September 2020).

Fischer, R., and Maurer, R. (1978). Droughtresistance in springwheat cultivars. 1: Grain yieldresponse. *Aust. J. Agr Res.* 29, 897–912. doi: 10.1071/AR9780897

Guellim, A., Catterou, M., Chabrerie, O., Tetu, T., Hirel, B., Dubois, F., et al. (2019). Ben; kichey, t. identification of phenotypic and physiological markers of salt stress tolerance in durum wheat (Triticum durum desf.) through integrated analyses. *Agronomy* 9, 844. doi: 10.3390/agronomy9120844

Hanci, F., and Cebeci, E. (2015). Comparison of salinity and drought stress effects on some morphological and physiological parameters in onion (Allium cepa l.) during early growth phase. *Bulg. J. Agric. Sci.* 21, 1204–1210.

Hanci, F., and Cebeci, E. (2018). Improvement of abiotic stress tolerance in onion: Selection studies under salinity conditions. *Int J Eng Sci.* 7 (9), 45–58. doi: 10.9790/1813-0709015458

Hanci, F., Cebeci, E., and Fidanci, A. A. (2016). Rapid screening method for salt stress tolerance of onion genotypes. *J. Appl. Hortic.* 18, 39–43. doi: 10.37855/jah.2016.v18i01.09

Jahromi, F., Aroca, R., Porcel, R., and Ruiz-Lozano, J. M. (2008). Influence of salinity on the *in vitro* development of glomus intraradices and on the *in vivo* physiological and molecular responses of mycorrhizal lettuce plants. *Microb. Ecol.* 55, 45–53. doi: 10.1007/s00248-007-9249-7

Janki, P., Vekaria, L., Hl, S., Parmar, K. B., and HP, P. (2020). Effect of saline irrigation water on growth and yields of onion (Allium cepa l.) varieties. *Int. J. Chem. Stud.* 8, 966–969. doi: 10.22271/chemi.2020.v8.i4g.9726

Kadayifci, A., Tuylu, G. I., Ucar, Y., and Cakmak, B. (2005). Crop water use of onion (Allium cepa l.) in Turkey. *Agric. Water Manage.* 72, 59–68. doi: 10.1016/j.agwat.2004.08.002

Kamran, M., Parveen, A., Ahmar, S., Malik, Z., Hussain, S., Chattha, M. S., et al. (2019). An overview of hazardous impacts of soil salinity in crops, tolerance mechanisms, and amelioration through selenium supplementation. *Int. J. Mol. Sci.* 21, 148. doi: 10.3390/ijms21010148

Khan, M. A. (2003). "Halophyte seed germination: Success and pitfalls," in *Proceedings of the international symposium on optimum resource utilization in salt affected ecosystems in arid and semi arid regions* Cairo, Egypt: Desert research centre, 346–358.

Khan, M. A. A., Alam, M. A., Yousuf, M. N., Raihan, H. Z., Rahman, M. A., and Brahma, S. (2022). Evaluation of short day local and exotic onion genotypes. *Bangladesh J. Agric.* 47, 27–43. doi: 10.3329/bjagri.v47i2.63324

Koyro, H.-W., Lieth, H., and Eisa, S. S. (2008). "Salt tolerance of chenopodium quinoa willd., grains of the Andes: Influence of salinity on biomass production, yield, composition of reserves in the seeds, water and solute relations," in *Mangroves and halophytes: Restoration and utilisation*, vol. 43 . Eds. M. Garcia Sucre and B. Herzog (Dordrecht: Springer Netherlands), 133–145.

Lee, J., Min, B., Yoon, S., Lee, M., Kim, H., and Hong, K. A. (2019). Multiple-regression model of bulb onion yield in response to meteorological conditions in gyeongsangnam province, republic of Korea. *Acta Hortic.* 1251, 81–90. doi: 10.17660/ActaHortic.2019.1251.10

Maas, E. V., and Hoffman, G. J. (1977). Crop salt tolerance - current assessment. *ASCE J. Irrig Drain Div* 103, 115–134. doi: 10.1061/jrcea4.0001137

Malik, Y. S., and Singh, K. (1977). Pandita ML effect of salinity on germination of onion varieties. *Haryana J. Hortic. Sci.* 6, 67–72.

Mangal, J. L., Lal, S., and Hooda, P. S. (1989). Salt tolerance of the onion seed crop. *J. Hortic. Sci.* 64, 475–477. doi: 10.1080/14620316.1989.11515980

Parvin, G. A., Ali, M. H., Fujita, K., Abedin, M. A., Habiba, U., and Shaw, R. (2017). "Land use change in southwestern coastal Bangladesh: Consequence to food and water supply," in *Proceedings of the land use management in disaster risk reduction. disaster risk reduction*. Eds. M. Banba and R. Shaw (Tokyo: Springer).

Paudel, D., Dhakal, S., Parajuli, S., Adhikari, L., Peng, Z., Qian, Y., et al. (2020). "Chapter 38 - use of quantitative trait loci to develop stress tolerance in plants," in *Plant life under changing environment*. Eds. D. K. Tripathi, V. Pratap Singh, D. K. Chauhan, S. Sharma, S. M. Prasad, N. K. Dubey and N. Ramawat (United States: Academic Press), 917–965, ISBN: .

Pitman, M. G., and Läuchli, A. (2006). "Global impact of salinity and agricultural ecosystems," in *Salinity: Environment - plants - molecules*. Eds. A. Läuchli and U. Lüttge (Dordrecht: Springer), 3–20.

Qadir, M., Quillérou, E., Nangia, V., Murtaza, G., Singh, M., Thomas, R. J., et al. (2014). Economics of salt-induced land degradation and restoration. *Nat. Resour. Forum* 38, 282–295. doi: 10.1111/1477-8947.12054

Rahman, A. K. M. M., Ahmed, K. M., Butler, A. P., and Hoque, M. A. (2018). Influence of surface geology and micro-scale land use on the shallow subsurface salinity in deltaic coastal areas: A case from southwest Bangladesh. *Environ. Earth Sci.* 77. doi: 10.1007/s12665-018-7594-0

R Core Team R (2021). *A language and environment for statistical computing*. Vienna: R Foundation for Statistical Computing. URL: https://www.R-project.org.

Regessa, M., Hachicha, M., Mansour, M., Nahdi, H., and Kheder, M. (2010). Response of onion to salinity. *Afr. J. Plant Sci. Biotechnol.* 4, 7–12.

Regessa, M., Gemechis, A., and Chala, E. (2022). Growth, physiology and yield of onion (Allium cepa l.) under salt stress. *Greener J. Agricultural Sci.* 12 (2), 154–167.

Sanwal, S. K., Kesh, H., Kumar, A., Dubey, B. K., Khar, A., Rouphael, Y., et al. (2022). Salt tolerance potential in onion: Confirmation through physiological and biochemical traits. *Plants* 11, 3325. doi: 10.3390/plants11233325

Shabala, S. (2013). Learning from halophytes: Physiological basis and strategies to improve abiotic stress tolerance in crops. *Ann. Bot.* 112, 1209–1221. doi: 10.1093/aob/mct205

Shoaib, A., Meraj, S., Nafisa,, Khan, K. A., and Javaid, M. A. (2018). Influence of salinity and fusarium oxysporum as the stress factors on morpho-physiological and yield attributes in onion. *Physiol. Mol. Biol. Plants an Int. J. Funct. Plant Biol.* 24, 1093–1101. doi: 10.1007/s12298-018-0570-z

Slavich, P. G., and Petterson, G. H. (1993). Estimating the electrical conductivity of saturated paste extracts from 1:5 soil, water suspensions and texture. *Soil Res.* 31, 73–81. doi: 10.1071/SR9930073

SRDI (2010). *Saline soils of Bangladesh* (Ministry ofAgriculture, Dhaka: Soil Resources Development Institute).

Sta-Baba, R., Bkheder, M., Chaar, H., and Harrabi, M. (2005). Identification des critères de sélection pour l'adaptation variétale d'oignon (Allium cepa l. *Rev. Inst. Nat. Agr. Tunisie* 20, 141–159.

Sta-Baba, R., Hachicha, M., Mansour, M., Nahdi, H., and Kheder, B. M. (2010). Response of onion to salinity. *Afr. J. Plant Sci. Biotechnol. ©2010* 4, 7–12.

Star Business Report (2022). Onion production increased by 27%: Razzaque. *Dly. Star*.

Sudha, G., and Riazunnisa, K. (2015). EFFECT OF SALT STRESS (NaCl) ON MORPHOLOGICAL PARAMETERS OF ONION (Allium cepa l.) SEEDLINGS. *Int. J. plant Anim. Environ. Sci.* 5, 125–128.

Takahashi, F., Tilbrook, J., Trittermann, C., Berger, B., Roy, S. J., Seki, M., et al. (2015). Comparison of leaf sheath transcriptome profiles with physiological traits of bread wheat cultivars under salinity stress. *PLoS One* 10, e0133322. doi: 10.1371/journal.pone.0133322

Uçarlı, C. (2021). Effects of salinity on seed germination and early seedling stage. *Abiotic Stress Plants* 211. doi: 10.5772/intechopen.93647

Ullah, A., and Bano, A. (2019). Role of PGPR in the reclamation and revegetation of saline land. *Pakistan J. Bot.* 51, 27–35. doi: 10.30848/PJB2019-1(43

Venâncio, J. B., Dias, N.da S., de Medeiros, J. F., de Morais, P. L. D., do Nascimento, C. W. A., Neto, O. N. de S., et al. (2022). Yield and morphophysiology of onion grown under salinity and fertilization with silicon. *Sci. Hortic. (Amsterdam).* 301, 111095. doi: 10.1016/j.scienta.2022.111095

Wahid, A., Perveen, M., Gelani, S., and Basra, S. M. A. (2007). Pretreatment of seed with H2O2 improves salt tolerance of wheat seedlings by alleviation of oxidative damage and expression of stress proteins. *J. Plant Physiol.* 164, 283–294. doi: 10.1016/j.jplph.2006.01.005

Wang, W., Vinocur, B., and Altman, A. (2003). Plant responses to drought, salinity and extreme temperatures: Towards genetic engineering for stress tolerance. *Planta* 218, 1–14. doi: 10.1007/s00425-003-1105-5

Wickham, H. (2009). *Ggplot2: Elegant graphics for data analysis* (Verlag New York: Springer), ISBN: .

Yaron, B., and Mokady, R. A. (1962). Technique for conducting pot experiments with saline water. *Plant Soil* 17, 392–398. doi: 10.1007/BF01377676

Yeo, A. (1998). Predicting the interaction between the effects of salinity and climate change on crop plants. *Sci. Hortic. (Amsterdam).* 78, 159–174. doi: 10.1016/S0304-4238(98)00193-9

Zafar, S., Ashraf, M. Y., Niaz, M., Kausar, A., and Hussain, J. (2015). Evaluation of wheat genotypes for salinity tolerance using physiological indices as screening tool. *Pakistan J. Bot.* 47, 397–405.

frontiers | Frontiers in Plant Science

TYPE Hypothesis and Theory
PUBLISHED 09 June 2023
DOI 10.3389/fpls.2023.1156514

OPEN ACCESS

EDITED BY
Shuvasish Choudhury,
Assam University, India

REVIEWED BY
Lakshmi Narayana Vemireddy,
Acharya N. G. Ranga Agricultural University, India
Sangeeta Srivastava,
Indian Institute of Sugarcane Research (ICAR), India

*CORRESPONDENCE
Guangyuan He
hegy@hust.edu.cn
Yin Li
yinli2021@hust.edu.cn
Xiaoyuan Chen
chenxy2@163.com

†These authors have contributed equally to this work

RECEIVED 01 February 2023
ACCEPTED 26 April 2023
PUBLISHED 09 June 2023

CITATION
Zhao M, Du C, Zeng J, Gao Z, Zhu Y, Wang J, Zhang Y, Zhu Z, Wang Y, Chen M, Wang Y, Chang J, Yang G, He G, Li Y and Chen X (2023) Integrated omic analysis provides insights into the molecular regulation of stress tolerance by partial root-zone drying in rice.
Front. Plant Sci. 14:1156514.
doi: 10.3389/fpls.2023.1156514

Integrated omic analysis provides insights into the molecular regulation of stress tolerance by partial root-zone drying in rice

Minhua Zhao[1†], Canghao Du[2†], Jian Zeng[1†], Zhihong Gao[1], Yongyong Zhu[1], Jinfei Wang[1], Yupeng Zhang[1], Zetao Zhu[1], Yaqiong Wang[2], Mingjie Chen[2], Yuesheng Wang[2], Junli Chang[2], Guangxiao Yang[2], Guangyuan He[2*], Yin Li[2*] and Xiaoyuan Chen[1*]

[1]Henry Fok School of Biology and Agriculture, Guangdong Engineering Technology Research Center for Efficient Utilization of Water and Soil Resources in North Region, Shaoguan University, Shaoguan, Guangdong, China, [2]The Genetic Engineering International Cooperation Base of Chinese Ministry of Science and Technology, Key Laboratory of Molecular Biophysics of Chinese Ministry of Education, College of Life Science and Technology, Huazhong University of Science and Technology, Wuhan, Hubei, China

Partial root-zone drying (PRD) is an effective water-saving irrigation strategy that improves stress tolerance and facilitates efficient water use in several crops. It has long been considered that abscisic acid (ABA)-dependent drought resistance may be involved during partial root-zone drying. However, the molecular mechanisms underlying PRD-mediated stress tolerance remain unclear. It's hypothesized that other mechanisms might contribute to PRD-mediated drought tolerance. Here, rice seedlings were used as a research model and the complex transcriptomic and metabolic reprogramming processes were revealed during PRD, with several key genes involved in osmotic stress tolerance identified by using a combination of physiological, transcriptome, and metabolome analyses. Our results demonstrated that PRD induces transcriptomic alteration mainly in the roots but not in the leaves and adjusts several amino-acid and phytohormone metabolic pathways to maintain the balance between growth and stress response compared to the polyethylene glycol (PEG)-treated roots. Integrated analysis of the transcriptome and metabolome associated the co-expression modules with PRD-induced metabolic reprogramming. Several genes encoding the key transcription factors (TFs) were identified in these co-expression modules, highlighting several key TFs, including TCP19, WRI1a, ABF1, ABF2, DERF1, and TZF7, involved in nitrogen metabolism, lipid metabolism, ABA signaling, ethylene signaling, and stress regulation. Thus, our work presents the first evidence that molecular mechanisms other than ABA-mediated drought resistance are involved in PRD-mediated stress tolerance. Overall, our results provide new insights into PRD-mediated osmotic stress tolerance, clarify the molecular regulation induced by PRD, and identify genes useful for further improving water-use efficiency and/or stress tolerance in rice.

KEYWORDS

RNA-Seq, metabolomics, omics analysis, rice, osmotic stress, regulation of gene expression, transcription factors, partial root-zone drying (PRD)

Introduction

The adverse impacts of abiotic stresses (such as drought, high salinity, cold, and high light intensity stress) on crop growth and production have becoming greater than before, threatening global food security (Suzuki et al., 2014). Developing new varieties with improved abiotic stress resistance and applying new cultivation techniques are important approaches to attenuate effects of stress on crop production. Recent climate changes have led to globally imbalanced rainfall and droughts (FAO, 2019). Drought stress has become particularly impactful in global agriculture, causing a loss of ~$30 billion in crop production (Gupta et al., 2019). In addition, agricultural activities will require more water to feed the world's population, which is predicted to reach ~10 billion by 2050 (United Nations, 2011; Koncagül et al., 2018).

The partial root-zone drying (PRD) technique represents a water-saving irrigation strategy to sustain crop growth with limited water resources but without significant yield loss (Mehrabi and Sepaskhah, 2019). The PRD approach has been successful for several major crops, including wheat, rice, maize, potato, and tomato (Kang et al., 2000; Saeed et al., 2008; Ahmadi et al., 2010; Sepaskhah and Ahmadi, 2012; Casa and Rouphael, 2014; Gao et al., 2021). In principle, the PRD technique splits the root system into two parts: one part of the root system in dry soil responds to drought stress and induces related signal transduction, whereas the other part of the root system maintains a normal water status to sustain plant growth (Khalil and Grace, 1993).

When the root system senses drought conditions, hydraulic and abscisic acid (ABA)-related signals are sent, both of which can mediate long-distance root-to-shoot communication to trigger a series of changes at the physiological, metabolic, and gene expression levels (Zhang et al., 2012; Gorgues et al., 2022). The small peptide CLAVATA3/EMBRYO-SURROUNDING REGIONRELATED 25 (CLE25) is synthesized and transported to the leaf tissue to augment ABA biosynthesis and signaling and to induce the expression of downstream stress-responsive genes (Sah et al., 2016; Takahashi et al., 2018). ABA signaling also leads to stomatal closure, which reduces water transpiration (Chen et al., 2020). Water scarcity also causes secondary stresses in plant tissues, such as osmotic and oxidative stresses (Zhang et al., 2012). It has been reported that PRD works for crops in which stomatal movements are sensitive to ABA (Dbara et al., 2016) and that PRD can decrease water use by 50% in grapevines (Collins et al., 2010).

Although PRD is useful for improving stress tolerance and limiting the use of water resources, the underlying mechanisms remain elusive. Previous physiological studies employed PRD experiments to investigate the response of rice seedlings to mild and severe drought treatments and demonstrated the involvement of both ABA and hydraulic signals in this process (Siopongco et al., 2008; Siopongco et al., 2009). However, we hypothesized that PRD-mediated stress tolerance might involve complex stress regulatory networks other than the ABA-dependent pathway. Several important questions regarding PRD-mediated stress tolerance remain unanswered: (1) what major changes occur in drying roots and well-watered roots, respectively, at the molecular level; (2) by which mechanisms does PRD mediate water and nutrient resource utilization to maintain growth with reduced water availability; (3) what are the important genes involved in this process, and can these genes be utilized in genetic improvement for better stress tolerance or water-use efficiency?

In the present study, rice seedlings were used as a research model to obtain evidence supporting our hypothesis and gain insights into PRD-mediated stress tolerance. Rice (*Oryza sativa* L.) was chosen for several reasons. (1) Rice is one of the most important crops globally, and Asia is a prominent producer and consumer of rice (Muthayya et al., 2014); (2) Except for the upland cultivars, rice plants are usually grown in paddy fields and have shallow root systems, demanding a large amount of water to maintain growth (Samson et al., 2002; Yu et al., 2020); (3) When drought occurs, the root system of rice is exposed to anaerobic flooding and aerobic drought conditions alternately, somewhat mimicking the PRD experiment. In this study, we combined physiological measurements, transcriptomics, and metabolomics to characterize the early response of rice seedlings to polyethylene glycol (PEG)-induced stress and PRD-mediated stress tolerance. Integrated omics analysis and our customized transcription factor (TF)-centric method helped to identify several key TFs and target genes involved in metabolic reprogramming during stress- or PRD-mediated tolerance. This provided important candidate genes that warrant functional studies on their roles in the regulation and tolerance of osmotic stress.

Materials and methods

Experimental design

In the present study, "MeiXiangZhan No.2", a representative elite fragrant rice variety widely cultivated in South China, was used (Mo et al., 2017). After seeds germination, the seedlings were cultivated at 32°C (12 h day and 12 h night) in the growth chamber until the four-leaf stage. To investigate the molecular mechanisms involved in PRD-mediated stress tolerance, a hydroponic experimental system was established to partially mimic the osmotic conditions of drought stress and PRD (Figure 1A). A set of three experiments was performed in triplicate: (1) the non-treated control experiment (abbreviated as "NT"): the rice seedlings at the four-leaf stage were hydroponically cultivated in growth tubes containing Hoagland nutrient solution (pH 5.5) that was changed every two days; (2) the PRD experiment: the rice seedlings were hydroponically cultivated with the roots separated into two growth tubes; half of the roots were grown in the Hoagland nutrient solution (abbreviated as the PRD treatment) and the other half were grown in PEG solution (100 g/L (m/v) PEG-6000) (abbreviated as the PRDPEG treatment); (3) the PEG treatment experiment: the rice seedlings were hydroponically cultivated in the same PEG solution as in he PRDPEG treatment. In the experiment, PEG, a widely used non-ionic, nonpenetrating high-molecular-weight molecule to induce osmotic stress of root tissues was chosen to mimic the water deficit conditions which rice plants under drought stress in the field may be experienced (Agrawal et al., 2016; Ogbaga et al., 2020). All the rice seedlings were cultivated in

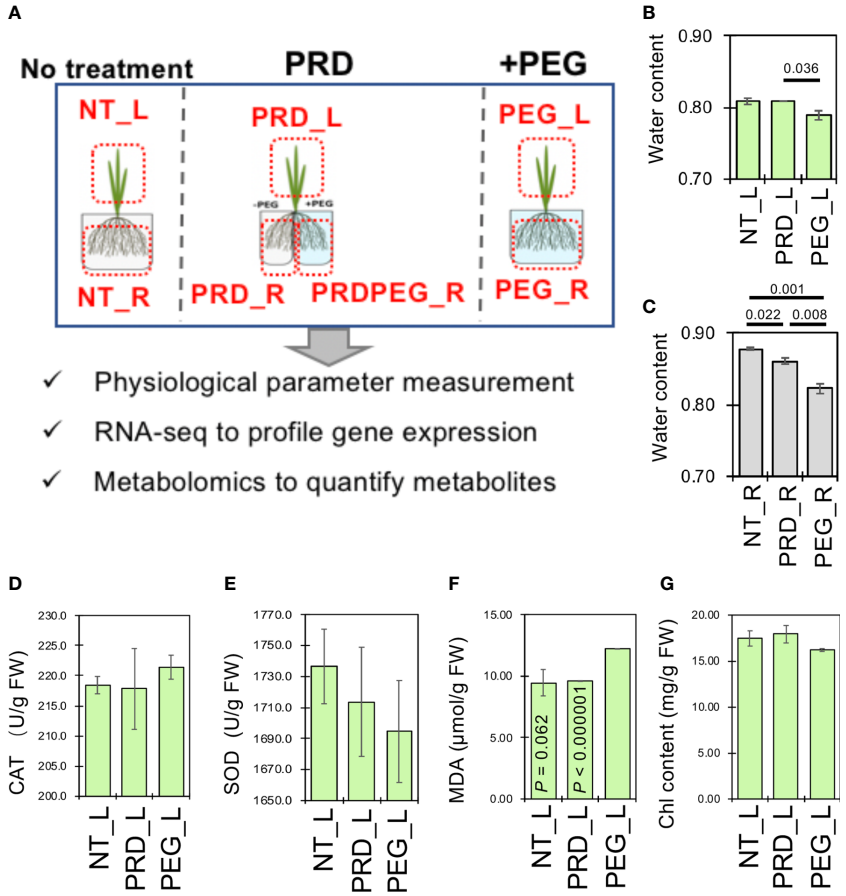

FIGURE 1
Partial root-zone drying attenuates the osmotic stress-induced water loss in the root. **(A)** Schematic diagram showing the experimental design to reveal the mechanism of enhanced osmotic-stress tolerance caused by PRD. The relative water contents of the leaf **(B)** and root samples **(C)**, the content of catalase (CAT, **(D)**, superoxide dismutase (SOD, **(E)**, malonic dialdehyde (MDA, **(F)** and chlorophyll **(G)** were measured to reflect the physiological status of the leaf tissues. All measurements were performed in triplicates. Statistical difference was determined by pair-wise comparison between the leaf or root samples by using Student's *t*-test ($P < 0.05$).

three replicates in a growth chamber of 24°C and a photoperiod of 14/10 h of day/night. To minimize potential differences between individual plants, each replicate comprised 12 rice plants that were randomly placed among replicates to remove positional effects on plant growth in the chamber. All plants were treated for six days, and then the mature leaves and roots were sampled, snap-frozen in liquid nitrogen, and stored at −80°C. Within each replicate, the leaf or root tissues were collected from 12 plants and pooled to form three samples (for the leaf and root tissues, respectively) with each sample used for physiological parameter measurements, RNA-seq, and metabolome analysis, respectively.

Measurement of physiological parameters

Relative water content (RWC) was measured according to Wei et al. (2014). The dehydrated leaves were soaked in distilled water for 4 h, and the turgid weight was recorded. The leaves were dried at 80°C for 48 h to measure the total dry weight. RWC was calculated as follows: RWC = (desiccated weight − DW)/(TW − DW). Chlorophyll content was determined using a UV spectrophotometric method (Feng et al., 2019). The malondialdehyde (MDA), catalase (CAT), and superoxide dismutase (SOD) levels were measured using assay kits (Nanjing Jiancheng Bioengineering Institute, Nanjing, China) (Qiu et al., 2021).

Transcriptome analysis

Total RNA was extracted using TRIzol reagent. The quality of the extracted RNA samples was examined using agarose gel electrophoresis, a NanoDrop 2000, and an Agilent 2100 Bioanalyzer. Standard protocols for the BGI genomic DNBSEQ-T7 platform were used to construct rice mRNA libraries. RNA-seq libraries were sequenced to generate 150-bp pair-end reads. For sequence quality control, Cutadapt and the FASTX-Toolkit (http://hannonlab.cshl.edu/fastx_toolkit/) were used to trim low-quality base pairs, as previously described (Li et al., 2019a). Clean quality-filtered reads were mapped to the rice reference genome (*var.*

Nipponbare IRGSP v1.0) using HISAT2 v2.0.1-beta with default parameters (Kawahara et al., 2013). Only uniquely-mapped reads were retained, and the read count matrix was subjected to differential expression analysis with DEseq2 using the following criteria: fold change ≥ 2 and a false discovery rate (FDR)-adjusted P-value < 0.05. The fragments per kilobase of exons per million mapped sequence reads (FPKM) were calculated for each gene model using RSEM (Li and Dewey, 2011). Genes with at least five mapped reads and an average FPKM ≥ 1 for the three replicates were considered to be expressed. The RNA statistics are provided in the supplementary file (Supplementary Table S7).

Quasi-targeted metabolome analysis

Quasi-targeted metabolomic analysis was performed to identify and quantify metabolites in rice samples, according to previous studies with modifications (Ali et al., 2008; Mark et al., 2010; Yang et al., 2014). The details of this process are described below.

Metabolites extraction

Tissues (100 mg) were individually grounded in liquid nitrogen, and the homogenate was resuspended in 500 μL prechilled 80% methanol by vortexing. The samples were incubated on ice for 5 min and centrifuged at 15,000 × *g* and 4°C for 20 min. A fraction of the supernatant was diluted to a final concentration containing 53% methanol with LC-MS grade water. Then, the samples were transferred to a fresh Eppendorf tube and then were centrifuged at 15000 × *g* and 4°C for 20 min. Finally, the supernatant was analyzed using an LC-MS/MS system analysis (Zhou et al., 2021; Peng et al., 2022).

HPLC-MS/MS analysis

The LC-MS/MS analyses were performed using an ExionLC AD system (SCIEX, Framingham, MA, USA) coupled with a QTRAP 6500+ mass spectrometer (SCIEX). Samples were injected onto an Xselect HSS T3 (2.1×150 mm, 2.5 μm) column and eluted using a 20-min linear gradient at a flow rate of 0.4 mL/min for the positive/negative polarity mode. Eluent A was 0.1% formic acid-water, while eluent B was 0.1% formic acid-acetonitrile (Ali et al., 2008). The solvent gradient was set as follows: 2% B, 2 min; 2–100% B, 15.0 min; 100% B, 17.0 min; 100–2% B, 17.1 min; 2% B, 20 min. The QTRAP 6500+ mass spectrometer was operated in positive polarity mode with curtain gas of 35 psi, collision gas of medium, ion spray voltage of 5500 V, temperature of 550 °C, ion source gas of 1:60, and ion source gas of 2:60. QTRAP 6500+ mass spectrometer was operated in negative polarity mode with the following parameters: curtain gas of 35 psi, collision gas of medium, ion-spray voltage of −4500 V, temperature of 550 °C, ion source gas of 1:60, ion source gas of 2:60.

Metabolites identification and quantification

The detection of experimental samples using multiple reaction monitoring (MRM) was based on an in-house database (Zhang et al., 2022a). More than 3200 commercially available purified standard compounds were registered on an LC-MS/MS platform in the in-house library of Novogene Co., Ltd. (Beijing, China) to determine their characteristics. Retention time (RT) with a narrow RT window, accurate mass match to the library entries (+/− 0.005 amu), Q1 (parent ion), Q3, and the MS/MS forward and reverse scores between the experimental data and authentic standards were applied as criteria to accurately identify biochemicals (Want et al., 2012; Sellick et al., 2011). The data files generated using HPLC-MS/MS were processed using SCIEX OS (v1.4) to integrate and correct the peaks with the following parameter settings: minimum peak height, 500; signal/noise ratio, 5; Gaussian smoothing width, 1. The area of each peak represents the relative contents of the corresponding substances.

Metabolomic data analysis

The identified metabolites were annotated using the Kyoto Encyclopedia of Genes and Genomes (KEGG) database (Luo et al., 2015), the Human Metabolome Database (HMDB) database (Yuan et al., 2012) and the Lipidmaps database (Barri and Dragsted, 2013). Principal component analysis (PCA) and partial least squares discriminant analysis (PLS-DA) were performed using metaX63. We applied a univariate analysis (*t*-test) to calculate statistical significance (*P*-value). The metabolites with variable important in projection value VIP > 1 and *P*-value < 0.05 and log2 (fold change) ≥ 1 or ≤ -1 were considered to be differential metabolites. Z-scores were calculated for each differential metabolite to obtain its relative abundance (Supplementary Table S5) and were used for k-means clustering analysis to reveal the representative trend within each group of differentially expressed metabolites (DEMs). KEGG enrichment analysis was performed for the DEMs using a relatively loose threshold ($P < 0.1$), as the metabolome data tended to capture a small fraction of all metabolites in the tissue.

Integrated analysis of transcriptome and metabolome data

Differentially expressed genes (DEGs) obtained from the RNA-seq analysis were subjected to K-means clustering to identify co-expression groups (also known as modules) in which genes are expressed in a similar trend. Many of them tend to share similar functions, are located in the same/related pathways, or have regulatory relationships. K-means clustering analysis, rather than weighted co-expression network analysis (WGCNA), was selected because the limited sample number may result in an unsatisfactory performance for WGCNA (Langfelder and Horvath, 2008; Langfelder et al., 2011). Figure of merit analysis was performed prior to k-means clustering to determine the appropriate number of clusters and ensure the performance of the k-means analysis (Supplementary Figure S1) (Yeung et al., 2001). Pearson's correlation analysis was used to link the co-expression modules and corresponding metabolic clusters.

Enrichment analysis was performed for each module using Gene Ontology (GO) annotation with ClusterProfiler (Supplementary Table S3) to obtain functional insights into the

co-expression modules (Supplementary Table S3) (Wu et al., 2021). The MapMan annotation of the rice genes was downloaded and used to understand the functions of the genes regulated by TFs and regulators (Usadel et al., 2009). Annotated transcription factors in the rice genome were obtained from planTFDB (Jin et al., 2014).

To perform TF-centric analysis, planTFDB-annotated TFs within the co-expression modules were searched using the FunRicegenes database to obtain related functional studies (Yao et al., 2018; Huang et al., 2022). Only TFs or regulators (e.g., TZF7) studied using transgenic or mutant lines were chosen for further analysis. The TFs were separated into two types: (1) representative target genes available: TFs without genome-wide expression analysis data or expression data not available, and the studies of these TFs included functional evidence of the downstream target genes; (2) genome-wide target genes available: TFs with genome-wide expression analysis data available to retrieve the TF's target genes or regulated genes. For the second type, the genome-wide target genes of a certain TF were retrieved from the studies (Supplementary Table S7) to compare whether the target genes were enriched in a particular co-expression module by using a hypergeometric test with R (Li et al., 2019a; Tu and Li, 2020). When the significantly enriched ($P_{hypergeometric} < 0.01$) target genes and the corresponding TF were within the same module or meta-module, we presumed that the TF likely regulates the target genes.

Statistic analysis

Statistical analysis of the physiological parameters was performed with R using *Student*'s t-test ($P < 0.05$).

Results and discussion

Physiological changes during the partial root-zone drying and osmotic stress treatments

When osmotic stress occurs, roots have difficulty absorbing water to sustain growth, which in turn triggers hydraulic signals and other chemical and phytohormone signals (e.g., the ABA signal) to the ground tissues to reduce water loss. Osmotic stress usually decreases relative water content and dry weight (Rahman et al., 2023). The relative water content was measured in the leaf and root tissues to examine the effects of PEG- and PRD-treatments (Figures 1A–C). Interestingly, significant water loss in the leaves was only induced in the PEG treatment (~0.79) and not in the PRD treatment (~0.81; Figure 1B). In contrast, PRD-treated roots had an intermediate water content (~0.86), which was significantly lower than that of the non-treated roots (0.88), but higher than that of the PEG-treated roots (0.82; Figure 1C), suggesting that the PRD strategy indeed mitigated osmotic stress or led to osmotic stress tolerance.

Osmotic stress concomitantly disrupts antioxidant defenses due to the higher production of reactive oxygen species (ROS). It could lead to membrane lipid peroxidation indicated by the high amount of MDA and activities of antioxidant enzymes such as SOD and CAT significantly regulated. Furthermore, levels of oxidative stress markers were measured to support this conclusion. In the leaf tissues, non-treated and PRD-treated leaves (NT_L and PRD_L, respectively) appeared to have relatively higher superoxide dismutase enzyme activity (albeit not significantly) but lower catalase enzyme activity when compared to PEG-treated leaves (Figures 1D, E). Untreated and PRD-treated leaves also showed lower MDA content than the PEG-treated leaves, indicating less membrane lipid damage (Figure 1F).

Moreover, osmotic stress signals have been reported to regulate photosynthesis, carbohydrate production, and energy metabolism (Shu et al., 2010). The chlorophyll contents of the untreated and PRD-treated leaves were higher than that of the PEG-treated leaves, indicating PRD-mediated stable photosynthesis (Figure 1G). Overall, the PRD treatment attenuated PEG-induced osmotic stress in plants: the PRD-treated roots were somewhat affected by the osmotic stress while the PRD-treated leaves may have a similar physiological status compared to that of the control leaves, reflected by the results of relative water content, and chlorophyll and MDA contents.

Transcriptome analysis

To obtain molecular insights into the PRD-mediated stress tolerance, replicates of seven samples (NT_L, NT_R, PRD_L, PRD_R, PRDPEG_R, PEG_L, and PEG_R; suffix L and R indicating leaves and roots, respectively) were subjected to transcriptome and metabolome analyses. RNA-seq identified approximately 17000 and 21000 genes expressed in the leaf and root samples, respectively (the genes with an average FPKM >= 1 were considered as expressed as described in the methods section. Supplementary Table S1). Differential expression analyses of the leaf and root samples led to 6459 differentially expressed genes (DEGs)(the expression matrix is provided in Supplementary Table S2). PCA revealed the following: (1) the leaf samples without treatment or those treated with PRD or PEG could not be well separated; (2) in the PRD experiment, the non-treated root (PRD_R) samples were grouped with the control roots (NT_R), whereas the PRD-treated root (PRDPEG_R) samples were clustered with the PEG-treated roots (PEG_R) (Figure 2A). This suggests that in the PRD treatment, the roots not experiencing osmotic stress had transcriptomes similar to that of the control plants.

To further dissect the group of genes that may explain the transcriptomic differences induced by PEG or PRD treatment, DEGs were clustered by the k-means approach, yielding ten co-expression modules (i.e., M1 to M10 in Figure 3A; Supplementary Figure S1), with each of the representative expression patterns shown in Figure 3. In the gene modules M2, M3, and M7, the gene expression between the root samples was not significantly different, whereas a much larger number of DEGs (i.e., 4058 genes from the M5 to M10 modules) did not show differential expression among the leaf samples, consistent with the PCA results that the PRD or PEG treatments influenced more genes in the roots than in the leaves. In the modules where genes were differentially expressed

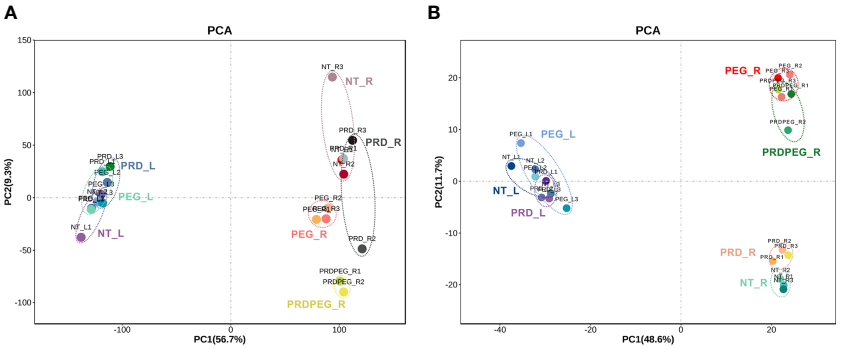

FIGURE 2
Principal component analysis (PCA) results for the transcriptomic data **(A)** and metabolomic data **(B)**. The abbreviations for the samples used hereafter: NT_L, non-treatment leaf samples; PRD_L, the leaf samples treated by PRD; PEG_L, the leaf samples treated by PEG; NT_R, the nontreatment root samples; PEG_R, the root samples treated by PEG; PRD_R, the root samples from the PRD treatment without PEG-induced osmotic stress; PRDPEG_R, the root samples from the PRD treatment with PEG-induced osmotic stress.

among the leaf samples (i.e., M1, M2, M3, and M4), the genes exhibited similar expression trends in PEG_L and PRD_L, which were upregulated or downregulated simultaneously (Figures 3B–E). In contrast, the genes in modules M8, M9, and M10 showed the highest expression in PEG_R, intermediate expression in PRDPEG_R, and lowest expression in both NT_R and PRD_R. Particularly, M5 had high expression exclusively in PRDPEG_R, suggesting that this group of genes represents the unique transcriptomic feature of PRDPEG_R, possibly explaining adjustments or communications between the root zones from the untreated and PRDPEG-treated parts. Furthermore, these modules were grouped into three meta-modules (MMA, MMB, and MMC) by calculating the correlations between the module expression patterns (Supplementary Figure S2). The MMA generally included three modules: M1, M2, and M4, in which M2 and M4 were positively correlated but negatively associated with M1. MMB included M5, M6, and M7, whereas MMC included M8, M9, and M10. In the MMA, the genes were mainly differentially expressed between leaf samples, possibly explaining the transcriptomic differences between NT_L and PEG_L/PRDPEG_L (Figures 1B–D).

Metabolome analysis

To gain a more comprehensive insight into metabolism during PEG and PRD treatments, quasi-targeted metabolomics was employed to identify and profile the metabolites (Zhang et al, 2022a). In the leaf samples, 1230 metabolites were identified, of which 1184 were reproducibly quantified (CV between replicates < 0.8) (Supplementary Table S4). In the root samples, 1057 metabolites were identified, with 944 metabolites reproducibly quantified (Supplementary Table S5). Pairwise comparison of the metabolite quantities within the leaf and root samples identified 216 DEMs in the leaf and 508 DEMs in the root, yielding a total of 633 DEMs, 73 leaf-specific metabolites, and 121 root-specific metabolites (Figure 4A; Supplementary Table S6). The larger number of DEMs in the roots than in the leaves further supports the findings based on our physiological and transcriptomic data: the leaf samples had a relatively more stable physiological status than the root samples. PCA result showed that: (1) PC1 and PC2 corresponded to the differences between tissues and treatments, respectively; (2) the metabolic status of the leaf samples (i.e., NT_L, PEG_L, and PRD_L) were similar between each other, while the root metabolic profiles were differentiated probably by the treatments. According to the PCA results, the PRD_R samples appeared to have an intermediate metabolic status between those of NT_R and PEG_R, with PRDPEG_R showing a distinct metabolic pattern (Figure 2B). A similar pattern between transcriptome- and metabolome-based PCAs emphasizes that the root, not the leaf, is the main tissue where reprogramming, either induced by PEG or PRD, occurs at the transcriptomic and metabolic levels.

K-means clustering enabled the DEMs falling into ten metabolic clusters (C1 to C10), as well as one cluster for leaf-specific metabolites and one cluster for root-specific metabolites (Figure 4A). The representative dynamics of each cluster is shown in Figures 4B–K. Because metabolic differences in the root may largely account for PRD-mediated stress tolerance, we highlight two types of metabolic dynamics: (1) the metabolites are highly abundant in NT_R and PRD_R, but in low abundance in PRDPEG_R and PEG_R (i.e., C1 and C5); (2) these metabolites are present at high levels in PRDPEG_R and PEG_R but at low levels in NT_R and PRD_R (i.e., C2, C3, C4, C6, C7, and C8). Also, the metabolites that differed for the comparisons "NT_R vs. PEG_R," "NT_R *vs* PRDPEG_R," or those that differed when comparing PRD_R with PRDPEG_R or with PEG_R drawn our attentions. KEGG enrichment analysis for these sets of DEMs identified several metabolic terms associated with primary metabolisms, such as glycolysis/gluconeogenesis, pyruvate metabolism, fructose and mannose metabolism, and chlorophyll metabolism (Figure 4L). In particular, the KEGG enrichment results demonstrated that the differences between NT_R vs. PEG_R/PRDPEG_R and PRD_R vs. PEG_R/PRDPEG_R lie in nitrogen and amino acid metabolic pathways, such as valine, leucine, and isoleucine biosynthesis, and alanine, aspartate, and glutamate metabolism. In contrast, the metabolic differences between NT_L vs. PEG_L/PRD_L reside not only in primary metabolic pathways

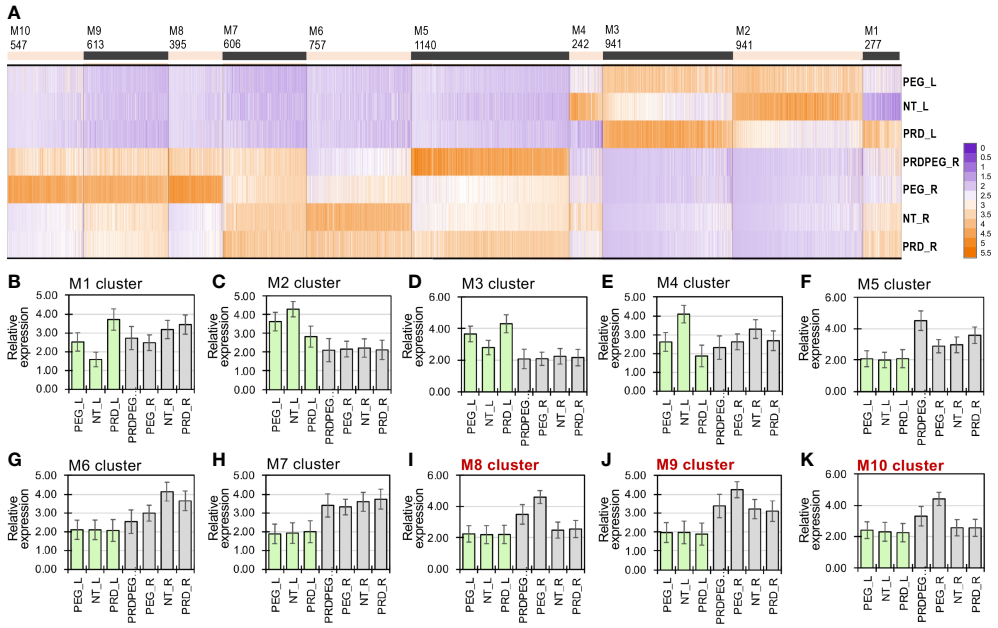

FIGURE 3
Transcriptomic analysis revealing major differences between the root samples subjected to the osmotic stress (PEG) and partial root-zone drying (PRD) **(A)**. The representative expression patterns of each module are shown in Figures **(B–K)**. The co-expression modules M8, M9 and M10 differed between PRD_R and PRDPEG_R are highlighted in red.

(e.g., chlorophyll and amino acid metabolism) but also in secondary metabolism (monoterpenoid synthesis) and pathways associated with ROS scavenging (glutathione metabolism) (Figure 4M). Therefore, our analyses revealed metabolic reprogramming in PEG-induced roots and, more importantly, in PRD-treated roots, suggesting a role for such reprogramming in PRD-mediated osmotic stress tolerance.

Integrated omics analysis highlights metabolic reprogramming in the PRD-treated roots and identifies important transcription factors and candidate genes

To pinpoint the DEGs associated with the observed metabolic reprogramming under the PEG or PRD treatments, the gene co-expression modules were linked with the metabolic clusters using correlation analysis (Figure 5). Gene module M1 was positively correlated with metabolic clusters C2 and C4 but negatively correlated with C7. Gene module M4 was positively correlated with metabolic clusters C1 and C3 but negatively correlated with clusters C4 and C9. The module M5 was associated with the metabolic clusters C9 and C10. In addition, M8 and M10 were linked to the metabolic clusters C6 to C10. Among the identified DEMs, the abundance of several phytohormone compounds differed between the samples. For example, indole-3-acetic acid (IAA) was significantly higher in PEG_R than in PRD_R and NT_R (Figure 6A). Interestingly, the active form of cytokinin (trans-zeatin) was detected in the leaf tissues, with NT_L and PRD_L both having high levels of trans-zeatin but PEG_L having a low trans-zeatin content (Figure 6B). Additionally, a less active form of cytokinin (N6-isopentenyl adenine-9-glucoside, iP9G) was decreased in PEG_L and PRD_L when compared with NT_L (Hallmark and Rashotte, 2020; Chen et al., 2021). Cytokinin appears in several active forms (such as isopentenyl adenine (iP) or trans-zeatin(tZ)) and is involved in various processes related to cell division, leaf development and senescence, and abiotic stress resistance (Honig et al., 2018; Liu et al., 2020). More recently, a study has demonstrated that iP9G acts as a less active cytokinin compound and plays a role in delaying leaf senescence (Hallmark and Rashotte, 2020). The higher abundance of cytokinin metabolites in PRD_L could explain its physiological status similar to the non-treated leaves. Besides, in the root samples, NT_R had the lowest level of salicylic acid (SA), while PRD_R showed increased SA content. Similarly, in the leaf, NT_L exhibited low SA content, while PEG_R and PRD_R showed high levels of SA (Figure 6C), suggesting that SA signaling, and response might be involved in stress response and/or tolerance. Several metabolites associated with the metabolism of auxin, cytokinin, gibberellic acid, and ABA exhibited confound changes, implying complex regulation or coordination of the phytohormone metabolism and signaling during the response and adaptation to the osmotic stress (Supplementary Figure S3).

To substantiate the relationship between transcriptional regulation and metabolic reprogramming during osmotic stress tolerance, a transcription factor (TF)-centric approach was employed: (1) the transcription factor-encoding genes were annotated in the gene co-expression modules with particular focuses on those TFs in the modules highly correlated with the metabolic clusters (e.g., M1, M4, M5, M8, M9, and M10) (Jin et al.,

10.3389/fpls.2023.1156514

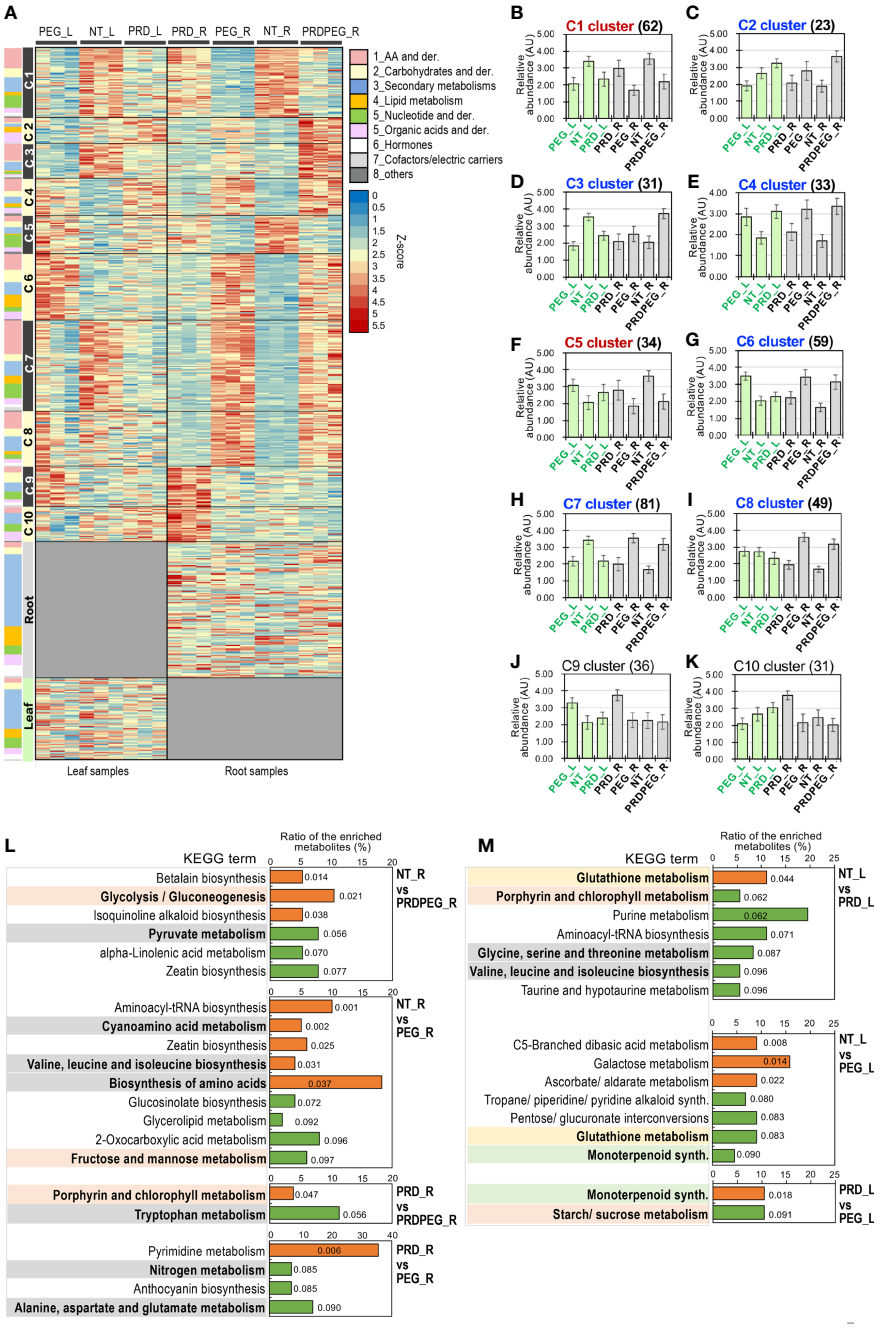

FIGURE 4
Metabolomic analysis revealing major differences between the root samples subjected to the osmotic stress (PEG) and PRD. **(A)** The heatmap of differential metabolites and those specifically detected in leaves or roots, with the classification of the metabolites indicated using color-codes as shown in the illustration. K-means clustering identified a total of ten metabolic clusters, namely C1, C2, C3, C4, C5, C6, C7, C8, C9 and C10. **(B)** The metabolic dynamic of the cluster C1. **(C)** The metabolic dynamic of the cluster C2. **(D)** The metabolic dynamic of the cluster C3. **(E)** The metabolic dynamic of the cluster C4. **(F)** The metabolic dynamic of the cluster C5. **(G)** The metabolic dynamic of the cluster C6. **(H)** The metabolic dynamic of the cluster C7. **(I)** The metabolic dynamic of the cluster C8. **(J)** The metabolic dynamic of the cluster C9. **(K)** The metabolic dynamic of the cluster C10. The number of metabolites for each cluster are indicated in the bracket. The clusters indicating high metabolic abundance for the NT_R and PRD_R samples but low abundance for the PEG_R samples are written in red, while the clusters indicating low metabolic abundance for the NT_R and PRD_R samples but high abundance for the PEG_R samples are written in blue. **(L, M)** KEGG enrichment analysis of the differential metabolites reflects differences in primary and secondary metabolism between the control, PEG-treated and PRD-treated samples. Comparison of the enriched KEGG metabolic pathways in the roots and leaves are shown in Figures 4A, B, respectively. The metabolic pathways related to amino acids/nitrogen, carbohydrates or secondary metabolism are highlighted in grey, light red and green backgrounds, respectively. P values for the enriched KEGG terms are indicated by colors (orange indicating $P<0.05$, and green indicating $P> 0.05$ and <0.1).

2017); (2) By taking advantage of the numerous functional studies in rice, "TF- target genes – downstream affected metabolites" were mapped in our expression modules and metabolic clusters (Yao et al., 2018; Huang et al., 2022); (3) a collection of rice TFs with their regulated genes or potential target genes reported were used for enrichment analysis to reveal if any set of TF's target genes is

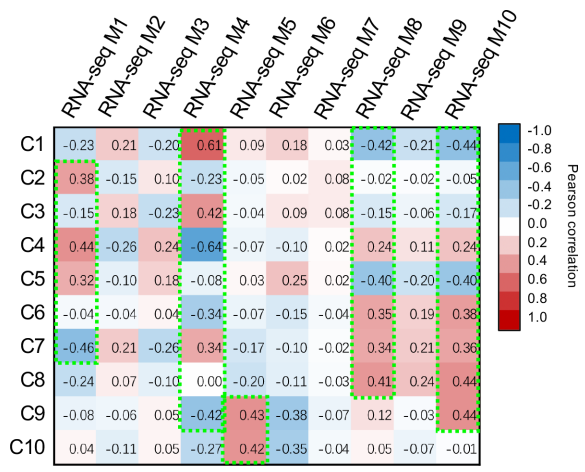

FIGURE 5
Pearson's correlation analysis identifies the association between metabolic clusters and gene expression modules.

significantly enriched in a co-expression module in a genome-wide manner (details in the Method section "Integrated analysis of transcriptome and metabolome data") (Supplementary Table S7).

Using these customized analysis approaches, we uncovered a complex coordination between primary metabolism (especially nitrogen transport and assimilation), ion transport and assimilation, and secondary metabolism in leaf and root tissues. First, two genes encoding NIN-like transcription factors (NIN-LIKE PROTEIN 1 and 3, NLP1 and NLP3, respectively) showed high expression levels in NT_L but lower expression in PEG_L and PRD_L (Figure 7A). PEG-treated roots also exhibited high OsNLP1 expression. Consistent with the upregulation of OsNLP1 in PEG_R, OsNLP1 is one of the major TFs involved in nitrogen utilization and transportation in rice and is primarily responsive to nitrogen deficiency (Alfatih et al., 2020). Indeed, the expression levels of OsNLP1's primary target genes, the ammonium transporter OsAMT1.1 and the nitrate transporter OsNRT1.1B, were highly correlated with OsNLP1 (Figure 7B). OsAMT1.1 is a prominent member of the OsAMT family that controls ammonium uptake and assimilation and positively affects rice plants' development and growth (Hoque et al., 2006; Ranathuge et al., 2014). In contrast, OsNRT1.1b is one of the major genes contributing to nitrate assimilation and divergence of NUE between japonica and indica rice subspecies, with several OsNRT1.1b natural variations being successfully used in rice breeding (Hu et al., 2015). In addition, OsNLP3 is highly expressed in the OsNLP family, with the highest expression levels detected in the green tissues (Zhang et al., 2022b). Correlated with OsNLP3 expression, the primary target genes of OsNLP3, encoding a set of nitrate reductase and nitrite reductase (i.e., OsNIA1, OsNIA2, and OsNIR1, respectively), were highly expressed in NT_L, but dramatically decreased in PEG_L and PRD_L (Tang et al., 2012b; Kabange et al., 2021), indicating that the nitrogen utilization ability in both PEG_L and PRD_L was probably compromised, while PRD_L leaves did not exhibit clear changes in several important physiological parameters (Figure 1).

In line with the expression patterns of the nitrogen-related TF OsNLP1 and its target genes observed in the root samples, it is found that most of the amino acids (AA) and AA derivatives exhibited similar abundances between NT_R and PRD_R, but in contrast to those in PRDPRG_R and PEG_R (Figure 7C). Nitrogen-rich AAs (glutamine and asparagine) are key to root-to-shoot nitrogen transportation, and their levels reflect nitrogen utilization and supply status (Hildebrandt et al., 2015; Galil et al., 2016). Importantly, both glutamine and asparagine were significantly abundant in NT_R and PRD_R but were lower in PRDPRG_R and PEG_R. By contrast, many amino acids and AA derivatives were present at low abundance in PEG_R and PRDPEG_R compared to those in NT_R/PRD_R, including branched-chain amino acids (valine, leucine, and isoleucine) and the S-containing AA methionine (Figure 7C). Together with the expression patterns of OsNLP1, OsNLP3, and their target genes in both the leaves and roots, these results indicate that nitrogen transport and assimilation are likely impaired in PEG and PRDPEG tissues, leading to systemic adjustments in multiple amino acid metabolic pathways.

Second, PEG-treated roots (PEG_R) showed significant upregulation of the Fe-deficiency-induced TFs IRO2 and IRO3 (ion-related transcription factors, IRO) (Ogo et al., 2011; Wang et al., 2021) (Figure 7A). Consistent with the expression patterns of OsIRO2 and OsIRO3, a group of key genes involved in Fe absorption and translocation was upregulated in PEG_R but not in the other root samples (Ogo et al., 2007). This pattern of OsIRO2/3 and its downstream target genes suggests that PEG-induced stress may lead to deficiencies in ion transportation and assimilation.

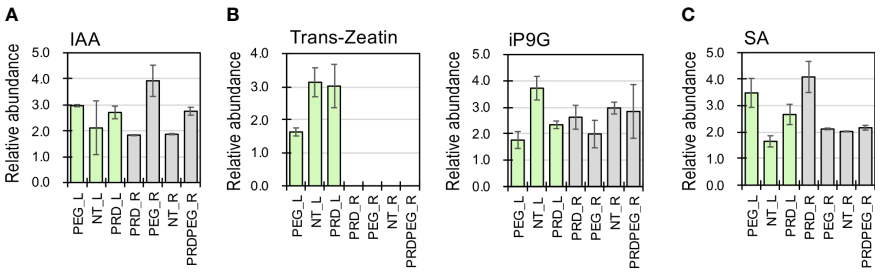

FIGURE 6
The relative abundance of several phytohormones (auxin, **(A)**; cytokinin, trans-Zeatin and iP9G, **(B)**; and salicylic acid, **(C)** detected using metabolomics.

10.3389/fpls.2023.1156514

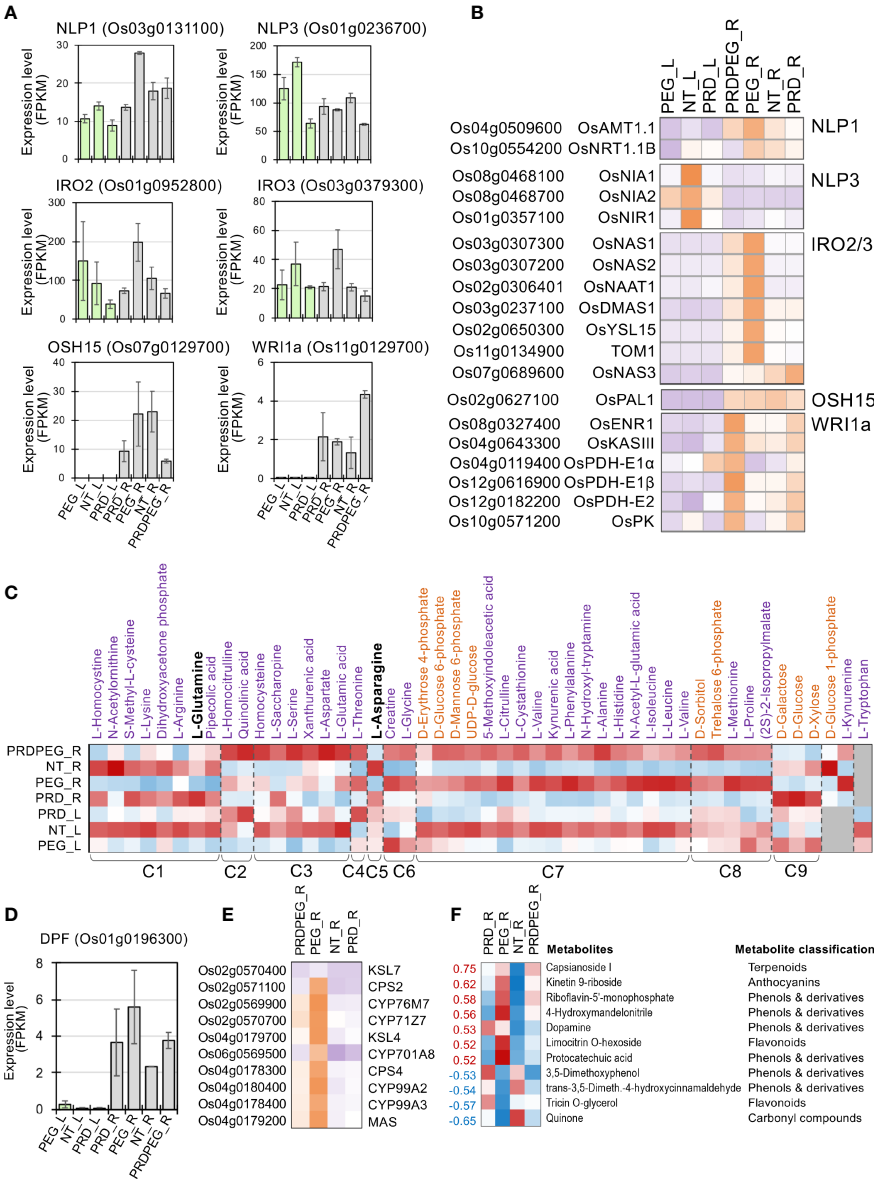

FIGURE 7
The metabolic reprogramming induced by PEG or PRD treatment and the underlying transcription factors. **(A)** Expression profiles of several key transcription factor genes (i.e., NLP1, NLP3, IRO2, IRO3, OSH15, and WRI1a) with validated functions in nitrogen utilization, ion transport and secondary metabolic pathways. **(B)** The expression profiles of the major target genes for NLP1, NLP3, IRO2, IRO3, OSH15, and WRI1a, respectively, in the PEG and PRD-treated samples. **(C)** Representative metabolites of amino acid and sugar metabolism showed dramatic changes, with PRD_R resembling the metabolic status of NT_R to maintain the supply of amino acids and sugars. Secondary metabolic pathways were affected **(F)** by either the PRD or PEG treatment partly through the differential expression of DPF **(D)**, a transcription factor controlling terpenoid biosynthesis, and its major target genes **(E)**.

Third, changes in primary and secondary metabolic pathways were observed at both the transcriptome and metabolome levels. The *Oryza Sativa* Homeobox 15 gene (OSH15) encodes a class I KNOX protein involved in phenylpropanoid and lignin biosynthesis and organ development (Yoon et al., 2017). Indeed, the *PAL1* gene, which encodes the rate-limiting enzyme of phenylpropanoid biosynthesis, phenylalanine ammonia lyase 1 (PAL1) (Jun et al., 2018; Li et al., 2019b), shared a similar expression pattern with *OsOSH15*, which was highly expressed in NT_R and PEG_R, but lower in PRD_R and PRDPEG_R, implying repressed secondary metabolism to flavonoids and monolignol/lignin. In contrast, the *diterpenoid phytoalexin factor* (*DPF*) gene and its target genes related to the biosynthesis of diterpenoid phytoalexins (DPs) were highly expressed in PEG_R, moderately expressed in PRD_R and PRDPEG_R, and weakly expressed in NT_R (Yamamura et al., 2015) (Figures 7D, E). In addition, a group of phenol and terpenoid metabolites was up- or down-regulated, which correlated well with the changes observed at the transcriptional level (Figure 7F). The upregulation of terpenoid biosynthesis may be caused by PEG-induced stress but is more

likely to reflect a reprogramming of secondary metabolites, in which terpenoid biosynthetic pathways related to pathogen defense are upregulated. Phenylpropanoid/lignin biosynthetic pathways are repressed to coordinate limited metabolic resources for stress response and adaptation.

In addition to stress-induced adjustments in nitrogen and secondary metabolism, osmolytes often accumulate in the root tissue in response to drought or osmotic stresses (Gorgues et al., 2022). Proline and sorbitol were highly accumulated in PEG_R and PRDPEG_R but remained at low levels in the NT_R and PRD_R samples (Figure 7C). In particular, a high level of proline was detected in PEG_L, indicating that proline is a major osmolyte in both leaves and roots that copes with PEG-induced osmotic stress. Another stress-related sugar metabolite, trehalose 6-phosphate, was abundant in PEG_R and PRDPEG_R. Unlike these stress-induced metabolites, sugars associated with primary metabolisms (especially glycolysis/gluconeogenesis), such as glucose, galactose, and glucose 1-phosphate, were low in PEG_R and PRDPEG_R but were low in NT_R and PRD_R (Figure 7C). This suggests that carbohydrate metabolism is likely to be affected by PEG treatment. This coordination between the metabolic pathways of carbohydrates, nitrogen/amino acids, and secondary compounds is at least partly controlled at the transcriptional level, with several functionally validated TFs (OsNLP1, OsNLP3, OsIRO2, OsIRO3, OsDPF, and OsOSH15) having clear roles in this coordination.

To fully utilize the TF-centric analysis approach, functional studies of rice TFs were systematically searched, in which the TF-regulated or targeted genes were identified by comparing the TF transgenic line to the wild type using RNA-seq or chromatin immunoprecipitation sequencing (ChIP-seq) analysis (Su et al., 2010; Li et al., 2011; Wan et al., 2011; Tang et al., 2012a; Fang et al., 2014; Lee et al., 2015; Zhang et al., 2017; Xu et al., 2018; Zhang et al., 2018; Wang et al., 2019; Liu et al., 2021; Guo et al., 2022; Li et al., 2022; Wei et al., 2022). Several sets of the target genes for a total of 12 TFs were collected, including one stress-induced RNA-binding protein, tandem CCCH zinc finger 7, and TZF7 (Supplementary Table S7) and these gene sets were compared with the identified co-expression modules, with a significant overlap between a gene set and a module determined using a hypergeometric test ($P < 0.01$) (Figure 8) (Li et al., 2019a; Tu and Li, 2020). As expected, the TFs and their target genes tend to be significantly enriched within the same meta-modules (the modules with positively or negatively correlated co-expression patterns), highlighting a number of TFs involved in the transcriptional regulation, such as TCP19 (Teosinte branched1/Cincinnata/proliferating cell factor 19) (Liu et al., 2021), ABF1 (ABRE binding factor 1) (Zhang et al., 2017), ABF2 (ABRE binding factor 2) (Tang et al., 2012a), CCA1 (CIRCADIAN CLOCK ASSOCIATED 1), LG2 (LUGULELESS 2) (Li et al., 2022; Wei et al., 2022), TZF7 (Guo et al., 2022) and DERF1 (drought-responsive ethylene response factor 1) (Wan et al., 2011) (shown in green boxes in Figure 8). As osmotic or drought stress occurs, the key stress-responsive phytohormone ABA begins to accumulate, mainly

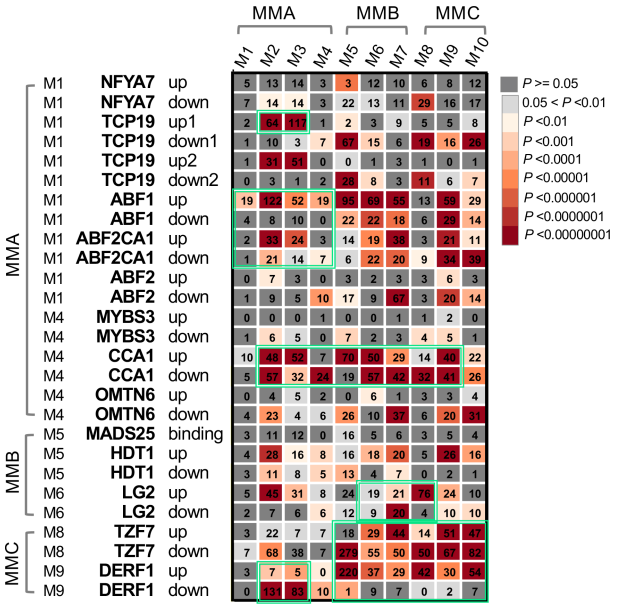

FIGURE 8
Significant overlaps between TF-target genes and the expression modules highlight several important transcriptional regulators in the modules. The heatmap shows the hypergeometric p values between TF-target genes and each of the ten expression modules, with dark grey indicating $P < 0.05$ and light grey indicating $0.05 < P < 0.01$. Representative TFs in these modules and their potential regulated genes in each module are shown in the pie chart, with the representative MapMan functional terms listed for each set of TF-target genes. MMA, MMB, and MMC stand for the meta-module A, B, and C, respectively, which are provided in Supplementary Figure S2.

in the leaf tissue, triggering its signal transduction and activating stress-related genes through several ABA-downstream TFs (Song et al., 2016; Chen et al., 2020). As expected, two major ABA-responsive TFs (i.e., ABF1 and ABF2) were highly expressed in PEG_L and PRD_L but not in NT_L (Figures 9D, G), and their upregulated genes were largely detected in modules M1 to M4 (Figures 9E, H). Interestingly, TCP19, which has been reported to be associated with rice nitrogen use efficiency (NUE) (Liu et al., 2021), was highly expressed in PRD-treated samples (PRD_L and PRDPEG_R). Given the distinct expression patterns of the other nitrogen-responsive genes (e.g., NLP1, NLP3, and their target genes) between NT-, PEG-treated-, and PRD-treated plants, and the similar metabolic changes in amino acid metabolism between NT_R and PRD_R, TCP19 might be a key regulator of nitrogen reprogramming in PRD-treated plants to coordinate root-to-shoot nitrogen allocation. Similarly, nitrogen reprogramming reflects the transcriptional regulation of multiple nitrogen transporters through several key TFs. Our analysis revealed that OsCCA1 (also known as N-mediated heading date 1, Nhd1) showed high expression exclusively in the untreated leaf and root tissues, which directly activated the ammonium transporter (OsAMT1;3) and the dual-affinity nitrate transporter (OsNRT2.4) to modulate nitrogen use

10.3389/fpls.2023.1156514

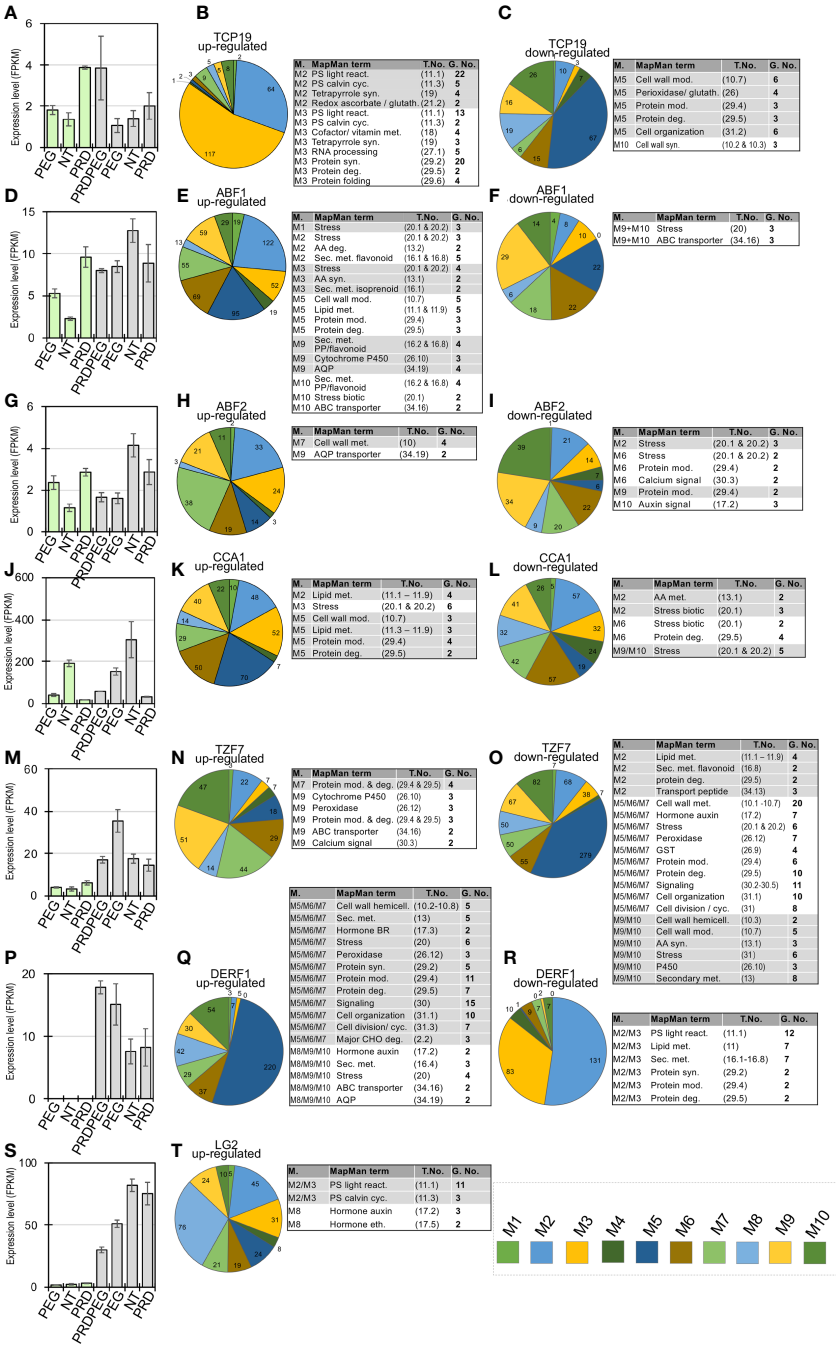

FIGURE 9
Profiling of the important transcription factors and regulators involved in the stress response and metabolic reprogramming during the PRD or PEG treatments. This diagram shows a total of seven selected transcription factors and regulators and their target genes or regulated genes in the coexpression modules (details in the Methods), with the expression profiles for TCP19, ABF1, ABF2, CCA1, TZF7, DERF1, LG2 shown in **(A, D, G, J, M, P, S)**, respectively. The up-regulated genes of TCP19, ABF1, ABF2, CCA1, TZF7, DERF1 and LG2 in each module are shown in pie charts in **(B, E, H, K, N, Q, T)**, respectively, with the genes annotated to be associated with stress and metabolic functional terms listed in the companion tables. The down-regulated genes of TCP19, ABF1, ABF2, CCA1, TZF7 and DERF1 in each module are shown in pie charts in **(C, F, I, L, O, R)**, respectively, with the genes annotated to be associated with stress and metabolic functional terms listed in the companion tables. In each table, the modules, MapMan-annotated term, term number (abbreviated as 'T. No.'), and gene number (abbreviated as 'G. No.') of the TFregulated genes are provided.

efficiency (NUE) and root growth (Li et al., 2022; Wei et al., 2022). In contrast, the RNA-binding protein OsTZF7, belonging to the tandem CCCH zinc finger (TZF) family, was highly expressed in PEG-treated roots. OsTZF7 is an essential component of stress granules associated with the post-transcriptional regulation of mRNAs during stress and is responsive to drought stress and ABA signaling (Guo et al., 2022). Thus, TZF7 likely represents evidence of a PEG-induced ABA response that is distinct from the transcriptional regulation

mediated by ABF1 and ABF2 in the leaf. We also detected similar expression patterns between NT_R and PRD_R for important transcription factors involved in stress tolerance and growth. OsDERF1 represents a novel ERF transcriptional cascade that modulates drought response through ethylene biosynthesis (Wan et al., 2011). Indeed, OsDERF1 remained at low expression levels in NT_R and PRD_R, with several hundred OsDERF1 target genes related to protein synthesis and cell wall metabolism that were well correlated in the MMC meta-module (Figures 8A, 9P–R). LIGULELESS2 (LG2) is another key transcription factor involved in leaf organogenesis; however, its role in root development remains elusive (Wang et al., 2021). The upregulated expression of LG2 in NT_R and PRD_R, together with its regulated genes, suggests that LG2 may play a role in maintaining root growth.

Besides, the differentially expressed genes identified in this work were compared with the rice meta-quantitative trait loci (MQTLs) that are known to involved in drought-related traits (Khahani et al., 2021). In particular, several MQTL regions related to root architecture-related traits were focused, including RDR (ratio of deep rooting), RDW (root dry weight), RL (root length), RN (root number), and RT (root thickness). 745 DEGs in our study were found to be co-localized with the MQTLs (Supplementary Tables S9, S10). Interestingly, the four drought-tolerance MQTL regions do not enrich the DEGs, whereas four, two four, and one MQTL regions associated with RT, RN, RDW and RDR traits are significantly enriched with the DEGs related to PRD-mediated stress tolerance. Several stress-related regulators identified in the present study were found in these MQTL regions, such as ABF1, TZF7, NF-YA7, and OMTN6 (Supplementary Table S9). Thus, the DEGs co-localized with drought related MQTLs may represent a useful source of candidate genes associated with drought tolerance in rice. Combining the results of TF-centric analysis and MQTL analysis, several regulators involved in stress response and metabolic changes (ABF1, ABF2, CCA1, DERF1, IRO2/3, LG2, NLP1, TCP19, TZF7, WRI1a) could be prioritized as major candidate genes for identifying rice genotypes with better PRD-mediated stress tolerance, while the DEGs co-localized with the drought related MQTL regions also deserving future investigations.

Conclusion

In this study, we integrated the results from physiological, transcriptome, and metabolome analyses. Our results demonstrated that PRD induces transcriptomic changes primarily in the roots but not in the leaves and adjusts several amino-acid and phytohormone metabolic pathways to maintain the balance between growth and stress responses. To the best of our knowledge, this is the first report to employ an integrated omics analysis to decipher the molecular regulation underlying the PRD technique. Our results established a link between transcriptional regulation and PRD-induced metabolic reprogramming. More importantly, transcription factors were identified in these co-expression modules, highlighting several key TFs, such as TCP19, WRI1a, ABF1, ABF2, DERF1, and TZF7, involved in nitrogen metabolism, lipid metabolism, ABA signaling, ethylene signaling, and stress regulation (summarized in Figure 10). These identified regulators and the associated transcriptional and metabolic changes strongly support the involvement of other mechanisms (such as metabolic reprogramming) in PRD-mediated stress tolerance. It is also worth mentioning that the main aim was to provide evidence for the hypothesis mentioned in the Introduction. However, more molecular experiments are necessary to validate the detailed functions of each regulator in the PRD process. Overall, our results provide new insights into PRD-mediated osmotic stress tolerance, clarify the molecular regulation induced by PRD, and identify genes useful for further improving water-use efficiency and/or stress tolerance in rice.

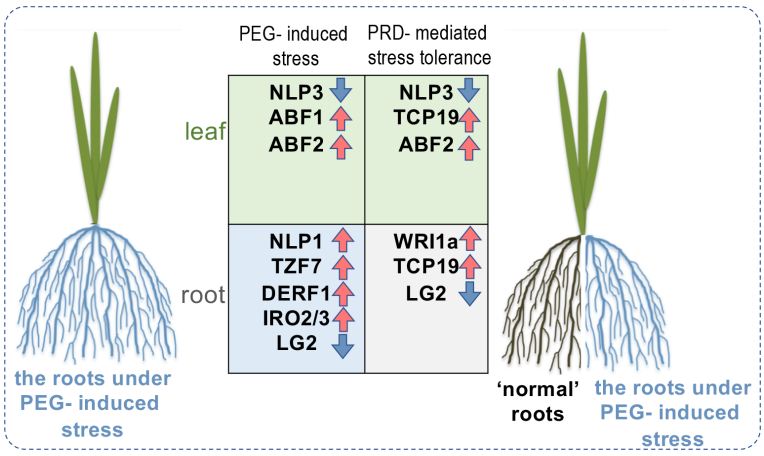

FIGURE 10
Proposed model illustrating the molecular differences between PEG-stressed and PRD-mediated stress-tolerant rice seedlings, highlighting a couple of potentially involved key regulators including not only the transcription factors (*e.g.*, ABF1, ABF2) downstream of ABA signaling pathway, but also several regulators related to metabolism and nutrient uptake (*e.g.*, NLP3, TCP19, WRI1a).

Data availability statement

The original contributions presented in the study are publicly available. This data can be found here: NCBI Short Read Archive (SRA), accession number PRJNA936260 (https://www.ncbi.nlm.nih.gov/sra/?term=PRJNA936260).

Author contributions

Conceptualization, JZ, YL, and XC. Experiments and methodology, MZ, CD, JZ, ZG, YYZ, JW, YPZ, YL, and YaW. Data acquisition and analyses, YaW, MC, YuW, JC, GY, and GH. Bioinformatic analyses, MZ, CD, JZ, and YL. Writing—original draft preparation, MZ, CD, YL, and XC. Writing—review and editing, MZ, CD, YL, and XC. Supervision, YL, and XC. Project administration, JZ, JC, GY, GH, YL, and XC. Funding acquisition, JZ, YL, and XC. All authors contributed to the article and approved the submitted version.

Funding

This work was supported by the Guangdong Basic and Applied Basic Research Foundation (2018A030307075, 2021A1515011236, 2023A1515011736, 2023A1515010336), Guangdong Science and Technology Program (2019B121201004), Research Platform Project of Education Department of Guangdong Province (2020KCKXTD037, 2021GCZX001, 2022ZDZX4047), National Innovative Training Program for College Students (202110576016), National Natural Science Foundation of China (32272126, 31901537), the Fundamental Research Funds for Central Universities, HUST (2021XXJS070, 3004170157), Wuhan Knowledge Innovation Project (2022020801010073) and the Opening fund of Guangdong Provincial Key Laboratory of Utilization and Conservation of Food and Medicinal Resources in Northern Region (FMR2022001Z).

Acknowledgments

We would like to express our appreciation to the editor and reviewers for their time and efforts to improve the quality of our manuscript.

Conflict of interest

The authors declare that the research was conducted in the absence of any commercial or financial relationships that could be construed as a potential conflict of interest.

Publisher's note

Supplementary material

The Supplementary Material for this article can be found online at: https://www.frontiersin.org/articles/10.3389/fpls.2023.1156514/full#supplementary-material

References

Agrawal, L., Gupta, S., Mishra, S. K., Pandey, G., Kumar, S., Chauhan, P. S., et al. (2016). Elucidation of complex nature of PEG induced drought-stress response in rice root using comparative proteomics approach. *Front. Plant Sci.* 7 1466. doi: 10.3389/fpls.2016.01466

Ahmadi, S. H., Andersen, M. N., Plauborg, F., Poulsen, R. T., Jensen, C. R., Sepaskhah, A. R., et al. (2010). Effects of irrigation strategies and soils on field-grown potatoes: gas exchange and xylem ABA. *Agric. Water Manage.* 97, 1486–1494. doi: 10.1016/j.agwat.2010.05.002

Alfatih, A., Wu, J., Zhang, Z. S., Xia, J., Jan, S. U., Yu, L., et al. (2020). Rice NIN-LIKE PROTEIN 1 rapidly responds to nitrogen deficiency and improves yield and nitrogen use efficiency. *J. Exp. Bot.* 71, 6032–6042. doi: 10.1093/jxb/eraa292

Ali, M., Brian, A. W., Kenneth, M., Lorian, S., and Barbara, W. (2008). Mapping and quantifying mammalian transcriptomes by RNA-seq. *Nat. Methods* 5, 621–628. doi: 10.1038/nmeth.1226

Barri, T., and Dragsted, L. O. (2013). UPLC-ESI-QTOF/MS and multivariate data analysis for blood plasma and serum metabolomics: effect of experimental artefacts and anticoagulant. *Analytica Chimica Acta* 768, 118–128. doi: 10.1016/j.aca.2013.01.015

Casa, R., and Rouphael, Y. (2014). Effects of partial root-zone drying irrigation on yield, fruit quality, and water-use efficiency in processing tomato. *J. Hortic. Sci. Biotechnol.* 89, 389–396. doi: 10.1080/14620316.2014.11513097

Chen, K., Li, G., Bressan, R. A., Song, C. P., Zhu, J., and Zhao, Y. (2020). Abscisic acid dynamics, signaling, and functions in plants. *J. Integr. Plant Biol.* 62, 25–54. doi: 10.1111/jipb.12899

Chen, L., Zhao, J., Song, J., and Jameson, P. E. (2021). Cytokinin glucosyl transferases, key regulators of cytokinin homeostasis, have potential value for wheat improvement. *Plant Biotechnol. J.* 19, 878–896. doi: 10.1111/pbi.13595

Collins, M. J., Fuentes, S., and Barlow, E. W. (2010). Partial rootzone drying and deficit irrigation increase stomatal sensitivity to vapour pressure deficit in anisohydric grapevines. *Funct. Plant Biol.* 37, 128–138. doi: 10.1071/FP09175

Dbara, S., Haworth, M., Emiliani, G., Mimoun, M. B., Gómez-Cadenas, A., and Centritto, M. (2016). Partial root-zone drying of olive (*Olea europaea* var.'Chetoui') induces reduced yield under field conditions. *PLoS One* 11, e0157089. doi: 10.1371/journal.pone.0157089

Fang, Y., Xie, K., and Xiong, L. (2014). Conserved miR164-targeted NAC genes negatively regulate drought resistance in rice. *J. Exp. Bot.* 65, 2119–2135. doi: 10.1093/jxb/eru072

FAO (2019). *Proactive approaches to drought preparedness – where are we now and where do we go from here* (Rome: Food and Agriculture Organization of the United Nations, FAO). Available at: https://www.fao.org/policy-support/tools-and-publications/resources-details/en/c/1242198/.

Feng, J., Wang, , Wu, Y., Luo, Q., Zhang, Y., Qiu, D., et al (2019). TaSnRK2.9, a Sucrose Non-fermenting 1-Related Protein Kinase Gene, Positively Regulates Plant Response to Drought and Salt Stress in Transgenic Tobacco. *Front. Plant Sci.* 9, 2003. doi: 10.3389/fpls.2018.02003

Galil, G., Amir, R., and Fernie, A. R. (2016). The regulation of essential amino acid synthesis and accumulation in plants. *Annu. Rev. Plant Biol.* 67, 153–178. doi: 10.1146/annurev-arplant-043015-112213

Gao, Z., Lin, Y., Zhang, Y., Liang, J., Luo, W., and Chen, X. (2021). Growth and ion content in rice seedling xylem sap under different water stresses and nitrogen forms. *Acta Agriculturae Boreali-Sinica* 36, 146–153. Available at: https://kns.cnki.net/kcms2/article/abstract?v=3uoqIhG8C44YLTlOAiTRKibYlV5Vjs7iy_Rpms2pqwbFRRUtoUImHc9uZAUAaM9XPZSmp3u_I1tLNPrdqPJpgJYRuJEuRaln&uniplatform=NZKPT

Gorgues, L., Li, X., Maurel, C., Martiniere, A., and Nancy, P. (2022). Root osmotic sensing from local perception to systemic responses. *Stress Biol.* 2, 36. doi: 10.1007/s44154-022-00054-1

Guo, C., Chen, L., Cui, Y., Tang, M., Guo, Y., Yi, Y., et al. (2022). RNA Binding protein OsTZF7 traffics between the nucleus and processing Bodies/Stress granules and positively regulates drought stress in rice. *Front. Plant Sci.* 13, 802337. doi: 10.3389/fpls.2022.802337

Gupta, A., Rico-Medina, A., and Cano-Delgado, A. I. (2019). The physiology of plant response to drought. *Science* 368, 266–269. doi: 10.1126/science.aaz7614

Hallmark, H. T., and Rashotte, A. M. (2020). Cytokinin isopentenyladenine and its glucoside isopentenyladenine-9G delay leaf senescence through activation of cytokinin-associated genes. *Plant Direct* 10, 1–15. doi: 10.1002/pld3.292

Hildebrandt, T. M., Nesi, A. N., Araujo, W. L., and Braun, H. (2015). Amino acid catabolism in plants. *Mol. Plant* 8, 1563–1579. doi: 10.1016/j.molp.2015.09.005

Honig, M., Plihalova, L., Husickova, A., Nisler, J., and Dolezal, K. (2018). Role of cytokinins in senescence, antioxidant defense and photosynthesis. *Int. J. Mol. Sci.* 19 (12), 4045. doi: 10.3390/ijms19124045

Hoque, M. S., Masle, J., Udvardi, M. K., Ryan, P. R., and Upadhyaya, N. M. (2006). Over-expression of the rice *OsAMT1-1* gene increases ammonium uptake and content, but impairs growth and development of plants under high ammonium nutrition. *Funct. Plant Biol.* 33, 153–163. doi: 10.1071/FP05165

Hu, B., Wang, W., Ou, S., Tang, J., Li, H., Che, R., et al. (2015). Variation in *NRT1.1B* contributes to nitrate-use divergence between rice subspecies. *Nat. Genet.* 47, 7–834. doi: 10.1038/ng.3337

Huang, F., Jiang, Y., Chen, T., Li, H., Fu, M., Wang, Y., et al. (2022). New data and new features of the FunRiceGenes (Functionally characterized rice genes). database: 2021 update. *Rice* 15, 23. doi: 10.1186/s12284-022-00569-1

Jin, J., Tian, F., Yang, D., Meng, Y., Kong, L., Luo, J., et al. (2017). PlantTFDB 4.0: toward a central hub for transcription factors and regulatory interactions in plants. *Nucl. Acids Res.* 45, D1040–D1045. doi: 10.1093/nar/gkw982

Jin, J., Zhang, H., Kong, L., Gao, G., and Luo, J. (2014). PlantTFDB 3.0: a portal for the functional and evolutionary study of plant transcription factors. *Nucl. Acids Res.* 42, D1182–D1187.

Jun, S. Y., Sattler, S. A., Cortez, G. S., Vermerris, W., Sattler, S. E., and Kang, C. (2018). Biochemical and structural analysis of substrate specificity of a phenylalanine ammonia-lyase. *Plant Physiol.* 176, 1452–1468. doi: 10.1104/pp.17.01608

Kabange, N. R., Park, S., Lee, J., Shin, D., Lee, S., Kwon, Y., et al. (2021). New insights into the transcriptional regulation of genes involved in the nitrogen use efficiency under potassium chlorate in rice (*Oryza sativa* l.). *Int. J. Mol. Sci.* 22, 2192. doi: 10.3390/ijms22042192

Kang, S. Z., Shi, P., Pan, Y. H., Liang, Z. S., Hu, X. T., and Zhang, J. (2000). Soil water distribution, uniformity and water-use efficiency under alternate furrow irrigation in arid areas. *Irrig. Sci.* 19, 181–190. doi: 10.1007/s002710000019

Kawahara, Y., de la Bastide, M., Hamilton, J. P., Kanamori, H., McCombie, W. R., Ouyang, S., et al. (2013). Matsumoto, T. improvement of the oryza sativa nipponbare reference genome using next generation sequence and optical map data. *Rice.* 6, 4. doi: 10.1186/1939-8433-6-4

Khahani, B., Tavakoi, E., Shariati, V., and Rossini, L. (2021). Meta−QTL and ortho −MQTL analyses identified genomic regions controlling rice yield, yield−related traits and root architecture under water deficit conditions. *Sci. Rep.* 11, 6942. doi: 10.1038/s41598-021-86259-2

Khalil, A. A., and Grace, J. (1993). Does xylem sap ABA control the stomatal behavior of water-stressed sycamore (*Acer pseudoplatanus* l.) seedlings? *Environ. Exp. Bot.* 44, 1127–1134. doi: 10.1093/jxb/44.7.1127

Koncagül, E., Tran, M., Connor, R., and Uhlenbrook, S. (2018). *World water development report 2020 – water and climate change* (UNESCO WWAP). Available at: https://www.unwater.org/news/un-world-water-development-report-2020-'water-and-climate-change.

Langfelder, P., and Horvath, S. (2008). WGCNA: an r package for weighted correlation network analysis. *BMC Bioinform.* 9, 559. doi: 10.1186/1471-2105-9-559

Langfelder, P., Luo, R., Oldham, M. C., and Horvath, S. (2011). Is my network module preserved and reproducible? *PLoS Comp. Biol.* 7, e1001057. doi: 10.1371/journal.pcbi.1001057

Lee, D., Kim, H. I., Jang, G., Chung, P. J., Jeong, J. S., Kim, Y. S., et al. (2015). The NF-YA transcription factor OsNF-YA7 confers drought stress tolerance of rice in an abscisic acid independent manner. *Plant Sci.* 241, 199–210. doi: 10.1016/j.plantsci.2015.10.006

Li, B., and Dewey, C. N. (2011). RSEM: accurate transcript quantification from RNA-seq data with or without a reference genome. *BMC Bioinform.* 12, 1–16. doi: 10.1186/1471-2105-12-323

Li, C., Huang, L., Xu, C., Zhao, Y., and Zhou, D. (2011). Altered levels of histone deacetylase OsHDT1 affect differential gene expression patterns in hybrid rice. *PLoS One* 6, e21789. doi: 10.1371/journal.pone.0021789

Li, Y., Tu, M., Feng, Y., Wang, W., and Messing, J. (2019a). Common metabolic networks contribute to carbon sink strength of sorghum internodes: implications for bioenergy improvement. *Biotechnol. Biofuel.* 12, 274. doi: 10.1186/s13068-019-1612-7

Li, Y., Wang, W., Feng, Y., Min, T., Wittich, P. E., Bate, N. L., et al. (2019b). Transcriptome and metabolome reveal distinct carbon allocation patterns during internode sugar accumulation in different sorghum genotypes. *Plant Biotechnol. J.* 17, 472–487. doi: 10.1111/pbi.12991

Li, K., Zhang, S., Tang, S., Zhang, J., Dong, H., Yang, S., et al. (2022). The rice transcription factor Nhd1 regulates root growth and nitrogen uptake by activating nitrogen transporters. *Plant Physiol.* 189, 1608–1624. doi: 10.1093/plphys/kiac178

Liu, Y., Wang, H., Jiang, Z., Wang, W., Xu, R., Wang, Q., et al. (2021). Genomic basis of geographical adaptation to soil nitrogen in rice. *Nature* 590, 600–623. doi: 10.1038/s41586-020-03091-w

Liu, Y., Zhang, M., Meng, Z., Wang, B., and Chen, M. (2020). Research progress on the roles of cytokinin in plant response to stress. *Int. J. Mol. Sci.* 21, 6574. doi: 10.3390/ijms21186574

Luo, P., Dai, W., Yin, P., Zeng, Z., Kong, H., Zhou, L., et al. (2015). Multiple reaction monitoring-ion pair finder: a systematic approach to transform non-targeted mode to pseudo-targeted mode for metabolomics study based on liquid chromatography-mass spectrometry. *Anal. Chem.* 87, 5050–5055. doi: 10.1021/acs.analchem.5b00615

Mark, D. R., Davis, J. M., and Gordon, K. S. (2010). EdgeR: a bioconductor package for differential expression analysis of digital gene expression data. *Bioinform.* 26, 139–140. doi: 10.1093/bioinformatics/btp616

Mehrabi, F., and Sepaskhah, A. R. (2019). Partial root zone drying irrigation, planting methods and nitrogen fertilization influence on physiologic and agronomic parameters of winter wheat. *Agric. Water Manage.* 223, 105688. doi: 10.1016/j.agwat.2019.105688

Mo, Z., Lei, S., Ashraf, U., Khan, I., Li, Y., Pan, S., et al. (2017). Silicon fertilization modulates 2-acetyl-1-pyrroline content, yield formation and grain quality of aromatic rice. *J. Cereal Sci.* 75, 17–24. doi: 10.1016/j.jcs.2017.03.014

Muthayya, S., Sugimoto, J. D., Montgomery, S., and Maberly, G. F. (2014). An overview of global rice production, supply, trade, and consumption. *Ann. NY Acad. Sci.* 1324, 7–14. doi: 10.1111/nyas.12540

Ogbaga, C. C., Athar, H., Amir, A., Bano, H., and Chater, C. C. (2020). Clarity on frequently asked questions about drought measurements in plant physiology. *Sci. Afric.* 8, e00405. doi: 10.1016/j.sciaf.2020.e00405

Ogo, Y., Itai, R. N., Kobayashi, T., Aung, M. S., Nakanishi, H., and Nishizawa, N. K. (2011). OsIRO2 is responsible for iron utilization in rice and improves growth and yield in calcareous soil. *Plant Mol. Biol.* 75, 593–605. doi: 10.1007/s11103-011-9752-6

Ogo, Y., Itai, R. N., Nakanishi, H., Kobayashi, T., Takahashi, M., Mori, S., et al. (2007). The rice bHLH protein OsIRO2 is an essential regulator of the genes involved in fe uptake under fe deficient conditions. *Plant J.* 51, 366–377. doi: 10.1111/j.1365-313X.2007.03149.x

Peng, Z., Wang, Y., Zuo, W., Gao, Y., Li, R., Yu, C., et al. (2022). Integration of metabolome and transcriptome studies reveals flavonoids, abscisic acid, and nitric oxide comodulating the freezing tolerance in liriope spicata. *Front. Plant Sci.* 12, 764625. doi: 10.3389/fpls.2021.764625

Qiu, D., Hu, W., Zhou, Y., Xiao, J., Hu, R., Wei, Q., et al. (2021). TaASR1-d confers abiotic stress resistance by affecting ROS accumulation and ABA signaling in transgenic wheat. *Plant Biotechnol. J.* 19, 1588–1601. doi: 10.1111/pbi.13572

Rahman, A., Alam, M. U., Hossain, M. S., Mahmud, J. A., Nahar, K., Fujita, M., et al. (2023). Exogenous Gallic acid confers salt tolerance in rice seedlings: modulation of ion homeostasis, osmoregulation, antioxidant defense, and methylglyoxal detoxification systems. *Agronomy-Basel* 13, 16. doi: 10.3390/agronomy13010016

Ranathuge, K., El-Kereamy, A., Gidda, S., Bi, Y. M., and Rothstein, S. J. (2014). *AMT1,1* transgenic rice plants with enhanced $NH4^{(+)}$ permeability show superior growth and higher yield under optimal and suboptimal $NH4^{(+)}$ conditions. *J. Exp. Bot.* 65, 965–979. doi: 10.1093/jxb/ert458

Saeed, H., Grove, I. G., Kettlewell, P. S., and Hall, N. W. (2008). Potential of partial rootzone drying as an alternative irrigation technique for potatoes (*Solanum tuberosum*). *Ann. Appl. Biol.* 152, 71–80. doi: 10.1111/j.1744-7348.2007.00196.x

Sah, S. K., Reddy, K. R., and Li, J. (2016). Abscisic acid and abiotic stress tolerance in crop plants. *Front. Plant Sci.* 7, 571. doi: 10.3389/fpls.2016.00571

Samson, B. K., Hasan, M., and Wade, L. J. (2002). Penetration of hardpans by rice lines in the rainfed lowlands. *Field Crops Res.* 76, 175–188. doi: 10.1016/S0378-4290(02)00038-2

Sellick, C. A., Hansen, R., Stephens, G. M., Goodacre, R., and Dickson, A. J. (2011). Metabolite extraction from suspension cultured mammalian cells for global metabolite profiling. *Nat. Protoc.* 6, 1241–1249. doi: 10.1038/nprot.2011.366

Sepaskhah, A. R., and Ahmadi, S. H. (2012). A review on partial root-zone drying irrigation. *Int. J. Plant Prod.* 4, 241–258. doi: 10.1111/j.1757-1707.2010.01052.x278r2010

Shu, L., Ding, W., Wu, J., Feng, F., Luo, L., and Mei, H. (2010). Proteomic analysis of rice leaves shows the different regulations to osmotic stress and stress signals. *J. Integr. Plant Biol.* 52, 981–995. doi: 10.1111/j.1744-7909.2010.00986.x

Siopongco, J., Sekiya, K., Yamauchi, A., Egdane, J., Ismail, A. M., and Wade, L. J. (2008). Stomatal responses in rainfed lowland rice to partial soil drying: evidence for root signals. *Plant Prod. Sci.* 11, 28–41. doi: 10.1626/pps.11.28

Siopongco, J., Sekiya, K., Yamauchi, A., Egdane, J., Ismail, A. M., and Wade, L. J. (2009). Stomatal responses in rainfed lowland rice to partial soil drying: comparison of two lines. *Plant Prod. Sci.* 12, 17–28. doi: 10.1626/pps.12.17

Song, L., Huang, C. S., Wise, W., Castanon, R., Nery, J. R., Chen, H., et al. (2016). A transcription factor hierarchy defines an environmental stress response network. *Science* 354, aag1550. doi: 10.1126/science.aag1550

Su, C., Wang, Y., Hsieh, T. H., Lu, C., Tseng, T. H., and Yu, S. (2010). A novel MYBS3-dependent pathway confers cold tolerance in rice. *Plant Physiol.* 153, 145–158. doi: 10.1104/pp.110.153015

Suzuki, N., Rivero, R. M., Shulaev, V., Blumwald, E., and Mittler, R. (2014). Abiotic and biotic stress combinations. *New Phytol.* 203, 32–43. doi: 10.1111/nph.12797

Takahashi, F., Suzuki, T., Osakabe, Y., Betsuyaku, S., Kondo, Y., Dohmae, N., et al. (2018). A small peptide modulates stomatal control *via* abscisic acid in long-distance signaling. *Nature* 556, 235–238. doi: 10.1038/s41586-018-0009-2

Tang, Z., Fan, X., Li, Q., Feng, H., Miller, A. J., Shen, Q., et al. (2012b). Knockdown of a rice stelar nitrate transporter alters long-distance translocation but not root influx. *Plant Physiol.* 160, 2052–2063. doi: 10.1104/pp.112.204461

Tang, N., Zhang, H., Li, X., Xiao, J., and Xiong, L. (2012a). Constitutive activation of transcription factor OsbZIP46 improves drought tolerance in rice. *Plant Physiol.* 158, 1755–1768. doi: 10.1104/pp.111.190389

Tu, M., and Li, Y. (2020). Profiling alternative 3' untranslated regions in sorghum using RNA-seq data. *Front. Genet.* 11, 556749. doi: 10.3389/fgene.2020.556749

United Nations. (2011) *Department of economic and social affairs, population division, world population prospects: the 2010 revision, volume I: comprehensive tables*. Available at: www.un.org/en/development/desa/population/publications/pdf/trends/WPP2010/WPP2010_Volume-I_Comprehensive-Tables.pdf.

Usadel, B., Poree, F., Nagel, A., Lohse, M., Czedik-Eysenberg, A., and Stitt, M. (2009). A guide to using MapMan to visualize and compare omics data in plants: a case study in the crop species, maize. *Plant Cell Environ.* 32, 1211–1229. doi: 10.1111/j.1365-3040.2009.01978.x

Wan, L., Zhang, J., Zhang, H., Zhang, Z., Quan, R., Zhou, S., et al. (2011). Transcriptional activation of OsDERF1 in OsERF3 and OsAP2-39 negatively modulates ethylene synthesis and drought tolerance in rice. *PloS One* 6, e25216. doi: 10.1371/journal.pone.0025216

Wang, R., Liu, C., Chen, Z., Song, S., and Wang, X. (2021). *Oryza sativa* LIGULELESS 2s determine lamina joint positioning and differentiation by inhibiting auxin signaling. *New Phytol.* 229, 1832–1839. doi: 10.1111/nph.16970

Wang, W., Ye, J., Ma, Y., Wang, T., Shou, H., and Zheng, L. (2020). OsIRO3 plays an essential role in iron deficiency responses and regulates iron homeostasis in rice. *Plants* 9, 1095. doi: 10.3390/plants9091095

Want, E. J., Masson, P., Michopoulos, F., Wilson, I. D., Theodorids, G., Plumb, R. S., et al. (2012). Global metabolic profiling of animal and human tissues *via* UPLC-MS. *Nat. Protoc.* 8, 17–32. doi: 10.1038/nprot.2012.135

Wei, S., Hu, W., Deng, X., Zhang, Y., Liu, X., Zhao, X., et al. (2014). A rice calcium-dependent protein kinase OsCPK9 positively regulates drought stress tolerance and spikelet fertility. *BMC Plant Biol.* 14, 133. doi: 10.1186/1471-2229-14-133

Wei, H., Xu, H., Su, C., Wang, X., and Wang, L. (2022). Rice CIRCADIAN CLOCK ASSOCIATED 1 transcriptionally regulates ABA signaling to confer multiple abiotic stress tolerance. *Plant Physiol.* 190, 1057–1073. doi: 10.1093/plphys/kiac196

Wu, T., Hu, E., Xu, S., Chen, M., Guo, P., Dai, Z., et al. (2021). clusterProfiler 4.0: a universal enrichment tool for interpreting omics data. *Innovation* 2, 100141. doi: 10.1016/j.xinn.2021.100141

Xu, N., Chu, Y., Chen, H., Li, X., Wu, Q., Jin, L., et al. (2018). Rice transcription factor OsMADS25 modulates root growth and confers salinity tolerance *via* the ABA-mediated regulatory pathway and ROS scavenging. *PloS Genet.* 14, e1007662. doi: 10.1371/journal.pgen.1007662

Yamamura, C., Mizutani, E., Okada, K., Nakagawa, H., Fukushima, S., Tanaka, A., et al. (2015). Diterpenoid phytoalexin factor, a bHLH transcription factor, plays a central role in the biosynthesis of diterpenoid phytoalexins in rice. *Plant J.* 84, 1100–1133. doi: 10.1111/tpj.13065

Yang, L., Gordon, K. S., and Wei, S. (2014). FeatureCounts: an efficient general purpose program for assigning sequence reads to genomic features. *Bioinform* 7, 923–930. doi: 10.1093/bioinformatics/btt656

Yao, W., Li, G., Yu, Y., and Ouyang, Y. (2018). funRiceGenes dataset for comprehensive understanding and application of rice functional genes. *GigaScience* 7, 1–9. doi: 10.1093/gigascience/gix119

Yeung, K. Y., Haynor, D. R., Ruzzo, W. L., and Horvath, S. (2001). Validating clustering for gene expression data. *Bioinform* 17, 309–318. doi: 10.1093/bioinformatics/17.4.309

Yoon, J., Cho, L., Antt, H. W., Koh, H., and An, G. (2017). KNOX protein OSH15 induces grain shattering by repressing lignin biosynthesis genes. *Plant Physiol.* 174, 312–325. doi: 10.1104/pp.17.00298

Yu, S., Ali, J., Zhang, C., Li, Z., and Zhang, Q. (2020). Genomic breeding of green super rice varieties and their deployment in Asia and Africa. *Theor. Appl. Genet.* 133, 1427–1442. doi: 10.1007/s00122-019-03516-9

Yuan, M., Breitkopf, S. B., Yang, X., and Asara, J. M. (2012). A positive/negative ion-switching, targeted mass spectrometry-based metabolomics platform for bodily fluids, cells, and fresh and fixed tissue. *Nat. Protoc.* 7, 872–881. doi: 10.1038/nprot.2012.024

Zhang, C., Li, C., Liu, J., Lv, Y., Yu, C., Li, H., et al. (2017). The OsABF1 transcription factor improves drought tolerance by activating the transcription of COR413-TM1 in rice. *J. Exp. Bot.* 68, 4695–4707. doi: 10.1093/jxb/erx260

Zhang, Z., Mu, X., Cao, Q., Shi, Y., Hu, X., and Zheng, H. (2022a). Honeybee gut lactobacillus modulates host learning and memory behaviors *via* regulating tryptophan metabolism. *Nat. Commun.* 13, 2037. doi: 10.1038/s41467-022-29760-0

Zhang, Z., Xia, J., Alfatih, A., Song, Y., Huang, Y., Sun, L., et al. (2022b). Rice NIN-LIKE PROTEIN 3 modulates nitrogen use efficiency and grain yield under nitrate-sufficient conditions. *Plant Cell Environ.* 45, 1520–1536. doi: 10.1111/pce.14294

Zhang, G., Xu, N., Chen, H., Wang, G., and Huang, J. (2018). OsMADS25 regulates root system development *via* auxin signaling in rice. *Plant J.* 95, 1004–1022. doi: 10.1111/tpj.14007

Zhang, H., Zhu, J., Gong, Z., and Zhu, J. (2012). Abiotic stress responses in plants. *Nat. Rev. Genet.* 23, 104–119. doi: 10.1038/s41576-021-00413-0

Zhou, J., Tian, L., Wang, S., Li, H., Zhao, Y., Zhang, M., et al. (2021). Ovary abortion induced by combined waterlogging and shading stress at the flowering stage involves amino acids and flavonoid metabolism in maize. *Front. Plant Sci.* 12, 778717. doi: 10.3389/fpls.2021.778717

frontiers | Frontiers in Plant Science

TYPE Original Research
PUBLISHED 21 July 2023
DOI 10.3389/fpls.2023.1224334

OPEN ACCESS

EDITED BY
Debojyoti Moulick,
Independent Researcher, Kolkata, India

REVIEWED BY
Sanjay Singh Rathore,
Indian Agricultural Research Institute (ICAR), India
Sukamal Sarkar,
Ramakrishna Mission Vivekananda Educational and Research Institute, India

*CORRESPONDENCE
Abdus Sattar
asattar@rpcau.ac.in

RECEIVED 17 May 2023
ACCEPTED 03 July 2023
PUBLISHED 21 July 2023

CITATION
Sattar A, Nanda G, Singh G, Jha RK and Bal SK (2023) Responses of phenology, yield attributes, and yield of wheat varieties under different sowing times in Indo-Gangetic Plains.
Front. Plant Sci. 14:1224334.
doi: 10.3389/fpls.2023.1224334

Responses of phenology, yield attributes, and yield of wheat varieties under different sowing times in Indo-Gangetic Plains

Abdus Sattar[1]*, Gangadhar Nanda[2], Gulab Singh[1], Ratnesh Kumar Jha[1] and Santanu Kumar Bal[3]

[1]Centre for Advance Studies on Climate Change, Dr. Rajendra Prasad Central Agricultural University, Pusa, India, [2]Department of Agronomy, Dr. Rajendra Prasad Central Agricultural University, Pusa, India, [3]AICRP on Agrometeorology, ICAR-Central Research Institute for Dryland Agriculture, Hyderabad, India

A field experiment with wheat was conducted at Pusa (25.98°N, 85.67°E, 52 m amsl), Bihar (middle Gangetic plains of India), to assess the responses of phenology, yield attributes, and yield to growing season temperature and heat stress. For this purpose, wheat was planted on five dates (viz., 15 November, 25 November, 5 December, 15 December, and 25 December) for three consecutive years (viz., 2014–2015, 2015–2016, and 2016–2017) with three prominent cultivars of the region (viz., RAU-3711, HD-2824, and HD-2733). Five dates of sowing represent different wheat-growing micro-environments as imposed by varying sowing dates encompassing the entire sowing window. The study observed the significant effect of sowing dates on phenophase duration. In general, with progress in the date of sowing, tiller initiation was delayed, while the reverse trend was observed for later growth phases. Sowing environments significantly influenced the number of effective tillers m–2. Average numbers of effective tillers (ET) m–2 for the wheat sown during 15–25 November were almost 11.6% higher than those of the 25 December sown crop. Grain filling duration (GFD) showed a declining trend with the advancement of sowing dates due to increased thermal load on the crop during the reproductive period. 15 November planted crop exhibited the highest GFD (47 days), which was shortened significantly beyond 25 November, signifying agrometeorological non-suitability of wheat sowing beyond this window. Wheat sown on 25 November recorded the highest grain yield (3.21 Mg ha–1), 48.61% higher than the 25 December sown crop due to the congenial thermal regime. In this context, we have identified optimal and sub-optimal conditions to escape heat stress for higher wheat productivity. Moreover, the sum of deviation of temperature from optimum thresholds, computed for sensitive growth phases (50% flowering to physiological maturity), helped us to identify heat stress and its impact on wheat. Genotype-by-environment (GGE) biplot analysis revealed that RAU-3711 was found to be the most stable cultivar. A decrease in the yield of wheat by 4.9% to 12.0%, sown during November, and 33.8% to 42.4%, sown during December, is predicted in 2050-51 and 2080-81, respectively, under RCP 4.5.

KEYWORDS

wheat, phenology, yield, sowing window, heat stress, simulation, CERES-wheat

1 Introduction

Wheat is the most important staple food crop in the world. It also plays a vital role in food security for millions of people in India and occupies approximately 30.6 million hectares area with a total production of 98.5 million tonnes (FAO, 2017) contributing approximately 43% to the country's granary (Bapuji Rao et al., 2015). India is the second largest producer of wheat after China with approximately 12% share in global wheat production. In recent years, rising temperature due to climate change has been a cause of concern for sustainable wheat production in India, more specifically over Indo-Gangetic Plains stretching a vast area from Punjab in the West and Bihar in the East. The concern is real regarding the negative effect of warming on the phenology and yield of crops (Xiao et al., 2012; Wang et al., 2013). Under such a situation, several adaptation measures, viz., wheat sowing by zero tillage, growing new heat-resistant cultivars, and changing planting schedules, are being taken up by policymakers and farmers. Wheat production in Indo-Gangetic Plains is vulnerable to short-term temperature extremes (Lobell et al., 2012). Prevalence of dry westerly wind and sudden rise of temperature during the fag end of the growing season tends to shorten the grain filling period (Garg et al., 2013; Sandhu et al., 2016; Vashisth et al., 2020) and negatively impact grain setting of wheat (Sattar and Srivastava, 2021). It significantly affects growth and photosynthetic efficiency (Wang et al., 2011) and consequently reduces biomass and productivity (Farooq et al., 2011). Grain number, which is determined from 30 days before flowering until shortly after flowering, and grain size, dependent on grain filling (Lobell et al., 2012), crop duration, and crop biomass, together tend to decide the final yield of the crop.

Phenology is an integral part of crop weather models, which is used to specify the appropriate time and rate of specific phasic development processes (Singh et al., 2001). In this context, studying crop phenology vis-à-vis thermal regime in the field and the integrated effect of weather on yield assumes significance to bring in proper resilience against the adverse impact of high temperature on crop growth. Varying dates of sowing expose the crop in a year to different temperatures during its growing period, which helps properly understand the response of phenology to ambient temperature (Vijaya et al., 2015). Xiao et al. (2013) showed that changes in the phenological phases of winter wheat are strongly related to temperature trends. Given the potential impacts of global warming on yield, the study of phenology assumes great importance due to its impacts on productivity and farming practices (Xiao et al., 2012; Wang et al., 2013). Temperature plays a great role in modifying the enzymatic functions of plants and causes a change in phenology, which is directly related to yield (Zhu et al., 2018).

Temperature-based agrometeorological indices, viz., growing degree day (GDD), helio-thermal unit (HTU), and photo-thermal units (PTU), have a direct relationship with the growth and yield of crops. Accordingly, these indices along with thermal efficiencies are important parts of understanding the responses of phenology and yield to growing season temperature. Heat stress manifested by the occurrence of significantly higher than normal temperatures for 15–25 days during the reproductive period of wheat in the *rabi* (winter) season of 2021–2022 caused a significant reduction of grain yield in India (Bal et al., 2022). Against the backdrop of the problem of terminal heat stress and variable wheat yield, we hypothesized that by optimizing sowing dates, wheat can be grown under a congenial thermal regime, thus offsetting the negative impacts.

Since temperature significantly influences wheat yield, it would be prudent to simulate future yield under a projected climatic scenario. Future wheat yield can be simulated by different crop simulation models. The CERES-Wheat model of Hoogenboom et al. (2019) is the most widely used crop growth model, and it is an effective tool to quantify the effects of cultivar, climate, soil, and management on wheat growth across the globe. It can be effectively used to simulate yield in the projected climate (Shen et al., 2022). Keeping in mind the above facts, an attempt has been made in this article to evaluate the responses of phenology and yield of wheat to growing season temperature and heat stress. A systematic study on this aspect for a region like the middle Gangetic Plains of eastern India appeared to be meager. In this context, the objectives of the investigation were set i) to quantify the impact of varying thermal regimes induced by varying sowing environments on crop phenology and yield ii) to optimize the exact sowing environment of wheat based on the response of phenology and yield to growing season thermal regime.

2 Materials and methods

2.1 Study location

The field experiment was carried out at the University Farm of Dr. Rajendra Prasad Central Agricultural University, Pusa (25.98°N, 85.67°E, 52 m), Bihar, located in the middle Gangetic plains of India.

2.2 Climate and soil

The region experiences a sub-humid subtropical monsoon climate. It has four major seasons, viz., summer (March–May), monsoon (June–September), post-monsoon (October–November), and winter (December–February). The average annual rainfall of the area is approximately 1,230 mm. Approximately 85% of rainfall occurs during the *kharif* (monsoon) season. May is the warmest summer month of the year with a daily maximum temperature of 37°C–41°C, while the coldest winter month is January with a daily minimum temperature of 5°C–8°C. December, January, and February are the main winter months in the region. Temperature decreases significantly from November, which becomes lowest in January. Increasing temperature from March onward heralds the commencement of the summer season. Locally, the period from 15 October to 15 March is called *rabi* season, in which important irrigated crops such as wheat, maize, potato, mustard, cauliflower, cabbage, and chickpea are grown.

The soil of the experimental field has sandy loam soil, which is the dominant soil textural class of the region. The physicochemical properties of the experimental soil are given in Table 1.

TABLE 1 Physio-chemical properties of soils of the experimental field.

S. no.	Specifics/parameters	Initial value
1.	Sand (%)	55.94
2.	Silt (%)	31.85
3.	Clay (%)	12.20
4.	Textural class	Sandy loam
5.	Electrical conductivity (dS m^{-1})	2.94
6.	pH	8.28
7.	Organic carbon (%)	0.47
8.	Available N (kg ha^{-1})	241.0
9.	Available P (kg ha^{-1})	17.18
10.	Available K(kg ha^{-1})	160.0
11.	Available Zn (kg ha^{-1})	1.33

2.3 Methodology

The experiment was conducted over three wheat growing seasons, viz., *rabi* (winter) seasons of 2014–2015, 2015–2016, and 2016–2017. The crop was planted on five dates every year (viz., 15 November (D1), 25 November (D2), 5 December (D3), 15 December (D4), and 25 December (D5)) with three prominent cultivars (viz., RAU-3711, HD-2824, and HD-2733) of the region in factorial randomized block design with three replications. The sowing was staggered to impose heat stress on the crop at critical growth phases. Recommended package of practices as followed by the farmers of the region was adopted. The crop was grown under irrigated conditions, and three irrigations were applied 21 days after sowing (DAS), 45 DAS, and 75 DAS. Nitrogen, phosphorus, and potassium at 120, 60, and 40 kg ha^{-1} were applied. All P and K and a half dose of N were applied at sowing as basal dose. The remaining half dose of N was top dressed in two equal splits at crown root initiation and boot stages. Hand weeding was carried out in the field to keep the field weed free. No infestation of insect pests was observed on the crop. Hence, no pesticide was applied during the period of the experiment. The occurrence of phenological events like tillering, booting, flowering, milk, dough, and physiological maturity in Julian Day was recorded from each plot, and average dates of these phases were calculated over the years and used for analysis. GDD, also known as heat unit (HU), was calculated at different phenological stages of the crop.

Growing degree-day is defined as the mean temperature above the base temperature. Mathematically, the GDD was computed by using the following equation (Nuttonson, 1955; Sastry and Chakravarty, 1982) at different phenological stages of the crop.

$$GDD = \Sigma [[T_{max} + T_{min}]/2 - T_b],$$

where GDD is the growing degree day (day °C), T_{max} is the daily maximum temperature (°C), T_{min} is the daily minimum temperature (°C), and T_b is the base temperature (°C); the base temperature was taken as 5°C (Nuttonson, 1955; Amrawat et al., 2013).

Helio-thermal unit was calculated by multiplying GDD and daily bright sunshine hours (BSS). BSS for a particular day as recorded by the sunshine recorder in the Agrometeorological Observatory was used in the estimation of HTU. The sum of HTU for the duration of each phenophase was calculated by using the following equation (Sastry and Chakravarty, 1982), and accumulated HTU at physiological maturity was calculated as follows:

$$HTU = GDD \times n,$$

where n is the actual duration of bright sunshine hours.

Accumulated PTUs at physiological maturity were calculated by multiplying GDD with the length of maximum possible sunshine hours (Nuttonson, 1955; Sastry and Chakravarty, 1982). It is mathematically expressed as PTU = GDD × N, where N is the maximum possible sunshine hours.

Heat use efficiency (HUE), helio-thermal use efficiency (HTUE), and photo-thermal use efficiency (PTUE) were calculated following Singh and Khushu (2012).

$$HUE\ (Kg\ ha^{-1}\ °C\ day^{-1}) = \frac{Grain\ yield\ (Kg\ ha^{-1})}{Accumulated\ GDD\ (°C\ day)},$$

$$PTUE\ (Kg\ ha^{-1}\ °C\ day\ hour^{-1}) = \frac{Grain\ yield\ (Kg\ ha^{-1})}{Accumulated\ PTU\ (°C\ day\ hour)},$$

$$HTUE\ (Kg\ ha^{-1}\ °C\ day\ hour^{-1}) = \frac{Grain\ yield\ (Kg\ ha^{-1})}{Accumulated\ HTU\ (°C\ day\ hour)}.$$

Daily weather data on maximum and minimum temperatures for the growing season were collected from the nearby Agrometeorological Observatory, Dr. Rajendra Prasad Central Agricultural University, Pusa, Bihar.

Observations on yield attributes, viz., effective tillers per m^{-2}, number of grains per spike, and test weight (1,000-grain), were taken from the net plot area. To determine the test weight of grains, 1,000 seeds from each plot were counted and dried until a constant weight was obtained. The crop was harvested manually with the help of a sickle from the net plot area. After the removal of excess moisture from grains of each plot, the grain yield and straw yield (kg per plot) were recorded after taking weight by open pan electronic balance, which was later converted to Mg ha^{-1}. The harvest index (%) was calculated by dividing economic yield (grain) by the biological yield (grain + straw), as follows:

$$Harvest\ Index\ (\%) = \frac{Economic\ yield\ (Mg\ ha^{-1})}{Biological\ yield\ (Mg\ ha^{-1})} \times 100.$$

Grain filling duration (GFD) was calculated by counting the number of calendar days from 50% flowering to physiological maturity. The grain filling rate (GFR) was calculated by dividing the grain yield (kg ha^{-1}) by GFD (days).

Pearson's correlation coefficients between grain yield, grain filling duration, and its rate, and yield attributes and weather parameters were computed (Gomez and Gomez, 1984). The sum of deviations of maximum and minimum temperatures from optimum thresholds was calculated at critical growth phases for each date of sowing, and based on the largest deviations, heat stress

was identified for the crop sown on different sowing dates. In this study, the sum of deviation from optimum thresholds of maximum temperature and minimum temperature for the sensitive growth phases, viz., flowering to milking and flowering to maturity, was calculated by taking 25°C and 12°C as optimum threshold maximum and minimum temperature, respectively, for flowering to milking (F-Mlk) and 27°C and 14°C as threshold maximum and minimum temperatures for flowering to maturity (F-Mat) stages (Sattar et al., 2020 and Sattar and Srivastava, 2021).

The data on crop phenology, yield, and other parameters were subjected to appropriate statistical analysis through SPSS software (version 17.0), and the significance of mean values was compared using the least significant difference values (Gomez and Gomez, 1984).

Genotype-by-environment (GGE) biplot analysis was carried out using R software version 4.2.3 with the help of the GGE Biplots package to visualize and interpret the multi-environment data and performance of varieties (Saeidnia et al., 2023). Each sowing date was considered a test environment. Accordingly, five test environments were used for testing the varieties. Variety with higher yield and stability, and which-won-where pattern were visualized for studying the higher yield producing variety under different sowing environments.

We also used the CERES-Wheat model (DSSAT v. 4.75) to simulate wheat yields for the years 2050-51 and 2080-81 using the Intergovernmental Panel on Climate Change (IPCC)) AR5 scenario of Representative Concentration Pathway 4.5 (RCP 4.5). Soil data, crop management data, and weather data of the site were used as necessary inputs to run the CERES-Wheat model. For simulation purposes, the model required a set of genetic coefficients pertaining to the phenology and growth of wheat. The genetic coefficients of wheat cultivars, namely, RAU-3711, HD-2824, and HD-2733, were estimated by the genetic sub-model of the DSSAT with repeated interactions until a close match between simulated and observed parameters of phenology and yield was obtained (Table 2). With the use of RCP 4.5, the average projected yield based on these varieties for 2050-51 and 2080-81 is discussed in the article. The yield of wheat varieties grown during 2014–2015 was considered as a baseline for comparison with the projected yield.

3 Results and discussion

3.1 Wheat phenology and grain filling duration under varying sowing environments

The phenological development of a crop is the most important biological footprint of climate change and warming impact. The study of crop phenology has important implications to understand crop response and adaptation to climate change (Tao et al., 2022). In the present study, crop micro-environment as imposed by different dates of sowing significantly influenced thermal days required to achieve different phonological stages, viz., tiller initiation, booting, 50% flowering, milking, dough, and maturity (Tables 3, 4). It extended from 26 to 38, 61 to 79, 82 to 97, 81 to 104, 99 to 132, and 106 to 139 days to reach tiller initiation, booting, 50% flowering, milking, dough, and maturity, respectively, over the experimentation period (2014–2015 to 2016–2017). Many authors (Tao et al., 2012; Li et al., 2021; Tao et al., 2022) opined that the phenology of crops is intricately related to crop management, sowing dates, and cultivars. In the Indo-Gangetic Plains, forced maturity of wheat due to a sudden rise in ambient temperature is common during the post-heading phase of the crop (Ram et al., 2012). Hence, quantification of the exact duration of phenological stages in a particular crop-growing environment and their impact on the yield is very important (Amrawat et al., 2013). This is more pertinent concerning the effect of changing climate on crop phenology (Liu et al., 2018). In the present study, the crop planted on 15 November took 78, 91, 100, 130, and 138 days to achieve booting and 50% flowering, milking, dough, and maturity stages, respectively, which were significantly higher than the rest of the sowing dates. However, the highest days to reach tiller initiation (37) were associated with the crop planted on 25 December (D5), which was significantly higher than the rest of the sowing dates. Days to tiller initiation varied from 27 days in D2 to 37 days in D5 (Table 2). In general, with progress in the date of sowing, tiller initiation was delayed. However, a reverse trend was recorded for days before booting. Tillering stage of the crop sown on later dates

TABLE 2 Genetic coefficient (GC) of wheat varieties.

S. no.	Genetic coefficients	GC of wheat varieties		
		RAU-3711	HD 2824	HD 2733
1.	PIV: days at optimum vernalizing temperature required to complete vernalization	14	17	18
2.	PID: percentage reduction in development rate in a photoperiod 10 h shorter than the threshold relative to the threshold	39	42	44
3.	P5: grain filling (excluding lag) phase duration	535	495	520
4.	PHINT: interval between successive leaf tip appearances	95	95	95
5.	G1: kernel number per unit canopy weight at anthesis (mg/g)	20	22	17
6.	G2: standard kernel size under optimum conditions (mg)	36	37	34
7.	G3: standard non-stressed dry weight (total including grain) of a single tiller at maturity (g)	1.5	1.5	1.5

TABLE 3 Phenology of wheat (thermal days) as affected by sowing environment and cultivars.

Date of sowing (D)	Tiller initiation				Booting				50% Flowering			
	2014–15	2015–16	2016–17	Average	2014–15	2015–16	2016–17	Average	2014–15	2015–16	2016–17	Average
D1	31b	26c	27c	28cd	79a	79a	75a	78a	90a	97a	86a	91a
D2	30b	26c	26c	27d	74b	76b	73b	74b	86b	89b	83b	86b
D3	31b	27bc	30b	29c	69c	69c	73b	70c	78c	79c	82b	80c
D4	37a	28b	31b	32b	66d	65d	66c	66d	76c	74d	79c	76d
D5	38a	35a	36a	37a	61e	65d	61d	62e	72d	75d	73d	73e
Cultivars (C)												
RAU-3711	33	28	30	30ns	67b	70b	69b	69b	77b	82b	79b	79b
HD-2824	34	28	30	31ns	71a	71ab	69b	71a	82a	83a	81a	82a
HD-2733	34	28	30	31ns	71a	72a	70a	71a	81a	83a	82a	82a
D × C	NS	NS	NS	NS	NS	NS	NS	NS	NS	NS	S	NS

Values with at least a common letter down the column are not significantly different from each other according to LSD test ($p< 0.05$).
LSD, least significant difference; S, significant; NS, non-significant; D1, 15 November; D2, 25 November; D3, 5 December; D4, 15 December; D5, 25 December.

encountered lower temperatures. There was a difference of 16 days to complete booting for D1 and D5. Similarly, days to 50% flowering showed a declining trend as that of the booting stage, and D1 took 91 days to attain 50% flowering, which was significantly higher than that of all other dates of sowing. There was a difference of 18 days to reach 50% flowering for D1 and D5. A similar trend was also observed for the milking, dough, and maturity stages. There was a difference of 18, 29, and 30 calendar days to reach the milking, dough, and maturity stages, respectively, between D1 and D5. D1 took 138 days to reach the maturity stage, while all other dates took significantly lower days to reach the maturity stage. The 3-year average data revealed that the duration of different phenophases differed significantly due to cultivars except for tiller initiation (Tables 3, 4). Systematic and accurate records of crop phenological data along with information on cultivars and management practices allow researchers to study the effects of weather on crop productivity based on actual weather data (Tao et al., 2012; Palosuo et al., 2015; Tao et al., 2017). This helps in better understanding the impact of adaptation mechanisms and studying the impact of future climate on crop production. Sattar et al. (2020) reported a reduced duration of crop phenology in response to elevated temperature. Late-sown crops had to encounter higher temperatures during critical phenophases. Out of three cultivars, HD-2733 and HD-2824 registered a similar number of days to complete different phenophases. In contrast, RAU-3711 availed significantly lesser days to attain booting (69), 50% flowering (79), milking (88), dough (114), and maturity (114) stages when compared to HD-2824 and HD-2733.

TABLE 4 Phenology of wheat (thermal days) as affected by sowing environment and cultivars.

Date of sowing (D)	Milking				Dough				Physiological maturity			
	2014–15	2015–16	2016–17	Average	2014–15	2015–16	2016–17	Average	2014–15	2015–16	2016–17	Average
D1	100a	104a	96a	100a	128a	132a	131a	130a	135a	139a	139a	138a
D2	94b	95b	91b	93b	120b	122b	123b	122b	127b	129b	130b	129b
D3	85c	88c	91b	88c	111c	114c	118c	115c	118c	121e	123c	121c
D4	85c	84d	88c	86d	106d	106d	112d	108d	113d	113d	118d	115d
D5	81d	83d	81d	82e	99e	100e	103e	101e	106e	107e	110e	108e
Cultivars (C)												
RAU-3711	86b	91	88b	88b	110b	116a	117	114b	118	123a	123	121c
HD-2824	91a	91	90a	90a	114a	114b	117	115ab	120a	121b	124	122b
HD-2733	90a	91	91a	90a	114a	115ab	118	116a	121a	122ab	125	123a
D × C	NS	NS	NS	NS	NS	NS	NS	NS	NS	S	NS	NS

Values with at least a common letter down the column are not significantly different from each other according to LSD test ($p< 0.05$).
LSD, least significant difference; S, significant; NS, non-significant; D1, 15 November; D2, 25 November; D3, 5 December; D4, 15 December; D5, 25 December.

10.3389/fpls.2023.1224334

Grain filling duration and grain filling rate of wheat were significantly affected during 3 years of experimentation (Table 5). GFD, in general, showed a declining trend with the advancement of sowing dates. D1 had a grain filling duration of 47 days, which was significantly higher than all other dates of sowing. The minimum grain filling duration (34 days) was associated with D5. Delayed sowing beyond D3 significantly reduced the GFD across varieties except for RAU-3711, which gave statistically similar GFD when compared with the highest GFD for 2015–2016. Kheiri et al. (2021) reported that variations in the length of the grain filling period contributed to significant changes in the grain yield of wheat cultivars *Sardari* and *Azar2* in Iran. A 5°C increase in temperature above 20°C increased the rate of grain filling and shortened the grain filling duration by 12 days in wheat (Yin et al., 2009). In this study, the highest GFR for 2014–2015, 2015–2016, and 2016–2017 was recorded with D2 (111 kg ha^{-1} day^{-1}), D3 (55 kg ha^{-1} day^{-1}), and D3 (63 kg ha^{-1} day^{-1}), respectively. The pooled data indicated that the grain filling rate increased up to D3 and then started declining up to D5, implying that wheat yield decreased sharply beyond D3. This might be due to increased thermal load on the crop, which is manifested in terms of higher accumulation of GDD due to delayed sowing. Chen et al. (2018) reported a shortening of the reproductive period due to an increase in GDD and extreme temperature (34°C) degree days (EDD). The highest GFD was recorded with the cultivar RAU-3711 (Table 5), whereas HD-2824 recorded the highest GFR. Exposing the crop to higher temperatures at critical growth phases tends to significantly affect phenophase duration and crop yield (Parya et al., 2010). Poudel et al. (2021) reported that the optimum temperature during the anthesis and grain filling stage ranges from 12°C to 22°C. High temperatures greater than 22°C during anthesis to grain maturity reduced grain yield due to a decrease in grain filling duration (Joshi et al., 2007). Shortening of grain filling duration is a serious problem in wheat owing to higher average temperature during the post-heading period (Lobell et al., 2012; Garg et al., 2013).

3.2 Yield attributes, yield, and harvest index under varying sowing environments

The date of sowing produced a significant effect on the number of effective tillers per m^2. D2 generated the highest number of effective tillers among all the dates of sowing (Table 6). The reduced number of tillers for the crop sown after 25 November might be due to the survival of less number of tillers under high-temperature conditions. Temperature decides the tiller initiation process in the axils of the basal leaves of wheat plants, and under unfavorable thermal regimes, the process of development of tillers either slows down or stops (Rahman et al., 2009). In our study, the impact of heat stress on the number of effective tillers was clearly visible. During 2014–2015, which did not experience any heat stress, effective tillers per m^2 were observed to be the maximum (489.3), which was significantly higher as compared to that of the other two seasons. However, under the unfavorable thermal regime, the effective tillers per m^2 reduced to 285.6 during 2015–2016 (Supplementary Table 1). The highest number of grains per spike was recorded with D3 for average data (Table 6). However, due to variations in temperature regime during the post-heading to grain filling period in different growing seasons, the maximum number of grains per spike was found to differ substantially from year to year. Considering test weight, it showed a declining trend with the advancement of sowing date, perhaps due to increased thermal load on the crop, causing grain shrinkage under the production of reactive oxygen species, reduced pollen tube development, increased pollen mortality, and grain abortion (Nawaz et al., 2013; Dubey et al., 2019). Among the years, the crop during 2014–2015 recorded the highest test weight (40.7 g), which was significantly higher than the other 2 years. The lowest test weight (30.4) was noted during 2015–2016, wherein the crop faced severe heat stress (Supplementary Table 1). In the case of cultivars, the highest number of effective tillers per m^2 was associated with HD-2733 for all the years of experimentation, showing thermo-tolerant

TABLE 5 Effect of sowing environment and cultivars on grain filling duration and rate.

Date of sowing (D)	Grain filling duration (days)				Grain filling rate (kg ha^{-1} day^{-1})			
	2014–15	2015–16	2016–17	Average	2014–15	2015–16	2016–17	Average
D1	45a	42a	53a	47a	90b	53a	53b	66bc
D2	41b	40b	47b	43b	111a	54a	61a	75a
D3	41b	42a	41c	41b	105a	55a	63a	74a
D4	37c	39b	39d	38c	104a	47a	59a	70ab
D5	33d	33c	37e	34d	105a	36b	49b	64c
Cultivars (C)								
RAU-3711	40ns	40a	44ns	42a	94b	50ab	58ns	67b
HD-2824	38ns	39b	43ns	40b	106a	53a	56ns	72a
HD-2733	40ns	39b	42ns	40b	109a	45b	58ns	71ab
D × C	NS	S	NS	NS	NS	NS	S	S

Values with at least a common letter down the column are not significantly different from each other according to LSD test ($p < 0.05$).
LSD, least significant difference; S, significant; NS, non-significant; D1, 15 November; D2, 25 November; D3, 5 December; D4, 15 December; D5, 25 December.

10.3389/fpls.2023.1224334

TABLE 6 Yield attributes of wheat as affected by sowing environment and cultivars.

Date of sowing (D)	Effective tillers per m^2				No. of grains per spike				Test weight (g)			
	2014–15	2015–16	2016–17	Average	2014–15	2015–16	2016–17	Average	2014–15	2015–16	2016–17	Average
D1	431b	330	337a	366a	46a	44	52	47	46.6a	32.0a	33.1a	37.2a
D2	513a	291	298ab	367a	45a	41	49	45	44.4a	32.9a	34.0a	37.1a
D3	474ab	293	290bc	352ab	44ab	46	53	48	41.2b	31.3a	32.3a	34.9a
D4	453ab	239	250c	314b	40bc	45	53	46	38.6b	28.8ab	29.9ab	32.4b
D5	426b	276	284bc	329ab	38c	44	52	45	32.8c	26.9b	27.6b	29.1b
Cultivars (C)												
RAU-3711	411b	286	294ab	331b	45	49a	57a	50a	42.4a	28.8	29.7	33.6
HD-2824	476a	265	267b	336b	42	43b	50b	45b	39.3b	31.6	32.6	34.5
HD-2733	491a	306	313a	370a	42	40b	48b	43b	40.4ab	30.8	31.9	34.4
D × C	NS	NS	S	NS	NS	NS	NS	NS	S	NS	NS	NS

Values with at least a common letter down the column are not significantly different from each other according to LSD test ($p< 0.05$).
LSD, least significant difference; S, significant; NS, non-significant; D1, 15 November; D2, 25 November; D3, 5 December; D4, 15 December; D5, 25 December.

characteristics, and thus, this cultivar resisted the negative impact of seasonal temperature increase on active tillering. Similarly, cultivars caused significant variation in the number of grains per spike except for 2014. Poudel et al. (2020) recorded heat stress-induced reduction in tiller number and spikelets per spike in wheat, resulting in poor grain yield. Higher day length reduced the spikelet number by decreasing the initiation period (Masoni et al., 2001; Arduni et al., 2009). Owing to the differential thermal regime experienced by wheat planted under different sowing windows, grain yield was found to be significantly affected (Table 7). Grain yield increased from D1 to D2/D3 and then declined down to D5 over 3 years of experimentation. For a higher yield of wheat (>4.0 Mg ha^{-1}) in the region, it is necessary that the period from flowering to dough stage must be completed by 15 March, beyond which yield decreases significantly (0.5 Mg ha^{-1} per week) due to high-temperature stress. The optimal and sub-optimal conditions for wheat growth based on yields, normal weather of congenial, and a heat stress year are given in Figure 1. The maximum grain yield was achieved with D2 for 2014–2015 and 2016–2017 (4.55 and 2.87 Mg ha^{-1}, respectively), while D3 gave the highest grain yield for 2015–2016 (2.31 Mg ha^{-1}). Average data of 3 years showed that D2 produced the highest grain yield (3.21 Mg ha^{-1}), 48.61% higher than D5 (2.16 Mg ha^{-1}). Grain yield obtained with D2 and D3 were statistically similar. Among the years, the highest grain yield was observed in 2014–2015 (4.03 Mg ha^{-1}), which was significantly higher than the other 2 years (Supplementary Table 1). However, the lowest grain yield was observed in 2015–2016 (1.96 Mg ha^{-1}). The crop during this year experienced the highest heat stress (Figure 2). Higher grain yield during 2014–2015 compared to the rest of the years could be ascribed to a congenial thermal regime that favored the production of higher effective tillers per m^2 (489.3) and test weight (40.7 g). Dubey et al. (2019) reported yield loss of wheat at New Delhi by 70, 29, and 77 kg ha^{-1} per day due to delay in sowing beyond the first week of November in varieties, viz., HD-2932, WR-544 and HD-2967 respectively. In one study conducted by Poudel et al. (2021), the grain yield of wheat was reduced by 47.6% under heat-stress conditions.

The interaction effect of sowing date and varieties were found significant for grain yield. Hence, genotype plus GGE biplot analysis shows the magnitude and pattern of the genotype–environment interaction effect among the genotypes in a graphical way. It revealed that the first two principal components (PCs) accounted for 70.37% and 28.56% variation of genotype + genotype–environment sum of squares, explaining a total of 98.93% variation (Figures 3, 4). The which-won-where pattern of the interaction between the date of sowing and varieties for grain yield (Figure 3) showed that variety RAU-3711 produced the highest grain yield when sown on 25 November (D2). Similarly, HD-2824 produced the highest grain yield when sown on 5 December (D3) and 15 December (D4). However, HD-2733 produced the highest grain yield when sown on 15 November (D1) and 25 December (D5). The average grain yield and stability performance of varieties are graphically depicted through the average environment coordination method (Figure 4), which helped in identifying the highest-yielding and most stable variety. The single-arrowed line that passes through the origin of the biplot and points toward higher mean values is the AEC abscissa, whereas the other line in the graph depicts the AEC ordinate. The variety farthest from the origin on the positive side of the AEC abscissa has the highest grain yield, and that farthest from the origin on the negative side of the AEC abscissa has the lowest grain yield. Therefore, the variety HD-2824 recorded the highest grain yield followed by HD-2733 and RAU-3711. However, the greater the absolute length of the projection of a variety, the less stable it is. As per Figure 4, the variety RAU-3711 was the most stable among the three varieties.

Straw yield followed a similar trend as grain yield for yearly data, but average data showed both D2 and D3 recorded the same straw yield (5.46 Mg ha^{-1}), which was 30% higher than that of the crop planted on D5 (Table 7). Biological yield (BY) increased from

TABLE 7 Grain yield of wheat as affected by sowing environment and cultivars.

Date of sowing (D)	Grain yield (Mg ha^{-1})				Straw yield (Mg ha^{-1})				Biological yield (Mg ha^{-1})				Harvest index (%)			
	2014–15	2015–16	2016–17	Average	2014–15	2015–16	2016–17	Average	2014–15	2015–16	2016–17	Average	2014–15	2015–16	2016–17	Average
D1	4.06b	2.24a	2.78b	3.03b	6.16a	4.49ab	5.19a	5.28a	10.22bc	6.73a	7.59ab	8.18a	39.96bc	33.21a	38.37	37.18ab
D2	4.55a	2.20a	2.87a	3.21a	6.45a	4.58ab	5.35a	5.46a	10.99a	6.78a	7.70a	8.49a	41.36a	32.46a	39.09	37.64a
D3	4.25ab	2.31a	2.57c	3.04ab	6.19a	4.91a	5.27a	5.46a	10.44ab	7.21a	7.74a	8.46a	40.62ab	32.14a	33.99	35.58bc
D4	3.80c	1.86b	2.30d	2.65c	5.77b	3.92bc	4.64a	4.78b	9.56cd	5.77b	6.63b	7.32b	39.69bc	32.33a	35.08	35.70b
D5	3.49c	1.18c	1.82e	2.16d	5.51b	3.38bc	3.70b	4.20c	9.00d	4.55c	4.96c	6.17c	38.62c	25.83b	36.84	33.76c
Cultivars (C)																
RAU-3711	3.77b	2.04a	2.53a	2.78	5.83b	4.52	5.14	5.16	9.60b	6.56a	7.33a	7.83	39.13b	30.55	36.28	35.32
HD-2824	4.02ab	2.09a	2.42b	2.84	5.85b	4.30	4.82	4.99	9.87b	6.38ab	7.05ab	7.77	40.66a	32.52	35.19	36.12
HD-2733	4.30a	1.74b	2.46b	2.83	6.36a	3.96	4.52	4.95	10.66a	5.69b	6.39b	7.58	40.35a	30.51	38.57	36.48
D × C	NS	S	S	S	S	NS	NS	S	S	S	S	S	S	NS	S	S

Values with at least a common letter down the column are not significantly different from each other according to LSD test ($p < 0.05$).
LSD, least significant difference; S, significant; NS, non-significant; D1, 15 November; D2, 25 November; D3, 5 December; D4, 15 December; D5, 25 December.

10.3389/fpls.2023.1224334

FIGURE 1
Optimal and sub-optimal conditions during flowering to grain filling stage for higher yield of wheat.

D1 to D2/D3 and then declined to D5 over 3 years of experimentation. It followed a similar pattern as that of grain yield, perhaps due to the partitioning of photosynthates synchronized linearly with temperature variation. The highest BY for 2014, 2015, and 2016 and average data was recorded with D2, D3, D3, and D2, respectively. Average data showed that BY increased from D1 to D2 and then started declining. The highest BY was recorded with D2 (8.49 Mg ha^{-1}), which was comparable with that of D3 (8.46 Mg ha^{-1}) and D1 (8.18 Mg ha^{-1}). D2 recorded 37.60% higher BY than D5. Delayed sowing shortens the crop growth duration and, consequently, the amount of radiation interception by the crop canopy. In response to this, biomass and yield tend to decrease significantly for the late-sown crop (Tao et al., 2015). The date of sowing significantly influenced the harvest index during 2014 and 2015 and for average data. For 2014–2015 and average data, it increased till D2, after which it started declining. However, for 2015–2016, it declined with the advancement of sowing dates. The highest harvest index for 2014–2015, 2015–2016, 2016–2017, and average data was recorded with D2, D1, D2, and D2, respectively. Varieties caused significant yield variation during 3 years of experimentation (Table 7). The highest grain yield for 2014–2015, 2015–2016, and 2016–2017 were obtained with HD-2733 (4.30 Mg ha^{-1}), HD-2824 (2.09 Mg ha^{-1}), and RAU-3711 (2.53 Mg ha^{-1}), respectively. Similarly, the straw yield was significantly affected only during 2014–2015, where HD-2733 recorded a significantly higher straw yield (6.36 Mg ha^{-1}) than

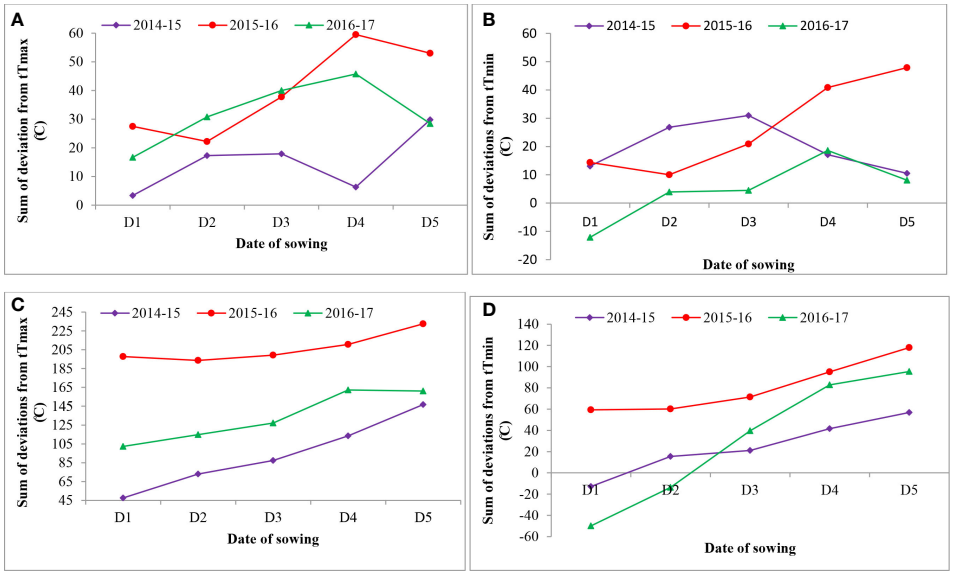

FIGURE 2
Effect of sowing environment on sum of deviations from threshold maximum and minimum temperature from flowering to milking stage **(A, B)** and flowering to maturity stage **(C, D)** in wheat. tTmax, threshold maximum temperature; tTmin, threshold minimum temperature.

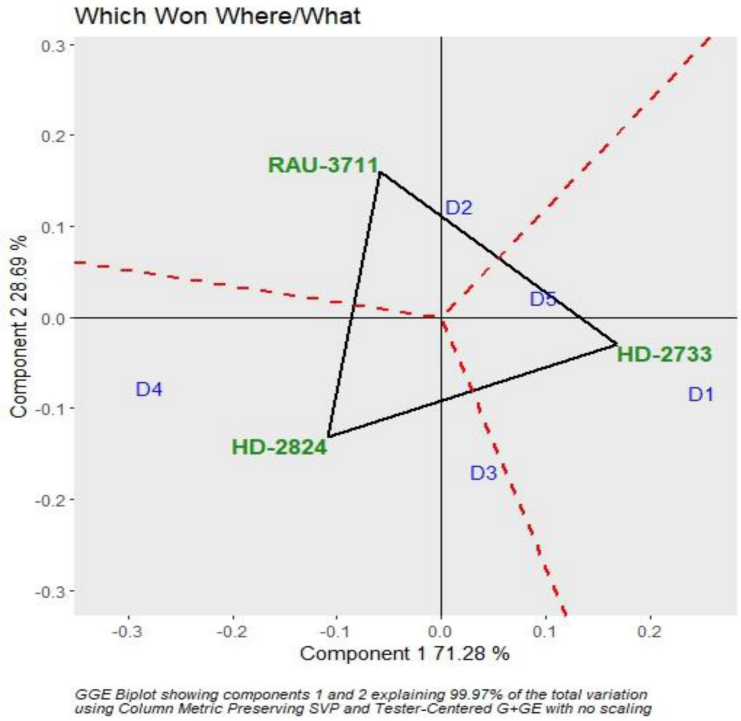

FIGURE 3
Polygon view of GGE biplot depicting varietal performance under various sowing dates. GGE, genotype by environment.

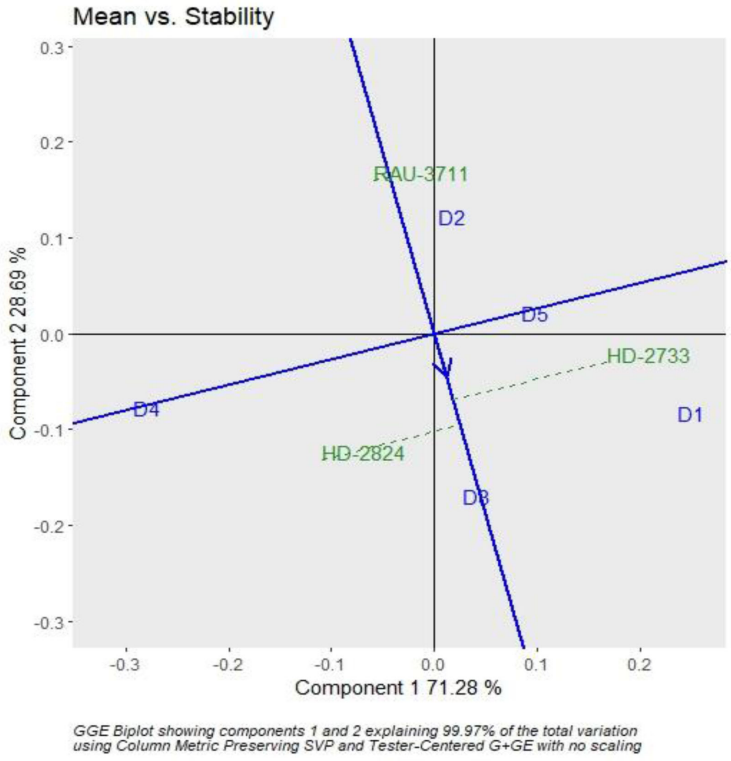

FIGURE 4
GGE biplot depicting the ranking of wheat varieties based on grain yield performance and stability. GGE, genotype by environment.

the other two varieties. The average data showed that the effect of cultivar was non-significant for straw yield. The effect of varieties on BY was significant for 2014–2015, 2015–2016, and 2016–2017. However, for average data, it was non-significant. The highest BY for 2014–2015, 2015–2016, and 2016–2017 was observed with HD-2733, RAU-3711, and RAU-3711, respectively.

Varieties had a non-significant effect on harvest index (HI) except for the years 2014–2015 (Table 7). The highest HI for 2014–2015 was recorded with HD-2824 (40.66), which was comparable with HD-2733 (40.35). Similarly, HD-2824, HD-2733, and HD-2733 recorded the highest HI for 2015–2016, 2016–2017, and average data. When the sowing was delayed beyond 25 November, late-sown crops had to experience higher temperatures during the period of experimentation. HI decreased for later sown crops due to exposure to high temperatures. Dubey et al. (2019) linked the reduction of HI under the late sown condition of wheat with the greenness index and grain filling period under heat stress. High temperature during the grain filling period shrinks the size of grains in wheat apart from reduced grain filling duration (Asseng et al., 2011; Lobell et al., 2012; Tao et al., 2015). In wheat, the period from the onset of spike initiation to flowering is very sensitive to temperature acceleration, and it seems to be the main reason for the reduction in sink size under high-temperature conditions, resulting in poor grain yield (Poudel et al., 2021). However, a normal sowing window provides an opportunity to accumulate more biomass as compared to late sowing due to a longer growing period, which helps produce a higher grain yield (Singh and Pal, 2003; Dar Eajaz et al., 2018).

3.3 Influence of sowing environment on the accumulation of agrometeorological indices

Air temperature modifies the enzymatic functions of plants and causes a change in phenology, which is directly related to yield (Zhu et al., 2018). The effect of temperature on crops can be effectively explained through the GDD concept. Hence, agrometeorological indices, viz., GDDs and photo-thermal index, have great practical significance in evaluating phenology and growth parameters (Streck et al., 2008; Kumar et al., 2010). Sub-optimal photo-thermal regimes during crop growing season have a profound impact on crop yield. Considering heat unit accumulation by wheat sown on different dates, it was observed that accumulated HU varied at 264°C–445°C, 640°C–917°C, 804°C–1,156°C, 926°C–1,269°C, 1,309°C–1,808°C, and 1,456°C–1,960°C days for tiller initiation, booting, 50% flowering, milking, dough, and maturity, respectively, over the experimentation period (Tables 8, 9). The average data showed that the D1 accumulated 408°C, 894°C, 1,056°C, 1,190°C, 1,709°C, and 1,860°C days for completion of tiller initiation, booting, 50% flowering, milking, dough, and maturity stages of wheat, respectively, which were significantly higher than rest of the sowing dates. Similarly, accumulated PTUs and HTU at physiological maturity were found to vary significantly with sowing environments and cultivars (Table 10). In order to harness the maximum benefits of the ambient thermal environment for higher yield, it is vital that sowing is completed at the right time. Inappropriate sowing dates cause varied weather conditions, especially in terms of the thermal requirement and radiation received by the crop canopy. In this context, an agrometeorological index such as GDD integrates phenological behavior with the thermal regime since it has a direct relation with the growth and development of crops (Mishra et al., 2007).

The date of sowing significantly affected HUE during all the years of experimentation (Table 11). HUE increased up to D2 and thereafter declined until D5 during 2014–2015 and 2016–2017, but for 2015–2016 and average data, it increased up to D3 and thereafter declined until D5. PTUE and HTUE were observed to be higher for the crop planted from 25 November to 5 December. Progressive delay in sowing corresponded to an increase in temperature, causing a shortening of the crop growing period leading to lower yield and higher accumulated HU. Dar Eajaz et al. (2018) linked lower thermal use efficiency of delayed sown wheat beyond the optimum window to lower yield under high moisture stress.

3.4 Stress identification and evaluation for adaptation

The sums of deviation from optimum thresholds of maximum temperature and minimum temperature for sensitive growth phases, viz., flowering to milking and flowering to maturity, were correlated with grain filling duration and grain yield to identify the degree of association and impact of heat stress. Data revealed that the sum of deviation from threshold maximum temperature (tTmax) for the F-Mlk period varied between 3.4°C in D1 in 2014–2015 and 59.5°C in D4 in 2015–2016 (Figure 2). The highest sum of deviation from tTmax for the F-Mlk period for 2014–2015, 2015–2016, and 2016–2017 was recorded with D5 (29.8°C), D4 (59.5°C), and D4 (45.8°C), respectively. Late sowing (D4 and D5) had a higher sum of deviation from tTmax during F-Mlk than the crop sown on D1 or D2 or D3 in general. The sum of deviation from threshold minimum temperature (tTmin) for the F-Mlk period varied between −12.1°C in D1 for 2016–2017 and 47.9° C in D5 for 2015–2016 (Figure 2). The highest sum of deviation from tTmin for the F-Mlk period for 2014, 2015, and 2016 was recorded with D3 (31.0°C), D5 (47.9°C), and D4 (18.6°C), respectively. The sum of deviation from tTmax for the F-Mat period varied from 47.6°C in D1 in 2014 to 232.5°C for D5 in 2015 (Figure 2). The highest sum of deviation from tTmax for the F-Mat period for 2014–2015, 2015–2016, and 2016–2017 was recorded with D5 (146.8°C), D5 (232.5°C), and D4 (162.2°C), respectively. Delaying the sowing operation increased the magnitude of the sum of deviation from tTmax for the F-Mat period. Late sowing (D4 and D5) had a higher sum of deviation from tTmax during F-Mat than the crop sown on D1 or D2 or D3. The sum of deviation from threshold minimum temperature (tTmin) for the F-Mat period varied between −49.9°C in D1 for 2016–2017 and 117.9°C in D5 for 2015–2016 (Figure 2). During the wheat growing season of 2008–2009, the accumulated sum of deviation from normal was negatively associated with the grain yield of wheat, and the number of tillers per m^2 was reduced by

TABLE 8 Growing degree day (heat unit) (°C days) at different phenophases of wheat as influenced by sowing environments and cultivars.

Date of sowing (D)	Tiller initiation stage				Booting stage				50% Flowering stage			
	2014–15	2015–16	2016–17	Average	2014–15	2015–16	2016–17	Average	2014–15	2015–16	2016–17	Average
D1	445a	400a	380b	408a	855a	917a	910a	894a	975a	1,156a	1,038a	1,056a
D2	351b	335b	325d	337c	761b	840b	841b	814b	906b	1,031b	961b	966b
D3	315d	281c	334cd	310d	696c	718d	807c	740c	804c	885d	956b	882c
D4	331cd	264d	339c	312d	657d	684e	752d	698d	826c	824e	963b	871c
D5	350bc	341b	394a	362b	640e	755c	712e	702d	817c	933c	912c	887c
Cultivars (C)												
RAU-3711	356	324	351	344	687c	769b	793c	750b	823b	958b	941c	907b
HD-2824	367	324	359	350	747a	786a	803b	779a	893a	964ab	969b	942a
HD-2733	353	325	353	344	732b	793a	817a	781a	880a	975a	989a	948a
D × C	NS	NS	NS	NS	NS	NS	NS	NS	NS	NS	S	NS

Values with at least a common letter down the column are not significantly different from each other according to LSD test ($p< 0.05$).
LSD, least significant difference; S, significant; NS, non-significant; D1, 15 November; D2, 25 November; D3, 5 December; D4, 15 December; D5, 25 December.

30%–35% due to high-temperature stress, lowering grain yield by 25%–30% (Anonymous, 2009). The highest sum of deviation from tTmin for the F-Mat period for 2014–2015, 2015–2016, and 2016–2017 was recorded with D5 (56.9°C, 117.9°C, and 95.4°C, respectively). Like tTmax during F-Mat, late sowing (D4 and D5) produced a higher sum of deviation from tTmin during F-Mat than sowing on D1, D2, or D3. The higher sum of deviation from thresholds due to the occurrence of high temperature during the post-heading period as a result of late sowing tends to accelerate the crop senescence and consequently shorten the duration (Dias and Lidon, 2009; Talukder et al., 2014). The greater the sum of deviation, the higher the heat stress experienced by the crop. This caused grain yield to reduce for later sown crops (beyond 25 November). At sensitive growth stages, such as flowering to milking, greater head load as manifested by the higher accumulation of sum of deviation (SD) enhanced canopy temperature (Siebert and Ewert, 2014), disrupted pollination, and caused pollen sterility, reducing the number of grains, consequently leading to reduced grain yield (Wheeler, 2012; Tao et al., 2015). The plots of maximum and minimum temperatures against the normal during three wheat growing seasons of the experimental period indicated that high temperatures during the reproductive and grain-filling period of wheat led to poor yield and yield attributes during 2015–2016 (Figure 5). For comparison with other years, maximum and minimum temperatures against the normal values are given in Supplementary Figure 1.

The correlation between grain yield, grain filling duration, and its rate and yield attributes with the sum of deviations from

TABLE 9 Growing degree day (heat unit) (°C days) at different phenophases of wheat as influenced by sowing environments and cultivars.

Date of sowing (D)	Milking stage				Dough stage				Physiological maturity stage			
	2014–15	2015–16	2016–17	Average	2014–15	2015–16	2016–17	Average	2014–15	2015–16	2016–17	Average
D1	1,128a	1,269a	1,172a	1,190a	1,574a	1,808a	1,746a	1,709a	1,730a	1,960a	1,890a	1,860a
D2	1,041b	1,132b	1,088b	1,087b	1,461b	1,651b	1,619b	1,577b	1,613b	1,805b	1,769b	1,729b
D3	926d	1,027d	1,086b	1,013c	1,362c	1,538c	1,576e	1,492c	1,512c	1,688c	1,692c	1,630c
D4	954c	1,008e	1,106b	1,022c	1,340c	1,443d	1,558e	1,447d	1,487cd	1,617d	1,707c	1,604d
D5	953c	1,086c	1,029c	1,023c	1,309d	1,451d	1,465d	1,408e	1,456d	1,617d	1,623d	1,565e
Cultivars (C)												
RAU-3711	954c	1,101b	1,076b	1,044b	1,354b	1,590a	1,587	1,510b	1,515b	1,750a	1,727	1,664b
HD-2824	1,033a	1,103a	1,098a	1,078a	1,435a	1,565b	1,590	1,530a	1,577a	1,725b	1,736	1,679ab
HD-2733	1,015b	1,110a	1,114a	1,080a	1,438a	1,579ab	1,601	1,539a	1,587a	1,737ab	1,746	1,690a
D × C	NS	NS	NS	NS	NS	NS	NS	NS	NS	NS	NS	NS

Values with at least a common letter down the column are not significantly different from each other according to LSD test ($p< 0.05$).
LSD, least significant difference; S, significant; NS, non-significant; D1, 15 November; D2, 25 November; D3, 5 December; D4, 15 December; D5, 25 December.

TABLE 10 Effect of sowing environment and cultivars on accumulated PTU and HTU by wheat.

Date of sowing (D)	Accumulated PTU (°C day hour)				Accumulated HTU (°C day hour)			
	2014–15	2015–16	2016–17	Average	2014–15	2015–16	2016–17	Average
D1	19,313a	22,132a	21,377	20,941a	7,809a	10,158a	10,263a	9,410a
D2	18,208b	20,430b	19,976	19,538b	7,207b	9,857b	9,421b	8,828c
D3	17,157c	19,222c	17,525	17,968c	7,147b	9,575c	9,602b	8,775c
D4	17,109c	18,434e	19,610	18,384bc	7,625a	9,642c	10,372a	9,213b
D5	16,848c	18,727d	18,792	18,122c	7,763a	10,014ab	10,268a	9,348a
Cultivars (C)								
RAU-3711	17,191b	19,977a	18,632	18,600	7,218b	9,949a	9,919	9,029b
HD-2824	17,911a	19,585b	19,774	19,090	7,610a	9,746b	9,974	9,110ab
HD-2733	18,079a	19,806a	19,962	19,282	7,703a	9,853ab	10,061	9,206a
D × C	NS	S	NS	NS	NS	NS	NS	NS

Values with at least a common letter down the column are not significantly different from each other according to LSD test ($p< 0.05$).
LSD, least significant difference; PTU, photo-thermal unit; HTU, helio-thermal unit; D1, 15 November; D2, 25 November; D3, 5 December; D4, 15 December; D5, 25 December.

threshold maximum and minimum temperature from flowering to milking stage and flowering to maturity stage in wheat is presented in Figure 6. The correlation study indicated that grain yield was negatively and significantly affected by the sum of deviation (SD) from tTmax for F-Mat (SDTmaxF-Mat) (−0.804***) and the sum of deviation from tTmax for F-Mlk (SDTmaxF-Mlk) (−0.663***) followed by the sum of deviation from tTmin from F-Mat (SDTminF-Mat) (−0.593***). Sattar et al. (2020) observed that maximum temperature, minimum temperature, and bright sunshine hour occurring during 50% flowering to milking and 50% flowering to maturity phases of wheat demonstrated a negative correlation with grain yield.

Similarly, SDTminF-Mat (−0.791***), the sum of deviation from tTmin from F-Mlk (SDTminF-Mlk) (0.592***), SDTmaxF-Mat (−0.436**), and SDTmaxF-Mlk (−0.359*) negatively and significantly impacted the grain filling duration. SDTmaxF-Mat (−0.672***), SDTmaxF-Mlk (−0.56***), and SDTminF-Mat (−0.372*) negatively and significantly impacted the grain filling rate. Liu et al. (2018) observed a significant negative correlation of the phase duration of wheat with mean temperature. Effective tillers per m^2, which positively and significantly affected GY (0.843***), were negatively and significantly affected by SDTmaxF-Mat (−0.62***), SDTmaxF-Mlk (0.594***), and SDTminF-Mat (−0.382**). Test weight, which positively and significantly affected GY (0.822**), was negatively and significantly affected by SDTmaxF-Mat (−0.786***), SDTmaxF-Mlk (−0.723***), and SDTminF-Mat (−0.583***). However, the number of grains per spike did not vary significantly by these

TABLE 11 Effect of sowing environment and cultivars on HUE, PTUE, and HTUE of wheat.

Date of sowing (D)	HUE (kg/°C days)				PTUE (kg/°C day hour)				HTUE (kg/°C day hour)			
	2014–15	2015–16	2016–17	Average	2014–15	2015–16	2016–17	Average	2014–15	2015–16	2016–17	Average
D1	2.34b	1.15b	1.47b	1.65b	0.21b	0.10a	0.13	0.15	0.52b	0.22ab	0.27b	0.34b
D2	2.82a	1.22ab	1.62a	1.89a	0.25a	0.11a	0.14	0.17	0.63a	0.22ab	0.30a	0.39a
D3	2.81a	1.37a	1.52b	1.90a	0.25a	0.12a	0.30	0.22	0.59a	0.24a	0.27b	0.37a
D4	2.55b	1.15b	1.35c	1.68b	0.22b	0.10a	0.12	0.15	0.50bc	0.19b	0.22c	0.30c
D5	2.39b	0.73c	1.12d	1.42c	0.21b	0.06b	0.10	0.12	0.45c	0.12c	0.18d	0.25d
Cultivars (C)												
RAU-3711	2.49b	1.16a	1.46a	1.71	0.22	0.10ab	0.23	0.18	0.53	0.21a	0.26a	0.33
HD-2824	2.56ab	1.20a	1.39b	1.72	0.22	0.11a	0.12	0.15	0.53	0.21a	0.24b	0.33
HD-2733	2.71a	1.00b	1.40b	1.70	0.24	0.09b	0.12	0.15	0.56	0.18b	0.25ab	0.33
D × C	NS	S	S	S	NS	S	NS	NS	NS	S	S	S

Values with at least a common letter down the column are not significantly different from each other according to LSD test ($p< 0.05$).
LSD, least significant difference; HUE, heat use efficiency; PTUE, photo-thermal use efficiency; HTUE, helio-thermal use efficiency; S, significant; NS, non-significant; D1, 15 November; D2, 25 November; D3, 5 December; D4, 15 December; D5, 25 December.

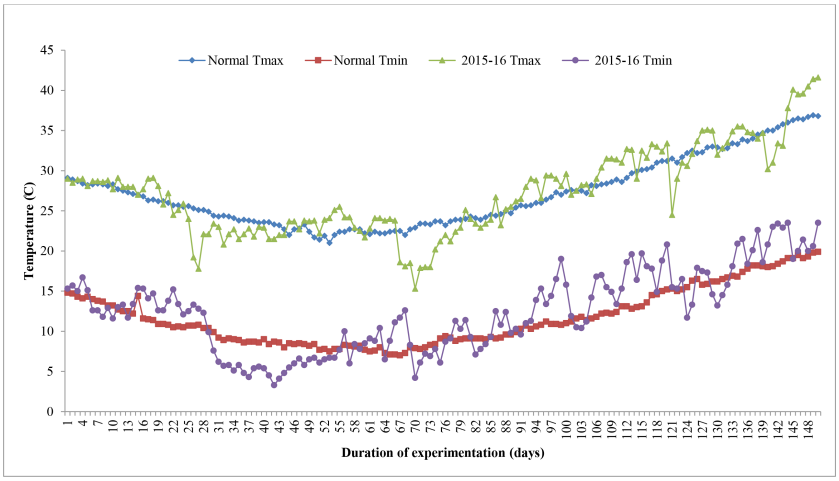

FIGURE 5
Variation of actual maximum temperature (Tmax) and minimum temperature (Tmin) during wheat growing seasons of 2015–2016 along with normal.

deviations SD from tTmax and tTmin, implying that this plant parameter is genetic and is not affected by temperature variation. Arduni et al. (2009) hypothesized that day length affects spikelet initiation and number. From the present study, it was revealed that SDTmaxF-Mat, SDTmaxF-Mlk, and SDTminF-Mat negatively impact the number of effective tillers per m^2, which is one of the most important yield attributes of wheat. Similarly, SDTmaxF-Mat, SDTmaxF-Mlk, and SDTminF-Mat negatively impact test weight and grain filling rate. Similarly, SDTmaxF-Mat, SDTmaxF-Mlk, SDTminF-Mat, and SDTminF-Mlk negatively impact grain filling duration. The strategy should be such that grain filling duration is completed before the onset of critical temperature thresholds of 29°C–30°C (Dubey et al., 2019; Sattar and Srivastava, 2021). In a study conducted by Hatfield et al. (2011), cereal grain yield was found to decrease between 4.1% and 10% due to an increase in the seasonal average temperature by 1° C. In the present study, excess thermal load computed in terms of the cumulative sum of deviation from thresholds provided an important criterion for assessing the impact of thermal stress on crop yield. Tao et al. (2017) highlighted the importance of different impacts of maximum and minimum temperatures during different growth stages of winter wheat, as well as the

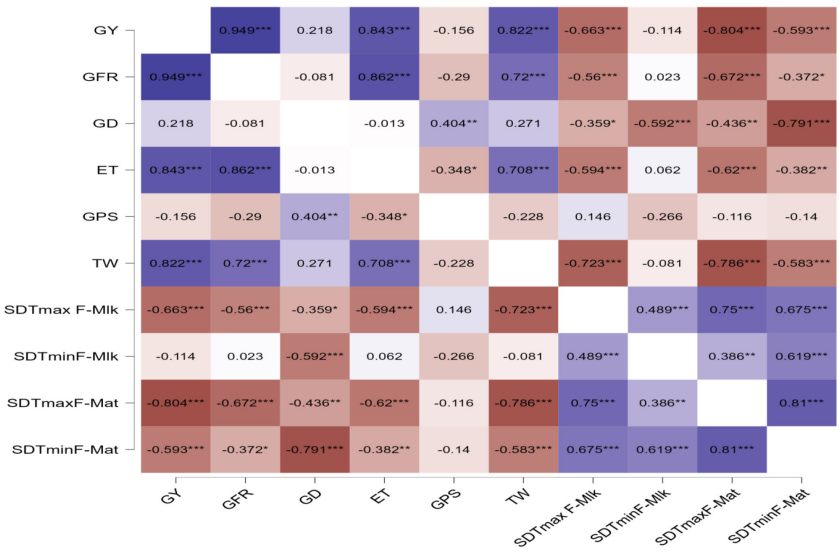

FIGURE 6
Correlation between grain yield, grain filling duration, and its rate and yield attributes with sum of deviations from threshold maximum and minimum temperature from flowering to milking stage and flowering to maturity stage in wheat. * p< 0.05, ** p< 0.01, *** p< 0.001. GY, grain yield; GFR, grain filling rate; GD, grain filling duration; ET, number of effective tillers per m^2; GPS, number of grains per spike; TW, test weight; tTmax, threshold maximum temperature; tTmin, threshold minimum temperature; SDTmaxF-Mlk, sum of deviation from tTmax for F-Mlk; SDTminF-Mlk, sum of deviation from tTmin from F-Mlk; SDTmaxF-Mat, sum of deviation from tTmax for F-Mat; SDTminF-Mat, sum of deviation from tTmin from F-Mat.

importance of management (e.g., shift of sowing date) and cultivars' shift in adapting to climate change in the major wheat growing region.

3.5 Simulating the future yield of wheat by CERES-wheat model

The projected yields of wheat for the year 2050-51 and 2080-81 simulated through the CERES-wheat DSSAT model is presented in Figure 7, which revealed that during 2050-51, the predicted wheat yield will vary from 3.07 to 3.88 Mg ha^{-1} across different sowing dates from 15 November to 25 December. Considering the projected yield for 2080-81, a significant decrease was observed, and it is predicted to range between 2.01 and 3.25 Mg ha^{-1}. For the crop planted during November and December, a decrease in yield by 4.9% to 12.0% and 33.8% to 42.4% is predicted during 2050-51 and 2080-81, respectively (Figure 8). Chhabra and Haris (2014) also reported a decline in wheat yield in the region by 3.6%–13% in 2050 and 14.1%–40% in 2080. The grain yield of wheat was projected to decline in Pakistan by 7%–18% in 2050 and 9%–30% in 2090 under RCP 4.5 (Ishaque et al., 2023). In view of the significant decrease in wheat yield in the future, effective mitigation and adaptation measures will be required to sustain wheat production in the region.

4 Conclusion

The responses of phenology, yield, and yield attributing characters of wheat to differential thermal regimes are critically evaluated in this article, and we found that the crop response did vary significantly across different sowing environments. Excess thermal load computed in terms of the cumulative sum of deviation from critical thresholds provided a useful criterion for assessing the effect of heat stress on wheat yield in association with various agrometeorological indices such as GDDs, HTU, and accumulated PTU. Differential sowing dates generated varied weather patterns especially in terms of the thermal requirement

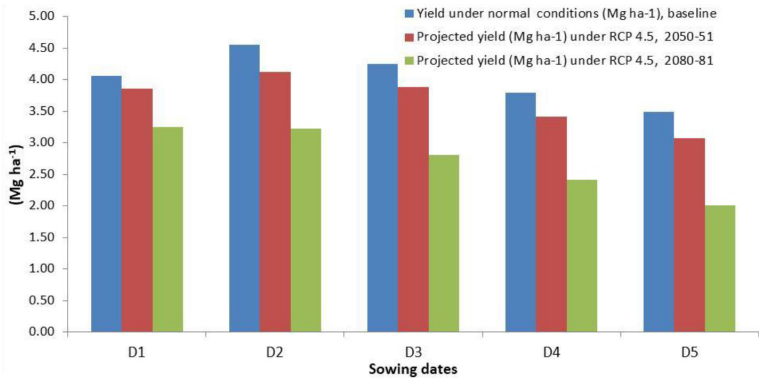

FIGURE 7
Predicted yield of wheat for 2050-51 and 2080-81 on different sowing dates by CERES-Wheat model under RCP 4.5. D1, 15 November; D2, 25 November; D3, 5 December; D4, 15 December; D5, 25 December.

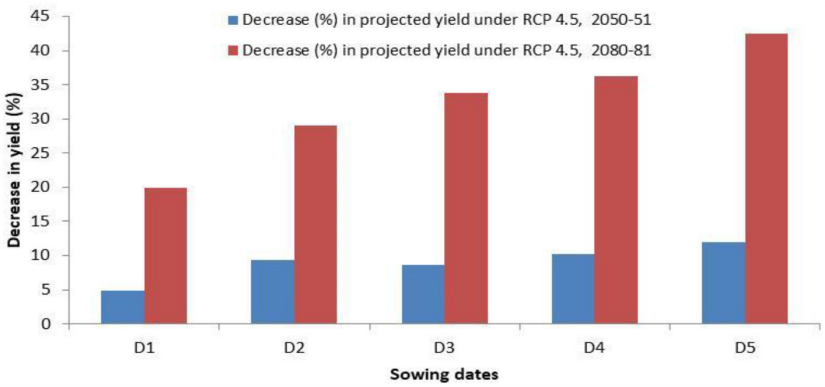

FIGURE 8
Decrease (%) in wheat yield in 2050-51 and 2080-81 on different sowing dates by CERES-Wheat model under RCP 4.5. D1, 15 November; D2, 25 November; D3, 5 December; D4, 15 December; D5, 25 December.

during the growing period of wheat. For a higher yield of wheat (>4.0 Mg ha^{-1}) in the region, it is necessary that grain filling is completed by 15 March, beyond which yield decreases substantially (0.5 Mg ha^{-1} per week) due to high-temperature stress. The optimal and sub-optimal conditions for wheat growth stressed the importance of the manipulation of sowing dates. Hence, it is necessary that wheat is planted at appropriate times for higher productivity. Critical responses of wheat phenology, yield, and yield attributing characters to varying sowing environments indicated that tactical decisions by the wheat growers keeping heat stress in mind would form an important guiding factor for wheat farming. Heat stress during the post-heading period is a serious climatic constraint for successful wheat production in the region. Since wheat growth is very sensitive to temperature, farmers in the area would be advised to finish their wheat planting before 25 November. Accordingly, shifting the planting time from the window of 25 November–10 December, which is usually practiced by 80% of wheat growers of the region to the window as prescribed in this study (i.e., finishing wheat sowing before 25 November), would be an important adaptation option for realizing higher yield and mitigating the negative impact of terminal heat stress on wheat growth and productivity. GGE biplot analysis indicated that RAU-3711 performed better when sown on 25 November (D2), whereas HD-2824 and HD-2733 performed better under 5 December (D3) and 15 December (D4) and 15 November (D1) and 25 December (D5). Wheat yield is predicted to decline significantly in 2050-51 and 2080-81 under RCP 4.5 scenario. Further studies using different models with a range of cultivars and management practices are needed to evaluate the impact of future climate change on wheat yield in the region.

Data availability statement

The original contributions presented in the study are included in the article/Supplementary Material. Further inquiries can be directed to the corresponding author.

Author contributions

Conceptualization: AS. Methodology: AS, GN, SKB. Data curation: AS, GN, GS, SKB. Original draft: AS, GN. Writing, review, and editing: AS, GN, RKJ, SKB, GS. Visualization: AS, GN. All authors contributed to the article and approved the submitted version.

Acknowledgment

The work has been carried out under the All India Coordinated Research Project on Agrometeorology (AICRPAM) funded by the Indian Council of Agricultural Research (ICAR), New Delhi. Sincere thanks are due to the authority of Dr. Rajendra Prasad Central Agricultural University for providing the necessary facilities for carrying out the research under the project.

Conflict of interest

The authors declare that the research was conducted in the absence of any commercial or financial relationships that could be construed as a potential conflict of interest.

Publisher's note

All claims expressed in this article are solely those of the authors and do not necessarily represent those of their affiliated organizations, or those of the publisher, the editors and the reviewers. Any product that may be evaluated in this article, or claim that may be made by its manufacturer, is not guaranteed or endorsed by the publisher.

Supplementary material

The Supplementary Material for this article can be found online at: https://www.frontiersin.org/articles/10.3389/fpls.2023.1224334/full#supplementary-material

References

Amrawat, T., Solanki, N. S., Sharma, S. K., Jajoria, D. K., and Dotaniya, M. L. (2013). Phenology growth and yield of wheat in relation to agrometeorological indices under different sowing dates. *Afr. J. Agricutural Res.* 8 (49), 6366–6374. doi: 10.5897/AJAR2013.8019

Anonymous (2009). *Annual Progress Report, All India Coordinated Research Project on Agrometeorology* Vol. 52 (RAU, Pusa, Bihar: Indian Council of Agricultural Research).

Arduni, I., Ercoli, L., Mariotti, M., and Masoni, A. (2009). Sowing Date Affect Spikelet Number and Grain Yield of Durum Wheat. *Cereal Res. Commun.* 37 (3), 469–478. doi: 10.1556/CRC.37.2009.3.16

Asseng, S., Foster, I., and Turner, N. C. (2011). The impact of temperature variability on wheat yields. *Global Change Biol.* 17, 997–1012. doi: 10.1111/j.1365-2486.2010.02262.x

Bal, S. K., Prasad, J. V. N. S., and Singh, V. K. (2022). *Heat wave 2022 Causes, impacts and way forward for Indian Agriculture* Vol. 50 (Hyderabad, Telangana, India: Technical Bulletin No. ICAR/CRIDA/ TB/01/2022, ICAR-Central Research Institute for Dryland Agriculture).

Bapuji Rao, B., Santhibhushan Chowdary, P., Sandeep, V. M., Pramod, V. P., and Rao, V. U. M. (2015). Spatial analysis of the sensitivity of wheat yields to temperature in India. *Agric. For. Meteorol.* 200, 192–202. doi: 10.1016/j.agrformet.2014.09.023

Chen, Y., Zhang, Z., Tao, F., Palosuot, T., and Rötter Reimund, P.. (2018). Impacts of heat stress on leaf area index and growth duration of winter wheat in the North China Plain. *Field Crops Res.* 222, 230–237. doi: 10.1016/j.fcr.2017.06.007

Chhabra, V., and Haris, A. A. (2014). Temperature Trends and their impact on rabi crops in changing climatic scenario of Bihar. *Sch. J. Agric. Vet. Sci.* 1 (4A), 230–234.

Dar Eajaz, A., Brar, A. S., and Yousuf, A. (2018). Growing degree days and heat use efficiency of wheat as influenced by thermal and moisture regimes, Jour. *Agrometeorol.* 20 (2), 168–170. doi: 10.54386/jam.v20i2.535

Dias, A. S., and Lidon, F. C. (2009). Evaluation of grain filling rate and duration in bread and durum wheat, under heat stress after anthesis. *J. Agron. Crop Sci.* 195, 137–147. doi: 10.1111/j.1439-037X.2008.00347.x

Dubey, R., Pathak, H., Singh, S., Chakraborty, B., Thakur, A. K., and Fagodia, R. K. (2019). Impact of Sowing Dates on Terminal Heat Tolerance of Different Wheat (Triticum aestivum L.) Cultivars. *Natl. Acad. Sci. Lett.* 42, 445–449. doi: 10.1007/s40009-019-0786-7

FAO. (2017). *Food and Agriculture Organization of the United Nations*. Available at: http://FAOSTAT.fao.org.

Farooq, M., Bramley, H., Palta, J. A., and Siddique, K. H. (2011). Heat stress in wheat during reproductive and grain-filling phases. *Crit. Rev. Plant Sci.* 30 (6), 491–507. doi: 10.1080/07352689.2011.615687

Garg, D., Sareen, S., Dalal, S., Tiwari, R., and Singh, R. (2013). Grain filling duration and temperature pattern influence on the performance of wheat genotypes under late planting. *Cereal Res. Commun.* 41, 500–507. doi: 10.1556/CRC.2013.0019

Gomez, K. A., and Gomez, A. A. (1984). *Statistical procedures for agricultural research* (Hoboken: Wiley).

Hatfield, J. L., Boote, K. J., Kimball, B. A., Ziska, L. H., Izaurralde, R. C., Ort, D., et al. (2011). Climate impact on agriculture: implications for crop production. *J. Agron.* 103, 351–370. doi: 10.2134/agronj2010.0303

Hoogenboom, G., Porter, C. H., Shelia, V., Boote, K. J., Singh, U., White, J. W., et al. (2019). *Decision Support System for Agrotechnology Transfer (DSSAT) Version 4.7.5* (Florida, USA: DSSAT Foundation, Gainesville). Available at: https://DSSAT.net.

Ishaque, W., Osman, R., Hafiza, B. S., Malghani, S., Zhao, B., Zu, M., et al. (2023). Quantifying the impacts of climate change on wheat phenology, yield, and evapotranspiration under irrigated and rainfed conditions. *Agric. Water Manage.* 275. doi: 10.1016/j.agwat.2022.108017

Joshi, A. K., Mishra, B., Chatrath, R., Ferrara, G. O., and Singh, R. P. (2007). Wheat improvement in India: present status, emerging challenges and future prospects. *Euphytica* 157 (3), 431–446. doi: 10.1007/s10681-007-9385-7

Kheiri, M., Soufizadeh, S., Moghaddam, S. M., and Ghaffari, A. (2021). Exploring the Impact of Weather Variability on Phenology, Length of Growing Period, and Yield of Contrast Dryland Wheat Cultivars. *Agric. Res.* 10 (4), 556–568. doi: 10.1007/s40003-020-00523-x

Kumar, R., Ramesh, K., Singh, R. D., and Prasad, R. (2010). Modulation of wild marigold (Tagetes minuta L.) phenophases towards the varying temperature regimes - a field study. *J. Agrometeorol.* 12, 234–240. doi: 10.54386/jam.v12i2.1313

Li, L., Wang, B., Feng, P., Wangh, H., He, Q., Wang, Y., et al. (2021). Crop yield forecasting and associated optimum lead time analysis based on multi-source environmental data across China. *Agric. For. Meteorol.* 308-309, 108558. doi: 10.1016/j.agrformet.2021.108558

Liu, Y., Chen, Q., Ge, Q., Dai, J., and Dou, Y. (2018). Effects of climate change and agronomic practice on changes in wheat phenology. *Climate Change* 150, 273–287. doi: 10.1007/s10584-018-2264-5

Lobell, D. B., Sibley, A., and Ortiz-Monasterio, J. I. (2012). Extreme heat effects on wheat senescence in India. *Nat. Clim. Change* 2, 186–189. doi: 10.1038/nclimate1356

Masoni, A., Arduini, I., Mariotti, M., Ercoli, L., and Bonari, E. (2001). Number of spikelets and leaf appearance rate in durum wheat as affected by temperature, daylength and nitrogen availability. *Agricol. Medit.* 131, 57–65.

Mishra, A. K., Tripathi, P., Mishra, S. R., and Kumar, R. (2007). Heat uni requirement of wheat cultivars as affected by moisture application frequencies. *Jour. Agrometeorol.* 2, 295–298. doi: 10.54386/jam.v9i2.1147

Nawaz, A., Farooq, M., Cheema, S. ,. A., and Wahid, A. (2013). Differential response of wheat cultivars to terminal heat stress. *Int. J. Agric. Biol.* 15, 1354–1358.

Nuttonson, M. Y. (1955). *Wheat climate relationship and the use of phenology in ascerting the thermal and photo thermal requirement of wheat* Vol. 388 (Washington DC, USA: American Institute of crop ecology).

Palosuo, T., Rötter, R. P., Salo, T., Peltonen-Sainio, P., Tao, F., and Lehtonen, H. (2015). Effects of climate and historical adaptation measures on barley yield trends inFinland. *Clim. Res.* 65, 221–236. doi: 10.3354/cr01317

Parya, M., Nath, R., Mazumder, D., and Chakraborty, P. K. (2010). Effect of thermal stress on wheat productivity in West Bengal, Jour. *Agrometeorol.* 12 (2), 217–220. doi: 10.54386/jam.v12i2.1309

Poudel, M. R., Ghimire, S., Pandey, M. P., Krishnahari, D., Bahadur, T. D., Paudel, H. K., et al. (2020). Evaluation of wheat genotypes under irrigated, heat stress and drought conditions. *J. Biol. Today's World* 9 (1), 1–3.

Poudel, P. B., Poudel, M. R., and Puri, R. R. (2021). Evaluation of heat stress tolerance in spring wheat (Triticum aestivum L.) genotypes using stress tolerance indices in western region of Nepal. *J. Agric. Food Res.* 5, 100179. doi: 10.1016/j.jafr.2021.100179

Rahman, M. ,. A., Chikushi, J., Yoshida, S., and Karim, A. J. M. S. (2009). Growth and yield components of wheat genotypes exposed to high temperature stress under control environment. *Bangladesh J. Agric. Res.* 34 (3), 360–372.

Ram, H., Singh, G., Mavi, G. S., and Sohu, V. S. (2012). Accumulated heat unit requirement and yield of irrigated wheat (Triticum aestivum L.) varieties under different crop growing environment in central Punjab. *J. Agrometeorol.* 14, 147–153. doi: 10.54386/jam.v14i2.1414

Saeidnia, F., Taherian, M., and Nazeri, S. M. (2023). Graphical analysis of multi-environmental trials for wheat grain yield based on GGE-biplot analysis under diverse sowing dates. *BMC Plant Biol.* 23, 198. doi: 10.1186/s12870-023-04197-9

Sandhu, S. S., Prabhjyot-Kaur, T. ,. P., Patel, S. R., Rajinder, P., Solanki, N. S., Ramesh., K., et al. (2016). Effect of intra-seasonal temperature on wheat at different locations of India: A study using CERES-Wheat model. *J. Agrometeorol.* 18 (2), 222–233. doi: 10.54386/jam.v18i2.939

Sastry, P. S. N., and Chakravarty, N. K. (1982). Energy summation indices for wheat crop in India. *Agric. Meteorol.* 27 (1-2), 45–48. doi: 10.1016/0002-1571(82)90018-8

Sattar, A., Singh, G., Singh, S., Kumar, M., Kumar, P. V., and Bal, S. K. (2020). Evaluating temperature thresholds and optimizing sowing dates of wheat in Bihar. *J. Agrometeorol.* 22 (2), 158–164. doi: 10.54386/jam.v22i2.156

Sattar, A., and Srivastava, R. C. (2021). Modelling climate smart rice-wheat production system in the middle Gangetic plains of India. *Theor. Appl. Climatology* 144, 77–91. doi: 10.1007/s00704-020-03497-6

Shen, H., Wang, Yu., Jiang, K., Li, S., Huang, D., Wu, J., et al. (2022). Simulation modeling for effective management of irrigation water for winter wheat Agricultural. *Water Manage* 269. doi: 10.1016/j.agwat.2022.107720

Siebert, S., and Ewert, F. (2014). Future crop production threatened by extreme heat. *Environ. Res. Lett.* 9, 041001. doi: 10.1088/1748-9326/9/4/041001

Singh, M., and Khushu, M. K. (2012). Growth and yield prediction of wheat in relation to agroclimatic indices under irrigated and rainfed condition. *J. Agrometeorol.* 14 (1), 63–66. doi: 10.54386/jam.v14i1.1386

Singh, S., and Pal, M. (2003). Growth, yield and phonological response of wheat cultivars to delayed sowing. *Indian J. Plant Physiol.* 8, 277–287.

Singh, A. K., Tripathi, P., and Mishra, S. R. (2001). Phenology, growing degree-days and phasic development model of wheat under rice-wheat cropping system. *Ind. J. Agril. Sci.* 71 (6), 363–366.

Streck, N. A., Lago, I., Gabriel, L. F., and Samboranha, F. K. (2008). Simulating maize phenology as a function of air temperature with a linear and a nonlinear model. *Pesquisa Agropecuária Bras.* 43, 449–455. doi: 10.1590/S0100-204X2008000400002

Talukder, A. S. M. H., Mcdonald, G. K., and Gill, G. S. (2014). Effect of short-term heat stress prior to flowering and early grain set on the grain yield of wheat. *Field Crop Res.* 160, 54–63. doi: 10.1016/j.fcr.2014.01.013

Tao, F., Xiao, D., Zhang, S., Zhang, Z., and Rotter, R. P. (2017). Wheat yield benefited from increases in minimum temperature in theHuang-Huai-Hai Plain of China in the past three decades. *Agric. For. Meteorol.* 239, 1–14. doi: 10.1016/j.agrformet.2017.02.033

Tao, F. L., Zhang, S., and Zhang, Z. (2012). Spatiotemporal changes of wheat phenology in China under the effects of temperature, day length and cultivar thermalcharacteristics. *Eur. J. Agron.* 43, 201–212. doi: 10.1016/j.eja.2012.07.005

Tao, F., Zhang, L., Zhang, Z., and Chen, Y. (2022). Climate warming outweighed agricultural managements in affecting wheat phenology across China during 1981-2018. *Agric. For. Meteorol.* 316, 108865. doi: 10.1016/j.agrformet.2022.108865

Tao, F., Zhao, Z., Shuai, Z., and Reimund, R. (2015). Heat stress impacts on wheat growth and yield were reduced in theHuang-Huai-Hai Plain of China in the past three decades Europ. *J. Agron.* 71, 44–52. doi: 10.1016/j.eja.2015.08.003

Vashisth, A., Goyal, A., and Krishnan, P. (2020). Effect of weather variability on growth and yield of wheat crop under semi-arid region of India. *J. Agrometeorol.* 22 (2), 124–131. doi: 10.54386/jam.v22i2.152

Vijaya, K. P., Rao, V. U. M., Bhavani, O., Dubey, A. P., Singh, C. B., and Venkateswarlu, B. (2015). Sensitive growth stages and temperature thresholds in wheat (Triticum aestivum L.) for index-based crop insurance in the Indo-Gangetic Plains of India *J. Agric. Sci.*, 154 (2), 321–333. doi: 10.1017/ S0021859615000209

Wang, J., Wang, E., Feng, L., Yin, H., and Yu, W. (2013). Phenological trends of winter wheat in response to varietal and temperature changes in the North China Plain. *Field Crops Res.* 144(2013), 135–144. doi: 10.1016/j.fcr.2012.12.020

Wang, J., Wang, E., Yang, X., Zhang, F., and Yin, H. (2011). Increased yield potential of wheat–maize cropping system in the North China Plain by climate change adaptation. *Climat Change* 113, 825–840. doi: 10.1007/s10584-011-0385-1

Wheeler, T. (2012). Wheat crops feel the heat. *Nat. Clim. Change* 2, 152–153. doi: 10.1038/nclimate1425

Xiao, D., Tao, F., Liu, Y., Shi, W, Wang, M, Liu, F, et al. (2013). Observed changes in winter wheat phenology in the North China Plain for 1981–2009. *Int. J. Biometeorol.* 57 (2), 275–285. doi: 10.1007/s00484-012-0552-8

Xiao, D., Tao, F., Liu, Y., Shi, W., Wang, M., Liu, F, et al. (2012). Observed changes in winter wheat phenology in the North China Plain for 1981–2009. *Int. J. Biometeorol* 57, 275–285. doi: 10.1007/s00484-012-0552-8

Yin, X., Guo, W., and Spiertz, J. H. (2009). Aquantitative approach to characterizesink—source relationships during grain filling in contrasting wheat genotypes. *Field Crops Res.* 114, 119–126. doi: 10.1016/j.fcr.2009.07.013

Zhu, P., Jin, Z., Zhuang, Q., Ciais, P., Bernacchi, C., Wang, X., et al. (2018). The important but weakening maize yield benefit of grain filling prolongation in the US Midwest. *Glob. Change Biol.* 24, 4718–4730. doi: 10.1111/gcb.14356

frontiers | Frontiers in Plant Science

TYPE Original Research
PUBLISHED 02 August 2023
DOI 10.3389/fpls.2023.1165113

OPEN ACCESS

EDITED BY
Shuvasish Choudhury,
Assam University, India

REVIEWED BY
Elsayed Mansour,
Zagazig University, Egypt
Owais Ali Wani,
Sher-e-Kashmir University of Agricultural Sciences and Technology of Kashmir, India
Jiban Shrestha,
Nepal Agricultural Research Council, Nepal

*CORRESPONDENCE
Ahmed M. S. Elfanah
ahmed.elfanah@arc.sci.eg
Magdi T. Abdelhamid
magdi.elsayed@ag.tamu.edu

RECEIVED 13 February 2023
ACCEPTED 07 July 2023
PUBLISHED 02 August 2023

CITATION
Elfanah AMS, Darwish MA, Selim AI, Elmoselhy OMA, Ali AM, El-Maghraby MA and Abdelhamid MT (2023) Hyperspectral reflectance and agro-physiological traits for field identification of salt-tolerant wheat genotypes using the genotype by yield*trait biplot technique. *Front. Plant Sci.* 14:1165113. doi: 10.3389/fpls.2023.1165113

Hyperspectral reflectance and agro-physiological traits for field identification of salt-tolerant wheat genotypes using the genotype by yield*trait biplot technique

Ahmed M. S. Elfanah[1,2]*, Mohamed A. Darwish[1], Adel I. Selim[3], Omnya M. A. Elmoselhy[1], Abdelraouf M. Ali[3,4], Maher A. El-Maghraby[1] and Magdi T. Abdelhamid[5,6]*

[1]Wheat Research Department, Field Crops Research Institute, Agricultural Research Center, Giza, Egypt, [2]Food Crops Research Institute, Yunnan Academy of Agricultural Sciences, Kunming, China, [3]National Authority for Remote Sensing and Space Sciences (NARSS), Cairo, Egypt, [4]Department of Environmental Management, Institute of Environmental Engineering, People's Friendship University of Russia (RUDN University), Moscow, Russia, [5]Botany Department, National Research Centre, Cairo, Egypt, [6]Department of Soil and Crop Sciences, Texas A&M University, College Station, TX, United States

Introduction: Salinity is the abiotic obstacle that diminishes food production globally. Salinization causes by natural conditions, such as climate change, or human activities, e.g., irrigation and derange misuse. To cope with the salinity problem, improve the crop environment or utilize crop/wheat breeding (by phenotyping), specifically in spread field conditions. For example, about 33 % of the cropping area in Egypt is affected by salinity.

Methods: Therefore, this study evaluated forty bread wheat genotypes under contrasting salinity field conditions across seasons 2019/20 and 2020/21 at Sakha research station in the north of Egypt. To identify the tolerance genotypes, performing physiological parameters, e.g., Fv/Fm, CCI, Na+, and K+, spectral reflectance indices (SRIs), such as NDVI, MCARI, and SR, and estimated salinity tolerance indices based on grain yield in non-saline soil and saline soil sites over the tested years. These traits (parameters) and grain yield are simultaneously performed for generating GYT biplots.

Results: The results presented significant differences ($P \leq 0.01$) among the environments, genotypes, and their interaction for grain yield (GY) evaluated in the four environments. And the first season for traits, grain yield (GY), plant height (PH), harvest index (HI), chlorophyll content index (CCI), chlorophyll fluorescence parameter Fv/Fm, normalized difference vegetation index (NDVI) in contrasting salinity environments. Additionally, significant differences were detected among environments, genotypes, and their interaction for grain yield along with spectral reflectance indices (SRIs), e.g., Blue/Green index (BIG2), curvature index (CI), normalized difference vegetation index (NDVI), Modified simple ratio (MSR). Relying on the genotype plus genotype by environment (GGE) approach,

genotypes 34 and 1 are the best for salinity sites. Genotypes 1 and 29 are the best from the genotype by stress tolerance indices (GSTI) biplot and genotype 34. Genotype 1 is the best from the genotype by yield*trait (GYT) method with spectral reflectance indices.

Discussion: Therefore, we can identify genotype 1 as salinity tolerant based on the results of GSTI and GYT of SRIs and recommend involvement in the salinity breeding program in salt-affected soils. In conclusion, spectral reflectance indices were efficiently identifying genotypic variance.

KEYWORDS

salinity tolerance indices, bread wheat, GGE biplots, GYT biplots, physiological traits, hyperspectral reflectance indices

1 Introduction

Soil salinity is an abiotic stressor and is considered one of the biggest obstacles to decreasing food production globally (Sardouie-Nasab et al., 2014; Tao et al., 2021; Quamruzzaman et al., 2022), impeding the breeding and releasing of cultivars (Bailey-Serres et al., 2019; Reynolds and Braun, 2022). It impacts more than 20%–40% of irrigated land (Ghonaim et al., 2021; Quamruzzaman et al., 2022). About 33% of the cropping area in Egypt is affected by salinity (Stavi et al., 2021; Morsy et al., 2022). Salinization is caused by either natural conditions (climate change) or human activities (anthropogenic, such as irrigation misuse) (Shabala et al., 2014; Stavi et al., 2021; Morsy et al., 2022). Reusing about 10 billion m^3 of drainage water is considered a salinization source to increase soil salinity and reflects the limited water resources in Egypt (Mohamed, 2017). Hence, salinity is coped with through either crop environment management or crop improvement (breeding) (Rady et al., 2016; Alharbi et al., 2021; Morsy et al., 2022).

Wheat (*Triticum aestivum* L.) is a dominant cultivated cereal crop worldwide that has a role to play in food security. It contributes approximately 20% of human calories and protein (Reynolds and Braun, 2022). The total production is about 750 million tons annually. Nearly 9 million tons in Egypt is produced from 1.3 million hectares of wheat-cultivated areas (FAOSTAT, 2021). Breeding for stress tolerance acquires whether select tolerant genotype or maintenance of the environmental factors, such as reclamation of the soil, for example, adding gypsum to the soil (Stavi et al., 2021; Morsy et al., 2022), application of potassium fertilizer to enhance the salt-tolerance (Dawood et al., 2014), foliar spray of glutathione as an antioxidant with an organic biostimulant to improve the physiological and metabolic adaptation to salinity (ur Rehman et al., 2021) or improving wheat under biotic stress such as disease (Msundi et al., 2021), drought stress (Schneider et al., 1997; Abdelhakim et al., 2021), and salinity stress (Aycan et al., 2021; Ghonaim et al., 2021; Moustafa et al., 2021). In contrast, the selection (phenotyping) for stress tolerance purposes relies on the integration of multiple disciplines, not only agronomic traits (grain yield) but also physiological traits (Na^+ and K^+) (Oyiga et al., 2016; Tao et al., 2021) and hyperspectroscopic measurements (normalized difference vegetation index (NDVI) (Ali et al., 2018; Moghimi et al., 2018; Bruning et al., 2020). Salinity tolerance is a complex phenomenon controlled by several physiological traits and processes and genetic factors (Gizaw et al., 2018) and influenced by growth stages and open field conditions (Haq et al., 2010; Moghimi et al., 2018; Bruning et al., 2020). For breeding for wheat saline soil tolerance purposes, Sardouie-Nasab et al. (2014) reported field screening for 100 bread wheat genotypes under saline and non-saline conditions to identify tolerant genotypes utilizing salt tolerance indices (STIs) and principal component analysis (PCA). Moreover, several researchers (Hinojosa et al., 2019; Mohammadi et al., 2022) have screened a large set of genotypes and then selected appropriate genotypes for field stress evaluation.

Remote sensing technologies and spectral instruments create valuable spectral information in many wavelength bands throughout the electromagnetic spectrum, particularly visible, near-infrared, and shortwave, and provide spectral reflectance indices. These approaches are powerful tools for identifying chemical and physical plant structures and functions and are considered rapid, high-throughput, non-destructive, and accurate plant vegetation measurements (Reynolds et al., 2012; Sun et al., 2019; Bruning et al., 2020). Additionally, these techniques utilize spectral reflectance indices (SRIs) and phenotypic data (Gizaw et al., 2018). Plant phenotyping under field conditions and based on SRIs enables breeders to select improved vigorous and high-yielding genotypes (Hinojosa et al., 2019). Spectral reflectance indices assist in exploring various traits of plant vigor and performance and rely on visible (400–700 nm wavelength) and near-infrared spectra (>700 nm wavelengths), which are employed in plant phenotyping and screening, for example, NDVI (Santana et al., 2021), leaf greenness, and pigment abundance (Reynolds et al., 2012; Hinojosa et al., 2019). For instance, several vegetation indices were calculated based on canopy spectral properties, particularly for plants under stress, indicating agro-morphological traits indirectly (El-Hendawy et al., 2019), and the SRIs correlated with genotype Sakha 93 more than Sakha 61 for growth and grain yield. Sun et al. (2019) reported that applying canopy reflectance in

winter wheat changed the canopy water content in different water regimes.

Physiological traits measured by instruments such as chlorophyll fluorescence are estimated as the Fv/Fm ratio (Hinojosa et al., 2019), and the chlorophyll content index (CCI) has been confirmed in plant phenotyping as a physiological trait measured by Opti-Sciences OS30p+ and Opti-Sciences CCM 200+ devices, respectively. For example, photosynthetic parameters decrease under saline conditions, which benefits the selection of salinity-tolerant genotypes (Munns and Gilliham, 2015; Tao et al., 2021). Additionally, Wu et al. (2015) pointed out the positive correlation between chlorophyll content and plant salt tolerance in barley and wheat (Tao et al., 2021). They reported that detecting chlorophyll fluorescence in the early growth stage is beneficial to preventing plant biomass loss under high-salinity treatment (El-Hendawy et al., 2019). In addition, researchers have reported that genotype selection based on genotype by trait (GT) biplots, including soil plant analysis development (SPAD) reading with agronomic traits, is an effective tool (Mohammadi, 2019; Kendal, 2020; Mohammadi and Amri, 2021). Salinity stress negatively influences chlorophyll fluorescence (Zarco-Tejada et al., 2003; Kalaji and Guo, 2008). On the other hand, physiological traits estimated in the laboratory that reflect a salinity-tolerant genotype include minimal Na^+ concentration, higher K^+ accumulation perfectly maintaining osmotic pressure in roots and shoots, and maximal photosystem (PSII) activities, resulting in producing higher biomass specifically under salinity stress (Oyiga et al., 2016; Morsy et al., 2022; Quamruzzaman et al., 2022).

STIs are used extensively in breeding programs (Sardouie-Nasab et al., 2014; Sabouri et al., 2022), and several applications compute them, such as *i*PASTIC (Pour-Aboughadareh et al., 2019). This online software generates several selection parameters, e.g., tolerance index (TOL) (Rosielle and Hamblin, 1981), mean productivity stress (MP) (Rosielle and Hamblin, 1981), STI (Fernandez, 1992), geometric mean productivity (GMP) (Fernandez, 1992), harmonic mean (HM) (Bidinger et al., 1987), stress susceptibility index (SSI) (Fischer and Maurer, 1978), yield index (YI), yield stability index (YSI) (Bouslama and Schapaugh, 1984), and relative stress index (Fischer and Wood, 1979). In addition, the combination of significant indices (CSI) (Sabouri et al., 2022) is proposed based on calculated means in contrasting conditions such as irrigated and non-irrigated environments. These parameters assist the breeders in selecting tolerant genotypes in cases studied to generate PCA, GT, and genotype by yield*trait (GYT) biplots (Sabouri et al., 2022; Bakhshi and Shahmoradi, 2023) for several crops.

The beneficial use of SRIs in wheat breeding programs is essential to recognize their relationship with agronomic traits (Santana et al., 2021). The GT and GYT biplot approaches (Yan et al., 2007; Yan and Frégeau-Reid, 2018; Darwish et al., 2023; Elfanah et al., 2023) allow breeders and statisticians to distinguish the correlation of traits and combinations, as well as the genotype rank and stability of these traits or GYT combinations. Furthermore, these biometrical techniques for identifying stress-tolerant genotypes rely on STIs. For example, GT, GYT, and genotype by yield*STI (GYSI) were employed to select barley drought-tolerant genotypes (Bakhshi and Shahmoradi, 2023), wheat breeds for stress tolerance (Mohammadi, 2019; Msundi et al., 2021; Zulfiqar et al., 2021), and other crops such as rice breeds for drought (Sabouri et al., 2022), barley (Kendal, 2020; Bakhshi and Shahmoradi, 2023), common bean genotypes (Sofi et al., 2022), and soybean (Kurbanov et al., 2023). Moreover, the GT model with SRIs in corn treated with nitrogen levels to identify trait relationships was used (Santana et al., 2021).

This study selected 40 elite genotypes based on evaluation of the previous season in multi-location trials. The selected genotypes were assessed in multisite and multi-season open fields under saline soil and non-saline conditions. The estimated characteristics were agronomic traits, physiological traits, STI computing parameters, and SRI. This study aims i) to evaluate and characterize 40 genotypes under saline and non-saline conditions to select salinity-tolerant genotypes and ii) to measure GYT using SRIs to assist wheat breeders in selecting genotypes positively correlated with grain yield to recommend the release of a new variety or to include it in a breeding program.

2 Materials and methods

2.1 Plant materials and experimental site

There were 40 genotypes selected from a local breeding program and exotic materials of CIMMYT yield trials, e.g., 39th ESWYT, 26th SAWYT, 26th HRWYT, and 8th SATYN (evaluated in multiple locations in Egypt in the 2017/18 season). These genotypes comprised 38 advanced breeding lines evaluated with two recently released cultivars, Misr 3 and Sakha 95, shown in Table S1.

Two separate field trials were carried out at the Sakha Agricultural Research Station, Kafr El-Sheikh, Egypt (latitude 31°5′ N and longitude 30°56′E) in two successive cropping seasons, viz., 2019/2020 and 2020/2021. The Elhamrawy farm (part of the Sakha Agricultural Research Station) possesses saline soil with heavy clay (electrical conductivity (EC) ranging from 8.0 to 10.0 dS m^{-1}), which could be classified as strongly saline soil. In addition, the Elnataf farm (another part of the Sakha Agricultural Research Station) is non-saline soil with heavy clay (EC ranging from 0.5 to 1.5 dS m^{-1}), which could be classified as non-saline soil. Both experiments were irrigated with fresh water from an irrigation channel from the River Nile passing through the experimental area with pH 7.35 and EC of 0.41 dS m^{-1} using a surface irrigation system. Each experiment received five irrigations per season.

There were 40 genotypes planted in an alpha lattice experimental design with three replicates. Each plot consisted of six rows, 20 cm apart and 3.0 m long. Furthermore, the recommended phosphorus fertilizer dose was 35 kg P ha^{-1} before wheat sowing. At the same time, nitrogen fertilizer was added as 180 kg N ha^{-1} at each environment's sowing and tillering stage. The sowing date was in

TABLE 1 Some chemical characteristics of soil in non-saline soil and saline soil at the experimental sites before sowing in the 2019/2020 and 2020/2021 seasons.

1111	EC	pH	SAR	Soluble cations Meq/L				Soluble anions Meq/L			
	(dS/m)	(1:2.5)		Na^+	Ca^{++}	Mg^{++}	K^+	CO_3^-	HCO_3^-	Cl^-	SO_4^{2-}
Non-saline/2020/2021	1.50	7.32	–	26.9	8.43	4.0	4.5	0.0	3.0	20.2	20.6
Saline/2019/2020	10.21	7.81	15.73	62.5	18.9	15.8	1.1	0.0	4.1	49.5	44.7
Saline/2019/2020	8.81	7.79	12.92	56.6	14.3	11.7	0.7	0.0	4.0	41.8	37.5
Saline/2020/2021	10.11	7.86	16.21	68.2	20.5	14.9	0.9	0.0	6.1	50.8	47.6
Saline/2020/2021	8.26	7.80	14.58	56.2	17.2	12.5	0.8	0.0	6.2	42.3	38.2

EC, the electrical conductivity of saturated extracts used (EC_e); pH, soil acidity; SAR, sodium adsorption ratio.

the third week of November. These procedures are according to the Ministry of Agriculture, and Land Reclamation, Egypt. Some chemical characteristics of saline soil and non-saline sites in the 2019/2020 and 2020/2021 seasons are shown in Table 1.

2.2 The first season measured traits

The agronomic traits measured were days to maturity (DM), days to heading (DH), plant height (PH), number of spikes m^{-1} (SM), biomass or biological yield (BY), and grain yield (GY) kg h^{-1}. Canopy temperature (CT) was obtained using a near-infrared temperature sensor (CEM DT 8835 infrared and K-type thermometer) at the completed flowering stage of each plot from 1:00 p.m. to 2:00 p.m. on a cloudless day. NDVI was measured by a field portable NDVI sensor (GreenSeeker® handheld crop sensor, Trimble Navigation Limited, Westminster, CO, USA). NDVI was measured between 11:30 a.m. and 2:00 p.m. The CCI was determined by a chlorophyll content meter (Opti-Sciences, Inc., CCM 200 plus) from the blade flag leaf (three readings per plot) at a completed flowering stage between 11 a.m. to 2 p.m. on a sunny day. Chlorophyll fluorescence (Fv/Fm) was estimated by a portable chlorophyll fluorometer (Opti-Sciences, $OS30p_+$).

2.3 The second season measured traits

The agronomic traits measured were GY kg h^{-1}. Additionally, the flame apparatus measured flag leaf concentrations of Na^+ and K^+. The leaf samples were collected from each plot at the end of the flowering stage. Furthermore, CT was measured as mentioned in the first season.

2.4 Spectroscopic measurements

2.4.1 Spectral device

The hyperspectral reflectance of the wheat canopy was measured using a portable backpack ASD spectroradiometer (Analytical Spectral Devices Inc., Boulder, CO, USA), which captured the reflectance from 350 to 2,500 wavelength using an optical fiber probe. The measurement was within ±2 h of solar noon under cloudless conditions. Spectral reflectance indices and calculated equations are presented in Table 2.

2.4.2 Ceptometer

A ceptometer (model AccuPAR LP-80, Decagon Devices, Pullman, USA) was utilized to measure the leaf area index (LAI)

TABLE 2 Spectral reflectance indices and calculation equations.

Vegetation index	Abbreviation	Formula	Reference
Normalized difference vegetation index	NDVI	$(R_{800} - R_{670})/(R_{800} + R_{670})$	(Rouse et al., 1974)
Modified chlorophyll absorption reflectance index	MCARI	$((R_{701} - R_{670}) - 0.2\ (R_{701} - R_{550})) \times (R_{701}/R_{670})$	(Gamon and Surfus, 1999)
Leaf chlorophyll index	LCI	$(R_{850}) - (R_{710})/(R_{850}) + (R_{680})$	(Pu et al., 2008)
Curvature index	CI	$R_{675} \times R_{690}/R^2_{683}$	(Zarco-Tejada et al., 2003)
Triangular vegetation index	TVI	$0.5(120\ (R_{750} - R_{550}) - 200\ (R_{670} - R_{550}))$	(Rouse et al., 1974)
Simple ratio	SR	R800/R670	(Birth and McVey, 1968)
Modified simple ratio	MSR	(R750 − R445)/(R705 − R445)	(Sims and Gamon, 2002)
Photochemical reflection index	PRI	(R531 − R570)/(R531 + R570)	(Gamon et al., 1992)
Red edge position	REP	RRE = R670+R780/2 REP = 700 + 40X (RRE − R700)/(R740 − R700)	(Guyot and Baret, 1988)
Blue/green index	BIG2	R450/R550	(Zarco-Tejada et al., 2005)
Plant senescence reflectance index	PSRI	(R680-R500)/R750	(Gitelson et al., 2001)

twice in early flowering and the middle of grain filling stages (LAI A and LAI B) within ±2 h of solar noon under cloudless conditions.

2.5 Salinity tolerance/sensitive indices

The grain yield means of 40 genotypes for non-saline soil (Yp) and saline soil (Ys) over two seasons were obtained to calculate the STIs. Based on these means, the stress tolerance indices were analyzed by the *i*PASTIC software (Pour-Aboughadareh et al., 2019). Additionally, Microsoft Excel calculates the newest index, CSI (Sabouri et al., 2022). Consequently, salinity tolerance/sensitive indices and equations are illustrated in Table 3. In addition, the grain yield means of non-saline soil (Yp) and saline soil (Ys) and grain yield over two sites over 2 years GY_E of 40 genotypes, and salinity tolerance/sensitive indices are shown in Table 4.

2.6 Statistical analyses

Analysis of variance (ANOVA) data were collected for all characters separately in seasons 2019/20 and 2020/21 over two sites (saline and non-saline soil). Combined data of grain yield over two sites and two seasons (environments) and genotype by environment (GGE) biplots for grain yield over environments were accomplished according to Yan et al. (2000) and Yan et al. (2007). Statistical analysis was conducted through GenStat 19th edition (VSN International Ltd., Hemel Hempstead, UK). Additionally, a GYT biplot model was created based on grain yield and other agronomic and physiological traits (e.g., Fv/Fm) averaged over the saline and non-saline soil sites and season 2019/20 of the 40 genotypes. Hence, a genotype by trait table was generated, and then GYT combinations were computed by multiplying GY and all traits because high values are desirable except for DH and DM; they are divided by GY for the same reason (the multiplication operation is opposite of division) (Yan and Frégeau-Reid, 2018). At the same time, the second season GY and SRI (e.g., NDVI) utilized as traits along with Na^+ and K^+ were measured in the saline soil experiment only. However, salinity tolerance index values were used to depict genotype by salt tolerance index (GSTI) biplots (Yan and Frégeau-Reid, 2008); data were normalized before analyses as follows:

$$Y_{ij} = \frac{T_{ij} - \overline{T}_j}{S_j}$$

where Y_{ij} is the standardized genotype value *i* for yield–trait combination *j*, T_{ij} is the original value of genotype *i* for yield–trait combination *j*, $\overline{T}_j$ is the mean of genotype *i* for yield–trait combination *j*, and S_j is the standard deviation for yield–trait combination *j*, by GenStat 19th edition.

The traits normalized in Microsoft Excel to make a radar chart are as follows:

$$X_N = \frac{(X_O - X_{MIN})}{(X_{MAX} - X_{MIN})}$$

where X_N is the normalized value, X_O is the original value, and X_{MAX} and X_{MIN} are the minimum and maximum values of the trait, respectively. This procedure obtains the traits as unitless in the case where they are compared. Origin (Pro), version 2021 (Origin Lab Corporation, Northampton, MA, USA) was utilized to illustrate radar charts.

TABLE 3 Salinity tolerance/sensitive indices and equations.

Stress index	Formula	Desirable value	Reference
Tolerance	$TOL = Yp - Ys$	Minimum	(Rosielle and Hamblin, 1981)
Stress susceptibility index	$SSI = \frac{1-(Ys/Yp)}{1-(\overline{Y}s/\overline{Y}p)}$	Minimum	(Fischer and Maurer, 1978)
Geometric mean productivity	$GMP = \sqrt{Yp \times Ys}$	Maximum	(Fernandez, 1992)
Stress tolerance index	$STI = \frac{Ys \times Yp}{(\overline{Y}s)^2}$	Maximum	(Fernandez, 1992)
Harmonic mean	$HM = \frac{2(Ys \times Yp)}{Ys + Yp}$	Maximum	(Bidinger et al., 1987)
Mean productivity	$MP = \frac{Yp + Ys}{2}$	Maximum	(Rosielle and Hamblin, 1981)
Yield index	$YI = \frac{Ys}{\overline{Y}s}$	Maximum	(Gavuzzi et al., 1997)
Yield stability index	$YSI = \frac{Ys}{Yp}$	Maximum	(Bouslama and Schapaugh, 1984)
Relative stress index	$RSI = \frac{(Ys/Yp)}{(Ys/Yp)}$	Maximum	(Fischer and Wood, 1979)
Combination of significant indices	$CSI = \frac{1}{2}(\sum_j^n rYp\,.\,index_j \times index_{ij} + \sum_j^n rYs\,.\,index_j \times index_{ij})$	Maximum	(Sabouri et al., 2022)

10.3389/fpls.2023.1165113

TABLE 4 Grain yield means of non-saline sites Yp and saline soil sites Ys and grain yield over two sites for 2 years GY_E of 40 genotypes and salinity tolerance/sensitive indices.

Genotype	Yp	Ys	TOL	MP	GMP	HM	SSI	STI	YI	YSI	RSI	CSI	Rank	GY_E
1	9,313	7,983	1,330	8,648	8,622	8,596	0.44	0.86	1.26	0.86	1.26	16,469.4	1	8,648[†] [a]
2	9,464	6,866	2,598	8,165	8,061	7,958	0.85	0.75	1.09	0.73	1.07	15,401.6	29	8,605 [ab]
3	8,715	5,977	2,738	7,346	7,217	7,091	0.98	0.60	0.95	0.69	1.01	13,792	31	8,432 [abc]
4	9,236	5,736	3,500	7,486	7,278	7,077	1.18	0.61	0.91	0.62	0.92	13,913.9	34	8,374 [abc]
5	7,961	5,431	2,530	6,696	6,575	6,457	0.99	0.50	0.86	0.68	1.01	12,565.1	22	8,320 [abc]
6	9,664	6,417	3,248	8,040	7,875	7,712	1.05	0.71	1.01	0.66	0.98	15,049.6	12	8,218 [a-d]
7	7,995	6,092	1,903	7,044	6,979	6,915	0.74	0.56	0.96	0.76	1.12	13,333.1	21	8,188 [a-e]
8	10,857	5,225	5,633	8,041	7,531	7,054	1.61	0.65	0.83	0.48	0.71	14,425.7	37	8,168 [a-e]
9	9,319	6,257	3,062	7,788	7,636	7,487	1.02	0.67	0.99	0.67	0.99	14,592.2	2	8,165 [a-e]
10	8,775	6,896	1,879	7,836	7,779	7,723	0.67	0.70	1.09	0.79	1.16	14,860.8	11	8,094 [a-e]
11	10,152	6,036	4,116	8,094	7,828	7,571	1.26	0.71	0.95	0.59	0.88	14,967.9	33	8,094 [a-e]
12	9,737	6,700	3,038	8,218	8,077	7,938	0.97	0.75	1.06	0.69	1.01	15,434.1	36	8,069 [a-e]
13	8,222	5,909	2,313	7,065	6,970	6,876	0.88	0.56	0.93	0.72	1.06	13,317.7	8	8,041 [a-e]
14	9,640	5,982	3,659	7,811	7,594	7,382	1.18	0.66	0.95	0.62	0.91	14,516.5	6	8,040 [a-e]
15	8,633	6,210	2,423	7,421	7,322	7,224	0.87	0.62	0.98	0.72	1.06	13,989.7	30	8,032 [a-e]
16	8,887	6,709	2,178	7,798	7,722	7,646	0.76	0.69	1.06	0.75	1.11	14,752.2	40	8,014 [a-e]
17	9,580	6,205	3,375	7892	7,710	7,532	1.10	0.68	0.98	0.65	0.95	14,736	23	7,999 [a-e]
18	7,945	6,755	1,190	7350	7,326	7,302	0.47	0.62	1.07	0.85	1.25	13,993.8	19	7,937 [a-e]
19	9,456	6,418	3,038	7937	7,790	7,646	1.00	0.70	1.01	0.68	1.00	14,886.5	32	7,924 [a-f]
20	9,576	6,047	3,529	7811	7,609	7,413	1.15	0.67	0.96	0.63	0.93	14,545.7	17	7,892 [a-f]
21	9,692	6,685	3,007	8188	8,049	7,912	0.97	0.75	1.06	0.69	1.02	15,380.7	10	7,836 [a-f]
22	9,354	7,286	2,068	8320	8,255	8,191	0.69	0.79	1.15	0.78	1.15	15,771.4	20	7,811 [a-f]
23	9,924	6,075	3,850	7999	7,764	7,536	1.21	0.69	0.96	0.61	0.90	14,843.8	14	7,811 [a-f]
24	9,487	5,263	4,225	7375	7,066	6,770	1.39	0.58	0.83	0.55	0.82	13,516.3	16	7,798 [a-f]
25	8,911	5,832	3,080	7371	7,209	7,050	1.08	0.60	0.92	0.65	0.96	13,777.6	28	7,797 [a-f]
26	8,849	6,441	2,408	7645	7,549	7,455	0.85	0.66	1.02	0.73	1.07	14,424.3	38	7,794 [a-f]
27	9,149	5,979	3,171	7564	7,396	7,232	1.08	0.63	0.95	0.65	0.96	14,135.3	9	7,787 [a-f]
28	10,050	5,544	4,506	7797	7,464	7,146	1.40	0.64	0.88	0.55	0.81	14,279.1	26	7,645 [a-f]
29	9,902	7,308	2,594	8605	8,507	8,410	0.82	0.83	1.16	0.74	1.09	16,252.9	35	7,612 [a-f]
30	9,861	6,203	3,659	8032	7,821	7,615	1.15	0.70	0.98	0.63	0.93	14,949.8	27	7,564 [a-f]
31	10,666	6,197	4,469	8432	8,130	7,839	1.30	0.76	0.98	0.58	0.86	15,547.5	4	7,486 [a-f]
32	9,890	5,957	3,933	7924	7,676	7,435	1.24	0.68	0.94	0.60	0.89	14,675.5	15	7,421 [b-f]
33	9,495	6,692	2,803	8094	7,971	7,851	0.92	0.73	1.06	0.70	1.04	15,231.6	24	7,375 [b-f]
34	9,787	6,960	2,827	8374	8,253	8,135	0.90	0.78	1.10	0.71	1.05	15,770.2	25	7,371 [c-f]
35	9,346	5,879	3,467	7613	7,412	7,218	1.15	0.63	0.93	0.63	0.93	14,169.5	18	7,350 [c-f]
36	10,045	6,093	3,952	8069	7,823	7,585	1.22	0.71	0.96	0.61	0.89	14,957.4	3	7,346 [b-f]
37	8,947	7,389	1,559	8168	8,130	8,093	0.54	0.76	1.17	0.83	1.22	15,531.3	13	7,065 [def]
38	9,844	5,745	4,099	7795	7,520	7,256	1.30	0.65	0.91	0.58	0.86	14,381	7	7,043 [def]

(Continued)

TABLE 4 Continued

Genotype	Yp	Ys	TOL	MP	GMP	HM	SSI	STI	YI	YSI	RSI	CSI	Rank	GY_E
39	8,066	5,820	2,247	6943	6,851	6,761	0.87	0.54	0.92	0.72	1.06	13,090.7	39	6,943 ^{ef}
40	8,276	7,753	523	8014	8,010	8,005	0.20	0.74	1.23	0.94	1.38	15,299.2	5	6,696 ^{f}
CV%														12.12

†Mean values within the same column for each trait with the same lowercase letter are not significantly different according to the least significant difference (LSD) at P ≤ 0.05. The rank of genotypes was based on GY_E combined analysis. TOL, tolerance index; MP, mean productivity stress; STI, tolerance index; GMP, geometric mean productivity; HM, harmonic mean; SSI, stress susceptibility index; YI, yield index; YSI, yield stability index; RSI, relative stress index; CSI, combination of significant indices.

3 Results

3.1 The estimated trait summary and mean performance

A summary of the studied traits measured in the 2019/2020 season is revealed in Table S2. The results revealed different minimum, maximum, and mean performance and genotype mean squares (MS Geno.) of non-saline and saline locations. There is significant difference between genotypes of all characters in non-saline and saline conditions, except for BY, CT, harvest index (HI), and SM for a non-saline soil site, which is in contrast with CT and SM in saline soil condition. Additionally, the CV of non-saline soil ranged from 2.01 for DM to 20.65% for SM. However, in the saline soil condition, CV ranged from 1.6 for DM to 25.89% for SM. Moreover, the rank of genotypes according to their mean performance for all studied characters was revealed.

Table S3 summarizes the SRIs and GYs estimated across non-saline and saline conditions in the 2020/2021 season. The data are minimum, maximum, and means of all SRIs and GYs. Additionally, the mean square of genotypes and significant differences among them in all SRI and GY except in non-saline soil sites' blue/green index (BIG2), modified simple ratio (MSR), SR, LAI A, and LAI B. However, in the saline soil site's, there are no significant differences among genotypes for SRI, such as modified chlorophyll absorption reflectance index (MCARI), LAI A, LAI B, and K/Na. In addition, high-ranked genotypes according to SRI mean performance were demonstrated.

The means of two non-saline soil sites (Yp) and saline soil sites (Ys) for the 40 genotypes were calculated over both studied seasons. Grain yield means ranged from 7,945 kg h^{-1} for genotype 18 to 10,857 kg h^{-1} for genotype 8 of non-saline soil sites. At the same time, the saline soil sites range from 5,225 kg h^{-1} of genotype 8 to 7,983 kg h^{-1} of genotype 1 (Figure S1). The results revealed that genotypes 1, 40, 37, 29, 33, 34, and 22 recorded the highest means and lowest fluctuations across seasons. In contrast, genotypes 8, 11, 23, 24, 28, and 31 had high fluctuations across environments over seasons (Figure S1).

TABLE 5 Analysis of variance (mean square) of agronomic and physiological traits of 40 genotypes evaluated under non-saline and saline soil sites in the 2019/2020 season.

Source of variation	DF	BY	DH	DM	Fv/Fm	GY	HI
ENV	1	1.36E+08**	8,166**	16,335**	0.000006^{NS}	1.58E+08**	1301**
REP:ENV	4	21,945,141	24.667	16.338	0.003626	2,155,530	219.86
BLK:REP:ENV	54	15,134,375	28.743	26.861	0.002444	1,298,744	68.53
GEN	39	9,105,748*	85.646**	51.2**	0.002373*	1,775,095**	51.82*
ENV:GEN	39	8,000,302^{NS}	6.786^{NS}	4.805^{NS}	0.002529**	1,801,470**	27.51^{NS}
Residual	102	5,465,161	5.193	7.388	0.001429	1,011,245	33.23
CV (%)		14.86	2.35	1.86	5.34	13.59	11.97
Source of variation	DF	NDVI	PH	SM	CCI	CT	
ENV	1	0.41917**	2,767**	415,751**	170.33**	4.692*	
REP:ENV	4	0.005033	55.42	16,460	115.43	23.718	
BLK:REP:ENV	54	0.007038	71.61	5,185	30.74	3.455	
GEN	39	0.010857**	168.53**	7,872^{NS}	37.29**	2.044*	
ENV:GEN	39	0.005503*	23.13**	6,528^{NS}	17.28^{NS}	1.564^{NS}	
Residual	102	0.003382	11.46	6,172	10.95	1.217	
CV (%)		10.84	3.44	24.26	10.42	4.36	

DF, degrees of freedom; ENV, environment (sites by season); GEN, genotype; REP, replication; BLK, block; BY, biological yield; DH, days to heading; DM, days to maturity; Fv/Fm, chlorophyll fluorescence; GY, grain yield; CT, canopy temperature; HI, harvest index; NDVI, normalized difference vegetation index; PH, plant height; SM^2, number of spikes per square meter; CCI, chlorophyll content index; CV, coefficient of variation; MS Geno., mean square of genotypes; * and **, significance levels of P≤0.05 and P≤0.01; NS, no significant difference.

3.2 The studied trait combined data analyses

Table 5 shows the combined ANOVA for the agronomic and physiological studied traits in the 2019/2020 season under non-saline and saline soil sites. The effect due to sites significantly varied from site to site for all traits except for Fv/Fm. In addition, the genotype component has a significant variation for all studied characters except SM. In comparison, the effect of genotype by sites for BY, DH, DM, HI, SM, CCI, and CT was insignificant in contrast with other traits.

Based on the combined data of non-saline and saline soil sites (environments) presented in Table 6, the environment significantly varied for all traits, e.g., grain yield and spectral reflectance indices. Furthermore, there is significant variation among genotypes examined in the 2020/2021 season for all traits except photochemical reflection index (PRI), plant senescence reflectance index (PSRI), red edge position (REP), SR, and LAI A. However, the interaction between environment and genotype was insignificant for most traits except BIG2, CI, GY, MSR, and NDVI.

The combined analysis of variance for grain yield traits over all sites and seasons (four environments) is demonstrated in Table S4. The data revealed significant differences among environments, genotypes, and environments by genotypes with significance levels ($P \leq 0.01$) along with CV 12.12%.

3.3 The comparison of the estimated traits and contrasting sites in both seasons

The mean performance of the agronomic and physiological traits of the 40 genotypes tested in non-saline soils versus saline soils in the 2019/2020 season is illustrated in a radar chart (Figure 1A). The results show that the same score was recorded for traits such as NDVI, days to heading (HD), and CCI for both sites, while the days to maturity, BY, and PH values of the non-

TABLE 6 Analysis of variance (mean square) of agronomic traits and spectral reflectance indices of the 40 genotypes evaluated in both non-saline and saline soil sites 2020/2021 season.

Source of variation	DF	BIG2	CI	GY	LCI	MCARI
ENV	1	0.076932**	0.012939*	1.14E+09**	0.125417**	0.000986**
REP:ENV	4	0.004917	0.0198	48,250,956	0.002748	3.14E−05
BLK:REP:ENV	54	0.000575	0.005866	4,077,516	0.000995	9.44E−05
GEN	39	0.000614**	0.005434*	1,669,177**	0.001398**	0.000112*
ENV:GEN	39	0.000615**	0.005677**	1,895,697**	0.000771^{NS}	7.37E−05^{NS}
Residual	102	0.000362	0.003238	786,465	0.000638	6.79E−05
CV (%)		2.95	−7.43	10.76	4.92	14.67
Source of variation	DF	MCARI 1	MSR	NDVI	PRI	PSRI
ENV	1	0.055588**	874.4954**	0.089744**	0.00352**	0.000823**
REP:ENV	4	0.005258	55.1711	0.003795	0.000621	0.000232
BLK:REP:ENV	54	0.002963	0.7201	0.000866	3.61E−05	7.17E−06
GEN	39	0.003111**	0.1974**	0.000969**	1.78E−05^{NS}	1.79E−05^{NS}
ENV:GEN	39	0.001688^{NS}	0.2015**	0.000716*	1.78E−05^{NS}	1.79E−05^{NS}
Residual	102	0.001396	0.1022	0.000454	2.03E−05	1.32E−05
CV (%)		14.67	5.09	13.17	2.87	−31.8
Source of variation	DF	REP	SR	TVI	LAI1A	LAI B
ENV	1	369.3083**	30,984.33**	101.93**	753.3372**	164.309**
REP:ENV	4	23.2046	1,946.206	8.339	36.0375	43.632
BLK:REP:ENV	54	0.3795	19.943	4.5	0.9701	2.426
GEN	39	0.3205^{NS}	0.2446^{NS}	4.764**	0.5044^{NS}	0.981^{NS}
ENV:GEN	39	0.3161^{NS}	0.2177^{NS}	2.825^{NS}	0.3914^{NS}	1.087^{NS}
Residual	102	0.2573	0.2769	2.193	0.3817	1.095
CV (%)		0.07	2.54	5.29	11.75	23.38

DF, degrees of freedom; ENV, environment (sites by season); GEN, genotype; REP, replication; BLK, block; GY, grain yield. * and **, significance levels of P≤0.05 and P≤0.01; NS, no significant difference.

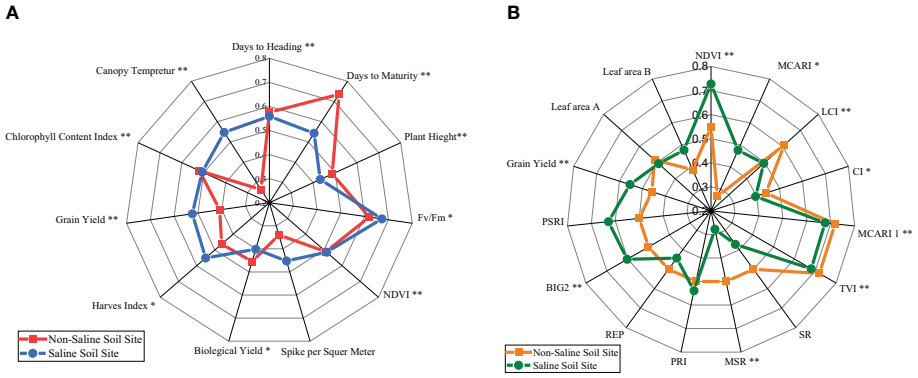

FIGURE 1
(A) Radar chart of the mean performance of the agronomic and physiological traits of 40 genotypes under non-saline and saline conditions evaluated in the 2019/2020 season. * and **, significance levels of $P \leq 0.05$ and $P \leq 0.01$, respectively, of genotype mean square. Fv/Fm, chlorophyll fluorescence; NDVI, normalized difference vegetation index. **(B)** Radar chart of the mean performance of grain yield (GY) and spectral reflectance indices along with LAI A and B, measured on 15 and 30 March 2021, for 40 genotypes under non-saline and saline conditions in the 2020/2021 season. * and **, significance levels of $P \leq 0.05$ and $P \leq 0.01$, respectively, of genotype mean square.

saline soil site tend to be greater than those of the saline soil site. In contrast, GY, HI, CT, SM, and chlorophyll fluoresce (Fv/Fm) had the highest means for the saline site. The genotypes varied significantly ($P \leq 0.01$) in combined data for all revealed traits except SM.

The means of spectral reflectance indices and grain yield averaged over the 40 genotypes in the two sites (non-saline soils and saline soils) in the 2020/2021 season are displayed in Figure 1B. The saline soil site recorded higher values than the non-saline soil site for SRIs, such as NDVI, MCARI, PRI, BIG2, PSRI, leaf area B, and GY, while other indices are the opposite, except for triangular vegetation index (TVI), MCARI 1, and leaf area A, which had almost the same means as the two sites. The genotypes varied significantly ($P \leq 0.01$) in combined data of both sites for all shown traits and SRIs except PRI, REP, SR PSRI, and leaf areas A and B.

3.4 GGE biplots for grain yield over the four environments

Figure 2A presents the which-won-where of the GGE biplot view for the grain yield data of the 40 genotypes over all sites and seasons (four environments). Genotype 34 (1 close to 34) is the best one. It is located on the polygon vertices in sector content saline sites of two years. On the other hand, genotypes 40 and 6 are the winners in the non-saline soils in the first season of 2019/20, but genotype 37 (16 close to 37) is the winner in the non-saline soils' second season of 2020/21. Principal components PC1 and PC2 explained 67.68% of the total variation of environments (E), genotypes (G), and G by E interaction. In the site of the saline soils (if we extend a vector from the biplot origin to points of saline sites), there was an acute angle between them. Thus, these sites are highly correlated in contrast to non-saline sites.

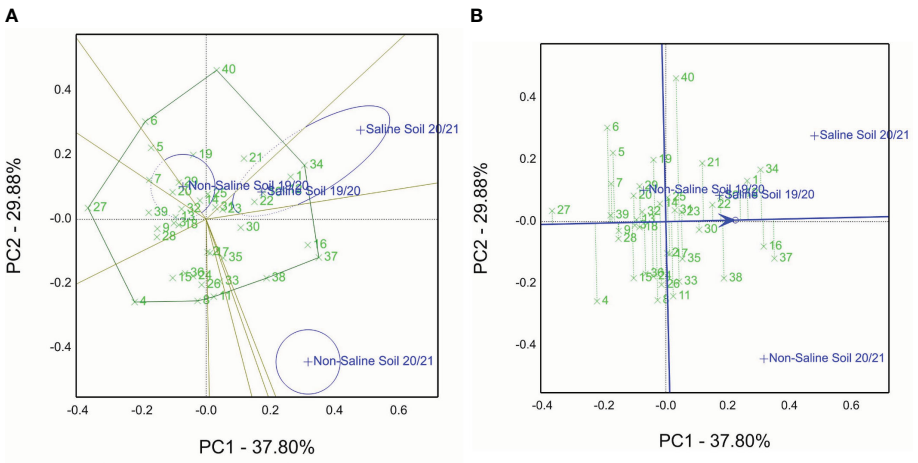

FIGURE 2
(A) Which-won-where GGE biplot view of the grain yield of 40 genotypes evaluated in non-saline and saline conditions in the 2019/2020 and 2020/2021 seasons (four environments). **(B)** Mean vs. stability view of the GGE biplot of 40 genotypes tested across non-saline and saline conditions in the 2019/2020 and 2020/2021 seasons (four environments).

From the 40 genotype entries, genotype 37, followed by 16, 34, 1, and 12, is the top-ranked genotype evaluated under non-saline soils and saline soils of the cropping seasons, whereas genotype 27 ranked as the lowest genotype (Figure 2B). Furthermore, the five selected genotypes are located close to the line with an arrow and possess short projections. This means that the stable genotypes across the four investigated environments compared with genotypes 40, 4, and 6 pointed away from the average tester coordination (ATC) line.

3.5 The estimation of salt tolerance indices and their GT biplots

The GT view was obtained to produce Figure 3A (GSTI) based on values of Table 4 using the grain yield (Yp) of non-saline soil sites and saline soil sites (Ys) over both seasons, their combined data over four environments (GYE), and salt tolerance/susceptibility indices. The findings reveal that genotypes 1, 29, 31, 34, 22, and 12 recorded the highest means of grain yield (Table 4). Moreover, genotypes 1 and 29 are the winning genotypes for salinity indices such as Ys, YI, MP, STI, HM, CSI, and GMP. On the other hand, genotype 8 is the winning genotype based on RC, SSI, and TOL susceptibility indices and non-saline soil sites' mean (Yp), and genotype 40 is the winner for YSI and RSI. Additionally, the sum of PC1 is 60.33% plus PC2 39.48%, equal to 99.8% of total variations, and it indicates the salinity tolerance indices STI and GY calculated from each other (Figure 3A).

According to the view of the GSTI biplot for average tester coordination, ATC is revealed in Figure 3B. The top-ranked genotypes are 1, followed by 29, 34, 22, and 31, while the poorest is genotype 5. Genotypes 29 and 34 had a strong performance and were close to the ATC line (short projection) compared with genotypes 40 and 18.

Table S5 reveals that the genotypes' ranks rely on STI and grain yield in non-saline soil (Yp) and saline soil sites (Ys). The results show that genotype 1 is the top-ranked one for Ys, MP, GMP, HM, STI, and YI. However, the opposing genotype 5 is the last ranked one for the same indices. On the other hand, genotype 8 recorded the lowest ranks for Ys, TOL, SSI, YI, YSI, and RSI. On the other hand, genotype 40 had the highest rank for the TOL, SSI (salinity tolerant), YSI, and RSI parameters. SR and AR are the sum and average of all ranks, and genotype 1 demonstrated the best one with values of 40 and 3.6. Nevertheless, genotype 24 recorded 391 and 35.5, respectively. The findings in Figure 3A confirmed these results.

The tester vector view of the GSTI biplot is depicted in Figure S2. The acute angle between STI vectors reflects the strength of the relationship or correlation and vice versa. For example, the angle between RSI and TOL indices indicates a negative correlation, while MP and GMP are highly positively correlated. These findings in Figure S2 are confirmed by numerical values such as the correlation coefficient for RSI, and TOL is $r = -0.98$ in contrast to MP and GMP recorded $r = 0.97$. Moreover, the relation between RSI and YSI is identically confirmed by the same indices located on the same point (Figure S2).

3.6 The GYT biplots for agronomic and physiological traits and SRI of both seasons

The GYT view is presented in Figure 4A. Based on the grain yield and other agronomic and physiological traits, the average of each genotype was evaluated under non-saline and saline sites in the 2019/2020 season. Hence, the GT table (two-way table) was

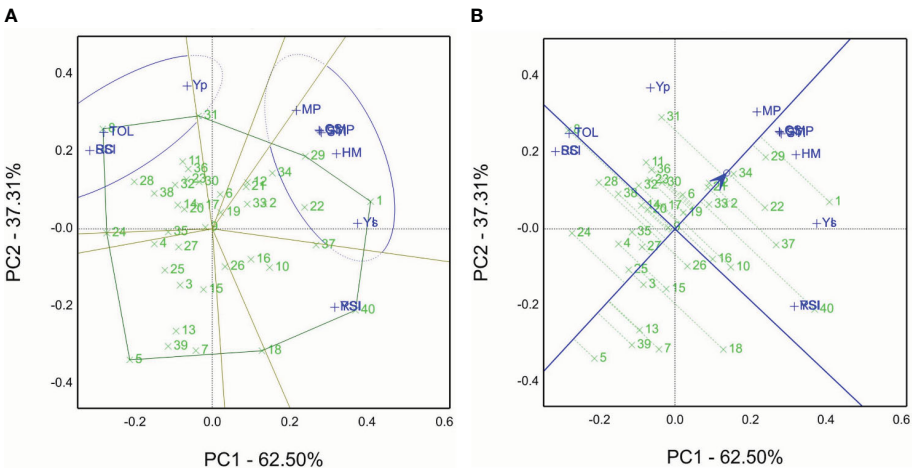

FIGURE 3
(A) Which-won-where view of the GSTI biplot of grain yield Yp in non-saline soil sites and Ys in saline soil sites in the 2019/2020 and 2020/2021 seasons of 40 genotypes with salinity tolerance indices, viz., tolerance index (TOL), mean productivity (MP), stress tolerance index (STI), geometric mean productivity (GMP), harmonic mean (HM), stress susceptibility index (SSI), yield index (YI), yield stability index (YSI), relative stress index (RSI), and combination of significant indices (CSI). **(B)** The average tester coordination view of the GSTI biplot of grain yield Yp in non-saline soil sites and Ys in saline soil sites in the 2019/2020 and 2020/2021 seasons of 40 genotypes with salinity tolerance indices, i.e., tolerance index (TOL), mean productivity (MP), stress tolerance index (STI), geometric mean productivity (GMP), harmonic mean (HM), stress susceptibility index (SSI), yield index (YI), yield stability index (YSI), relative stress index (RSI), and combination of significant indices (CSI).

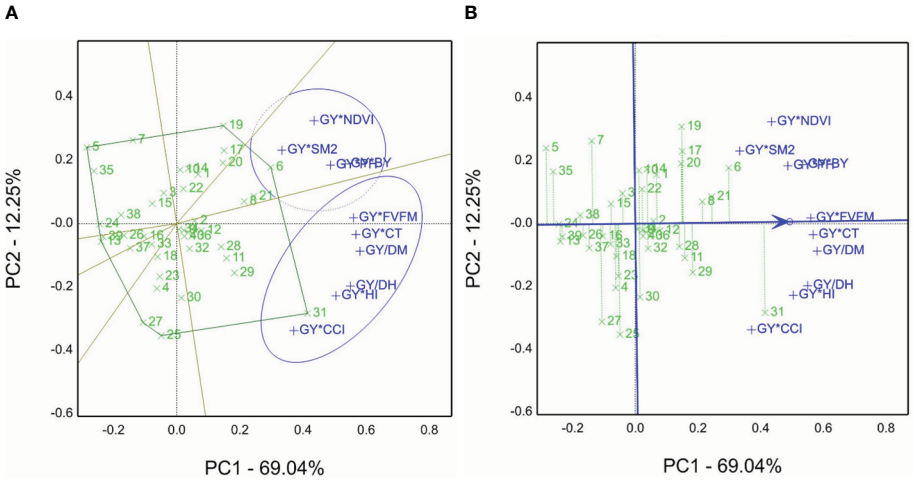

FIGURE 4
(A) Which-won-where view of the genotype by yield*trait (GYT) biplot of agronomic and physiological traits, e.g., BY, biological yield; DH, days to heading; DM, days to maturity; Fv/Fm, chlorophyll fluorescence; GY, grain yield; CT, canopy temperature; HI, harvest index; NDVI, normalized difference vegetation index; PH, plant height; SM2, number of spikes m^{-1}; and CCI, chlorophyll content index, to create the combinations of 40 genotypes evaluated in normal and saline sites in the 2019/2020 season. **(B)** The average tester coordination view of the genotype by yield*trait (GYT) biplot of agronomic and physiological traits, e.g., BY, biological yield; DH, days to heading; DM, days to maturity; Fv/Fm, chlorophyll fluorescence; GY, grain yield; CT, canopy temperature; HI, harvest index; NDVI, normalized difference vegetation index; PH, plant height; SM2, number of spikes per square meter; and CCI, chlorophyll content index, to generate the combinations of 40 genotypes evaluated in normal and saline sites in the 2019/2020 season.

generated, and then GYT combinations were normalized and calculated. Genotype 31 won the GY*Fv/Fm, GY*CT, GY/DH, GY/DM, GY*HI, and GY*CCI combinations. However, genotype 6 is the best for the GY*NDVI, GY*SM2, GY*PH, and GY*BY combinations. The sum of PC1 and PC2 accounted for 81.29% of total variations.

The GYT results are revealed in Figure 4B. The 40 genotypes' ranking is 31>6>8>21>8>29, and genotype 5 is the lowliest genotype according to GYT combinations. However, the genotype placed close to the ATC line tended to be superior and had a balanced trait profile, e.g., genotypes 21 and 8 and vice versa, based on that view of the first season biplot data.

For the 2020/2021 season, the grain yield averaged for the 40 genotypes and non-saline and saline sites were combined to produce the GYT combinations (data normalized before analyses) using SRIs. Genotype 1 was selected as the winner for most combinations, genotype 34 for the GY*MCARI combination, genotype 5 for the GY*CI combination, genotype 3 for the GY*PSRI combination, and genotype 12 for GY/Na combination (the minimum is the desirable value) (Figure 5A).

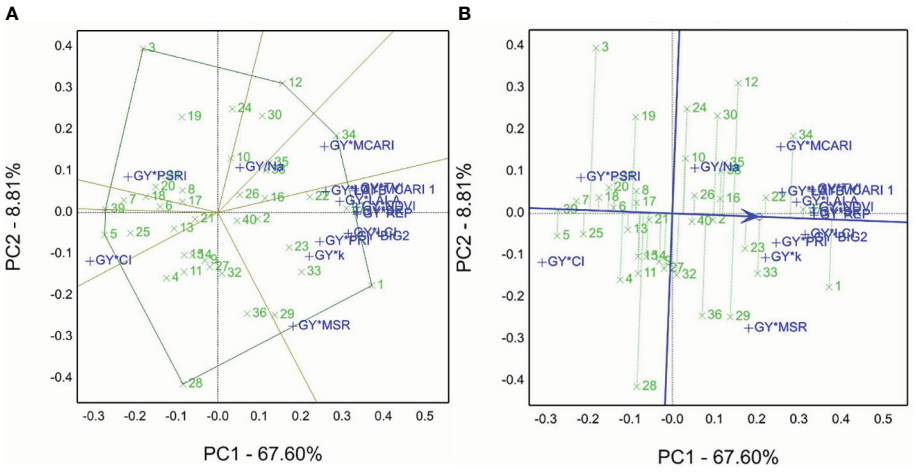

FIGURE 5
(A) Which-won-where view of the genotype by yield*trait (GYT) biplot of grain yield averaged in non-saline and saline soil sites with spectral reflectance indices to generate the combinations of 40 genotypes evaluated in the 2020/2021 season. **(B)** The average tester coordination view of the genotype by yield*trait (GYT) biplot of grain yield averaged non-saline and saline soil sites with spectral reflectance indices to generate the combinations of 40 genotypes evaluated in the 2020/2021 season.

In the GYT biplot findings of the 2020/2021 season, the ATC (Figure 5B) demonstrated the best-ranked genotypes, e.g., genotype 1 followed by 37, 34, 22, 33. In contrast, genotype 5 had the lowest performance based on the GYT combinations with spectral reflectance indices, and genotypes 37 and 22 tended to be superior to 12 and 29. Thus, refer to the closeness and farness of the genotype location from the ATC line. The sum of contributions for PC1 and PC2 accounted for 76.14% of overall variations.

4 Discussion

Salinity tolerance varies from one specie to another, but the species' tolerance mechanisms are similar to drought tolerance (Munns and Tester, 2008). Thus, we selected elite genotypes from CIMMYT drought trials, viz., SAWYT and SATYN, besides the yield potentiality trials, to identify salinity-tolerant genotypes evaluated under the open field conditions, as shown in Table S1. Several researchers (Sardouie-Nasab et al., 2014; Hinojosa et al., 2019; Mohammadi et al., 2022) have screened a large set of genotypes and then selected appropriate genotypes for field stress evaluation. They used different traits, agronomic characters, physiological traits, spectral reflectance indices, and STIs. In this study, relying on the GGE approach, genotypes 34 and 1 are the best for saline soil sites (Figure 2A). Genotypes 1 and 29 (Figure 3A) and genotype 34 (Figure 3B) are the best from the GSTI view. Genotype 1 is the best from the GYT view with SRI (Figures 5A, B). Therefore, genotype 1 could be identified as salt tolerant based on the STI and SRI results, shown in Figures 3A, B, 5A, B and Table S5.

Salinity tolerance is a complex phenomenon controlled by several physiological functions and genetic factors (Gizaw et al., 2018) and influenced by growth stages and open field conditions (Haq et al., 2010; Oyiga et al., 2016; Tao et al., 2021). The appropriate design, alpha lattice, was used to reduce the experimental error generated and analyzed by GenStat, especially, in salinity-affected fields (acquired for genotype evaluation). Findings of grain yield data presented in Table S4 (combined) over the four studied environments showed significant differences for environments, genotypes, and their interaction, which are similar to other reports (Ali et al., 2012; Enyew et al., 2021; Msundi et al., 2021; El-Hendawy et al., 2022). Additionally, similar findings were pointed out for the combined data and GGE biplot by (Enyew et al., 2021; Darwish et al., 2022; Darwish et al., 2023). Tables 5, 6 show significant differences in genotypes, environments, and their interactions for most studied traits over season by season separately. These findings agree with the results of agronomic traits (Enyew et al., 2021) and chlorophyll fluorescence (Fv/Fm) in quinoa crop (Hinojosa et al., 2019). In contrast, spectral reflectance index results agree with other reports (Prasad et al., 2007; El-Hendawy et al., 2019; Sun et al., 2019) regarding BIG2, CI, MSR, and NDVI as shown in Table 6.

The GGE, GT, and GYT models facilitate the mission of plant breeders to select tolerant genotypes for biotic and abiotic stresses. Based on the grain yield, other agronomic and physiological traits were averaged over the non-saline and saline soil sites, a genotype by trait table was generated, and then GYT combinations were normalized and calculated. Multiplication of GY and all traits was done compute the combinations because high values are desirable except for DH and DM. Multiplication of GY and all traits was done to compute the combinations because high values are desirable. However, DH and DM are divided by GY for the same reason (the multiplication operation is the opposite of division) (Yan and Frégeau-Reid, 2018). This study used GT analysis to address salinity tolerance indices generated from the *i*PASTIC online software (Table 4) and produced the GSTI biplots shown in Figure 3A, Figure S2, and Figure 3B and then identified genotypes 1 and 29 as salt-tolerant genotypes, while genotype 40 had yield stability. These findings agreed with the results of other reports (Yan and Frégeau-Reid, 2008; Mohammadi, 2019; Msundi et al., 2021; Santana et al., 2021; Zulfiqar et al., 2021). Salinity tolerance indices were calculated using the *i*PASTIC application based on grain yield in non-saline and saline soil sites over the years, and all the indices were employed to generate the GSTI biplots shown in Figure 3A and Figure S2. Other researchers, in this regard, obtained similar results (Mohammadi, 2019; Santana et al., 2021; Sabouri et al., 2022).

All traits measured of 40 genotypes were used to compare non-saline soil and saline soil sites. The traits data normalized by maximum and minimum values (to convert the raw data of traits into unitless values) and averaged of traits in a radar chart, e.g., for GY of the saline site recorded average higher than non-saline site in Figures 1A, B it may reflect the amount of variation in saline sites. These findings were similar to the results of several agronomic and physiological traits recorded by Al-Ashkar et al. (2019); Yang et al. (2020); Mohan et al. (2021); Yang et al. (2022), and Rebouh et al. (2023). In the same context, the wheat nitrogen deficit did not impact the Fv/Fm ratio (Gioia et al., 2015). However, sowing depth influences the grain yield of wheat (Amram et al., 2015).

The salt-tolerant genotype may have a minimal Na^+ concentration, a higher K^+ accumulation, a nicely maintained osmotic pressure in its roots and shoot, and maximal photosystem (PSII) activities, producing higher biomass specifically under salinity stress (Oyiga et al., 2016; Quamruzzaman et al., 2022). Accordingly, genotype 1 possesses a higher accumulation of K^+ and the best rank of GY in saline soil sites in both seasons (Tables S2, S3). However, genotype 10 recorded the lowest Na^+ concentration and K^+:Na^+ ratio and BY in the saline soil site (Table S3). These findings are consistent with those obtained in other reports (Oyiga et al., 2016; Morsy et al., 2022; Quamruzzaman et al., 2022). Genotype 12 was the best according to the GY/Na^+ combination (Figure 5A), while genotype 1 was the best from the GY*K^+ combination of the GYT biplot.

Remote sensing technologies and spectral instruments create valuable spectral information in many wavelength bands throughout the electromagnetic spectrum, particularly visible, near-infrared, and shortwave, and provide spectral reflectance indices. These approaches are becoming extremely powerful tools for identifying chemical and physical plant structures and functions by non-destructive methods and rapid and precise measurements (Reynolds et al., 2012; Bruning et al., 2020; El-Hendawy et al., 2022). Additionally, GGE, GT, and GYT biplots are other powerful tools in

plant breeding for screening many genotypes and identify the best one, specifically under stress conditions. For example, researchers (Mohammadi et al., 2022) screened 220 durum wheat genotypes for drought tolerance. They used GT biplots to identify drought-tolerant genotypes; authors (Enyew et al., 2021) used GGE biplots to discriminate and select among 320 sorghum genotypes. At the same time, other researchers (Santana et al., 2021) used spectral reflectance indices and GT biplots to identify high-yielding corn genotypes evaluated under low- and high-nitrogen applications. Researchers (Elfanah et al., 2023) pointed out the selection of salt-tolerant wheat genotypes based on pots and lysimeter systems (sandy soil) identified employing STI and SRI parameters. In the current study, genotype 1 is the best one from the GYT view with SRI (Figures 5A, B) in saline soil (clay field).

Salinity stress reduces chlorophyll fluorescence (Fv/Fm), CCI, and NDVI (Oyiga et al., 2016; Quamruzzaman et al., 2022). However, the CCI value increased in plants under salinity conditions (Hasanuzzaman et al., 2018; Quamruzzaman et al., 2022). This value reflects the degradation of chlorophyll in salt-treated plants as well as reduced cell size and concentration of chlorophyll content in mesophyll tissues. In the present study, genotype 31 is the best one from the GYT biplot view based on GY*Fv/Fm, GY*CT, and GY*CCI, while it is genotype 6 in the same view for GY*NDVI (Figures 4A, B).

5 Conclusions

In conclusion, we used different selection criteria, physiological parameters, and spectral reflectance indices and estimated salinity tolerance indies simultaneously with grain yield. In this study, the results demonstrated significant differences ($p \leq 0.01$) among the environments, genotypes, and their interaction for GY evaluated in the four environments. Moreover, in the first season, the traits GY, PH, HI, CCI, chlorophyll fluorescence parameter Fv/Fm, and NDVI were measured in contrasting salinity environments. Additionally, significant differences were detected among environments, genotypes, and their interaction for grain yield along with SRIs, e.g., BIG2, curvature index (CI), NDVI, and MSR. Moreover, based on the GGE approach, genotypes 34 and 1 are the best performing in saline soil sites. Genotypes 1 and 29 and genotype 34 are the best from the GSTI biplot. Genotype 1 is the best from the GYT method with spectral reflectance indices. Therefore, we can identify genotype 1 as salt tolerant based on the results of GSTI and SRI and recommend including it in salinity breeding programs.

Data availability statement

The raw data supporting the conclusions of this article will be made available by the authors, without undue reservation.

Author contributions

All authors listed have made a substantial, direct, and intellectual contribution to the work, and approved it for publication.

Conflict of interest

The authors declare that the research was conducted in the absence of any commercial or financial relationships that could be construed as a potential conflict of interest.

Publisher's note

Supplementary material

The Supplementary Material for this article can be found online at: https://www.frontiersin.org/articles/10.3389/fpls.2023.1165113/full#supplementary-material

SUPPLEMENTARY FIGURE 1
The tester vector view of GSTI biplot view of grain yield Yp in normal sites and Ys in stress sites in season 2019/2020 and 2020/2021 of 40 genotypes with salinity tolerance indices, e.g., Tolerance index TOL, Mean Productivity MP, Stress Tolerance Index STI, Geometric Mean Productivity GMP, Harmonic Mean HM, Stress Susceptibility Index SSI, Yield Index YI, Yield Stability Index YSI, Relative Stress Index RSI, and Combination of Significant Indices CSI.

SUPPLEMENTARY FIGURE 2
Correlation coefficient and diagram of grain yield Yp and Ys in non-saline and saline soil sites, respectively, averaged across 2019/2020 and 2020/2021 seasons with stress tolerance/sensitive indices STI.

References

Abdelhakim, L. O. A., Rosenqvist, E., Wollenweber, B., Spyroglou, I., Ottosen, C.-O., and Panzarová, K. (2021). Investigating combined drought-and heat stress effects in wheat under controlled conditions by dynamic image-based phenotyping. *Agronomy* 11 (2), 364. doi: 10.3390/agronomy11020364

Ali, A.M., Aboelghar, M.A., El-shirbeny, M.A., and Salem, N.H. (2018). Comparative analysis of some winter crops area estimation using landsat-8 and sentinal-2 satellite imagery. *Asian Journal of Agriculture and Biology* 16 (2), 189–197.

Al-Ashkar, I., Alderfasi, A., El-Hendawy, S., Al-Suhaibani, N., El-Kafafi, S., and Seleiman, M. F. (2019). Detecting salt tolerance in doubled haploid wheat lines. *Agronomy* 9 (4), 211. doi: 10.3390/agronomy9040211

Alharbi, B. M., Elhakem, A. H., Alnusairi, G. S., Soliman, M. H., Hakeem, K. R., Hasan, M. M., et al. (2021). Exogenous application of melatonin alleviates salt stress-induced decline in growth and photosynthesis in Glycine max (L.) seedlings by improving mineral uptake, antioxidant and glyoxalase system. *Plant Soil Environ.* 67 (4), 208–220. doi: 10.17221/659/2020-PSE

Ali, A. M., Aboelghar, M. A., El-shirbeny, M. A., and Salem, N. H. (2018). Comparative analysis of some winter crops area estimation using landsat-8 and sentinal-2 satellite imagery. *Asian J. Agric. Biol.* 6 (2), 189–197.

Ali, Z., Salam, A., Azhar, F. M., Khan, I. A., Khan, A. A., Bahadur, S., et al. (2012). The response of genetically distinct bread wheat genotypes to salinity stress. *Plant Breed.* 131 (6), 707–715. doi: 10.1111/j.1439-0523.2012.02002.x

Amram, A., Fadida-Myers, A., Golan, G., Nashef, K., Ben-David, R., and Peleg, Z. (2015). Effect of GA-sensitivity on wheat early vigor and yield components under deep sowing. *Front. Plant Sci.* 6, 487. doi: 10.3389/fpls.2015.00487

Aycan, M., Baslam, M., Asiloglu, R., Mitsui, T., and Yildiz, M. (2021). Development of new high-salt tolerant bread wheat (Triticum aestivum L.) genotypes and insight into the tolerance mechanisms. *Plant Physiol. Biochem.* 166, 314–327. doi: 10.1016/j.plaphy.2021.05.041

Bailey-Serres, J., Parker, J. E., Ainsworth, E. A., Oldroyd, G. E., and Schroeder, J. I. (2019). Genetic strategies for improving crop yields. *Nature* 575 (7781), 109–118. doi: 10.1038/s41586-019-1679-0

Bakhshi, B., and Shahmoradi, S. S. (2023). Simultaneous selection of high-yielding and drought-tolerant barley landraces using GT, GYT and GYSI methodologies. *Cereal Res. Commun.* 51 (1), 237–248. doi: 10.1007/s42976-022-00290-1

Bidinger, F., Mahalakshmi, V., and Rao, G. D. P. (1987). Assessment of drought resistance in pearl millet (Pennisetum americanum (L.) Leeke). II. Estimation of genotype response to stress. *Aust. J. Agric. Res.* 38 (1), 49–59. doi: 10.1071/AR9870049

Birth, G. S., and McVey, G. R. (1968). Measuring the color of growing turf with a reflectance spectrophotometer 1. *Agron. J.* 60 (6), 640–643. doi: 10.2134/agronj1968.00021962006000060016x

Bouslama, M., and Schapaugh, W.Jr (1984). Stress tolerance in soybeans. I. Evaluation of three screening techniques for heat and drought tolerance 1. *Crop Sci.* 24 (5), 933–937. doi: 10.2135/cropsci1984.0011183X002400050026x

Bruning, B., Berger, B., Lewis, M., Liu, H., and Garnett, T. (2020). Approaches, applications, and future directions for hyperspectral vegetation studies: an emphasis on yield-limiting factors in wheat. *Plant Phenome J.* 3 (1), e20007. doi: 10.1002/ppj2.20007

Darwish, M. A., Elkot, A. F., Elfanah, A., Selim, A. I., Yassin, M. M., Abomarzoka, E. A., et al. (2023). Evaluation of wheat genotypes under water regimes using hyperspectral reflectance and agro-physiological parameters via genotype by yield* trait approaches in sakha station, delta, egypt. *Agriculture* 13 (7), 1338. doi: 10.3390/agriculture13071338

Darwish, M., Mohamed, M., AbdEl-Rady, A., Ghalab, E., and Elfanah, A. M. S. (2022). Estimation of AMMI and GGE biplots for some bread and durum wheat genotypes. *J. Plant Production* 13 (3), 75–83. doi: 10.21608/JPP.2022.131275.1103

Dawood, M. G., Abdelhamid, M. T., and Schmidhalter, U. (2014). Potassium fertiliser enhances the salt-tolerance of common bean (Phaseolus vulgaris L.). *J. Hortic. Sci. Biotechnol.* 89 (2), 185–192. doi: 10.1080/14620316.2014.11513067

Elfanah, A. M., Darwish, M. A., Selim, A. I., Shabana, M. M., Elmoselhy, O. M., Khedr, R. A., et al. (2023). Spectral reflectance indices' performance to identify seawater salinity tolerance in bread wheat genotypes using genotype by yield* trait biplot approach. *Agronomy* 13 (2), 353. doi: 10.3390/agronomy13020353

El-Hendawy, S., Al-Suhaibani, N., Elsayed, S., Alotaibi, M., Hassan, W., and Schmidhalter, U. (2019). Performance of optimized hyperspectral reflectance indices and partial least squares regression for estimating the chlorophyll fluorescence and grain yield of wheat grown in simulated saline field conditions. *Plant Physiol. Biochem.* 144, 300–311. doi: 10.1016/j.plaphy.2019.10.006

El-Hendawy, S., Al-Suhaibani, N., Mubushar, M., Tahir, M. U., Marey, S., Refay, Y., et al. (2022). Combining hyperspectral reflectance and multivariate regression models to estimate plant biomass of advanced spring wheat lines in diverse phenological stages under salinity conditions. *Appl. Sci.* 12 (4), 1983. doi: 10.3390/app12041983

Enyew, M., Feyissa, T., Geleta, M., Tesfaye, K., Hammenhag, C., and Carlsson, A. S. (2021). Genotype by environment interaction, correlation, AMMI, GGE biplot and cluster analysis for grain yield and other agronomic traits in sorghum (Sorghum bicolor L. Moench). *PloS One* 16 (10), e0258211. doi: 10.1371/journal.pone.0258211

FAOSTAT (2021). Available at: https://www.fao.org/worldfoodsituation/csdb/en/ (Accessed June 14, 2022).

Fernandez, G. C. (1992). "Effective selection criteria for assessing plant stress tolerance," in *Proceeding of the International Symposium on Adaptation of Vegetables and other Food Crops in Temperature and Water Stress*, Shanhua, Taiwan, Aug. 13-16. 257–270.

Fischer, R., and Maurer, R. (1978). Drought resistance in spring wheat cultivars. I. Grain yield responses. *Aust. J. Agric. Res.* 29 (5), 897–912. doi: 10.1071/AR9780897

Fischer, R., and Wood, J. (1979). Drought resistance in spring wheat cultivars. III.* Yield associations with morpho-physiological traits. *Aust. J. Agric. Res.* 30 (6), 1001–1020. doi: 10.1071/AR9791001

Gamon, J., Penuelas, J., and Field, C. (1992). A narrow-waveband spectral index that tracks diurnal changes in photosynthetic efficiency. *Remote Sens. Environ.* 41 (1), 35–44. doi: 10.1016/0034-4257(92)90059-S

Gamon, J., and Surfus, J. (1999). Assessing leaf pigment content and activity with a reflectometer. *New Phytol.* 143 (1), 105–117. doi: 10.1046/j.1469-8137.1999.00424.x

Gavuzzi, P., Rizza, F., Palumbo, M., Campanile, R., Ricciardi, G., and Borghi, B. (1997). Evaluation of field and laboratory predictors of drought and heat tolerance in winter cereals. *Can. J. Plant Sci.* 77 (4), 523–531. doi: 10.4141/P96-130

Ghonaim, M. M., Mohamed, H. I., and Omran, A. A. (2021). Evaluation of wheat (Triticum aestivum L.) salt stress tolerance using physiological parameters and retrotransposon-based markers. *Genet. Resour. Crop Evol.* 68, 227–242. doi: 10.1007/s10722-020-00981-w

Gioia, T., Nagel, K. A., Beleggia, R., Fragasso, M., Ficco, D. B. M., Pieruschka, R., et al. (2015). Impact of domestication on the phenotypic architecture of durum wheat under contrasting nitrogen fertilization. *J. Exp. Bot.* 66 (18), 5519–5530. doi: 10.1093/jxb/erv289

Gitelson, A. A., Merzlyak, M. N., and Chivkunova, O. B. (2001). Optical properties and nondestructive estimation of anthocyanin content in plant leaves¶. *Photochem. Photobiol.* 74 (1), 38–45. doi: 10.1562/0031-8655(2001)074<0038:OPANEO>2.0.CO;2

Gizaw, S. A., Godoy, J. G. V., Garland-Campbell, K., and Carter, A. H. (2018). Using spectral reflectance indices as proxy phenotypes for genome-wide association studies of yield and yield stability in Pacific Northwest winter wheat. *Crop Sci.* 58 (3), 1232–1241. doi: 10.2135/cropsci2017.11.0710

Guyot, G., and Baret, F. (1988). "Utilisation de la haute resolution spectrale pour suivre l'etat des couverts vegetaux," in *Spectral Signatures of Objects in Remote Sensing* 287, 279.

Haq, T. U., Gorham, J., Akhtar, J., Akhtar, N., and Steele, K. A. (2010). Dynamic quantitative trait loci for salt stress components on chromosome 1 of rice. *Funct. Plant Biol.* 37 (7), 634–645. doi: 10.1071/FP09247

Hasanuzzaman, M., Shabala, L., Zhou, M., Brodribb, T. J., Corkrey, R., and Shabala, S. (2018). Factors determining stomatal and non-stomatal (residual) transpiration and their contribution towards salinity tolerance in contrasting barley genotypes. *Environ. Exp. Bot.* 153, 10–20. doi: 10.1016/j.envexpbot.2018.05.002

Hinojosa, L., Kumar, N., Gill, K. S., and Murphy, K. M. (2019). Spectral reflectance indices and physiological parameters in quinoa under contrasting irrigation regimes. *Crop Sci.* 59 (5), 1927–1944. doi: 10.2135/cropsci2018.11.0711

Kalaji, M., and Guo, P. (2008). Chlorophyll fluorescence: a useful tool in barley plant breeding programs. *Photochem. Res. Prog.* 29, 439–463.

Kendal, E. (2020). Evaluation of some barley genotypes with geotype by yield* trait (GYT) biplot method. *Poljoprivreda i Sumarstvo* 66 (2), 137–150. doi: 10.17707/AgricultForest.66.2.13

Kurbanov, R., Panarina, V., Polukhin, A., Lobachevsky, Y., Zakharova, N., Litvinov, M., et al. (2023). Evaluation of field germination of soybean breeding crops using multispectral data from UAV. *Agronomy* 13 (5), 1348. doi: 10.3390/agronomy13051348

Moghimi, A., Yang, C., Miller, M. E., Kianian, S. F., and Marchetto, P. M. (2018). A novel approach to assess salt stress tolerance in wheat using hyperspectral imaging. *Front. Plant Sci.* 9, 1182. doi: 10.3389/fpls.2018.01182

Mohamed, N. N. (2017). Management of salt-affected soils in the Nile Delta. *Nile Delta* 50, 265–295. doi: 10.1007/698_201

Mohammadi, R. (2019). Genotype by yield* trait biplot for genotype evaluation and trait profiles in durum wheat. *Cereal Res. Commun.* 47 (3), 541–551. doi: 10.1556/0806.47.2019.32

Mohammadi, R., and Amri, A. (2021). Agronomic performance and genotype× Moisture conditions interaction for morpho-physiological traits in durum wheat. *Crop Breeding Genet. Genomics* 3 (1), 1-25. doi: 10.20900/cbgg20210002

Mohammadi, R., Cheghamirza, K., Geravandi, M., and Abbasi, S. (2022). Assessment of genetic and agro-physiological diversity in a global durum wheat germplasm. *Cereal Res. Commun.* 50, 1–10. doi: 10.1007/s42976-021-00143-3

Mohan, A., Grant, N. P., Schillinger, W. F., and Gill, K. S. (2021). Characterizing reduced height wheat mutants for traits affecting abiotic stress and photosynthesis during seedling growth. *Physiologia Plantarum* 172 (1), 233–246. doi: 10.1111/ppl.13321

Morsy, S., Elbasyoni, I. S., Baenziger, S., and Abdallah, A. M. (2022). Gypsum amendment influences performance and mineral absorption in wheat cultivars grown in normal and saline-sodic soils. *J. Agron. Crop Sci.* 208 (5), 675–692. doi: 10.1111/jac.12598

Moustafa, E. S., Ali, M. M., Kamara, M. M., Awad, M. F., Hassanin, A. A., and Mansour, E. (2021). Field screening of wheat advanced lines for salinity tolerance. *Agronomy* 11 (2), 281. doi: 10.3390/agronomy11020281

Msundi, E. A., Owuoche, J. O., Oyoo, M. E., Macharia, G., Singh, R. P., and Randhawa, M. S. (2021). Identification of bread wheat genotypes with superior grain yield and agronomic traits through evaluation under rust epiphytotic conditions in Kenya. *Sci. Rep.* 11 (1), 21415. doi: 10.1038/s41598-021-00785-7

Munns, R., and Gilliham, M. (2015). Salinity tolerance of crops–what is the cost? *New Phytol.* 208 (3), 668–673. doi: 10.1111/nph.13519

Munns, R., and Tester, M. (2008). Mechanisms of salinity tolerance. *Annu. Rev. Plant Biol.* 59, 651–681. doi: 10.1146/annurev.arplant.59.032607.092911

Oyiga, B. C., Sharma, R., Shen, J., Baum, M., Ogbonnaya, F., Léon, J., et al. (2016). Identification and characterization of salt tolerance of wheat germplasm using a multivariable screening approach. *J. Agron. Crop Sci.* 202 (6), 472–485. doi: 10.1111/jac.12178

Pour-Aboughadareh, A., Yousefian, M., Moradkhani, H., Moghaddam Vahed, M., Poczai, P., and Siddique, K. H. (2019). iPASTIC: An online toolkit to estimate plant abiotic stress indices. *Appl. Plant Sci.* 7 (7), e11278. doi: 10.1002/aps3.11278

Prasad, B., Carver, B. F., Stone, M. L., Babar, M., Raun, W. R., and Klatt, A. R. (2007). Genetic analysis of indirect selection for winter wheat grain yield using spectral reflectance indices. *Crop Sci.* 47 (4), 1416–1425. doi: 10.2135/cropsci2006.08.0546

Pu, R., Gong, P., and Yu, Q. (2008). Comparative analysis of EO-1 ALI and Hyperion, and Landsat ETM+ data for mapping forest crown closure and leaf area index. *Sensors* 8 (6), 3744–3766. doi: 10.3390/s8063744

Quamruzzaman, M., Manik, S. N., Livermore, M., Johnson, P., Zhou, M., and Shabala, S. (2022). Multidimensional screening and evaluation of morpho-physiological indices for salinity stress tolerance in wheat. *J. Agron. Crop Sci.* 208 (4), 454–471. doi: 10.1111/jac.12587

Rady, M. M., Mounzer, O., Alarcón, J., Abdelhamid, M., and Howladar, S. (2016). Growth, heavy metal status and yield of salt-stressed wheat (Triticum aestivum L.) plants as affected by the integrated application of bio-, organic and inorganic nitrogen-fertilizers. *J. Appl. Bot. Food Qual.* 89, 21-28.

Rebouh, N., Mohamed, E. S., Polityko, P., Dokukin, P., Kucher, D., Latati, M., et al. (2023). Towards improving the precision agriculture management of the wheat crop using remote sensing: A case study in Central Non-Black Earth region of Russia. *Egyptian J. Remote Sens. Space Sci.* 26 (3), 505–517. doi: 10.1016/j.ejrs.2023.06.007

Reynolds, M. P., and Braun, H.-J. (2022). *Wheat improvement: food security in a changing climate.* (Springer Nature).

Reynolds, M., Pask, A., and Mullan, D. (2012). *Physiological breeding I: interdisciplinary approaches to improve crop adaptation.* (Mexico, D.F.: CIMMYT).

Rosielle, A., and Hamblin, J. (1981). Theoretical aspects of selection for yield in stress and non-stress environment 1. *Crop Sci.* 21 (6), 943–946. doi: 10.2135/cropsci1981.0011183X002100060033x

Rouse, J. W. Jr., Haas, R. H., Deering, D., Schell, J., and Harlan, J. C. (1974). Monitoring the vernal advancement and retrogradation (green wave effect) of natural vegetation. https://ntrs.nasa.gov/citations/19750020419

Sabouri, A., Dadras, A. R., Azari, M., Saberi Kouchesfahani, A., Taslimi, M., and Jalalifar, R. (2022). Screening of rice drought-tolerant lines by introducing a new composite selection index and competitive with multivariate methods. *Sci. Rep.* 12 (1), 2163. doi: 10.1038/s41598-022-06123-9

Santana, D. C., Flores, M., Cotrim, M. F., Rodrigues, E. V., Santos, A.d., Teodoro, L. P. R., et al. (2021). Genotype× trait biplot and canonical correlations for spectral and agronomic traits in corn. *Agron. J.* 113 (2), 1197–1204. doi: 10.1002/agj2.20581

Sardouie-Nasab, S., Mohammadi-Nejad, G., and Nakhoda, B. (2014). Field screening of salinity tolerance in Iranian bread wheat lines. *Crop Sci.* 54 (4), 1489–1496. doi: 10.2135/cropsci2013.06.0359

Schneider, K. A., Rosales-Serna, R., Ibarra-Perez, F., Cazares-Enriquez, B., Acosta-Gallegos, J. A., Ramirez-Vallejo, P., et al. (1997). Improving common bean performance under drought stress. *Crop Sci.* 37 (1), 43–50. doi: 10.2135/cropsci1997.0011183X003700010007x

Shabala, S., Bose, J., and Hedrich, R. (2014). Salt bladders: do they matter? *Trends Plant Sci.* 19 (11), 687–691. doi: 10.1016/j.tplants.2014.09.001

Sims, D. A., and Gamon, J. A. (2002). Relationships between leaf pigment content and spectral reflectance across a wide range of species, leaf structures and developmental stages. *Remote Sens. Environ.* 81 (2-3), 337–354. doi: 10.1016/S0034-4257(02)00010-X

Sofi, P. A., Saba, I., Ara, A., and Rehman, K. (2022). Comparative efficiency of GY* T approach over GT approach in genotypic selection in multiple trait evaluations: case study of common bean (Phaseolus vulgaris) grown under temperate Himalayan conditions. *Agric. Res.* 11 (3), 373–381. doi: 10.1007/s40003-021-00577-5

Stavi, I., Thevs, N., and Priori, S. (2021). Soil salinity and sodicity in drylands: A review of causes, effects, monitoring, and restoration measures. *Front. Environ. Sci.* 330. doi: 10.3389/fenvs.2021.712831

Sun, H., Feng, M., Xiao, L., Yang, W., Wang, C., Jia, X., et al. (2019). Assessment of plant water status in winter wheat (Triticum aestivum L.) based on canopy spectral indices. *PloS One* 14 (6), e0216890. doi: 10.1371/journal.pone.0216890

Tao, R., Ding, J., Li, C., Zhu, X., Guo, W., and Zhu, M. (2021). Evaluating and screening of agro-physiological indices for salinity stress tolerance in wheat at the seedling stage. *Front. Plant Sci.* 12, 646175. doi: 10.3389/fpls.2021.646175

ur Rehman, H., Alharby, H. F., Bamagoos, A. A., Abdelhamid, M. T., and Rady, M. M. (2021). Sequenced application of glutathione as an antioxidant with an organic biostimulant improves physiological and metabolic adaptation to salinity in wheat. *Plant Physiol. Biochem.* 158, 43–52. doi: 10.1016/j.plaphy.2020.11.041

Wu, H., Shabala, L., Zhou, M., Stefano, G., Pandolfi, C., Mancuso, S., et al. (2015). Developing and validating a high-throughput assay for salinity tissue tolerance in wheat and barley. *Planta* 242, 847–857. doi: 10.1007/s00425-015-2317-1

Yan, W., and Frégeau-Reid, J. (2008). Breeding line selection based on multiple traits. *Crop Sci.* 48 (2), 417–423. doi: 10.2135/cropsci2007.05.0254

Yan, W., and Frégeau-Reid, J. (2018). Genotype by yield* trait (GYT) biplot: a novel approach for genotype selection based on multiple traits. *Sci. Rep.* 8 (1), 8242. doi: 10.1038/s41598-018-26688-8

Yan, W., Hunt, L. A., Sheng, Q., and Szlavnics, Z. (2000). Cultivar evaluation and mega-environment investigation based on the GGE biplot. *Crop Sci.* 40 (3), 597–605. doi: 10.2135/cropsci2000.403597x

Yan, W., Kang, M. S., Ma, B., Woods, S., and Cornelius, P. L. (2007). GGE biplot vs. AMMI analysis of genotype-by-environment data. *Crop Sci.* 47 (2), 643–653. doi: 10.2135/cropsci2006.06.0374

Yang, M.-D., Leghari, S. J., Guan, X.-K., Ma, S.-C., Ding, C.-M., Mei, F.-J., et al. (2020). Deficit subsurface drip irrigation improves water use efficiency and stabilizes yield by enhancing subsoil water extraction in winter wheat. *Front. Plant Sci.* 11, 508. doi: 10.3389/fpls.2020.00508

Yang, Y., Li, N., Wu, Y., Liu, B., Li, S., Tao, L., et al. (2022). Key phenotypes related to wheat grain yield in a two-site multicultivar test. *Agron. J.* 114 (5), 2874–2885. doi: 10.1002/agj2.21098

Zarco-Tejada, P. J., Berjón, A., López-Lozano, R., Miller, J. R., Martín, P., Cachorro, V., et al. (2005). Assessing vineyard condition with hyperspectral indices: Leaf and canopy reflectance simulation in a row-structured discontinuous canopy. *Remote Sens. Environ.* 99 (3), 271–287. doi: 10.1016/j.rse.2005.09.002

Zarco-Tejada, P. J., Pushnik, J., Dobrowski, S., and Ustin, S. (2003). Steady-state chlorophyll a fluorescence detection from canopy derivative reflectance and double-peak red-edge effects. *Remote Sens. Environ.* 84 (2), 283–294. doi: 10.1016/S0034-4257(02)00113-X

Zulfiqar, S., Ishfaq, S., Ikram, M., Nawaz, M. A., and Rahman, M.-u. (2021). Characterization of gamma-rays-induced spring wheat mutants for morphological and quality traits through multivariate and GT Bi-plot analysis. *Agronomy* 11 (11), 2288. doi: 10.3390/agronomy11112288

frontiers | Frontiers in Plant Science

TYPE Systematic Review
PUBLISHED 25 August 2023
DOI 10.3389/fpls.2023.1221288

OPEN ACCESS

EDITED BY
Akbar Hossain,
Bangladesh Wheat and Maize Research Institute, Bangladesh

REVIEWED BY
Muhammad Adnan Akram,
Lanzhou University, China
Biswajit Pramanick,
Dr. Rajendra Prasad Central Agricultural University, India

*CORRESPONDENCE
Rentao Liu
nxuliu2012@126.com
Hongwei Xu
xuhongwei16@sicau.edu.cn

†These authors share first authorship

RECEIVED 09 June 2023
ACCEPTED 09 August 2023
PUBLISHED 25 August 2023

CITATION
Qu Q, Wang Z, Gan Q, Liu R and Xu H (2023) Impact of drought on soil microbial biomass and extracellular enzyme activity. *Front. Plant Sci.* 14:1221288. doi: 10.3389/fpls.2023.1221288

Impact of drought on soil microbial biomass and extracellular enzyme activity

Qing Qu[1,2†], Zhen Wang[1†], Quan Gan[3], Rentao Liu[1*] and Hongwei Xu[3*]

[1]Breeding Base for State Key Laboratory of Land Degradation and Ecological Restoration in Northwestern China, Key Laboratory of Restoration and Reconstruction of Degraded Ecosystems in Northwestern China of Ministry of Education, Ningxia University, Yinchuan, China, [2]Institute of Soil and Water Conservation, Chinese Academy of Sciences and Ministry of Water Resources, Yangling, China, [3]College of Forestry, Sichuan Agricultural University, Chengdu, China

Introduction: With the continuous changes in climate patterns due to global warming, drought has become an important limiting factor in the development of terrestrial ecosystems. However, a comprehensive understanding of the impact of drought on soil microbial activity at a global scale is lacking.

Methods: In this study, we aimed to examine the effects of drought on soil microbial biomass (carbon [MBC], nitrogen [MBN], and phosphorus [MBP]) and enzyme activity (β-1, 4-glucosidase [BG]; β-D-cellobiosidase [CBH]; β-1, 4-N-acetylglucosaminidase [NAG]; L-leucine aminopeptidase [LAP]; and acid phosphatase [AP]). Additionally, we conducted a meta-analysis to determine the degree to which these effects are regulated by vegetation type, drought intensity, drought duration, and mean annual temperature (MAT).

Result and discussion: Our results showed that drought significantly decreased the MBC, MBN, and MBP and the activity levels of BG and AP by 22.7%, 21.2%, 21.6%, 26.8%, and 16.1%, respectively. In terms of vegetation type, drought mainly affected the MBC and MBN in croplands and grasslands. Furthermore, the response ratio of BG, CBH, NAG, and LAP were negatively correlated with drought intensity, whereas MBN and MBP and the activity levels of BG and CBH were negatively correlated with drought duration. Additionally, the response ratio of BG and NAG were negatively correlated with MAT. In conclusion, drought significantly reduced soil microbial biomass and enzyme activity on a global scale. Our results highlight the strong impact of drought on soil microbial biomass and carbon- and phosphorus-acquiring enzyme activity.

KEYWORDS

biogeochemical cycles, climate change, ecosystem function, ecosystem structure, soil microbial activity, soil microbial community

1 Introduction

With the intensification of climate warming, global precipitation patterns have changed considerably, affecting the structure, function, and biodiversity of terrestrial ecosystems (van der Molen et al., 2011; Lozano et al., 2021). Data indicate that the occurrence of future extreme weather events, such as rainfall or drought, will likely exhibit a trend of long duration and wide impact (Stott, 2016). In particular, drought will reduce soil moisture, which directly affects plant growth and photosynthesis, thereby affecting the versatility of soil ecosystems (Barnes et al., 2018; Li et al., 2022; Wan et al., 2022).

As the most active component of soil organic matter, the microbial biomass (carbon [MBC], nitrogen [MBN], and phosphorus [MBP]) is very sensitive to changes in the soil environment and can accurately reflect changes in soil carbon and nitrogen content (Wardle, 1998; Bastos et al., 2023). As an important component of soil biological activity, enzymes determine the intensity and direction of various biochemical processes in soil and are an indicator of soil fertility and vitality (Wang et al., 2023a). Soil microbial biomass content and enzyme activity exhibit a more rapid response to changes in soil moisture than to changes in other soil properties. For example, a decrease in soil water availability directly or indirectly affects the reproduction and activity of microorganisms (Ren et al., 2018; Chen et al., 2023). Therefore, exploring the effects of drought on microbial activity will contribute to our understanding of the structure and function of terrestrial ecosystems under various global precipitation patterns.

Previous studies have shown that prolonged drought limits vegetation growth and alters microbial community structure (Mishra et al., 2021; Peszek et al., 2021; Wang et al., 2023b). For example, Wang et al. (2021b) demonstrated that drought reduced plant primary productivity and biomass by 12.6% and 16.7%, respectively (Figure 1). A reduction in plant biomass directly affects the sources of energy for microorganisms (Song et al., 2019; Ge et al., 2022; Malik and Bouskill, 2022). Additionally, drought affects microbial activity by increasing osmotic stress and resource competition (Canarini et al., 2021; Xie et al., 2021; He et al., 2023). A decrease in soil water availability directly leads to the dehydration of some microorganisms, thereby reducing overall microbial activity, and even leading to the death and decomposition of some microorganisms (Zhang et al., 2023). In addition, lack of soil moisture affects the physiological characteristics of microorganisms and reduces their ability to acquire and utilise pairs (Sistla and Schimel, 2012), thus limiting their biological activity owing to a lack of energy. However, Sanaullah et al. (2011) found that drought did not substantially reduce the soil microbial biomass; however, this result may be related to the strong drought resistance of crops or local climatic conditions in this study. Therefore, uncertainties remain regarding the impacts of drought on microbial activity (Figure 1). A meta-analysis is urgently needed to determine these effects and to reveal the response of terrestrial biogeochemical cycles to changes in global precipitation patterns.

Drought intensity and duration are important factors affecting microbial activity (Sun et al., 2020). Moderate drought inhibits plant growth; however, an excessive reduction in soil water availability may lead to plant death (Hoover et al., 2014; Akram et al., 2020; Zang et al., 2020). A recent meta-analysis confirmed this conclusion (Wang et al., 2021b). Substantial reductions in plant biomass limit the availability of food sources for microorganisms (Brown et al., 2021). Furthermore, excessive drought damages soil properties, such as structure, porosity, and pH (Chen et al., 2020; Lozano et al., 2021; Peng et al., 2023), thereby creating environmental conditions that are unfavourable for the growth of microorganisms. Consequently, microbial metabolism, activity, and enzyme production are reduced (Manzoni et al., 2014; Fitzpatrick et al., 2017).

Furthermore, excessive drought damages soil properties, such as structure, porosity, and pH (Chen et al., 2020; Lozano et al., 2021; Peng et al., 2023), thereby creating environmental conditions that are unfavourable for the growth of microorganisms. Consequently, microbial metabolism, activity, and enzyme production are reduced (Manzoni et al., 2014; Fitzpatrick et al., 2017). For example, compared with those in forests, plants in croplands and grasslands typically have lower biomass and shallower root systems (Jian et al., 2015; Cheng et al., 2016); therefore, after drought, there are large differences in the effects on plant growth for each vegetation type, resulting in different impacts on soil microorganisms. However, owing to the complexity and heterogeneity of ecosystems (Hu et al., 2021; Wang et al., 2021a), our understanding of how drought affects soil microbial activity under different vegetation types is still incomplete. In addition, microbial activity is also regulated by climatic factors such as mean annual temperature (MAT) (Malik et al., 2020a). Moderate temperature increases can promote plant growth and accelerate soil nutrient turnover (Akram et al., 2022; Joly et al., 2023), but excessively high temperatures may exacerbate soil moisture loss (Qu et al., 2023), resulting in strong inhibition of microbial activity. Overall, research on the global-scale impacts of drought on microbial activity, especially in terms of drought intensity, drought duration, vegetation type, and MAT is lacking (Figure 1). This gap in the existing literature has limited our understanding of the impacts of increasing drought on ecosystem structure, function, and biodiversity under global climate change.

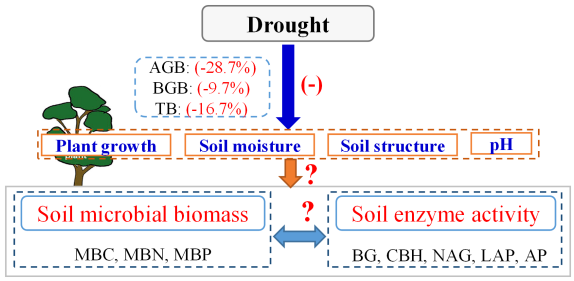

FIGURE 1
Conceptual framework showing impacts of drought on plant growth, soil microbial biomass, and enzyme activity. "+" and "-" indicate positive and negative effects, respectively. "?", unresolved by the previous study. Data on the effects of drought on plant biomass comes from the results of the previous meta-analysis (Wang et al., 2021b). AGB, above-ground biomass. BGB, below-ground biomass. TB, total biomass. MBC, soil microbial biomass carbon. MBN, microbial biomass nitrogen. MBP, microbial biomass phosphorus. BG, β-1, 4-glucosidase. CBH, β-D-cellobiosidase. NAG, β-1, 4-N-acetylglucosaminidase. LAP, L-leucine aminopeptidase.

Based on meta-analysis and published data, this study investigated the effects of drought on soil microbial activity. The specific aims of this study were to identify: (1) how drought affects soil microbial biomass and enzyme activity and (2) whether this effect is regulated by vegetation type (cropland, grassland, shrub, and forest), geographical location/continents (Asia, America, Europe, Oceania, and Africa), drought intensity, drought duration, and MAT. Our hypotheses were as follows: (1) Drought inhibits soil microbial activity due to adverse soil environmental conditions (e.g., reduced availability of energy sources and changes in physical structure) (Manzoni et al., 2014; Fitzpatrick et al., 2017). (2) The effect of drought on microbial activity is higher in croplands and grasslands than in forests owing to different plant growth characteristics (Clark et al., 2009). (3) Drought intensity and duration aggravate its negative effects on microbial activity because severe and prolonged droughts can cause plants to wither and die, thereby reducing plant biomass (Smith et al., 2009; Brown et al., 2021). The results of this study contribute to an improved understanding of the impact of drought on the structure, function, and biodiversity of terrestrial ecosystems.

2 Materials and methods

2.1 Data collection

We utilized the Web of Science, Google Scholar, and the China National Knowledge Infrastructure databases to search all relevant literature published prior to 2023. The search terms are listed in Supplementary Table 1. After a preliminary screening of titles and abstracts, the literature was evaluated again based on the following criteria: (1) A treatment group (drought) and control group (normal water supply) must be included. (2) The vegetation types, drought intensity, and drought duration must be identified. (3) At least one research index must be included (Supplementary Table 2). (4) The research should not include the interaction of multiple factors, such as nitrogen addition, warming, or carbon dioxide doubling. (5) If data for multiple soil layers were reported in the study, only the manifested soil index data were obtained. (6) The research must clarify the mean, sample size, and standard deviation (SD) of all variables. If no standard deviation was reported, it was calculated using the standard error (SE) as follows: $SD = SE\sqrt{N}$ (Fu et al., 2015). The screening steps are shown in Supplementary Figure 1. In addition, we collected data on longitude, latitude, MAT, mean annual precipitation (MAP), drought intensity, and drought duration. MAT, mean annual precipitation (MAP) are obtained directly from the article or from the WorldClim database (http://www.worldclim.org/).

2.2 Meta-analysis

The response ratio (RR) was used to measure the influence of drought on related variables (Hedges et al., 1999), and was calculated using the following formula:

$$\mathrm{RR} = \ln\left(\frac{\overline{X_t}}{\overline{X_c}}\right) = ln\overline{X_t} - ln\overline{X_c} \quad (1)$$

$$v = \frac{S_t^2}{n_t X_t^2} + \frac{S_c^2}{n_c X_c^2} \quad (2)$$

where, $\overline{X_t}$ and $\overline{X_c}$ are the mean values of the variables in the experimental and control groups, respectively; nt and nc are the sample sizes of the variables in the experimental and control groups, respectively; and St and Sc are the SD of the variables in the experimental and control groups, respectively.

The weighted response ratio (RR_{++}), 95% bootstrap confidence interval (CI), standard error $S(RR_{++})$, and weighting factor (w) were calculated using the random-effects model. If the 95% bootstrap CI was located to the left of the zero-carving line, it indicated that, compared with the control group, the treatment group had a negative effect on related research indicators; otherwise, it had a positive effect. When zero was included, drought had no significant influence on the corresponding variables. These values were calculated using the following equations:

$$RR_{++} = \frac{\sum_{i=1}^{m}\sum_{j=1}^{ki} W_{ij} RR_{ij}}{\sum_{i=1}^{m}\sum_{j=1}^{ki} W_{ij}} \quad (3)$$

$$95\%\mathrm{CI} = RR_{++} \pm 1.96 S(RR_{++}) \quad (4)$$

$$S(RR_{++}) = \sqrt{\frac{1}{\sum_{i=1}^{m}\sum_{j=1}^{ki} W_{ij}}} \quad (5)$$

$$w_{ij} = \frac{1}{\vartheta_i + \sigma^2} \quad (6)$$

where, ϑ_i and σ^2 are the variance of the data in the i-th study and the random variable that exists between the studies, respectively.

To describe the RR of each variable more intuitively and clearly, we converted the value to a percentage using the following formula:

$$\text{Effect size}(\%) = [exp(RR_{++}) - 1] \times 100\% \quad (7)$$

In this study, a linear mixed model was used to analyse whether the RRs of soil microbial biomass and enzyme activity were affected by vegetation type (cropland, grassland, shrub, and forest) and continents (Asia, America, Europe, Oceania, and Africa). "Study" was designated as the random effects component (Bates et al., 2015; Hao et al., 2022). The influence of the grouping variables on microbial activity was calculated using the random-effects model, which indicated heterogeneity in the group cumulative effect sizes (Q_M) (Gao et al., 2021; Xu et al., 2022a). Regression analysis was selected to study the relationships of the RRs of soil microbial biomass and enzyme activity with drought intensity, drought duration, and MAT. A funnel plot was used to assess potential publication bias (Supplementary Figure 2). The above processes were performed using the R v.4.0.2 metafor package. Both integrated and regression analysis diagrams were completed using Origin 9.0.

3 Results

3.1 Overview of the dataset

In total, 60 studies encompassing 250 data points and 12 variables were included in this study (Appendix Dataset 1, Supplementary Table 2). The sample sizes of cropland, grassland, shrub, and forest were 41, 92, 11, and 106, respectively. The distribution of the sample points is shown in Figure 2.

3.2 Overall effects

Drought significantly affected soil microbial biomass and enzyme activity, and the effects varied among different variables (Figure 3). Briefly, drought significantly decreased soil microbial biomass carbon (MBC), microbial biomass nitrogen (MBN), and microbial biomass phosphorus (MBP) by 22.7%, 21.2%, and 21.6%, respectively. Meanwhile, drought considerably decreased the activities of β-1, 4-glucosidase (BG) and acid phosphatase (AP) by 26.8% and 16.1%, respectively, but had a lesser effect on β-D-cellobiosidase (CBH), β-1, 4-N-acetylglucosaminidase (NAG), and L-leucine aminopeptidase (LAP). Additionally, drought markedly decreased the soil organic carbon (SOC) and total phosphorus (TP) by 6.5% and 7.6%, respectively. Overall, drought had a stronger inhibitory effect on soil microbial biomass and soil carbon- and phosphorus-acquiring enzyme activity and a weaker effect on soil nitrogen-acquiring enzyme activity.

3.3 Response of soil microbial biomass and enzyme activity to vegetation types and continents

The effects of drought on soil microbial biomass and enzyme activity are regulated by vegetation types (Figure 4; Supplementary Table 3). Briefly, drought negatively affected MBC and MBN in croplands (MBC: -30.2%; MBN: -36.1%) and grasslands (MBC: -12.1%; MBN: -15.6%), but it had less effect on these factors in shrubs and forests (Figure 4A). Drought negatively affected BG in croplands (-49.1%) and AP in croplands (-20.5%) and grasslands (-12.6%), whereas the effect on CBH and NAG were all neutral in grasslands and forests (Figure 4B). In addition, drought negatively affected SOC in croplands (-7.9%), grasslands (-6.3%), and forests (-6.4%) (Figure 4C).

In contrast, continents played a smaller role in regulating the effects of drought on soil microbial biomass and enzyme activity (Figure 5; Supplementary Table 4). Briefly, drought only negatively affected MBN in Asia (-22.9%), LAP in Europe (-65.2%), and AP in Asia (-15.4%), whereas the effects on other indices were neutral in all continents (Figures 5A–C).

3.4 Response of soil microbial biomass and enzyme activity to drought intensity and duration

Drought intensity had different effects on soil microbial biomass and enzyme activity (Figure 6). Briefly, the response ratio of BG, CBH, NAG, and LAP decreased significantly ($p < 0.05$) with increasing drought intensity, whereas the response ratio of soil microbial biomass did not show significant ($p > 0.05$) changes with increasing drought intensity (Figures 6A, B). Meanwhile, drought intensity did not significantly affect the response ratio of total nitrogen (TN) and TP ($p > 0.05$), but it was significantly negatively correlated with the response ratio of SOC and pH (Figure 6C).

Drought duration also showed different effects on soil microbial biomass and enzyme activity (Figure 6). Briefly, the response ratio of MBN, MBP, BG, CBH, NAG, and LAP decreased significantly ($p < 0.05$) with increasing drought duration, whereas the response ratio of MBC did not show significant ($p > 0.05$) changes with increasing drought duration (Figures 6D, E). Meanwhile, the

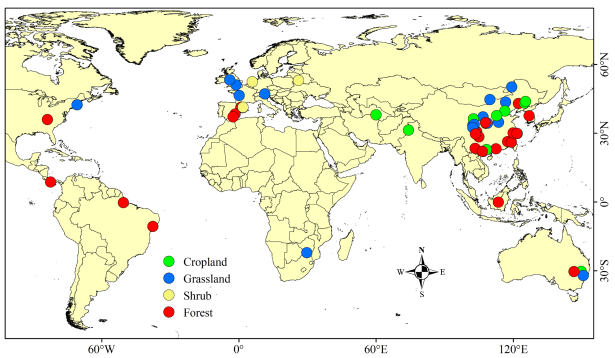

FIGURE 2
Global distribution of study sites used in this meta-analysis.

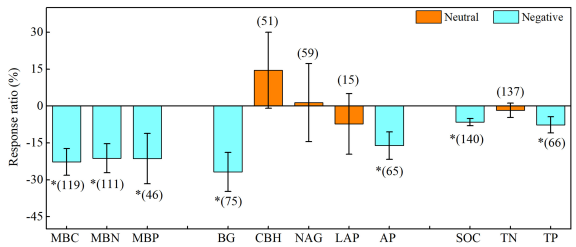

FIGURE 3
Effects of drought on soil microbial biomass, enzyme activity, and soil chemistry properties. Error bars denote the 95% confidence interval (CI). The number in parentheses indicates the sample size. * indicates that the impact of drought is considered as significant ($p < 0.05$). MBC, soil microbial biomass carbon. MBN, microbial biomass nitrogen. MBP, microbial biomass phosphorus. BG, β-1, 4-glucosidase. CBH, β-D-cellobiosidase. NAG, β-1, 4-N-acetylglucosaminidase. LAP, L-leucine aminopeptidase. AP, acid phosphatase. SOC, soil organic carbon. TN, total nitrogen. TP, total phosphorus.

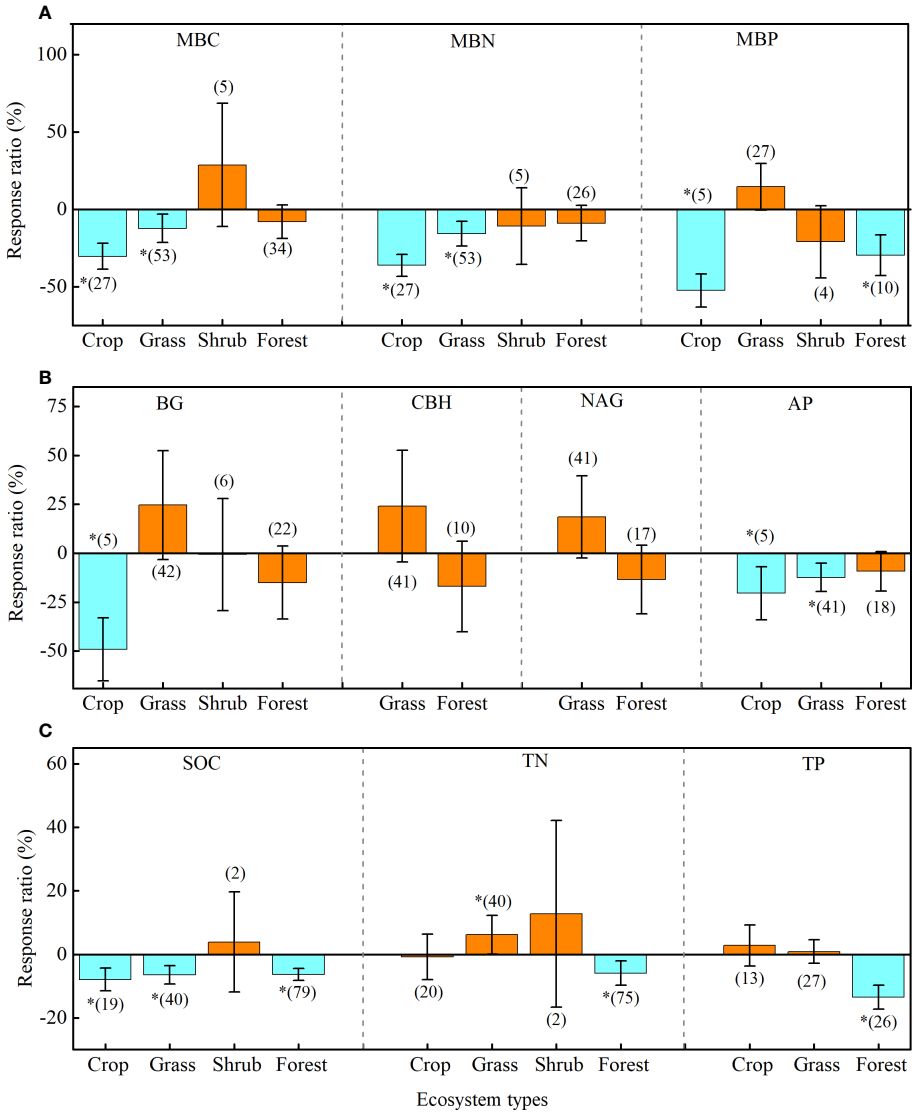

FIGURE 4
Effects of drought on soil microbial biomass **(A)**, enzyme activity **(B)**, and soil chemistry properties **(C)** of four ecosystem types: cropland (Crop), grassland (Grass), shrub, and forest. Error bars denote the 95% confidence interval (CI). The number in parentheses indicates the sample size. * indicates that the impact of drought is considered as significant ($p < 0.05$). MBC, soil microbial biomass carbon. MBN, microbial biomass nitrogen. MBP, microbial biomass phosphorus. BG, β-1, 4-glucosidase. CBH, β-D-cellobiosidase. NAG, β-1, 4-N-acetylglucosaminidase. LAP, L-leucine aminopeptidase. AP, acid phosphatase. SOC, soil organic carbon. TN, total nitrogen. TP, total phosphorus.

response ratio of SOC also decreased significantly with increasing drought duration (Figure 6F).

3.5 Response of soil microbial biomass and enzyme activity to MAT

The responses of soil microbial biomass and enzyme activity to drought were influenced by MAT (Figure 6). Briefly, the response ratio of MBP, BG, and NAG decreased significantly ($p < 0.05$) with MAT, whereas the response ratio of MBC, MBN, CBH, LAP, and AP did not show significant ($p > 0.05$) changes with MAT (Figures 6G, H). Meanwhile, the response ratio of SOC, TN, TP, and pH also decreased significantly with MAT (Figure 6I).

4 Discussion

4.1 Effect of drought on soil microbial biomass and enzyme activity

The frequent occurrence of droughts worldwide has greatly affected the structure, function, and biodiversity of terrestrial ecosystems (Williams and de Vries, 2020; Lozano et al., 2021). However, a comprehensive understanding of the impacts of drought on microbial activity is lacking, which has limited our understanding of the multifunctional nature of ecosystems. Thus, the current study provides direct global evidence that drought has substantially reduced soil microbial biomass (MBC, 22.7%; MBN, 21.2%; MBP, 21.6%) and enzyme activity (BG, 26.8%; AP, 16.1%)

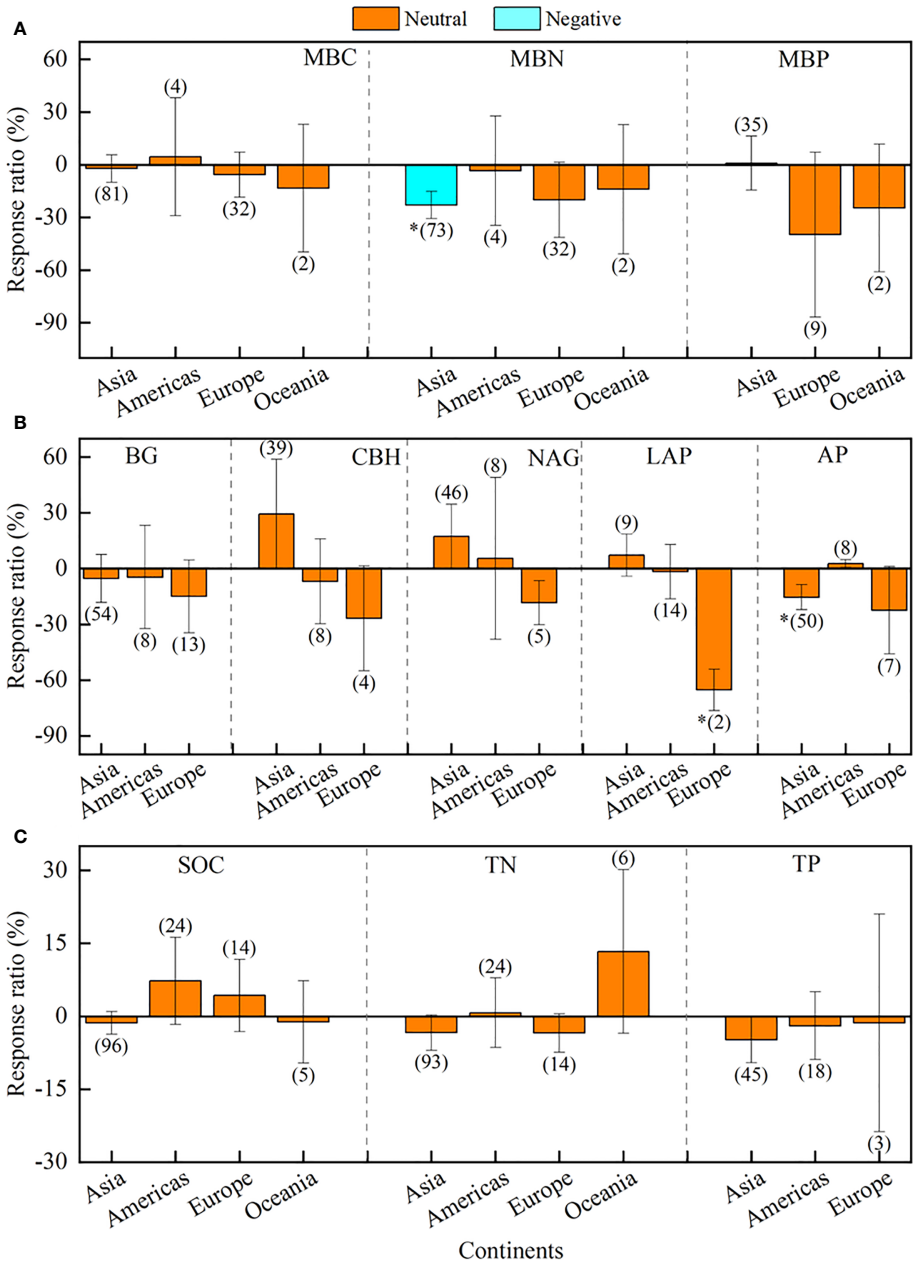

FIGURE 5
Effects of different continents of Asia, America, Europe, Oceania, and Africa on soil microbial biomass **(A)**, enzyme activity **(B)**, and soil chemistry properties **(C)**. Error bars denote the 95% confidence interval (CI). The number in parentheses indicates the sample size. * indicates that the impact of drought is considered as significant ($p < 0.05$). MBC, soil microbial biomass carbon. MBN, microbial biomass nitrogen. MBP, microbial biomass phosphorus. BG, β-1, 4-glucosidase. CBH, β-D-cellobiosidase. NAG, β-1, 4-N-acetylglucosaminidase. LAP, L-leucine aminopeptidase. AP, acid phosphatase. SOC, soil organic carbon. TN, total nitrogen. TP, total phosphorus.

(Figure 7). This phenomenon can be explained by the following four aspects: (1) Microorganisms have semi-permeable membranes, and the availability of soil moisture is essential for maintaining the survival and activity of microorganisms (Yan et al., 2021; Ge et al., 2022). In water-poor environments, microbial community transformation is slow, and lack of moisture may lead to microbial cracking or death (Schimel, 2018; Zhang et al., 2023). (2) Drought is generally believed to reduce plant biomass, soil litter content, and root activity, which in turn reduces the availability of food sources for microorganisms. Drought can also change the quality and amount of carbon sources available to microorganisms by reducing photosynthesis and plant growth (Malik et al., 2020b; Yan et al., 2023). Restriction of substrate concentration and availability and root exudates may be another important cause of reduced microbial activity (Ge et al., 2022; Malik and Bouskill, 2022). (3) Drought directly affects soil aeration, which in turn affects the decomposition of root exudates and organic matter and affects microbial activity and enzyme production by affecting soil physicochemical properties, and

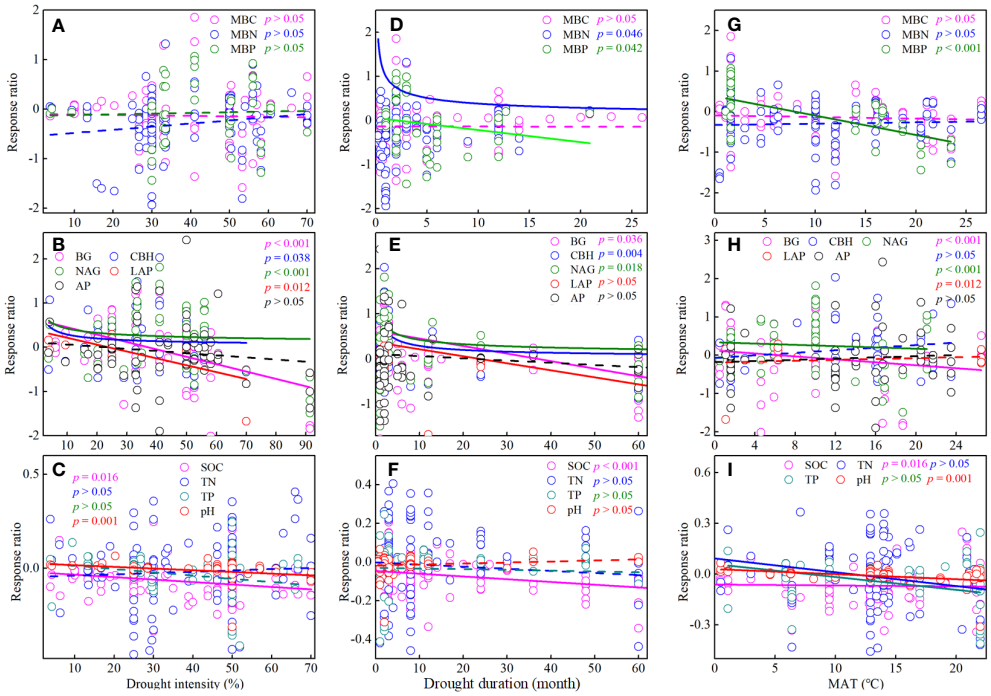

FIGURE 6
Effects of drought intensity **(A-C)**, drought duration **(D-F)**, and annual average temperature (MAT) **(G-I)** on soil microbial biomass, enzyme activity, and soil chemistry properties. MBC, soil microbial biomass carbon. MBN, microbial biomass nitrogen. MBP, microbial biomass phosphorus. BG, β-1, 4-glucosidase. CBH, β-D-cellobiosidase. NAG, β-1, 4-N-acetylglucosaminidase. LAP, L-leucine aminopeptidase. AP, acid phosphatase. SOC, soil organic carbon. TN, total nitrogen. TP, total phosphorus.

the diffusion of organic matter (Condit et al., 2013; Canarini et al., 2021; Quintana et al., 2023). (4) A decrease in soil moisture also reduces the ability of microorganisms to acquire and utilise resources (Sistla and Schimel, 2012), thus reducing their activity. Soil microorganisms are a key indicator of the ability of soils to conduct biogeochemical reactions (Battin et al., 2003; Agathokleous et al., 2020). The results of this study suggests that drought changes ecosystem structure and reduces the rate of material cycling.

4.2 Effect of vegetation types and continents on soil microbial biomass and enzyme activity

Owing to the complexity and heterogeneity of ecosystems, drought substantially reduced soil MBC and MBN as well as BG and AP activity in farmlands and grasslands. The results indicated that drought mainly inhibited soil microbial activity in farmlands and

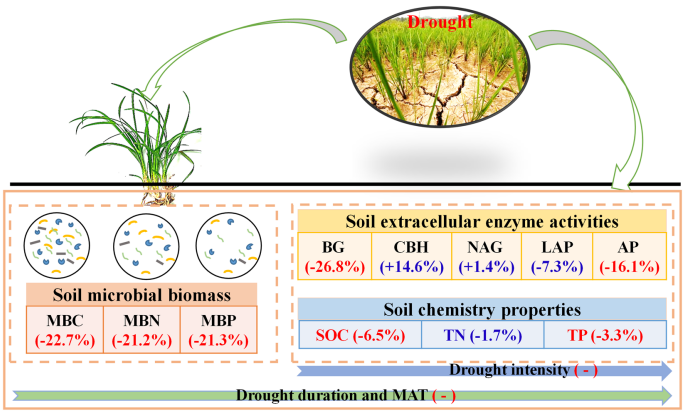

FIGURE 7
Conceptual framework showing impacts of drought on C soil microbial biomass, enzyme activity, and soil chemistry properties. "+" and "-" indicate positive and negative effects, respectively. Red and blue indicate significant and insignificant effects, respectively. Numbers in parentheses indicate percentage changes after drought. MBC, soil microbial biomass carbon. MBN, microbial biomass nitrogen. MBP, microbial biomass phosphorus. BG, β-1, 4-glucosidase. CBH, β-D-cellobiosidase. NAG, β-1, 4-N-acetylglucosaminidase. LAP, L-leucine aminopeptidase. AP, acid phosphatase. SOC, soil organic carbon. TN, total nitrogen. TP, total phosphorus.

grasslands but did not affect microbial biomass or enzyme activity in forests to the same degree. This outcome may be related to the distribution of the sample points. Rainfall distribution varies by ecosystem, and forests are mainly distributed in areas of heavy rainfall (the MAP of all forest sample points was 1174 mm), whereas cropland and grassland are mainly distributed in areas of low rainfall (the MAP of all cropland and grassland sample points was 480 mm and 807 mm, respectively) (Supplementary Figure 3). Previous studies have shown that rainfall is an important factor affecting microbial activity (Ren et al., 2018; Ochoa-Hueso et al., 2020). The low MAP of cropland and grassland may have had a superimposed effect on drought, aggravating the drought stress of the soil, and thus enhancing the inhibition of plant growth and microorganism activity. In contrast, the higher MAP in forests may have alleviated the decrease in soil moisture caused by drought stress and improved the physical structure of the soil to some degree, making it more suitable for microbial growth and reproduction, thus alleviating the negative effect of drought on microbial activity. This result also indicated that soil microorganisms in croplands were more sensitive to drought responses than those in forests, as well as more susceptible to soil moisture reduction. In this study, the samples were grouped by geographical location (Asia, America, Europe, Oceania, and Africa) to explore the influence of this factor in regulating the effects of drought. Notably, we found that the effects of drought on soil microbial biomass and enzyme activity were generally similar among different locations. This contradicts the conclusion of a previous study that geographical location affected microbial nutrient restriction and thus microbial activity (Xu et al., 2022b). This discrepancy may be due to the small number of samples in America, Oceania, and Africa in this study, which reduced the statistical power of our meta-analysis results.

4.3 Effect of drought intensity and duration on soil microbial biomass and enzyme activity

Knowledge on the effects of high-intensity drought stress, particularly those of drought duration, on soil microbial activity is lacking. In this analysis, global-scale data on the changes in microbial activity under different drought intensities and durations were collected, and it was determined that enzyme activity decreased with increasing drought intensity, and both microbial biomass and enzyme activity decreased with increasing drought duration (Figure 7). We propose the following explanations for these responses to drought. First, in a water-scarce environment, microbial community activity is low; however, with the intensification of drought stress, many microorganisms die, thus reducing enzyme production (Hoover et al., 2014; Zang et al., 2020). Second, drought inhibits plant growth. Severe and long-term drought causes plants to wilt and die, thereby reducing plant biomass, which lowers the quality of available carbon sources and nutrient content for microorganisms (Smith et al., 2009; Brown et al., 2021). Third, the worsening of drought stress may lead to soil cracking, land degradation, and changes in the physical environment of the soil (air, water, aggregate structure, etc.) (Fitzpatrick et al., 2017; Wan et al., 2023), making it unsuitable for the propagation and growth of microorganisms. Additionally, studies have indicated that soil microorganisms reduce the loss of nutrients and metabolism under long-term drought stress (Manzoni et al., 2014; Brown et al., 2021), thereby reducing microbial biomass and enzyme production capacity. With the intensification of global warming, the frequency and intensity of drought events worldwide have increased (Hoover et al., 2014), which has seriously impacted the structure, function, and biodiversity of terrestrial ecosystems (Barnes et al., 2018; Qu et al., 2023). The results of this study contribute to the overall understanding of ecosystem versatility under conditions of continuous global climate change.

4.4 Effect of MAT on soil microbial biomass and enzyme activity

In addition to rainfall, temperature patterns also affect soil microbial activity under drought stress. In this study, microbial activity decreased with increasing MAT, and the effect of drought on microbial activity changed from positive to negative with an increase in MAT. The analysis indicated that drought had a positive effect on microbial activity in low-temperature regions, whereas microbial activity was inhibited in warmer regions. Temperature affects microbial activity by influencing the soil temperature, soil physical structure, and plant growth (Billings and Ballantyne, 2013; Abirami et al., 2021). Moderate temperature increases can promote plant growth, accelerate litter decomposition, increase soil nutrient turnover rates (Cusack et al., 2010; Joly et al., 2023), and promote the growth and reproduction of microorganisms. In contrast, excessive temperature and drought superimpose these effects and may decrease the availability of soil water and reduce the turnover rate of soil nutrients (Xu et al., 2022b; Qu et al., 2023), thereby strongly inhibiting microbial activity. Soil microorganisms play an important role in material cycling in terrestrial ecosystems (Agathokleous et al., 2020). The results of this study highlight the impact of drought on soil microbial biomass and enzyme activity and the resulting effects on nutrient cycling processes in terrestrial ecosystems.

5 Conclusions

Our integrated analysis provided direct evidence that drought has significantly inhibited soil microbial activity globally. In particular, drought had a stronger inhibitory effect on soil microbial biomass and soil carbon- and phosphorus-acquiring enzyme activity and a weaker effect on soil nitrogen-acquiring enzyme activity. Furthermore, drought had a greater effect on microbial biomass than on soil enzyme activity. Additionally, our results revealed a negative correlation between microbial activity and drought intensity, drought duration, and MAT. Our results

contribute to the overall understanding of the structure and function of terrestrial ecosystems under global climate change.

Data availability statement

The original contributions presented in the study are included in the article/Supplementary Material, further inquiries can be directed to the corresponding author/s.

Author contributions

QQ, RL, and HX conceived and designed this meta-analysis. QQ, QG, and ZW analyzed the data. QQ drafted the original manuscript. RL and HX helped analyze the data and rewrote part of the manuscript. All authors contributed to the article and approved the submitted version.

Funding

This work was supported by the Open Fund for Key Lab. of Land Degradation and Ecological Restoration in Northwestern China of Ningxia University (LDER2023Z02), the Innovation Group Project of Natural Science Foundation of Ningxia Province (2023AAC01002), and the Innovation Group Project of Ningxia Science and Technology (2021RXTDLX01).

Acknowledgments

We would like to thank Sha Xue and Minggang Wang for providing statistics assistance.

Conflict of interest

The authors declare that the research was conducted in the absence of any commercial or financial relationships that could be construed as a potential conflict of interest.

Publisher's note

All claims expressed in this article are solely those of the authors and do not necessarily represent those of their affiliated organizations, or those of the publisher, the editors and the reviewers. Any product that may be evaluated in this article, or claim that may be made by its manufacturer, is not guaranteed or endorsed by the publisher.

Supplementary material

The Supplementary Material for this article can be found online at: https://www.frontiersin.org/articles/10.3389/fpls.2023.1221288/full#supplementary-material

References

Abirami, B., Radhakrishnan, M., Kumaran, S., and Wilson, A. (2021). Impacts of global warming on marine microbial communities. *Sci. Total Environ.* 791, 147905. doi: 10.1016/j.scitotenv.2021.147905

Agathokleous, E., Feng, Z., Oksanen, E., Sicard, P., Wang, Q., Saitanis, C. J., et al. (2020). Ozone affects plant, insect, and soil microbial communities: A threat to terrestrial ecosystems and biodiversity. *Sci. Adv.* 6, eabc1176. doi: 10.1126/sciadv.abc1176

Akram, M. A., Wang, X. T., Hu, W. G., Xiong, J. L., Zhang, Y. H., Deng, Y., et al. (2020). Convergent variations in the leaf traits of desert plants. *Plants* 9, 990. doi: 10.3390/plants9080990

Akram, M. A., Zhang, Y. H., Wang, X. T., Shrestha, N., Malik, K., Khan, I., et al. (2022). Phylogenetic independence in the variations in leaf functional traits among different plant life forms in an arid environment. *J. Plant Physiol.* 272, 153671. doi: 10.1016/j.jplph.2022.153671

Barnes, C. J., van der Gast, C. J., McNamara, N. P., Rowe, R., and Bending, G. D. (2018). Extreme rainfall affects assembly of the root-associated fungal community. *New Phytol.* 220, 1172–1184. doi: 10.1111/nph.14990

Bastos, T. R. D., Barreto-Garcia, P. A. B., Mendes, I. D., Monroe, P. H. M., and de Carvalho, F. F. (2023). Response of soil microbial biomass and enzyme activity in coffee-based agroforestry systems in a high-altitude tropical climate region of Brazil. *Catena* 230, 107270. doi: 10.1016/j.catena.2023.107270

Bates, D., Mächler, M., Bolker, B., and Walker, S. (2015). Fitting linear mixed-effects models using lme4. *J. Stat. Software* 67, 1–48. doi: 10.18637/jss.v067.i01

Battin, T. J., Kaplan, L. A., Denis Newbold, J., and Hansen, C. M. E. (2003). Contributions of microbial biofilms to ecosystem processes in stream mesocosms. *Nature* 426, 439–442. doi: 10.1038/nature02152

Billings, S. A., and Ballantyne, F. (2013). How interactions between microbial resource demands, soil organic matter stoichiometry, and substrate reactivity determine the direction and magnitude of soil respiratory responses to warming. *Glob. Change Biol.* 19, 90–102. doi: 10.1111/gcb.12029

Brown, R. W., Chadwick, D. R., Zang, H., and Jones, D. L. (2021). Use of metabolomics to quantify changes in soil microbial function in response to fertiliser nitrogen supply and extreme drought. *Soil Biol. Biochem.* 160, 108351. doi: 10.1016/j.soilbio.2021.108351

Canarini, A., Schmidt, H., Fuchslueger, L., Martin, V., Herbold, C. W., Zezula, D., et al. (2021). Ecological memory of recurrent drought modifies soil processes via changes in soil microbial community. *Nat. Commun.* 12, 5308. doi: 10.1038/S41467-021-25675-4

Chen, W., Meng, P. P., Feng, H., and Wang, C. Y. (2020). Effects of arbuscular mycorrhizal fungi on growth and physiological performance of catalpa bungei CAMey. *under Drought Stress. Forests* 11, 10. doi: 10.3390/f11101117

Chen, C., Singh, A., Yang, B., Wang, H., and Liu, W. (2023). Effect of termite mounds on soil microbial communities and microbial processes: Implications for soil carbon and nitrogen cycling. *Geoderma* 431, 116368. doi: 10.1016/j.geoderma.2023.116368

Cheng, J., Chu, P., Chen, D., and Bai, Y. (2016). Functional correlations between specific leaf area and specific root length along a regional environmental gradient in Inner Mongolia grasslands. *Funct. Ecol.* 30, 985–997. doi: 10.1111/1365-2435.12569

Clark, J. S., Campbell, J. H., Grizzle, H., Acosta-Martinez, V., and Zak, J. C. (2009). Soil microbial community response to drought and precipitation variability in the chihuahuan desert. *Microb. Ecol.* 57, 248–260. doi: 10.1109/82.532010

Condit, R., Engelbrecht, B. M. J., Pino, D., Perez, R., and Turner, B. L. (2013). Species distributions in response to individual soil nutrients and seasonal drought across a community of tropical trees. *Proc. Nat. Acad. Sci. U. S. A.* 110, 5064–5068. doi: 10.1073/pnas.1218042110

Cusack, D. F., Torn, M. S., McDowell, W. H., and Silver, W. L. (2010). The response of heterotrophic activity and carbon cycling to nitrogen additions and warming in two tropical soils. *Glob. Change Biol.* 16, 2555–2572. doi: 10.1111/j.1365-2486.2009.02131.x

Fitzpatrick, R. W., Mosley, L. M., Raven, M. D., and Shand, P. (2017). Schwertmannite formation and properties in acidic drain environments following exposure and oxidation of acid sulfate soils in irrigation areas during extreme drought. *Geoderma* 308, 235–251. doi: 10.1016/j.geoderma.2017.08.012

Fu, Z., Niu, S., and Dukes, J. S. (2015). What have we learned from global change manipulative experiments in China? A meta-analysis. *Sci. Rep.* 5, 12344. doi: 10.1038/srep12344

Gao, D., Bai, E., Yang, Y., Zong, S., and Hagedorn, F. (2021). A global meta-analysis on freeze-thaw effects on soil carbon and phosphorus cycling. *Soil Biol. Biochem.* 159, 108283. doi: 10.1016/j.soilbio.2021.108283

Ge, X., Wang, C., Wang, L., Zhou, B., Cao, Y., Xiao, W., et al. (2022). Drought changes litter quantity and quality, and soil microbial activities to affect soil nutrients in moso bamboo forest. *Sci. Total Environ.* 838, 156351. doi: 10.1016/j.scitotenv.2022.156351

Hao, J., Feng, Y., Wang, X., Yu, Q., Zhang, F., Yang, G., et al. (2022). Soil microbial nitrogen-cycling gene abundances in response to crop diversification: a meta-analysis. *Sci. Total Environ.* 838, 156621. doi: 10.1016/j.scitotenv.2022.156621

He, T., Dai, X., Li, W., Zhou, J., Zhang, J., Li, C., et al. (2023). Response of net primary productivity of vegetation to drought: A case study of Qinba Mountainous area, Chin-2018). *Ecol. Indic.* 149, 110148. doi: 10.1016/j.ecolind.2023.110148

Hedges, L. V., Gurevitch, J., and Curtis, P. S. (1999). The meta-analysis of response ratios in experimental ecology. *Ecology* 80, 1150–1156. doi: 10.1890/0012-9658(1999)080[1150:TMAORR]2.0.CO;2

Hoover, D. L., Knapp, A. K., and Smith, M. D. (2014). Resistance and resilience of a grassland ecosystem to climate extremes. *Ecology* 95, 2646–2656. doi: 10.1890/13-2186.1

Hu, W. G., Ran, J. Z., Dong, L. W., Du, Q. J., Ji, M. F., Yao, S. R., et al. (2021). Aridity-driven shift in biodiversity-soil multifunctionality relationships. *Nat. Commun.* 12, 1. doi: 10.1038/s41467-021-25641-0

Jian, S., Zhao, C., Fang, S., and Yu, K. (2015). The distribution of fine root length density for six artificial afforestation tree species in Loess Plateau of Northwest China. *For. Syst.* 24, e003. doi: 10.5424/fs/2015241-05521

Joly, F.-X., Scherer-Lorenzen, M., and Haettenschwiler, S. (2023). Resolving the intricate role of climate in litter decomposition. *Nat. Ecol. Evol.* doi: 10.1038/s41559-022-01948-z

Li, L., Qian, R., Liu, W., Wang, W., Biederman, J., Zhang, B., et al. (2022). Drought timing influences the sensitivity of a semiarid grassland to drought. *Geoderma* 412, 115714. doi: 10.1016/j.geoderma.2022.115714

Lozano, Y. M., Aguilar-Trigueros, C. A., Onandia, G., Maass, S., Zhao, T., and Rillig, M. C. (2021). Effects of microplastics and drought on soil ecosystem functions and multifunctionality. *J. Appl. Ecol.* 58, 988–996. doi: 10.1111/1365-2664.13839

Malik, A. A., and Bouskill, N. J. (2022). Drought impacts on microbial trait distribution and feedback to soil carbon cycling. *Funct. Ecol.* 36, 1442–1456. doi: 10.1111/1365-2435.14010

Malik, A. A., Martiny, J. B. H., Brodie, E. L., Martiny, A. C., Treseder, K. K., and Allison, S. D. (2020a). Defining trait-based microbial strategies with consequences for soil carbon cycling under climate change. *ISME J.* 14, 1–9. doi: 10.1038/s41396-019-0510-0

Malik, A. A., Swenson, T., Weihe, C., Morrison, E. W., Martiny, J. B. H., Brodie, E. L., et al. (2020b). Drought and plant litter chemistry alter microbial gene expression and metabolite production. *ISME J.* 14, 2236–2247. doi: 10.1038/s41396-020-0683-6

Manzoni, S., Schaeffer, S. M., Katul, G., Porporato, A., and Schimel, J. P. (2014). A theoretical analysis of microbial eco-physiological and diffusion limitations to carbon cycling in drying soils. *Soil Biol. Biochem.* 73, 69–83. doi: 10.1016/j.soilbio.2014.02.008

Mishra, A., Alnahit, A., and Campbell, B. (2021). Impact of land uses, drought, flood, wildfire, and cascading events on water quality and microbial communities: A review and analysis. *J. Hydrol.* 596, 125707. doi: 10.1016/j.jhydrol.2020.125707

Ochoa-Hueso, R., Arca, V., Delgado-Baquerizo, M., Hamonts, K., Pineiro, J., Serrano-Grijalva, L., et al. (2020). Links between soil microbial communities, functioning, and plant nutrition under altered rainfall in Australian grassland. *Ecol. Monogr.* 90 (4), e01424. doi: 10.1002/ecm.1424

Peng, Y. M., Xu, H. S., Wang, Z., Li, L., Shang, J. Y., Li, B. G., et al. (2023). Effects of intercropping and drought on soil aggregation and associated organic carbon and nitrogen. *Soil Use Manage.* 39, 316–328. doi: 10.1111/sum.12866

Peszek, L., Zgrundo, A., Noga, T., Kochman-Kedziora, N., Poradowska, A., Rybak, M., et al. (2021). The influence of drought on diatom assemblages in a temperate climate zone: A case study from the Carpathian Mountains, Poland. *Ecol. Indic.* 125, 83–95. doi: 10.1016/j.ecolind.2021.107579

Qu, Q., Xu, H., Ai, Z., Wang, M., Wang, G., Liu, G., et al. (2023). Impacts of extreme weather events on terrestrial carbon and nitrogen cycling: A global meta-analysis. *Environ. pollut.* 319, 120996. doi: 10.1016/j.envpol.2022.120996

Quintana, J. R., Martin-Sanz, J. P., Valverde-Asenjo, I., and Molina, J. A. (2023). Drought differently destabilizes soil structure in a chronosequence of abandoned agricultural lands. *Catena* 222, 106871. doi: 10.1016/j.catena.2022.106871

Ren, C., Chen, J., Lu, X., Doughty, R., Zhao, F., Zhong, Z., et al. (2018). Responses of soil total microbial biomass and community compositions to rainfall reductions. *Soil Biol. Biochem.* .116, 4–10. doi: 10.1016/j.soilbio.2017.09.028

Sanaullah, M., Blagodatskaya, E., Chabbi, A., Rumpel, C., and Kuzyakov, Y. (2011). Drought effects on microbial biomass and enzyme activities in the rhizosphere of grasses depend on plant community composition. *Appl. Soil Ecol.* 48, 38–44. doi: 10.1016/j.apsoil.2011.02.004

Schimel, J. P. (2018). Life in dry soils: effects of drought on soil microbial communities and processes. *Annu. Rev Ecol Evol S.*49, 409–432.

Sistla, S. A., and Schimel, J. P. (2012). Stoichiometric flexibility as a regulator of carbon and nutrient cycling in terrestrial ecosystems under change. *New Phytol.* 196, 68–78. doi: 10.1111/j.1469-8137.2012.04234.x

Smith, M. D., Knapp, A. K., and Collins, S. L. (2009). A framework for assessing ecosystem dynamics in response to chronic resource alterations induced by global change. *Ecology* 90, 3279–3289. doi: 10.1890/08-1815.1

Song, J., Wan, S., Piao, S., Knapp, A. K., Classen, A. T., Vicca, S., et al. (2019). A meta-analysis of 1,119 manipulative experiments on terrestrial carbon-cycling responses to global change. *Nat. Ecol. Evol.* 3, 1309–1320. doi: 10.1038/s41559-019-0958-3

Stott, P. (2016). How climate change affects extreme weather events Research can increasingly determine the contribution of climate change to extreme events such as droughts. *Science* 352, 1517–1518. doi: 10.1126/science.aaf7271

Sun, Y., Liao, J., Zou, X., Xu, X., Yang, J., Chen, H. Y. H., et al. (2020). Coherent responses of terrestrial C:N stoichiometry to drought across plants, soil, and microorganisms in forests and grasslands. *Agr. For. Meteorol.* 292, 108104. doi: 10.1016/j.agrformet.2020.108104

van der Molen, M. K., Dolman, A. J., Ciais, P., Eglin, T., Gobron, N., Law, B. E., et al. (2011). Drought and ecosystem carbon cycling. *Agr. For. Meteorol.* 151, 765–773. doi: 10.1016/j.agrformet.2011.01.018

Wan, Q., Li, L., Liu, B., Zhang, Z., Liu, Y., and Xie, M. (2023). Different and unified responses of soil bacterial and fungal community composition and predicted functional potential to 3 years' drought stress in a semiarid alpine grassland. *Front. Microbiol.* 14. doi: 10.3389/fmicb.2023.1104944

Wan, W., Liu, Z., Li, J., Xu, J., Wu, H., and Xu, Z. (2022). Spatiotemporal patterns of maize drought stress and their effects on biomass in the Northeast and North China Plain from 2000 to 2019. *Agr. For. Meteorol.* 315, 108821. doi: 10.1016/j.agrformet.2022.108821

Wang, B., An, S., Liang, C., Liu, Y., and Kuzyakov, Y. (2021a). Microbial necromass as the source of soil organic carbon in global ecosystems. *Soil Biol. Biochem.* 162, 108422. doi: 10.1016/j.soilbio.2021.108422

Wang, L., Hamel, C., Lu, P. A., Wang, J. Y., Sun, D. D., Wang, Y. J., et al. (2023a). Using enzyme activities as an indicator of soil fertility in grassland-an academic dilemma. *Front. Plant Sci.* 14. doi: 10.3389/fpls.2023.1175946

Wang, C., Sun, Y., Chen, H. Y. H., Yang, J., and Ruan, H. (2021b). Meta-analysis shows non-uniform responses of above- and belowground productivity to drought. *Sci. Total Environ.* 782, 146901. doi: 10.1016/j.scitotenv.2021.146901

Wang, H., Wang, Y., Kang, C., Wang, S., Zhang, Y., Yang, G., et al. (2023b). Drought stress modifies the community structure of root-associated microbes that improve Atractylodes lancea growth and medicinal compound accumulation. *Front. Plant Sci.* 13. doi: 10.3389/fpls.2022.1032480

Wardle, D. A. (1998). Controls of temporal variability of the soil microbial biomass: A global-scale synthesis. *Soil Biol. Biochem.* 30, 1627–1637. doi: 10.1016/S0038-0717(97)00201-0

Williams, A., and de Vries, F. T. (2020). Plant root exudation under drought: implications for ecosystem functioning. *New Phytol.* 225, 1899–1905. doi: 10.1111/nph.16223

Xie, J., Dawwam, G. E., Sehim, A. E., Li, X., Wu, J., Chen, S., et al. (2021). Drought stress triggers shifts in the root microbial community and alters functional categories in the microbial gene pool. *Front. Microbiol.* 12. doi: 10.3389/fmicb.2021.744897

Xu, H., Liu, Q., Wang, S., Yang, G., and Xue, S. (2022a). A global meta-analysis of the impacts of exotic plant species invasion on plant diversity and soil properties. *Sci. Total Environ.* 782, 152286. doi: 10.1016/j.scitotenv.2021.152286

Xu, H., Qu, Q., Li, G., Liu, G., Geissen, V., Ritsema, C. J., et al. (2022b). Impact of nitrogen addition on plant-soil-enzyme C-N-P stoichiometry and microbial nutrient limitation. *Soil Biol. Biochem.* 170, 108714. doi: 10.1016/j.soilbio.2022.108714

Yan, Z., Kang, E., Zhang, K., Li, Y., Hao, Y., Wu, H., et al. (2021). Plant and soil enzyme activities regulate CO2 efflux in alpine peatlands after 5 years of simulated extreme drought. *Front. Plant Sci.* 12. doi: 10.3389/fpls.2021.756956

Yan, S., Weng, B., Jing, L., and Bi, W. (2023). Effects of drought stress on water content and biomass distribution in summer maize(Zea mays L.). *Front. Plant Sci.* 14. doi: 10.3389/fpls.2022.1032480

Zang, Y., Min, X., Resco de Dios, V., Ma, J., and Sun, W. (2020). Extreme drought affects the productivity, but not the composition, of a desert plant community in Central Asia differentially across microtopographies. *Sci. Total Environ.* 717, 137251. doi: 10.1016/j.scitotenv.2020.137251

Zhang, X., Bilyera, N., Fan, L., Duddek, P., Ahmed, M. A., Carminati, A., et al. (2023). The spatial distribution of rhizosphere microbial activities under drought: water availability is more important than root-hair-controlled exudation. *New Phytol.* 237, 780–792. doi: 10.1111/nph.18409

frontiers | Frontiers in Plant Science

TYPE Correction
PUBLISHED 21 March 2024
DOI 10.3389/fpls.2024.1393574

OPEN ACCESS

EDITED AND REVIEWED BY
Pedro Piedras,
University of Cordoba, Spain

*CORRESPONDENCE
Rentao Liu
nxuliu2012@126.com
Hongwei Xu
xuhongwei16@sicau.edu.cn

†These authors share first authorship

RECEIVED 29 February 2024
ACCEPTED 14 March 2024
PUBLISHED 21 March 2024

CITATION
Qu Q, Wang Z, Gan Q, Liu R and Xu H (2024) Corrigendum: Impact of drought on soil microbial biomass and extracellular enzyme activity.
Front. Plant Sci. 15:1393574.
doi: 10.3389/fpls.2024.1393574

Corrigendum: Impact of drought on soil microbial biomass and extracellular enzyme activity

Qing Qu[1,2†], Zhen Wang[1†], Quan Gan[3], Rentao Liu[1*] and Hongwei Xu[3*]

[1]Breeding Base for State Key Laboratory of Land Degradation and Ecological Restoration in Northwestern China, Key Laboratory of Restoration and Reconstruction of Degraded Ecosystems in Northwestern China of Ministry of Education, Ningxia University, Yinchuan, China, [2]Institute of Soil and Water Conservation, Chinese Academy of Sciences and Ministry of Water Resources, Yangling, China, [3]College of Forestry, Sichuan Agricultural University, Chengdu, China

KEYWORDS

biogeochemical cycles, climate change, ecosystem function, ecosystem structure, soil microbial activity, soil microbial community

A Corrigendum on:

Impact of drought on soil microbial biomass and extracellular enzyme activity

By Qu Q, Wang Z, Gan Q, Liu R and Xu H (2023) Front. Plant Sci. 14:1221288. doi: 10.3389/fpls.2023.1221288

Text Correction

In the published article, there was an error. In the published article, there was a mistake in the formula. The formula was displayed as "SD =√SE". The correct statement is "SD = SE$\sqrt{N}$".

A correction has been made to 2 Materials and methods, 2.1 Data collection. This sentence previously stated:

"If no standard deviation was reported, it was calculated using the standard error (SE) as follows: SD =√SE (Fu et al., 2015)."

The corrected sentence appears below:

"If no standard deviation was reported, it was calculated using the standard error (SE) as follows: SD = SE$\sqrt{N}$ (Fu et al., 2015)."

The authors apologize for this error and state that this does not change the scientific conclusions of the article in any way. The original article has been updated.

Publisher's note

frontiers | Frontiers in Plant Science

TYPE Review
PUBLISHED 28 August 2023
DOI 10.3389/fpls.2023.1232675

OPEN ACCESS

EDITED BY
Debojyoti Moulick,
Independent researcher, Kolkata, India

REVIEWED BY
Biswajit Pramanick,
Dr. Rajendra Prasad Central Agricultural University, India
Swati Hazra,
Sharda University, India

*CORRESPONDENCE
Anteneh Agezew Melash
antenehagezew2008@gmail.com

RECEIVED 31 May 2023
ACCEPTED 27 July 2023
PUBLISHED 28 August 2023

CITATION
Melash AA, Bogale AA, Bytyqi B, Nyandi MS and Ábrahám ÉB (2023) Nutrient management: as a panacea to improve the caryopsis quality and yield potential of durum wheat (*Triticum turgidum* L.) under the changing climatic conditions. *Front. Plant Sci.* 14:1232675. doi: 10.3389/fpls.2023.1232675

Nutrient management: as a panacea to improve the caryopsis quality and yield potential of durum wheat (*Triticum turgidum* L.) under the changing climatic conditions

Anteneh Agezew Melash[1,2]*, Amare Assefa Bogale[3], Bekir Bytyqi[1], Muhoja Sylivester Nyandi[1] and Éva Babett Ábrahám[4]

[1]Kálmán Kerpely Doctoral School of Crop Production and Horticultural Science, University of Debrecen, Debrecen, Hungary, [2]Department of Horticulture, College of Agriculture and Environmental Science, Debark University, Debark, Ethiopia, [3]Institute of Crop Production, Hungarian University of Agriculture and Life Sciences, Gödöllő, Hungary, [4]Faculty of Agricultural, Food Sciences and Environmental Management, Institute of Crop Sciences, University of Debrecen, Debrecen, Hungary

The increasing human population and the changing climate, which have given rise to frequent drought spells, pose a serious threat to global food security, while identification of high-yielding drought-tolerant genotypes coupled with nutrient management remains a proficient approach to cope with these challenges. An increase in seasonal temperature, recurring drought stress, and elevated atmospheric CO_2 are alarmingly affecting durum wheat production, productivity, grain quality, and the human systems it supports. An increase in atmospheric carbon dioxide can improve wheat grain yield in a certain amount, but the right amount of nutrients, water, and other required conditions should be met to realize this benefit. Nutrients including nitrogen, silicon, and sulfur supply could alleviate the adverse effects of abiotic stress by enhancing antioxidant defense and improving nitrogen assimilation, although the effects on plant tolerance to drought stress varied with nitrogen ionic forms. The application of sewage sludge to durum wheat also positively impacts its drought stress tolerance by triggering high accumulation of osmoregulators, improving water retention capacity in the soil, and promoting root growth. These beneficial effect of nutrients contribute to durum wheat ability to withstand and recover from abiotic stress conditions, ultimately enhance its productivity and resilience. While these nutrients can provide benefits when applied in appropriate amounts, their excessive use can lead to adverse environmental consequences. Advanced technologies such as precision nutrient management, unmanned aerial vehicle-based spraying, and anaerobic digestion play significant roles in reducing the negative effects associated with nutrients like sewage sludge, zinc, nanoparticles and silicon fertilizers. Hence, nutrient management practices offer significant potential to enhance the caryopsis quality and yield

potential of durum wheat. Through implementing tailored nutrient management strategies, farmers, breeders, and agronomists can contribute to sustainable durum wheat production, ensuring food security and maintaining the economic viability of the crop under the changing climatic conditions.

KEYWORDS

durum wheat, nutrient management, grain quality, yield, enrichment of CO2, drought, water logging, temperature

1 Introduction

Durum wheat *(Triticum turgidum* L.*)*, a commonly cultivated form of allotetraploid, holds particular significance due to its essential role in the production of semolina, a key ingredient for pasta and macaroni manufacturing (Bin et al., 2017; Andrej et al., 2021). The capacity of durum wheat to produce high-quality foodstuffs is strongly determined by the content and composition of grain storage proteins, which form a viscoelastic network called gluten that is formed when flour is hydrated and mixed into a dough (Koga et al., 2016). This network allows the dough to stretch and retain its shape during pasta and macaroni processing, such as kneading and extrusion. Although durum wheat offers such enormous economic and industrial benefits, the yield, grain protein, and mineral concentration may wane in the future due to changing climatic circumstances (Ben et al., 2021). Globally, durum wheat production accounts for 5% of the total wheat production, cultivated across 16 million hectares of planting area (Beres et al., 2020). However, only 13% of the world's arable land is suitable for durum wheat cultivation, and as a result of climate change, the suitable area may have decreased by 19% and 48% in the middle and end of the century, respectively (Andrej et al., 2021). These changes could intensify extreme meteorological and hydrological events, including drought, waterlogging, and heat waves, which have also increased persistently in terms of both frequency and intensity (Seneviratne et al., 2012; Yu et al., 2018).

The changing climatic conditions pose a substantial threat to crop production, including durum wheat, as they give rise to significant alterations in phytochemical, physiological, and biochemical processes. These changes can have severe repercussions, impacting both the yield of durum wheat and the surrounding environment. A shift in climatic conditions such as high temperatures and drought stress has turned out to be the most important constraining factor for the crop production sector, where a substantial effect is frequently observed at the later developmental phases (Ben et al., 2021). It has been observed that, up to a certain concentration, atmospheric CO_2 enrichment could increase yield and grain starch accumulation, but it also negatively affects the nutritional profile of grains, such as the protein and mineral content of most cereals (Asseng et al., 2019; Ben et al., 2021). However, the mechanisms behind these additive and antagonistic effects remain obscure, although common understanding ascribes the dilution effect as the primary cause of the decline in grain nutritional profile (Santos et al., 2023). Identification of drought-tolerant and high-yielding cultivars combined with proper nutrient management could be an effective approach to reduce these challenges (Boudjabi et al., 2015; Ma et al., 2017; Melash et al., 2019). Indeed, this approach may necessitate an understanding of crop response to water stress as well as crop responsiveness to the applied nutrients (Shew et al., 2020).

Identifying the resilience of yield and grain quality under changing climatic conditions is of utmost importance in effectively addressing the challenges posed by CO_2 enrichment, drought, and high temperature stresses. Hence, understanding the temporal and spatial scales of the consequences of these stressors is important for developing effective adaptation and mitigation strategies. It has been proven that unless global efforts to reduce greenhouse gas emissions are promptly and significantly intensified, the effects of climate change will be more profound on future durum wheat production. This could further constrain the harvestable yield and morphometric traits of wheat, often through a decrease in important yield attribute traits such as, the number of seeds per spike, grain weight, and spike length (Hasan and Tacettin, 2010). However, there has been relatively limited consideration of potential climate impacts on malnutrition through mechanisms such as changing the nutrient content of food products (Santos et al., 2023). These climate-induced shifts impact on suitable growing areas, grain yield, and nutritional composition, necessitating a comprehensive understanding and eventual adoption of efficient and sustainable nutrient management techniques to stabilize production and adapt the entire food supply chain.

Nutrient management emerges as a promising panacea to counterbalance the negative impacts of changing climatic conditions on durum wheat cultivation (Melash and Ábrahám, 2022). Advanced site-specific technologies and techniques allow for the precise customization of nutrient applications, considering factors like timing, rate, and placement, to optimize durum wheat productivity while minimizing environmental impacts (Kizilgeci et al., 2021). The application of precision nutrient management to durum wheat has demonstrated encouraging results, leading to improved grain yield and protein content. Moreover, precision nutrient management not only enhances crop yield and income but also promotes the efficient utilization of nutrients and water while reducing greenhouse gas (GHG) emissions (Sadhukhan et al., 2023). In the broader context of agriculture, implementing nutrient

management strategies based on a nutrient expert approach has also shown considerable benefits. This approach has resulted in a significant reduction of 1.44 million tons in nitrogen fertilizer use and a decrease of 5.34 million tons of CO_2 equivalent emissions annually in addition to increasing yield of crops such as rice and wheat (Sapkota et al., 2021). This reduction reflects a more precise and efficient use of nitrogen inputs, ensuring that crops receive the optimal amount of nutrients, reducing wastage, and mitigating potential environmental impacts. The strategic utilization of nitrogen fertilizer offers a significant potential for enhancing grain yield and bolstering crop stress tolerance. Nitrogen plays a crucial role in maintaining leaf water potential, facilitating photosynthetic activities, and fortifying antioxidative defense mechanisms, thus contributing to crop performance (Abid et al., 2016). In the context of drought stress and associated challenges in wheat crop, the application of silicon, seaweed extracts, sewage sludge, and zinc-containing fertilizers has been found to effectively alleviate the inhibitory effects of abiotic stressors (Boudjabi et al., 2015; Coskun et al., 2016; Ma et al., 2017). Hence, incorporating zinc-containing fertilizers, sewage sludge, and silicon-based nutrients into the cultivation system of durum wheat can provide several benefits including optimizing nutrient availability, promoting plant health, and enhancing the crop's resilience to changing climatic conditions.

The protagonists of nutrient management technologies have been reported in various studies as a potential agronomic solution to enhance yield and grain quality traits under the current climate change scenarios (Sapkota et al., 2021). However, fertilizer management practices alone cannot single-handedly mitigate climate change effects on durum wheat productivity but rather should be viewed as a vital component of a comprehensive set of climate-smart agricultural strategies. Hence, adopting precision agriculture techniques, integrating organic and inorganic fertilizers, and implementing supportive policies can optimize nutrient use, reduce greenhouse gas emissions, enhance soil carbon sequestration, and promote sustainable agricultural systems. Indeed, scientific verification has shown that the integration of farmyard manure along with additional silicon based fertilizers enhances growth, increases grain yield, improves nutrient uptake, crop quality, and boosts nitrogen-use efficiency of the crop (Naik et al., 2022). Through a comprehensive analysis of existing research this review article aims to achieve two primary objectives. Firstly, it seeks to identify knowledge gaps, challenges, and opportunities associated with fertilizer management in durum wheat production. The article could therefore provide valuable recommendations for future research and policy development in this field, with the ultimate goal of optimizing fertilizer use and improving agricultural practices. Secondly, it aims to examine the effectiveness of nutrient management strategies in enhancing the yield, physiology, and grain nutritional composition of durum wheat under abiotic stress conditions and promoting sustainable agricultural systems. By assessing the outcomes of different nutrient management approaches the article can contribute to the development of sustainable agricultural system that promote resilient crop production. Through these objectives, the article can universally serve as a valuable resource for agronomists, researchers, and farmers alike, facilitating better decision making and fostering advancements in durum wheat cultivation for improved food security and sustainable agricultural practices under the changing climatic scenarios.

2 Methodology

A comprehensive search of the literature has been conducted to identify relevant studies and publications related to the topic of interest. The search was performed across various electronic databases such as PubMed, Scopus, Web of Science, and Google Scholar. Keywords and terms used in the search included the terms climate change, drought, waterlogging, durum wheat varieties in combination with the terms qualitative and qualitative traits. The initial search yielded a total of 236 articles, which were then screened based on their titles and abstracts for relevance to the topic under investigation. After the initial screening, a more detailed evaluation of the selected articles was conducted and included studies that met the following inclusion criteria: online accessibility, written language, and most importantly, primary data. Studies that did not meet the inclusion criteria or were duplicates were excluded. The full texts of the selected articles were obtained and reviewed for their relevance to the research question and the quality of the methodology employed.

The selected studies encompassed a wide range of experimental designs, including randomized controlled trials, long-term observational studies, and field and greenhouse experiments as well. In order to provide a comprehensive analysis, studies investigating the effects of various fertilizer types, including synthetic fertilizers, organic amendments, and bio-fertilizers, and their role under changing climatic conditions were included in this review. The overall findings of the included studies are summarized and presented in a narrative format, highlighting the key trends, patterns, and knowledge gaps in the literature.

3 Building a resilient future: evaluating the resilience of yield and grain quality in a changing climate

3.1 Unveiling the impact of drought-induced stress on grain yield and quality

The change in rainfall pattern could increase short-run crop failures and cause long-run reduction in production. This is primarily due to the adverse effect it can have on morphometric characteristics and associated yield-attributed traits of crops. The harmful effect of drought stress on grain yield can be significantly amplified when it occurs with the presence of various other climatic parameters, as illustrated in Figure 1 (Pradhan et al., 2012; Qaseem et al., 2019). Its cohabitation and concurrent effect can have a synergistic, antagonistic, or hypo-additive effect on yield and other associated yield attribute traits (Prasad et al., 2011). Heat and drought-induced stress significantly affect the rate of wheat

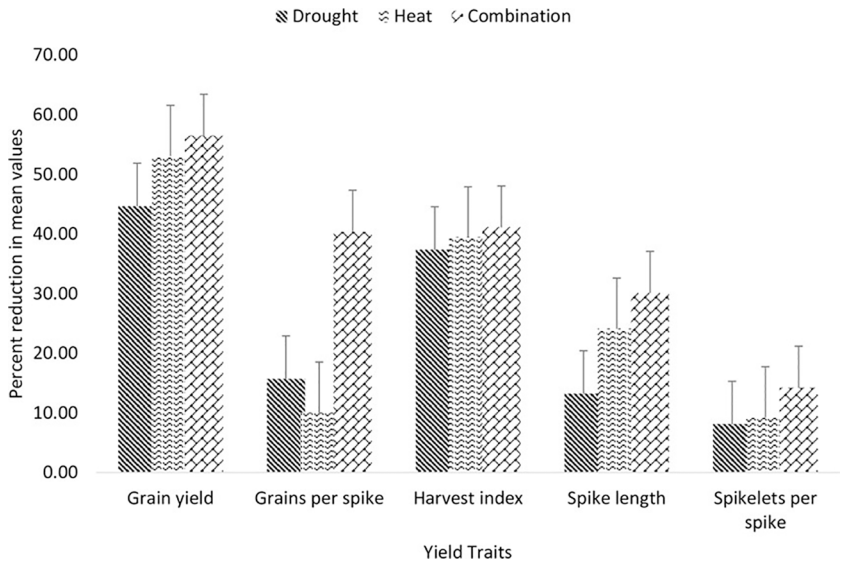

FIGURE 1
illustrates a percentage reduction in grain yield and associated traits of wheat genotypes evaluated under drought, heat, and combinations of both stress treatments (Qaseem et al., 2019).

growth and development, and under such conditions, wheat species could complete their developmental cycle much faster than under normal conditions (Ghazi, 2012). However, the crop might have a short duration with fewer days to accumulate more assimilates during their entire developmental cycle (Erda et al., 2005; Wahid et al., 2007). This effect initiates various physiological processes, such as a decreased rate of photosynthesis coupled with abnormal respiration, stomata closure, and high leaf temperature, leading to a diminished potential for biomass production (Mittler, 2006; Qaseem et al., 2019). Hence understanding the effect of heat and drought stress on durum wheat growth and development is crucial for developing strategies to mitigate their negative impacts and ensure sustainable production in changing environments.

The austerity and negative impact instigated by drought stress are usually unforeseeable, as they are also controlled by multiple factors, including patterns in rainfall, the water-retaining ability of the soil, and a water deficit due to a high crop transpiration rate (Yan et al., 2016). The combination of these factors contributes to the complex nature of drought and its impact on the entire agricultural system. These situations further aggravate the drought stress and influence the overall productivity of crops by affecting the relationships with water-soluble nutrients and eventually causing a substantial decline in grain yield due to the impairment of the photosynthetic process (Rakshit et al., 2020; Gebrewahid et al., 2021). These results universally indicate that drought stress is not solely determined by absence or deficiency of rainfall; it also depends on how the available water is retained in the soil and the rate at which the crop consume water through transpiration. Although grain yield is a multifarious amalgamation of diverse yield-attributed traits, drought-mediated yield reduction could account for up to 50% of the total grain production (Ben et al., 2021). Pollen abortion, a decrease in the amount of conserved food, and the formation of sterile tillers are the main factors contributing to a decrease in grain formation during dry climatic conditions (Duggan et al., 2005; Sinclair and Jamieson, 2006; Ji et al., 2010). The higher deposition of abscisic acid in the spike, triggered by drought stress, has also been found to potentially reduce the pollination capacity of the ovary, leading to significant seed abortion and a decline in seed set (Weldearegay et al., 2012). These results indicate the importance of developing improved durum wheat varieties that possess enhanced resistance to drought stress; thus, the utilization of novel molecular markers and their successful integration into breeding programs is a valuable approach to achieving maximum production.

Water stress during the critical growth stages of wheat, such as flowering and grain filling, can be particularly detrimental. These stages are crucial for the development and filling of grains, and any water shortage during this time can result in reduced morphometric traits, such as plant height, the number of tillers, biomass yield, and grain weight, which could decrease along with the grain filling rate (Nouri et al., 2011). A substantial decline in leaf area and photosynthesis activity was also detected under drought stress, which eventually intensified to reduce the number of leaves per plant, leaf size, and longevity (Shao et al., 2008). This could be due to the limitation of leaf extension under water stress conditions to balance the absorbed water by the root and the water status of plant tissue (Nezhadahmadi et al., 2013). While the effect of drought stress is a complex issue, the specific outcomes can vary depending on various factors, such as the duration and intensity of drought events, plant health conditions, nutritional status, varietal differences, and growth stages at which crops are exposed to drought and the environmental conditions in which crops are grown (Sun et al., 2017; Yu et al., 2018).

3.1.1 Drought stress and grain protein content: understanding the complex relationship

The grain protein content plays a multifaceted role, particularly in relation to both drought conditions and in the context of food products. Higher grain protein concentration is not only improving the quality of end-use products but also enhance survival of the cells against stress conditions due to its role in stabilizing the membranes (Jamshidi et al., 2020). Higher protein content in grains can help crops maintain metabolic functions, sustain growth, and enhance drought tolerance, as proteins are involved in various physiological processes, including enzymatic reactions, cellular signaling, and stress responses (Merewitz et al., 2011). However, establishing a clear and consistent relationship between drought stress and grain quality attributes in durum wheat has indeed posed challenges, despite substantial research efforts (Flagella et al., 2010; Gebrewahid et al., 2021). The absence of a "one-size-fits-all" model for the impact of drought stress on durum wheat, could be a reflection of the complex nature of drought stress and the varied responses observed across different crop ecotypes and genotype-by-environment (G × E) interactions. The presence of additional factors and methodological differences among previous studies can contribute to the challenge of establishing a simple one-dimensional model for drought stress alone and make it difficult to consolidate research findings into a single model.

The relationship between drought and grain protein content could vary depending on the durum wheat varieties, the pedoclimatic conditions of the growing environment, and their interaction (Melash and Ábrahám, 2022). The interactions and synergistic effects between these factors further complicate the prediction and management of drought stress. In some cases, drought stress significantly decreases the grain protein content, to an extent that varies with the degree and timing of the drought events as well (Flagella et al., 2010; Gebrewahid et al., 2021). Gene expression of storage protein fractions such as gliadin, glutenin, -gliadin, and -gliadin has also been downregulated when the cropping season experiences a dry spell (Yang et al., 2011; Begcy and Walia, 2015). The decreased grain protein concentration in water-limited environments can be primarily attributed to the limited availability and assimilation of nitrogen, which is an essential component of storage grain proteins (Zia et al., 2021). This negative consequence of the drought effect, along with poor caryopsis quality, could further constrain the strength of the dough and its stability, such as loaf volume and valorimetric values (Tsenov et al., 2015).

While a number of studies suggest a negative effect of drought stress on durum wheat grain protein content, there are also controversial findings and alternative perspectives. It has been observed that grain protein content can be significantly ameliorated when wheat crops are subjected to drought stress (Flagella et al., 2010; Ahsan et al., 2022). The improved grain protein content and associated quality traits under such a scenario could be due to the reduction in grain starch accumulation (Barnabas et al., 2008), and the limited starch accumulation allows for a higher concentration of nitrogen per unit of starch in the grains (Stone and Nicolas, 1998). The decreased starch accumulation could be due to a decrease in amylose composition, which causes the loose packaging in the starch granules (Prathap et al., 2019). The loss of packaging in the starch granules can further influence grain functional properties, such as the ability to form gels and thickening properties, in food and industrial applications. Additionally, the shortening of grain filling stages under drought conditions could also result in reduced starch accumulation in the developing grains due to early senescence of the crop (Prathap et al., 2019). Early senescence in crops results in a reduction in their photosynthetic capacity of crops, which further exacerbating the limited supply of assimilates required for grain filling and starch synthesis (Sehgal et al., 2018). It is, therefore, very important to consider all involved production factors when studying and managing the impact of drought stress on grain protein content to develop targeted mitigation strategies and breeding programs aimed at improving protein content under water-limited environmental conditions.

3.1.2 Drought stress affects nitrogen assimilation to result in poor phytochemical composition

When evaluating the effect of drought stress on durum wheat productivity, it is important to consider various factors that directly influences overall crop performance. Impairment in symbiotic nitrogen fixation under drought conditions has been observed due to improvement in oxygen diffusion resistance in root bacteroides; resulting in reduced nitrogenase activity that may potentially decrease the availability of nitrogen for the biosynthesis of proteins (Sehgal et al., 2018). There is convincing evidence that the change in composition of protein subunits owing to drought and seasonal heat stress is principally due to alterations in the amount of accumulated nitrogen at the grain filling stage (Triboï et al., 2003; Urban et al., 2018). Investigating the impact of drought stress and associated extreme events under a range of nitrogen doses on physiological traits and other attributes could provide important insights in the development of drought tolerant wheat varieties (Teixeira et al., 2014). This indicates that, although grain protein quality largely depends on the varietal performance, it may be affected by environmental-induced factors (Gebrewahid et al., 2021).

The reduction in mineral accumulation such as iron, zinc, nitrogen, phosphorus, and total protein content in developing grains due to drought stress has also been observed in a wide range of crops (Sehgal et al., 2018). The low phytochemical composition observed in crops under drought stress is often characterized by lower levels of secondary metabolites such as phenolics, flavonoids, alkaloids, and terpenoids. These compounds play crucial roles in crops defense against various environmental stressors, as well as in providing health benefits to humans when consumed as part of a plant-based diet (Bindu et al., 2021). This can have implications for plant growth, development, drought tolerance, and the nutritional and therapeutic properties of plants. Hence, understanding these effects is important for crop management practices and the development of strategies to mitigate the impacts of drought on the physiology and phytochemical composition of durum wheat.

While there is general knowledge about the importance of nitrogen in growth development and phytochemical composition of crops, the intricate interactions between variable nitrogen rate, nitrogen source, drought stress, and specific phenological phases of durum wheat are still an active area of research. An investigation that examines the impact of drought stress under variable nitrogen doses on resource use efficiency, physiological traits, and other associated traits can provide valuable insights for developing drought-tolerant crop varieties (Teixeira et al., 2014). Hence, conducting a comprehensive evaluation of the combined effect of nitrogen deficiency and drought stress can provide a valuable insights into the physiological, biochemical, and phytochemical responses of durum wheat varieties to drought stress. This evaluation can also help elucidate how these responses interact with nitrogen availability, thus agronomists, and durum wheat breeders can develop crop varieties that are more resilient and adaptable to the changing climatic conditions.

3.2 Unravelling the heat puzzle: decoding the impact of high temperature stress on crop yields

Higher temperature stress eventually reduces harvestable yield while encouraging weed and pest proliferation. In most cases, crops could respond to high-temperature stress in two different phases. The first stage is based on the intrinsic tolerance to high temperature-induced damage, known as basal thermos-tolerance, while the second stage involves resource mobilization and gene expression changes to deal with heat stress related injury, known as acquired thermos-tolerance (Bento et al., 2017). High temperatures have been observed to cause disruptions in the structure and function of chloroplasts, a reduction in chlorophyll content, and the inactivation of chloroplast enzymes, resulting in decreased photosynthesis activity in wheat (Yang et al., 2002). Increased temperature stress during the reproductive stage may also have an impact on spike fertility and, as a result, grain yield (De Storme and Geelen, 2014). It has been worth mentioning that pollen formation in wheat is a heat-sensitive process, and high temperature-induced pollen sterility often occurs due to irregularities during microsporogenesis (Jäger et al., 2008; Narayanan, 2018).

While elevated carbon dioxide levels can influence certain aspect of crop performance, it's overall effect on physiology, grain quality, and yield, the overall effect is universally considered to be smaller compared to the challenges posed by high-temperature stress (Ben et al., 2021) (Figure 2). This effect triggers a decline in global wheat production of about 4.1 to 6.4% for each degree escalation in temperature (Liu et al., 2016; Ashwani et al., 2020). Wheat crops grown under warmer climatic conditions are more susceptible to significant grain yield losses than wheat cultivated in cooler climatic conditions (Sommer et al., 2013). However, it is worth noting that there is general consensus that in high latitude regions, spring wheat production would benefit from a warmer climate through an extension of the growing season (Sommer et al., 2013). such a huge grain yield loss under warmer or dry climatic conditions could be due to negative water and energy balances resulting from limited water availability and imbalanced energy inputs, which can offset the positive effect of elevated CO_2 on stomatal conductance, which leads to net losses in soil water content, affecting wheat physiology and eventually grain yield (Helman and Bonfil, 2022). The potential losses in grain yield associated with warmer climatic conditions in wheat crops necessitate careful consideration of climate change impacts and the implementation of appropriate management practices and breeding strategies.

In certain situation, the combination of reduced cooling caused by lower transpiration rates and an increased leaf area index (LAI) can lead to unexpectedly higher water losses in plants (Helman and Bonfil, 2022). In a wet growing environment, varieties with a higher LAI and radiation use efficiency could benefit from the increased availability of water and solar radiation. A higher LAI allows for greater light interception and photosynthetic activity, leading to increased biomass production and subsequently higher number of

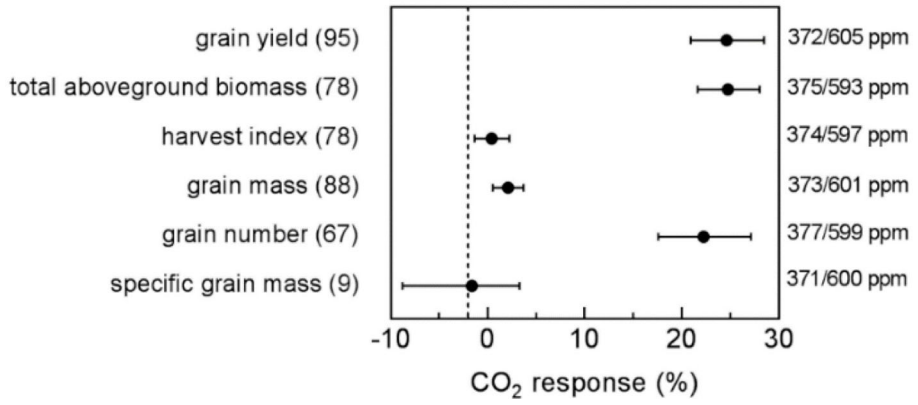

FIGURE 2
The eCO2 effect on wheat yield components (grain yield, harvest index, grain mass, grain number, total aboveground biomass, and specific grain mass) using aCO2 as the reference. The number of observation pairs is given within the brackets. The average concentration level for ambient and elevated CO2 treatments is given on the right y-axis (aCO2/eCO2).

grain and yield. On the other hand, under hot and dry climatic conditions, short maturing varieties with high grain dry-matter potential and stay-green capacity tend to perform better (Padovan et al., 2020). The shorter maturation periods could allow the crop to complete their life cycle prior to the onset of server stress, while grain dry-matter potential ensures efficient utilization of available resources for grain production. Hence, understanding the genetic basis for variation in phenology and other adaptive morphometric traits could enable wheat breeders and agronomists to predict grain yield risk factors, such as drought and heat, and thereby improve agronomic crop management practices.

3.3 Enrichment of atmospheric carbon dioxide effect on qualitative and quantitative agronomic traits

The composition of durum wheat grain encompasses various nutrients, such as proteins, carbohydrates, minerals, and phytochemicals, which collectively contribute to its nutritional and market value of the harvested product (Melash and Ábrahám, 2022). This diverse array of components collectively contributes to the nutritional quality and market value of harvested durum wheat. The concentration can be influenced by a number of factors such as nitrogen availability and environmental conditions. Lower carbon dioxide (CO_2) concentrations, for instance, has been shown to have an impact on the physiology and metabolome of mature grains. These changes in grain nutrient composition can subsequently affect the nutritional status of the grain (Wang J. et al., 2021). Higher CO_2 levels can increase morphometric traits and grain yield in crops, primarily due to their positive effect on stimulating photosynthetic activities (Erda et al., 2005). It has been proven that an increment in CO_2 up to 550 ppm (parts per million) can consistently increase both biomass and grain yields by about 5–15% (Ainsworth and Long, 2005). However, a nonlinear response to elevated carbon dioxide levels has been observed in some studies, where the stimulation of grain and biomass yield starts to diminish at around 600 ppm of CO_2 (Fitzgerald et al., 2016). This nonlinear response suggests that there might be a saturation point beyond which further increases in CO_2 do not provide additional yield benefits in crops; although the specific threshold at which this occurs can vary depending on crop ecotype, temperature and seasonal water availability

Increased atmospheric CO_2 levels and their interactions with other production limiting factors, such as water availability and nitrogen supply, can strongly modulate crop growth responses and result in a wide range of growth responses, typically spanning between 0% and 50% (Erda et al., 2005). The coexistence of elevated carbon dioxide and high temperature stress can have negative effects on wheat varieties, leading to reduced biomass and grain yield, perhaps due to a reduction in the number of spikes per plant (Galani et al., 2022). This implies that while elevated CO_2 levels can initially stimulate photosynthesis, enhance grain yield and biomass production, the combined effects of heat and drought stress can override these benefits and lead to reduced grain yield (Ben et al., 2021). It means that the combined effect of multiple abiotic stress factors can be more detrimental to durum grain protein content and yield than individual stressors alone.

The detrimental impact of elevated CO_2 on crop grain yield has been extensively studied (Figure 3), shedding light on the intricate mechanisms and physiological responses involved. However, little is known about how it may affect the nutritional composition of wheat grains, despite the fact that it is a vital aspect of food security (Haddad et al., 2016; Asseng et al., 2019). The changes in chemical composition observed in crops, such as a decrease in leaf nitrogen concentration and an increase in the carbon-to-nitrogen (C/N) ratio, could be strongly associated with increasing CO_2 concentration (Wieser et al., 2008; De Santis et al., 2021). This effect is thought to occur because, as CO_2 levels increase, crops can

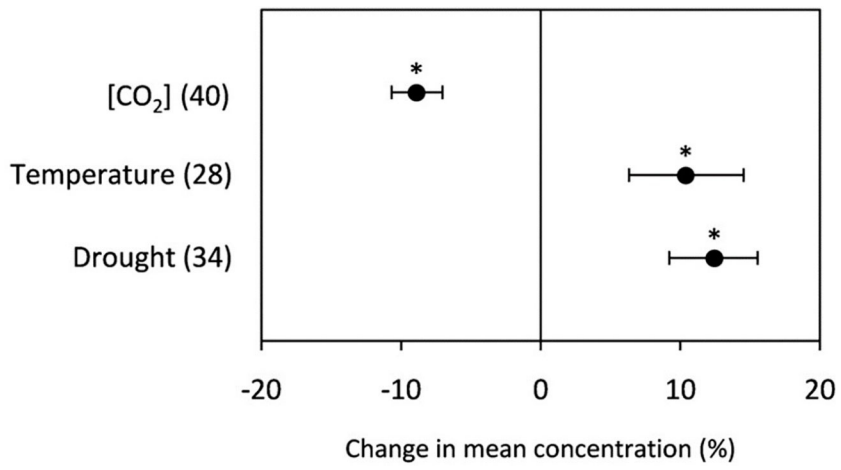

FIGURE 3
The change in grain protein content of wheat grown under high temperatures, elevated CO2, and drought stress conditions The numerical data in the parentheses indicates, the number of observations, and the error bars indicate the 95% CI, while the single asterisk (*) indicates a statistically significant difference between the observations at $p < 0.05$.

more easily convert the excess carbon into carbohydrates, which can lead to a dilution of protein levels in the grain. When grain protein content is reduced under elevated CO_2 levels while total yield production remains relatively constant, there is a dilution effect, resulting in lower grain protein content on a per-unit basis (Thompson et al., 2019). There has been an estimated decrease in grain protein content of about 1.08% for each 1 t ha^{-1} yield increment under elevated CO_2 conditions (Galani et al., 2022). It means that as crop yields increase, there is a corresponding decrease in grain protein content, particularly under elevated CO_2 conditions. This could have significant implications for food security and the market value of the product, as protein is an important nutrient for human health and industrial purposes; thus, it is an important factor to consider in breeding and food production programs (Melash and Ábrahám, 2022).

3.4 Dynamic in quantitative and qualitative agronomic traits under waterlogging stress

Water logging, which occurs when soil becomes water-saturated and oxygen is limited, can have a number of negative effects on crop growth, development, and grain protein content (Ren et al., 2014; Chao et al., 2022). This is because waterlogging can reduce the availability and uptake of nitrogen by plants, which is an essential nutrient for the production of storage proteins (Otie et al., 2019). When plants are waterlogged, the roots may not be able to take up nitrogen from the soil (Kaur et al., 2020a), or the nitrogen in the soil may be transformed into a form that is not readily available to plants. As a result, the plants may not be able to produce as much protein, or the protein content they do produce may be of lower quality. This can have a negative impact on the nutritional quality and commercial value of the grain. However, enhanced grain protein content has been observed, while starch concentration was decreased under waterlogging conditions occurred at maturity (Wang J. et al., 2021). Higher grain protein content under such conditions could be due to inhibition of carbohydrate transformation into starch in the developing wheat grain (Zhou et al., 2018). This means that, although an increase in grain protein content is a possible response, it is not always consistent under waterlogged conditions.

When durum wheat experiences water logging, the crop undergoes a series of physiological and biochemical changes to cope with the existing stress conditions. These changes often include alterations in physio-morphological traits, such as biomass production, grain weight, and photosynthetic activity, due to restrictions in the availability of oxygen to the roots (Arguello et al., 2016). A decrease in photosynthesis could limit the ability of crops to produce energy and assimilate carbon dioxide, resulting in a slower growth rate and a lower harvestable yield. Waterlogging situations can also induce the formation of adventitious roots in durum wheat (Tian et al., 2021). These roots arise above the waterlogged zone and serve as a strategy to overcome oxygen deprivation in the root zone. A suppressed root respiration, decreased root activity, and energy shortage have also been observed under waterlogged soil as compared to well-drained conditions (Pan et al., 2021). The impaired root system under waterlogged conditions could further limit the ability of crops to absorb essential nutrients, leading to nutrient deficiencies. Inadequate nutrient uptake affects wheat growth and reduces shoot growth, ultimately resulting in grain yield loss (Herzog et al., 2016). Hence, to avert grain yield and quality loss under waterlogging conditions, agronomists, plant breeders, and researchers focus on the development of crop varieties with improved tolerance to excess water, such as deep root systems, enhanced photosynthetic efficiency, and better nutrient uptake capacities. Additionally, agronomic practices such as proper drainage, crop rotation, and soil management can minimize the negative impacts of waterlogging on crop productivity.

A switch from aerobic respiration to anaerobic respiration due to waterlogging can also decrease the grain yield by preventing culms from generating spikes, slowing spikelet formation, decreasing the number of spikelets $spike^{-1}$, the formation of florets $spikelet^{-1}$, and the number of kernels $spike^{-1}$ (Pampana et al., 2016). However, the actual yield loss under waterlogging conditions could vary widely depending on the durum wheat varieties, their tolerance to waterlogging, the variation in the growing environment, and the duration and severity of waterlogging (Cotrozzi et al., 2021). In some cases, yield losses could be moderate, ranging from 19% to 30%, while in severe and prolonged waterlogging conditions, yield losses can exceed 55% or even lead to total crop failure (Marti et al., 2015; Pampana et al., 2016). Extended waterlogging conditions and anaerobic respiration could further trigger the accumulation of toxic metabolites such as lactic acid, ethanol, and aldehydes, along with increases in reactive oxygen species, resulting in cell death and crop senescence (Pan et al., 2021). Inhibited gaseous exchange capacity under waterlogging conditions could also cause a rapid buildup or plant hormone degradation and further influence the waterlogging tolerance of crops (Kuroha et al., 2018; Pan et al., 2021).

It has been globally estimated that approximately 10-12% of the agricultural area is affected by waterlogging or severe soil drainage constraints (Kaur et al., 2020b). In the United States, for example, flooding poses a significant hazard and has been ranked as the second most impactful abiotic stress factor, following drought, in terms of crop production losses over a 12-year period (Kaur et al., 2020b). These constraints pose significant challenges to agricultural productivity and sustainability in affected regions. A long-term research study conducted in China also revealed that the grain yield of wheat cultivars showed a steady improvement over the years. However, it was observed that the rate of yield improvement was lower under waterlogging conditions compared to normal watering conditions. Under normal watering conditions, the grain yield increased by 53 kg ha^{-1} per year (equivalent to a yearly improvement of 0.6%), while under waterlogging treatment, the increase was 35 kg ha^{-1} per year (equivalent to a yearly improvement of 0.51%) from 1967 to 2010 (Ding et al., 2020). The research conducted in China, although specific to the wheat cultivars in that region, provides a general indication that as wheat cultivars are continuously developed and improved over time, there is a tendency for their overall waterlogging tolerance to decline. This observation has broader implications for wheat breeding programs and the selection of traits prioritized during cultivar development.

The detrimental impact of waterlogging on the quality, yield, and physiological aspects of wheat universally highlights the need to devise effective mitigation strategies. Addressing these constraints requires a combination of management strategies tailored to a particular or specific conditions. These may include implementing improved drainage systems, raised bed planting, ensuring land leveling, optimizing the sowing period, adaptive nutrient management and utilizing plant growth-promoting substances (Figure 4) (Pramanick et al., 2023). The use of raised beds has proven to be significant in high rainfall regions, as observed in Victoria, Australia. The substantial yield increases observed for both wheat (50%) and barley (30%) in Victoria demonstrate the effectiveness of raised beds as an agronomic measure in mitigating the adverse effects of waterlogging in high rainfall areas (Manik et al., 2019). In addition to the agronomic based mitigation interventions, the contemporary advancements in biotechnology, including functional genomics, offer promising approaches to identify specific genes or QTL (Quantitative Trait Loci) associated with waterlogging tolerance in wheat. Genome modification techniques are also employed to enhance wheat's capacity to withstand waterlogging conditions substances (Pramanick et al., 2023). These biotechnological interventions play a significant role in the development of novel wheat cultivars with improved tolerance to waterlogging.

3.5 Biofortification of crops as influenced by the changing climate

The nutritional functional diversity of the cropping system, which is based on both on-farm durum wheat species diversity and nutritional composition, holds significant potential to address malnutrition and associated health complications. However, increasing demand for nutritious, safe, and healthy food because of a growing population and changing climatic conditions; pledge to maintain biodiversity and other resources pose a major challenge to the crop production sector (Dwivedi et al., 2017). Micronutrient deficiency, such as zinc malnutrition, has been observed to affect more than 17% of the world population, and enrichment of the atmospheric carbon dioxide significantly lowers grain zinc concentration by about 9.1% (Soares et al., 2019). This reduction may further affect about 138 million people and place them at a new risk of zinc deficiency by 2050 (Myers et al., 2015; Soares et al., 2019).

When wheat crops are grown under elevated CO_2 conditions, wheat tend to accumulate a higher level of carbohydrate and enhance yield, but with reduced concentrations of certain minerals such as zinc and iron by about 3% and 5%, respectively (Richard et al., 2022). This result highlights that climate change adaptation strategies that benefit grain yield may not always have a positive effect on grain qualitative traits, thus putting further pressure on global quality wheat production (Asseng et al., 2019). A recent meta-analysis also showed a significant decline in grain Zn, Fe, S, Ca, Mg, P, Mn, K, and Mo with increasing CO_2 concentration (Ben et al., 2021). The decreased grain mineral concentration could be primarily attributed to changes in plant physiology, such as a decrease in the pace of transpiration rate, i.e., linked to stomatal closure due to long-term exposure to elevated CO_2, since higher CO_2 could reduce the mass flow in the soil toward roots, which diminishes the availability of mobile minerals in the rhizosphere (Loladze, 2002). However, higher grain zinc and iron deposition has been observed under high temperature conditions, offsetting the

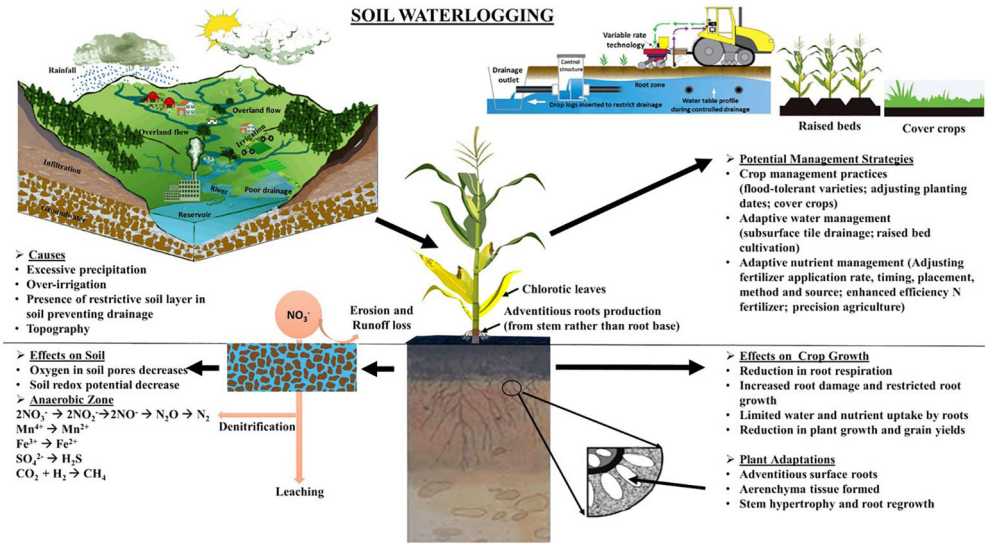

FIGURE 4
Illustrates a depiction of the causes of soil waterlogging, its impact on crop production nitrogen losses, and potential approaches for managing these issue (Kaur et al., 2020b).

decrease in grain mineral concentration due to elevated carbon dioxide (Wang et al., 2020). Although the specific mechanism behind this response is not yet fully understood, it could be attributed to improved drought induced transportation of trace elements, leading to higher grain mineral concentrations (Ge et al., 2010). Addressing these issues generally requires a multifaceted approach, such as breeding crop varieties that are more efficient in micronutrient uptake and allocation, optimizing nutrient management approaches, and considering agronomic practices that can enhance the availability of mineral nutrients in the root zone. It has been also observed that the coexistence of abiotic stress on nutrient composition had a positive effect on gluten, Fe, Zn, and protein, showing respective increases of 19.11%, 14.42%, 7.20%, and 4.60%. However, the decrease in yield offset the concentration gains in other nutrients, leading to a decrease in K (-32.08%), Mn (-21.65%), P (-13.12%), and Mg (-7.66%) (Figure 5). This result highlights the trade-off between nutrient yield and overall grain yield when subjected to abiotic stress. While certain nutrients such as gluten, Fe, Zn, and protein showed improvements in yield, the decrease in yield can offset the gains in concentration for other essential nutrients.

4 The climate-nutrient nexus: managing nutrient inputs for sustainable agriculture in a changing climate

4.1 Nitrogen application under drought condition: from risk to resilience

Nitrogen application under drought conditions is a crucial aspect of agronomic practices, transforming the concept of risk into resilience. Improving crop resistance to heat and drought stressors through plant breeding and adjustments in agronomic practices such as site-specific nutrient management, time of sowing, and proper nitrogen fertilization are thought to be useful in climate change adaptation (Van Ittersum et al., 2013). Nitrogen metabolism such as, ion absorption, nitrogen assimilation, amino acid synthesis, and protein synthesis are very important drought tolerance indicators (Li et al., 2020). Increasing nitrogen application up to a certain level may alleviate drought-induced stress by increasing root osmotic regulators, stimulating the acceleration of root biomass

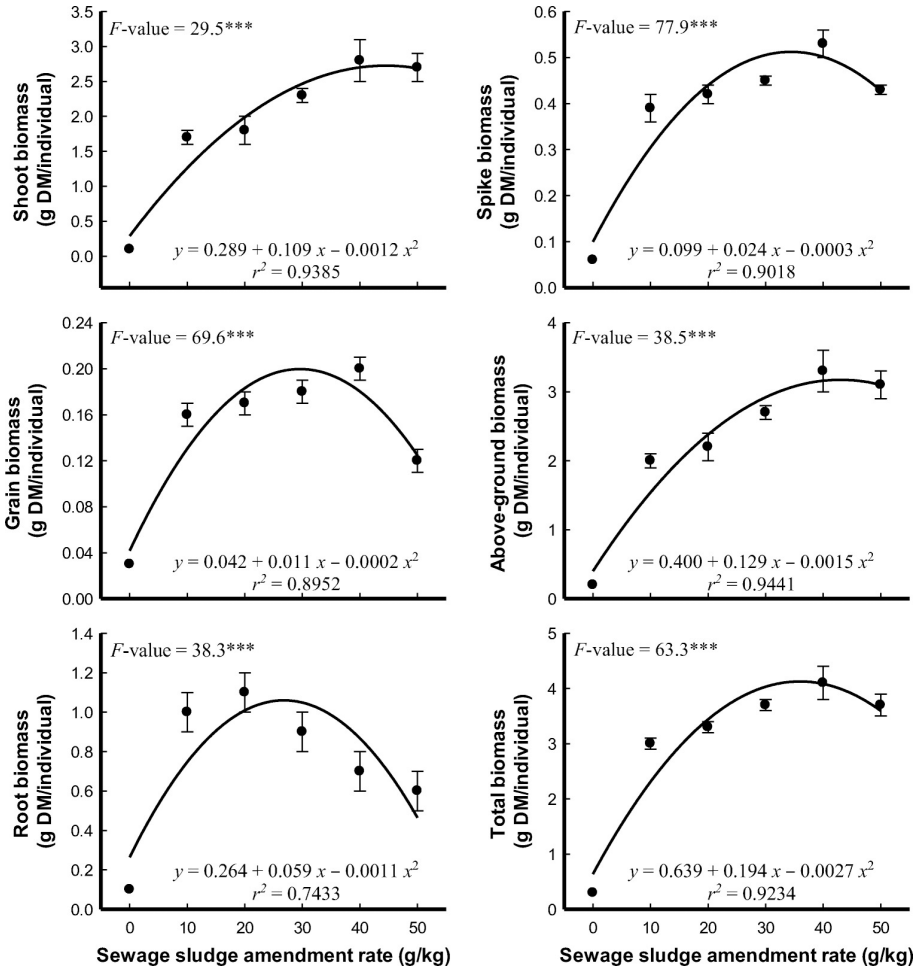

FIGURE 5
Effects of different sewage sludge amendment rates on the biomass of wheat harvested after 80 days (means ± standard error, n = 24). F values represent a one-way ANOVA and degrees of freedom (df) = 5. ***P<0.001 (Eid et al., 2019).

accumulation, and enhancing nitrogen assimilation ability, which would reduce moisture limitations (Xiong et al., 2018). In the presence of mild drought stress, application of nitrogen fertilizer at a higher dose has been demonstrated to enhance the plasticity expression of root development (Tran and Kano-Nakata, 2014). Integrated nitrogen, phosphorus, and potassium applications also profoundly increase osmoprotectant accumulation and activity of both nitrogen absorption and antioxidant enzymes to increase wheat grain production and drought tolerance (Shabbir et al., 2016). However, it is important to note that excessive nitrogen application can have negative impacts on plant growth and development, including reduced drought tolerance (Liu et al., 2016). This suggests that the regulatory function of nitrogen in drought-induced stress tolerance of plants is dependent on the severity of the stress, nitrogen amount, and crop species variation (Xiong et al., 2018). Hence, it is essential to apply nitrogen in appropriate amounts and at the right time to maximize its benefits for the growth and development of durum wheat.

Nitrogen application at the appropriate timing and amount can aid in the development of stress defense mechanisms while also promoting normal crop growth (Chang and Liu, 2016). Under proper nitrogen fertilization, plants can produce adequate antioxidant enzyme activity and osmotic adjustment by generating proline accumulation to alleviate drought-induced physiological damage (Li et al., 2020). In a universal agreement, higher nitrogen metabolism enhances the drought resistance level of crop plants (Zhong and Cao, 2017). It means that higher levels of nitrate transport and assimilation could subsidise to improve the drought induced stress tolerance level of crops (Zhong and Chen, 2015). Hence, implementing innovative agronomic techniques and harnessing the potential of nitrogen-based fertilizers could enhance durum wheat productivity, adapt to challenging climatic conditions, and ultimately transition the crop sector from a vulnerable state to one of resilience. However, to the best of our knowledge, the nitrogen effect under varying drought stress levels at various intensities of abiotic stress and the phenological plasticity of durum wheat are not clearly understood, which may require a comprehensive investigation at a refined molecular level.

4.2 Harnessing nanoparticles: revolutionary solutions for mitigating crop abiotic stress

The past few decades have seen significant structural modifications in agricultural cultivation systems that are intended to improve how crops respond to diverse abiotic stresses. The use of nanoparticles in agricultural production systems has been observed as advantageous for both environmental stewardship and crop productivity enhancement. Nanoparticles are small molecular aggregates with dimensions of 1–100 nm. These tiny particles may easily enter the plant cells through both above-ground organs, such as the cuticle, epidermis, stomata, and hydathodes; and underground organs, including root tips, cortex, lateral roots, and wounds (El-Saadony et al., 2022). Due to their high reactivity, nanomaterials exhibit efficient nutrient absorption for plants, resulting in greater utilization efficacy and minimal losses in comparison to conventional fertilizers (Avila-Quezada et al., 2022).

Nanoparticles have been frequently reported to improve growth, development, grain quality, and yield of crops under a range of abiotic stress conditions. It has been observed that a proper soil-based application of analcite nanoparticles enhances the germination and morphometric traits of wheat, particularly under dry climatic conditions (Hossain et al., 2021). Improved germination percentages have also been observed in other crops following the application of ZnO-based nanoparticles (Sedghi et al., 2013). Nanoparticles such as Cu-based fertilization influence various physio-morphological traits such as biomass yield, chlorophyll concentration, carotenoid contents, leaf water content, and anthocyanin, particularly under dry climatic conditions (van Nguyen et al., 2022). An increase in wheat morphometric traits due to the application of Cu and Zn nanoparticles could be due to improvements in antioxidant enzyme activity and relative moisture content, which ultimately reduce the effects of drought stress (Taran et al., 2017; Semida et al., 2021). Through adjusting these processes, nanoparticle-based fertilization could help crops adapt to drought stress and maintain both yield and grain protein concentration in the current climate change scenarios.

Under drought conditions, the application of silicon dioxide (SiO_2) nanoparticles has been found to increase the shoot length, and relative water content while reducing superoxide radical formation, and membrane damage (Turgeon, 2010). This is attributed to the ability of SiO_2 nanoparticles to improve water uptake and retention, thus reducing the negative impacts of water stress on the growth, development, and grain quality of crops. When silicon dioxide (SiO_2) and titanium dioxide (TiO_2) nanoparticles are simultaneously applied, significant improvements in grain yield and stress tolerance levels of crops have been observed (Shallan et al., 2016). The enhanced grain yield following SiO_2 fertilization can be attributed to various factors, including improved photosynthesis, stomatal conductance, and stress tolerance of crops (Ashkavand et al., 2015). However, the effectiveness of nanoparticle fertilization in enhancing drought tolerance and improving grain yield can be influenced by nutrient application methods. It has been observed in some studies that foliar application of titanium dioxide nanoparticles can enhance grain yield and stress tolerance in wheat more effectively than other application methods (Jaberzadeh et al., 2013). Additionally, the application of zinc-based nanoparticles has shown potential for increasing grain zinc concentration along with improving grain yield, proline, glycine betaine, free amino acids, protein content, and other yield-related traits (Dapkekar et al., 2018; Ghani et al., 2022). Zinc-based nanoparticle applications have additional effects beyond the nutrient supply, such as enhanced nutrient uptake, increased photosynthetic activity, and improved water use efficiency; these specific effects can contribute to the overall improvement of grain yield, protein content, carbohydrate metabolism, and other yield-related traits (Verma et al., 2022a).

Drought stress could also negatively affect the nutrient absorption and utilization efficiency of plants, including essential nutrients like nitrogen, phosphorus, and potassium (Raza et al., 2023). However, the application of silicon-based nanofertilizers has been shown to have positive effects on soil nutrient availability,

including nitrogen, phosphorus, and potassium (Rizwan et al., 2019). This effect ensures that crops have access to necessary essential nutrients, particularly in water-limited environments, stimulating plant growth, yield, and grain protein content. It has also been shown to have beneficial effects in reducing the accumulation of heavy metals, such as cadmium (Cd), under drought conditions and improving the drought tolerance of crops by initiating different pathways (Khan et al., 2019). It is also worth mentioning that climatic extremes such as drought, salt, and waterlogging could enhance the production of reactive oxygen species (ROS), leading to oxidative stress (Hasanuzzaman et al., 2020). This action impaired water uptake, disrupting biological membranes, ionic imbalance, oxidative damage and nutritional imbalance, reducing cell division and expansion, lipid metabolism rate of photosynthesis and consequently impairing yield attribute traits (Kumari et al., 2022). Through neutralizing ROS and stabilizing cell membranes, silicon-based nanoparticles could contribute to reducing the damaging effects of ROS on wheat cells (Hussain et al., 2019). This could have a significant positive effect on durum wheat physiology, such as enhanced stress tolerance, improved crop health, and vigorous growth.

The other important nutrient that has gained attention as a mitigation solution for climate change is nitrogen-based nanoparticles due to their ability to enhance nitrogen use efficiency and reduce nitrogen losses. It has been shown to offer potential positive benefits in terms of tillering capacity, crop health, vigorous growth, and leaf colour changes, i.e., from light yellow to green (Kumar et al., 2022a). Alteration of the life colour impels that adequate application of nitrogen based nanoparticles could maintain the greenness of crops, which caused the crop to mature at its proper time and promoted proper development of the grains, and grain protein content remained high. Nitrogen-based fertilization also improves antioxidant defense mechanisms and reduces drought-induced oxidative damage by promoting the synthesis and activity of antioxidant enzymes such as superoxide dismutase (SOD) and peroxidase (POD), thus improving photosynthesis and crop stress tolerance levels (Raza et al., 2022). The improved photosynthesis could, in turn, increase carbon assimilation and energy availability, which are important for crop growth and drought stress tolerance. Although nanoparticles have a positive effect on overall crop productivity, the optimum concentration and sources of nanoparticles may vary depending on specific growing conditions and wheat varieties. Thus, extensive and rigorous field trials are necessary before widespread adaptation of nanoparticle-based fertilization approaches aimed at improving crop yield and grain protein content under changing climate scenarios.

4.3 Revitalizing agriculture with silicon-based fertilizers for enhanced productivity and environmental sustainability

Revitalizing agriculture through the use of silicon-based fertilizers has emerged as a promising strategy to support overall growth and development of crops, such as by enhancing photosynthetic efficiency and limiting electrolytic leakage under changing climatic conditions (Mir et al., 2022). Although it is not classified as an essential nutrient for all crops, a number of reports indicate the critical role of silicon in enhancing crop abiotic and biotic stress tolerance, such as drought, salt, freezing, nutrient imbalance, and radiation damage (Wang M. et al., 2021). Application of silicon under drought conditions has increased the photosynthesis rate, stomatal conductance, and antioxidant defense compared to plants grown without silicon application, which leads to efficient energy conversion and increased biomass production (Ali et al., 2019). It also enhances the crop's ability to withstand drought stress by maintaining root growth and improving water transport (Yan et al., 2016). The effects of which are attributed to the increased antioxidant defense and decreased oxidative stress induced by silicon fertilization (Gunes et al., 2007). This means that proper application of silicon-based fertilizers could allow wheat crops to explore or access water from deeper soil layers in a water-limited environment.

Through enhancing photosynthetic activity, increasing the efficiency of nutrient uptake, delaying senescence, improving stomatal responses, and enhancing drought tolerance silicon fertilization enables plants to maintain higher biomass and grain yield production under abiotic stress condition (Schaller et al., 2021; Irfan et al., 2023). Improved morphometric and physiological traits, such as gas exchange capacity, total root length, surface area of the root, volume of the root, and plant height, dry matter, have been observed following silicon application under drought conditions (Irfan et al., 2023; Chen et al., 2011). A larger silicon mediated root surface area could facilitate enhanced water and nutrient absorption, which is particularly important when soil moisture availability is limited. This silicon-mediated change in root development could further improve root endodermal silicification and suberization (Fleck et al., 2011). The enhanced silicification of the endodermis could contribute to improved water and nutrient uptake efficiency by restricting the passive flow of water and solutes.

While the exact mechanisms of how silicon enhances seed germination under drought conditions are still being studied, several research studies have reported positive effects on the stimulation of seed germination and spikelet sterility in wheat (Hameed et al., 2013). In addition to its effect on grain yield, proper fertilization with silicon could maintain or even increase the protein content of durum wheat under drought conditions (Kutasy et al., 2023). Because, silicon enhances the activity of enzymes involved in nitrogen metabolism, this leads to improved nitrogen uptake, assimilation, and translocation within the plant. This, in turn, can contribute to higher grain protein accumulation. Hence, the positive effects of silicon on physiology, yield formation, nutrient uptake, and grain quality substantiate the need to include these essential nutrients in the cultivation system of durum wheat under changing climatic conditions. An intimation to adapt silicon as a remedial measure under changing climatic conditions, is evident from the upregulation of genes involved in adaptation mechanisms such as phytohormone metabolism and cell wall synthesis upon supplementation of silicon fertilizers (Haddad et al., 2019).

The presence of silicon in plant tissues can enhance the crop's ability to withstand drought stress through several mechanisms, such as the antioxidant system and reducing drought-induced oxidative stress (Gunes et al., 2007). It has been observed that the application of silicon-based fertilizers exhibits improved wheat resistance to drought stress, particularly in silicon-accumulating varieties compared to non-silicon-accumulating crops (Thorne et al., 2021). However, in plant species that are less effective at accumulating silicon, the application of silicon can still have positive effects in countering drought stress, such as tomato and canola (Wang M. et al., 2021). These suggest that both accumulators and non-accumulators could benefit from silicon fertilization, and even low levels of Si accumulation can contribute to improved plant performance under drought conditions (Katz, 2014). A higher drought tolerance level in silicon-accumulated varieties could be due to reduced transpiration, increased water uptake, regulating stomatal behaviour, enhanced antioxidant activity, and improved photosynthesis following silicon application (Wang M. et al., 2021).). These traits could therefore contribute to the ability of silicon-accumulated wheat varieties to better withstand and recover from abiotic stress, ultimately leading to improved grain yield and resilience in water-limited environments.

4.4 From waste management to climate solutions: sewage sludge fertilization as an adaptive agricultural approach

The application of sewage sludge could be considered an adaptive agricultural approach with potential benefits for both waste management and climate solutions. In the presence of abiotic stress, such as drought stress, the availability of water is very limited, and crops like durum wheat may not be able to absorb nutrients from the soil effectively. The use of sewage sludge has been found to improve the water-holding capacity of soil, which can improve the seasonal drought stress tolerance of durum wheat (Boudjabi et al., 2015; Debiase et al., 2016). In recent years, sewage sludge fertilization has gained interest and recognition due to its nutrient content, organic matter contribution, and cost-effectiveness in comparison to synthetic fertilizers (Inmaculada et al., 2007; Boudjabi et al., 2015). It contains substantial amounts of nutrients essential for plant growth, including nitrogen, phosphorus, and organic carbon (Fytili and Zabaniotou, 2008). Through improving nutrient availability and mitigating the effects of drought stress, sewage sludge fertilization can also contribute to an increase in grain protein, and amino acids content, resulting in improved nutritional quality of wheat (Mazen et al., 2010).

When applied as fertilizer, sewage sludge releases nutrients gradually, ensuring sustained supply to the crops over an extended growing season (Muter et al., 2022). The slow release of sewage sludge fertilizers could be more advantageous, particularly in dry land farming where drought is a serious factor, as it allows plants to access essential nutrients steadily in a water-limited environment (Muter et al., 2022). Additionally, augmenting sewage sludge fertilizers has improved the grain yield of durum wheat, through which sludge-based fertilization allows root growth and helps to explore deep into the soil and absorb more water, thus enabling the crop to avoid the seasonal water stress effect (Sonia et al., 2019). Improved water utilization efficiency could help durum wheat plants maintain physiological processes, minimize stress, and allocate resources efficiently. The water stress reduction role of sewage sludge application has been confirmed, through which sludge based fertilization improves water retention capacity, regulates chlorophyll a, and enhances aboveground biomass production (Boudjabi et al., 2015). However, when sewage sludge is applied in excess, it could increase osmotic stress, perhaps due to the hydrophilic effect of organic matter contained in the sludge (Boudjabi et al., 2015). Higher growth parameters and biomass yield have been observed (Figure 6), particularly under low concentrations of sludge application, which further decreases the risk of heavy metal toxicity (Eid et al., 2019). Inversely, the application of sewage sludge-based fertilization, particularly at higher doses, have showed a synergistic effect that mitigates drought stress in other crop plants. This effect is attributed to the increased accumulation of osmoregulators, which assist plants in coping with water scarcity (Oustani et al., 2015). However, responsible application practices should be followed to ensure the safe and effective utilization of sewage sludge as a fertilizer (Oustani et al., 2015). These results universally indicated that improper or excessive application of sewage sludge can have a negative consequence including nutrient imbalance, heavy metal accumulation, and environmental pollution. Hence, regular monitoring soil and plant samples can provide valuable insights into nutrient levels and potential heavy metal accumulations of wheat, enabling timely corrective measures if needed (Feszterová et al., 2021).

The use of sewage sludge fertilizers can have significant agronomic benefits, such as providing nutrients such as nitrogen, ammonium, potassium, and zinc and thus improving soil quality (Marin and Rusănescu, 2023). When sewage sludge is applied to the soil, it can indeed improve soil organic matter (SOM) content, nutrient contents, soil porosity, bulk density, aggregate stability, and available water holding capacity (Simões-Mota et al., 2022). This improvement could be attributed to several factors, such as the high moisture content of sewage sludge and the presence of soil organic matter (Achkir et al., 2023). This can be particularly beneficial in drought conditions, as the soil can hold more moisture, providing a reservoir for plant growth and reducing seasonal water stress. However, the presence of higher organic matter in sewage sludge can stimulate microbial populations, leading to increased microbial respiration and subsequent water consumption (Hechmi et al., 2020). It clearly indicates that if the soil is already experiencing drought conditions, this increased demand for moisture could further stress crops and reduce their growth and yield potential. Hence, it is very important to consider the balance between the positive effects of sewage sludge application on moisture retention and the potential negative consequences associated with increased microbial activity and soil moisture demand, particularly under drought conditions.

The application of sewage sludge can also provide cost benefits by reducing the need for mineral fertilizers and promoting economically beneficial crop production (Silva et al., 2022).

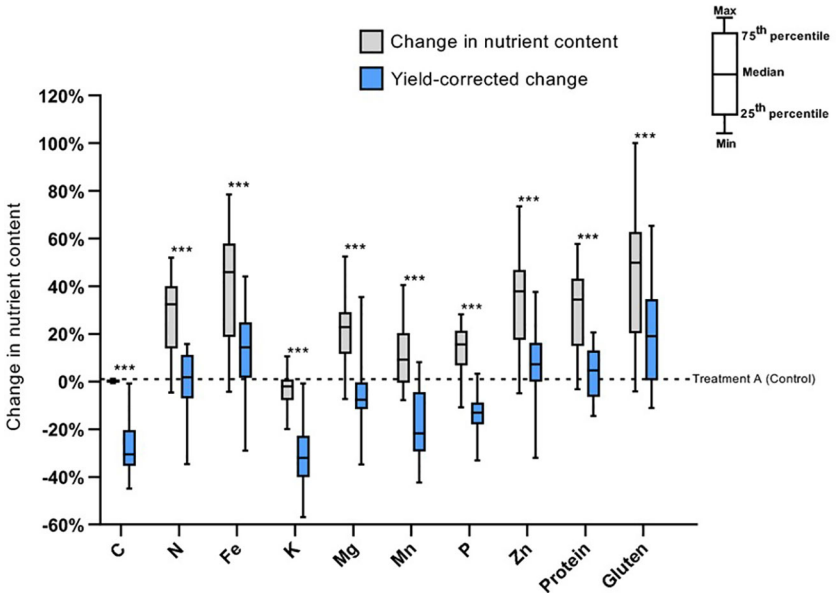

FIGURE 6
Illustrates the average percentage change in nutritional composition and yield associated nutrient content of wheat varieties under the co-existence of abiotic stress compared to the control. NB: "A" stands for ambient CO2, lower temperature settings, and no O3 addition (control). The bars indicated with *** refer to a significant difference at p = 0.001 between the normal and yield-corrected nutrient content (Galani et al., 2022).

Previous studies have shown that the application of sewage sludge can save up to 25% of mineral fertilizer requirements, and its combined application with inorganic fertilizers proved economically beneficial for cereal production (Ankush et al., 2021). While sewage sludge can provide benefits as a fertilizer, it is important to consider and address the potential risks associated with its use. Because sewage sludge may contain heavy metals, and organic pollutants that accumulate in soils and transfer to crops and groundwater if not properly managed (Healy et al., 2016).

4.5 Zinc-infused fertilizers: cultivating resilient harvests amidst changing climate

The need for improved compatibility between food security and environmental stewardship is of considerable urgency under the current climate change scenarios. Several studies have shown that zinc deficiency can result in reduced crop yields and lower protein content in grain (Melash et al., 2019). This is because zinc is necessary for the synthesis of enzymes that are involved in nitrogen metabolism, which is essential for protein production in crops. Under changing climate conditions, such as increased temperature and rainfall variability, crop growth and development can be negatively affected. However, the use of zinc-containing fertilizers has been shown to mitigate some of the negative effects of changing climate conditions on crop yields and grain protein content (Tao et al., 2018). These effect could be achieved through supporting nutrient limitations and physiological process such as improved photosynthesis pigment, active oxygen scavenging substances, and a reduction in lipid peroxidation under drought condition (Ma et al., 2017). This implies a huge grain yield and quality reduction would occur under the co-existence of soil zinc deficiency, and drought conditions have been observed to have a more profound effect on decreasing the yield and quality of wheat grain (Bagci et al., 2007).

Drought stress could be alleviated through the proper application of zinc-containing fertilizers, and this effect may be attributed to its ability to detoxify reactive oxygen species (ROS) generation and increase antioxidant enzymes (Wang and Jin, 2007; Sofy, 2015). It has been also observed that the application of various levels of zinc resulted in a significant increase in catalase, superoxide dismutase, peroxidase, and ascorbate peroxidase activities at 40% water holding capacity, where water availability is limited (Sattar et al., 2022). This result suggests that zinc fertilization can enhance the antioxidant defense mechanism of wheat crops, enabling them to better cope with water deficit-induced oxidative stress. However, the effectiveness of zinc-containing fertilization can vary depending on the method of application, particularly in enhancing the drought tolerance level and yield performance of wheat crops. The use of zinc priming alone or in amalgamation with zinc foliar-based application has been found to improve the regulated dissipation of excess energy in wheat. This effect was profound, with zinc priming alone increasing the regulated dissipation by over two-fold, and when coupled with zinc foliar application, the increase reaches three-fold under drought conditions (Pavia et al., 2019). Late-season foliar application of zinc under drought conditions could also improve photosynthesis activity, pollen viability, the number of fertile spikes, the number of grains per spike, the water-use efficiency of the wheat crop, and grain zinc concentration (Karim et al., 2012). Applying zinc-based fertilizer has also improved yield and grain zinc concentration by about 10.5 and 15.8%, 22.6 and 9.7%, and 28.2 and 32.8% under adequate water supply, moderate

drought, and severe drought, respectively (Ma et al., 2017). The enhancement in yield and grain zinc concentration was maximum under severe drought conditions, which implies that soil-based zinc fertilization may be particularly beneficial in improving wheat crop performance during periods of drought stress.

4.6 Seaweed extracts and climate resilience: how marine-based fertilizers can strengthen agricultural systems

The modern crop production system is facing a critical challenge due to extreme environmental changes. These changes are posing a serious challenge to the crop production sector, necessitating the development of trailblazing strategies for sustainable agriculture and food security. The use of seaweed extracts as a natural and sustainable plant growth promoter is gaining increasing attention, in recent years. It contains various compounds such as cytokinins, auxins, and betaines that have been shown to improve the water-use efficiency and stress tolerance of crops (Ali et al., 2022). The seaweed extracts are also abundant in phytohormones, sterols, carbohydrates, polysaccharides, sugars, polyphenols, vitamins, lipids, amino acids, peptides, proteins, macronutrients, and micronutrients that can potentially enhance plant growth and yield (Shukla et al., 2019). These substances could improve photosynthesis activities, nutrient uptake, resiliency, crop development, and soil health, allowing crops to better withstand drought conditions (Deolu-Ajayi et al., 2022). Seaweed extracts have been found to enhance root growth, carotenoids, and tissue water content, which can help crops access water and essential nutrients more efficiently under dry climatic conditions (Ali et al., 2022). An increase in the aggregation of soil particles, soil nutrient availability, aeration, and water-holding capacity has been observed following the application of soluble alginates from seaweeds and protein hydrolysates (Colla et al., 2017).

The application of seaweed extracts improves the drought tolerance of wheat by improving water retention capacity, enhancing root growth, and increasing photosynthesis activity (Sharma et al., 2019). The ability of seaweed extracts to enhance the antioxidant activity of reactive oxygen species scavenging enzymes, such as superoxide dismutase, peroxidases, catalases, and phenolic antioxidants could explain the potential of seaweed application to improve crop stress tolerance (Kumar et al., 2013; Deolu-Ajayi et al., 2022). Important physiological traits such as chlorophyll content were also improved following the application of seaweed extracts by ameliorating the biogenesis of chloroplasts and decreasing chlorophyll degradation (Jannin et al., 2013). This effect could be due to the up-regulated genes that are strongly linked with photosynthesis, cell metabolism, stress response, and S and N metabolism (Jannin et al., 2013). This result universally implies that by protecting photosynthetic tissues from damage, seaweed extracts can help durum wheat varieties maintain and produce energy from sunlight, even in water-scarce environments. Although, effectiveness of seaweed extracts and their method of action in crops are still not well understood, the application of seaweed extracts in stimulating yield, promoting vegetative growth, and ameliorating grain protein content under stress conditions indicates that it is more essential to encourage adoption by durum wheat producing farmers, particularly in drought-prone areas.

The seaweed extract can maintain the water balance of crops and reduce water loss through transpiration. Studies have shown that application of seaweed extracts under drought conditions can improve wheat grain yield by up to 8.04% (Najafi Vafa et al., 2022). This could be due to enhanced crop drought tolerance through improving water retention capacity, reducing transpiration, and enhancing the activity of antioxidant enzymes that protect crops against drought-induced oxidative stress. A vital function of seaweed extracts in maintaining absorption of soil nutrients by crops, stimulated the growth and enhanced plant resistance to abiotic stress could be the cause of such a huge yield advantage (Chen et al., 2021). It has also been observed that the application of seaweed extracts increases the freezing tolerance of crops other than wheat, such as barley, with an increase in winter hardiness (Ganesan et al., 2015). The attenuation effect of seaweed extracts against drought, cold, and salinity stress effects has been shown to be mediated through enhanced root morphology, a build-up of non-structural carbohydrates, which improved storage of energy, enhanced metabolism, and water adjustments, as well as the build-up of proline (Ganesan et al., 2015).

When wheat is grown under elevated atmospheric carbon dioxide, the crop tends to allocate more resources to photosynthesis and less to nitrogen composition, which can result in decreased grain protein content (Tcherkez et al., 2020). Offsetting resource allocation between photosynthesis and protein synthesis has been observed following the application of seaweed extracts under certain conditions, resulting in higher storage proteins in the grain (Deolu-Ajayi et al., 2022). Additionally, the application of seaweed extracts can also improve grain yield and protein content in crops grown under waterlogged conditions. This is thought to be due to stimulating water retention, soil aeration, and nutrient availability, thereby promoting grain nutritional composition (Deolu-Ajayi et al., 2022). Priming wheat seeds with extracts of U. linza or C. officinalis has shown positive effects on chlorophyll content, carotenoid levels, sugar accumulation, protein synthesis, and lipid metabolism (Arun et al., 2023). Seaweed priming enhances protein and sugar contents by facilitating the absorption of major elements, notably magnesium, which activates chlorophyll synthesis and boosts photosynthetic rates (Hamouda et al., 2022).

The foliar spray of seaweed extract has been reported to be effective in improving the performance of wheat varieties under drought conditions. This treatment has been correlated with numerous positive effects, such as the improvement of compatible osmolytes, antioxidant compounds, and genetic variation in non-coding chloroplast DNA regions like the trnL intron and psbA-tnH (Ali et al., 2022). This suggests that seaweed extracts could be a

promising agronomic strategy for improving the drought tolerance of crops, which is becoming increasingly important under the current climate change scenarios and water scarcity. A number of studies further suggest that seaweed extracts may increase the production of stress response genes in plants through several mechanisms, such as hormonal regulation, antioxidant activity, and enhanced nutrient availability. Enhanced stress response genes such as Na+/K+ transporters and late embryogenesis abundant (LEA) proteins, including dehydrins, and aquaporins, have been observed following seaweed extract application under abiotic stress conditions (Goñi et al., 2018; Rasul et al., 2021). Although the precise mechanism by which seaweed extracts increase the production of stress response genes in plants is not yet fully understood and may depend on the specific extract and varieties used, these mechanisms suggest that seaweed extracts can provide multiple benefits to crops under stress conditions.

5 The feasibility, environmental risk, and mitigation strategies of nutrient-based climate interventions

Nutrient based climate change interventions in agriculture have gained attention as potential strategies to mitigate greenhouse gas emissions and adapt to changing climatic conditions (Kumar et al., 2022b). These interventions involve application of fertilizers, and altering agricultural practices to enhance carbon sequestration, nutrient availability, reduce nitrous oxide, and improve overall soil health (Hassan et al., 2022b). However, prior to implementing such interventions on large scale, it is crucial to thoroughly asses their feasibility, potential environmental risk, and develop effective mitigation strategies to ensure long term sustainability. When considering the feasibility and environmental risks of using nutrients such as silicon, sewage sludge, zinc and sulphur for climate interventions, it is also essential to evaluate factors such as nutrient availability, local regulations and guidelines, potential impacts on water quality and soil health, and overall sustainability of the practices. Implementing these interventions should be done with careful planning, monitoring, and adherence to best management practices to minimize any negative environmental consequences (Muter et al., 2022).

The environmental implications of sewage sludge (SS) in various disposal scenarios, such as landfill disposal, agricultural use, and other applications, have garnered significant attention. The energy consumption during the treatment of SS is the primary contributor to global warming, accounting for over 50% of the impact (Muter et al., 2022). The disposal of sludge in agricultural areas primarily contributes to terrestrial acidification, and freshwater ecotoxicity, global warming, eutrophication, and acidification (Rorat et al., 2019). Additionally, the transportation of SS to agricultural areas has been identified as a significant factor influencing terrestrial and freshwater ecotoxicity, as well as ozone formation in terrestrial ecosystems. The toxicity associated with SS is often linked to the presence of toxic heavy metals such as Cr, Pb, Ni, Hg and Cd because industrial wastewater is mixed with sewage (Mañas and de las Heras, 2021; Muter et al., 2022). Hence, the selection of an appropriate waste treatment method plays a crucial role in mitigating the environmental impact associated with sewage sludge application. Various methods, including anaerobic digestion, pyrolysis, and supercritical water oxidation, have been identified as effective approaches for reducing the environmental risks associated with SS (Teoh and Li, 2020). Anaerobic digestion, for instance, allows for the conversion of organic matter in SS into biogas, cost effective, minimizing greenhouse gas emissions and reducing the potential for global warming (Rorat et al., 2019; Teoh and Li, 2020). Additionally, composting or co-composting with other biodegradable wastes and additives is an important treatment method for SS, enabling a significant reduction in volume and minimal emissions of hazardous substances, making it environmentally acceptable when compared to incineration (Sugurbekova et al., 2023). It has been also observed that applying sewage sludge at lower doses presents minimal risks to the environment, while simultaneously enhancing the grain yield and quality of crops. Hence, carefully determining the appropriate dosage, the potential negative impacts associated with SS application can be mitigated, ensuring that the benefits outweigh the risks.

Although further research is needed to fully understand the long-term effects of nanoparticles, NPs based crop fertilization possess distinct characteristics in comparison to conventional fertilizers (Lina et al., 2023). These unique attributes contribute to a gradual and sustainable absorption of nutrients by crops, primarily because of their high surface-to-volume ratio and reduced nutrient loss (Tarafder et al., 2020). In compression, the conventional fertilizer applications, such as nitrogenous, phosphates, and potassium-based have been found to have low efficiency rates, with nitrogenous fertilizers ranging from 20 to 50%, phosphates ranging from 10 to 25%, and potassium ranging from 35 to 40% (Avila-Quezada et al., 2022). This inefficiency can lead to a significant volume of fertilizers being applied in agricultural practices. However, nanofertilizers offer active sites that facilitate a greater number of biological activities, thereby enhancing the efficiency of nutrient absorption by plants (Feregrino-Pérez et al., 2018). Moreover, NPs also contribute to the improvement of soil fertility and create a favourable environment for the growth of beneficial microorganisms within the soil (Thavaseelan and Priyadarshana, 2021). As a result, nanofertilizers provide sustainable solutions to address issues of environmental pollution and climate change (Solanki et al., 2015). Additionally, the use of NFs presents economic benefits by minimizing the leaching and volatilization of conventional fertilizers. Leaching and volatilization contribute to nutrient loss and environmental pollution, thus reducing these processes could offer a cleaner technology for the environment and provide an attractive proposition for agricultural producers (Avila-Quezada et al., 2022). However, if nanoparticles

are not properly managed NFs could adversely affect plants through multiple mechanisms. These include DNA damage, the formation of reactive oxygen species (ROS), interaction with nuclear proteins, chromosomal abnormalities, a decrease in DNA repair mechanisms, and the occurrence of genetic defects. For instance, studies have shown that NiO NPs can penetrate the DNA of plants, causing irreversible damage to their cells (Faisal et al., 2013; Verma et al., 2022b). Similarly, when Co_3O_4 NPs were applied to crops, it resulted in apoptosis (cell death) in their cells (Faisal et al., 2016). Furthermore, the use of ZnO NPs has been found to have detrimental effects on the membrane integrity, chromosomal structure, and DNA strand stability in various plant species (Faisal et al., 2016; Bhardwaj et al., 2022). Despite the remarkable efficiency and ease of application, nanofertilizers are accompanied by certain limitations, including complicated production processes, fragile transport, and dosage-sensitive efficiency, which are currently impeding the widespread adoption of nanofertilizers in agriculture (Kalwani et al., 2022). Nevertheless, concerning economic feasibility, nanoparticles have the potential to be economically viable and less environmentally toxic compared to some other alternatives (Upadhayay et al., 2023).

While nutrient based climates change interventions offer potential benefits, nutrients could also carry certain environmental risks that needs to be managed. Application of nutrients, such as silicon, and zinc-based fertilizers are an essential for plants, and silicon-based fertilizers have been developed to enhance plant growth, increase resistance to pests and diseases, and improve abiotic stress tolerance. Silicon inhibits the toxicity caused by heavy metals, protecting plants from their detrimental effects and plays a crucial role in activating soil phosphorus (P), making it more readily available for plants (Imran et al., 2021). This activation process enhances the absorption of P by plant roots, along with other essential nutrients. The positive influence of Si in enhancing crop yield, improving crop resilience, and addressing the challenges of sustainable agriculture and food provision, emphasizing the need for its wider adoption in modern agriculture (Barão, 2023). However, it is important to consider the potential for silicon accumulation in soil, which may affect soil properties and nutrient availability. The application of zinc containing fertilizers in crops has been found to yield several beneficial effects. These advantages include enhanced zinc grain accumulation and protection against cadmium (Cd) uptake and transfer through the roots and xylem-to-phloem pathways (Hassan et al., 2022a). While zinc is an essential micronutrient for plants and offers numerous benefits when applied in appropriate doses, excessive levels can negatively impact foliage and crop yields (Xu et al., 2021). Additionally, improper application can result in zinc leaching into water bodies, causing water pollution (Singh et al., 2022). Hence, proper dosage and application practices, along with regular soil testing, are necessary to prevent the adverse effects associated with zinc-infused fertilizers. In recent years, unmanned aerial vehicle-based spraying (UAV-based spraying) has emerged as a safer, cleaner, and more efficient method for the targeted application of zinc-containing fertilizers. This technology reduces zinc input, increases the recovery rate, and minimizes the risk of fertilizer residue (Xu et al., 2021). This technology expands the options for fertilizing crops and facilitates the production of highly Zn-biofortified grain while optimizing input costs for farmers.

6 Conclusions

The changing climate poses a significant threat to crops, including durum wheat, and sustainable adaptation strategies are necessary to maintain food and nutritional security. This comprehensive review article provides a comprehensive overview of the current understanding of nutrient management in durum wheat cultivation under changing climatic conditions. Identifying knowledge gaps and exploring advanced strategies, contribute to the existing literature and provide valuable insights for researchers, agronomists, and farmers alike. It is crucial for future research to focus on investigating the specific nutrient requirements of durum wheat under different climate scenarios and evaluating the effectiveness of innovative nutrient management practices to ensure sustainable and resilient wheat production. Implementing precision farming techniques, optimizing fertilizer application rates and timing, and utilizing precision nutrient delivery systems are potential strategies to maximize farm profitability, efficiency and mitigate the adverse effects of climate variability on durum wheat production. However, the coexistence effect of climatic parameters on nutrient uptake, translocation, grain quality, yield and assimilation mechanisms within durum wheat crops remains poorly understood. Therefore, future research should focus on unraveling these intricacies to develop targeted nutrient management strategies for maximizing grain quality and yield. As the traditional nutrient management practices are also insufficient in addressing the complex challenges posed by climate change, there is a need for advanced nutrient management strategies to mitigate the negative impacts of the changing climate conditions on durum wheat. Hence, adopting innovative approaches such as precision agriculture, controlled-release fertilizers, and site-specific nutrient management can optimize nutrient availability, uptake efficiency, and utilization by durum wheat plants. A continuous research, technological advancements, and farmer education are key to successfully addressing these challenges and realizing the benefits of nutrient management in durum wheat production.

Author contributions

All authors listed have made a substantial, direct, and intellectual contribution to the work, and approved it for publication. All authors contributed to the article and approved the submitted version.

Funding

This work was supported by the Tempus Public Foundation (Hungary) within the framework of the Stipendium Hungaricum Scholarship Programme, supported by the Ministry of Science and Higher Education (MoSHE https://www.moshe.gov.et/) of Ethiopia and Debark University (https://dku.edu.et/).

Acknowledgments

The authors would like to thank their respective institutions for their support. We would also like to thank the library at University of Debrecen, Hungary, for providing the valuable online resources and comprehensive databases.

Conflict of interest

The authors declare that the research was conducted in the absence of any commercial or financial relationships that could be construed as a potential conflict of interest.

Publisher's note

All claims expressed in this article are solely those of the authors and do not necessarily represent those of their affiliated organizations, or those of the publisher, the editors and the reviewers. Any product that may be evaluated in this article, or claim that may be made by its manufacturer, is not guaranteed or endorsed by the publisher.

References

Abid, M., Tian, Z., Ata-Ul-Karim, S. T., Cui, Y., Liu, Y., Zahoor, R., et al. (2016). Nitrogen Nutrition Improves the Potential of Wheat *(Triticum aestivum L.)* to Alleviate the Effects of Drought Stress during Vegetative Growth Periods. *Front. Plant Sci.* 7. doi: 10.3389/fpls.2016.00981

Achkir, A., Aouragh, A., El Malfmqhi, M., Labjar, N., Bouch, M. E., Ouahidi, M. L., et al. (2023). Implication of sewage sludge increased application rates on soil fertility and heavy metals contamination risk. *Emerg. Contam.* 9 (1), 100200. doi: 10.1016/j.emcon.2022.100200

Ahsan, J., Nadeem, A., Javed, A., Amir, H., Muhammad, A., Ashraf, S. A., et al. (2022). Grain yield, chlorophyll and protein contents of elite wheat genotypes under drought stress. *J. King Saud Univ. Sci.* 34(7), 102279. doi: 10.1016/j.jksus

Ainsworth, E. A., and Long, S. P. (2005). What have we learned from fifteen years of Free Air Carbon Dioxide Enrichment (FACE)? A meta-analytic review of the responses of photosynthesis, canopy properties and plant production to rising CO_2. *New Phytol.* 165, 351–372. doi: 10.1111/j.1469-8137.2004.01224.x

Ali, S., Rizwan, M., Hussain, A., urRehman, M. Z., Ali, B., Yousaf, B., et al. (2019). Silicon nanoparticles enhanced the growth and reduced the cadmium accumulation in grains of wheat (Triticumaestivum L.). *Plant Physiol. Biochem.* 140, 1–8. doi: 10.1016/j.plaphy.2019.04.041

Ali, A. H., Said, E. M., and Abdelgawad, Z. A. (2022). The role of seaweed extract on improvement drought tolerance of wheat revealed by osmoprotectants and DNA (cpDNA) markers. *Braz. J. Bot.* 45, 857–867. doi: 10.1007/s40415-022-00820-5

Andrej, C., Andrea, T., Matteo, Z., and Conxita, R. (2021). Global loss of climatically suitable areas for durum wheat growth in the future. *Environ. Res. Lett.* 16(10), 104049. doi: 10.1088/1748-9326/ac2d68

Ankush, P. R., Singh, V., Diwedi, A., Popat, R. C., Kumari, S., Kumar, N., et al. (2021). Sewage sludge impacts on yields, nutrients and heavy metals contents in pearl millet–wheat system grown under saline environment. *Int. J. @ Plant Prod.* 15, 93–105. doi: 10.1007/s42106-020-00122-4

Arguello, M. N., Mason, R. E., Roberts, T. L., Subramanian, N., Acuna, A., Addison, C. K., et al. (2016). Performance of soft red winter wheat subjected to field soil waterlogging: grain yield and yield components. *Field Crops Res.* 194, 57–64. doi: 10.1016/j.fcr.2016.04.040

Arun, M. N., Kumar, R. M., Nori, S., Sreedevi, B., Padmavathi, G., Revathi, P., et al. (2023). Biostimulant properties of marine bioactive extracts in plants: incrimination toward sustainable crop production in rice. *Intechopen.*. doi: 10.5772/intechopen.108640

Ashkavand, P., Tabari, M., Zarafshar, M., Tomášková, I., and Struve, D. (2015). Effect of SiO_2 nanoparticles on drought resistance in hawthorn seedlings. *For. Res. Pap.* 76, 350–359. doi: 10.1515/frp-2015-0034

Ashwani, P., Dhankher, O. P., and Christine, H. F. (2020). Mitigating the impact of climate change on plant productivity and ecosystem sustainability. *J. Experm. Bota.* 71 (2, 451–456. doi: 10.1093/jxb/erz518

Asseng, S., Martre, P., Maiorano, A., Rötter, R. P., O'Leary, G. J., Fitzgerald, G. J., et al. (2019). Climate change impact and adaptation for wheat protein. *Glob Change Biol.* 25, 155–173. doi: 10.1111/gcb.14481

Avila-Quezada, G., Ingle, A., Golińska, P., and Rai, M. (2022). Strategic applications of nano-fertilizers for sustainable agriculture: Benefits and bottlenecks. *Nanotechnology Rev.* 11, 1,2123–1,2140. doi: 10.1515/ntrev-2022-0126

Bagci, S. A., Ekiz, H., Yilmaz, A., and Cakmak, I. (2007). Effects of zinc deficiency and drought on grain yield of field-grown wheat cultivars in central anatolia. *J. Agron. Crop Sci.* 193, 198–206. doi: 10.1111/j.1439-037X.2007.00256.x

Barão, L. (2023). The use of si-based fertilization to improve agricultural performance. *J. Soil Sci. Plant Nutr.* 23, 1096–1108. doi: 10.1007/s42729-022-01106-1

Barnabas, B., Jager, K., and Feher, A. (2008). The effect of drought and heat stress on reproductive processes in cereals. *Plant Cell Environ.* 31, 11–38. doi: 10.1111/j.1365-3040.2007.01727.x

Begcy, K., and Walia, H. (2015). Drought stress delays endosperm development and mis regulates genes associated with cytoskeleton organization and grain quality proteins in developing wheat seeds. *Plant Sci.* 240, 109–119. doi: 10.1016/j.plantsci.2015.08.024

Ben, M. S., Soba, D., Zhou, B., Loladze, I., Morales, F., and Aranjuelo, I. (2021). Climate change, crop yields, and grain quality of C_3 cereals: A meta-analysis of $[CO_2]$, temperature, and drought effects. *Plants* 10, 1052. doi: 10.3390/plants10061052

Bento, M., Pereira, S. G., Viegas, W., and Silva, M. (2017). Durum wheat diversity for heat stress tolerance during inflorescence emergence is correlated to TdHSP101C expression in early developmental stages. *PloS One* 12, 12. doi: 10.1371/journal.pone.0190085

Beres, B. L., Rahmani, E., Clarke, J. M., Grassini, P., Pozniak, C. J., Geddes, C. M., et al. (2020). A systematic review of durum wheat: enhancing production systems by exploring genotype, environment, and management (G × E × M) synergies. *Front. Plant Sci.* 11. doi: 10.3389/fpls.2020.568657

Bhardwaj, A. K., Arya, G., Kumar, R., Hamed, L., Pirasteh-Anosheh, H., Jasrotia, P., et al. (2022). Switching to nanonutrients for sustaining agroecosystems and environment: The challenges and benefits in moving up from ionic to particle feeding. *J. Nanobiotechnology.* 20, 19. doi: 10.1186/s12951-021-01177-9

Bin, X. F., Kun, W., Brigitte, D., Dale, T., and Shin, N. (2017). Kernel vitreousness and protein content: Relationship, interaction and synergistic effects on durum wheat quality. *J. Cere. Sci.* 78, 2–9. doi: 10.1016/j.jcs.2017.07.005

Bindu, Y., Abhimanyu, J., Md Samiur, R., and Om Prakash, N. (2021). Secondary metabolites in the drought stress tolerance of crop plants: A review. *Gene Rep.* 23, 101040. doi: 10.1016/j.genrep.2021.101040

Boudjabi, S., Kribaa, M., and Chenchouni, H. (2015). Growth, physiology and yield of durum wheat *(Triticum durum)* treated with sewage sludge under water stress conditions. *Excli J.* 14, 320–334. doi: 10.17179/excli2014-715

Chang, Z., and Liu, Y. (2016). Effects of cytokinin and nitrogen on drought tolerance of creeping bentgrass. *PloS One* 11, e0154005. doi: 10.1371/journal.pone.0154005

Chao, H., Weiqiang, Z., Hui, W., Yang, G., Shoutian, M., Anzhen, Q., et al. (2022). Effects of waterlogging at different stages on growth and ear quality of waxy maize. *Agric. Water Manage.* 266, 107603. doi: 10.1016/j.agwat.2022.107603

Chen, D., Zhou, W., Yang, J., Ao, J., Huang, Y., Shen, D., et al. (2021). Effects of seaweed extracts on the growth, physiological activity, cane yield and sucrose content of sugarcane in China. *Front. Plant Sci.* 12. doi: 10.3389/fpls.2021.659130

Chen, W., Yao, X., Cai, K., and Chen, J.. (2011). Silicon alleviates drought stress of rice plants by improving plant water status, photosynthesis and mineral nutrient absorption. *Biol. Trace Elem. Res.* 142, 67–76. doi: 10.1007/s12011-010-8742-x

Colla, G., Hoagland, L., Ruzzi, M., Cardarelli, M., Bonini, P., Canaguier, R., et al. (2017). Bio stimulant action of protein hydrolysates: unraveling their effects on plant physiology and microbiome. *Front. Plant Sci.* 8. doi: 10.3389/fpls.2017.02202

Coskun, D., Britto, D. T., Huynh, W. Q., and Kronzucker, H. J. (2016). The role of silicon in higher plants under salinity and drought stress. *Front. Plant Sci.* 7. doi: 10.3389/fpls.2016.01072

Cotrozzi, L., Lorenzini, G., Nali, C., Pisuttu, C., Pampana, S., and Pellegrini, E. (2021). Transient waterlogging events impair shoot and root physiology and reduce grain yield of durum wheat cultivars. *Plants* 10, 2357. doi: 10.3390/plants10112357

Dapkekar, A., Deshpande, P., Oak, M. D., Paknikar, K. M., and Rajwade, J. M. (2018). Zinc use efficiency is enhanced in wheat through nano fertilization. *Sci. Rep.* 8 (1), 6832. doi: 10.1038/s41598-018-25247-5

Debiase, G., Montemurro, F., Fiore, A., Rotolo, C., Farrag, K., Miccolis, A., et al. (2016). Organic amendment and minimum tillage in winter wheat grown in Mediterranean conditions: Effects on yield performance, soil fertility and environmental impact. *Euro. J. Agron.* 75, 149–157. doi: 10.1016/j.eja.2015.12.009

Deolu-Ajayi, A. O., Meer, I. M., Werf, A., and Karlova, R. (2022). The power of seaweeds as plant biostimulants to boost crop production under abiotic stress. *Plant Cell Environ.* 45, 2537–2553. doi: 10.1111/pce.14391

De Santis, M. A., Soccio, M., Laus, M. N., and Flagella, Z. (2021). Influence of drought and salt stress on durum wheat grain quality and composition: A review. *Plants* 10, 2599. doi: 10.3390/plants10122599

De Storme, N., and Geelen, D. (2014). The impact of environmental stress on male reproductive development in plants: biological processes and molecular mechanisms. *Plant Cell Environ.* 37(1), 1–18. doi: 10.1111/pce.12142

Ding, J., Liang, P., Wu, P., Zhu, M., Li, C., Zhu, X., et al. (2020). Effects of waterlogging on grain yield and associated traits of historic wheat cultivars in the middle and lower reaches of the Yangtze River, China. *Field Crops Res.* 246, 107695. doi: 10.1016/j.fcr.2019.107695

Duggan, B., Richards, R., Van Herwaarden, A., and Fettell, N. (2005). Agronomic evaluation of a tiller inhibition gene (tin) in wheat. I. Effect on yield, yield components, and grain protein. *Aust. J. Agric. Res.* 56, 169–178. doi: 10.1071/AR04152

Dwivedi, S. L., Van Bueren, E. T. L., Ceccarelli, S., Grando, S., Upadhyaya, H. D., and Ortiz, R. (2017). Diversifying food systems in the pursuit of sustainable food production and healthy diets. *Trends Plant Sci.* 22 (10), 842–856. doi: 10.1016/j.tplants.2017.06.011

Eid, E. M., Alrumman, S. A., El-Bebany, A. F., Fawy, K. F., Taher, M. A., Hesham, A. E. L., et al. (2019). Evaluation of the potential of sewage sludge as a valuable fertilizer for wheat *(Triticum aestivum L.)* crops. *Environ. Sci. pollut. Res.* 26, 392–401. doi: 10.1007/s11356-018-3617-3

El-Saadony, M. T., Saad, A. M., Soliman, S. M., Salem, H. M., Desoky, E. S. M., Babalghith, A. O., et al. (2022). Role of nanoparticles in enhancing crop tolerance to abiotic stress: A comprehensive review. *Front. Plant Sci.* 13. doi: 10.3389/fpls.2022.946717

Erda, L., Xiong, W., Ju, H., Xu, Y., Li, Y., Bai, L., et al. (2005). Climate change impacts on crop yield and quality with CO_2 fertilization in China. Phil. *Trans. R. Soc B.* 360, 2149–2154. doi: 10.1098/rstb.2005.1743

Faisal, M., Saquib, Q., Alatar, A. A., Al-Khedhairy, A. A., Ahmed, M., Ansari, S. M., et al. (2016). Cobalt oxide nanoparticles aggravate DNA damage and cell death in eggplant via mitochondrial swelling and NO signaling pathway. *Biol. Res.* 49, 1–13. doi: 10.1186/s40659-016-0080-9

Faisal, M., Saquib, Q., Alatar, A. A., Al-Khedhairy, A. A., Hegazy, A. K., and Musarrat, J. (2013). Phytotoxic hazards of NiO-nanoparticles in tomato: A study on mechanism of cell death. *J. Hazard. Mater.* 250, 318–332. doi: 10.1016/j.jhazmat.2013.01.063

Feregrino-Pérez, A. A., Magaña-López, E., Guzmán, C., and Esquivel, K. (2018). A general overview of the benefits and possible negative effects of the nanotechnology in horticulture. *Sci. Hortic.* 238, 126–137. doi: 10.1016/j.scienta.2018.03.060

Feszterová, M., Porubcová, L., and Tirpáková, A. (2021). The monitoring of selected heavy metals content and bioavailability in the soil-plant system and its impact on sustainability in agribusiness food chains. *Sustainability* 13, 7021. doi: 10.3390/su13137021

Fitzgerald, G. J., Tausz, M., O'Leary, G., Mollah, M. R., Tausz-Posch, S., Seneweera, S., et al. (2016). Elevated atmospheric $[CO_2]$ can dramatically increase wheat yields in semi-arid environments and buffer against heat waves. *Glob. Chang Biol.* 22(6), 2269–2284. doi: 10.1111/gcb.13263

Flagella, Z., Giuliani, M. M., Giuzio, L., Volpi, C., and Masci, S. (2010). Influence of water deficit on durum wheat storage protein composition and technological quality. *Eur. J. Agron.* 33, 197–207. doi: 10.1016/j.eja.2010.05.006

Fleck, A. T., Nye, T., Repenning, C., Stahl, F., Zahn, M., and Schenk, M. K. (2011). Silicon enhances suberization and lignification in roots of rice (Oryza sativa). *J. Exper. Bota.* 62(6), 2001–2011. doi: 10.1093/jxb/erq392

Fytili, D., and Zabaniotou, A. (2008). Utilization of sewage sludge in EU application of old and new methods—A review. *Renew. Sustain. Energy Rev.* 12, 116–140. doi: 10.1016/j.rser.2006.05.014

Galani, Y. J., Hansen, E. M., Droutsas, I., Holmes, M., Andrew, J. C., Teis, N. M., et al. (2022). Effects of combined abiotic stresses on nutrient content of European wheat and implications for nutritional security under climate change. *Sci. Rep.* 12, 5700. doi: 10.1038/s41598-022-09538-6

Ganesan, S., Vadivel, K., and Jayaraman, J. (2015). Sustainable crop disease management using natural products. *CABI.* doi: 10.1079/9781780643236.0160

Ge, T. D., Sui, F. G., Nie, S., Sun, N. B., Xiao, H., and Tong, C. L. (2010). Differential responses of yield and selected nutritional compositions to drought stress in summer maize grains. *J. Plant Nutt.* 33, 1811–1818. doi: 10.1080/01904167.2010.503829

Gebrewahid, L., Mengistu, D. K., Tsehaye, Y., Aberha, A., and Aberra, D. A. (2021). Variability among Ethiopian durum wheat genotypes grown under different climatic conditions of Tigray for some agronomic and grain-quality traits. *J. Crop Improv.* 35(2), 184–203. doi: 10.1080/15427528.2020.1806979

Ghani, M. I., Saleem, S., Rather, S. A., Rehmani, M. S., Alamri, S., Rajput, V. D., et al. (2022). Foliar application of zinc oxide nanoparticles: An effective strategy to mitigate drought stress in cucumber seedling by modulating antioxidant defense system and osmolytes accumulation. *Chemosphere* 289, 133202. doi: 10.1016/j.chemosphere.2021.133202

Ghazi, N. A. (2012). Phenological development-yield relationships in durum wheat cultivars under late-season high-temperature stress in a semiarid environment. *Int. Sch. Res. Notices.* 7, 456856. doi: 10.5402/2012/456856

Goñi, O., Quille, P., and O'Connell, S. (2018). Ascophyllum nodosumextract biostimulants and their role in enhancing tolerance to drought stress in tomato plants. *Plant Physiol. Biochem.* 126, 63–73. doi: 10.1016/j.plaphy.2018.02

Gunes, A., Pilbeam, D. J., Inal, A., Bagci, E. G., and Coban, S. (2007). Influence of silicon on antioxidant mechanisms and lipid peroxidation in chickpea (*Cicer arietinum* L.) cultivars under drought stress. *J. Plant Interact.* 2, 105–113. doi: 10.1080/17429140701529399

Haddad, L., Hawkes, C., Webb, P., Thomas, S., Beddington, J., Waage, J., et al. (2016). A new global research agenda for food. *Nat.* 540, 30–32. doi: 10.1038/540030a

Haddad, C., Trouverie, J., Arkoun, M., Yvin, J.-C., Caïus, J., Brunaud, V., et al. (2019). Silicon supply affects the root transcriptome of *Brassica napus* L. *Planta* 249, 1645–1651. doi: 10.1007/s00425-019-03120-7

Hameed, A., Sheikh, M. A., Jamil, A., and Basra, S. M. (2013). Seed priming with sodium silicate enhances seed germination and seedling growth in wheat *(Triticum aestivum L.)* under water deficit stress induced by polyethylene glycol. *Pak. J. Life Soc Sci.* 11, 19–24.

Hamouda, M. M., Saad-Allah, K. M., and Gad, D. (2022). Potential of seaweed extract on growth, physiological, cytological and biochemical parameters of wheat *(Triticum aestivum L.)* seedlings. *J. Soil Sci. Plant Nutr.* 22(2, 1818–1831. doi: 10.1007/s42729-022-00774-3

Hasan, K., and Tacettin, Y. (2010). The Effect of Drought Stress on Grain Yield, Yield Components and some Quality Traits of Durum Wheat *(Triticum turgidum ssp. durum)* Cultivars. *Not. Bot. Hortic. Agrobot. Cluj.* 38(1, 164–170. doi: 10.15835/nbha3814274

Hasanuzzaman, M., Bhuyan, M. B., Zulfiqar, F., Raza, A., Mohsin, S. M., Mahmud, J. A., et al. (2020). Reactive oxygen species and antioxidant defense in plants under abiotic stress: Revisiting the crucial role of a universal defense regulator. *Antioxidants* 9(8, 681. doi: 10.3390/antiox9080681

Hassan, M. U., Aamer, M., Mahmood, A., Awan, M. I., Barbanti, L., Seleiman, M. F., et al. (2022a). Management strategies to mitigate N_2O emissions in agriculture. *Life* 12, 439. doi: 10.3390/life12030439

Hassan, M. U., Nawaz, M., Mahmood, A., Shah, A. A., Shah, A. N., Muhammad, F., et al. (2022b). The role of zinc to mitigate heavy metals toxicity in crops. *Front. Environ. Sci.* 1712. doi: 10.3389/fenvs.2022.990223

Healy, M. G., Fenton, O., Forrestal, P. J., Danaher, M., Brennan, R. B., and Morrison, L. (2016). Metal concentrations in lime stabilised, thermally dried and anaerobically digested sewage sludges. *J. Waste Manage.* 48, 404–408. doi: 10.1016/j.wasman.2015.11.028

Hechmi, S., Hamdi, H., Mokni-Tlili, S., Zoghlami, I. R., Khelil, M. N., Benzarti, S., et al. (2020). Carbon mineralization, biological indicators, and phytotoxicity to assess the impact of urban sewage sludge on two light-textured soils in a microcosm. *J. Environ. Qual.* 49(2, 460–471. doi: 10.1002/jeq2.20011

Helman, D., and Bonfil, D. J. (2022). Six decades of warming and drought in the world's top wheat-producing countries offset the benefits of rising CO_2 to yield. *Sci. Rep.* 12, 7921. doi: 10.1038/s41598-022-11423-1

Herzog, M., Striker, G. G., Colmer, T. D., and Pedersen, O. (2016). Mechanisms of waterlogging tolerance in wheat – a review of root and shoot physiology. *Plant Cell Environ.* 39, 1068–1086. doi: 10.1111/pce.12676

Hossain, A., Skalicky, M., Brestic, M., Maitra, S., Ashraful Alam, M., Syed, M. S., et al. (2021). Consequences and mitigation strategies of abiotic stresses in wheat *(Triticum aestivum L.)* under the changing climate. *Agronomy* 11, 241. doi: 10.3390/agronomy11020241

Hussain, A., Rizwan, M., Ali, Q., and Ali, S. (2019). Seed priming with silicon nanoparticles improved the biomass and yield while reduced the oxidative stress and cadmium concentration in wheat grains. *Environ. Sci. pollut. Res.* 26, 7579–7588. doi: 10.1007/s11356-019-04210-5

Imran, K., Samrah, A. A., Muhammad, R., Shafaqat, A., Muhammad, J. H., Marian, B., et al. (2021). Effects of silicon on heavy metal uptake at the soil-plant interphase: A review. *Ecotoxicol. Environ. Saf.* 222, 112510. doi: 10.1016/j.ecoenv.2021.112510

Inmaculada, P. M., Carmen, A., Carlos, G., Alfredo, P., and Manuel, S. D. (2007). Effect of water deficit on microbial characteristics in soil amended with sewage sludge or inorganic fertilizer under laboratory conditions. *Bioresource Techno.* 98(1, 29–37. doi: 10.1016/j.biortech.2005.11.026

Irfan, M., Maqsood, M. A., Mahboob, W., Sarwar, N., Hafeez, O. B. A., Hussain, S., et al. (2023). Silicon nutrition in plants under water-deficit conditions: overview and prospects. *Water* 15, 739. doi: 10.3390/w15040739

Jaberzadeh, A., Moaveni, P., Tohidi Moghadam, H. R., and Zahedi, H. (2013). Influence of bulk and nanoparticles titanium foliar application on some agronomic traits, seed gluten and starch contents of wheat subjected to water deficit stress. *Not. Bot. Horti. Agrobot.* 41, 201–207. doi: 10.15835/nbha4119093

Jäger, K., Fábián, A., and Barnabás, B. (2008). Effect of water deficit and elevated temperature on pollen development of drought sensitive and tolerant winter wheat *(Triticum aestivum L.)* genotypes. *Acta Biol. Szegediensis.* 52, 1, 67–71.

Jamshidi, G. K., Moosavi, S. S., Amirmahani, F., Fatemeh, S., and Maryam, N. (2020). Assessment of changes in growth traits, oxidative stress parameters, and enzymatic and non-enzymatic antioxidant defense mechanisms in Lepidium draba plant under osmotic stress induced by polyethylene glycol. *Protoplasma* 257, 459–473. doi: 10.1007/s00709-019-01457-0

Jannin, L., Arkoun, M., Etienne, P., Laîné, P., Goux, D., Garnica, M., et al. (2013). Brassica napus growth is promoted by ascophyllum nodosum (L.) Le Jol. seaweed extract: microarray analysis and physiological characterization of N, C, and S metabolisms. *J. Plant Growth Regul.* 32, 31–52. doi: 10.1007/s00344-012-9273-9

Ji, X., ShIran, B., Wan, J., Lewis, D. C., Jenkins, C. L., Condon, A. G., et al. (2010). Importance of pre-anthesis anther sink strength for maintenance of grain number during reproductive stage water stress in wheat. *Plant Cell Environ.* 33, 926–942. doi: 10.1111/j.1365-3040.2010.02130.x

Kalwani, M., Chakdar, H., Srivastava, A., Pabbi, S., and Shukla, P. (2022). Effects of nanofertilizers on soil and plant-associated microbial communities: Emerging trends and perspectives. *Chemosphere* 287, 132107. doi: 10.1016/j.chemosphere.2021.132107

Karim, M. R., Zhang, Y. Q., Zhao, R. R., Chen, X. P., Zhang, F. S., and Zou, C. Q. (2012). Alleviation of drought stress in winter wheat by late foliar application of zinc, boron, and manganese. J. *Plant Nutr. Soil Sci.* 175, 142–151. doi: 10.1002/jpln.201100141

Katz, O. (2014). Beyond grasses: the potential benefits of studying silicon accumulation in non-grass species. *Front. Plant Sci.* 5. doi: 10.3389/fpls.2014.00376

Kaur, G., Nelson, K. A., Motavalli, P. P., and Singh, G. (2020a). Adaptation to early-season soil waterlogging using different nitrogen fertilizer practices and corn hybrids. *Agronomy* 10, 378. doi: 10.3390/agronomy10030378

Kaur, G., Singh, G., Motavalli, P. P., Nelson, K. A., Orlowski, J. M., and Golden, B. R. (2020b). Impacts and management strategies for crop production in waterlogged or flooded soils: A review. *J. Agron.* 112(3, 1475–1501. doi: 10.1002/agj2.20093

Khan, Z. S., Rizwan, M., Hafeez, M., Ali, S., Javed, M. R., and Adrees, M. (2019). The accumulation of cadmium in wheat *(Triticum aestivum)* as influenced by zinc oxide nanoparticles and soil moisture conditions. *Environ. Sci. pollut. Res.* 26, 19859–19870. doi: 10.1007/s11356-019-05333-5

Kizilgeci, F., Yildirim, M., Islam, M. S., Ratnasekera, D., Iqbal, M. A., and Sabagh, A. E. (2021). NorMalized difference vegetation index and chlorophyll content for precision nitrogen management in durum wheat cultivars under semi-arid conditions. *Sustainability* 13, 3725. doi: 10.3390/su13073725

Koga, S., Böcker, U., Moldestad, A., Tosi, P., Shewry, P. R., Mosleth, E. F., et al. (2016). Influence of temperature during grain filling on gluten viscoelastic properties and gluten protein composition. *J. Sci. Food Agric.* 96, 122–130. doi: 10.1002/jsfa.7068

Kumar, A., Dillip, K. S., Shiladitya, D., Ajay, S., Jayanarayanan, K., Girish, C. K., et al. (2022a). Nutrient management may reduce global warming potential of rice cultivation in subtropical India. *Curr. Opin. Environ. Sustain.* 4, 100169. doi: 10.1016/j.crsust.2022.100169

Kumar, M., Reddy, C. R. K., and Jha, B. (2013). The ameliorating effect of Acadian marine plant extract against ionic liquids-induced oxidative stress and DNA damage in marine macroalga *Ulva lactuca*. *J. Appl. Phycol.* 25, 369–378. doi: 10.1007/s10811-012-9871-8

Kumar, A., Singh, K., Verma, P., Singh, O., Panwar, A., Singh, T., et al. (2022b). Effect of nitrogen and zinc nano fertilizer with the organic farming practices on cereal and oil seed crops. *Sci. Rep.* 12, 6938. doi: 10.1038/s41598-022-10843-3

Kumari, V. V., Banerjee, P., Verma, V. C., Sukumaran, S., Chandran, M. A. S., Gopinath, K. A., et al. (2022). Plant nutrition: an effective way to alleviate abiotic stress in agricultural crops. *Int. J. Mol. Sci.* 23, 8519. doi: 10.3390/ijms23158519

Kuroha, T., Nagai, K., Gamuyao, R., Wang, D. R., Furuta, T., Nakamori, M., et al. (2018). Ethylene-gibberellin signaling underlies adaptation of rice to periodic flooding. *Science* 361, 181–186. doi: 10.1126/science.aat1577

Kutasy, E., Diósi, G., Buday-Bódi, E., Nagy, P. T., Melash, A. A., Forgács, F. Z., et al. (2023). Changes in Plant and Grain Quality of Winter Oat *(Avena sativa L.)* Varieties in Response to Silicon and Sulphur Foliar Fertilisation under Abiotic Stress Conditions. *Plants* 12, 969. doi: 10.3390/plants12040969

Li, S., Lili, Z., Shalom, D. A., Guochang, D., Min, S., Sipan, W., et al. (2020). Nitrogen supply enhances the physiological resistance of Chinese fir plantlets under polyethylene glycol (PEG)-induced drought stress. *Sci. Rep.* 10, 7509. doi: 10.1038/s41598-020-64161-7

Lina, M. A., Salim, F. B., and Mahroos, B. (2023). Perspective chapter: application of nanotechnology solutions in plants fertilization and environmental remediation. *IntechOpen*. doi: 10.5772/intechopen.1001441

Liu, B., Asseng, S., Müller, C., Ewert, F., and Elliott, J. (2016). Similar estimates of temperature impacts on global wheat yield by three independent methods. *Nat. Clim. Change*. doi: 10.1038/nclimate3115

Loladze, I. (2002). Rising atmospheric CO_2 and human nutrition: Toward globally imbalanced plant stoichiometry? *Trends Ecol. Evol.* 17, 457–461. doi: 10.1016/S0169-5347(02)02587-9

Ma, D., Sun, D., Wang, C., Ding, H., Qin, H., Hou, J., et al. (2017). Physiological responses and yield of wheat plants in zinc-mediated alleviation of drought stress. *Front. Plant Sci.* 8. doi: 10.3389/fpls.2017.00860

Mañas, P., and de las Heras, J. (2021). Sewage sludge to fertilise durum wheat: effects on crop and soil. Humic substance. *IntechOpen*. doi: 10.5772/intechopen.95896

Manik, S. N., Pengilley, G., Dean, G., Field, B., Shabala, S., and Zhou, M. (2019). Soil and crop management practices to minimize the impact of waterlogging on crop productivity. *Front. Plant Sci.* 10. doi: 10.3389/fpls.2019.00140

Marin, E., and Rusănescu, C. O. (2023). Agricultural use of urban sewage sludge from the wastewater station in the municipality of alexandria in rOmania. *Water* 15, 458. doi: 10.3390/w15030458

Marti, J., Savin, R., and Slafer, G. A. (2015). Wheat yield as affected by length of exposure to waterlogging during stem elongation. *J. Agro. Crop Sci.* 201, 473–486. doi: 10.1111/jac.12118

Mazen, A., Faheed, F. A., and Ahmed, A. F. (2010). Study of potential impacts of using sewage sludge in the amendment of desert reclaimed soil on wheat and jews mallow plants. *Braz. Arch. Biol. Technol.* 53, 917–930. doi: 10.1590/S1516-89132010000400022

Melash, A. A., and Ábrahám, É.B. (2022). Barriers and levers to enhance end-use functional properties of durum wheat *(Triticum turgidum L.)* grain: An agronomic implication. *Heliyon* 8 (5), e09542. doi: 10.1016/j.heliyon.2022.e09542

Melash, A. A., Dejene, K. M., Dereje, A. A., and Alemtsehay, T. (2019). The influence of seeding rate and micronutrients foliar application on grain yield and quality traits and micronutrients of durum wheat. *J. Cereal Sci.* 85, 221–227. doi: 10.1016/j.jcs.2018.08.005

Merewitz, E. B., Gianfagna, T., and Huang, B. (2011). Protein accumulation in leaves and roots associated with improved drought tolerance in creeping bentgrass expressing an ipt gene for cytokinin synthesis. *J. Exp. Bot.* 62 (15), 5311–5333. doi: 10.1093/jxb/err166

Mir, R. A., Bhat, B. A., Yousuf, H., Islam, S. T., Raza, A., Rizvi, M. A., et al. (2022). Multidimensional role of silicon to activate resilient plant growth and to mitigate abiotic stress. *Front. Plant Sci.* 13. doi: 10.3389/fpls.2022.819658

Mittler, R. (2006). Abiotic stress, the field environment and stress combination. *Trends Plant Sci.* 11, 15–19. doi: 10.1016/j.tplants.2005.11.002

Muter, O., Dubova, L., Kassien, O., Cakane, J., and Alsina, I. (2022). Application of the sewage sludge in agriculture: soil fertility, technoeconomic, and life-cycle assessment. *IntechOpen*. doi: 10.5772/intechopen.104264

Myers, S. S., Wessells, K. R., Kloog, I., Zanobetti, A., and Schwartz, J. (2015). Effect of increased concentrations of atmospheric carbon dioxide on the global threat of zinc deficiency: a modelling study. *Lancet Glob.* 3(10, 639–645. doi: 10.1016/S2214-109X(15)00093-5

Naik, B. S., Sharma, S. K., Pramanick, B., Chaudhary, R., Yadav, S. K., Tirunagari, R., et al. (2022). Silicon in combination with farmyard manure improves the productivity, quality and nitrogen use efficiency of sweet corn in an organic farming system. *Silicon* 14(10, 5733–5743. doi: 10.1007/s12633-022-01818-0

Najafi Vafa, Z., Sohrabi, Y., Mirzaghaderi, G., and Heidari, G. (2022). Soil microorganisms and seaweed application with supplementary irrigation improved physiological traits and yield of two dryland wheat cultivars. *Front. Plant Sci.* 13. doi: 10.3389/fpls.2022.855090

Narayanan, S. (2018). Effects of high temperature stress and traits associated with tolerance in wheat. *J. Sci.* 2(3, 177–186. doi: 10.15406/oajs.2018.02.00067

Nezhadahmadi, A., Prodhan, Z. H., and Faruq, G. (2013). Drought tolerance in wheat. *Sci. World J.* 2013, 610721. doi: 10.1155/2013/610721

Nouri, A., Etminan, A., Teixeira da Silva, J. A., and Mohammadi, R. (2011). Assessment of yield, yield related traits and drought tolerance of durum wheat genotypes *(Triticum turgidum* var. *durum Desf.). Aust. J. @ Crop Sci.* 5, 1, 8–1,16. doi: 10.14720/aas.2021.117.2.2021

Otie, V., An, P., Idorenyin, U., and Egrinya, E. (2019). Brassinolide effects on maize *(Zea mays L.)* growth and yield under waterlogged conditions. *J. Plant Nutr.* 42(8, 954–969. doi: 10.1080/01904167.2019.1584220

Oustani, M., Halilat, M. T., and Chenchouni, H. (2015). Effect of poultry manure on the yield and nutriments uptake of potato under saline conditions of arid regions. *Emir. J. Food Agric.*, 106–120. doi: 10.9755/ejfa.v27i1.17971

Padovan, G., Martre, P., Semenov, M. A., Masoni, A., Bregaglio, S., Ventrella, D., et al. (2020). Understanding effects of genotype × environment × sowing window interactions for durum wheat in the Mediterranean basin. *Field Crops Res.* 259, 107969. doi: 10.1016/j.fcr.2020.107969

Pampana, S., Masoni, A., and Arduini, I. (2016). Grain yield of durum wheat as affected by waterlogging at tillering. *Cereal Res. Commun.* 44, 706–716. doi: 10.1556/0806.44.2016.026

Pan, J., Sharif, R., Xu, X., and Chen, X. (2021). Mechanisms of waterlogging tolerance in plants: research progress and prospects. *Front. Plant Sci.* 11. doi: 10.3389/fpls.2020.627331

Pavia, I., Roque, J., Rocha, L., Ferreira, H., Castro, C., Carvalho, A., et al. (2019). Zinc priming and foliar application enhances photoprotection mechanisms in drought-stressed wheat plants during anthesis. *Plant Physiol. Biochem.* 140, 27–42. doi: 10.1016/j.plaphy.2019.04.028

Pradhan, G. P., Prasad, P. V., Fritz, A. K., Kirkham, M. B., and Gill, B. S. (2012). Effects of drought and high temperature stress on synthetic hexaploidy wheat. *Funct. Plant Biol.* 39, 190–198. doi: 10.1071/FP11245

Pramanick, B., Dubey, R., Kesarwani, A., Bera, A., Bhutia, K. L., Kumar, M., et al. (2023). "Advancement in mitigating the effects of waterlogging stress in wheat," in *Abiotic stresses in wheat* (Cambridge: Academic Press), 339–355. doi: 10.1016/B978-0-323-95368-9.00013-8

Prasad, P., Pisipati, S., Momčilović, I., and Ristic, Z. (2011). Independent and combined effects of high temperature and drought stress during grain filling on plant yield and chloroplast ef-tu expression in spring wheat. *J. Agro. Crop Sci.* 197, 430–441. doi: 10.1111/j.1439-037X.2011.00477.x

Prathap, V., Kishwar, A., Archana, S., Chandrapal, V., Veda, K., Viswanathan, C., et al. (2019). Starch accumulation in rice grains subjected to drought during grain filling stage. *Plant Physiol. Biochem.* 142, 440–451. doi: 10.1016/j.plaphy.2019.07.027

Qaseem, M. F., Qureshi, R., and Shaheen, H. (2019). Effects of Pre-Anthesis Drought, Heat and Their Combination on the Growth, Yield and Physiology of diverse Wheat *(Triticum aestivum L.)* Genotypes Varying in Sensitivity to Heat and drought stress. *Sci. Rep.* 9, 6955. doi: 10.1038/s41598-019-43477-z

Rakshit, A., Singh, H. B., Singh, A. K., Singh, U. S., and Fraceto, L. (2020). *New frontiers in stress management for durable agriculture* (Berlin: Springer). doi: 10.1007/978-981-15-1322-0

Rasul, F., Gupta, S., Olas, J. J., Gechev, T., Sujeeth, N., and Mueller-Roeber, B. (2021). Priming with a seaweed extract strongly improves drought tolerance in arabidopsis. *Int. J. Mol. Sci.* 22, 1469. doi: 10.3390/ijms22031469

Raza, A., Salehi, H., Rahman, M. A., Zahid, Z., Madadkar Haghjou, M., Najafi-Kakavand, S., et al. (2022). Plant hormones and neurotransmitter interactions mediate antioxidant defenses under induced oxidative stress in plants. *Front. Plant Sci.* 13. doi: 10.3389/fpls.2022.961872

Raza, M. A. S., Zulfiqar, B., Iqbal, R., Muzamil, M. N., Aslam, M. U., Muhammad, F., et al. (2023). Morpho-physiological and biochemical response of wheat to various treatments of silicon nano-particles under drought stress conditions. *Sci. Rep.* 13(1, 2700. doi: 10.1038/s41598-023-29784-6

Ren, B. C., Zhang, J. W., Li, X., Fan, X., Dong, S. T., Zhao, B., et al. (2014). Effect of waterlogging on grain filling and quality of summer maize. *Can. J. Plant Sci.* 94, 23–31. doi: 10.4141/cjps2013-175

Richard, D. S., Sufia, A., Sarah, G., Martin, W. B., and Klaus, K. (2022). The potential impact of climate change on the micronutrient-rich food supply. *Adv. Nutr.* 13(1, 80–100. doi: 10.1093/advances/nmab104

Rizwan, M., Ali, S., Ali, B., Adrees, M., Arshad, M., Hussain, A., et al. (2019). Zinc and iron oxide nanoparticles improved the plant growth and reduced the oxidative stress and cadmium concentration in wheat. *Chemosphere* 214, 269–277. doi: 10.1016/j.chemosphere.2018.09.120

Rorat, A., Courtois, P., Vandenbulcke, F., and Lemiere, S. (2019). *Sanitary and environmental aspects of sewage sludge management* (Oxford, UK: Industrial and Municipal Sludge (Butterworth-Heinemann), 55–180. doi: 10.1016/B978-0-12-815907-1.00008-8

Sadhukhan, R., Kumar, D., Sen, S., Sepat, S., Ghosh, A., Shivay, Y. S., et al. (2023). Precision nutrient management in zero-till direct-seeded rice influences the productivity, profitability, nutrient, and water use efficiency as well as the environmental footprint in the indo gangetic plain of India. *Agriculture* 13, 784. doi: 10.3390/agriculture13040784

Santos, C. S., Habyarimana, E., and Vasconcelos, M. W. (2023). The impact of climate change on nutrient composition of staple foods and the role of diversification in increasing food system resilience. *Front. Plant Sci.* 14. doi: 10.3389/fpls.2023.1087712

Sapkota, T. B., Jat, M. L., Rana, D. S., Khatri-Chhetri, A., Jat, H. S., Bijarniya, D., et al. (2021). Crop nutrient management using nutrient expert improves yield, increases farmers' income and reduces greenhouse gas emissions. *Sci. Rep.* 11, 1564. doi: 10.1038/s41598-020-79883-x

Sattar, A., Wang, X., Ul-Allah, S., Sher, A., Ijaz, M., Irfan, M., et al. (2022). Foliar application of zinc improves morpho-physiological and antioxidant defense mechanisms, and agronomic grain biofortification of wheat *(Triticum aestivum L.)* under water stress. *Saudi J. Biol. Sci.* 29(3, 1699–1706. doi: 10.1016/j.jcs.2019.03.007

Schaller, J., Scherwietes, E., Gerber, L., Vaidya, S., Kaczorek, D., Pausch, J., et al. (2021). Silica fertilization improved wheat performance and increased phosphorus concentrations during drought at the field scale. *Sci. Rep.* 11(1, 20852. doi: 10.1038/s41598-021-00464-7

Sedghi, M., Mitra, H., and Sahar, T. (2013). Effect of nano zinc oxide on the germination of soybean seeds under drought stress. *Ann. West Univ. Timi¸s. Ser. Biol.* 16, 73–78.

Sehgal, A., Sita, K., Siddique, K. H. M., Kumar, R., Bhogireddy, S., and Varshney, R. K. (2018). Drought or/and heat-stress effects on seed filling in food crops: impacts on functional biochemistry, seed yields, and nutritional quality. *Front. Plant Sci.* 9. doi: 10.3389/fpls.2018.01705

Semida, W. M., Abdelkhalik, A., Mohamed, G. F., Abd El-Mageed, T. A., Abd El-Mageed, S. A., Rady, M. M., et al. (2021). Foliar application of zinc oxide nanoparticles promotes drought stress tolerance in eggplant. *(Solanum melongena L.). Plants* 10, 421. doi: 10.3390/plants10020421

Seneviratne, S. I., Nicholls, N., Easterling, D., Goodess, C. M., Kanae, S., Kossin, J., et al. (2012). "Changes in climate extremes and their impacts on the natural physical environment,"," in *Managing the risks of extreme events and disasters to advance climate change adaptation: special report of the intergovernmental panel on climate change*. Eds. C. B. Field, V. Barros, T. F. Stocker and Q. Dahe (Cambridge: Cambridge University Press), 109–230. doi: 10.1017/CBO9781139177245.006

Shabbir, R. N., Waraich, E. A., Ali, H., Nawaz, F., Ashraf, M. Y., Ahmad, R., et al. (2016). Supplemental exogenous NPK application alters biochemical processes to improve yield and drought tolerance in wheat (Triticum aestivum L.). *Environ. Sci. pollut. Res.* 23, 2651–2662. doi: 10.1007/s11356-015-5452-0

Shallan, M. A., Hassan, H. M., Namich, A. A., and Ibrahim, A. A. (2016). Biochemical and physiological effects of TiO_2 and SiO_2 nanoparticles on cotton plant under drought stress. *Res. J. Pharm. Biol. Chem. Sci.* 7, 1540–1551.

Shao, H. B., Chu, L. Y., Jaleel, C. A., and Zhao, C. X. (2008). Water-deficit stress-induced anatomical changes in higher plants. *C. R. Biol.* 331(3, 215–225. doi: 10.1016/j.crvi.2008.01.002

Sharma, S., Chen, C., Khatri, K., Rathore, M. S., and Pandey, S. P. (2019). Gracilaria dura extract confers drought tolerance in wheat by modulating abscisic acid homeostasis. *Plant Physiol. Biochem.* 136, 143–154. doi: 10.1016/j.plaphy.2019.01.015

Shew, A. M., Tack, J. B., Nalley, L. L., and Chaminuka, P. (20204408). Yield reduction under climate warming varies among wheat cultivars in South Africa. *Nat. Commun.* 11, 1. doi: 10.1038/s41467-020-18317-8

Shukla, P. S., Mantin, E. G., Adil, M., Bajpai, S., Critchley, A. T., and Prithiviraj, B. (2019). Ascophyllum nodosum-based biostimulants: sustainable applications in agriculture for the stimulation of plant growth, stress tolerance, and disease management. *Front. Plant Sci.* 10. doi: 10.3389/fpls.2019.00655

Silva, R. D., Jalal, A., Nascimento, R. E., Elias, N. C., Kawakami, K. C., Abreu-Junior, C. H., et al. (2022). Composted sewage sludge application reduces mineral fertilization requirements and improves soil fertility in sugarcane seedling nurseries. *Sustainability* 14, 4684. doi: 10.3390/su14084684

Simões-Mota, A., Virto, I., and Poch, R. M. (2022). Effects of long-term sewage sludge application to a calcareous soil structure. *Soil Use Manage.* 38, 1693–1704. doi: 10.1111/sum.12838

Sinclair, T., and Jamieson, P. (2006). Grain number, wheat yield, and bottling beer: an analysis. *Field Crops Res.* 98, 60–67. doi: 10.1016/j.fcr.2005.12.006

Singh, A., Sharma, A., Verma, R. K., Chopade, R. L., Pandit, P. P., Nagar, V., et al. (2022). *Heavy metal contamination of water and their toxic effect on living organisms* (IntechOpen). doi: 10.5772/intechopen.105075

Soares, J. C., Santos, C. S., Carvalho, S. M., Pintado, M. M., and Vasconcelos, M. W. (2019). Preserving the nutritional quality of crop plants under a changing climate: importance and strategies. *Plant Soil* 443, 1–26. doi: 10.1007/s11104-019-04229-0V

Sofy, M. R. (2015). Application of salicylic acid and zinc improves wheat yield through physiological processes under different levels of irrigation intervals. *Int. J. Plant Res.* 5, 136–156. doi: 10.5923/j.plant.20150505.06

Solanki, P., Bhargava, A., Chhipa, H., Jain, N., and Panwar, J. (2015). "Nanofertilizers and their smart delivery system," in *Nanotechnologies in food and agriculture*. Eds. M. Rai, C. Ribeiro, L. Mattoso and N. Duran (Cham, Switzerland: Springer), 81–101. doi: 10.1007/978-3-319-14024-7_4

Sommer, R., Glazirina, M., Yuldashev, T., Otarov, A., Ibraeva, M., Martynova, L., et al. (2013). Impact of climate change on wheat productivity in Central Asia. *Agric. Ecosyst. Environ.* 178, 78–99. doi: 10.1016/j.agee.2013.06.011

Sonia, B., Mohammed, K., and Haroun, C. (2019). Sewage sludge fertilization alleviates drought stress and improves physiological adaptation and yield performances in Durum Wheat *(Triticum durum)*: A double-edged sword. *J. King Saud Uni. Sci.* 31(3, 336–344. doi: 10.1016/j.jksus.2017.12.012

Stone, P., and Nicolas, M. (1998). Comparison of sudden heat stress with gradual exposure to high temperature during grain-filling in two wheat varieties difference in heat tolerance. II. Fractional protein accumulation. *Aust. J. Plant Physiol.* 25, 1–11. doi: 10.1071/PP9950935

Sugurbekova, G., Nagyzbekkyzy, E., Sarsenova, A., Danlybayeva, G., Anuarbekova, S., Kudaibergenova, R., et al. (2023). Sewage sludge management and application in the form of sustainable fertilizer. *Sustainability* 15, 6112. doi: 10.3390/su15076112

Sun, P., Zhang, Q., Cheng, C., Singh, V. P., and Shi, P. J. (2017). ENSO induced drought hazards and wet spells and related agricultural losses across Anhui Province, China. *Nat. Hazards.* 89, 963–983. doi: 10.1007/s11069-017-3002-4

Tao, Z. Q., Wang, D. M., Chang, X. H., Wang, Y. J., Yang, Y. S., and Zhao, G. C. (2018). Effects of zinc fertilizer and short-term high temperature stress on wheat grain production and wheat flour proteins. *J. Integr. Agric.* 17(9, 1979–1990. doi: 10.1016/S2095-3119(18)61911-2

Tarafder, C., Daizy, M., Alam, M. M., Ali, M. R., Islam, M. J., Islam, R., et al. (2020). Formulation of a hybrid nanofertilizer for slow and sustainable release of micronutrients. *ACS Omega.* 5(37, 23960–23966. doi: 10.1021/acsomega.0c03233

Taran, N., Storozhenko, V., Svietlova, N., Batsmanova, L., Shvartau, V., and Kovalenko, M. (2017). Effect of zinc and copper nanoparticles on drought resistance of wheat seedlings. *Nanoscale Res. Lett.* 12, 60. doi: 10.1186/s11671-017-1839-9

Tcherkez, G., Ben Mariem, S., Larraya, L., García-Mina, J. M., Zamarreño, A. M., Paradela, A., et al. (2020). Elevated CO_2 has concurrent effects on leaf and grain metabolism but minimal effects on yield in wheat. *J. Exp. Bot.* 7119, 5990–6003. doi: 10.1093/jxb/eraa330

Teixeira, E. I., George, M., Herreman, T., Brown, H., Fletcher, A., and Chakwizira, E. (2014). The impact of water and nitrogen limitation on maize biomass and resource-use efficiencies for radiation, water and nitrogen. *Field Crops Res.* 168, 109–118. doi: 10.1016/j.fcr.2014.08.002

Teoh, S. K., and Li, L. Y. (2020). Feasibility of alternative sewage sludge treatment methods from a lifecycle assessment (LCA) perspective. *J. Clean. Prod.* 247, 119495. doi: 10.1016/j.jclepro.2019.119495

Thavaseelan, D., and Priyadarshana, G. (2021). Nanofertilizer use for sustainable agriculture. *J. Res. Technol.Eng.* 2(1, 41–59.

Thompson, M., Gamage, D., Ratnasekera, D., Perera, A., Martin, A., and Seneweera, S. (2019). Effect of elevated carbon dioxide on plant biomass and grain protein concentration differs across bread, durum and synthetic hexaploid wheat genotypes. *J. Cereal Sci.* 87, 103–110. doi: 10.1016/j.jcs.2019.03.007

Thorne, S. J., Hartley, S. E., and Maathuis, F. J. (2021). The effect of silicon on osmotic and drought stress tolerance in wheat landraces. *Plants* 10, 814. doi: 10.3390/plants10040814

Tian, L., Zhang, Y., Chen, P., Zhang, F., Li, J., Yan, F., et al. (2021). How does the waterlogging regime affect crop yield? A global meta-analysis. *Front. Plant Sci.* 12. doi: 10.3389/fpls.2021.634898

Tran, T. T., and Kano-Nakata, M. (2014). Nitrogen application enhanced the expression of developmental plasticity of root systems triggered by mild drought stress in rice. *Plant Soil.* 378, 139–152. doi: 10.1007/s11104-013-2013-5

Triboï, E., Martre, P., and Triboï-Blondel, A. M. (2003). Environmentally-induced changes in protein composition in developing grains of wheat are related to changes in total protein content. *J. Exp. Bota.* 54(388, 1731–1742. doi: 10.1093/jxb/erg183

Tsenov, N., Atanasova, D., Stoeva, I., and Tsenova, E. (2015). Effects of drought on grain productivity and quality in winter bread wheat. *Bulg. J. Agric. Sci.* 21, 592–598.

Turgeon, R. (2010). The puzzle of phloem pressure. *Plant Physiol.* 154, 578–581. doi: 10.1104/pp.110.161679

Upadhayay, V. K., Chitara, M. K., Mishra, D., Jha, M. N., Jaiswal, A., Kumari, G., et al. (2023). Synergistic impact of nanomaterials and plant probiotics in agriculture: A tale of two-way strategy for long-term sustainability. *Front. Microbiol.* 14. doi: 10.3389/fmicb.2023.1133968

Urban, O., Hlaváová, M., Klem, K., Novotna, K., Rapantova, B., Smutna, P., et al. (2018). Combined effects of drought and high temperature on photosynthetic characteristics in four winter wheat genotypes. *Field Crop Res.* 223, 137–149. doi: 10.1016/j.fcr.2018.02.029

Van Ittersum, M. K., Cassman, K. G., Grassini, P., Wolf, J., Tittonell, P., and Hochman, Z. (2013). Yield gap analysis with local to global relevance - a review. *Field Crops Res.* 143, 4–17. doi: 10.1016/j.fcr.2012.09.009

van Nguyen, D., Nguyen, H. M., Le, N. T., Nguyen, K. H., Nguyen, H. T., Le, H. M., et al. (2022). Copper nanoparticle application enhances plant growth and grain yield in maize under drought stress conditions. *J. Plant Growth Regul.* 41, 364–375. doi: 10.1007/s00344-021-10301-w

Verma, K. K., Song, X. P., Joshi, A., Rajput, V. D., Singh, M., Sharma, A., et al. (2022a). Nanofertilizer possibilities for healthy soil, water, and food in future: An overview. *Front. Plant Sci.* 13. doi: 10.3389/fpls.2022.865048

Verma, K. K., Song, X. P., Joshi, A., Tian, D. D., Rajput, V. D., Singh, M., et al. (2022b). Recent trends in nano-fertilizers for sustainable agriculture under climate change for global food security. *Nanomaterials* 12(1, 173. doi: 10.3390/nano12010173

Wahid, A. S., Gelani, M. A., and Foolad, M. R. (2007). Heat tolerance in plants: an overview. *Environ. Exp. Bot.* 61(3, 199–223. doi: 10.1016/j.envexpbot.2007.05.011

Wang, H., and Jin, J. (2007). Effects of zinc deficiency and drought on plant growth and metabolism of reactive oxygen species in maize *(Zea mays L.). Agric. Sci. China.* 6, 988–995. doi: 10.1016/S1671-2927(07)60138-2

Wang, J., Li, L., Lam, S. K., Liu, X., and Pan, G. (2020). Responses of wheat and rice grain mineral quality to elevated carbon dioxide and canopy warming. *Field Crops Res.* 249, 107753. doi: 10.1016/j.fcr.2020.107753

Wang, M., Wang, R., Mur, L. A. J., Ruan, J., Shen, Q., and Guo, S. (2021). Functions of silicon in plant drought stress responses. *Hortic. Res.* 8, 254. doi: 10.1038/s41438-021-00681-1

Wang, J., Yuxiang, M., Tianqi, H., Weiping, L., and Dalei, L. (2021). Water and heat stresses during grain formation affect the physicochemical properties of waxy maize starch. *J. Sci. Food Agric.* 101 (4), 1331–1339. doi: 10.1002/jsfa.10743

Weldearegay, D. F., Yan, F., Jiang, D., and Liu, F. (2012). Independent and combined effects of soil warming and drought stress during anthesis on seed set and grain yield in two spring wheat varieties. *J. Agron. Crop Sci.* 198, 245–253. doi: 10.1111/j.1439-037X.2012.00507.x

Wieser, H., Manderscheid, R., Erbs, M., and Weigel, H. J. (2008). Effects of elevated atmospheric CO_2 concentrations on the quantitative protein composition of wheat grain. *J. Agric. Food Chem.* 56, 6531–6535. doi: 10.1021/jf8008603

Xiong, X., Chang, L., Khalid, M., Zhang, J., and Huang, D. (2018). Alleviation of Drought Stress by Nitrogen Application in Brassica campestris ssp. Chinensis L. *Agrono.* 8, 66. doi: 10.3390/agronomy8050066

Xu, M., Liu, M., Liu, F., Zheng, N., Tang, S., Zhou, J., et al. (2021). A safe, high fertilizer-efficiency and economical approach based on a low-volume spraying UAV loaded with chelated-zinc fertilizer to produce zinc-biofortified rice grains. *J. Clean. Prod.* 323, 129188. doi: 10.1016/j.jclepro.2021.129188

Yan, W., Zhong, Y., and Shangguan, Z. (2016). A meta-analysis of leaf gas exchange and water status responses to drought. *Sci. Rep.* 6, 20917. doi: 10.1038/srep20917

Yang, F., Jorgensen, A. D., Li, H. W., Sondergaard, I., Finnie, C., and Svensson, B. (2011). Implications of high-temperature events and water deficits on protein profiles in wheat *(Triticum aestivum L.* cv. *Vinjett)* grain. *Proteom.* 11(9, 1684–1695. doi: 10.1002/pmic.201000654

Yang, J., Sears, R. G., and Gill, B. S. (2002). Genotypic differences in utilization of assimilate sources during maturation of wheat under chronic heat and heat shock stresses. *Euphytica* 125(2, 179–188. doi: 10.1023/A:1015882825112

Yu, H., Zhang, Q., Sun, P., and Song, C. (2018). Impact of droughts on winter wheat yield in different growth stages during 2001–2016 in Eastern China. *Int. Disaster Risk Sci.* 9, 376–391. doi: 10.1007/s13753-018-0187-4

Zhong, C., and Cao, X. (20171079). Nitrogen metabolism in adaptation of photosynthesis to water stress in rice grown under different nitrogen levels. *Front. Plant Sci.* 8. doi: 10.3389/fpls.2017.01079

Zhong, L., and Chen, D. (2015). AtTGA4, a bZIP transcription factor, confers drought resistance by enhancing nitrate transport and assimilation in Arabidopsis thaliana. *Biochem. Biophys. Res. Commun.* 457, 433–439. doi: 10.1016/j.bbrc.2015.01.009

Zhou, Q., Huang, M., Xin, H., Jing, L., Xiao, W., Jian, C., et al. (2018). Effect of post-anthesis waterlogging on biosynthesis and granule size distribution of starch in wheat grains. *Plant Physiol. Biochem.* 132, 222–228. doi: 10.1016/j.plaphy.2018.08.035

Zia, R., Nawaz, M. S., Siddique, M. J., Hakim, S., and Imran, A. (2021). Plant survival under drought stress: Implications, adaptive responses, and integrated rhizosphere management strategy for stress mitigation. *Microbiol. Res.* 242, 126626. doi: 10.1016/j.micres.2020.126626

frontiers | Frontiers in Plant Science

TYPE Original Research
PUBLISHED 10 November 2023
DOI 10.3389/fpls.2023.1239860

OPEN ACCESS

EDITED BY
Debojyoti Moulick,
Independent Researcher, Kolkata, India

REVIEWED BY
Rainer Hofmann,
Lincoln University, New Zealand
Artur Nosalewicz,
Polish Academy of Sciences, Poland

*CORRESPONDENCE
Bahram Heidari
bheidari@shirazu.ac.ir

RECEIVED 14 June 2023
ACCEPTED 24 October 2023
PUBLISHED 10 November 2023

CITATION
Shariatipour N, Shams Z, Heidari B and Richards C (2023) Genetic variation and response to selection of photosynthetic and forage characteristics in Kentucky bluegrass (*Poa pratensis* L.) ecotypes under drought conditions.
Front. Plant Sci. 14:1239860.
doi: 10.3389/fpls.2023.1239860

Genetic variation and response to selection of photosynthetic and forage characteristics in Kentucky bluegrass (*Poa pratensis* L.) ecotypes under drought conditions

Nikwan Shariatipour [1], Zahra Shams [2], Bahram Heidari [1]* and Christopher Richards [3]

[1]Department of Plant Production and Genetics, School of Agriculture, Shiraz University, Shiraz, Iran, [2]Department of Horticulture Science, School of Agriculture, Shiraz University, Shiraz, Iran, [3]United States Department of Agriculture, The Agricultural Research Service, National Laboratory for Genetic Resources Preservation, Fort Collins, CO, United States

Introduction: Evaluation of the effects of water-limited conditions on the photosynthetic characteristics and forage yield is important for enhancing the forage productivity and drought tolerance in Kentucky bluegrass (*Poa pratensis* L.).

Methods: In the present study, 100 P. *pratensis* ecotypes collected from different geographical areas in Iran were assessed under well-watered and drought stress conditions. Genetic variation and response to selection for the photosynthetic characteristics [i.e., net photosynthesis rate (A), stomatal conductance (g_s), transpiration rate (T_r), chlorophyll content (Chl), and photochemical efficiency (Fv/Fm)] and forage yield [fresh forage yield (FY) and dry forage yield (Dy)] traits were analyzed during the 2018 and 2019 growing seasons.

Results and discussion: Drought stress had negative effects on evaluated photosynthesis parameters and significantly reduced dry and fresh forage yields. On average, FY with a 45% decrease and g_s with a 326% decrease under drought stress conditions showed the highest reduction rate among forage yield and photosynthesis traits, respectively. Genotypic coefficients of variation (GCV) for FY were lower under drought stress. The estimates of heritability, genetic advance, and genetic advance as percentage of mean showed the predominance of additive gene action for the traits. Overall, the results showed that "Ciakhor", "Damavand", "Karvandan", "Basmenj", "Abr2", "Abrumand", "Borhan", "Hezarkanian", "LasemCheshmeh", "Torshab", and "DoSar" have higher forage yield production with little change between two irrigation regimes, which makes them promising candidates for developing high-yielding drought-tolerant varieties through breeding programs.

KEYWORDS

ecotype, forage yield, genetic advance, Kentucky bluegrass, photosynthesis

Introduction

Nowadays, climate changes that severely affect plant growth shift from monsoon patterns and global warming to drought more intensely and frequently. As a detrimental abiotic stress for plant growth, drought threatens production in agriculture in most countries and geographical regions (Liu et al., 2022a). Drought has periodically affected agricultural productivity in Iran, which is one of the countries suffering from low precipitation and water shortages. Iran's climate, with the exception of the northern coastal areas and western parts, is mainly arid and semi-arid, with high temperatures up to +50°C and 240 mm average annual rainfall (Heshmati, 2007; Amiri and Eslamian, 2010). Such conditions can lead to shortage of water resources and additional challenges for water distribution that can limit crop production in Iran (Noorisameleh et al., 2020).

Crop production losses caused by drought are the most important and damaging of all abiotic stresses (Seleiman et al., 2021). Photosynthesis plays a central role in plant growth and crop productivity and has become a major focus of research on abiotic stress (Gururani et al., 2015; Kebbas et al., 2015; Li et al., 2015; Liu et al., 2017; Fang et al., 2018; Zhang et al., 2022). The stomatal (stomatal closure due to decreased CO_2 intake) or nonstomatal (low photosynthetic rate in mesophyll tissue) responses, or both, are considered as the main factors responsible for decreased photosynthesis during drought stress (Varone et al., 2012; Ghotbi-Ravandi et al., 2014). Stomatal closure that restricts the diffusion of CO_2 into the mesophyll of leaves is an essential response to decrease evaporative water loss (Cornic, 2000). Evaluation of adaptive photosynthetic responses of plants can facilitate breeding efforts directed toward developing tolerant varieties for challenging and water-limited environmental conditions (Fahad et al., 2015; Saud et al., 2014; Torres-Ruiz et al., 2015; Liang et al., 2020; Yang et al., 2021).

Kentucky bluegrass (*Poa pratensis* L.) as a perennial grass with good spring green-up and forage quality is well suited for animal grazing. The grazing tolerance of this plant species is better than other cool-season forage grasses, which makes it an ideal species for permanent pastures. Kentucky bluegrass, unlike most cool season grasses, spreads by rhizomes, which helps it fill in open areas and produce a denser sod, which makes it ideal for erosion control. In addition, *P. pratensis* is more drought tolerant than many other grass species, which makes it a suitable candidate forage crop in arid and semi-arid areas. Previous studies determined that *P. pratensis* has a native distribution that spans different climatic regions of Iran, especially in the western and northern regions along the Zagros and Alborz Mountain ranges (Shariatipour et al., 2022; Ghanbari et al., 2023). The profusion of potential Kentucky bluegrass ecotypes provides high phenotypic and genotypic diversity for better stability against the adverse climate change effects (Shariatipour et al., 2022). Better understanding of differential physiological responses to water-limited conditions is important for the unraveling stress tolerance mechanisms and managing breeding strategies to identify stress-tolerant Kentucky bluegrass genotypes. In the Zhang et al. (2019) study, the "Wildhorse" cultivar of Kentucky bluegrass was exposed to drought stress and results indicated that drought stress led to cell membrane damage, resulting in decline in photosynthetic rate, chlorophyll content, and visual quality in Kentucky bluegrass. In another study, the contribution of silicate in the photosynthesis regulation and related metabolic pathways was investigated in Kentucky bluegrass (cv. "Arcadia") tested under drought stress (Saud et al., 2016). Additionally, the effect of foliar application of cytokinin and potassium on stimulation of stomatal opening and resumption of photosynthesis in the recovery process of Kentucky bluegrass plants exposed to long-term drought stress was investigated (Hu et al., 2013). Analysis of genetic variation in Kentucky bluegrass has shown that simultaneous selection may be possible for important characters for the development of superior turf types (Berry et al., 1969). Results of the Wang and Huang (2003) study demonstrated the genotypic variation for abscisic acid (ABA) accumulation and physiological parameters in four cultivars of Kentucky bluegrass tested under drought stress. In the Merewitz et al. (2010) study, evaluation of agronomic traits and recovery of Kentucky bluegrass genotypes demonstrated variation in response of genotypes to drought stress and the potential for the development of hybrids with improved drought tolerance and performance during recovery. However, most previous studies focused on the agronomy of this species as a turf grass and did not assess the role of genetic variation of photosynthesis activities in response to drought stress in Kentucky bluegrass. Therefore, our objectives were to (1) analyze the effects of drought stress on photosynthesis parameters and forage yield traits; and (2) estimate genetic variation, heritability, and efficiency of response to selection of photosynthetic variation for the improvement of drought tolerance in a collection of Kentucky bluegrass ecotypes from Iran.

Materials and methods

Plant material

Plan material consisted of 176 wild Kentucky bluegrass ecotypes that were collected from different geographical areas in Iran (Shariatipour et al., 2022). The collected samples are not threatened species in Iran and were identified following the NCBI Taxonomy descriptions (https://www.ncbi.nlm.nih.gov/Taxonomy/Browser/wwwtax.cgi?lvl=0&id=4545). Each clone sample containing 10 to 15 tillers was collected from a depth of 40 cm of soil and transferred to plastic pots for clonal propagation in a greenhouse. After pre-evaluation of the whole population, 100 viable accessions were selected for growing in the field and further phenotypic evaluation.

Experimental design and drought stress treatment

The rhizomes of the selected accessions were grown in the Shiraz University field research station at Bajgah (52° 35 N and 39°

Abbreviations: A, net photosynthesis rate; g_s, stomatal conductance; T_r, transpiration rate; Chl, chlorophyll content; Fv/Fm, photochemical efficiency; FY, fresh forage yield; DY, dry forage yield; GCV, genotypic coefficients of variation; PCV, phenotypic coefficients of variation; RCBD, randomized complete block design; ANOVA, analysis of variance; GLM, general linear model; GA, genetic advance; GAM, genetic advance as percentage of mean.

4 E, 1,810 m) over 2 years (2017–2018 and 2018–2019 seasons). The geographical information about the areas where the accessions collected is presented in Figure 1 and Supplementary Table S1. The long-term mean of maximum (22.95°C) and minimum (4.9°C) temperatures and mean annual precipitation of 394 mm generally without rain during the summer made supplemental irrigation necessary for growing the crop.

After field establishment, the germplasm panel was subjected to two irrigation regimes, one as a control with irrigation over the crop growing cycle and one as a drought stress treatment. The experiment was established in a randomized complete block design (RCBD) with two replications in each irrigation treatment. Each plot in the RCBD design contained one clone with a distance of 80 cm between clones. The plants continued to grow in the second year. The soil information used in the current study is shown in Table 1. The data showed that the soil had a clay loam texture. The soil water content (θ_i) in the root zone was measured to determine the net irrigation depth (d_n) following Eq. 1 (Israelsen and Hansen, 1962):

$$d_n = \sum_{i=1}^{n} (\theta_{FCi} - \theta_i) \times \Delta z_i \quad (1)$$

where

θ_{FCi} = the volumetric soil water content in layer i at field capacity

n = the number of soil layers

d_n = the net irrigation water depth (m)

θ_i = the volumetric soil water content in layer i

Δz_i = the thickness of soil in layer i (m)

Based on soil characteristic, n and i are considered 1 in this equation. Field capacity data were used for the irrigation efficiency of 90%, equal to 10% water loss, which was used to gain the gross irrigation water (d_g) based on Eq. 2 (Israelsen and Hansen, 1962):

$$d_g = d_n/0.9 \quad (2)$$

then, the 50% and 100% d_g were applied for drought stress and non-stress treatments, respectively (Israelsen and Hansen, 1962). Soil water content was constant in 2 years and a drip irrigation system with a weekly irrigation frequency was followed.

Measurements

Photosynthetic rate (A), stomatal conductance (g_s), and transpiration rate (T_r)

Four weeks after the rhizome establishment in the field and implementing drought stress treatment, all photosynthesis-related traits were measured in both irrigation regimes. Single-leaf A, g_s, and T_r were measured at 12:00–14:00 during sunny days in 10 to 12 whole fully expanded leaves using the LCi portable full-automatic photosynthetic measurement system (ADC Bio-Scientific, Ltd.,

FIGURE 1
The collection areas for *Poa pratensis* accessions in Iran. The green color indicates provinces and the purple circles represent the approximate location of the collected accessions.

10.3389/fpls.2023.1239860

TABLE 1 The physical characteristic of soil in the field used for evaluation of genetic diversity in *Poa pratensis* accessions.

Parameter	Unit	Soil depth (cm)	
		0-30	30-60
Field capacity (FC) (−0.033 MPa)	cm^3 cm^{-3}	32	33
Permanent wilting point (PWP) (−1.5 MPa)	cm^3 cm^{-3}	11	16
Bulk density (BD)	g cm^{-3}	1.31	1.37
Clay	%	36	39
Sand	%	25	27
Silt	%	39	34
Texture	–	Clay loam	Clay loam

Hertfordshire, UK). After stabilization in the chamber, all photosynthetic parameters of the leaves in each sample were recorded in 2-min intervals by the device All records were performed at 800 µmol m^{-2} s^{-1} photosynthetic photon flux density, which was the light saturation point for Kentucky bluegrass leaves as described by Saud et al. (2014).

Photochemical efficiency (Fv/Fm)

Expanded leaves were used for leaf photochemical efficiency as the ratio between variable and maximum fluorescence (Fv/Fm) in the non-energized state accomplished by exposure to darkness. After adaptation of selected leaves to darkness for 30 min, measurements were made on intact leaves with a chlorophyll fluorescence meter (Chlorophyll Fluorometer, OS-30p, Opti-sciences, Inc., USA). The light intensity for the readings was 3,500 µmol.

Chlorophyll content

Four weeks after implementing drought stress treatment, chlorophyll content was measured by soaking the expanded leaves (0.1 g) in dimethyl sulfoxide solution at 40°C for 48 h in plants tested under both irrigation treatments. Absorbance of the extracts was read out at 663 and 645 nm wavelength using a spectrophotometer (Epoch Microplate Spectrophotometer, BioTek Instruments, Inc., USA). These are expressed as mg g^{-1} dry leaf weight (Fu and Huang, 2001).

Forage yield traits

Forage yield was expressed as fresh- and dry-weight yield. FY was measured as the weight of fresh herbage harvested per plot, and after drying at 72°C for 48 h, the measured weight was expressed as DY.

Statistical and biometrical–genetic analyses

Analysis of variance (ANOVA) for the RCBD was carried out to examine significance of the years, irrigation regime (non- and drought stress), genotype effects and their interactions. The residual and predicted values for each trait were subjected to the ANOVA assumptions test. The expected mean squares of the general linear model (GLM) were used for variance component estimation (Table 2). In GLM, the effect of year was random, whereas accession and irrigation regime were fixed.

The phenotypic, genotypic, and environmental variances were estimated according to the expected value of mean square of the sources of variations in the ANOVA table described by Federer and Searle (1976) as follows (equation (Eqs. 3–5):

$$\sigma_g^2 = \frac{MS_g - MS_e}{r} \tag{3}$$

$$\sigma_e^2 = MS_e \tag{4}$$

$$\sigma_P^2 = \sigma_g^2 + \sigma_e^2 \tag{5}$$

where MS_g, MS_e, and r are genotypic mean square, error mean square, and the number of replications, respectively.

Phenotypic (PCV) and genotypic (GCV) coefficients of variation were estimated according to Burtone and De Vane (1953) (Eqs. 6 and 7):

$$PCV = \frac{\sqrt{\sigma_p^2}}{\mu} \times 100 \tag{6}$$

$$GCV = \frac{\sqrt{\sigma_g^2}}{\mu} \times 100 \tag{7}$$

where µ is the mean of population for the tested traits. The broad-sense heritability (h^2) which shows the contribution of the genetic variance in the phenotypic variation of a trait, was calculated according to method of Lush (1940) (Eq. 8):

$$h^2 = \frac{\sigma_g^2}{\sigma_p^2} \tag{8}$$

In the above equations, σ_P^2, σ_g^2 and σ_e^2 stand for the phenotypic, genotypic, and environmental variances, respectively.

The genetic advance (GA) and genetic advance as percentage of trait mean (GAM) were estimated according to Johnson et al. (1955) (Eqs. 9 and 10):

$$GA = k \times \sigma_e \times \frac{h^2}{100} \tag{9}$$

TABLE 2 Expected mean squares for photosynthetic parameters and forage yield traits across two environments (non- and drought stress) in *Poa pratensis* accessions.

Source of variation	Degree of freedom	Expected mean squares
Block	$r - 1 = 1$	
Genotype	$g - 1 = 99$	$\sigma_e^2 + r\sigma_g^2$
Error	$(r - 1)(g - 1) = 99$	σ_e^2

g, genotype; r, number of blocks; σ_e^2, error variance; σ_g^2, genotypic variance.

10.3389/fpls.2023.1239860

$$GAM = \frac{GA}{\mu} \times 100 \quad (10)$$

where the constant k is the standardized selection differential or selection intensity. The value of k at 5% proportion selected is 2.063.

The phenotypic and genotypic correlation coefficients were calculated (Eqs. 11 and 12) to determine the relationship of traits.

$$r_{p(XY)} = \frac{S_{p(XY)}}{S_{p(X)} \times S_{p(Y)}} \quad (11)$$

$$r_{g(XY)} = \frac{S_{g(XY)}}{S_{g(X)} \times S_{g(Y)}} \quad (12)$$

where $r_{p(XY)}$, $S_{p(XY)}$, $S_{p(X)}$, $S_{p(Y)}$, $S_{g(XY)}$, $r_{g(XY)}$, $S_{g(Y)}$, and $S_{g(X)}$ are the phenotypic correlation between traits X and Y, the phenotypic covariance between traits X and Y, the root of the phenotypic variance of trait X, the root of the phenotypic variance of trait Y, the genotypic correlation between traits X and Y, the genotypic covariance between traits X and Y, the root of the genotypic variance of trait Y, and the root of the genotypic variance of trait X, respectively. The key photosynthetic parameters associated with forage yield traits were determined using stepwise regression (Montgomery, 2006). A heatmap clustering was constructed based on the ward.D2 linkage algorithm and Manhattan distance metrics. Statistical analyses were performed using SAS version 9.4 (SAS Institute, Cary, NC, USA) and R *TraitStats* (Nitesh et al., 2020), *corrplot* (Wei et al., 2017), and *pheatmap* (Kolde and Kolde, 2018) packages.

Results

Analysis of variance and change of photosynthesis and forage yield traits under the well-watered and drought stress conditions

ANOVA was performed to assess the effects of year, genotype, irrigation regime, and their interactions following mean comparison for photosynthesis and forage-related traits (Table 3). Prior to ANOVA, the test of ANOVA assumptions indicated the additive effects of the components in the model. The results of ANOVA showed that main and interaction effects were significant for the traits (Table 3). Results of mean comparisons of photosynthetic parameters and forage yield traits for the two environments over the years are presented in Figure 2. Drought stress reduced forage yield and photosynthetic traits in both years. In addition, Kentucky bluegrass accessions had higher quantity for assessed traits especially for FY and DY in the second year (Figure 2). The FY with 43% and 46% losses was considerably reduced under drought stress in 2018 and 2019, respectively. The DY trait showed 24% and 29% (2019) reductions under drought -stress treatment in 2018 and 2019, respectively (Figure 2, Table 4). Photosynthetic traits especially A, g_s, and T_r showed high reduction in response to drought stress (Figure 2, Table 4). Analysis of distribution of traits showed that the genotypes had higher

TABLE 3 Source of variations and mean squares in combined analysis of variance (cANOVA) for traits assessed in non-stress and drought stress in 100 *Poa pratensis* accessions in 2018 and 2019.

Characters	Irrigation regime (Ir, df = 1)	Error I (df = 2)	Genotype (G) (df = 99)	(Ir × G) (df = 99)	Error II (df = 198)	Year (Y) (df = 1)	Y × Ir (df = 1)	Y × G (df = 99)	Y × G × Ir (df = 99)	Residual (df = 200)
FY	23,271,035.52***	5,115.25	116,521.07***	45,513.89***	5,482.94	87,757,778.53***	3,314,064.13***	39,434.88***	40,753.07***	3,020.60
DY	3,162,499.07***	898.29	50,298.39***	14,875.64***	2,200.59	31,668,496.63***	657,526.96***	15,778.87***	11,865.47***	1,711.00
A	22,172.99***	3.46	7.06***	1.79**	0.19	725.98***	18.04***	1.76***	1.47***	0.16
g_s	6.923***	0.011	0.005***	0.0021***	5.3 E-5	0.168***	0.036***	4.4 E-4***	4.5 E-4***	4.8 E-5
T_r	1,392.70***	0.384	0.644***	0.213***	0.008	18.650***	0.094***	0.092***	0.098***	0.005
Chl	1,949.94***	3.22	0.98***	0.33***	0.04	54.76**	0.35***	0.18***	0.19***	0.032
Fv/Fm	5.82***	0.05	0.015***	0.006***	4.5 E-4	0.61***	0.036***	0.0011***	0.0010***	2.9 E-4

** and *** represent non-significant and significant at $p < 0.01$ and $p < 0.001$, respectively. Ir, irrigation regime; G, genotype; Y, year, Error I = R(M); Error II = R × G(M); FY, forage fresh yield; DY, forage dry yield; A, net photosynthetic rate; g_s, stomatal conductance; T_r, transpiration rate; Chl, chlorophyll content; Fv/Fm, photochemical efficiency.

phenotypic variation for FY and DY in the second than in the first year. However, the genotypes represented relatively similar phenotypic variation for photosynthesis phenotypes over the 2 years (Figure 2). Evaluation of traits over treatments showed inconsistent response to irrigation treatments. Large differences in response of genotypes to irrigation treatments was observed for g_s where the genotypes had higher variation for g_s in drought stress treatment than in normal irrigation conditions (Figure 2). The highest decrease in photosynthesis-related traits belonged to A, which was 363.35% under drought stress in the first year, followed by g_s (346.56%) and T_r (309.98%). The Fv/Fm showed a lower increase (26.60%) while g_s with a 305.72% decrease showed higher reduction among photosynthetic traits under drought stress in the second year, followed by A (245.01%) and T_r (235.88) (Figure 2, Table 4).

The net photosynthesis rate (A) ranged from 0.96 to 18.22 μmol m^{-2} s^{-1}. "Ciakhor" under non-stress conditions in the second year and "GilanTappeh" in the first year and under drought stress treatment had the highest and lowest A, respectively (Supplementary Table S2). "Liqvan" (17.42 μmol m^{-2} s^{-1}) and "Noqan" (17.25 μmol m^{-2} s^{-1}): "Abrumand" (17.25 μmol m^{-2} s^{-1}) stood at the second and third rankings for A under non-stress treatment in 2019. The stomatal conductance ranged from 0.01 to 0.38 mol m^{-2} s^{-1}. The "Ciakhor" under non-stress conditions in the second year illustrated the highest g_s followed by "Liqvan" (0.37 mol m^{-2} s^{-1}) and "Noqan" (0.36 mol m^{-2} s^{-1}) in the second year and under a non-stress environment (Supplementary Table S2). The "GilanTappeh" (0.23 mol m^{-2} s^{-1}) and "Abr2" (4.98 mmol m^{-2} s^{-1}) showed the lowest and highest transpiration rate (T_r) under drought stress conditions in 2018 and non-stress in 2019, respectively. As presented in Supplementary Table S2, the chlorophyll content (Chl) varied from 5.75 mg g^{-1} dry weight to 12.02 mg g^{-1} dry weight. Among the assessed accessions, "Sarab" (12.02 mg g^{-1} dry weight) and "Abr2" (12.00 mg g^{-1} dry weight) showed higher Chl content in the second year and under the non-stress condition, whereas the lowest Chl belonged to "GillanTappeh" (5.75 mg g^{-1} dry weight) (Supplementary Table S2). Photochemical efficiency (Fv/Fm) ranged from 0.38 in the "Abbasabad" in 2018 under drought stress conditions to 0.85 in the "Ciakhor" in 2019 under non-stress conditions (Supplementary Table S2).

The mean for fresh (FY) and dry forage yields (DY) ranged from 332.50 g to 2,026.57 g (FY) and 175.54 g to 1,129.00 g (DY), respectively. "Ciakhor" in 2019 under non-stress and "GilanTappeh" under drought stress conditions in 2018 had the highest and lowest FY and DY, respectively (Supplementary Table S2).

Genetic advance and heritability estimates

The PCV and GCV estimated under non-stress and drought stress treatments are presented in Table 4. DY (24.61%, 20.29%) and g_s (47.18%, 41.52%) had the highest PCVs in both irrigation regimes

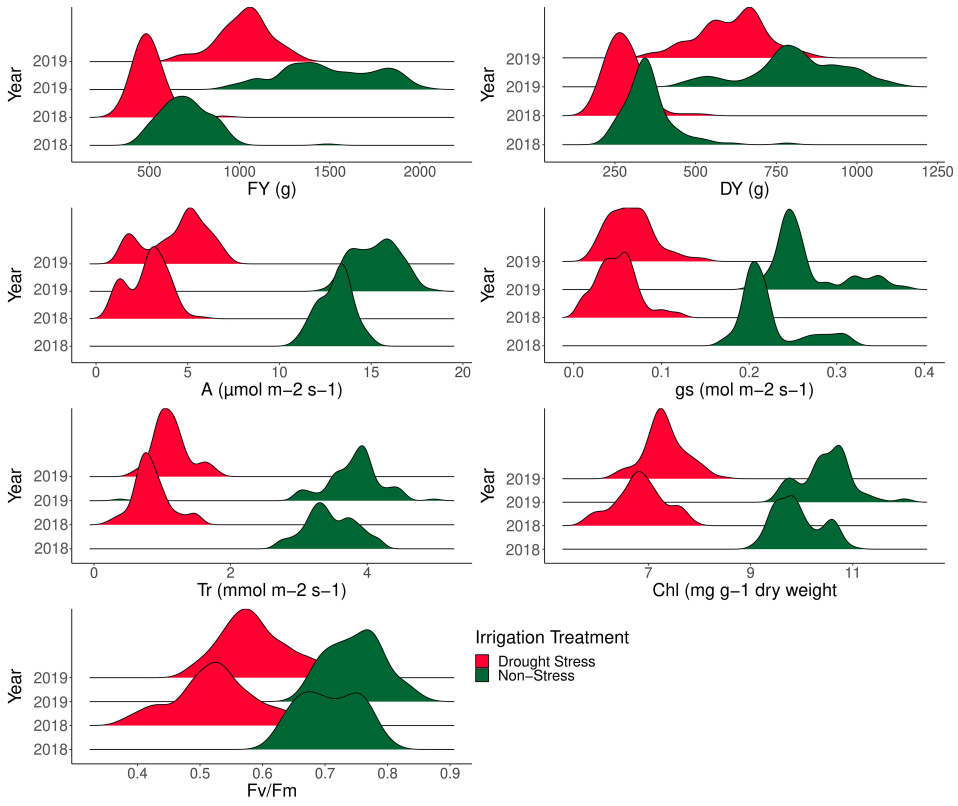

FIGURE 2
Phenotypic variation of 100 *Poa pratensis* accessions evaluated in non-stress and drought stress conditions over 2018 and 2019.

10.3389/fpls.2023.1239860

TABLE 4 Mean value, phenotypic coefficients of variation (PCV), genotypic coefficients of variation (GCV), broad-sense heritability (h_b^2), genetic advance (GA) and genetic advance as percentage of mean (GAM) of studied traits measured from 100 accessions of *Poa pratensis* evaluated in non-stress and drought stress environments during years 2018 and 2019.

Trait	Mean ± SE (2018)		Non-stress*									
			GCV (%)		PCV (%)		h_b^2(%) ± SE		GA		GAM (%)	
	Non-stress condition	Drought stress	2018	2019	2018	2019	2018	2019	2018	2019	2018	2019
FY	704.91^a ± 11.08	492.53^b ± 6.33	19.62	17.54	22.26	18.23	77.70	92.58	251.19	520.23	35.63	34.77
DY	349.11^a ± 6.06	280.70^b ± 4.76	19.97	19.35	24.61	20.19	65.83	91.88	116.51	307.41	33.37	38.22
A	13.04^a ± 0.06	2.82^b ± 0.08	6.43	7.72	7.02	8.23	83.87	88.09	1.58	2.28	12.13	14.93
g_s	0.22^a ± 0.002	0.05^b ± 0.002	15.84	15.23	16.23	15.53	95.21	96.28	0.07	0.08	31.83	30.79
T_r	3.46^a ± 0.02	0.84^b ± 0.02	10.26	13.33	10.51	13.47	95.37	97.94	0.71	1.03	20.64	27.18
Chl	9.92^a ± 0.03	6.84^b ± 0.04	4.37	4.55	4.73	4.82	85.36	89.24	0.83	0.93	8.32	8.86
Fv/Fm	0.71^a ± 0.003	0.52^b ± 0.005	6.48	5.50	6.94	6.05	87.06	82.72	0.09	0.08	12.45	10.31
Trait	Mean ± SE (2019)		Drought stress*									
			GCV (%)		PCV (%)		h_b^2(%) ± SE		GA		GAM (%)	
	Non-stress condition	Drought stress	2018	2019	2018	2019	2018	2019	2018	2019	2018	2019
FY	1,496.05^a ± 19.24	1,026.22^b ± 10.59	14.25	13.67	18.21	14.62	61.22	87.33	113.10	269.98	22.96	26.31
DY	804.37^a ± 11.46	621.29^b ± 7.73	19.48	16.43	24.01	17.64	65.82	86.80	91.36	195.94	32.55	31.54
A	15.25^a ± 0.09	4.42^b ± 0.12	36.11	36.29	39.81	37.31	82.27	94.59	1.90	3.21	67.46	72.70
g_s	0.26^a ± 0.003	0.07^b ± 0.002	46.54	39.66	47.18	41.52	97.34	91.25	0.05	0.05	94.60	78.05
T_r	3.79^a ± 0.02	1.13^b ± 0.02	31.23	21.60	32.04	23.54	94.97	84.22	0.53	0.46	62.69	40.83
Chl	10.48^a ± 0.04	7.32^b ± 0.03	6.63	5.32	7.49	5.62	78.40	89.74	0.83	0.76	12.10	10.39
Fv/Fm	0.75^a ± 0.005	0.59^b ± 0.004	11.90	9.48	12.68	9.85	88.05	92.57	0.12	0.11	22.99	18.78

FY, forage fresh yield; DY, forage dry weight; A, net photosynthetic rate; gs, stomatal conductance; Tr, transpiration rate; Chl, chlorophyll content; Fv/Fm, photochemical efficiency SE, standard error of the mean. Means with different letter are significantly different in each row, * All genetic variation parameters and heritabilities are significant at 0.05 probability level.

in 2018 and 2019, respectively. FY (22.26%, 18.23%) and A (39.81%, 37.31%) ranked next for PCV under non-stress conditions and drought stress environment in 2018 and 2019, respectively. Chl demonstrated the minimum value for PCV in both years and irrigation regimes (Table 4). In 2018, the GCV ranged from 4.37% (Chl) to 19.97% (DY) under non-stress treatment and from 6.63% (Chl) to 46.54% (g_s) under drought treatment. In 2019, DY (19.35%) and FY (17.54%) had the highest value for GCV under non-stress conditions while g_s (39.66%) and A (36.29%) had the highest GCV under drought treatments. The lowest GCV was observed for Chl (4.55%, 5.32%) in two growing seasons (Table 4).

The heritability estimates ranged from 65.83% (DY) to 95.37% (T_r) under non-stress treatment and from 61.22% (FY) to 97.34% (g_s) under drought stress environment in 2018 (Table 4). The estimated heritability for g_s (h_b^2 = 95.21%) under non-stress conditions and T_r (h_b^2 = 94.97%) under drought stress conditions were next in the rankings. In 2019, the heritability of assessed traits ranged from 82.72% for Fv/Fm to 97.94% for T_r under non-stress environment and from 84.22% for T_r to 94.59% for A under drought stress treatment. The forage yield traits (FY and DY) showed higher heritability in 2019 compared with 2018 under both irrigation regimes (Table 4). Furthermore, the photosynthetic traits showed high heritability with low change between two watering regimes across 2 years, while the heritability of FY and DY in 2018 was quite low in both conditions.

The FY in 2018 (251.19) and 2019 (520.23) presented the highest GA, while the lowest GA belonged to g_s (0.07) in 2018 and g_s (0.08) and Fv/Fm (0.08) in 2019 under non-stress treatment. Under drought conditions, the GA ranged from 0.05 for g_s to 113.10 for FY in 2018 and from 0.05 to 269.98 for the same traits in 2019. In 2018, GAM ranged from 8.32% for Chl to 35.63% for FY under non-stress conditions and from 12.10% for Chl to 94.60% for g_s under drought treatment. The DY (38.22%) and g_s (78.05%) demonstrated the highest GAM in 2019 under both irrigation regimes while the lowest GAM was observed in Chl (8.86%, 10.29%) in the same year and irrigation regimes (Table 4). The photosynthetic traits showed low GA with low change under non-stress and drought stress conditions over 2 years, while FY and DY represented high GA in both conditions with a significant change over the years (Table 4).

Correlation of traits

The correlation coefficients of forage yield traits and photosynthetic parameters under non-stress and drought stress treatments are shown in Figure 3. Under non-stress and drought stress conditions, net photosynthesis rate was strongly correlated with photosynthetic components (r_p and $r_g > 0.70$) except with Fv/Fm under normal conditions (Figure 3). High correlation coefficients were obtained among other phytochemical traits. For instance, g_s shows strong correlation with T_r ($r_p = 0.73$ and $r_g = 0.75$, non-stress; $r_p = 0.85$ and $r_g = 0.89$, drought stress) and Chl ($r_p = 0.72$ and $r_g = 0.77$, non-stress; $r_p = 0.83$ and $r_g = 0.90$, drought stress). T_r and Fv/Fm ($r_p = 0.64$ and $r_g = 0.66$, non-stress; $r_p = 0.82$ and $r_g = 0.89$, drought stress) and T_r and Chl content showed high correlations. High genotypic and phenotypic ($r_p = 0.82$; $r_g = 0.88$) correlations were obtained between A and Fv/Fm. Additionally, FY was strongly correlated with DY under both irrigation regimes (r_p and $r_g = 0.91$, non-stress; r_p and $r_g = 0.96$, drought stress). Photosynthetic parameters and forage yield were significantly correlated. Although Fv/Fm had low phenotypic and genotypic correlations with FY and FD under non-stress treatment, they showed strong correlation under drought stress treatment.

Both phenotypic and genotypic correlations of the photosynthetic parameters with FY and DY were higher under drought conditions compared with well-watered control. The results of stepwise regression analysis demonstrated that A, g_s, and T_r were the most important contributors to FY (R^2 = 64%) and DY (R^2 = 67%) variances in well-watered treatment (Table 5). Under drought stress conditions, 91% of the FY variation was explained by A, g_s, T_r, and Fv/Fm. The traits A, g_s, and T_r showed high contribution to the total phenotypic variation of DY (Table 5).

Clustering accessions

The dendrogram of heatmap clustering of tested *P. pratensis* accessions and evaluated traits under the two irrigation regimes is shown in Figure 4. Under non-stress conditions, the accessions were clustered into three distinct groups (Figure 4). In group I, the accessions showed high values for all assessed traits. Group II, which comprised 63 accessions, showed relatively moderate values for photosynthetic parameters and forage yield traits. Group III consisted of "MazraeBeed", "Abbasabad", "Losku", "Talesh", "Ashab", "Karimabad", "Chaleki", "Tazeabad", "Ghircanyon1", "BandarehAnzali", "SinavaCheshme", "Marian", "GilanTappeh", "Nowgaran", "Roodafshan", and "SheRiz" accessions had low levels for all measured traits (Figure 4).

Under drought stress treatment, the tested *P. pratensis* accessions were divided into three groups (Figure 4). Groups I and II represented the highest and lowest values for all measured traits, respectively. Group III comprised 60 accessions with relatively moderate values for forage yield traits and photosynthetic parameters (Figure 4). The result of cluster analysis showed that half of the tested accessions belonged to group II under non-stress conditions (Figure 4). Eight accessions were placed in group III under drought stress conditions (Figure 4) with moderate values for forage yield traits and photosynthetic parameters.

Several accessions placed in the clusters II and III (Figure 4) showed low and moderate values for the tested traits under non-stress but high forage yield (FY and DY) under drought stress conditions (Figure 4).

Discussion

Exploiting natural variation from field-collected natural populations can add variation needed to develop new variates.

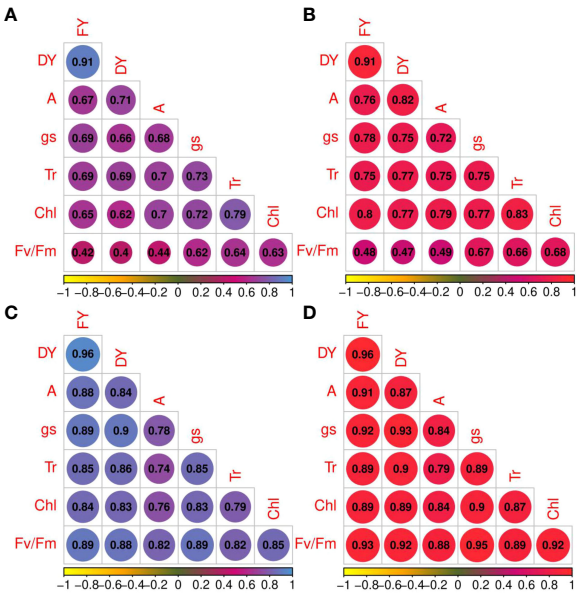

FIGURE 3
Phenotypic (blue color spectrum) and genotypic (red color spectrum) correlation coefficients for photosynthetic parameters and forage yield traits in 100 *Poa pratensis* accessions evaluated in non-stress **(A, B)** and drought stress **(C, D)** conditions.

10.3389/fpls.2023.1239860

TABLE 5 Results of stepwise regression analysis between photosynthetic parameters and forage yield traits (FY and DY) in *Poa pratensis* accessions evaluated in non-stress and drought stress conditions.

Treatment	FY					DY				
	Variable entered	Parameter estimate	Partial R^2	Model R^2	F value	Variable entered	Parameter estimate	Partial R^2	Model R^2	*F* value
Non-stress	g_s	1,641.45	0.5410	0.5410	12.54***	A	45.88	0.5841	0.5841	21.09***
	A	54.82	0.0775	0.6186	9.42**	T_r	67.37	0.0673	0.6515	7.64*
	T_r	109.43	0.0234	0.6421	6.31**	g_s	616.12	0.0193	0.6708	5.64**
	Intercept	−470.53	–	–	7.26**	Intercept	−460.40	–	–	22.20***
Drought stress	g_s	1,134.28	0.8329	0.8329	8.67**	g_s	1,312.13	0.8186	0.8186	23.28***
	A	31.33	0.0624	0.8953	38.32***	T_r	109.75	0.0368	0.8554	21.32***
	Tr	100.85	0.0150	0.9103	13.42**	A	13.00	0.0138	0.8692	10.16**
	Fv/Fm	279.99	0.0029	0.9132	3.16*	Intercept	213.98	–	–	243.23***
	Intercept	324.36	–	–	25.55***					

n.s., *, **, and *** represent non-significant, significant at $p < 0.05$, $p < 0.01$ and $p < 0.001$, respectively. FY, forage fresh yield; DY, forage dry yield; A, net photosynthetic rate; g_s, stomatal conductance; T_r, transpiration rate; Chl, chlorophyll content; Fv/Fm, photochemical efficiency.

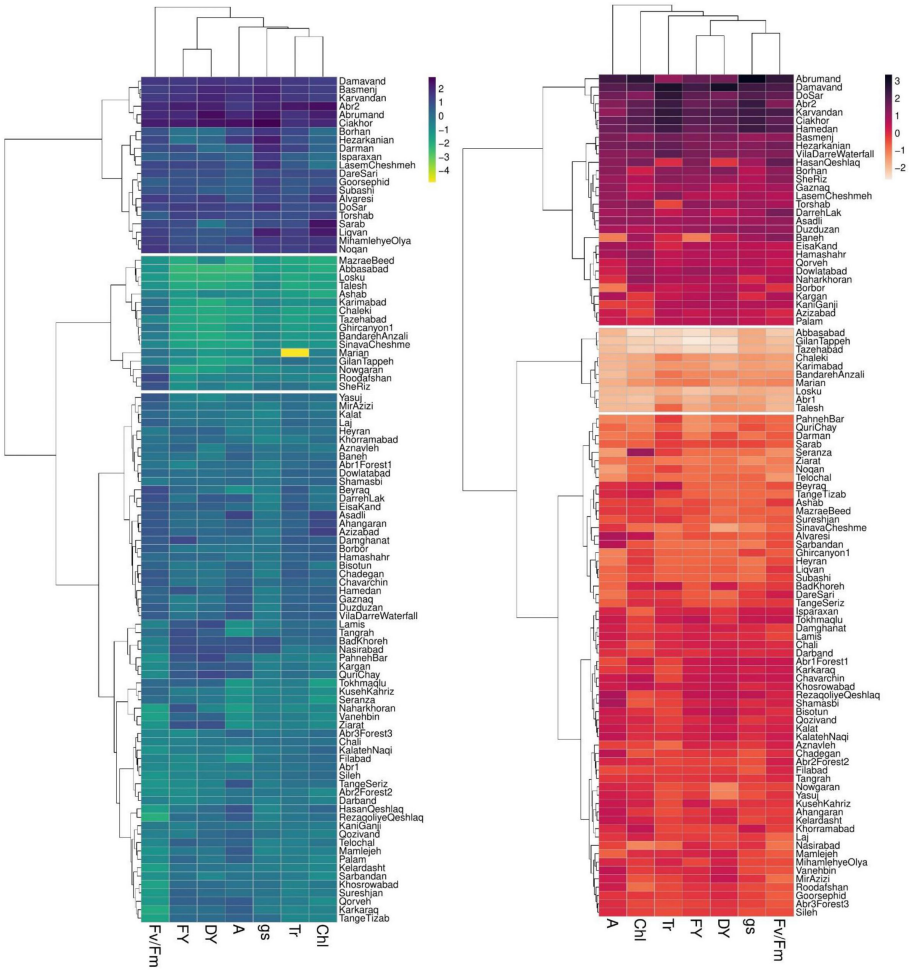

FIGURE 4
Two-dimensional heatmap dendrogram for 100 P. *pratensis* accessions tested for photosynthetic and forage yield traits under non-stress (blue dendrogram) and drought stress (red dendrogram). Dendrograms illustrate the relation between accessions (rows) and traits (columns) based on variations in color shades. FY, forage fresh yield; DY, forage dry yield; A, net photosynthetic rate; g_s, stomatal conductance; T_r, transpiration rate; Chl, chlorophyll content; Fv/Fm, photochemical efficiency.

Ecotype variation is the end point of sustained environmental selection, and using these accessions can reveal important and novel variation not available in commercial varieties. Natural variation in underexploited genetic resources such as plant ecotypes is a raw material for the development of new varieties and the continuity of breeding crops for different traits (Flood et al., 2011; Lawson et al., 2012). In the present study, photosynthetic parameters were significantly affected by the moisture regime that was in agreement with results of other studies for the same traits in Kentucky bluegrass (Hu et al., 2010; Hu et al., 2013; Saud et al., 2016; Zhang et al., 2019). The decrease in photosynthetic rate under drought stress is due to the decrease in the supply of water, which decreases the g_s under drought stress to reduce water loss and stomatal closure that then leads to reduced leaf transpiration and an insufficient supply of CO_2 (Chavers et al., 2009; Ghotbi-Ravandi et al., 2014; Roig-Oliver et al., 2021). Stomatal closure and photosynthesis are the most sensitive events against the adverse effects of drought stress (Quarrie and Jones, 1977; Meng et al., 1999; Xu and Zhou, 2008; Hu et al., 2013; Flexas and Carriqui, 2020). Under drought stress, plants regulate photosynthesis through the balance of water budget by reducing the T_r, which is an adaptive strategy to avoid the adverse effects of drought (Schreiber et al., 1995; Medrano et al., 2002; Zhang et al., 2022). The photochemical efficiency (Fv/Fm) has been shown as a sensitive indicator of plant photosynthetic performance (Guidi et al., 2019). Reduced Fv/Fm, which is an indicator of the efficiency of excitation energy captured by "open" PSII reaction centers, is associated with downregulation of photosynthesis or decreased photosystem II (PSII) efficiency (Souza et al., 2004; Guidi et al., 2019). The results of our study indicated significant reduction in Fv/Fm quantity under drought stress conditions, which was in line with results of the Fv/Fm ratio in drought compared to the non-stress condition in previous studies of Kentucky bluegrass (Abraham et al., 2008; McCann and Huang, 2008; Hu et al., 2010). Photosynthetic capacity is determined by leaf chlorophyll and photochemical reactions. It has been shown that leaf senescence, which expedites in response to the adverse effects of drought stress, decreases leaf Chl content (Wise and Naylor, 1987). Damage to chlorophyll is almost attributed to damage to membrane, which results in leaf senescence under water-limited conditions (Simon, 1974; Liu and Huang, 2000). In this study, significant reduction was found in Chl content under drought stress compared with the non-stress treatment, which was in line with results of changes in chlorophyll content in Kentucky bluegrass tested under water-limited conditions in the Saud et al. (2016) study. Results of our study showed that g_s, A, and T_r had higher reduction under drought compared with the *Chl* content, which shows chlorophyll content and photochemical efficiency that are less sensitive to water-limited conditions than stomatal components in Kentucky bluegrass. It has been shown that early inhibition of photosynthesis under water-limited conditions could be induced by stomatal closure and the possible damage to PSII (Hu et al., 2010). The forage yield of the evaluated *P. pratensis* accessions in this study was significantly decreased under drought stress conditions. The negative impact of drought stress on morphological traits including biomass has been documented in Kentucky bluegrass (Abraham et al., 2008; Liu et al., 2022b).

The particular source of phenotypic variation determines whether the trait has the ability to respond to natural/artificial selections and environmental changes (Byers et al., 2008). Our study showed that the Kentucky bluegrass genotypes had substantial variation for forage yield and several photosynthesis characters over the years and irrigation regimes. However, trait–irrigation treatment interaction was observed in our accessions. The g_s character showed higher phenotypic variation under drought stress conditions compared with normal irrigation treatment. Variation in plant materials is the key prerequisite to successful breeding programs and development of new varieties for use in different environmental conditions. Analysis of heritability and genetic advance helps breeders predict the potential of a population for the improvement of different traits in response to selection. In the current study, the majority of traits including FY, DY, A, g_s, and T_r showed moderate to high genetic variability (GCV and PCV), particularly under drought stress treatment, which shows the possibility of the trait improvement through direct and indirect selections. However, the results indicated low variability for Chl and Fv/Fm, suggesting the need for improvement of base population through cross breeding for these traits (Terfa and Gurmu, 2020). The small difference between the GCV and PCV values in our study was consistent with previous studies in different crops (Majidi et al., 2009; Jalata et al., 2011). All the tested traits in this study had relatively high heritability (61.22% to 97.94%), which is critical for successful phenotypic selection. Photosynthetic parameters showed higher heritability compared with forage yield phenotypes in our study. Thus, the association of photosynthesis and forage yield could help use photosynthetic parameters as a criterion for indirect selection for high-yielding varieties under drought stress conditions. Breeding through indirect selection could be more efficient than direct selection in the cases that selection for direct traits is complicated and when indirect traits show high heritability than direct ones (Blum, 2011; Shariatipour et al., 2022). Estimation of the genetic advance (GA) will help to predict selection progress that can be expected as result of exercising selection in a breeder germplasm. High heritability and moderate to high genetic advance were recorded for forage yield and photosynthesis traits except for Chl under non-stress treatment, indicating the predominance of additive gene action for these phenotypes. The use of mean-based genetic advance (GAM) coupled with high heritability helps breeders to better predict the resultant effect of selection for multiple traits compared with selections based on heritability estimates alone. It has been shown that traits with high heritability coupled with moderate genetic advance improved more easily than the traits showing lower GAM and heritability (Singh et al., 2016). The forage-related traits presented higher heritability, GA, and GAM in our population for the non-stress condition compared with drought treatment. According to Blum (2011), yield usually shows higher heritability and greater genetic advance through selection in an optimal environment than in stressed environments. The genotypic variation and the high heritability identified in the current study suggested the higher contribution of genetic components compared with environmental variance in the phenotypic variation of the tested traits. The higher contribution of genetic variance in

phenotypic variation accelerates the selection and development of new drought-tolerant varieties with higher forage yield production.

Information on the covariance of traits is useful for predicting how the selection pressure exerted on one trait will result in trade-offs for other traits (Mehri et al., 2009; Kole and Saha, 2013). The correlation of photosynthetic parameters in our study was in agreement with previous studies that have shown co-regulation of stomatal conductance (g_s) and photosynthesis in plants (Wong et al., 1979; Farquhar et al., 2001; Medrano et al., 2002). The correlation between photosynthetic parameters has been identified in different forage grasses (Fariaszewska et al., 2020; Mastalerczuk et al., 2022). The results of this study indicated that photosynthesis characteristics and forage yield traits were strongly correlated in both irrigation regimes, suggesting the effective role of these parameters in forage production in Kentucky bluegrass. Photosynthesis is the basis of biomass production in plants (Keller et al., 2022). It has been shown that photosynthetic CO_2 assimilation contributes to approximately 90% of dry matter of crop plants (Lawlor, 1995). In our study, photosynthesis, transpiration, and stomatal conductance had a direct positive effect on the forage yield production, which was in agreement with the results of the Staniak et al. (2018) study in Festulolium [*Festulolium braunii* (K. Richt) A. Camus] and alfalfa (*Medicago* × varia T. Martyn). Results of the Flexas and Carriqui (2020) study have shown that the ratio of g_m (mesophyll conductance) and g_s affects maximizing photosynthesis in plants. In the present study, the identified correlation between photosynthetic characteristics and forage yield phenotypes under drought stress treatment suggests the possibility of successful selection for both high forage yield and higher photosynthesis potential. The result of the interrelation analysis of the tested traits indicated the higher contribution of photosynthetic parameters to the observed variation in forage yield phenotypes (FY and DY) under drought stress environment compared with normal watering treatment, which suggests the critical role of photosynthesis parameters in yield under drought stress conditions (Harbinson and Yin, 2023).

Clustering individuals in a population that provides information about similarities of genotypes helps for selection and crosses between different groups for expanding genetic variation and development of new segregation populations. Results of cluster analysis in our study showed that the assessed accessions were divided into distinct high and low photosynthesis and forage yield groups. The development of a segregating population through crosses between accessions of two high and low productive groups helps in mapping quantitative traits loci and identifying markers associated with traits for use in marker-assisted selection programs in *P. pratensis*.

Conclusions

The results of our studies showed the significant effects of the watering regime on the photosynthesis system and forge yield traits. Among the tested photosynthetic parameters, stomatal conductance showed a higher correlation with forage yield, which can be suggested as an integrative parameter for identifying drought-tolerant varieties. This work provides supporting information for two research areas. One is the interrelationship of traits and the level of genetic variation for photosynthesis and forage-related traits under two moisture regimes. The other is information on heritability and gain from selection, which shows the potential of our *P. pratensis* population for the improvement of two different sets of traits. The wide variation observed for traits in the ecotypic variation sampled in the accessions tested helps to select good candidates and develop segregating populations through cross-breeding programs to breed drought-tolerant varieties with higher forage yield traits and identify information about QTLs of traits.

Data availability statement

The original contributions presented in the study are included in the article/Supplementary Material. Further inquiries can be directed to the corresponding author.

Author contributions

NS and ZS performed the experiment, conducted data analysis, and wrote the draft of article; BH conceived and designed the project, reviewed the statistical analyses, and edited the first and final draft of the manuscript; CR contributed to reviewing the analyses and provided critical advice on data analysis. All authors have read and approved the manuscript.

Acknowledgments

The authors gratefully acknowledge Shiraz University for providing a research field for this study. No grant was available to support this research.

Conflict of interest

The authors declare that the research was conducted in the absence of any commercial or financial relationships that could be construed as a potential conflict of interest.

Publisher's note

Supplementary material

The Supplementary Material for this article can be found online at: https://www.frontiersin.org/articles/10.3389/fpls.2023.1239860/full#supplementary-material

References

Abraham, E. M., Meyer, W. A., Bonos, S. A., and Huang, B. (2008). Differential responses of hybrid bluegrass and Kentucky bluegrass to drought and heat stress. *HortScience* 43 (7), 2191–2195. doi: 10.21273/HORTSCI.43.7.2191

Amiri, M. J., and Eslamian, S. S. (2010). Investigation of climate change in Iran. *J. Environ. Sci. Technol.* 3 (4), 208–216. doi: 10.3923/jest.2010.208.216

Berry, C. D., Glover, D. V., and Daniel, W. H. (1969). Phenotypic and genotypic variation and covariation of some quantitative turf characteristics in *Poa pratensis* L. *Crop Sci.* 9, 470–473. doi: 10.2135/cropsci1969.0011183X000900040025x

Blum, A. (2011). *Plant breeding for water-limited environments* (Boca Raton, FL: CRC).

Burtone, G. W., and De Vane, G. M. (1953). Estimating heritability in tall Fescus (*Festuca arundinaceae*) from replicated clonal material. *Agron. J.* 45, 478–481. doi: 10.2134/agronj1953.00021962004500100005x

Byers, D. (2008). Components of phenotypic variance. *Nat. Educ.* 1(1), 161.

Chavers, M. M., Flexas, J., and Pinheiro, C. (2009). Photosynthetics under drought and salt stress: Regulation mechanisms from whole plant to cell. *Ann. Bot.* 103, 551–560. doi: 10.1093/aob/mcn125

Cornic, G. (2000). Drought stress inhibits photosynthesis by decreasing stomatal aperture–not by affecting ATP synthesis. *Trends Plant Sci.* 5 (5), 187–188. doi: 10.1016/S1360-1385(00)01625-3

Fahad, S., Hussain, S., Bano, A., Saud, S., Hassan, S., Shan, D., et al. (2015). Potential role of phytohormones and plant growth-promoting rhizobacteria in abiotic stresses: consequences for changing environment. *Environ. Sci. pollut. Res.* 22, 4907–4921. doi: 10.1007/s11356-014-3754-2

Fang, X., Li, Y., Nie, J., Wang, C., Huang, K., Zhang, Y., et al. (2018). ffects of nitrogen fertilizer and planting density on the leaf photosynthetic characteristics, agronomic traits and grain yield in common buckwheat (*Fagopyrum esculentum* M.). *Field Crop Res.* 219, 160–168. doi: 10.1016/j.fcr.2018.02.001

Fariaszewska, A., Aper, J., Van Huylenbroeck, J., De Swaef, T., and Baert, J. (2020). Physiological and biochemical responses of forage grass varieties to mild drought stress under field conditions. *Int. J. Plant Prod.* 14, 335–353. doi: 10.1007/s42106-020-00088-3

Farquhar, G. D., Von Caemmerer, S., and Berry, J. A. (2001). Models of photosynthesis. *Plant Physiol.* 125 (1), 42–45. doi: 10.1104/pp.125.1.42

Federer, W.T., and Searle, S.R. (1976). Model considerations and variance component estimation in augmented completely randomized and randomized complete blocks designs-Preliminary Version. Cornell University, Ithaca, New York. Available at: https://hdl.handle.net/1813/32691

Flexas, J., and Carriqui, M. (2020). Photosynthesis and photosynthetic efficiencies along the terrestrial plant's phylogeny: lessons for improving crop photosynthesis. *Plant J.* 101, 964–978. doi: 10.1111/tpj.14651

Flood, P. J., Harbinson, J., and Aarts, M. G. M. (2011). Natural genetic variation in plant photosynthesis. *Trends Plant Sci.* 16(6), 327–335. doi: 10.1186/s13007-016-0113-y

Fu, J., and Huang, B. (2001). Involvement of antioxidants and lipid peroxidation in the adaptation of two cool-season grasses to localized drought. *Environ. Exp. Bot.* 45, 105–114. doi: 10.1016/S0098-8472(00)00084-8

Ghanbari, M. A., Salehi, H., and Jowkar, A. (2023). Genetic diversity assessment of Iranian Kentucky bluegrass accessions: II. Nuclear DNA content and its association with morphological and geographical features. *Mol. Biotechnol.* 65 (1), 84–96. doi: 10.1007/s12033-022-00534-9

Ghotbi-Ravandi, A. A., Shahbazi, M., Shariati, M., and Mulo, P. (2014). Effects of mild and severe drought stress on photosynthetic efficiency in tolerant and susceptible barley (*Hordeum vulgare* L.) genotypes. *J. Agron. Crop Sci.* 200, 403–415. doi: 10.1111/jac.12062

Guidi, L., Lo Piccolo, E., and Landi, M. (2019). Chlorophyll fluorescence, photoinhibition and abiotic stress: does it make any difference the fact to be a C3 or C4 species? *Front. Plant Sci.* 10. doi: 10.3389/fpls.2019.00174

Gururani, M. A., Venkatesh, J., and Tran, L. S. P. (2015). Regulation of photosynthesis during abiotic stress-induced photoinhibition. *Mol. Plant* 8 (9), 1304–1320. doi: 10.1016/j.molp.2015.05.005

Harbinson, J., and Yin, X. (2023). Modelling the impact of improved photosynthetic properties on crop performance in Europe. *Food Energy Secur.* 12 (1), e402. doi: 10.1002/fes3.402

Heshmati, G. A. (2007). Vegetation characteristics of four ecological zones of Iran. *Int. J. Plant Prod.* 1 (2), 215–224.

Hu, L., Wang, Z., and Huang, B. (2010). Diffusion limitations and metabolic factors associated with inhibition and recovery of photosynthesis from drought stress in a C3 perennial grass species. *Physiol. Plant* 139 (1), 93–106. doi: 10.1111/j.1399-3054.2010.01350.x

Hu, L., Wang, Z., and Huang, B. (2013). Effects of cytokinin and potassium on stomatal and photosynthetic recovery of Kentucky bluegrass from drought stress. *Crop Sci.* 53 (1), 221–231. doi: 10.2135/cropsci2012.05.0284

Israelsen, O. W., and Hansen, V. E. (1962). *Irrigation Principles and Practices* (Inc., New York: John Wiley & Sons), 448.

Jalata, Z., Ayana, A., and Zeleke, H. (2011). Variability, heritability and genetic advance for some yield and yield related traits in Ethiopian Barley (*Hordeum vulgare* L.) landraces and crosses. *Int. J. Plant Breed. Genet.* 5 (1), 44–52. doi: 10.3923/ijpbg.2011.44.52

Johnson, H. W., Robinson, H. F., and Comstock, R. E. (1955). Estimates of genetic and environmental variability in soybeans. *Agron. J.* 47, 314–318. doi: 10.2134/agronj1955.00021962004700070009x

Kebbas, S., Lutts, S., and Aid, F. (2015). Effect of drought stress on the photosynthesis of *Acacia tortilis* subsp. *raddiana* at the young seedling stage. *Photosynthetica* 53 (2), 288–298. doi: 10.1007/s11099-015-0113-6

Keller, B., Zimmermann, L., Rascher, U., Matsubara, S., Steier, A., and Muller, O. (2022). Toward predicting photosynthetic efficiency and biomass gain in crop genotypes over a field season. *Plant Physiol.* 188 (1), 301–317. doi: 10.1093/plphys/kiab483

Kolde, R., and Kolde, M. R. (2018) *Package 'pheatmap'. R package*. Available at: https://cran.microsoft.com/snapshot/2018-06-22/web/packages/pheatmap/pheatmap.pdf.

Kole, P. C., and Saha, A. (2013). Correlation coefficients of component characters with seed yield and their direct effects in path analysis in fenugreek grown under six environments. *J. Hortic. Forest.* 5, 17–20. doi: 10.5897/JHF12.020

Lawlor, D.W. (1995) The effects of water deficit on photosynthesis. *In Environment and Plant Metabolism* (ed. N. Smirnoff), pp. 129–160. Bios Scientific Publishers, Oxford.

Lawson, T., Kramer, D. M., and Raines, C. A. (2012). Improving yield by exploiting mechanisms underlying natural variation of photosynthesis. *Curr. Opin. Biotechnol.* 23 (2), 215–220. doi: 10.1016/j.copbio.2011.12.012

Li, C. X., Shen, H. Y., Wang, T., and Wang, X. L. (2015). ABA regulates subcellular redistribution of OsABI-LIKE2, a negative regulator in ABA signaling, to control root architecture and drought resistance in *Oryza sativa*. *Plant Cell Physiol.* 56, 2396–2408. doi: 10.1093/pcp/pcv154

Liang, G., Liu, J., Zhang, J., and Guo, J. (2020). Effects of drought stress on photosynthetic and physiological parameters of tomato. *J. Am. Soc Hortic. Sci.* 145 (1), 12–17. doi: 10.21273/JASHS04725-19

Liu, X., and Huang, B. (2000). Heat stress injury in relation to membrane lipid peroxidation in creeping bentgrass. *Crop Sci.* 40, 503–510. doi: 10.2135/cropsci2000.402503x

Liu, L., Wang, X., and Chang, C. (2022a). Toward a smart skin: Harnessing cuticle biosynthesis for crop adaptation to drought, salinity, temperature, and ultraviolet stress. *Front. Plant Sci.* 13. doi: 10.3389/fpls.2022.961829

Liu, W., Xie, F., Chen, Y., and Cui, G. (2022b). Growth and morphological responses of Kentucky bluegrass to homogeneous and heterogeneous soil water availabilities. *Agron* 12 (6) 1265. doi: 10.3390/agronomy12061265

Liu, J., Zhang, R., Zhang, G., Jing, G., and Zhi, D. (2017). Effects of soil drought on photosynthetic traits and antioxidant enzyme activities in *Hippophae rhamnoides* seedlings. *J. For. Res.* 28, 255–263. doi: 10.1007/s11676-016-0302-6

Lush, J. H. (1940). Intra-sire correlations or regressions of offspring on dam as a method of estimating heritability of characteristics. *J. Anim. Sci.* 1940 (1), 293–301. doi: 10.2527/jas1940.19401293x

Majidi, M. M., Mirlohi, A., and Amini, F. (2009). Genetic variation, heritability and correlations of agro-morphological traits in tall fescue (*Festuca arundinacea* Schreb.). *Euphytica* 167 (3), 323–331. doi: 10.1007/s10681-009-9887-6

Mastalerczuk, G., Borawska-Jarmułowicz, B., and Darkalt, A. (2022). Changes in the physiological and morphometric characteristics and biomass distribution of forage grasses growing under conditions of drought and silicon application. *Plants* 12 (1), 16. doi: 10.3390/plants12010016

McCann, S. E., and Huang, B. (2008). Drought responses of Kentucky bluegrass and creeping bentgrass as affected by abscisic acid and trinexapac-ethyl. *J. Am. Soc Hortic. Sci.* 133 (1), 20–26. doi: 10.21273/JASHS.133.1.20

Medrano, H., Escalona, J. M., Bota, J., Gulias, J., and Flexas, J. (2002). Regulation of photosynthesis of C3 plants in response to progressive drought: stomatal conductance as a reference parameter. *Ann. Bot.* 89 (7), 895–905. doi: 10.1093/aob/mcf079

Mehri, N., Fotovat, R., Saba, J., and Jabbari, F. (2009). Variation of stomata dimensions and densities in tolerant and susceptible wheat cultivars under drought stress. *J. Food Agric. Environ.* 7 (1), 167–170.

Meng, L., Li, L., Chen, W., Xu, Z., and Liu., L. (1999). Effect of water stress on stomatal density, length, width and net photosynthetic rate in rice leaves. *J. Shenyang Agric. Univ.* 30, 477–480.

Merewitz, E., Meyer, W., Bonos, S., and Huang, B. (2010). Drought stress responses and recovery of Texas× Kentucky hybrids and Kentucky bluegrass genotypes in temperate climate conditions. *Agron. J.* 102 (1), 258–268. doi: 10.2134/agronj2009.0328

Montgomery, D. C. (2006). *Introduction to linear regression analysis* (New York: John Wiley and Sons).

Nitesh, S. D., Patroti, P., and Parashuram, S. (2020) *Data Analysis with TraitStats. R packages*. Available at: https://cran.r-project.org/web/packages/TraitStats/TraitStats.pdf.

Noorisameleh, Z., Khaledi, S., Shakiba, A., Firouzabadi, P. Z., Gough, W. A., and Mirza, M. M. (2020). Comparative evaluation of impacts of climate change and droughts on river flow vulnerability in Iran. *Water Sci. Eng.* 13 (4), 265–274. doi: 10.1016/j.wse.2020.05.001

Quarrie, S. A., and Jones, H. G. (1977). Effects of abscisic acid and water stress on development and morphology of wheat. *J. Exp. Bot.* 28, 192–203. doi: 10.1093/jxb/28.1.192

Roig-Oliver, M., Fullana-Pericàs, M., Bota, J., and Flexas, J. (2021). Adjustments in photosynthesis and leaf water relations are related to changes in cell wall composition in Hordeum vulgare and Triticum aestivum subjected to water deficit stress. *Plant Sci.* 311, 111015. doi: 10.1016/j.plantsci.2021.111015

Saud, S., Li, X., Chen, Y., Zhang, L., Fahad, S., Hussain, S., et al. (2014). Silicon application increases drought tolerance of Kentucky bluegrass by improving plant water relations and morphophysiological functions. *Sci. World J.* 2014, 368694 doi: 10.1155/2014/368694

Saud, S., Yajun, C., Fahad, S., Hussain, S., Na, L., Xin, L., et al. (2016). Silicate application increases the photosynthesis and its associated metabolic activities in Kentucky bluegrass under drought stress and post-drought recovery. *Environ. Sci. pollut. Res.* 23, 17647–17655. doi: 10.1007/s11356-016-6957-x

Schreiber, U., Bilger, W., and Neubauer, C. (1995). "Chlorophyll Fluorescence as a Nonintrusive Indicator for Rapid Assessment of *In Vivo* Photosynthesis," in *Ecophysiology of Photosynthesis. Springer study Edition*, vol. 100 . Eds. E. D. Schulze and M. M. Caldwell (Berlin, Heidelberg: Springer). doi: 10.1007/978-3-642-79354-7_3

Seleiman, M. F., Al-Suhaibani, N., Ali, N., Akmal, M., Alotaibi, M., Refay, Y., et al. (2021). Drought stress impacts on plants and different approaches to alleviate its adverse effects. *Plants* 10 (2), 259. doi: 10.3390/plants10020259

Shariatipour, N., Heidari, B., Shams, Z., and Richards, C. (2022). Assessing the potential of native ecotypes of *Poa pratensis* L. for forage yield and phytochemical compositions under water deficit conditions. *Sci. Rep.* 12, 1121. doi: 10.1038/s41598-022-05024-1

Simon, E. W. (1974). Phospholipids and plant membrane permeability. *New Phytol.* 73, 377–420. doi: 10.1111/j.1469-8137.1974.tb02118.x

Singh, V. K., Sharma, V., Kumar, S. P., Chaudhary, M., Sharma, B., and Chauhan, M. P. (2016). Study on genetic variability, heritability and genetic advance for yield and its contributing traits in linseed (*Linum usitatissimum* L.). *Curr. Adv. Agric. Sci.* 8 (2), 192–194. doi: 10.5958/2394-4471.2016.00046.0

Souza, R. P., MaChado, E. C., Silva, J. A. B., Lagôa, A. M. M. A., and Silveira, J. A. G. (2004). Photosynthetic gas exchange, chlorophyll fluorescence and some associated metabolic changes in cowpea (Vigna unguiculata) during water stress and recovery. *Environ. Exp. Bot.* 51 (1), 45–56. doi: 10.1016/S0098-8472(03)00059-5

Staniak, M., Bojarszczuk, J., and Księżak, J. (2018). Changes in yield and gas exchange parameters in Festulolium and alfalfa grown in pure sowing and in mixture under drought stress. *Acta Agric. Scand. - B Soil Plant Sci.* 68 (3), 255–263. doi: 10.1080/09064710.2017.1390149

Terfa, G. N., and Gurmu, G. N. (2020). Genetic variability, heritability and genetic advance in linseed (*Linum usitatissimum* L) genotypes for seed yield and other agronomic traits. *Oil Crop Sci.* 5 (3), 156–160. doi: 10.1016/j.ocsci.2020.08.002

Torres-Ruiz, J. M., Diaz-Espejo, A., Perez-Martin, A., and Hernandez-Santana, V. (2015). Role of hydraulic and chemical signals in leaves, stems and roots in the stomatal behaviour of olive trees under water stress and recovery conditions. *Tree Physiol.* 35, 415–424. doi: 10.1093/treephys/tpu055

Varone, L., Ribas-Carbo, M., Cardona, C., Gallé, A., Medrano, H., Gratani, L., et al. (2012). Stomatal and non-stomatal limitations to photosynthesis in seedlings and saplings of Mediterranean species pre-conditioned and aged in nurseries: Different response to water stress. *Environ. Exp. Bot.* 75, 235–247. doi: 10.1016/j.envexpbot.2011.07.007

Wang, Z., and Huang, B. (2003). Genotypic variation in abscisic acid accumulation, water relations, and gas exchange for Kentucky bluegrass exposed to drought stress. *J. Am. Soc Hortic. Sci.* 128 (3), 349–355. doi: 10.21273/JASHS.128.3.0349

Wei, T., Simko, V., Levy, M., Xie, Y., Jin, Y., and Zemla, J. (2017). Package 'corrplot'. *Statistician* 56 (316), e24.

Wise, R. R., and Naylor, A. W. (1987). Chilling-enhanced photo-oxidation. The peroxidative destruction of lipids during chilling injury to photosynthesis and ultrastructure. *Plant Physiol.* 83, 278–282. doi: 10.1104/pp.83.2.272

Wong, S. C., Cowan, I. R., and Farquhar, G. D. (1979). Stomatal conductance correlates with photosynthetic capacity. *Nature* 282 (5737), 424–426. doi: 10.1038/282424a0

Xu, Z., and Zhou, G. (2008). Responses of leaf stomatal density to water status and its relationship with photosynthesis in a grass. *J. Exp. Bot.* 59, 3317–3325. doi: 10.1093/jxb/ern185

Yang, X., Lu, M., Wang, Y., Wang, Y., Liu, Z., and Chen, S. (2021). Response mechanism of plants to drought stress. *Horticulturae* 7 (3), 50. doi: 10.3390/horticulturae7030050

Zhang, X., Goatley, M., Wu, W., Ervin, E., and Shang, C. (2019). Drought-induced injury is associated with hormonal alteration in Kentucky bluegrass. *Plant Signal. Behav.* 14 (10), e1651607. doi: 10.1080/15592324.2019.1651607

Zhang, X., Liu, W., Lv, Y., Li, T., Tang, J., Yang, X., et al. (2022). Effects of drought stress during critical periods on the photosynthetic characteristics and production performance of Naked oat (*Avena nuda* L.). *Sci. Rep.* 12 (1), 11199. doi: 10.1038/s41598-022-15322-3

Frontiers in
Plant Science

Cultivates the science of plant biology and its applications

The most cited plant science journal, which advances our understanding of plant biology for sustainable food security, functional ecosystems and human health.

Discover the latest Research Topics

See more →

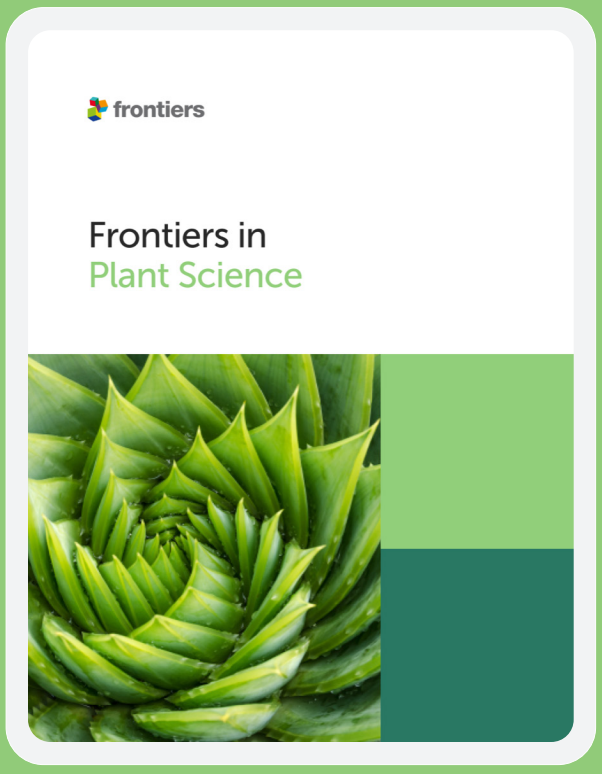

Frontiers

Avenue du Tribunal-Fédéral 34
1005 Lausanne, Switzerland
frontiersin.org

Contact us

+41 (0)21 510 17 00
frontiersin.org/about/contact